

---

Synthesis of functional glycoconjugates  
to explore structural aspects  
of carbohydrate recognition

---

Dissertation

zur Erlangung des Doktorgrades  
der Mathematisch-Naturwissenschaftlichen Fakultät  
der Christian-Albrechts-Universität zu Kiel  
vorgelegt von

Sven Ole Jaeschke  
aus Hamburg

Otto Diels-Institut für Organische Chemie  
Kiel 2021



*“Das Wichtigste ist,  
dass man nicht aufhört zu fragen.“*

Albert Einstein

---

Referentin: Prof. Dr. Thisbe K. Lindhorst

Koreferent: Prof. Dr. Frank D. Sönnichsen

Tag der mündlichen Prüfung: 07. März 2022

Die vorliegende Arbeit wurde unter Anleitung von  
Prof. Dr. Thisbe K. Lindhorst  
am Otto Diels-Institut für Organische Chemie  
der Christian-Albrechts-Universität zu Kiel  
im Zeitraum von  
November 2016 bis Dezember 2021 angefertigt.



Hiermit erkläre ich, Sven Ole Jaeschke, dass ich die vorliegende Arbeit selbstständig und nur unter Verwendung der angegebenen Quellen und Hilfsmittel angefertigt habe. Inhalt und Form dieser Arbeit sind eigenständig erarbeitet und verfasst worden. Die Arbeit ist unter Einhaltung der Regeln guter wissenschaftlicher Praxis der Deutschen Forschungsgemeinschaft entstanden. Weder die gesamte Arbeit noch Teile davon sind an anderer Stelle im Rahmen eines Prüfungsverfahrens eingereicht worden. Dies ist mein erster Promotionsversuch. Mir wurde kein akademischer Grad entzogen.

Kiel,

---

Sven Ole Jaeschke



Im Rahmen der Masterarbeit wurden bereits Teile des Kapitels 3 erarbeitet und in dieser Arbeit übernommen:

- Die Syntheseroute zu Verbindung **10** in Scheme 3.1
- Die Syntheseroute zu Verbindung **15** in Scheme 3.2
- Die Syntheseroute zu Verbindung **18** in Scheme 3.3

Die theoretischen Berechnungen im Kapitel 5 wurden von Prof. Dr. Alexander A. Auer (MPI für Kohlenforschung, Mülheim) durchgeführt.

Teile dieser Arbeit wurden bereits veröffentlicht:

- S. O. Jaeschke, T. K. Lindhorst, "*Versatile Synthesis of Diaminoxylosides via Iodosulfonamidation of Xylal Derivatives*", *Eur. J. Org. Chem.* **2021**, 2021, 6312-6318. (DOI: 10.1002/ejoc.202100792)
- S. O. Jaeschke, I. vom Sondern, T. K. Lindhorst, "*Synthesis of regioisomeric maltose-based Man/Glc glycoclusters to control glycoligand presentation in 3D space*", *Org. Biomol. Chem.* **2021**, 19, 7013-7023. (DOI: 10.1039/D1OB01150B)
- G. Despras, J. Hain, S. O. Jaeschke, "*Photocontrol over Molecular Shape: Synthesis and Photochemical Evaluation of Glycoazobenzene Macrocycles*", *Chem. Eur. J.* **2017**, 23, 10838-10847. (DOI: 10.1002/chem.201701232)



## Abstract

Cell surface glycoconjugates play an important role in many fundamental processes of cell recognition. For example, bacterial adhesion is mediated by carbohydrate-specific binding of bacterial lectins to the glycocalyx of host cells. The molecular and structural complexity of the glycocalyx is essential for its biological function but yet has not been understood in every detail. Thus, scientists are interested in developing new tools and methods to investigate the role of glycans in biological processes. Within the scope of this thesis multifunctional glycoconjugates were designed and synthesized to study in particular, the organization of multivalency and the conformational switching of monosaccharides in the context of carbohydrate recognition.

In the first part of this thesis, the organization of heteromultivalency is addressed in a bottom-up approach based on the synthesis of regioisomeric heterobivalent Man/Glc glycoclusters, which were derived from a multifunctional maltoside scaffold molecule. These glycoclusters were tested as inhibitors of lectin (FimH)-mediated bacterial adhesion and the results rationalized by molecular modelling. It turned out that especially the spatial orientation of the Man ligand essentially governs the inhibitory potency of the respective heteroglycocluster, whereas the glucose moiety contributes secondary interactions in complex with the bacterial lectin FimH.

In order to explore and control different monosaccharide conformations, xylose derivatives were investigated as conformational switches in the second part of this thesis. Accordingly, a new synthesis strategy of 2,4-diamino xyloside derivatives was explored based on xylals as key intermediates of the synthetic route. Danishefsky's iodosulfonamidation was utilized to achieve *xy/o*-configured conformational switches with high precision in stereo- and regiochemistry. Their  ${}^4C_1$  to  ${}^1C_4$  conformational equilibrium can be controlled by chelation of the 2- and 4-amino groups with zinc ions. Furthermore, the conformational equilibrium of 2,4-diamino xyloside derivatives was analyzed in greater detail by a combination of NMR spectroscopy and theoretical chemistry in collaboration.

In a last chapter, the xyloside conformational switch was used as basis for the synthesis of a bivalent cluster mannoside. Its controlled conformational switching between the  ${}^4C_1$  and the  ${}^1C_4$  conformation strongly influences the amplitude of Man ligand presentation. The biological effect of this kind of orientational control of ligand presentation was measured in a bacterial adhesion-inhibition assay, showing a significant functional difference.

Within these three sections this thesis revealed original architectures and synthetic routes for functional glycoconjugates, with whom effects of multivalency, and spatial ligand orientation were controlled and led to a better understanding of carbohydrate recognition.



## Kurzzusammenfassung

Glykokonjugate auf Zelloberflächen nehmen eine wesentliche Rolle in fundamentalen Zellerkennungsprozessen ein. Insbesondere die bakterielle Adhäsion ist bestimmt durch kohlenhydratspezifische Bindungen von bakteriellen Lektinen an die Glykokalyx von Wirtszellen. Die molekulare und strukturelle Komplexität der Glykokalyx ist essenziell für ihre biologische Funktion, jedoch bis jetzt nicht bis ins Detail verstanden. Demzufolge sind NaturwissenschaftlerInnen daran interessiert, neue Methoden und Instrumente zu schaffen, um die Rolle von Glykanen in biologischen Prozessen zu untersuchen. Im Rahmen dieser Arbeit wurden multifunktionale Glykokonjugate entwickelt und synthetisiert, um insbesondere die Organisation von Multivalenz und das konformationelle Schalten von Monosacchariden im Kontext der Kohlenhydraterkennung zu untersuchen.

Im ersten Teil dieser Thesis wurde die „Organisation von Heteromultivalenz“ in einem bottom-up Ansatz adressiert. Dazu wurden, basierend auf multifunktionalen Maltosescaffolds regioisomere heterobivalente Man/Glc Glykocluster dargestellt. Diese Glykocluster wurden als Inhibitoren von lektinvermittelter bakterieller Adhäsion (FimH) getestet und die Ergebnisse wurden mit Hilfe von Modellierungsexperimenten genauer untersucht. Es zeigte sich, dass besonders die räumliche Orientierung der Mannoseliganden essenziell für das Inhibitionspotential der jeweiligen Heteroglykocluster war. Zudem konnte festgestellt werden, dass die Glc-Einheit zu sekundären Cluster-Protein Wechselwirkungen mit dem Lektin FimH führte.

Um die unterschiedlichen Konformationen von Monosacchariden zu analysieren und zu kontrollieren, wurden im zweiten Teil dieser Thesis Xyloederivate als konformationelle Schalter untersucht. Dabei wurde eine neue Synthesestrategie für 2,4-Diaminoxyloside entwickelt, welche auf Xylalen als Schlüsselintermediaten basierte. Zudem wurde Danishefsky's Iodsulfonylamidierung implementiert, um *xylo*-konfigurierte konformationelle Schalter mit einer hoher Regio- und Stereospezifität darzustellen. Das vorliegende konformationelle Gleichgewicht von 2,4-Diaminoxylosiden zwischen  ${}^4C_1$  zu  ${}^1C_4$  lässt sich durch die Komplexierung von Zinkionen kontrollieren. Das konformationelle Gleichgewicht von 2,4-Diaminoxylosiden wurde mit einer Kombination aus NMR-Experimenten und einer Kollaboration mit der theoretischen Chemie genauer analysiert.

Im letzten Kapitel wurden, basierend auf den konformationell schaltbaren Xylosiden, bivalente Mannosidcluster synthetisiert. Das kontrollierte Schalten zwischen den  ${}^4C_1$  und  ${}^1C_4$  Konformationen beeinflusst die Amplitude der Mannosidligandenpräsentation immens. Die Auswirkungen dieser kontrollierten Kontrolle der Ligandenpräsentation wurde in bakteriellen

Adhäsions-Inhibitions-Assays bestimmt und zeigte einen signifikanten funktionalen Unterschied auf.

In den drei Abschnitten dieser Thesis konnten originelle Architekturen und Syntheserouten für funktionale Glykokonjugate aufgezeigt werden, mit denen Effekte der Multivalenz und der räumlichen Ligandenorientierung kontrolliert werden konnten. Diese Aspekte führen zu einem besseren Verständnis von Kohlenhydraterkennung.

## Table of contents

1	General introduction.....	1
1.1	Carbohydrates in the context of glycobiology.....	1
1.2	Multivalency effects.....	6
1.3	Conformations of pyranoses.....	9
1.4	Conformational equilibria and their analysis.....	13
1.5	Conformational switchable monosaccharides.....	16
2	How can carbohydrate-protein interactions be controlled? – The project idea.....	20
3	The effect of carbohydrate ligand presentation by maltose-based glycoclusters.....	22
3.1	Synthesis of heterobivalent maltose-based glycoclusters.....	27
3.2	Synthesis of homobivalent maltose-based glycoclusters.....	38
3.3	Biological testing.....	42
3.4	Molecular modelling.....	44
3.5	Conclusion.....	49
4	Conformational glycoswitches: Synthesis of 2,4-diamino xylosides.....	51
4.1	Synthesis of 2,4-diamino xylosides via thioglycosides.....	54
4.2	Starting from L-arabinose – the glycal approach.....	59
4.3	Following the glycal approach via iodosulfonamidation.....	69
4.4	2,4-Diamino xylosides as conformational switches.....	84
4.5	Conclusion.....	88
5	Solvent-dependent conformational equilibria and their analysis.....	90
5.1	Determination of coupling constants to describe conformations.....	91
5.2	Which conformers occur in solution?.....	97
5.3	Solvent-dependent conformational equilibria.....	100
5.4	Conclusion.....	105
6	Biphenyl xyloside clusters to control spatial ligand presentation.....	106
6.1	Synthesis of bis-biphenyl xyloside glycoclusters.....	108
6.2	Biological testing.....	114

6.3	Molecular modelling .....	116
6.4	The potential of orthogonal switchable glycoconjugates .....	122
6.5	Conclusion.....	125
7	What have we learned? – Concluding remarks.....	126
8	Experimental section.....	130
8.1	Materials and methods .....	130
8.2	Individual synthetic procedures .....	133
8.2.1	Synthetic procedures for chapter 3 .....	133
8.2.2	Synthetic procedures for chapter 4.1.....	166
8.2.3	Synthetic procedures for chapter 4.2.....	173
8.2.4	Synthetic procedures for chapter 4.3.....	189
8.2.5	Synthetic procedures for chapter 4.4.....	210
8.2.6	Synthetic procedures for chapter 6 .....	212
8.3	Biological tests.....	226
8.4	Computational methods.....	232
8.4.1	Molecular modelling with Schrödinger .....	232
8.4.2	DFT calculations .....	234
8.5	NMR spectra of synthesized compounds.....	238
9	References.....	297
	Abbreviations .....	320
	Danksagung.....	322

## 1 General introduction

Carbohydrates are essential components of all living organisms. Next to lipids, nucleotides, and proteins they play a central role in biochemical processes in health and disease.<sup>[1]</sup> The structural diversity of carbohydrates (glycans) is unequalled due to the stereochemical features of monosaccharides including the stereo- and regiochemistry of the glycosidic linkages leading to oligo- and polysaccharides. In addition, functional modifications, such as O-sulfatation, -acetylation, or -phosphorylation, as well as deoxy- and amino-deoxy functions contribute to the vast variety of glycans in nature and their biological functions.<sup>[2]</sup> In nature carbohydrates are products of photosynthesis, forming D-glucose from carbon dioxide and water. Subsequent biosynthetic steps of the plant cell metabolism lead to multiple modifications of D-glucose such as epimerization, resulting in the biosynthesis of diverse glycans. In mammalian organisms, carbohydrates have different crucial functions, such as energy production, energy storage and macromolecule fabrication. In addition, they are also involved in cell recognition,<sup>[3]</sup> cell communication and microbial colonization and invasion<sup>[4]</sup> either by commensal or pathogenic species.<sup>[1b]</sup> However, in the field of carbohydrate and glycobiological research many details of the impact of glycans remain unknown to date due to the enormous complexity of carbohydrate display on the cell surface.<sup>[5]</sup> Thus, additional synthetic as well as analytical tools for the study of glycan recognition and function are required, in order to better understand carbohydrate-dependent cell biology and to explore the diversity and structural boundary conditions of glycoconjugate function beyond what is known so far.<sup>[6]</sup>

### 1.1 Carbohydrates in the context of glycobiology

Cell surface glycans play a fundamental role in glycobiology, especially in processes such as cell recognition and cell adhesion. Cell recognition can occur when a counterpart (e.g., bacteria or viruses) recognizes a specific carbohydrate epitope as glycoligand on the surface of a cell membrane via special carbohydrate-binding proteins, so-called lectins (*vide infra*).<sup>[7]</sup> These carbohydrate-protein interactions depend on the stereochemistry and the conformation of glycoligands, their presentation in space and their multivalent organization.

The membrane of eukaryotic cells consists of different lipids, which are forming a bilayer surrounding the cell and protecting it from external influences such as pH changes or salts. Furthermore, various proteins are incorporated into this bilayer. They connect the innercellular and extracellular sites and function as receptors, ion channels or carrier proteins. At the extracellular site, the lipid bilayer of eukaryotic cells is functionalized with complex

inhomogenously arranged glycoconjugates, which are bound to proteins or lipids incorporated in the cell membrane. This thick layer of glycoconjugates (up to 100 nm or more) surrounds the whole cell and is thus called the “glycocalyx” (Figure 1.1).<sup>[8]</sup> The composition of the glycocalyx differs from cell type to cell type and thus is highly individual. In addition, the glycocalyx is dependent on the aging process and the physiological status of a cell.<sup>[9]</sup> For cancer cells it is observed that the expression of bulky glycoproteins is upregulated, which influences transmembrane receptor organization and function resulting in metastasis.<sup>[10]</sup>

The glycocalyx represents a site of first contact in many biological processes and interacts with a broad spectrum of external partners. These extracellular processes mediated by the glycocalyx have been extensively investigated. It was shown that glycoconjugates in form of glycoproteins or glycolipids play an important role in cellular processes, such as signaling,<sup>[3a]</sup> molecular recognition<sup>[11]</sup> and cell adhesion.<sup>[12]</sup> For example, glycoconjugates serve as attachment points for pathogenic organisms including bacteria or viruses. These adhesion processes are mediated by protein-protein interactions, carbohydrate-carbohydrate interactions and especially by protein-carbohydrate interactions, respectively. Many mechanistic details of glycocalyx functions are not fully understood to date and define an important research area in glycobiology.

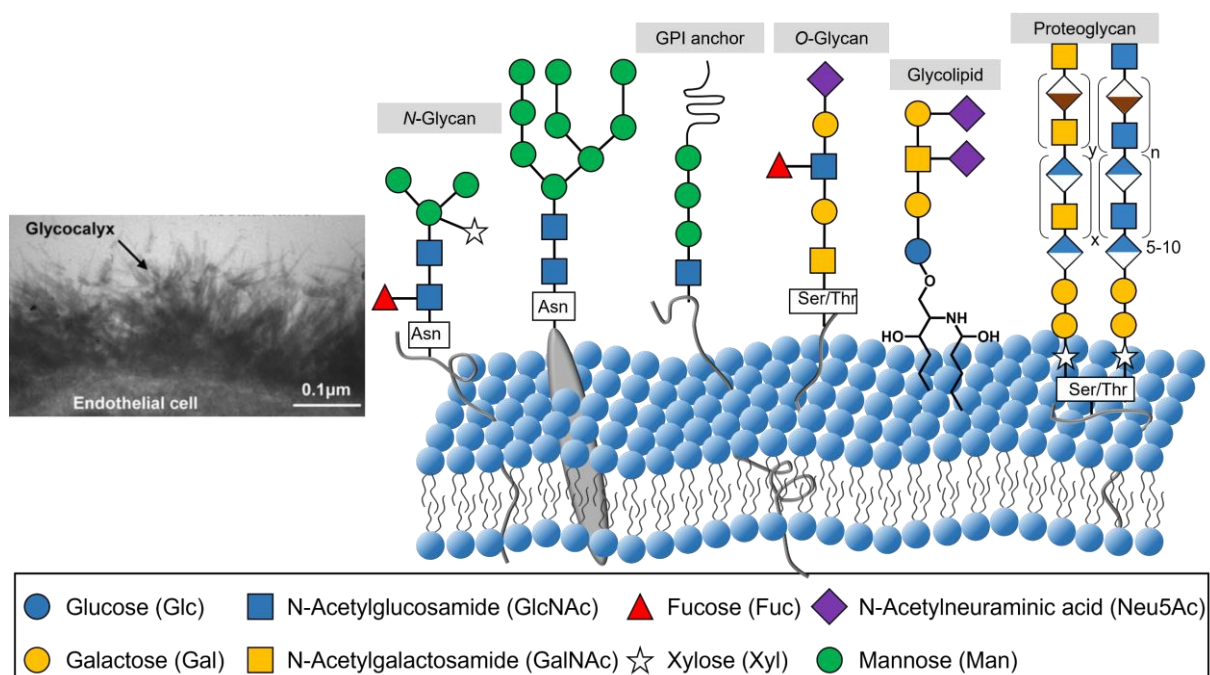


**Figure 1.1.** Electron micrograph of an endothelial cell (left) showing the glycocalyx.<sup>[13]</sup> A schematic overview of a eukaryotic cell membrane (right) shows the phospholipid bilayer and some basic glycan structures,<sup>[14]</sup> which are commonly linked to either membrane proteins (*N*-glycans, *O*-glycans, proteoglycans), GPI anchors or lipids. Carbohydrate moieties are depicted according to the convention introduced by the Consortium for Functional Glycomics (CFG).<sup>[15]</sup>

Glycocalyx components mainly consist of glycoproteins and glycolipids. In glycolipids, the lipid moiety is embedded into the cell membrane, projecting the glycoconjugate to the extracellular space.<sup>[16]</sup> But glycolipids can exist also in the lumen of the endoplasmic reticulum (ER). Often, the carbohydrate constituents of glycolipids are galactose or glucose residues as in the case of cerebroside. The oligosaccharide portions of gangliosides are more complex and typically contain sialic acid residues. Especially gangliosides are an important object of glycobiological research because they are part of cell signaling processes in the nervous system.<sup>[17]</sup>

Glycoproteins, on the other hand, are divided into two main groups, *N*- and *O*-glycoproteins. The *O*-glycans, bearing a *N*-acetylgalactosamine (GalNAc) moiety in its structure, are bound to the hydroxyl group of a side chain of serine (Ser) or threonine (Thr), respectively (Figure 1.1).<sup>[18]</sup> *O*-Glycans mainly occur in mucins, which are transmembrane proteins and can be found in mucous secretions.

*N*-Glycans form the most common group of glycoproteins. They are *N*-glycosidically linked to the side chain of an asparagine (Asn) residue of the protein. The common sequon for *N*-glycosylation is Asn-X-Ser or Asn-X-Thr (X is any amino acid except proline). In general, all *N*-glycans share the same core pentasaccharide, namely Man ( $\alpha$ 1,6) (Man ( $\alpha$ 1,3)) Man ( $\beta$ 1,4) GlcNAc ( $\beta$ 1,4) GlcNAc ( $\beta$ 1-Asn). With respect to the diverse functionalization of this core pentasaccharide, *N*-glycans are subdivided into three classes, those of the high-mannose type, where only mannose units are attached to the core structure, the complex type, in which several “antennae”, containing galactose and neuraminic acid are attached to the core structure, and those of the hybrid type, in which mannose units are attached to the Man ( $\alpha$ 1,6) branch and a complex-type antennae to the other branch of the core structure (Figure 1.2).<sup>[19]</sup>

Furthermore, *N*-glycans can be modified at the core structure with L-fucose ( $\alpha$ 1,6) or D-xylose ( $\beta$ 1,2), which can have an effect on glycan processing in various biological aspects (Figure 1.1 and Figure 1.2).<sup>[20]</sup> Thus, fucose itself plays an important role in recognition processes and supports specific carbohydrate-protein interactions.<sup>[21]</sup> On the other hand, core-xylose is an immunogenic motif and can often be found in plants. It has been observed that core xylosylation plays a significant role in food allergens and is present in glycans of parasitic nematodes.<sup>[22]</sup> In mammals, xylose is found in proteoglycans as part of the core structure.<sup>[23]</sup>

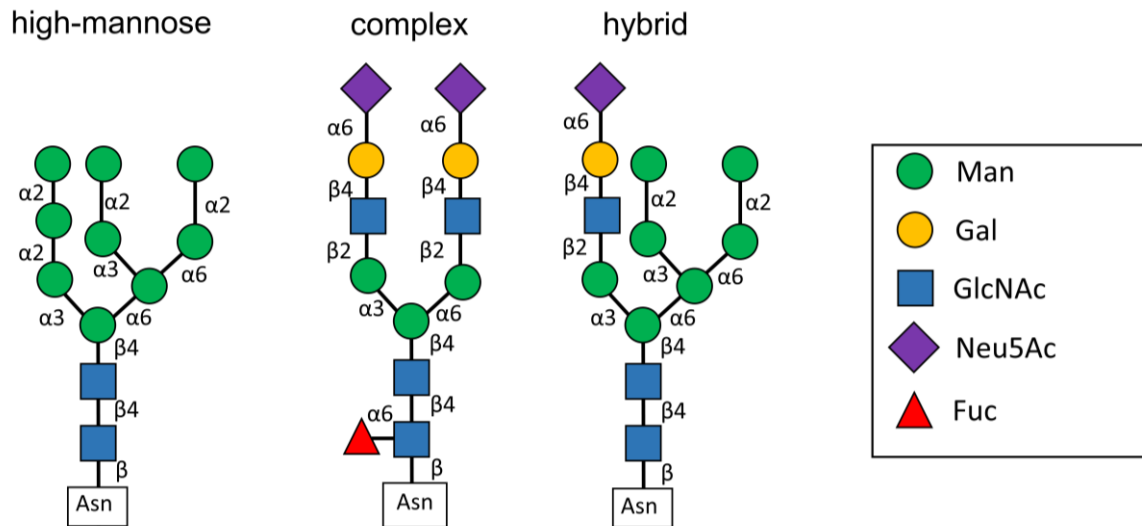


**Figure 1.2.** Schematic presentation of the three different types of *N*-glycans of the high-mannose, complex and hybrid type. All types share the same core pentasaccharide: Man ( $\alpha$ 1,6) (Man ( $\alpha$ 1,3)) Man ( $\beta$ 1,4) GlcNAc ( $\beta$ 1,4) GlcNAc ( $\beta$ 1,Asn). All carbohydrates are shown by the conventions of the Consortium for Functional Glycomics (CFG)<sup>[14-15]</sup> and the following abbreviations are used: Gal (galactose), Man (mannose), GalNAc (*N*-acetylgalactosamine), Neu5Ac (*N*-acetylneuraminic acid) and Fuc (L-fucose).<sup>[24]</sup> Figure adapted from the literature.<sup>[14]</sup>

The glycosylation of eukaryotic proteins is a complex co-translational modification affecting the solubility, charge, and conformation of the protein. Additionally, glycosylation provides carbohydrate ligands for specific recognition processes in cell-cell communication, signal transduction, and immune response.<sup>[25]</sup> Many of these processes are mediated by interactions with lectins.<sup>[26]</sup> Lectins are defined as carbohydrate-specific proteins, lacking an enzymatic or immune activity. They are present in all living organisms including viruses, bacteria and plants.<sup>[6b]</sup>

In 1936, a first conclusion about lectins and their carbohydrate-specific binding was drawn when concanavalin A (Con A) was isolated from jack beans by Sumner and Howell.<sup>[27]</sup> By further investigations, it could be clarified that lectins show similarities in their primary, or tertiary structures, respectively. Additionally, it was revealed that the interaction between lectins and carbohydrate ligands is non-covalent and reversible.<sup>[3a]</sup> The carbohydrate specificity of lectins is often based on a conserved amino acid sequence, which is forming the so-called carbohydrate recognition domain (CRD). The CRD of lectins recognizes terminal non-reducing carbohydrate motifs of glycans and forms complexes with such glycoepitopes. Their carbohydrate specificity discriminates between  $\alpha$ - and  $\beta$ -anomers, which is reflected in different binding affinities.<sup>[26]</sup> Due to their carbohydrate specificity, lectins are involved in several biological processes like cell-cell interactions in the immune system and in the adhesion of infectious agents to host cells.<sup>[4]</sup>

In particular, glycoconjugates of the glycocalyx enable the adhesion of commensal and pathogenic bacteria to eukaryotic cells, which is essential for mammals. The immune system needs those commensal bacteria to inhibit the colonization of pathogens. But if commensal bacteria colonize in regions where they normally do not occur, they can turn into pathogens.<sup>[28]</sup> One example of commensal bacteria are the Gram-negative *Escherichia coli* (*E. coli*), which colonize the gastrointestinal tract of mammals. Other *E. coli* strains, however are pathogens and responsible for a number of infectious diseases, such as urinary tract infections (uropathogenic *E. coli*, UPEC),<sup>[29]</sup> meningitis (neonatal meningitis causing *E. coli*, NMEC),<sup>[30]</sup> or diarrhoea (enterohemorrhagic *E. coli*, EHEC).<sup>[31]</sup> The adhesion of these bacteria occurs mainly via bacterial lectins, which are located either on the bacterial surface or are part of their adhesive organelles called fimbriae.<sup>[32]</sup> *E. coli* bacteria adhere to  $\alpha$ -D-mannoside residues on the surface of urothelial cells mediated by so-called type 1 fimbriae.<sup>[33]</sup> This type of fimbriae consists of the main structural subunit FimA forming the pilus rod, the subunits FimF and FimG, and the mannose-specific adhesin FimH, which is located at the tip of the fimbriae (Figure 1.3, A).<sup>[34]</sup> Fimbriae are connected to the periplasm via a complex with FimC and subunits can cross the bacterial membrane through a pore, formed by FimD.<sup>[35]</sup>

The first crystal structure of the FimH-FimC complex has revealed that the adhesin FimH consists of two domains, namely the FimH<sub>P</sub> pilus domain and the FimH<sub>L</sub> lectin domain. At the tip of the FimH<sub>L</sub> domain, the CRD of FimH is located, which specifically binds  $\alpha$ -D-mannosides.<sup>[34]</sup> The interactions between a mannose ligand and the FimH CRD were investigated in great detail and X-ray analysis revealed that the hydroxyl groups of the ligand interact through hydrogen bonds with the amino acid residues Phe1, Asn46, Asp47, Asp54, Gln133, Asn135, and Phe142. Furthermore, mannosides with an aromatic aglycone show increased affinity due to interactions with two tyrosine residues (Tyr48 and Tyr137) forming the so-called “tyrosine gate” at the entrance of the FimH CRD. These residues undergo  $\pi$ - $\pi$  interactions with the aromatic glycoconjugate, which improves the overall complexation of the ligand (Figure 1.3, B).<sup>[36]</sup> In addition to the interactions inside the CRD and with the tyrosine gate, the complexes between carbohydrate ligands and the lectin FimH can be influenced by secondary interactions with various regions in the periphery of the CRD.<sup>[37]</sup>

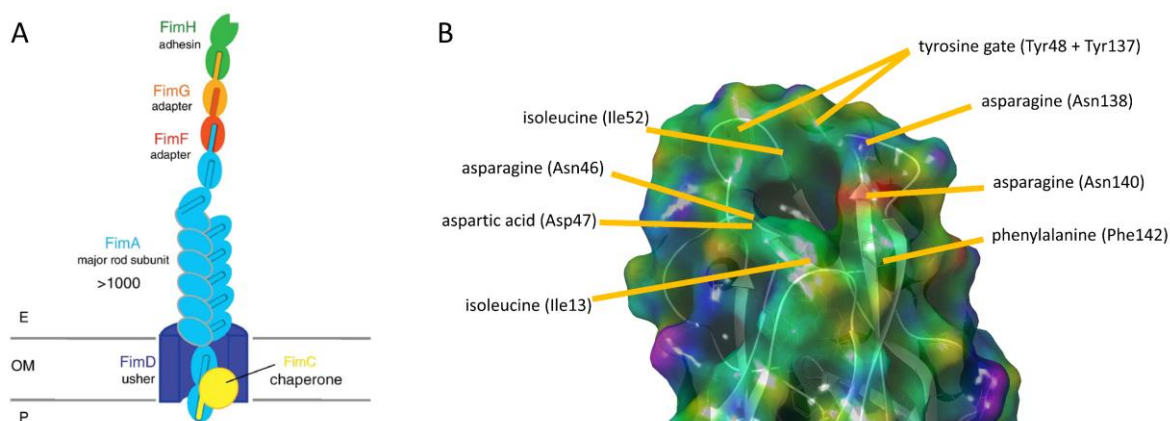


**Figure 1.3.** Schematic representation of the type 1 fimbriae, consisting of the fimbrial shaft and a flexible tip including the lectin FimH (A). (Figure adapted from literature.<sup>[35]</sup>) The CRD of FimH is specific for  $\alpha$ -D-mannosides and the “tyrosine gate” (Tyr48 and Tyr137) supports the interactions with the aromatic aglycone of synthetic ligands. (B) In the periphery of the CRD various other amino acids can exert secondary interactions with further moieties of, for example, glycoclusters. Rendered with Schrödinger (color code: positive charges in purple, neutral in green, negative charges in red).

FimH-mediated bacterial adhesion is a very well investigated process and can serve as a robust model system for the investigation of carbohydrate-protein interactions and some of their more novel aspects, such as ligand orientation or conformational effects.

## 1.2 Multivalency effects

An important characteristic of the glycocalyx is the multivalent presentation of glycoligands. Typical binding constants of singular lectin-carbohydrate interactions are in the millimolar or high micromolar range. However, as oligosaccharides are highly branched and glycoligands are presented as multiple copies,<sup>[38]</sup> carbohydrate recognition benefits from the fact that various simultaneous carbohydrate-lectin interactions can occur in a multivalent process adding several low affinities of singular interacting events to an overall high avidity.<sup>[39]</sup> Therefore, multivalent glycoconjugates have become valuable tools to investigate carbohydrate interactions. Already early studies by Y. C. Lee and co-workers have shown that a linear increase of ligand valency within a synthetic glycocluster can result in a logarithmic increase of binding avidity (combined strength of all carbohydrate-lectin interactions).<sup>[39b, 40]</sup> This effect has been called the “cluster effect”, corresponding to multivalent interaction of glycoligands with multiple CRDs of a lectin.<sup>[41]</sup>

It has turned out, that multivalency effects can have quite different reasons.<sup>[41]</sup> Kiessling and colleagues suggested several possible mechanisms for multivalency effects.<sup>[42]</sup> For example, a glycoconjugate carrying multiple ligands can bind to multiple binding sites of one receptor.

Therefore, the cost for the translational entropy that is needed for the first ligand-receptor interactions is paid with the affinity of the first contact and all following binding interactions can proceed without further translational entropy cost.<sup>[43]</sup> This enables multivalent ligands to bind simultaneously to oligomeric receptors, an effect that is called the chelation effect (Figure 1.4, A). Multivalent ligands can also act as activators of a signal transduction as they bind to multiple non oligomeric receptors on the cell surface. This process is facilitated by the diffusion of receptors in the fluid lipid bilayer and triggered by multivalent ligands (Figure 1.4, B). On the other hand, some receptor proteins possess binding subsites in addition to the CRD, providing additional interactions with multivalent ligands (Figure 1.4, C). High avidity can also be the result of a high local ligand concentration, which statistically affects the frequency of ligand-protein interactions (Figure 1.4, D).<sup>[44]</sup>

Many of the described multivalency effects occur with oligomeric lectins, bearing more than one CRD. However, the cluster effect can also be observed with the monomeric bacterial lectin FimH, a protein that forms just one CRD accommodating exactly one mannosyl residue. In this case, it has been suggested that a cluster effect is the result of a high concentration of mannosyl residues in the close neighborhood to the FimH CRD (Figure 1.4, D). Furthermore, the multivalency mechanism profits from the quick rebinding of mannoside residues after their release.<sup>[45]</sup>

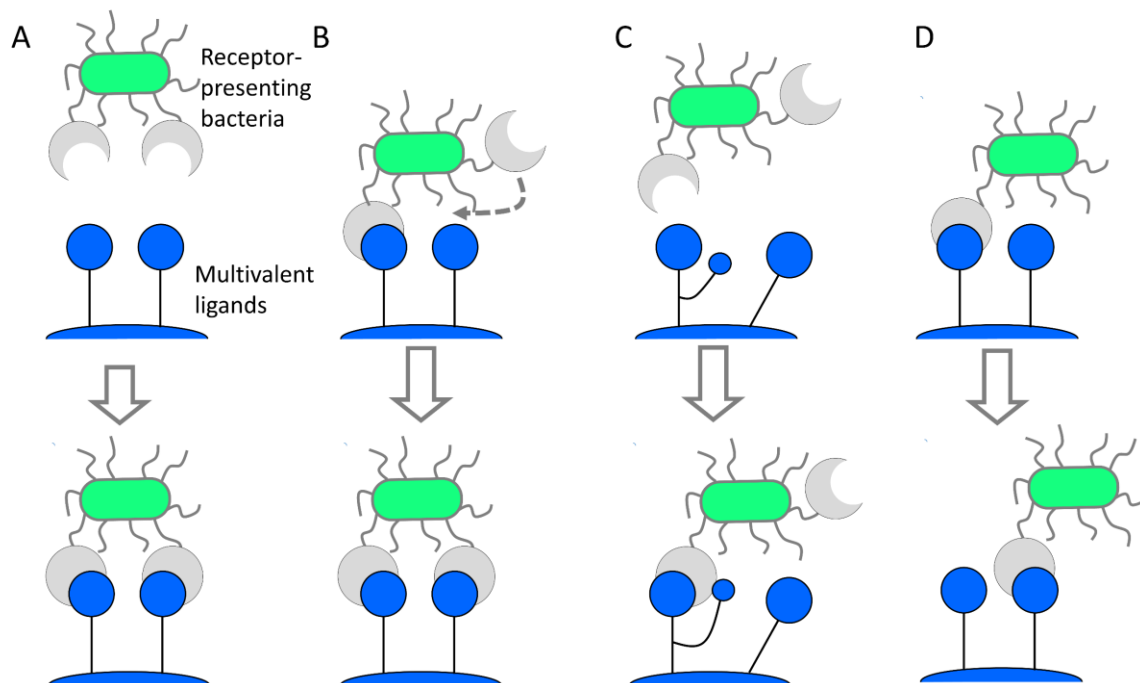


**Figure 1.4.** Illustration of possible mechanisms of multivalent ligand-receptor binding processes. The entropic chelate effect (A) increases affinity due to multiple binding events. Multivalent ligands can cluster multiple receptors (B). Secondary interactions support the ligand-receptor interactions (C). A high ligand concentration statistically favors binding events (D). Figure adapted from the literature.<sup>[42a]</sup>

Since it is important to study multivalency effects, a variety of multivalent glycomimetics have been developed, for example glycoclusters, glycopolymers, or glycodendrimers.<sup>[46]</sup> The majority of multivalent systems presents the same ligand in a multiple fashion and thus its concentration is locally increased.<sup>[47]</sup> However, the biological environment of the glycocalyx is defined by a heterogeneity of various ligands and hence several effects of carbohydrate recognition are excluded when just homomultivalent glycoclusters are studied.<sup>[48]</sup> Thus, heteromultivalent glycoconjugates have been taken into account for the investigation of carbohydrate recognition processes and indeed, significant heteromultivalent effects were observed and termed “heterocluster effect”.<sup>[49]</sup>

Hence, the group of García-Fernández pioneered the synthesis of heteromultivalent glycoclusters, paying tribute to the natural diversity of glycocalyx carbohydrates.<sup>[50]</sup> The group used  $\beta$ -cyclodextrin as a scaffold molecule and addressed the primary positions of the glucosides for functionalization with diverse carbohydrate ligands. A synthesis strategy was designed, which allowed the preparation of homo- and heteromultivalent glycoclusters with up to 21 sugar ligands and different sugar densities (Figure 1.5, A). In this way, heteroglycoclusters with Man/Glc and Man/Lac combinations were achieved, and the interaction of the targeted clusters with concanavalin A (ConA, Man/Glc specific) and peanut agglutinin (PNA, Lac specific) were studied using enzyme-linked lectin assays (ELLA), isothermal titration calorimetry (ITC) and surface plasmon resonance spectroscopy (SPR). While homovalent glycoclusters exhibited a multivalency effect as expected, this effect was often surpassed by heteromultivalent clusters depending on ligand density. The heterocluster effect was explained by secondary interactions between heterogeneous glycan moieties and the lectin surface, which can significantly influence binding.<sup>[50a]</sup> Subsequently, a variety of further heteromultivalent glycoconjugates were prepared<sup>[48]</sup> and heteroglycoclusters have become increasingly interesting in glycobiology as well as in drug design.<sup>[51]</sup>

Further investigations of the heterocluster effect addressed the precise presentation of carbohydrate ligands and their relative orientation to each other was addressed next. Thus, the group of Dumy and Renaudet proposed a combinatorial approach for the synthesis of a structurally diverse library of four monosaccharide ligands based on a tetrafunctional cyclopeptide scaffold.<sup>[52]</sup> By orthogonal ligation chemistry (oxime ligation, thiol-ene reaction, copper-catalyzed azide-alkyne cycloaddition and nucleophilic substitution) it was possible to achieve a defined distribution of carbohydrate ligands (Figure 1.5, B).<sup>[52c]</sup> Furthermore, this approach enables the synthesis of higher branched heteroglycoclusters by conjugation of multiple scaffolds. For a heteroglycocluster with two different ligands the group of Renaudet observed a heterocluster effect in the interactions with the lectins LecA and LecB.<sup>[52d]</sup>

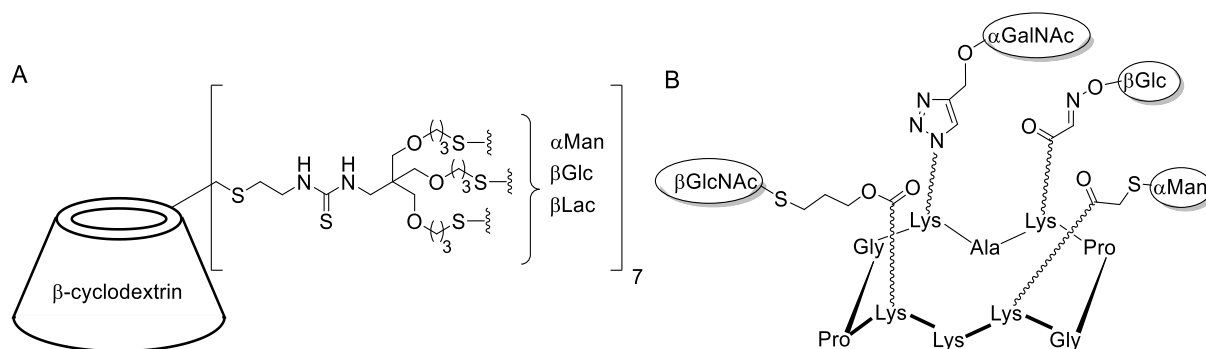


**Figure 1.5.** Examples of heteromultivalent glycoclusters. The functionalization of  $\beta$ -cyclodextrins with various carbohydrate ligands (Man, Lac, Glc) increases the affinity to lectins (A). Small tetrafunctional cyclic peptides are suitable scaffolds for the synthesis of heteromultivalent glycoclusters (B) by combinatorial chemistry to achieve a defined ligand distribution (Man, Glc, GalNAc, GlcNAc).

### 1.3 Conformations of pyranoses

Monosaccharides mainly exist as cyclic hemiacetals in the form of furanoses (5-membered ring) or pyranoses (6-membered ring), respectively. Especially the stereochemical details of monosaccharide substitution influence and govern the conformational properties of sugars.

Five main classes of ring conformations have been described, the chair (*C*), skew (*S*), boat (*B*), half-chair (*H*) and the envelope (*E*) conformation.<sup>[53]</sup> The shape of a particular conformer is referenced with respect to a plane, which is defined by four (*C*, *S*, *B*, *H*) or five (*E*), respectively, atoms of the ring (Figure 1.6). Atoms which are positioned above or below the ring plane are depicted in super- or subscript before and after the letter which defines the specific conformational type.

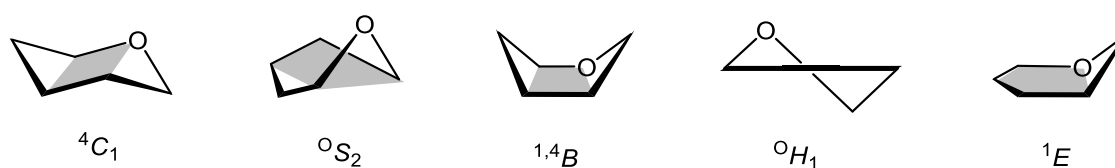


**Figure 1.6.** Schematic representation of chair (*C*), skew (*S*), boat (*B*), half-chair (*H*) and envelope (*E*) ring conformations of pyranoses. The shape of the ring conformation is referenced to a plane (grey), generated by 4 or 5 atoms, respectively, and specified by respective super- and subscripts.

The mathematical description of pyranose ring systems was introduced by Cremer and Pople in 1975 in their work about ring puckering coordinates.<sup>[54]</sup> They showed that every ring shape can be precisely devised by the definition of three coordination numbers, the Cremer-Pople parameters. For this, the puckering parameter *Q*, describing the degree of deviation of the atoms related to the plane, was defined. In addition, the angles  $\theta$  and  $\phi$  are used to define the

position of the conformation on the multidimensional surface of  $Q$  (Figure 1.7, A).<sup>[55]</sup> Hence, using the parameters  $Q$ ,  $\theta$  and  $\phi$  a spherical coordinate system is built for pyranose rings, where the poles are occupied by the two *chair* conformers  ${}^4C_1$  and  ${}^1C_4$ . The equator is defined by the *skew* and *boat* conformers and in between the *envelope* and *half-chair* conformations are positioned. The resulting Cremer-Pople plot is a theoretical and for every pyranose individual consideration for the occurring ring conformations and conformational interconversions of pyranoses. To track the conformational changes of pyranoses the British chemist Sir Fraser Stoddart constructed a two-dimensional projection of the conformational interconversion pathways (Figure 1.7, B).<sup>[56]</sup> On this map it is assumed that one of the three Cremer-Pople parameters is kept constant. Hence the interconversions can be described in two dimensions.

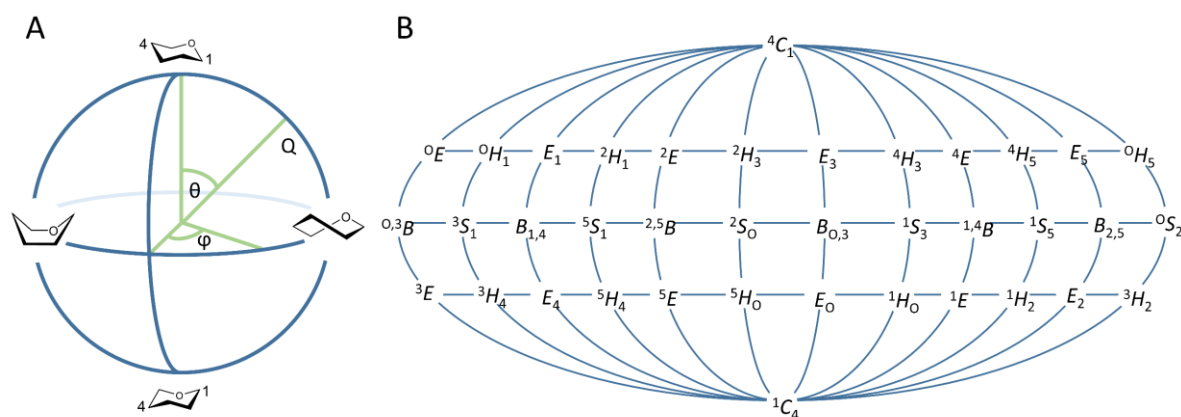


**Figure 1.7.** Cremer-Pople parameters  $Q$  (A) can describe ring conformations of pyranoses. Abbreviations:  $E$ : envelope,  $B$ : boat,  $C$ : chair,  $S$ : skew,  $H$ : half-chair.

The conformational preferences of pyranoses can be differently affected. On the one hand, electronic and sterical effects of the functional groups of a monosaccharide can influence the ring conformation. Additionally, also external stimuli can affect the ring conformation. One assumption for the preference for a specific ring conformation of a monosaccharide is that 1,3-diaxial interactions between functional groups (mainly OH groups) of a carbohydrate cause steric hindrance. This is also one reason why most D-configured aldohexoses (e.g., D-glucose, D-galactose, or D-mannose) exist as  ${}^4C_1$  conformers where most substituents are equatorially orientated. The conformational equilibrium of  $\beta$ -D-glucose lies far on the side of the  ${}^4C_1$  conformer owing to an energy barrier between the two chairs of  $\sim 5.70$  kcal/mol (Figure 1.8). On the other hand, for the same reason, L-sugars (e.g., L-rhamnose or L-fucose) can be found exclusively in the inverted  ${}^1C_4$  conformation.

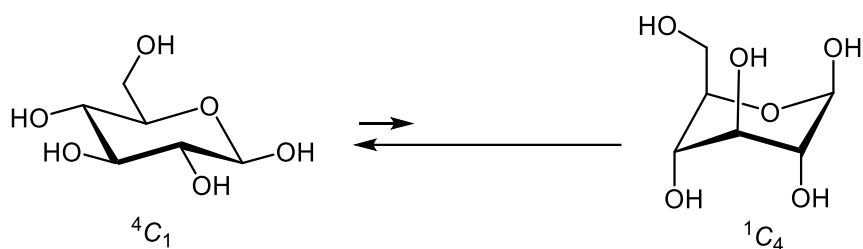


**Figure 1.8.** Natural occurring D-sugars (e.g., D-glucose) are mainly present in the  ${}^4C_1$  conformation due to high-equatorial orientated functional groups.

The energetically unfavored 1,3-diaxial interactions in monosaccharides can be overcome in different ways leading to a distortion of the preferred  ${}^4C_1$  conformation. For example, bulky vicinal protecting groups (e.g., silyl ethers) induce ring distortion and the conformation changes from the  ${}^4C_1$  to the  ${}^{1,4}B$  conformer as described by Bols et al. for the activity of super-armed glycosyl donors (Figure 1.9, A).<sup>[57]</sup> Another possibility to influence the regular chair conformation is the formation of bridging protecting groups, which were also introduced to affect the reactivity of monosaccharides. For example, the 1,2,4-O-acetyl orthoester derivative of glucose presented by Bochkov et al. is locked in the  $B_{1,4}$  conformation (Figure 1.9, B).<sup>[58]</sup> Yamada and co-workers showed that butenylene-bridged glucosides serve as “axial rich” glycosyl donors, such as the twisted glucose derivative depicted in Figure 1.9, C, showing a  ${}^3S_1$  conformation.<sup>[59]</sup>

In addition to the modification of the hydroxyl groups by protection chemistry also the anomeric effect has an influence on the conformation of sugars. It stabilizes the axial orientation of electron withdrawing groups at the anomeric center by hyperconjugation of non-bonding electrons of the endocyclic oxygen to the anti-bonding  $\sigma$  orbital of the bond between the anomeric carbon and the anomeric electronegative group. Thus, benzoylated  $\beta$ -D-xylosyl halides (e.g. bromide) are forced by an anomeric stabilization into the  ${}^1C_4$  conformation as shown by Lindner (Figure 1.9, D).<sup>[60]</sup> Also other interactions have an influence on the conformation of sugars such as intramolecular hydrogen bonds or charged and aromatic substituents, which give rise to dipole-dipole and  $\pi$ - $\pi$  interactions, respectively. Hence, L-iduronic acid, a constituent of heparin, shows high conformational flexibility depending on its degree of sulfation and can occur in  ${}^4C_1$ ,  ${}^1C_4$  or  ${}^2S_0$  conformation (Figure 1.9, E).<sup>[61]</sup>

While for most examples the *chair*, *skew* and *boat* conformations are the dominating forms, glycols exist in the *half-chair* conformation. Glycols are defined by a double bond between the anomeric center and C-2 and represent important and versatile building blocks in carbohydrate chemistry. The tri-O-acetylated D-glucal, for example, adopts a  ${}^4H_5$  *half-chair* conformation (Figure 1.9, F). This conformational features makes glucal amenable for an electrophilic attack from the  $\beta$ -face of the molecule.<sup>[62]</sup>

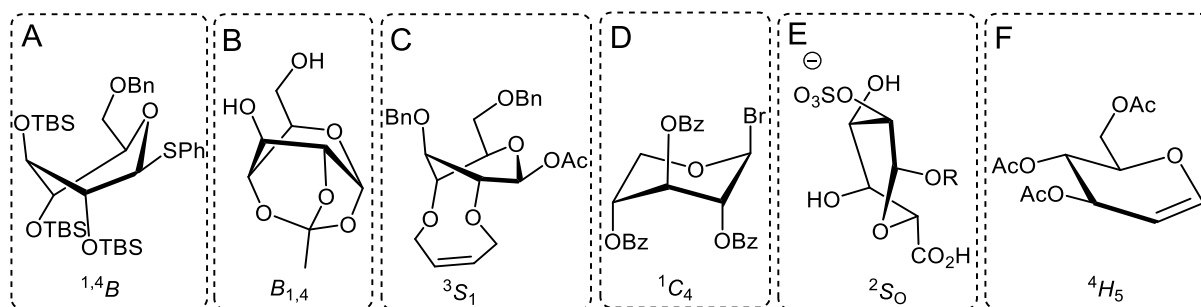


**Figure 1.9.** The main conformation of sugars can be distorted into other favored conformations by several modifications, for example bulky protecting groups (A), bridging units (B and C), the anomeric effect (D), charged substituents or unsaturated bonds (F).

Furthermore, some monosaccharides (e.g., D-altrose, D-idose or D-xylose) show small energy barriers between several energy minimum conformations.<sup>[63]</sup> Thus, without further modifications, they exist as a conformational equilibrium. Conformational equilibria are complicated to control, and their analysis is difficult to tackle.

However, the ring conformation of monosaccharides plays a significant role in many natural or synthetic processes. It affects carbohydrate recognition and the reactivity of molecules in numerous ways. For example, a strained conformation of a glycosyl donor influences the dissociation of the anomeric leaving group, the preorganization of intermediates and the stereochemical outcome of a glycosylation reaction.<sup>[64]</sup> Also enzymatic reactions such as glycoside cleavage and formation of glycosidic bonds proceed through various conformational changes of the carbohydrate substrates.<sup>[65]</sup> For example, the endo-1,4- $\beta$ -xylanases are enzymes, which are involved in the hydrolysis of hemi-cellulose, so-called xylan.<sup>[66]</sup> These enzymes perform the hydrolysis of xylan via a glycosyl-enzyme intermediate, which has an oxocarbenium ion character and occurs in the  $^{2,5}B$  conformation.<sup>[67]</sup> The group of Wilson could crystallize the reactive intermediate of the enzyme-xylan complex and X-ray analysis proved its  $^{2,5}B$  conformation in the active site (Figure 1.10, A).<sup>[68]</sup> Furthermore, the group of Blériot demonstrated that the  $^{2,5}B$  conformer of xylosides is enormously reactive in glycosylation reactions. By locking the *boat* conformation with a 2,5-ethyl bridge, various thioxylosides were prepared and tested in glycosylation reactions to show that derivatives in the  $^{2,5}B$  conformation reacted approximately 200 times faster than the respective  $^4C_1$  conformers (Figure 1.10, B).<sup>[69]</sup>

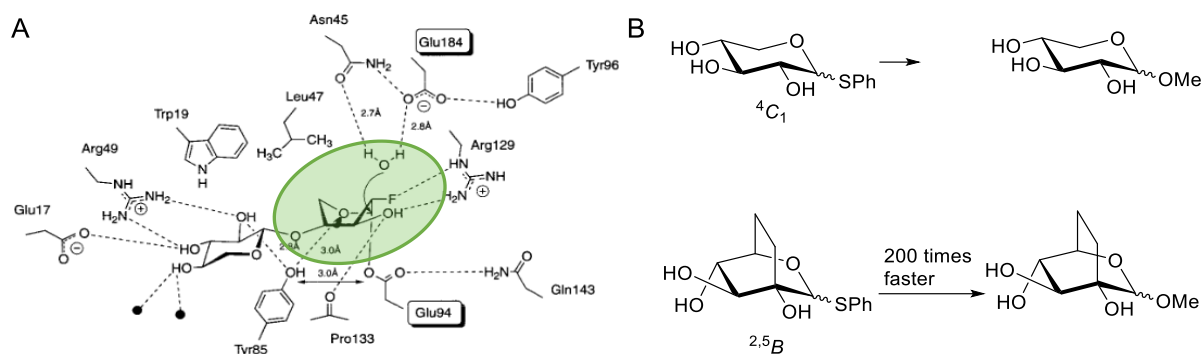


**Figure 1.10.** The enzyme-substrate complex that is formed during the hydrolysis of xylan contains a reactive  ${}^{2,5}B$  conformer as demonstrated by co-crystallization with endo-1,4- $\beta$ -xylanase (A); graphic adapted from the literature.<sup>[68]</sup> Thioxylosides locked in the  ${}^{2,5}B$  conformation show higher reactivity as glycosyl donors than the analogues in  ${}^4C_1$  conformation (B).<sup>[69]</sup>

## 1.4 Conformational equilibria and their analysis

In addition to the conformational analysis of monosaccharides, studying the conformations of oligo- and polysaccharides is important since conformational aspects of glycans are highly connected to their biological function. The conformational analysis of oligosaccharides is typically concentrated on the glycosidic bonds and their orientation, which is defined by three torsion angles ( $\phi$ ,  $\psi$ , and  $\omega$ ).<sup>[70]</sup> As mentioned earlier, also the conformational flexibility of the monosaccharide ring is an important feature in the context of glycobiology. Hence, the function of natural occurring carbohydrates such as furanosides in DNA<sup>[71]</sup> or the hexopyranose  $\alpha$ -L-idopA in heparin<sup>[72]</sup> are dependent on their conformational structure. Accordingly, the conformational analysis of monosaccharides, the theoretical prediction of occurring conformations and the influence of the ring conformation on molecular function is important.<sup>[73]</sup>

The conformation of monosaccharides is highly dependent on the presence of exocyclic groups. Thus, the potential energy landscape of monosaccharides differs for all pyranose species. The group of Beckham computed by high-level quantum mechanics in the gas phase the possible ring conformations of different carbohydrates and in addition determined the kinetic landscapes for conformational interconversions (Figure 1.11).<sup>[74]</sup> With these results it was possible to gain information about certain carbohydrate structures in enzyme-carbohydrate complexes, which could not be explained so far.<sup>[65b]</sup>

Especially the puckering of the pentose  $\beta$ -D-xylose is of interest, since its two stable chair conformers show a small energy barrier ( $\sim 2.3$  kcal/mol between  ${}^1C_4$  and  ${}^4C_1$ )<sup>[74]</sup> and thus conformational interconversions might occur.<sup>[75]</sup> In addition to the two isomeric chair conformations, the most kinetically accessible conformation is the  ${}^2S_0$  (Figure 1.11), which was also shown in NMR experiments by Rönns and co-workers.<sup>[76]</sup> The interconversion energies

along the equator are relatively low (0.5-5.6 kcal/mol). Thus, puckering from the  ${}^2S_0$  to other *skew* or *boat* conformers are also favored and can be found as reactive intermediates in enzyme-carbohydrate complexes. Furthermore, the Beckham group could calculate the electronic structures of various conformers, which gave more insights into the connections between conformational structures and reactivity.<sup>[74]</sup>

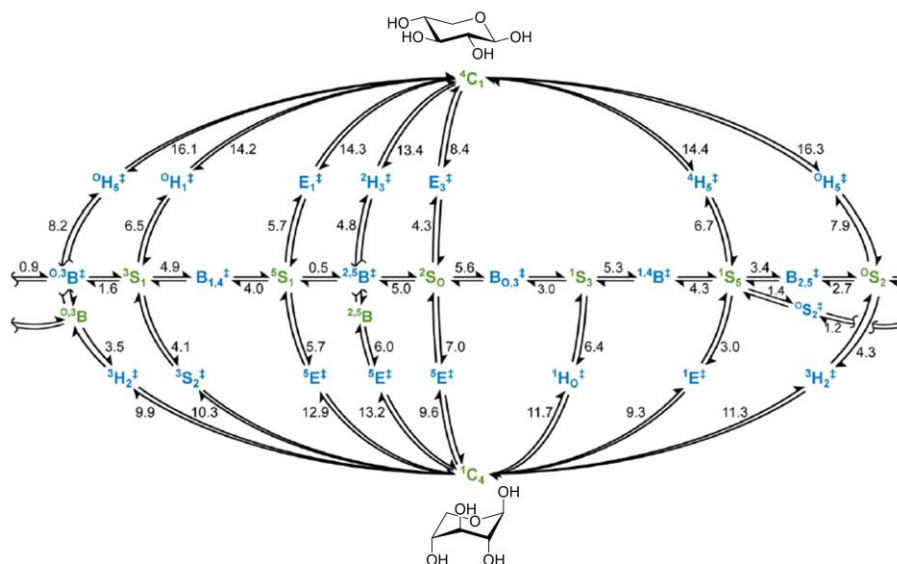


**Figure 1.11.** Computed puckering interconversions pathways for  $\beta$ -D-xylose at the CCSD(T)6-311+G(d,p) level of theory (298 K in kcal/mol). color code: green: local energy minimum; blue: transition state. Figure adapted from the literature.<sup>[74]</sup>

While the conformation of monosaccharides in protein-carbohydrate complexes is enormously affected by the structure of the active site of the protein, also other environmental parameters can have an influence on the conformation. In addition to the constitution of substituents also the presence of metal ions or solvent characteristics are important for the occurrence of carbohydrate conformers.<sup>[77]</sup> In unpolar solvents intramolecular interactions such as charge-dipole or dipole-dipole interactions are facilitated. The formation of intramolecular hydrogen bonds increases in solvents with a lower polarity.<sup>[75]</sup> Additionally, it has been shown that the anomeric effect for carbohydrates is of greater significance in unpolar solvents.

Widmalm and co-workers prepared naphthoyl  $\beta$ -D-xylosides in order to investigate their potency to inhibit the biosynthesis of glycosaminoglycans.<sup>[76]</sup> They figured out that these xylosides occurred in conformational equilibria in solution. In addition to the assumed  ${}^4C_1$  conformation also the inverted  ${}^1C_4$  and the  ${}^2S_0$  conformations could be found. Furthermore, a relationship between the conformer distribution and the polarity of the solvent, in which the sample was measured, was observed. In polar solvents (DMSO, MeOH) the  ${}^4C_1$  conformation was predominant, but for solvents with a lower polarity (benzene, chloroform) the population

of  ${}^4C_1$  was decreasing and the  ${}^1C_4$  and the  ${}^2S_0$  conformations were observed. This solvent-dependent conformational behavior was rationalized with intramolecular hydrogen bonds between the 2- and the 4-hydroxyl group, which could occur in the  ${}^1C_4$  conformation with all substituents in an axial orientation.<sup>[78]</sup>

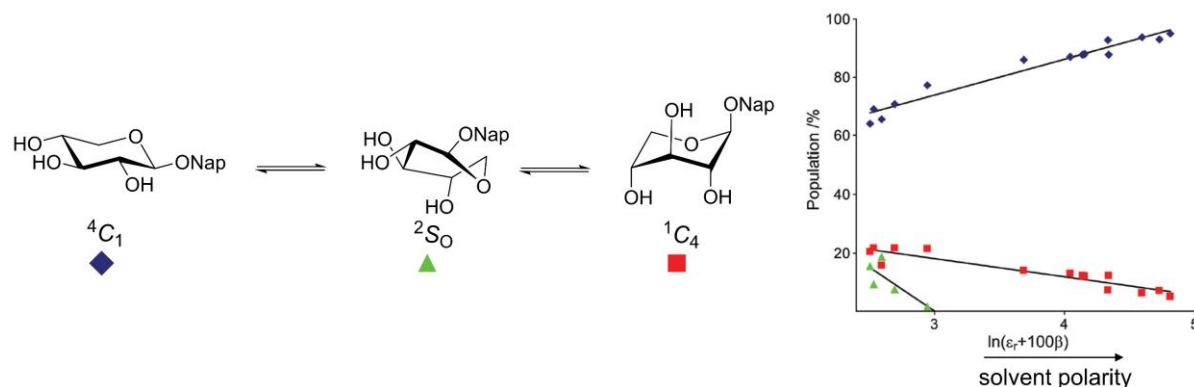


**Figure 1.12.** The conformational equilibrium of naphthoylexyloxy derivatives is dependent on the solvation environment and three conformers can occur. In polar solvents the  ${}^4C_1$  conformation is dominant, whereas the population of  ${}^1C_4$  and  ${}^2S_0$  increases in unpolar solvents. Figure adapted from the literature.<sup>[78]</sup>

For the analysis of conformational equilibria, it is important to know that the exchange rate ( $k_{ex}$ ) between two conformers is highly dependent on the temperature.<sup>[79]</sup> For the conformational interconversion from one conformer to another, an activation energy has to be paid to reach a transition state towards the next intermediate (Figure 1.13, A). These time-dependent processes can be studied by dynamic NMR spectroscopy.<sup>[79]</sup> Since the ring interconversion is a fast process ( $\sim 100$  ns), NMR spectroscopy of these molecular processes often displays a time-averaged signal of two or more conformers, so-called coalesced peaks. The occurrence of separated or coalesced peaks is dependent on the exchange rate ( $k_{ex}$ ) and the frequency difference between the nuclei in the respective conformers ( $\Delta\nu$ ). The relationship between these two parameters results in a coalescent spectrum when  $k_{ex}$  is 2.22 times ( $\pi/\sqrt{2}$ ) larger than  $\Delta\nu$  of the exchanging states. The temperature for the  $k_{ex}$  at the transition state between the conformers is called the coalescence temperature ( $T_c$ ). Since  $k_{ex}$  is temperature-dependent the spectral appearance varies with the temperature. Around the coalescence temperature NMR signals are broadened due to the Heisenberg uncertainty principle related to the energy states of the conformers. Above  $T_c$  one set of sharp signals is describing an average of the dynamic equilibrium. Otherwise below this temperature, the two signal sets of isomeric conformers are separated (Figure 1.13, B). Accordingly, NMR spectroscopy at low temperatures can lead to a separation of the signals and thus to coupling constants of the pure conformers.<sup>[80]</sup>

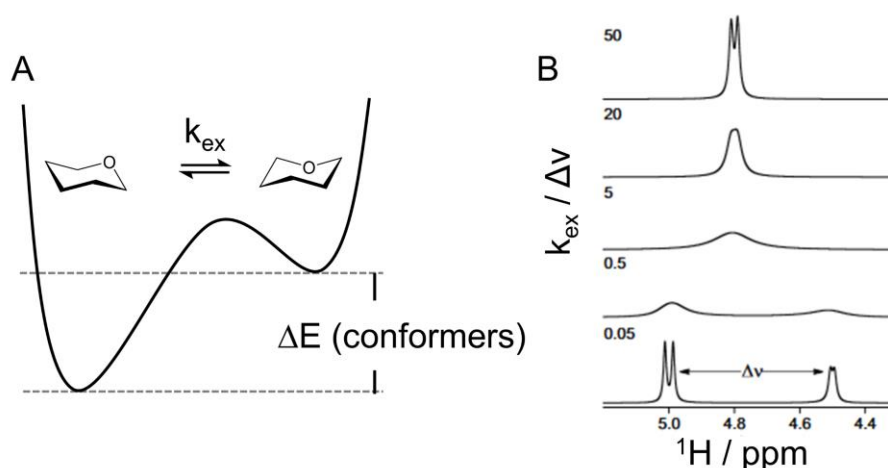


**Figure 1.13.** The conformational equilibrium between two pyranoside conformers is temperature-dependent (A). If both conformers are present at the same time, NMR spectroscopy can give time-average signal peaks for both conformers. Depending on  $k_{ex}$  the signals are separated or coalescent (B).

The conformation of pyranosides can be determined by NMR spectroscopy by measuring the coupling constants between the vicinal ring protons. Coupling constants can be affected by various parameters, such as geometric or electronic factors. For the theoretical prediction of coupling constants, the general Karplus equation for  $^3J_{H,H}$  couplings, derived by Haasnoot et al., takes the dihedral angle of two vicinal protons into account.<sup>[81]</sup> Furthermore, coupling constants are affected also by the electronegativity of substituents, the orbital hybridization, and the bond length.

## 1.5 Conformational switchable monosaccharides

For molecular switches it is important that the molecule can exist in two or more stable isomeric states. The transition between these states affects properties of the molecule depending on the distance between functional groups and their relative orientation (shape, size, polarity, complexing ability or biological activity).<sup>[82]</sup> The well-defined stereochemistry and the high degree of functionalization makes monosaccharides attractive as molecular switches for different applications.<sup>[83]</sup> However, conformational effects in sugar rings are difficult to control, to analyze, and finally to proceed reversibly, as it is required for molecular switches. In general, the pyranose ring has to be functionalized in a way that by addressing the functional group with an external stimulus the energy difference between two conformational states (which are in the same energetic range) can be overcome and the ring flip occurs. Only few examples of monosaccharide switches have been published so far.

One tool for triggering conformational change is the modification of the anomeric aglycone. It is known that axial arrangement of electron withdrawing groups prefer, stabilized by the anomeric effect with the endocyclic oxygen, the  ${}^4C_1$  conformation. Davis and co-workers showed that *N*-( $\alpha$ -D-xylosyl)-imidazole occurs in its unprotonated form in the  ${}^4C_1$  conformation as expected. Though, by protonation of the imidazolyl unit the anomeric effect is overwhelmed and a conformational change to the  ${}^1C_4$  conformer takes place (Figure 1.14, A)<sup>[84]</sup> so-called the reversed anomeric effect.<sup>[85]</sup> Coutrot and Busseron demonstrated that the conformation of a pyridinium mannoside can be switched in a supramolecular mannosyl [2]rotaxane.<sup>[86]</sup> If the macrocycle is not in the periphery of the aglycone pyridinium the mannosyl residue shows  ${}^1C_4$  conformation dedicated to the reversed anomeric effect. But if the macrocycle is shuttled towards the mannosyl residue by deprotonation, the positive pyridinium charge is shielded and the anomeric effect overwhelms again (Figure 1.14, B). This is resulting in a conformational change to the  ${}^4C_1$ , which is reversible by back shuttling of the macrocycle.

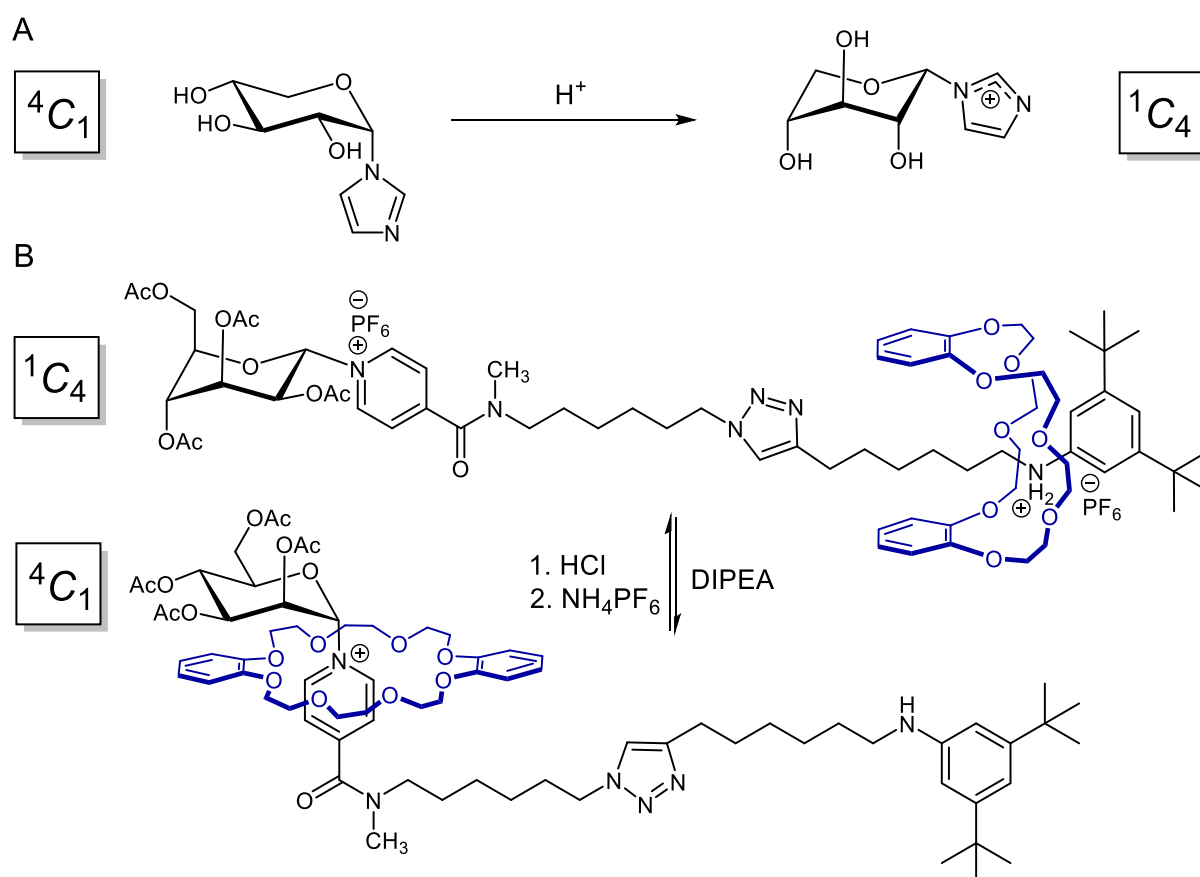


**Figure 1.14.** Carbohydrate based molecular switches which are triggered by a reversed anomeric effect. Protonation of the anomeric *N*-imidazolyl moiety leads to a ring flip of xylosides (A). The reversed anomeric effect of mannosides can also occur due to supramolecular [2]rotaxanes resulting again in a ring flip (B). Figure adapted from the literature.<sup>[84, 86]</sup>

Another tool for switching the conformation of monosaccharides is the complexation with metal ions. Thus, by the synthetic modification of carbohydrates to chelating agents stimuli-responsive surfactants are generated, which are interesting for material science.<sup>[87]</sup> By the functionalization of methyl  $\alpha$ -D-glucoside, Pedersen and co-workers presented a conformational switchable lipid (Figure 1.15)<sup>[88]</sup> where the 3- and 6-positions were modified with lipophilic alkyl chains and the 2- and 4-positions with pyridine residues. By the addition of zinc (II) cations a conformational flip from  ${}^4C_1$  to  ${}^1C_4$  was caused by complexation with the metal salt. The  ${}^1C_4$  conformation with all substituents in axial orientation is amphiphilic and can be incorporated into liposomes to encapsulate a fluorescent cargo, for example. This process is reversible by the addition of a stronger ligand (EDTA), which makes the lipid attractive for liposomal drug delivery systems.

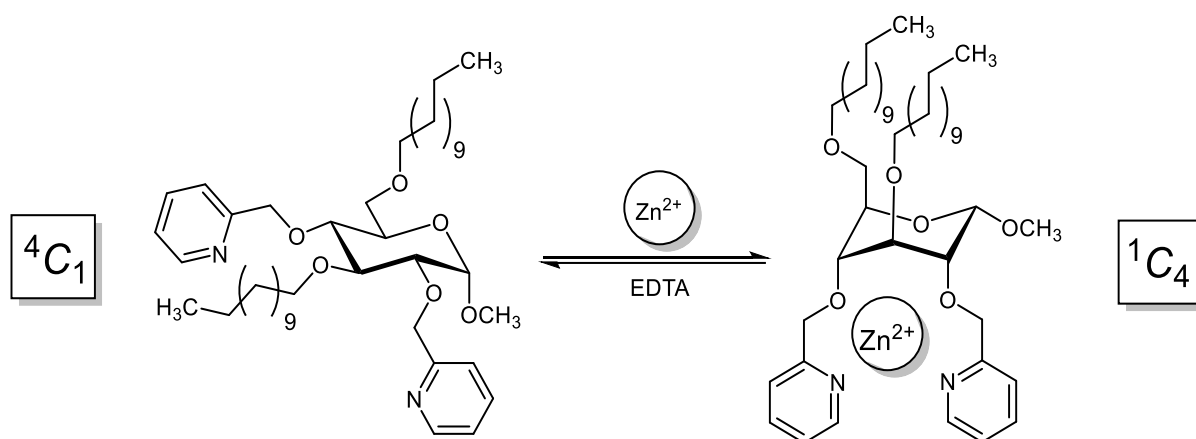


**Figure 1.15.** Conformational switchable glucoside-based lipid for the formation of liposomes.<sup>[88]</sup>

The ability of a monosaccharide to serve as a molecular switch is highly dependent on the energy difference between two stable conformers. For D-xylose the energy barriers for puckering interconversions between the chair conformers are low ( $\sim 2.3$  kcal/mol between  ${}^1C_4$  and  ${}^4C_1$ ).<sup>[74]</sup> By synthetic modifications of  $\beta$ -D-xylopyranosides the energy barrier between the conformers can be overcome and conformational switches can be achieved.<sup>[78, 89]</sup>

In 1999, Hashimoto and Yuasa employed the first conformational hinge based on a xylopyranoside.<sup>[90]</sup> By modification of D-xylose they synthesized 2,4-diamino xylosides which could be switched between their chair conformations by the chelation of metal (II) ions (Figure 1.16). The xyloside switches offer two further positions for functionalization (1- and 3-position) in order to transfer the conformational transition to a molecular function. First, trisaccharides with a central xylose hinge were synthesized and the switching ability was studied with different metal ions.<sup>[91]</sup> Next, the 1- and 3-position were modified with pyrene residues and the molecular switch was used as a metal specific excimer fluorescence sensor.<sup>[92]</sup> By a ring flip of the xyloside, the pyrene substituents are orientated in an axial position and can now exert  $\pi$ - $\pi$

interactions resulting in a fluorescence emission. On the other hand, the pyrene interactions stabilize also the corresponding  ${}^1C_4$  state. In addition, it was also shown that the conformational change can be triggered by protonation. Furthermore, Yuasa and co-workers presented a 2,4-diamino xyloside-based lipid and incorporated it into micelles by conformational switching.<sup>[93]</sup> Thus the incorporation and release of a drug were controlled by a hinged sugar.

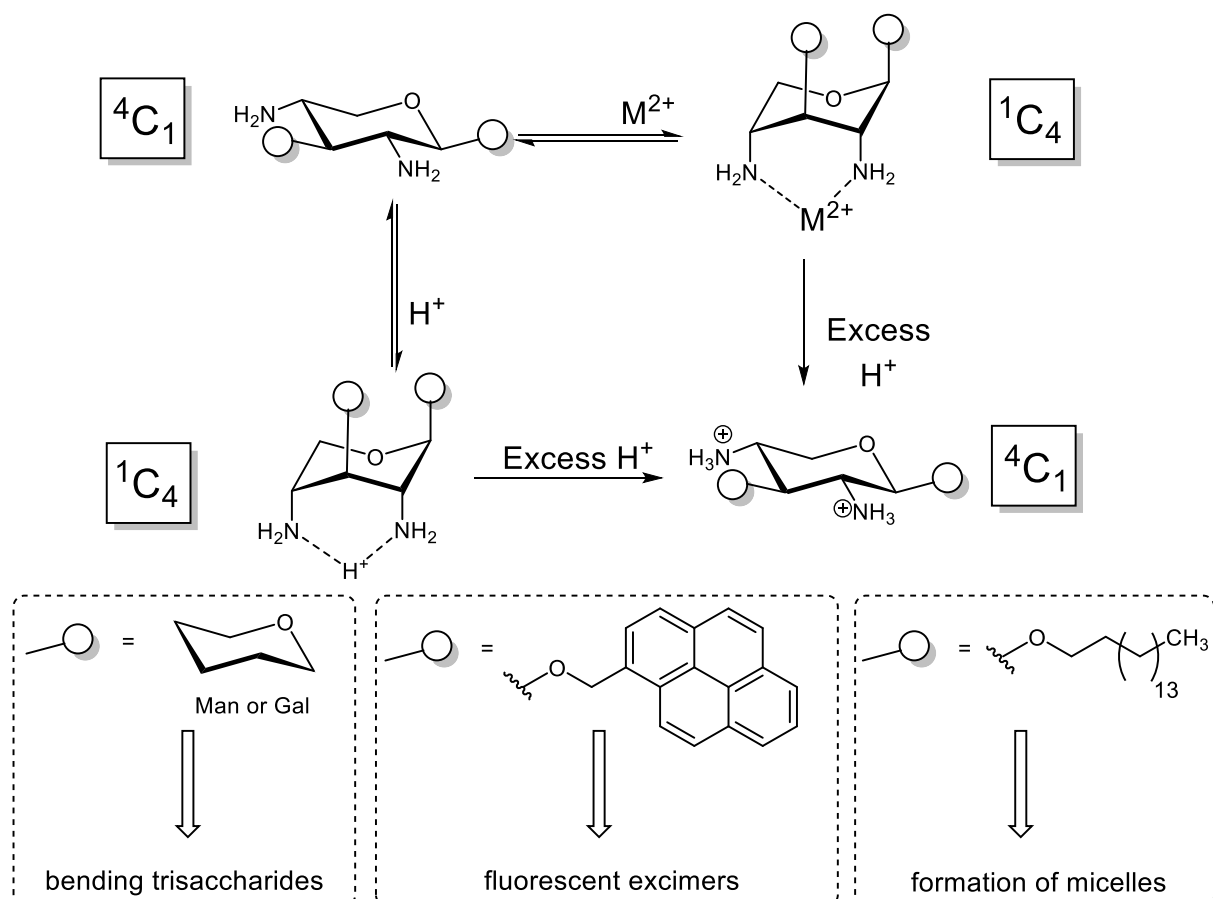


**Figure 1.16.** Hashimoto and Yuasa showed that 2,4-diamino xylosides can serve as molecular switches. The conformational transition from  ${}^4C_1$  to  ${}^1C_4$  is triggered by chelation of metal ions or protons. By varying the functional groups at the 1- and 3- position the xylosides can be used in various applications.

The fact that  $\pi$ - $\pi$  interactions between pyrene groups can stabilize conformations was also shown by Sakakibara and Ariga.<sup>[94]</sup> They employed a pyrene-functionalized methyl  $\beta$ -D-xyloside to flip the chair conformation of the sugar ring in a Langmuir monolayer by varying the surface pressure. The ring flip was detected by excimer emission of staggered pyrene residues, demonstrating that interactions between aromatic residues support conformational changes.

## 2 How can carbohydrate-protein interactions be controlled? – The project idea

Carbohydrate-protein interactions play a crucial role in many essential biological processes such as in the adhesion of bacteria to the glycocalyx of human cells, which is mediated by lectins. Strikingly, carbohydrate-protein interactions are crucial in both health and disease states of an organism.<sup>[1b]</sup> Hence, it is important to study carbohydrate recognition, which is dependent on ligand accessibility, multivalency effects, ligand density, and also the conformation of glycoligands. Tailor-made glycomimetics can help to address the meaning of specific parameters that influence carbohydrate recognition in a bottom-up approach rather than to tackle the complex orchestration of glycobiology top-down.

The project of this thesis is focused on two aspects of carbohydrate recognition, the organization and spatial distribution (“presentation”) of carbohydrate ligands and the conformation of xylosides in order to utilize them as conformational switches. For the first approach, a maltoside scaffold was designed and elaborated into regioisomeric Man/Glc heterobivalent glycoclusters. (Figure 2.1, chapter 3). The influence of the varying relative orientation of an  $\alpha$ -D-mannoside ligand versus a  $\beta$ -D-glucoside moiety was tested in bacterial adhesion-inhibition assays. The testing results were rationalized by molecular modelling studies.

In the second approach, diamino-xylosides were elaborated into conformational switches. A ring flip between the  ${}^4C_1$  and  ${}^1C_4$  conformation can be triggered by metal complexation of the two amino groups of the sugar ring. This “molecular machine”, a rather unexplored area in the glycosciences, can be utilized to, again, vary and control the relative orientation of two mannose ligands in space. Also in this case, for the biological testing *E. coli* bacteria were employed in adhesion-inhibition assays (Figure 2.1, chapter 4, 5 and 6). The results were rationalized by molecular modelling and molecular dynamics simulations. The work on the xyloside conformational switching project included two unexpected aspects. First, the synthesis of the target molecules proved to be very demanding and accordingly, a rich body of chemistry is described in chapter 4. Secondly, it became necessary to analyse conformational equilibria of certain xyloside derivatives, which could not be resolved by NMR spectroscopy. For this purpose, a cooperation was established with theoretical chemistry. Accordingly, the spectroscopic and theoretical analysis of xyloside conformational dynamics is described in chapter 5.

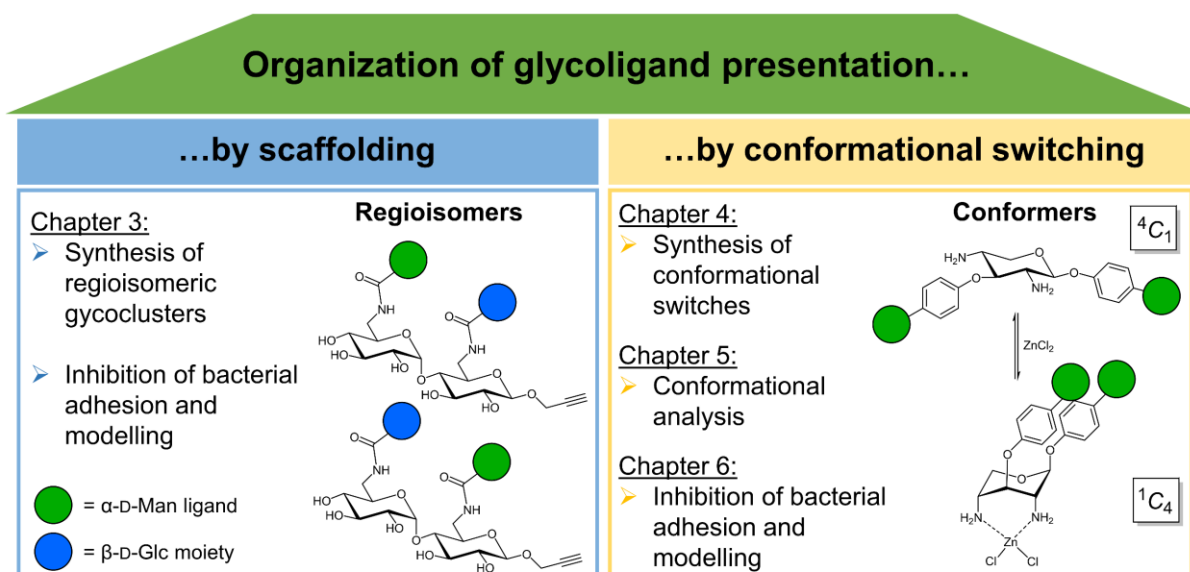


**Figure 2.1.** Overview about the tools to “organize glycoligand presentation” in carbohydrate recognition processes, which are discussed in the respective chapters.

### 3 The effect of carbohydrate ligand presentation by maltose-based glycoclusters

In addition to homo- and heteromultivalency, the three-dimensional (3D) presentation of carbohydrate ligands in a supramolecular context is an important parameter of carbohydrate recognition. Hence, the design of glycoclusters in which glycoligand presentation can be precisely controlled, such as on a surface (glycoarrays) or projected from a molecular scaffold, became important. Various scaffold molecules can be employed to organize multivalency in 3D space as they can provide a precise spatial orientation of carbohydrate ligands. In addition, functional scaffolds allow for the switching of carbohydrate spatial presentation between well-defined states. Assuming that within the glycocalyx, ligand presentation is likewise modulated to control biological function, functional glycoconjugates allow a valuable bottom-up approach to systematically study the effect of ligand orientation in carbohydrate recognition.<sup>[6b, 40, 95]</sup>

Pioneer work in this field has been performed by Strömberg and co-workers, who demonstrated that glycosphingolipids (GSL) can exist in different orientation relative to a membrane. They found that binding to different adhesin varies according to the spatial ligand presentation at the membrane.<sup>[95b]</sup> Hakomori has studied the assembly of glycoconjugates on surfaces and their interactions with adhesins.<sup>[95a, 96]</sup> Boons and co-workers demonstrated that the recognition of carbohydrate ligands by influenza virus hemagglutinin is modulated by their presentation within an array of complex branched *N*-glycans.<sup>[97]</sup>

Several other approaches were employed to address the organization of multivalency in the context of carbohydrate recognition.<sup>[47]</sup> Lindhorst and co-workers used photoresponsive azobenzene glycosides to control the spatial arrangement of glycoconjugates and to investigate the effect of different glycoligand orientation on carbohydrate recognition.<sup>[98]</sup> Hence, azobenzene glycosides were immobilized on a gold surface and the resulting glyco-SAMs were photoisomerized<sup>[99]</sup> to demonstrate that bacterial adhesion could be reversibly controlled by the isomerization status (*E* or *Z* configuration of the azo group) of the glycosylated surface and hence the orientation of the carbohydrate ligand.<sup>[98a]</sup> (Figure 3.1, A). Later, the same phenomenon was observed, when the glyco-SAMs were designed with rather rigid biphenyl azobenzene glycoconjugates as shown by Fast and colleagues.<sup>[98d]</sup> Control of glycoligand presentation using photoswitchable glycoconjugates could also be transferred to the surface of human mammary epithelial cells type-1 (HMEC-1). By metabolic oligosaccharide engineering Möckl and co-workers attached azobenzene mannosides to the cell surface by copper(I)-catalyzed azide alkyne cycloaddition (CuAAC, click reaction). Afterwards the bacterial adhesion of type 1-fimbriated *E. coli* bacteria to the HMEC-1 cells was investigated and the ligand orientation was controlled by irradiation with UV light. The experiment showed

higher bacterial binding for the *E*- than for the *Z*-state of the surface (Figure 3.1, B).<sup>[98b]</sup> Furthermore, Despras et al. demonstrated that HMEC-1 cells could also be functionalized with more complex multivalent azobenzene cluster mannosides and photoisomerized.<sup>[98c]</sup> The experiment once again showed that the *E*-isomer on a surface is a better ligand for bacterial adhesion than the *Z*-isomer.

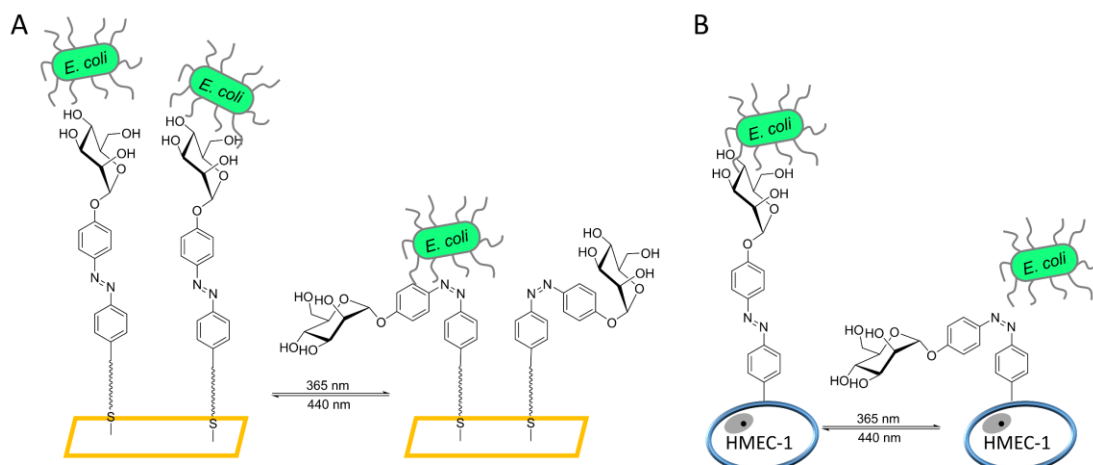


**Figure 3.1.** Presentation of different azobenzene glycoconjugates to influence bacterial adhesion of type 1 fimbriated *E. coli* bacteria. By isomerization of the azo group the spatial orientation of mannoside ligands on related to a gold (A)<sup>[98a]</sup> or human cell (HMEC-1, B)<sup>[98b]</sup> surface can be varied and thus bacterial adhesion controlled.

For the design of functional glycoclusters with varied ligand presentation in 3D space, the choice of the scaffold molecule is crucial as it defines the options for multifunctionality as well as for the 3D features of ligand presentation.<sup>[47]</sup> In previous work Brekalo et al. demonstrated that spatial ligand presentation by so-called pseudoenantiomeric heterobivalent glycoclusters is essential for carbohydrate recognition processes.<sup>[100]</sup> Based on D- and L-serine various glycocluster pairs were synthesized and tested as inhibitors of mannose-specific bacterial adhesion (Figure 3.2) to show that the differentiation in the stereochemistry of a focal point varied the inhibitory potency of Man/Glc glycoclusters significantly.

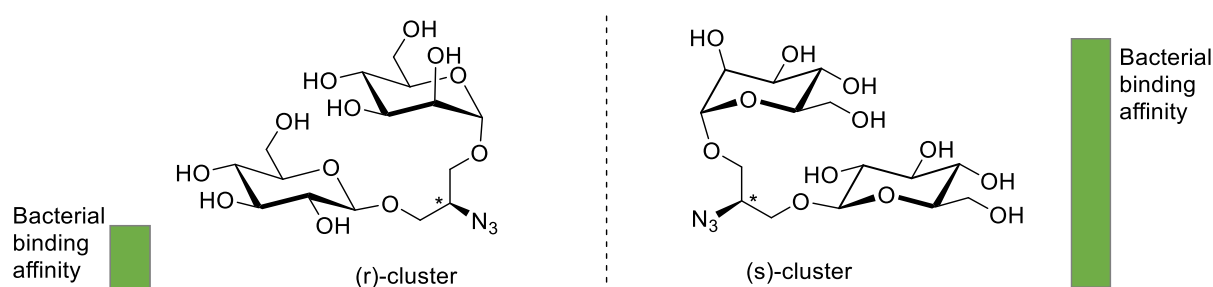


**Figure 3.2.** Representation of serine-based pseudoenantiomeric heterobivalent glycoclusters. The (s)-cluster shows a 20-fold higher biological activity to type 1 fimbriated bacteria than the (r)-cluster.<sup>[100]</sup>

For the multivalent presentation of carbohydrate ligands frequently also carbohydrate scaffolds were utilized.<sup>[101]</sup> Typically, glycoside scaffolds provide a rigid conformation, a defined stereochemistry, and in addition, their multifunctionality offers many possibilities for combinatorial derivatization. Furthermore, the biological compatibility of carbohydrates qualifies them as.<sup>[102]</sup> In recent years, Lindhorst and co-workers have frequently utilized carbohydrate scaffolds to generate various glycoclusters. First, homomultivalent glycoclusters of an A<sub>5</sub> type were achieved by uniform functionalization of all positions of a mono- or disaccharide, respectively.<sup>[103]</sup> These so-called “octopus glycosides”<sup>[104]</sup> were later complemented by the synthesis of AB<sub>4</sub>-type scaffold molecules.<sup>[105]</sup> Lindhorst and Gloe described a mannose-derived N<sub>3</sub>(NHBoc)<sub>4</sub>-type scaffold molecule which was utilized as tetravalent glycocluster in multivalency studies (Figure 3.4, A).

This work exemplifies the potential of carbohydrate scaffolds. The individual positions of the sugar rings allow for a facile heterogeneous functionalization of carbohydrate scaffolds (Figure 3.3).<sup>[106]</sup> For instance the anomeric position can be addressed individually by glycosylation and thus various functional moieties can be introduced as the aglycone of a glycoside scaffold. The primary hydroxyl group at the 6-position of hexapyranoses can be discriminated from the remaining secondary alcohols utilizing steric control of regioselectivity. Finally, the reactivity of the secondary hydroxyl groups is controlled by stereoelectronic factors of the respective saccharide (e.g., ring conformation and configuration of the hydroxyl groups). These differences in reactivity combined with a suitable protecting group strategy make it possible to orthogonally introduce functional groups at a carbohydrate scaffold.

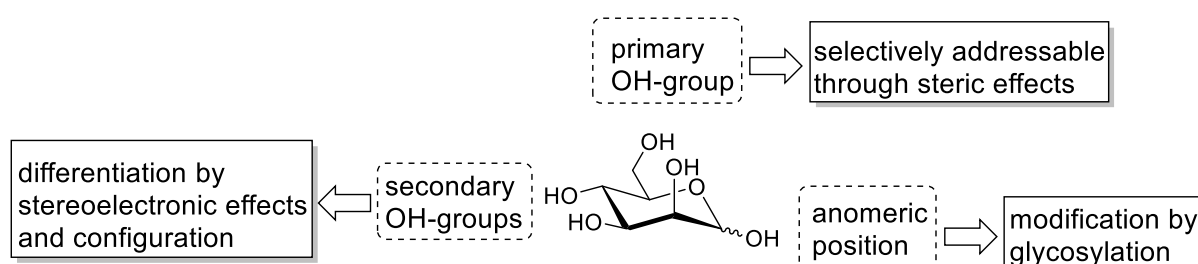


**Figure 3.3.** Selectively modification of carbohydrates to synthesize multifunctional scaffolds by differentiation of the hydroxyl groups.

Hence, even AB<sub>2</sub>-, ABC-, or ABCDE-type carbohydrate scaffold molecules can be achieved.<sup>[107]</sup> For the synthesis of a AB<sub>2</sub>-type scaffold Ciuk et al. allylated the 2- and 3-position of a respective mannoside (Figure 3.4, B). The corresponding scaffold was used for the synthesis of bivalent glycoclusters.<sup>[108]</sup> In the work of Patel et al. a ABC-type scaffold (Figure 3.4, C), based on galactose, served as a precursor in the synthesis of heteroglycoclusters bearing mannosyl, lactosyl and fucosyl moieties. Thus, the 6-hydroxyl group was replaced by an amino function and the three functional groups could be addressed by orthogonal ligation

chemistry.<sup>[107c]</sup> Opatz and colleagues used orthogonal protection to achieve a thioglucoside of the ABCDE-type (Figure 3.4, D)<sup>[109]</sup> which can be employed in combinatorial chemistry.<sup>[110]</sup>

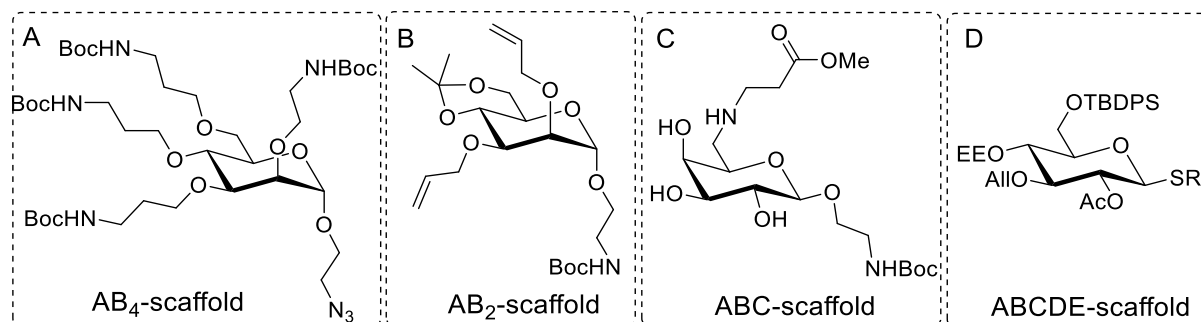


**Figure 3.4.** Carbohydrates can serve as scaffold molecules for the synthesis of glycoclusters. Their multifunctionality makes them suitable to be derivatized in various types. Abbreviations: All: allyl; TBDPS: *tert*-butyl di-phenyl silyl; EE: 1-ethoxy-ethyl.

Relying on the findings of Brekalo et al.,<sup>[100]</sup> the concept of a variable spatial presentation of Man- and Glc-ligands and the influence on bacterial adhesion was transferred to the disaccharide D-maltose as a scaffold molecule. D-Maltose serves as a privileged scaffold molecule for two reasons. First, its natural occurrence makes the system more biomimetic and on the other hand, the systematic functionalization of maltosides is easily accessible. Moreover, the structure of D-maltose offers the opportunity to vary the position of a Man ligand and the relative orientation of a respective Glc-moiety in order to investigate the influence of ligand presentation and secondary interactions with the lectin (Figure 3.5).

Hence, maltose was converted into a trifunctional scaffold of the ABC-type to allow ligation chemistry by naturally occurring amide bonds to attach an  $\alpha$ -D-mannopyranoside (Man) and a  $\beta$ -D-glucopyranoside (Glc) unit to the primary 6- and 6'-positions of the scaffold. With this requirement, a maltose scaffold was targeted with orthogonal protected or respectively masked amino groups at the 6- and 6'-position to allow amide coupling with carboxy functionalized glycoside ligands. In the master thesis of Jaeschke the concept of trifunctional maltose scaffolds was introduced and first attempts for the preparation were described.<sup>[111]</sup>

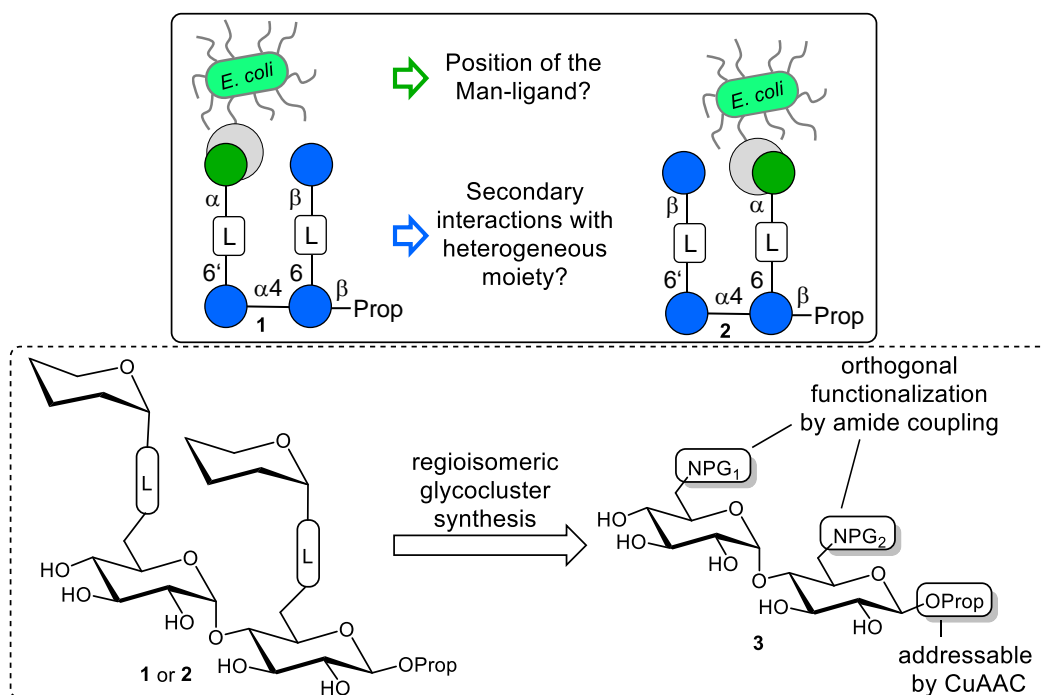


**Figure 3.5.** Maltose-based regioisomeric heterovalent glycoclusters for the investigation of carbohydrate-protein interactions. Heteroglycoclusters are based on a trifunctional propargyl  $\beta$ -D-maltoside **3**. Color code: Glc (blue); Man (dark green). Abbreviations: PG: protecting groups; L: linker; Prop: propargyl; CuAAC: copper-catalyzed azide alkyne cycloaddition.

Thus, two regioisomeric heterobivalent Man/Glc glycoclusters, **1** and **2** (Figure 3.5), were targeted where the sugar moieties are ligated to the maltoside scaffold via amide bonds. A propargyl functional group was chosen as aglycone part of the maltoside to allow for eventual conjugation of the glycocluster by click chemistry or its immobilization on surfaces. The prepared heterobivalent glycoclusters were tested as inhibitors of mannose-specific bacterial adhesion (FimH-mediated). In order to tease out the single effect of ligand scaffolding on carbohydrate recognition, various synthetic targets were targeted; (i) the synthesis of a trifunctional maltoside scaffold with orthogonal protected amino groups and (ii) regioisomeric glycoclusters with Man and Glc ligands and in addition a homobivalent cluster mannoside for comparison. Two key questions were addressed:

- Has the position of the Man ligand (6 or 6', respectively) an influence on FimH affinity?
- Does a sugar moiety in addition to a specific glycoligand support carbohydrate recognition, for example by secondary carbohydrate-lectin interactions?

The essence of this chapter was published:<sup>[112]</sup>

S. O. Jaeschke, I. vom Sondern, T. K. Lindhorst, "Synthesis of regioisomeric maltose-based Man/Glc glycoclusters to control glycoligand presentation in 3D space", *Org. Biomol. Chem.* **2021**, *19*, 7013-7023. (DOI: 10.1039/D1OB01150B)

### 3.1 Synthesis of heterobivalent maltose-based glycoclusters

For the synthesis of heteromultivalent glycoclusters **1** and **2**, a synthetic strategy was envisaged, which is divided into the synthesis of the trifunctional maltose scaffold on the one hand and its subsequent modification with synthetic  $\alpha$ -D-mannopyranoside and  $\beta$ -D-glucopyranoside ligands, respectively, at the primary 6- and 6'-positions of the maltoside scaffold leading to the two heterobivalent glycoclusters **1** and **2** with regioisomeric carbohydrate presentation.

The targeted maltoside scaffold **3** represents a trifunctional glycoside, containing an alkyne functionality in its aglycone part and two orthogonally protected amino functions, both derived from the primary hydroxyl groups present in maltose. Whereas the alkyne moiety offers the possibility for further ligation by Cu(I)-catalyzed 1,3-dipolar cycloaddition, for example the protected amino groups can be subsequently addressed by amide coupling reactions to achieve glycoclusters **1** and **2**, respectively.

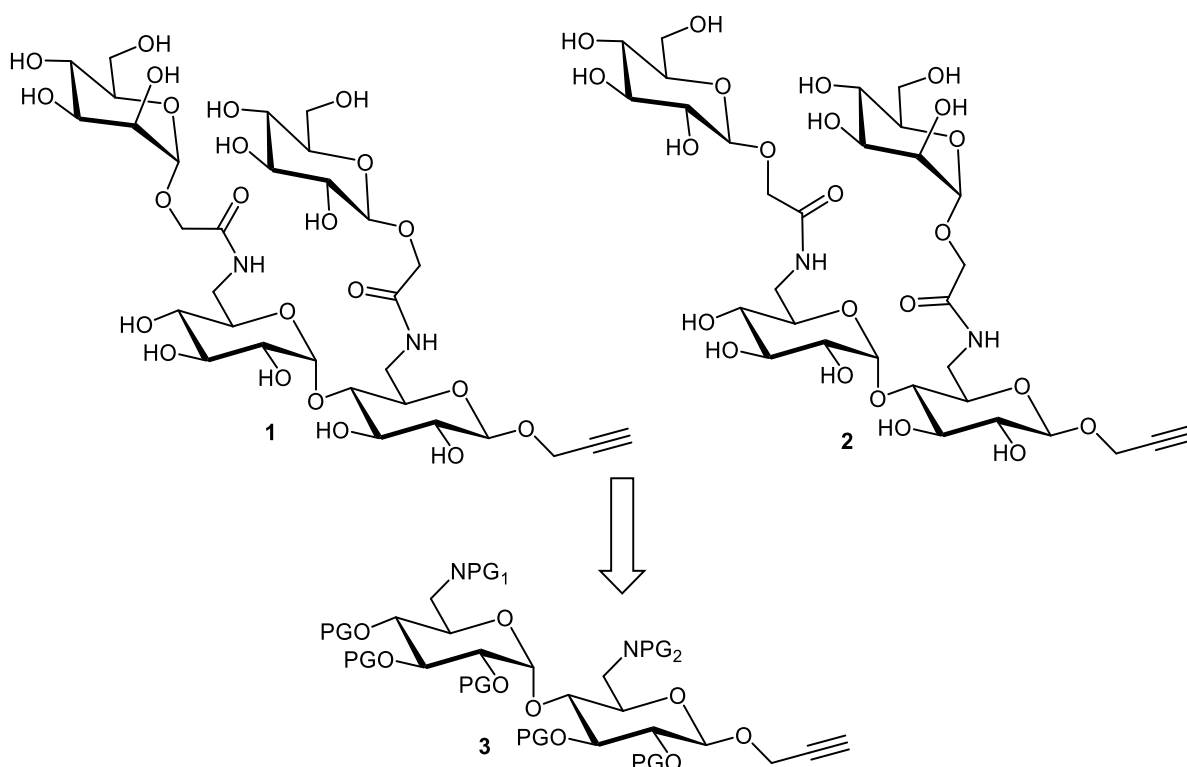


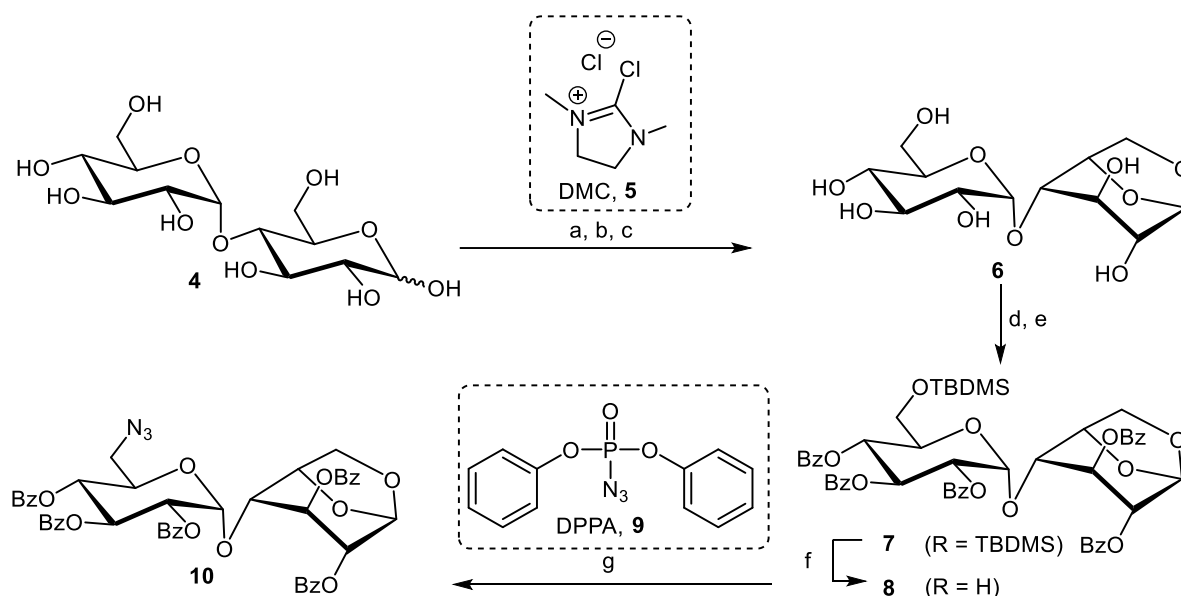
**Figure 3.6.** Heterobivalent maltose-based glycoclusters **1** and **2** were synthesized from a heterofunctionalized maltose scaffold **3**. PG = protecting group or masked amino function.

Since the synthesis of the trifunctional scaffold **3** requires orthogonal addressable amino groups at the 6- and 6'-position, first of all the primary hydroxyl groups of D-maltose (**4**) had to be differentiated and functionalized, respectively. The synthesis of multifunctional maltose scaffolds was started from D-maltose (**4**). In a first reaction step the disaccharide was

converted into the 1,6-anhydro derivative maltosan (**6**), in which both, the anomeric position and the primary 6-position are blocked. According to the work of Tanaka et al., the 1,6-anhydro derivative **6** was synthesized by treating D-maltose (**4**) with 2-chloro-1,3-dimethyl imidazolium chloride (**5**, DMC) in the presence of triethylamine in water.<sup>[113]</sup> Here, compared to the work of Tanaka, the purification of **6** was optimized by an additional acetylation step using acetic anhydride in pyridine. This procedure allowed easy removal of 1,3-dimethyl-2-imidazolidinone (DMI), which is a byproduct from **5**, by an aqueous workup. Subsequent deacetylation of the peracetylated intermediate under Zemplén conditions<sup>[114]</sup> gave **6** as a colorless solid in a yield of 94 % over three steps (Scheme 3.1). The <sup>1</sup>H NMR spectrum clearly showed that the chair conformation of the reducing sugar ring changes from the <sup>4</sup>C<sub>1</sub> to its <sup>1</sup>C<sub>4</sub> conformer. In comparison to the shape of maltose (**4**), the ring protons of **6** are in the <sup>1</sup>C<sub>4</sub> conformation in equatorial positions. This is indicated in the <sup>1</sup>H NMR spectrum by the relatively small coupling constants <sup>3</sup>J of ~0.5 to ~1 Hz, compared to ~9-10 Hz typically found for trans-diaxial coupling constants.

Having **6** in hand, functionalization of the 6'-position could be addressed in the next step as the anomeric and 6-hydroxyl group is blocked in the 1,6-anhydro ring. Because the direct introduction of an azide group by an Appel reaction or a Mitsunobu reaction with the unprotected **6** was not possible, it was necessary to implement a protecting group strategy. To obtain a maltose derivative in which only the 6'-position is unprotected, first this primary hydroxyl group of **6** was protected. Thus, the *tert*-butyldimethylsilyl ether protecting group (TBDMS) was used, because its introduction is regioselective for primary hydroxyl groups of the sugar ring. Therefore, according to a procedure of Jian et al., maltosan (**6**) was treated with *tert*-butyldimethylsilyl chloride (TBDMSCl) in pyridine at room temperature.<sup>[115]</sup> After complete conversion of the starting material the remaining free secondary hydroxyl groups were esterified with benzoyl chloride (BzCl) in the same pot. This one-pot procedure gave the TBDMS-protected maltosan **7** in a yield of 77 % over two steps. The silyl ether **7** was deprotected in tetrahydrofuran using tetra-*n*-butylammonium fluoride (TBAF), buffering the system with acetic acid, to achieve the pure 6'-hydroxy maltosan **8** after column chromatography in 92 % yield.

For the final functionalization of the 6'-OH group of **8** an azido group was introduced by a modified Mitsunobu reaction.<sup>[116]</sup> According to a procedure of Thompson and co-worker,<sup>[117]</sup> maltosan derivative **8** was treated with triphenylphosphine, diphenyl phosphoryl azide (**9**, DPPA) and diisopropyl azodicarboxylate (DIAD) at room temperature. The 6'-azido maltosan **10** was obtained clean in a yield of 72 % after column chromatography (Scheme 3.1).

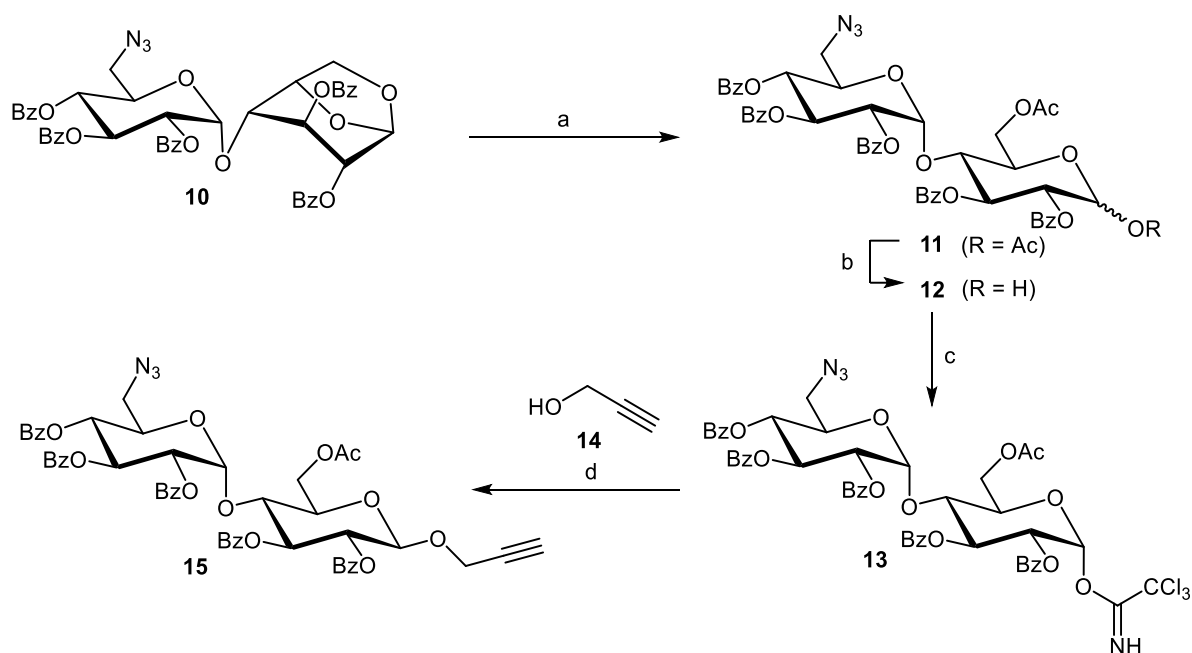


**Scheme 3.1.** Selective functionalization of the 6'-position of D-maltose (**4**) leading to azido maltose **10**. (a) Et<sub>3</sub>N, H<sub>2</sub>O, 0 °C→rt, 2 h; (b) Ac<sub>2</sub>O, pyridine, rt, 2.5 h; (c) NaOMe, MeOH, rt, 1 h, 94 % (over 3 steps); (d) TBDMSCl, pyridine, rt, 4 h; (e) BzCl, pyridine, rt, 1 h, 77 % (over 2 steps); (f) AcOH, TBAF, THF, 0 °C→rt, 16 h, 92 %; (g) PPh<sub>3</sub>, DIAD, dry THF, -15 °C→rt, 16 h, 72 %.

In the next step the anomeric position had to be functionalized. This was possible by the acetolysis of the 1,6-anhydro ring with acetic anhydride<sup>[118]</sup> yielding the corresponding 1,6-diacetate product which can in turn be selectively deprotected at the anomeric position and subsequently transformed into a glycosyl donor such as a trichloroacetimidate over three steps (Scheme 3.2).<sup>[119]</sup>

For the acetolysis, the 1,6-anhydro compound **10** was treated at room temperature with a mixture of acetic anhydride, acetic acid, and catalytic amounts of sulfuric acid (Scheme 3.2). After complete conversion into the 1,6-diacetate **11**, it was neutralized and the intermediate further taken in the next step without purification. Anomeric deprotection was achieved with hydrazinium acetate in dimethylformamide at 55 °C.<sup>[120]</sup> After complete conversion into the hemiacetal **12** it was washed in an aqu. workup and the intermediate taken in the following step without further purification. According to Schmidt *et al.*<sup>[121]</sup> the reducing maltose intermediate **12** was deprotonated with 1,8-diazabicycloundec-7-ene (DBU) and then treated with trichloroacetonitrile in dry dichloromethane<sup>[122]</sup> to furnish the addition product **13** after column chromatography in a yield of 68 % (over three steps). The achieved glycosyl donor allows introduction of a functional aglycone moiety as required for the preparation of a multifunctional maltose-based scaffold. Here, glycosylation of propargyl alcohol (**14**) allows further immobilization or other modifications by “click chemistry” (Scheme 3.2). Thus, **13** and propargyl alcohol (**14**) were treated with Lewis acid boron trifluoride diethyl etherate (BF<sub>3</sub>·Et<sub>2</sub>O)

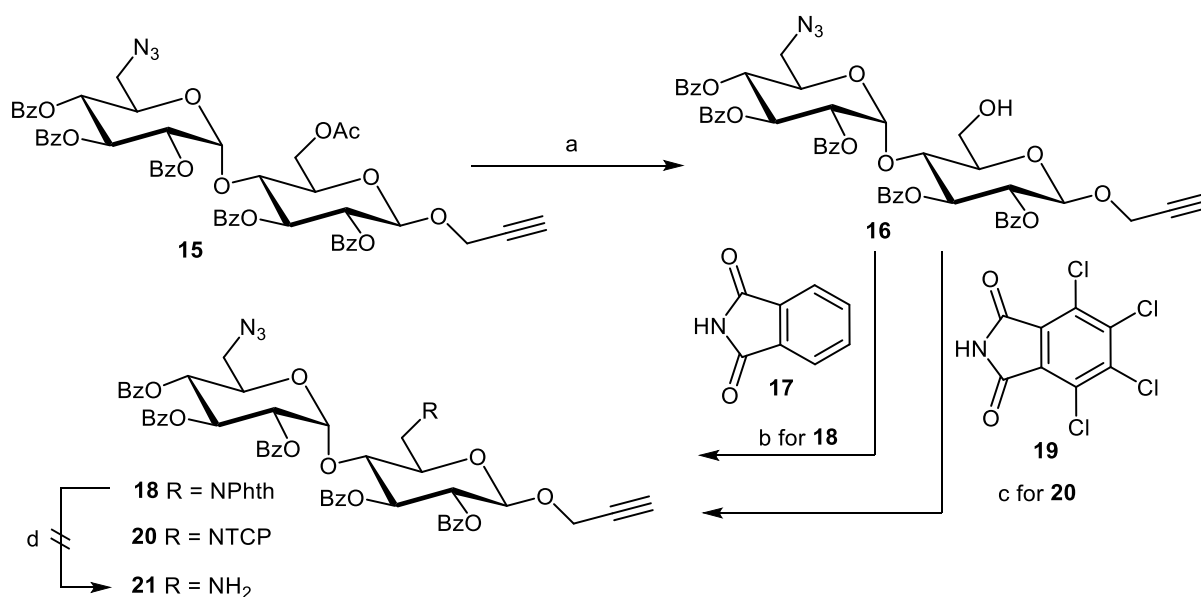
in  $\text{CH}_2\text{Cl}_2$  and the desired propargyl  $\beta$ -maltoside **15** was obtained in pure form in a yield of 91 % (Scheme 3.2).



**Scheme 3.2.** Synthesis of maltoside derivative **15** starting from 1,6-anhydro compound **10**. (a)  $\text{H}_2\text{SO}_4$ ,  $\text{Ac}_2\text{O}$ ,  $\text{AcOH}$  rt, 1 h; (b)  $\text{N}_2\text{H}_4 \cdot \text{AcOH}$ , DMF,  $55^\circ\text{C}$ , 2 h; (c) DBU,  $\text{Cl}_3\text{CCN}$ , dry  $\text{CH}_2\text{Cl}_2$ ,  $0^\circ\text{C} \rightarrow \text{rt}$ , 2 h, 68 % (over 3 steps); (d)  $\text{BF}_3 \cdot \text{Et}_2\text{O}$ , 3 Å MS, dry  $\text{CH}_2\text{Cl}_2$ ,  $0^\circ\text{C} \rightarrow \text{rt}$ , 2 h, 91 %.

In order to introduce a second orthogonal amino function at the 6-position of the maltosyl scaffold, the 6-*O*-acetyl protecting group of **15** had to be removed first. Ester protecting groups can easily be cleaved under basic conditions or according to Zemplén transesterification.<sup>[114]</sup> In addition, it is also possible to cleave ester protecting groups under acidic conditions. However, in this case, a method for the chemoselective cleavage of acetyl groups in the presence of benzoyl esters was sought. It is known that different ester groups have graded reactivities and that acetyl esters are more acid-labile than benzoyl esters.<sup>[123]</sup> Thus, according to Pornsuriyasak and co-worker<sup>[124]</sup> the *O*-acetyl group at the 6-position of **15** could be cleaved using acetyl chloride and methanol, producing hydrogen chloride (HCl) *in situ* (Scheme 3.3). The acid protonates the acetyl carbonyl function and thus cleavage of the *O*-acetyl group is facilitated, while the benzoyl ester is kept intact under these conditions. Decreasing the temperature to  $0^\circ\text{C}$  prevented an unwanted deprotection of benzoyl esters and the obtained 6-hydroxy-6'-azido-deoxy maltoside **16** was isolated in a yield of 76 %. For the orthogonal functionalization with a second amino group, phthalimide derivatives were introduced. Besides the fact that phthalimides are well-known precursors of amino functions, it is advantageous for the envisaged synthetic sequence that phthalimides are acidic enough to be used in Mitsunobu reactions as nucleophiles.<sup>[125]</sup>

Accordingly, first **16** was treated with phthalimide (**17**) according to the work of Walker et al.<sup>[126]</sup> Thus, under Mitsunobu conditions **16** was converted in the presence of triphenylphosphine and DIAD to yield phthalimido maltoside **18** in a yield of 70 % after purification on silica gel (Scheme 3.3). With the diamino maltoside **18** in hand, the selective deprotection of the phthalimido protecting group was attempted with the aim to keep the benzoyl esters intact. However, it turned out, that by treating **18** with hydrazine in ethanol the anomeric propargyl function was reduced and the benzoyl groups were cleaved. Thus, an alternative route for the amino group of the 6-position of **16** had to be found. To this end, the 6-amino function was introduced as tetrachlorophthalimide (**19**, TCP-NH). Tetrachlorophthaloyl protecting groups are well-known in carbohydrate chemistry because they can be removed under milder conditions than the respective phthalimides allowing the presence of ester protecting groups.<sup>[127]</sup> Due to the electron-withdrawing chlorine atoms the acidity of the imidic hydrogen is enhanced, which makes the TCP-NH (**19**) a more effective reagent in Mitsunobu reactions. According to a procedure of Fraser-Reid and co-worker<sup>[128]</sup> **16** was treated with triphenylphosphine and DIAD in the presence of TCP-NH (**19**). The corresponding maltoside derivative **20** could be isolated after column chromatography in a yield of 81 % (Scheme 3.3).

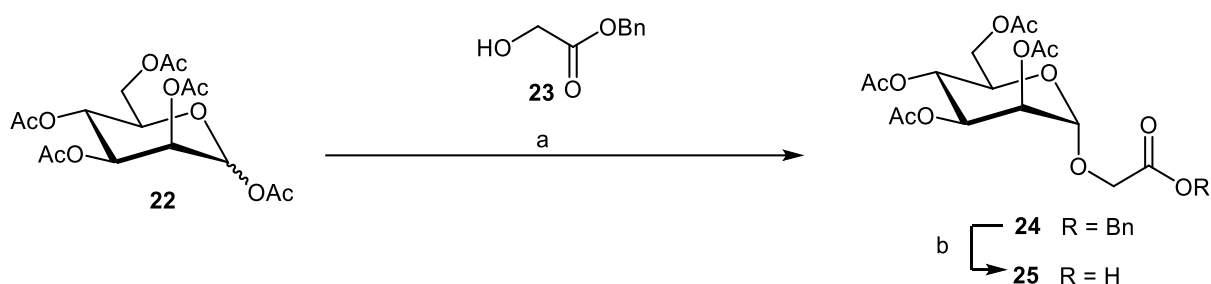


**Scheme 3.3.** Introduction of an orthogonal amino moiety at the 6-position of maltoside **16** by Mitsunobu reactions give the maltose-based scaffolds **18** and **20**. (a) AcCl, MeOH, CH<sub>2</sub>Cl<sub>2</sub>, 0 °C→rt, 16 h, 76 %; (b) PPh<sub>3</sub>, DIAD, dry THF, 0 °C→rt, 72 h, 70 %; (c) PPh<sub>3</sub>, DIAD, dry THF, 0 °C→rt, 16 h, 81 %; (d) N<sub>2</sub>H<sub>4</sub>·H<sub>2</sub>O, EtOH, 60 °C, 2h.

With the derivative **20** in hand, a maltose-based scaffold was achieved for the synthesis of heteromultivalent glycoclusters. To attach carbohydrate ligands to the multifunctional maltose scaffold **20** by amide coupling, two different carboxy-functionalized glycosides had to be synthesized. Amide conjugation was chosen owing to the natural character of this linkage

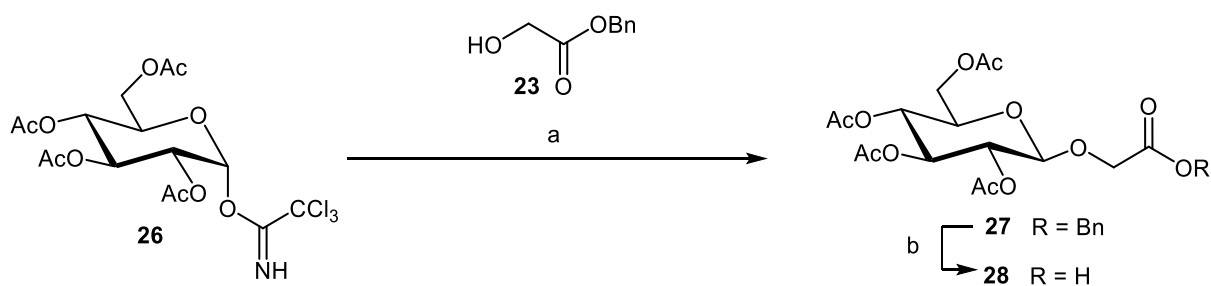
which is found in native glycopeptides. In addition, the short methylene linker in the aglycone makes the glycoclusters comparable with methyl  $\alpha$ -D-mannoside as a standard inhibitor for FimH in later bacterial binding studies.

The mannoside ligand **25**<sup>[129]</sup> was synthesized in two steps starting from the known mannoside peracetate **22**. According to a procedure of Kumar et al., **22** was used in a glycosylation reaction with  $\text{BF}_3 \cdot \text{Et}_2\text{O}$  as a promoter and benzyl glycolate (**23**) as a glycosyl acceptor at 0 °C. The corresponding mannoside **24** was isolated in a yield of 65 %. Then in a second step, the benzyl ester was cleaved by hydrogenation using palladium as a catalyst under a hydrogen atmosphere. After filtration over celite the free carboxylic acid **25** was obtained in quantitative yield (Scheme 3.4).



**Scheme 3.4.** Synthesis of mannoside carboxylic acid **25** starting from peracetylated mannoside **22**. (a)  $\text{BF}_3 \cdot \text{Et}_2\text{O}$ , 3 Å MS, dry  $\text{CH}_2\text{Cl}_2$ , 0 °C  $\rightarrow$  rt, 16 h, 65 %; (b)  $\text{H}_2$ , Pd/C, EE, rt, 2 h, quant.

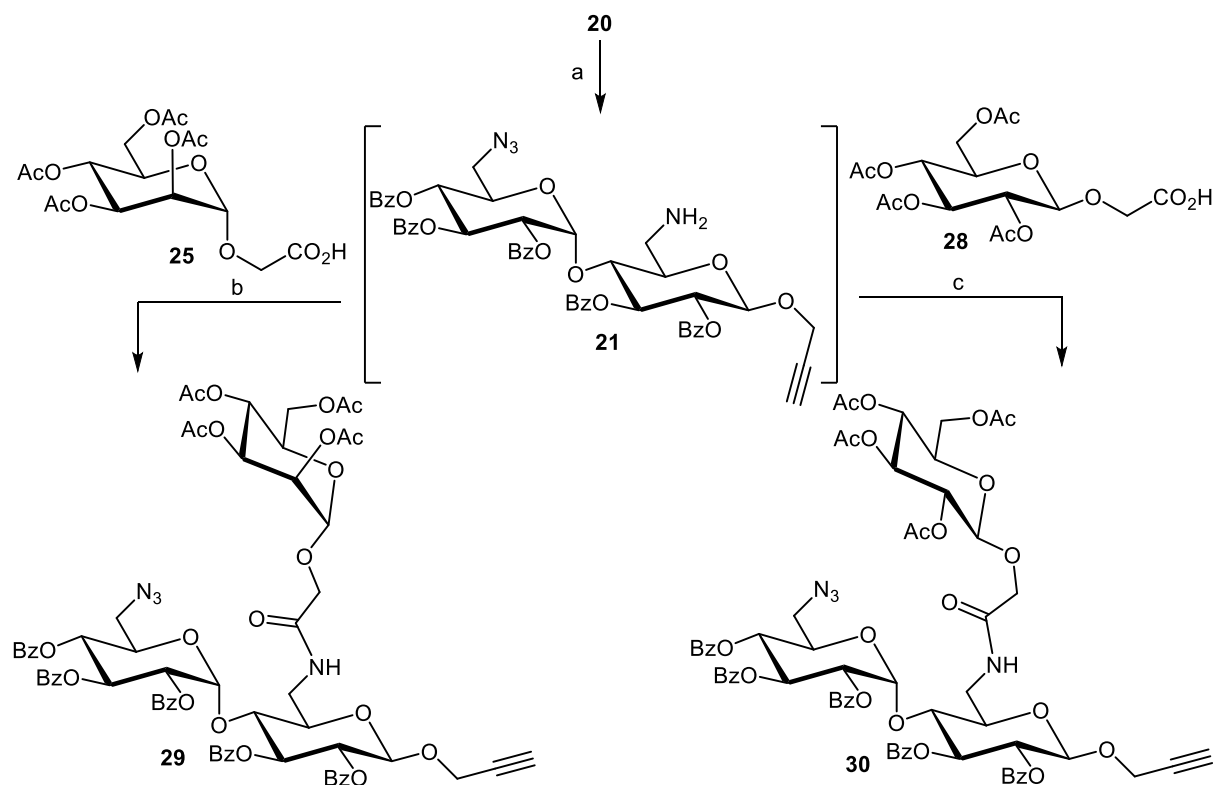
In an analogous sequence glucoside ligand **28** was synthesized starting from the known glucosyl trichloroacetimidate **26**.<sup>[121]</sup> According to a procedure of Wang et al., **26** was activated using  $\text{BF}_3 \cdot \text{Et}_2\text{O}$  and benzyl glycolate (**23**) was glycosylated in a yield of 87 %.<sup>[130]</sup> Afterwards the corresponding free carboxylic acid **28** was obtained by palladium-catalyzed hydrogenation of the benzyl ester **27** in quantitative yield (Scheme 3.5).



**Scheme 3.5.** Synthesis of glucose carboxylic acid **28** starting from glucose trichloroacetimidate (**26**). (a)  $\text{BF}_3 \cdot \text{Et}_2\text{O}$ , 3 Å MS, dry  $\text{CH}_2\text{Cl}_2$ , 0 °C  $\rightarrow$  rt, 16 h, 87 %; (b)  $\text{H}_2$ , Pd/C, EE, rt, 2 h, quant.

With the scaffold **20** and the ligand **25** and **28** in hand, the functionalization of the 6-position was performed in a two-step reaction. First, the TCP protecting group had to be cleaved. While

the selective deprotection of phthalimide **18** was not successful (Scheme 3.3) the more labile tetrachlorophthalimide could be removed under milder reaction conditions. According to a procedure of Fraser-Reid and co-workers **20** was treated with ethylenediamine in a mixture of acetonitrile and tetrahydrofuran at 50 °C.<sup>[131]</sup> The corresponding free amine **21** was obtained and used without any further purification in an amide coupling reaction with activated carboxylic acids **25** or **28** (Scheme 3.6). Here the conditions of the amide coupling required optimization of the activation reagents and the used solvents.



**Scheme 3.6.** Synthesis of maltose derivative **29** and **30** starting from **20**. (a) ethylenediamine, MeCN/THF, 50 °C, 1 h; (b) NHS, EDC·HCl, DMSO, rt, 16 h, 60 % (over 2 steps); (c) NHS, EDC·HCl, DMSO, rt, 16 h, 64 % (over 2 steps).

The optimization for the amide bond formation was performed with the mannoside ligand **25**. Accordingly, in all attempts, first the carboxylic acid was activated to an active ester at room temperature and afterwards the amine **21** was added for the conjugation (Table 3.1). In a first attempt **25** was activated according to a procedure of Hotha and co-worker<sup>[132]</sup> and **25** was treated with 1-ethyl-3-(3-dimethylaminopropyl)carbodiimide (EDC) and hydroxy benzotriazole (HOBt) in tetrahydrofuran, but after the addition of amine **21** and DIPEA the formation of the corresponding amide **29** was not observed. Changing the activation reagent as reported by Lindhorst and co-workers<sup>[133]</sup> from EDC to diisopropylcarbodiimide (DIC) in the presence of HOBt led to the formation of amide **29**, which was isolated in a poor yield of 30 % after column chromatography. To increase the yield of **29** another activation method had to be implemented.

In the next approach, following a procedure of Stoddart and co-worker, **25** was treated with *O*-benzotriazol-1-yl-*N,N,N',N'*-tetramethyluronium tetrafluoroborate (HBTU·BF<sub>4</sub>) in the presence of DIPEA.<sup>[134]</sup> After the addition of the free amine **21** the formation of amide **29** was observed. Isolation of **29** (34 %) showed that the yield was not changed significantly.

With these results in hand, it was tried to form active esters with *N*-hydroxysuccinimide (NHS) from the corresponding carboxylic acid **25**. First, according to Greatrex et al.<sup>[129]</sup> **25** was reacted with NHS and dicyclohexylcarbodiimide (DCC) in dimethylformamide. In fact, the targeted amide conjugate **29** was formed but it could not be purified by column chromatography and the <sup>1</sup>H NMR showed impurities of the urea side product of DCC. Thus, it was decided to change the activation reagent from DCC to the water-soluble EDC·HCl, whereas all side products could be removed by an aqu. workup. For this optimized reaction conditions, the amide **29** could be isolated in an increased yield of 57 %. Finally, in a last step the solvent was changed from DMF to dimethyl sulfoxide (DMSO), which resulted in a higher isolated yield of **29** (68 %). With this it was shown that the optimal conditions for the activation of **25** belong to the treatment with NHS and EDC in DMSO (Table 3.1).

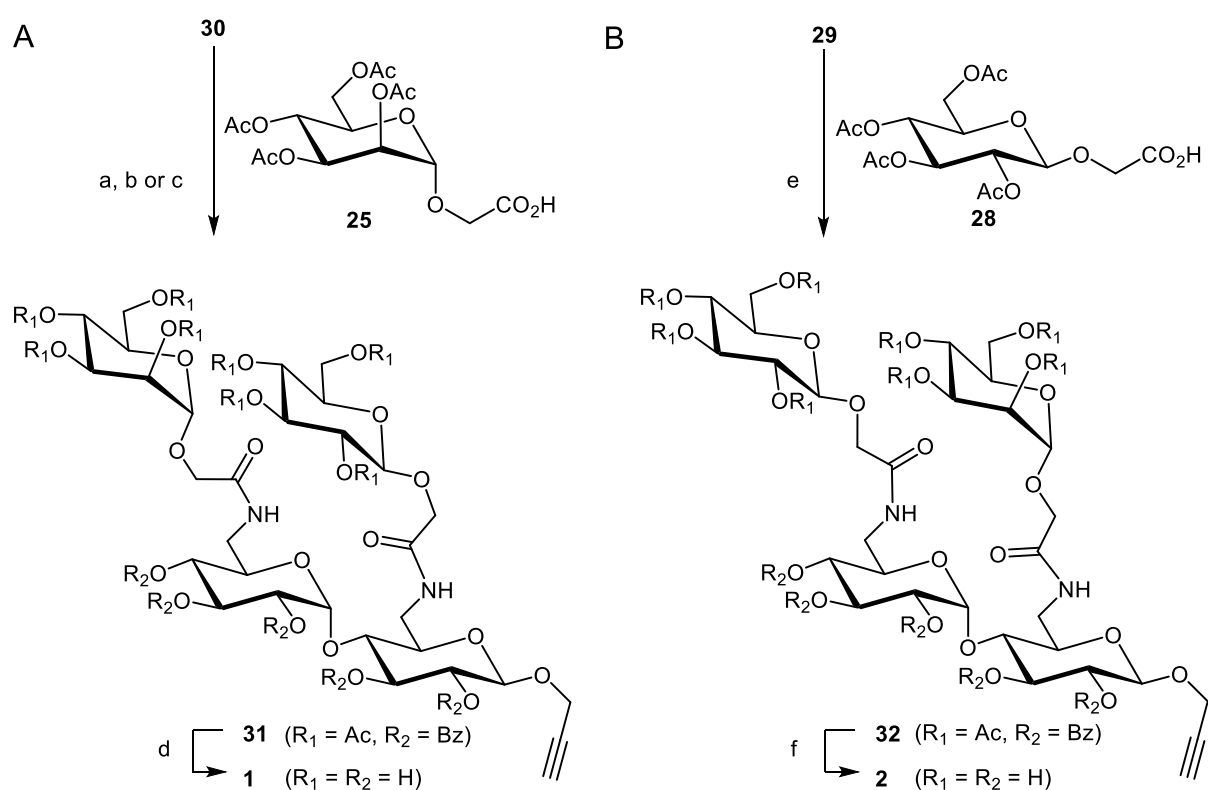
Employing these optimized conditions, the amide coupling of glucoside **28** with the free amine **21** gave the respective monovalent amide glycoconjugate **30** in a yield of 64 % after column chromatography (Table 3.1).

**Table 3.1.** Optimization of the amide bond formation between carboxylic acid **25** and **28** and amine **21**. All reactions were carried out at room temperature for 16 h.

Entry	Carbohydrate ligand	Coupling reagent	Solvent	Yield
1	Man-CO <sub>2</sub> H <b>25</b>	HOBt, EDC·HCl, DIPEA	THF	-
2	Man-CO <sub>2</sub> H <b>25</b>	DIC, HOBt, DIPEA	CH <sub>2</sub> Cl <sub>2</sub>	30 %
3	Man-CO <sub>2</sub> H <b>25</b>	HBTU·BF <sub>4</sub> , DIPEA	DMF	34 %
4	Man-CO <sub>2</sub> H <b>25</b>	NHS, DCC, DIPEA	DMF	not isolated
5	Man-CO <sub>2</sub> H <b>25</b>	NHS, EDC·HCl, DIPEA	DMF	57 %
6	Man-CO <sub>2</sub> H <b>25</b>	NHS, EDC·HCl, DIPEA	DMSO	68 %
7	Glc-CO <sub>2</sub> H <b>28</b>	NHS, EDC·HCl, DIPEA	DMSO	64 %

With the monovalent clusters **29** and **30** in hand, the heterobivalent glycoclusters **1** and **2** were targeted. Hence, the 6'-azido functional group in **29** and **30**, respectively, offers two different possibilities for amide bond formation. On one hand, reduction of the azide into the

corresponding amine provided the opportunity for amide coupling reactions, as described for the 6-position before. Unfortunately, reduction of azido cluster **30** favors intramolecular migration of the benzoyl ester protecting group of the 4'-position and give the corresponding benzoyl amide. To avoid this side reaction, the clusters **29** and **30** were functionalized by a Staudinger ligation. A Staudinger ligation as introduced by Saxon and Bertozzi<sup>[135]</sup> involves the reaction of an azide with a phosphine, which react to an aza-ylide after release of nitrogen.<sup>[136]</sup> The aza-ylide intermediate can be reacted with activated carboxylic acids to the corresponding amides. Hence, Staudinger ligation was performed for the functionalization of **30** and **29** with carboxylic acids **25**, respective **28**, employing optimized activation conditions (NHS/EDC) (Scheme 3.7).



**Scheme 3.7.** Synthesis of maltose-based heteroglycoclusters **1** (A) and **2** (B) by Staudinger ligation starting from clusters **30** and **29**, respectively. (a) NHS, EDC·HCl, PPh<sub>3</sub>, dry THF, 0 °C→rt, 16 h; (b) NHS, EDC·HCl, PBU<sub>3</sub>, dry THF, 0 °C→rt, 16 h, 32 %; (c) NHS, EDC·HCl, PMe<sub>3</sub>, dry THF, 0 °C→rt, 16 h, 68 %; (d) NaOMe, MeOH, rt, 2 h, 82 %; (e) NHS, EDC·HCl, PMe<sub>3</sub>, dry THF, 0 °C→rt, 16 h, 65 %; (f) NaOMe, MeOH, rt, 2 h, 88 %.

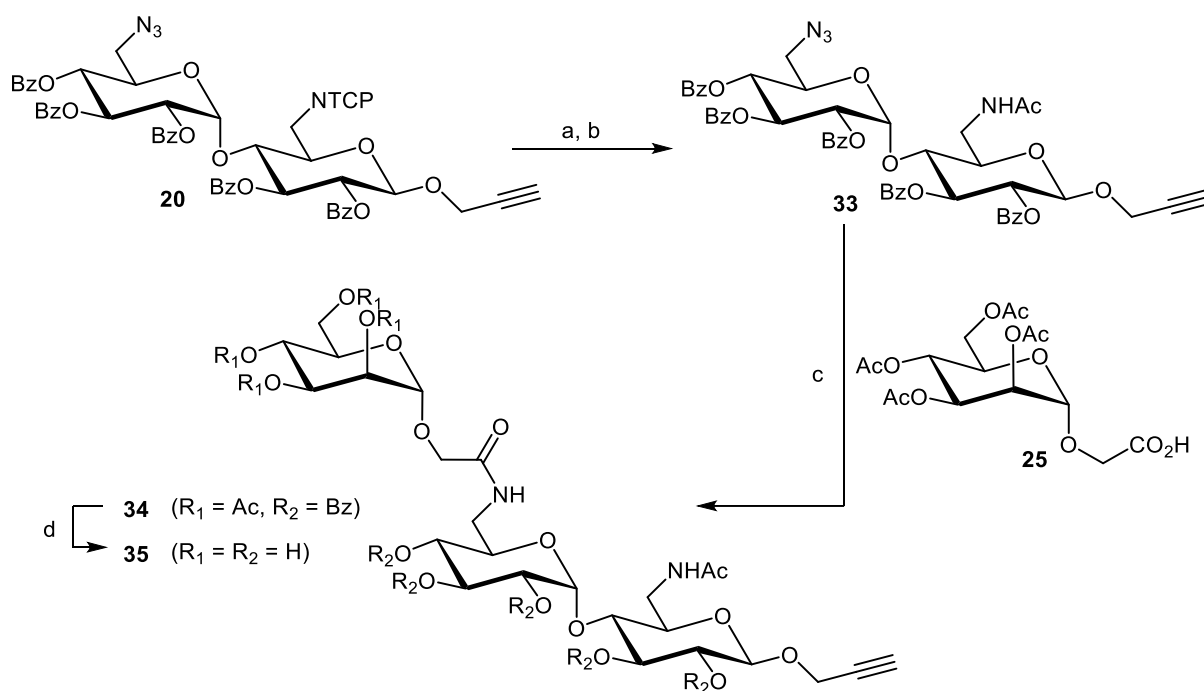
In a first attempt **25** and azide **30** were treated with PPh<sub>3</sub> but it was observed that no reaction took place, and the azido function was still intact (Scheme 3.7). Then, the reaction was performed with a more reactive phosphine and according to Mizuno et al. tributyl phosphine (PBU<sub>3</sub>) was utilized.<sup>[137]</sup> Thus, carboxylic acid **25** and azide **30** were treated with PBU<sub>3</sub> in dry tetrahydrofuran for 16 h and the targeted product **31** was isolated after column

chromatography in a poor yield of 32 %. In addition, also the benzoyl migration product was found as the major side product (45 %). To increase the yield of the amide **31** it was focused on the choice of the phosphine. Lindhorst and co-workers showed that the Staudinger ligation with trimethyl phosphine ( $\text{PMe}_3$ ) gave fair yields.<sup>[138]</sup> With this in mind **25** was added to azide **30** and treatment with  $\text{PMe}_3$  providing the targeted protected heterovalent glycocluster **31** in a good yield of 68 % (Scheme 3.7). These reaction conditions were further employed for the functionalization of **29** with glucoside carboxylic acid **28**. Here, treatment with  $\text{PMe}_3$  gave the heteroglycocluster **32** in a good yield of 65 %.

In a last step the ester protecting groups for both clusters had to be removed. Thus, under standard Zemplén transesterification conditions the clusters **31** and **32** were treated with sodium methoxide in methanol.<sup>[114]</sup> Neutralization, extraction and size exclusion chromatography provided the targeted heteroclusters in yields of 82 % for 6'- $\alpha$ -Man-6- $\beta$ -Glc **1** and 88 % for 6'- $\beta$ -Glc-6- $\alpha$ -Man **2** respectively (Scheme 3.7). Lyophilization of both compounds made them available for biological assays with *E. coli* bacteria.

In order to test whether heteromultivalent or scaffolding effects occur for protein carbohydrate interactions, a control substance **35** was designed (Scheme 3.8). Hence, the terminal 6'-position of scaffold **20** was functionalized with a carboxymethyl  $\alpha$ -D-mannoside, and the 6-position was *N*-acetylated. With this approach the influence of the presence of carbohydrate ligands at the 6-position can be investigated. On the other hand, the motive of an amido group at the 6-position is still present and has no effect on interactions of the glycocluster and the lectin FimH.

For the synthesis of this monovalent maltose cluster **35**, it was started from scaffold molecule **20**. In a first step the TCP protecting group was removed by treatment of **20** with ethylenediamine. Then, subsequently without any further purification the free amino group was acetylated by using acetic anhydride in the presence of pyridine and the 6-amido maltoside **33** was obtained in a yield of 70 % over two steps. With this maltoside in hand the 6'-position was derivatized in a Staudinger ligation reaction. Thus, following the optimized reaction conditions, the carboxymethyl mannoside **25** was activated with NHS and EDC·HCl and after the addition of maltoside **33** treatment with  $\text{PMe}_3$  gave the monovalent maltoside cluster **34** in a yield of 50 %. In a last step the ester protecting groups were cleaved under Zemplén transesterification conditions<sup>[114]</sup> to achieve the unprotected monovalent maltoside cluster **35** in a yield of 90 % after size exclusion chromatography (Scheme 3.8). Before **35** was used in a biological assay it was lyophilized.



**Scheme 3.8.** Synthesis of a monovalent maltose-based glycocluster **35** starting from scaffold **20**. (a) ethylenediamine, MeCN/THF, 50 °C, 1 h; (b) Ac<sub>2</sub>O, pyridine, rt, 16 h, 70 % (over 2 steps); (c) NHS, EDC·HCl, PMe<sub>3</sub>, dry THF, 0 °C→rt, 16 h, 50 %; (d) NaOMe, MeOH, rt, 2 h, 90 %.

With the heterogeneous functionalized maltose-based glycoclusters **1**, **2** and **35** in hand, their properties as inhibitors of bacterial adhesion could be tested. For such assays, the analogous homobivalent glycocluster, carrying two α-D-Man moieties was required.

### 3.2 Synthesis of homobivalent maltose-based glycoclusters

For the biological testing of the two heterobivalent maltose-based glycoclusters **1** and **2**, the homobivalent cluster mannoside **36** was required for comparison. For the synthesis of **36**, the diazide **37** was envisaged as starting material for a subsequent Staudinger ligation with the *manno*-configured carboxymethyl glycoside **25** (Figure 3.7).

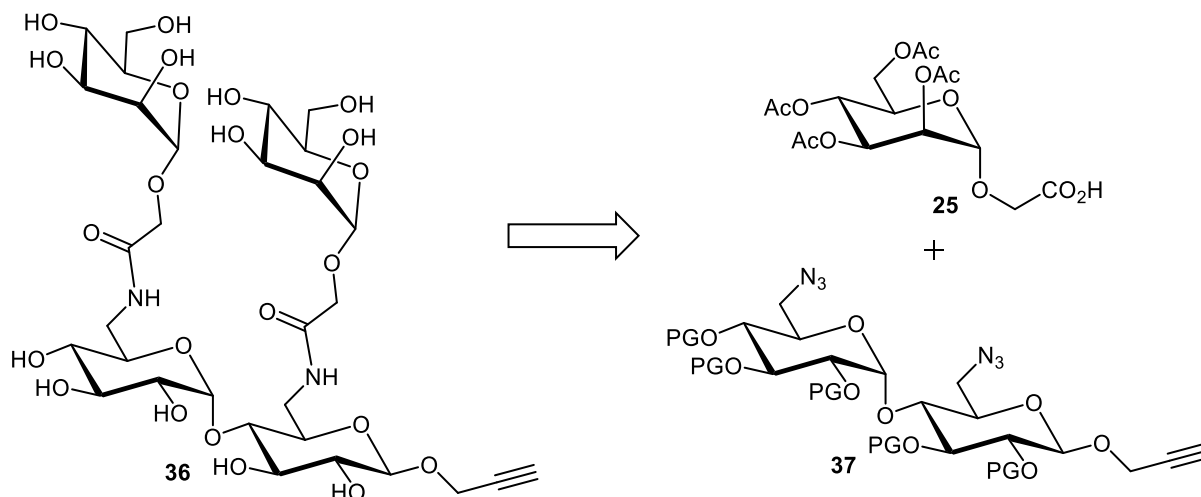
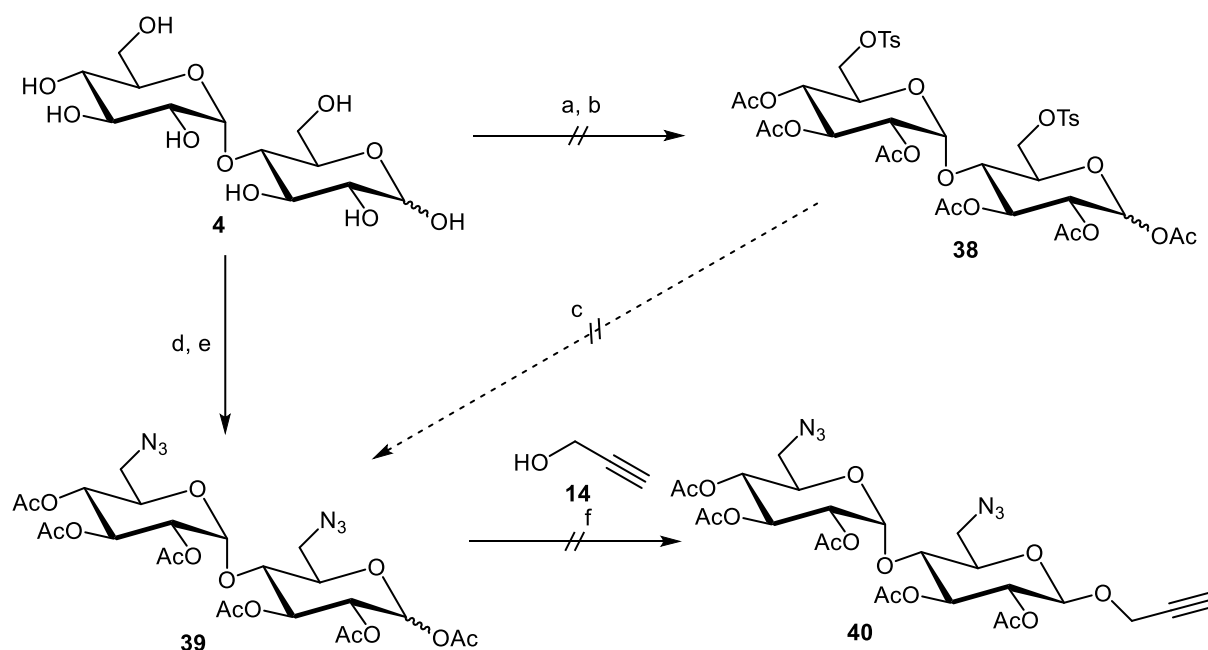


**Figure 3.7.** Homovalent maltose-based glycocluster **36** is synthesized from a homofunctionalized maltose scaffold **37** bearing two primary azido moieties, which can be addressed by Staudinger ligation. PG = protecting group.

For a first approach towards maltoside scaffold **37**, D-maltose (**4**) was treated with TsCl in pyridine according to Rolland et al.,<sup>[139]</sup> in order to achieve the bis-tosylate **38** after *in situ* acetylation and in the next step the targeted bis-azide **39** after nucleophilic substitution. However, this reaction sequence was not successful. In a second attempt, D-maltose (**4**) was treated with NaN<sub>3</sub> in the presence of triphenylphosphine (PPh<sub>3</sub>) and carbon tetrabromide (CBr<sub>4</sub>) in DMF according to Kovensky and co-workers.<sup>[140]</sup> After complete conversion of the starting material the remaining free hydroxyl groups were acetylated in the same pot and the desired diazido maltose **39** was obtained in a fair yield of 36 % over two steps. However, the synthesis failed in the following step as the BF<sub>3</sub>·Et<sub>2</sub>O-catalyzed glycosylation of propargyl alcohol (**14**) to gain the maltoside **40** did not work (Scheme 3.9).



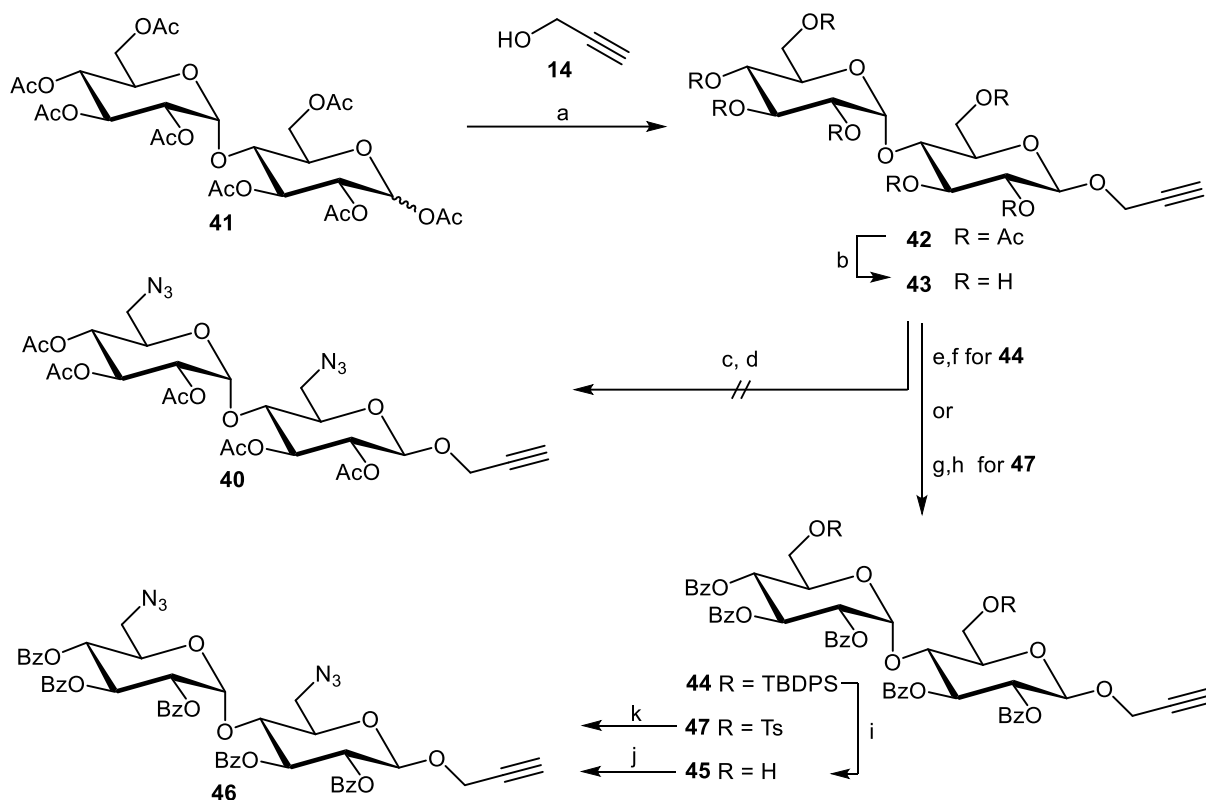
**Scheme 3.9.** Synthesis of diazido maltoside **40** starting from D-maltose (**4**). (a) TsCl, pyridine, 0 °C→rt, 2 h; (b) Ac<sub>2</sub>O, pyridine, rt, 16 h; (c) NaN<sub>3</sub>, DMF, 80 °C, 16 h; (d) NaN<sub>3</sub>, PPh<sub>3</sub>, CBr<sub>4</sub>, DMF, rt, 16 h; (e) Ac<sub>2</sub>O, pyridine, rt, 16 h, 36 % (over 2 steps); (f) BF<sub>3</sub>·Et<sub>2</sub>O, 3 Å MS, dry CH<sub>2</sub>Cl<sub>2</sub>, 0 °C→rt, 2 h.

As a consequence of these results, the glycosylation, starting from the literature-known maltose octaacetate **41**,<sup>[141]</sup> was performed first, delivering the propargyl maltoside **42** in a yield of 48 % after column chromatography (Scheme 3.10). Concomitantly with this work, Fletcher and co-workers in 2019 published the synthesis of **42** using the same reaction conditions.<sup>[142]</sup> With maltoside **42** in hand, the acetyl protecting groups were removed in the next step under Zemplén conditions<sup>[114]</sup> to obtain the unprotected maltoside **43** in quantitative yield. Unfortunately, also with the propargyl maltoside **43**, the regioselective azide functionalization with PPh<sub>3</sub>, CBr<sub>4</sub>, and NaN<sub>3</sub> according to Defaye and co-workers<sup>[143]</sup> did not give the desired bis-azide **40**.

As the Appel-analogous reaction of the propargyl maltoside **43** with NaN<sub>3</sub> does not work, the primary hydroxyl groups of the maltoside were first regioselective protected as TBDPS ethers to yield maltoside **44** after in situ-benzoylation (Scheme 3.10). According to Yan et al.<sup>[144]</sup> **43** was treated with *tert*-butyldiphenylsilyl chloride (TBDPSCI) and after full conversion of the starting material the remaining free hydroxyl groups were benzoylated in the same pot by the addition of BzCl yielding disilylether maltoside **44** in a yield of 74 % over two steps. Deprotection of the silyl ether protecting groups by treatment with tetra-*n*-butyl ammonium fluoride (TBAF) gave maltoside **45** in a yield of 87 % after purification by column chromatography. In a final step in a modified Mitsunobu reaction<sup>[116]</sup> the primary hydroxyl groups of **45** were turned into azide functional groups by treatment with PPh<sub>3</sub>, DPPA and DIAD

according to a procedure of Thompson and co-workers,<sup>[117]</sup> giving the bis-azide **46** in a good yield of 74 % after column chromatography (Scheme 3.10).

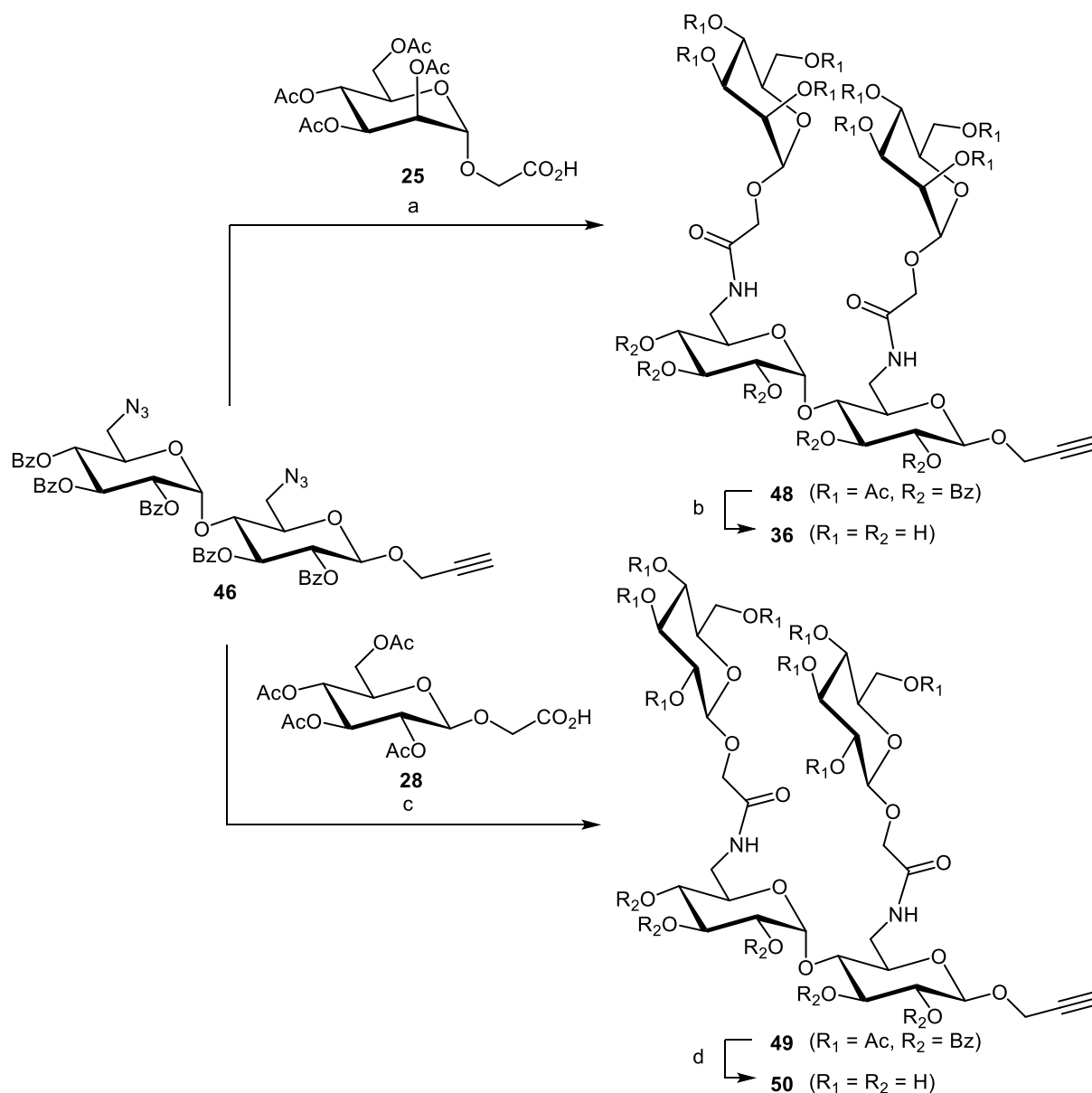
In order to reduce the number of reaction steps and increase the overall yield of **46** an alternative modification strategy was applied and, referring to the work of Takano and co-workers,<sup>[145]</sup> the primary OH groups of maltoside **43** were regioselectively tosylated. Accordingly, maltoside **43** was treated with tosyl chloride (TsCl) and by the addition of BzCl to the same pot the remaining secondary OH groups were esterified, which gave the bis-tosylated maltoside **47** in a yield of 67 % over two steps. In a nucleophilic substitution reaction, the bis-tosylate **47** was reacted with NaN<sub>3</sub> in DMF to obtain **46** in a yield of 84 % (Scheme 3.10).



**Scheme 3.10.** Synthesis of diazido maltoside **46** starting from peracetylated maltose **41**. (a) BF<sub>3</sub>·Et<sub>2</sub>O, 3Å MS, dry CH<sub>2</sub>Cl<sub>2</sub>, 0 °C→rt, 48 h, 48 %; (b) NaOMe, MeOH, rt, 2 h, quant.; (c) NaN<sub>3</sub>, PPh<sub>3</sub>, CBr<sub>4</sub>, DMF, rt, 16 h; (d) Ac<sub>2</sub>O, pyridine, rt, 16 h; (e) TBDPSCl, pyridine, 0 °C→rt, 4 h; (f) BzCl, pyridine, 0 °C→rt, 6 h, 74 % (of **44** over 2 steps); (g) TsCl, pyridine, 0 °C→rt, 2 h; (h) BzCl, pyridine, 0 °C→rt, 6 h, 67 % (for **47** over 2 steps); (i) AcOH, TBAF, THF, 0 °C→rt, 16 h, 87 %; (j) PPh<sub>3</sub>, DIAD, dry THF, -15 °C→rt, 16 h, 74 %; (k) NaN<sub>3</sub>, DMF, 80 °C, 16 h, 84 %.

Overall, the propargyl diazido maltoside **46** was obtained in five reaction steps from peracetylated maltose **41**. With this homobifunctional scaffold molecule in hand, it was now possible to address the 6- and 6'-position with carbohydrate ligands in a Staudinger ligation reaction for the preparation of homobivalent glycoclusters.

For the synthesis of the glycoclusters **36** and **50** the bis-azido maltoside **46** was conjugated with the two carboxymethyl glycosides **25**, respectively **28** in a Staudinger ligation. Employing the optimized reaction conditions, carboxymethyl mannoside **25** was activated by using NHS and EDC·HCl and after addition of bis-azido maltoside **46** treatment with  $\text{PMe}_3$  gave the bivalent maltoside cluster **48** in a yield of 56 % (Scheme 3.11). With **48** in hand the ester protecting groups were cleaved under Zemplén conditions<sup>[114]</sup> to achieve the unprotected bivalent maltoside cluster **36** in a yield of 77 % after size exclusion chromatography.



**Scheme 3.11.** Synthesis of maltose derivative **36** starting from **46**. (a) NHS, EDC·HCl,  $\text{PMe}_3$ , dry THF,  $0\text{ }^\circ\text{C}$ →rt, 16 h, 56 %; (b) NaOMe, MeOH, rt, 2 h, 77 %; (c) NHS, EDC·HCl,  $\text{PMe}_3$ , dry THF,  $0\text{ }^\circ\text{C}$ →rt, 16 h, 65 %; (d) NaOMe, MeOH, rt, 2 h, 79 %.

In accordance with the optimized Staudinger conditions also the  $6'\beta\text{-Glc-6}\beta\text{-Glc}$  glycocluster **49** was synthesized, using carboxymethyl glucoside **28** as a ligand, and the protected bivalent

glycocluster **49** was obtained in a yield of 65 %. Cleaving the ester protecting groups gave the bis-glucoside glycocluster **50** in a yield of 79 % after size exclusion chromatography on Sephadex (Scheme 3.11).

With the heterogeneous functionalized maltose-based glycoclusters **1**, **2** and **35** and the homogeneous cluster **36** in hand biological testing in bacterial adhesion-inhibition assays was performed.

### 3.3 Biological testing

To test the synthesized maltose-based glycoclusters **1**, **2**, **35** and **36** as ligands of the mannose-specific bacterial lectin FimH, adhesion-inhibition assays with *E. coli* were performed.<sup>[146]</sup> As mentioned earlier (cf. chapter 3.1), it was of interest to answer two main questions. First, the role of the relative position of the mannoside ligand at the maltose scaffold was addressed. Secondly, putative secondary interactions exerted by the glucose moiety in the heterobivalent glycoclusters were evaluated.

In the employed adhesion-inhibition assay<sup>[146]</sup> the inhibition of type 1 fimbriae-mediated adhesion of fluorescent *E. coli* to a mannan-coated surface is measured. The employed *E. coli* strain PKL1162 expresses GFP (green fluorescent protein) and hence, bacterial adhesion can be correlated to fluorescence read-out.<sup>[147]</sup> Testing of serially solutions of the maltose-based glycoclusters leads to dose-response inhibition curves of which IC<sub>50</sub> values were deduced. Because results measured with live bacteria can vary significantly between independent experiments, methyl  $\alpha$ -D-mannopyranoside (MeMan) was used as a reference ligand in each experiment. Therefore, inhibitory potencies of each synthetic ligand can be reported relative to MeMan (RIP values) and compared to each other (cf. Experimental section, chapter 8.3).

Figure 3.8 shows an example of inhibition curves as obtained with glycoclusters **1**, **2**, and MeMan tested on the same plate. Both glycoclusters show a higher inhibitory potency than MeMan and moreover the heterobivalent glycocluster **1**, carrying the Man ligand at the 6'-position of the maltoside scaffold is a better inhibitor of FimH-mediated bacterial adhesion than the regioisomeric glycocluster **2**.

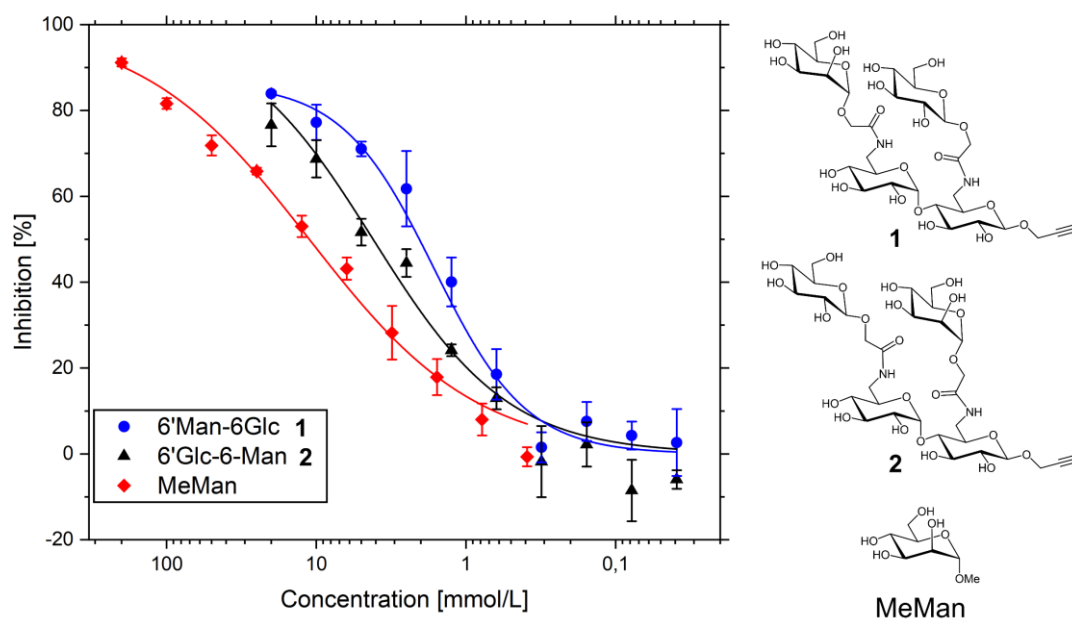


**Figure 3.8.** Inhibition curves obtained with maltosides **1** and **2** as inhibitors for type 1 fimbriae-mediated bacterial adhesion to a mannan-coated microtiter plate. MeMan was tested in parallel on the same plate. Sigmoidal concentration-response curves were fitted by non-linear regression. Error bars are standard deviations from triplicate values on one plate.

The  $IC_{50}$  values obtained, and the respective RIP values are compiled in Table 3.2. All tested glycocluster **1**, **2**, **35**, and **36**, showed a higher inhibitory potency than MeMan. The homobivalent glycocluster 6' $\alpha$ Man-6 $\alpha$ Man (**36**) showed the highest inhibitory potency (RIP = 8.01), which was 8-fold better than for MeMan. The regioisomeric glycoclusters 6' $\alpha$ Man-6 $\beta$ Glc (**1**) and 6' $\beta$ Glc-6 $\alpha$ Man (**2**) significantly difference in their inhibitory potencies, **2** showing a RIP value of 2.99 and **1** of 5.70 (Table 3.2). This almost twofold difference can be attributed to the effect of relative ligand positioning, in other words, the Man ligand presentation at the 6'-position of the maltoside scaffold (cluster **1**) is superior to ligation at the 6-position (cluster **2**).

The monovalent glycocluster **35** is a relevant control compound to test the effect of a 6-ligated glucose moiety. As the RIP of **35** (4.33) is somewhat lower than the RIP of **1** (5.70), the  $\beta$ -D-Glc moiety at the 6-position of the maltose glycocluster **1** seems to have a beneficial effect on FimH affinity of the ligand for FimH (Table 3.2). This finding parallels with the known heterocluster effect.<sup>[48, 148]</sup>

**Table 3.2.** Inhibitory potencies of the maltose-based glycoclusters **1**, **2**, **35**, and **36** as determined in adhesion-inhibition assays with type 1 fimbriated *E. coli* (pPKL1162).

Cluster	IC <sub>50</sub> <sup>a</sup> [mmol]	IC <sub>50</sub> MeMan <sup>b</sup> [mmol]	RIP <sup>c</sup>	Average RIP <sup>d</sup>
6'αMan-6αMan <b>36</b>	1.98 (±0.13)	14.57 (±1.58)	7.34 (±1.28)	8.03 (±1.34)
	2.08 (±0.15)	18.12 (±1.61)	8.71 (±1.40)	
6'αMan-6βGlc <b>1</b>	2.08 (±0.03)	12.39 (±1.19)	5.96 (±0.66)	5.70 (±0.77)
	2.05 (±0.15)	11.14 (±0.97)	5.44 (±0.87)	
6'βGlc-6αMan <b>2</b>	3.74 (±0.31)	12.39 (±1.19)	3.31 (±0.59)	2.99 (±0.57)
	4.17 (±0.48)	11.14 (±0.97)	2.67 (±0.54)	
6'αMan-6NHAc <b>35</b>	3.11 (±0.34)	13.43 (±0.77)	4.32 (±0.72)	4.33 (±0.65)
	2.06 (±0.12)	8.94 (±0.67)	4.34 (±0.58)	

<sup>a</sup> IC<sub>50</sub> values are average values of duplicate or triplicate results on one plate.

<sup>b</sup> IC<sub>50</sub> (MeMan) values are average values of triplicate results on the same plate.

<sup>c</sup> RIP values are based on the inhibitory potency of MeMan tested on the same microplate IP (MeMan) ≡ 1);  $RIP(\text{glycocluster}) = IC_{50}(\text{MeMan})/IC_{50}(\text{glycocluster})$ .

<sup>d</sup> RIP mean values of two independent experiments with error propagation.

With the outcome from the biological testing of the various maltose-based glycoclusters, it was of interest to explain the differences in the RIP values. Thus, the lectin-carbohydrate interactions were studied by molecular modelling.

### 3.4 Molecular modelling

For the investigation of the detailed binding process of the maltose-based glycoclusters to the lectin FimH docking studies with the Schrödinger software were performed.<sup>i</sup> In a first step the glycoclusters **1**, **2**, **35** and **36** were subjected to a docking study using the program *Glide*.<sup>[149]</sup> The glycocluster ligands were prepared by using *Maestro*<sup>[150]</sup> and then minimized by using *LigPrep*<sup>[151]</sup> with the OPLS3e force field.

<sup>i</sup> The modelling experiments were performed in a cooperation with Ingo vom Sondern, M.Sc. from the Lindhorst group.

Since the lectin FimH can occur in two different conformations, namely the open gate conformation (PDB code 1KLF)<sup>[152]</sup> and the closed gate conformation (PDB code 1UWF)<sup>[38a]</sup>, theoretical experiments for both conformers were performed. In case of the open gate the tyrosine residues Tyr48 and Tyr137 at the entrance of the CRD are more separated from each other and interaction with unpolar or aromatic aglycons of mannoside ligands can take place. For the docking both protein conformers were prepared with the implemented *Protein Preparation Wizard*.

Next, docking was performed in an extra precision mode, which fixed the lectin in a rigid conformation whereas the ligand is flexible during the docking process (cf. Experimental section, chapter 8.4.1). The top glide scoring results were then submitted to a MM-GBSA calculation<sup>[153]</sup> (molecular mechanics energies combined with generalized born and surface area continuum solvation), which gave binding energies for the four glycoclusters (Table 3.3). These binding energies were compared, and it turned out that the results for the closed gate conformation of the lectin FimH correlated better with the experimental RIP values than with the open gate conformation. In case of the open gate conformation the monovalent cluster **35** showed the best binding ( $-72.09 \text{ kcal mol}^{-1}$ ), which was in contrary to the biological results. On the other hand, molecular modelling with the closed gate conformer of FimH showed that heterobivalent cluster **1** was the best ligand ( $-89.52 \text{ kcal mol}^{-1}$ ) and clusters **35** and **36** showed second-best binding, which was in better accordance with the biological experiments (Table 3.3). Therefore, for further refinement of the molecular modelling using IFD, only the closed gate conformation of FimH (PDB code: 1UWF) was considered.

The binding of carbohydrate ligands to the lectin FimH is a highly dynamic event.<sup>[154]</sup> Hence, for the prediction of this recognition process an induced fit docking (IFD)<sup>[155]</sup> was performed, whereas next to the ligand also the receptor protein is allowed to adapt different conformations. The IFD calculations led to IFD scores, which described various binding poses. For every glycocluster the top five binding poses were selected by the best docking score and ranked by using the implemented *Metadynamics*.<sup>[156]</sup> Here a short molecular dynamics simulation of 10 ns was performed to determine the stability of the predicted binding modes by collective variables. It was shown by Clark et al. that a sampling by metadynamics is more precise in finding the correct protein-ligand complex than ranking only by docking score.<sup>[157]</sup> In the next step the most stable protein-carbohydrate complexes of each ligand were selected and subjected to a MM-GBSA calculation to determine the binding energies of the complexes, respectively. The results for the IFD calculations are shown in Table 3.3.

**Table 3.3.** Computed results from molecular modelling studies with the synthetic ligands **1**, **2**, **35**, and **36**. The best docking scores and corresponding binding energies (MM-GBSA) using Glide or induced fit docking (IFD) are listed. IFD poses were ranked using metadynamics and the most stable complex was selected for a MM-GBSA calculation to give IFD binding energies. Lower values suggest tighter FimH binding. RIP values (higher values relating to stronger FimH binding) are shown for comparison.

Glycocluster (RIP)	Glide score		Binding energy [kcal mol <sup>-1</sup> ] <sup>a</sup>		IFD score	IFD binding energy [kcal mol <sup>-1</sup> ] <sup>a</sup>
	1KLF	1UWF	1KLF	1UWF	1UWF	1UWF
6 <sup>1</sup> αMan-6αMan <b>36</b> (8.03)	-9.930	-12.391	-70.29	-59.82	-312.26	-87.90
6 <sup>1</sup> αMan-6βGlc <b>1</b> (5.70)	-10.044	-12.481	-57.71	-89.52	-312.32	-83.60
6 <sup>1</sup> βGlc-6αMan <b>2</b> (4.33)	-8.928	-11.218	-65.95	-53.34	-313.93	-81.14
6 <sup>1</sup> αMan-6NHAc <b>35</b> (2.99)	-9.839	-10.675	-72.09	-60.47	-310.64	-79.15

<sup>a</sup> best binding poses were used for the MM-GBSA calculations.

The theoretical binding energies, computed by IFD, were in excellent correlation with the observed RIP values from inhibition-adhesion assays (Figure 3.9). The linear relationship between the binding energy and the experimental RIP value underlines that IFD is a valid method to predict carbohydrate-protein interactions and their complexes. Glycocluster **36** showed the best binding (-87.90 kcal mol<sup>-1</sup>) and also for the heterobivalent glycoclusters **1** (-83.60 kcal mol<sup>-1</sup>) and **2** (-81.14 kcal mol<sup>-1</sup>) realistic binding energies were determined. In addition, the monovalent glycocluster **35** was predicted as the weakest ligand (-79.15 kcal mol<sup>-1</sup>), which was also in accordance with the experimental RIP value. These calculations led to a ranking of the glycocluster FimH affinity of **36** > **1** > **2** > **35**.

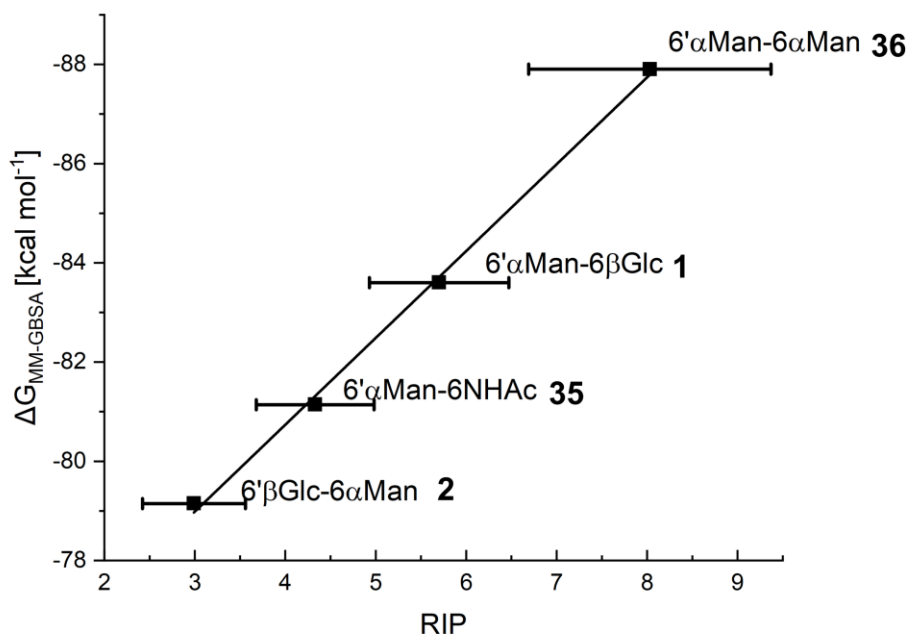


**Figure 3.9.** Comparison of computed binding energies from MM-GBSA<sup>[153]</sup> calculations with relative inhibitory potency (RIP) values from biological testing. Error bars are displayed for experimental RIP values (cf. Table 3.2). Higher RIP values and lower binding energies correspond to stronger binding. The computed results are in excellent correlation with the experimental results. Graphic adapted from literature.<sup>[112]</sup>

To figure out, what were the driving forces for the different binding energies, respective RIP values, of the maltose-based glycoclusters, the computed FimH-glycocluster complexes were inspected and the results for the clusters **1**, **2** and **36** are shown in Figure 3.10. All structures reveal that the  $\alpha$ -D-mannosyl ligand is buried in the CRD of the FimH bond by the typical hydrogen bond network with the CRD.<sup>[37b]</sup> The differences in binding affinity are assigned to secondary non-covalent interactions of the second (glycosyl) residue with the periphery of the CRD of FimH and to the ligand presentation by the maltoside scaffold (Figure 3.10, A). The binding poses of the glycoclusters could be divided into two categories. On one hand the glycocluster, where the mannosyl residue was ligated to the 6'-position (**1**, **35** and **36**), bond in the same way. The other category of glycoclusters was represented by **2**, bearing the mannosyl residue on the 6-position, respectively.

In case of glycoclusters **1**, **35** and **36** the more hydrophilic site of the maltose scaffold is oriented towards the tyrosine gate and interacts with it. The structures show also that comparing **1** and **36** the 6-positioned glycosyl residues (Man for **36** and Glc for **1**) interact with the same region of the protein surface around Asp140 (Figure 3.10, B) and the affinity for FimH differs in the hydrogen bond patterns. For the cluster **2** it is the other way round and a different binding mode with FimH is observed (Figure 3.10, B). The maltoside scaffold is orientated

towards the opposite direction, which has as consequence that the 6'-Glc residue is interacting with another region resulting in a lower affinity for FimH.

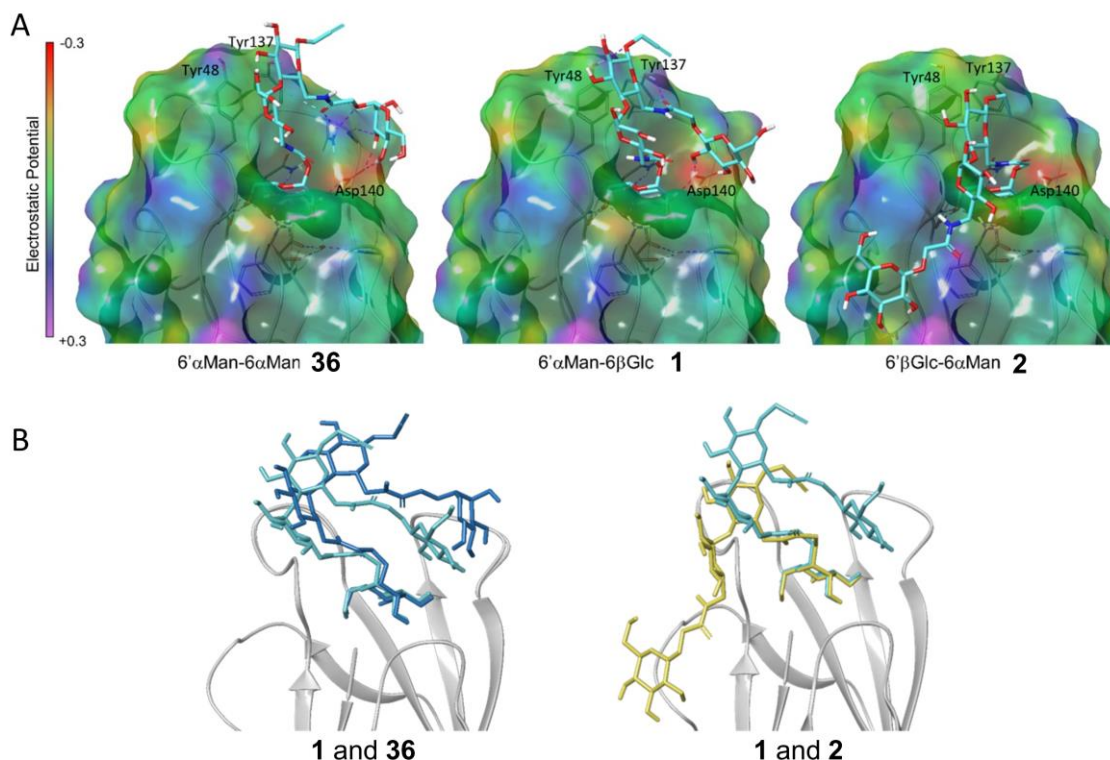


**Figure 3.10.** Connolly surface representations of selected FimH-glycocluster complexes as derived from induced fit docking (IFD) using the closed gate conformation of FimH (pdb: 1UWF).<sup>[38a]</sup> The maltose-based glycoclusters **1**, **2**, and **36** are depicted as stick models. Protein coloring represents the electrostatic potential of the surface (positive charges in purple, neutral in green, negative charges in red, cf. depicted color bar). Hydrogen bonds are indicated as dashed lines. Graphics adapted from literature.<sup>[112]</sup>

Following, the explicit hydrogen bond patterns of the glycoclusters with FimH were inspected (Figure 3.11). For the homobivalent glycocluster **36**, the 6-conjugated mannose moiety and the amide bond form additional hydrogen bonds to Asn138, Ser139, and Asp140 in complex with FimH. This interaction pattern looks similar for the heterobivalent glycocluster **1**, having a glucose moiety ligated at the 6-position of the maltoside scaffold (hydrogen bonds to Tyr137 and Asn140). Only the monovalent glycocluster **35**, which binds like glycoclusters **1** and **36**, is lacking in secondary interactions with Asp140 due to the missing carbohydrate at the 6-position. On the other hand, the heterobivalent glycocluster **2**, with the mannosyl ligand ligated to the 6-position, forms hydrogen bonds between the Glc residue and Asp100, which results in a lower affinity.

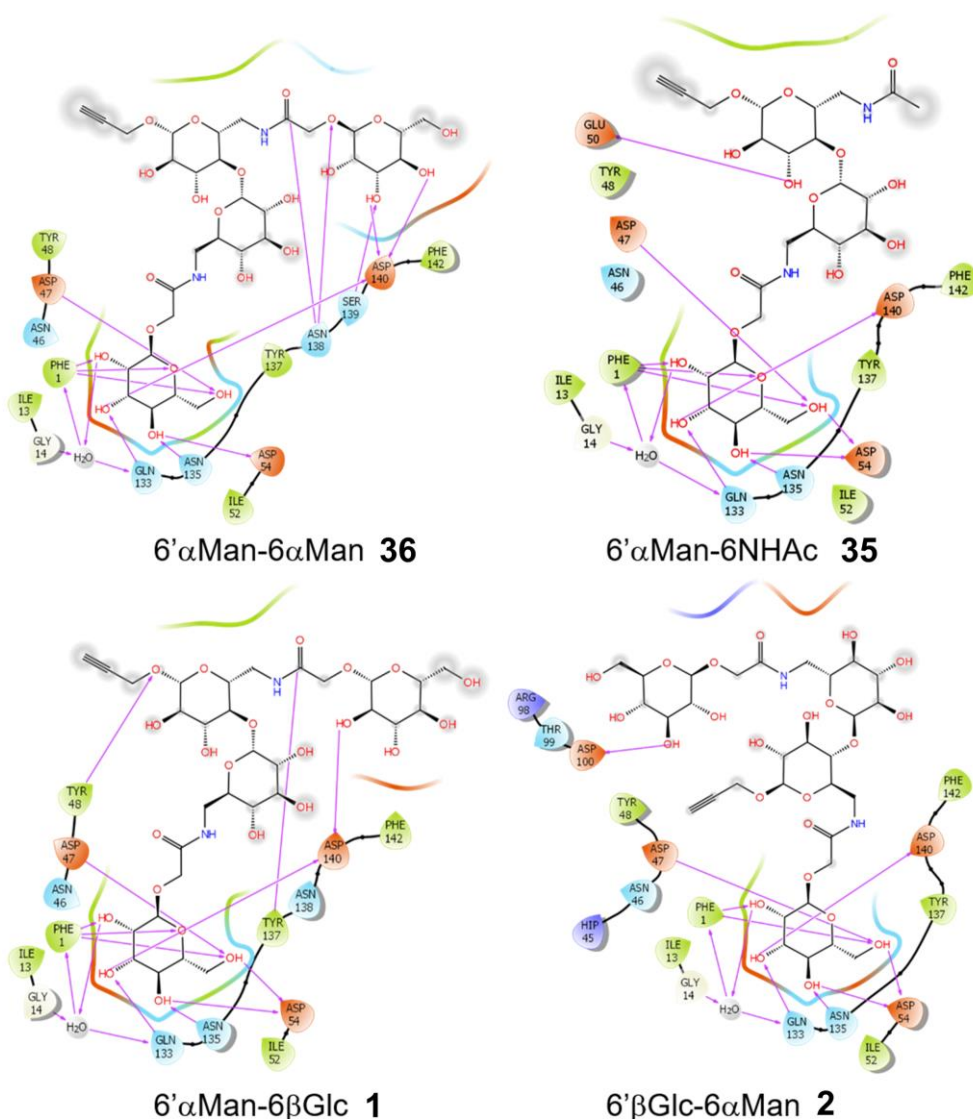


**Figure 3.11.** Two-dimensional representation of the most stable ligand-protein complexes from IFD for glycoclusters **1**, **2**, **35**, and **36**. The hydrogen bond network is shown in magenta. FimH amino acids are represented teardrop shaped. The mannose binding pocket as multi-colored line (interruption indicates solvent exposure). Grey shades indicated solvent exposure. Graphic adapted from literature.<sup>[112]</sup>

The molecular modelling and the predicted IFD binding energies supported the results from the biological experiments. It revealed the importance of the spatial Man ligand presentation by a maltoside scaffold and demonstrated that secondary interactions with additional glycoside moieties lead to higher lectin affinity.

### 3.5 Conclusion

This subproject was dedicated to the synthesis and testing of a series of novel maltose-based glycoclusters. A facile synthetic pathway led to a multifunctional maltoside scaffold, which

could further be functionalized by orthogonal ligation chemistry. The achieved heterobivalent Man/Glc glycoclusters (Figure 3.12) were employed to systematically explore the influence of the spatial presentation of a Man ligand versus a Glc moiety in a bottom-up approach. Biological testing was performed using an adhesion-inhibition assay with type 1-fimbriated *E. coli* and RIP values were determined for all synthetic glycoclusters. The measured effects were rationalized by molecular modelling of the FimH-glycocluster complexes allowing to estimate the importance of secondary interactions exerted by the Glc moiety.

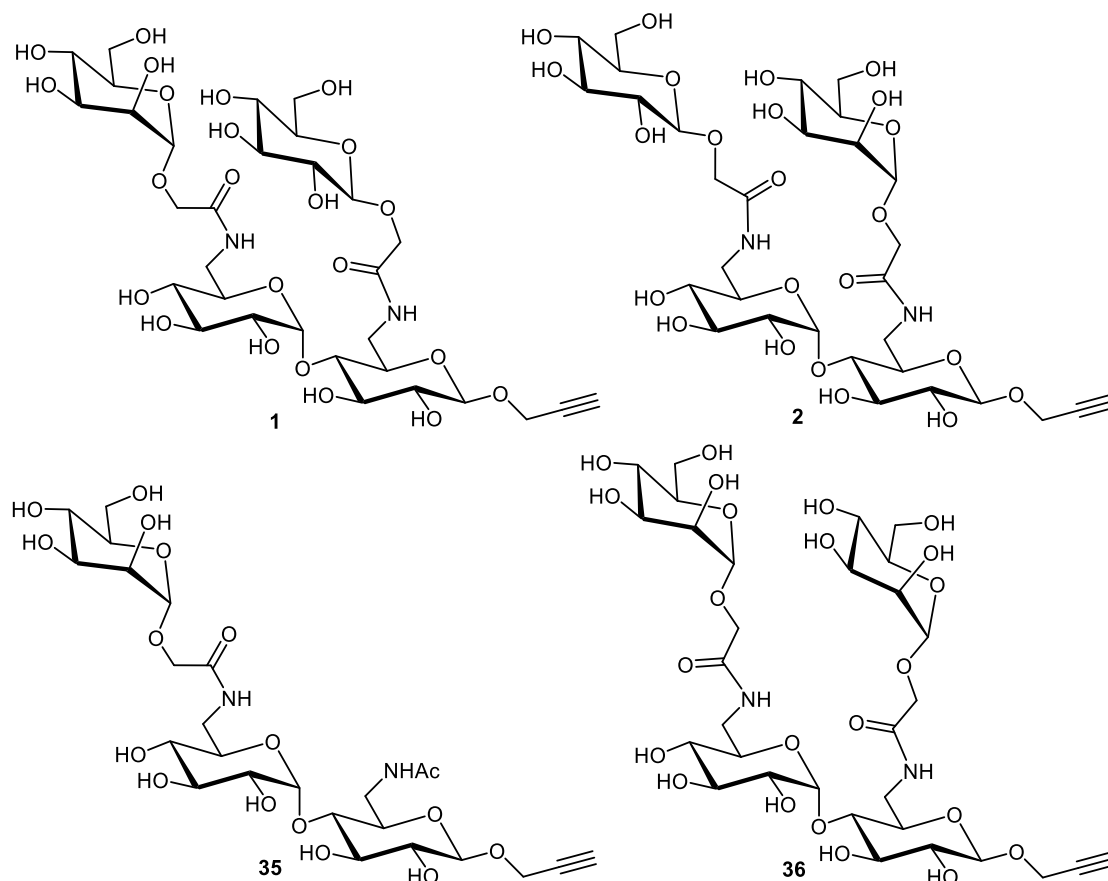


Figure 3.12. Overview of the synthesized maltose-based glycoclusters.

The testing results clearly showed that the presentation of the Man ligand at the 6'-position of the maltoside scaffold leads to better binding to the lectin FimH (**1** versus **2**). Furthermore, an additional sugar unit at the 6-position of the scaffold (Glc or Man) increases the affinity of the respective glycocluster. If this carbohydrate moiety is missing, the inhibitory potency decreases (**1** and **36** versus **35**). The results suggest that synthetic carbohydrate scaffolds may indeed mimic some of the complexity of natural glycoconjugates in order to vary glycoligand presentation in 3D space. Other than in a top-down approach exploring carbohydrate recognition with glycosylated cells, for example, carbohydrate scaffolds allow the investigation of specific principles of carbohydrate recognition, isolated from the overwhelming complexity of a more natural environment.

## 4 Conformational glycoswitches: Synthesis of 2,4-diamino xylosides

In addition to the regioisomeric ligand presentation by carbohydrate scaffolds, the spatial orientation of carbohydrate ligands can also be controlled by conformational switching. In biological processes conformational changes play a significant role as the function of macromolecules often is related to small conformationally switchable units. Conformational changes can be induced by multiple environmental factors such as ion concentration, pH value, temperature, phosphorylation, light or binding of a ligand. Often conformational changes in biological systems are the first step of cascade reactions such as in signalling. Many examples exist for conformational changes in nature.<sup>[158]</sup> While the induced conformational change by binding of insulin to its receptors is an example for peptide switches,<sup>[159]</sup> the conformation of the oligosaccharide heparin is highly dependent on the sulfation of the molecule.<sup>[61a, 160]</sup> It is known that the function of the glycocalyx is dependent on accessibility, multivalency and density of carbohydrate constituents. But also conformations of glycans have an effect on carbohydrate recognition processes.<sup>[5b, 42a]</sup> It has been demonstrated by Normark and co-workers that the orientation of glycosphingolipids plays an essential role in bacterial adhesion and the spatial orientation of glycoligands is a factor in the signaling between normal and malignant cell development.<sup>[95b]</sup>

To control the orientation of carbohydrate ligands in space, in this account monosaccharide scaffolds were utilized as conformational switchable units. Compared to molecular switches like azobenzene glycosides, the switching of monosaccharide conformation can be triggered by other stimuli, such as metal ions or pH value (cf. chapter 1.5). By synthetic modifications  $\beta$ -D-xylose the energy barrier between the chair conformers can be reduced and the pentose can be turned into a conformational switch. Thus, Yuasa and Hashimoto demonstrated that 2,4-diamino xylosides can suite as molecular switches by metal complexation (cf. chapter 1.5).<sup>[90]</sup>

In order to further study and utilize the conformational behavior of xylosides, for example to control spatial ligand presentation, 2,4-diamino  $\beta$ -D-xylosides were targeted as molecular switches (Figure 4.1). En route to conformational switches, xyloside **51** was designed as a key molecule. The amino functions at the 2- and 4-position serve as chelating functional groups, allowing to trigger a conformational interconversion by complexation of metal ions, as described by Yuasa.<sup>[90, 92a, 93]</sup> In addition, the 1- and 3-positions are modified with aryl moieties for two reasons. On the one hand, it was shown that aromatic  $\pi$ - $\pi$  interactions support the ring flip by stabilizing the  ${}^1C_4$  conformation (cf. chapter 1.5). On the other hand, the direct addition

of phenyl moieties transfers the conformational motion, due to their rigidity, to the mannosyl ligands in order to gain maximal control over spatial ligand presentation.

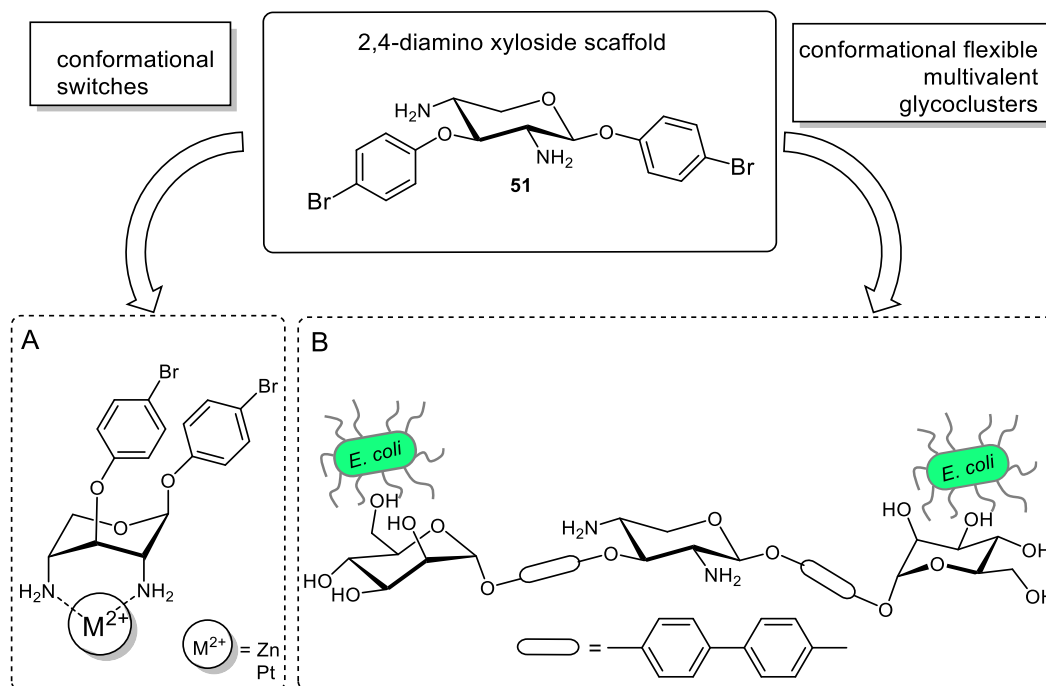


**Figure 4.1.** The synthesis of the 2,4-diamino xyloside **51** is a key intermediate for the investigation of conformational equilibria and switching, respectively. On the one hand, **51** represents a system where the conformational switching can be stimulated by metal cations (A). On the other hand, multivalent glycoclusters can be synthesized derived from **51** and their distance can be influenced depending on the chair conformation of the xyloside. This in turn can influence mannose-specific bacterial binding (B).

It was of interest to investigate designed diamino xyloside **51** for three reasons:

- The synthesis of diamino xylosides is a challenging task. A new convincing synthetic route was sought allowing for high precision regio- and stereoselectivity.
- It is of interest to study the conformational behavior of **51** and its ability as a molecular switch by the addition of metal ions.
- Finally, **51** serves as a scaffold for the synthesis of bivalent glycoclusters to study the effect of spatial ligand presentation using conformational switchable xylosides (chapter 6).

For the synthesis of aminosugar derivatives, such as **51**, various methods have been described over the years and often natural aminosugars (e.g., glucosamine) are used as starting material. Nevertheless, when amino moieties have to be introduced at other ring positions than the 2-position, appropriate reaction pathways have to be employed. Thus,  $S_N2$  substitution often is a suitable method. In substitution reactions, azides, phthalimides or sulfonamides have frequently been employed to replace an activated OH-group, leading to an inversion of configuration at the respective stereocenter.<sup>[161]</sup> However, also other

functionalization reactions for the introduction of amino groups like the Mitsunobu reaction or the addition to the glycal double bond have been implemented into the aminosugar chemistry.

For the synthesis of 2,4-diamino xylosides a previous method, published by Yuasa and Hashimoto, started from D-xylose (**52**).<sup>[90]</sup> First, D-xylose was converted in 5 steps into the corresponding methyl 4-mesyl- $\beta$ -D-xyloside **53**, which formed the precursor for the synthesis of the Černý epoxide **54**. Then, two azido functional groups were introduced via a tandem ring opening of **54** with sodium azide to give the 2,4-diazido xyloside **55**. At this point a disadvantage of the synthesis becomes apparent as regioisomeric diazides are obtained as side products in this reaction. Furthermore, for the modification of the aglycone in order to achieve other xylosides (**57**) than methyl xylosides (cf. Figure 1.16), further steps are required involving acetolysis of **55** and conversion into suitable xylosyl donors **56** (trichloroacetimidate or chloride). In glycosylation reactions the desired xylosides are obtained as anomeric mixtures because of the lack of anomeric control of the 2-azido group of **56** (Figure 4.2).<sup>[90, 91b, 92b]</sup>

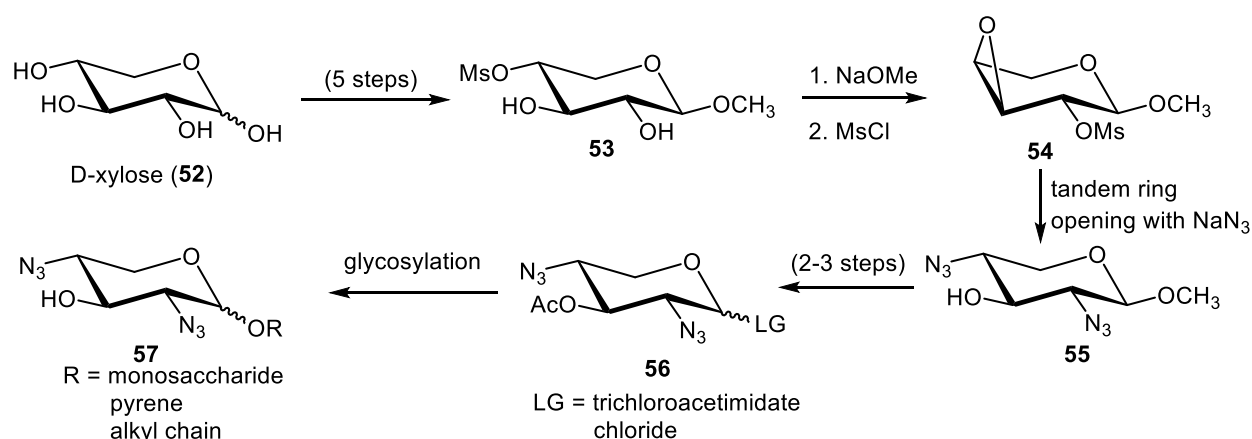


**Figure 4.2.** Literature-known synthetic route to achieve masked 2,4-diamino xylosides **57** starting from D-xylose (**52**).<sup>[90]</sup> The Černý epoxide **54** is reached in 7 steps and then a tandem ring opening reaction delivers the diazide **55**. In order to exchange the aglycone moiety another 3-4 steps are required where stereoselectivity is not ensured. MS: mesyl, LG: leaving group.

In order to overcome the weaknesses of this established synthesis of 2,4-diamino xylosides, a new synthetic pathway was envisaged. Thus, first it was tried to optimize the stereospecificity for the glycosylation reaction and reduce the number of reaction steps. Accordingly, the synthetic route via Černý epoxides was carried out with thioxylosides.

The essence of this chapter was published:<sup>[162]</sup>

S. O. Jaeschke, T. K. Lindhorst, "Versatile Synthesis of Diaminoxylosides via Iodosulfonamidation of Xylal Derivatives", *Eur. J. Org. Chem.* **2021**, 2021, 6312-6318. (DOI: 10.1002/ejoc.202100792).

#### 4.1 Synthesis of 2,4-diamino xylosides via thioglycosides

For the synthesis of 2,4-diamino xylosides a synthetic strategy was envisaged which was based on Černý epoxides, but for the modification of the anomeric center another approach was implemented. While in the previous work of Yuasa and Hashimoto the conversion of the anomeric position to a glycosyl donor and respective glycosylation took place at a late stage of the synthetic sequence, in this account a thioglycoside was utilized, which was prepared at the beginning of the synthetic pathway. Thioglycosides serve as potent glycosyl donors in the glycosylation of unreactive glycosyl acceptors. Furthermore, thioglycosides can be introduced early in the synthesis sequence, since they are stable as anomeric protecting groups under several reaction conditions.<sup>[163]</sup>

Once the thioxyloside was synthesized, the Černý epoxide **60** was prepared which is the key intermediate of this synthetic approach (Figure 4.3). Accordingly, in a tandem ring opening reaction with sodium azide the 2,4-diazido thioxyloside **61** was targeted, which serves as a xylosyl donor for the challenging stereoselective  $\beta$ -glycosylation reaction of 4-bromophenol. Since also in this account the 2-position is bearing an azido masked amino function, no neighbouring group effect can assist in a stereoselective glycosylation. For the  $\beta$ -selective glycosylation of 2-azido glycosides it is known that stereoselectivity can be increased by the use of coordinating solvents (e.g., MeCN) or ionic liquids. Furthermore, the 3-position had to be functionalized by *O*-arylation with a 4-bromophenyl residue (Figure 4.3). Since the synthesis of the 2,4-diamino xylosides is highly dependent on the reactivity of intermediate **60**, the synthetic work was first focused on the synthesis of this Černý epoxide.

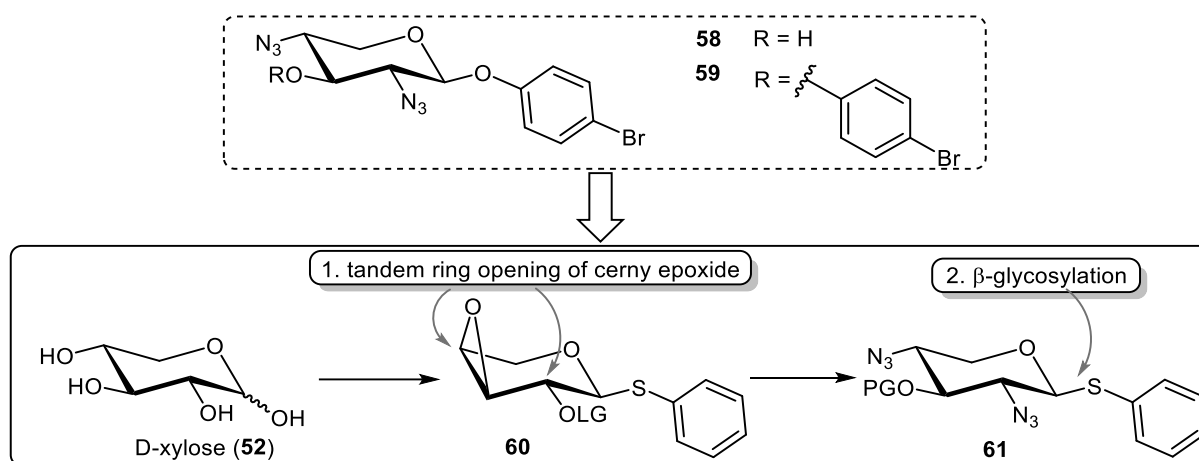
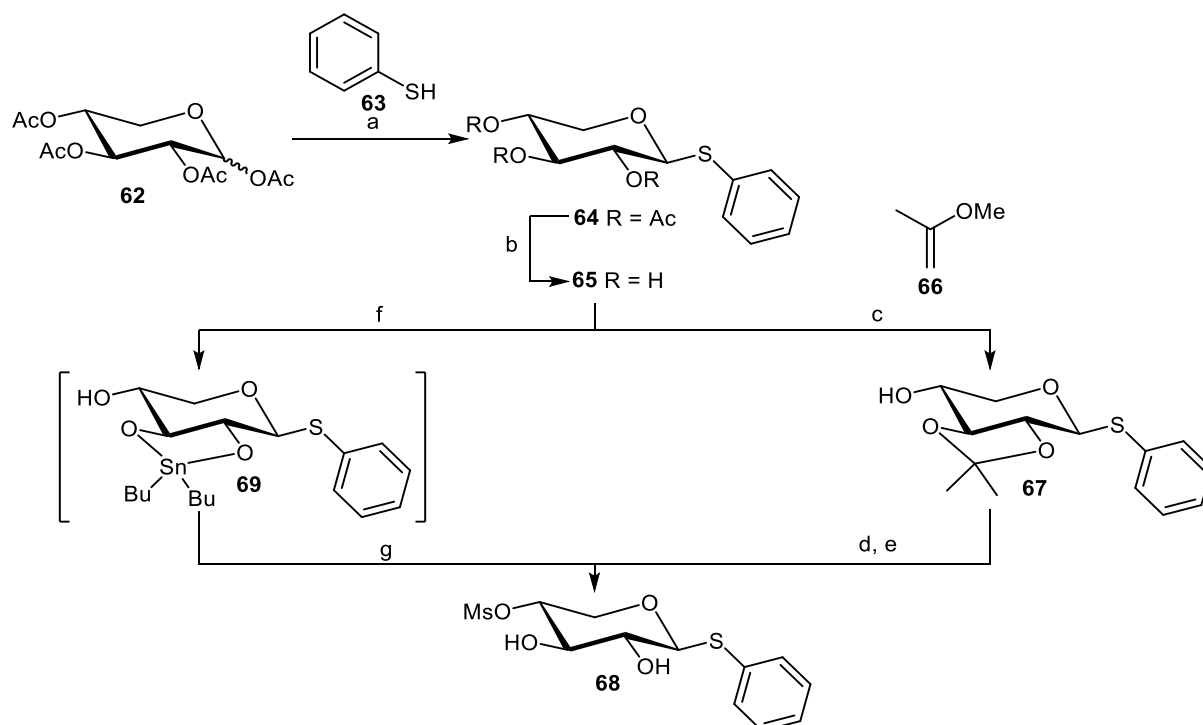


**Figure 4.3.** Synthesis of azide masked 2,4-diamino xylosides **58** and **59** by a nucleophilic tandem ring opening of Černý epoxide **60**. Thioxyloside **61** serves as a glycosyl donor for further glycosylation of an aromatic aglycone. The synthetic pathway starts from the monosaccharide D-xylose (**52**) LG: leaving group; PG: protecting group.

The synthesis of Černý epoxides was started from known peracetylated D-xylose (**62**) and in a  $\text{BF}_3 \cdot \text{Et}_2\text{O}$ -promoted glycosylation reaction with thiophenol (**63**) the desired thioglycoside **64** was obtained after column chromatography in a yield of 70 % (Scheme 4.1).<sup>[164]</sup> Cleaving the acetyl protecting groups under Zemplén transesterification conditions gave the unprotected thioglycoside **65** in high yield.<sup>[165]</sup> For the formation of Černý epoxides it is necessary to regioselectively introduce a leaving group at the 4-position. First a 2,3-isopropylidene protecting group was installed, and the 4-OH group was converted into a mesylate. Accordingly, **65** was treated with 2-methoxypropene (**66**) in the presence of a catalytical amount of camphor sulfonic acid to give the corresponding acetal **67** in a yield of 57 %.<sup>[166]</sup> Then, in a two-step reaction, first **67** was treated with  $\text{MsCl}$  in pyridine and in a second step the acetal protecting group was cleaved under acidic conditions with acetic acid, yielding the targeted mesylated thioxyloside **68** in 72 % over 2 steps (Scheme 4.1).

To increase the yield of **68** and to decrease the number of reaction steps thioglycoside **68** was synthesized in a different approach. Thus, thioglycoside **65** was treated with dibutyltin oxide ( $\text{Bu}_2\text{SnO}$ ) to form the stannylidene intermediate **69**, which was not further purified and subsequently treated with  $\text{MsCl}$  in  $\text{CH}_2\text{Cl}_2$ . An advantage of this reaction is that during the mesylation  $\text{HCl}$  is produced *in situ*, which leads to deprotection of the tin acetal. The targeted thioxyloside **68** was obtained after two steps in a yield of 80 % (Scheme 4.1).

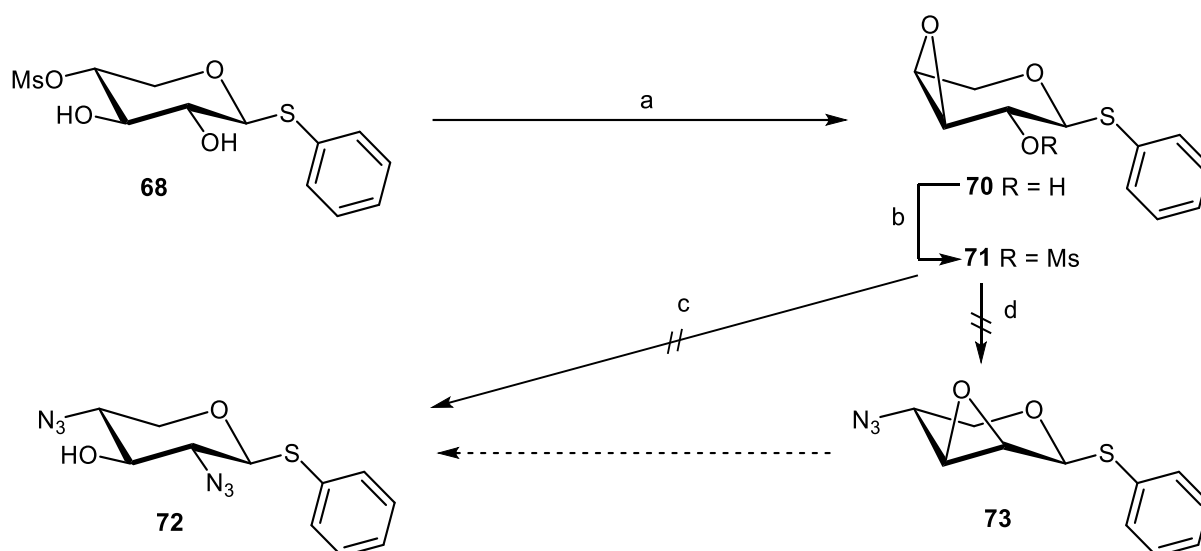


**Scheme 4.1.** Synthesis of thioxyloside **68** starting from peracetylated xylose **62**. (a)  $\text{BF}_3 \cdot \text{Et}_2\text{O}$ , dry  $\text{CH}_2\text{Cl}_2$ ,  $0^\circ\text{C} \rightarrow \text{rt}$ , 16 h, 70 %; (b)  $\text{NaOMe}$ ,  $\text{MeOH}$ ,  $\text{rt}$ , 1 h, 96 %; (c) CSA, dry  $\text{DMF}$ ,  $\text{rt}$ , 4 h, 57 %; (d)  $\text{MsCl}$ , pyridine,  $\text{rt}$ , 16 h; (e)  $\text{AcOH}$ ,  $60^\circ\text{C}$ , 4 h, 72 % (over two steps); (f)  $\text{Bu}_2\text{SnO}$ , dioxane,  $100^\circ\text{C}$ , 3 h; (g)  $\text{MsCl}$ , dry  $\text{CH}_2\text{Cl}_2$ ,  $0^\circ\text{C} \rightarrow \text{rt}$ , 16 h, 80 % (over two steps).

Next, thioxyloside **68** was converted into the corresponding Černý epoxide **70**.<sup>[167]</sup> In general, anhydro sugars serve as important intermediates for the derivatization of carbohydrates and especially small oxirane rings (intramolecular epoxides) show a high reactivity. The reactivity of an epoxide is also highly dependent on the position of the anhydro ring, the general steric arrangement and the conformation of the substrate.<sup>[168]</sup> By nucleophilic opening of carbohydrate epoxides functional groups like fluorides,<sup>[169]</sup> amines<sup>[170]</sup> or alkoxides<sup>[171]</sup> can be introduced in a regio- and stereospecific way. Also for the synthesis of 4-azido-4-deoxy xylosides it is known that ring opening reactions of 3,4-epoxids are promising.<sup>[172]</sup>

To achieve the diazide **72**, by epoxide opening, the 3,4-L-arabinosyl epoxide **70** was required. Thus, **68** was treated with sodium methoxide in methanol<sup>[167]</sup> and by an intramolecular nucleophilic attack, the 3,4-L-arabinosyl epoxide **70** was formed and isolated in an excellent yield of 94 % (Scheme 4.2). To force a tandem epoxide opening to introduce two azido moieties, it was necessary to convert the 2-OH group of **70** into a sulfonate leaving group. Thus, **70** was treated with MsCl in the presence of pyridine and the corresponding mesylate **71** was obtained in a yield of 89 %. However, it was not stable to moisture and cannot be stored in the freezer since degradation occurred. Nevertheless, with derivative **71** in hand, two different synthetic strategies for its derivatization were pursued. In the first approach the regioselective tandem epoxide ring opening of the Černý epoxide **71** by the nucleophilic attack of an azide was applied.<sup>[172]</sup> The nucleophilic attack of the azide at the 4-position results in an equatorial hydroxide intermediate at the 3-position. In a following intramolecular S<sub>N</sub>2 reaction the 2-mesylate can be replaced and the corresponding 2,3-anhydro lyxoside **73** is formed, which can be opened regioselectively by a second azide leading to the 2,4-diazido xyloside **72** (Scheme 4.2).<sup>[172]</sup> According to a procedure of Hashimoto and co-workers **71** was treated with sodium azide in toluene and water at 140 °C, but only decomposition of the starting material was observed. Also, reactions at lower temperatures did not show a conversion to the targeted diazide **72**.

In order to open the 3,4-epoxide **71** regioselectively with an azide moiety, it was tried to avoid the cascade reaction of **71** to **72**. It is known from the work of Voelter and co-workers that epoxides like **71** can be opened under mild conditions by the use of Lewis acids and the displacement of the C-2-leaving group and the formation of **72** can be avoided.<sup>[173]</sup> Accordingly, following a procedure of Banaszek et al,<sup>[174]</sup> **71** was treated with trimethylsilyl azide (TMSN<sub>3</sub>) and BF<sub>3</sub>·Et<sub>2</sub>O, but as shown before, again the formation of the desired product **73** was not accomplished and decomposition of **71** was obtained (Scheme 4.2).



**Scheme 4.2.** Synthesis of thioxyloside **72** starting from thioxyloside **68**. (a) NaOMe, MeOH, 0 °C, 2 h, 94 %; (b) MsCl, pyridine, dry CH<sub>2</sub>Cl<sub>2</sub>, rt, 1 h, 89 %; (c) NaN<sub>3</sub>, TBAB, toluene/H<sub>2</sub>O, 140 °C, 16 h; (d) TMSN<sub>3</sub>, BF<sub>3</sub>·Et<sub>2</sub>O, rt, 2 h, CH<sub>2</sub>Cl<sub>2</sub>.

In the tandem ring opening of epoxide **71** in order to yield **72**, various side reactions can occur (Figure 4.4). While the nucleophilic epoxide opening of the 3,4-epoxide **74** to the 2,3-epoxide intermediate **75** by an azide is regioselective, the reaction of **75** with sodium azide can give the 2- or 3-azido-functionalized regioisomers **76** and **77**, respectively.<sup>[175]</sup> In the presence of nucleophiles, the C-2 leaving group can be substituted in a classical S<sub>N</sub>2 reaction, yielding thioxyloside **78** with an inverted C-2 stereocenter.

Finally, in case of 2-sulfonated thioglycosides a migration of the anomeric thio group can take place. By an intramolecular nucleophilic rearrangement of the activated 2-position the episulfonium ion **79** is formed, which is in equilibrium with the lyxosyl carbenium ion **79b**. The attack of an external nucleophile gives an anomeric mixture of lyxoside **80**.<sup>[176]</sup> This sulfanyl migration reaction can take place under various conditions. Nevertheless, high temperatures and strong nucleophiles like azides, are supporting the rearrangement as described by Pale<sup>[177]</sup> and Liptak.<sup>[178]</sup> In addition to the activated 2-position also the ring strain of the 3,4-oxirane ring of the pyranose **74** can lead to the 1,2-sulfanyl migration. However, this side reaction also explains the instability of thioarabinoside **71** and its sensitivity to moisture.

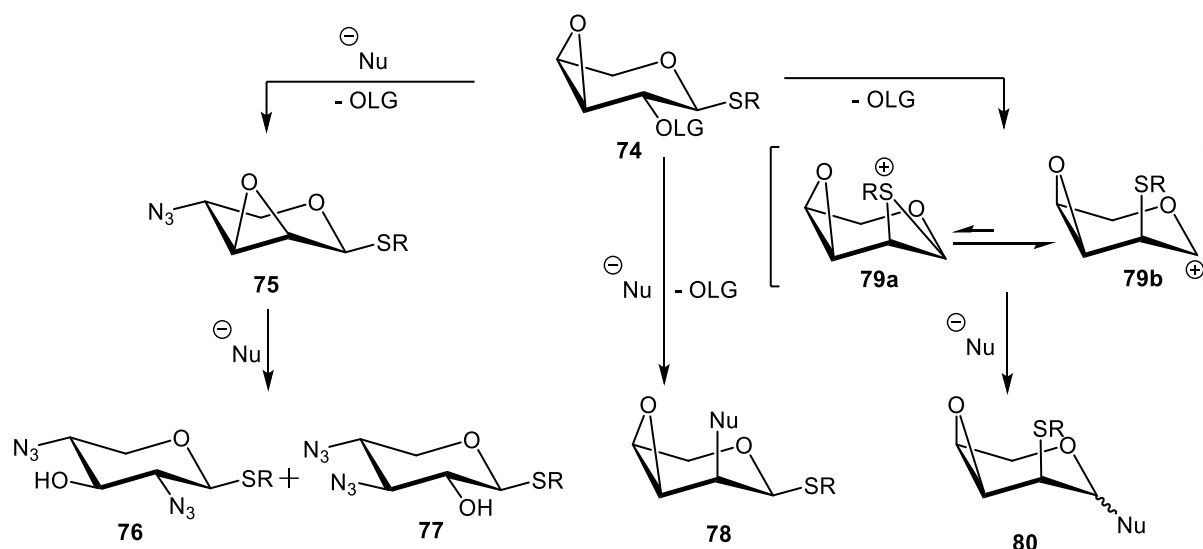


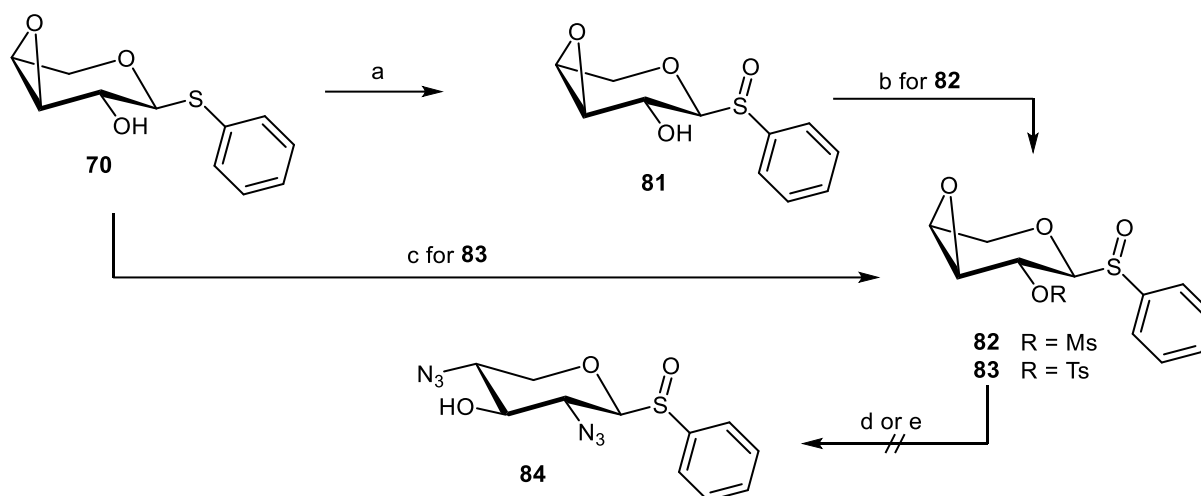
**Figure 4.4.** In addition to the unregiospecific opening of the 3,4-epoxide **74** also side reactions can occur. An unwanted substitution of the 2-positioned leaving group can give the axial substitution product **78**. Thioglycosides with a leaving group at the 2-position can undergo a sulfanyl migration via a cyclic intermediate **79a**, which can be opened by a nucleophile to lead **80**. LG: leaving group.

Since an intramolecular sulfanyl migration had to be avoided, the synthetic strategy had to be altered. Next to thioglycosides also glycosyl sulfoxides are potent glycosyl donors for the glycosylation of aromatic glycosyl acceptors. They are activated by triflic anhydride at low temperatures in the presence of a nucleophilic acceptor.<sup>[179]</sup> In addition, an intramolecular migration of a sulfoxide moiety should not occur.<sup>[180]</sup> In the following, the epoxy-thioglycosides were converted into the respective sulfoxides.

The synthesis of glycosyl sulfoxides started from the thio arabinoside **70** with an oxidation using *meta*-chloroperbenzoic acid (*m*CPBA). According to a procedure of Carpintero et al.,<sup>[181]</sup> **70** was treated with 1.0 equ. *m*CPBA in  $\text{CH}_2\text{Cl}_2$  and the corresponding sulfoxide **81** was obtained in a fair yield of 53 %. Next, **81** was treated with MsCl in the presence of pyridine and the respective mesylate **82** was isolated in a yield of 76 %. The sulfoxide with a 2-tosyl group **83** was synthesized in a one pot procedure starting from **70**. Thus, in accordance to a procedure of Sauv e and co-workers,<sup>[182]</sup> **70** was treated with TsCl in the presence of potassium iodide and silver oxide. After full conversion of the starting material, *m*CPBA was added and the tosylated sulfoxide **83** was obtained in a yield of 48 % over two steps. For all sulfoxides only the formation of a single stereoisomer was observed. However, the configuration of the sulfur stereocenter (R or S) could not be assigned.<sup>[183]</sup>

With the two sulfoxides **82** and **83** in hand, the opening of the epoxide was attempted. In a first experiment, **82** was treated with  $\text{NaN}_3$  (9.0 equ.) at 140 °C. Here, decomposition of the starting material was observed and attempts to perform the reaction at lower temperatures (80 °C,

60 °C) showed the same result. Next, it was tried to open the epoxide via activation with a Lewis acid. Thus, **82** was treated with  $\text{TMSN}_3$  and  $\text{BF}_3 \cdot \text{Et}_2\text{O}$ , but also this approach was not successful as the targeted diazido xylosyl sulfoxide **84** could not be obtained (Scheme 4.3).



**Scheme 4.3.** Synthesis of xylosyl sulfoxides **82** and **83** as precursors for the synthesis of 2,4-diazido xylosyl sulfoxide **84**. (a) *m*CPBA,  $\text{CH}_2\text{Cl}_2$ ,  $-78\text{ }^\circ\text{C}$ , 30 min, 53 %; (b) MsCl, pyridine, dry  $\text{CH}_2\text{Cl}_2$ ,  $0\text{ }^\circ\text{C} \rightarrow \text{rt}$ , 16 h, 76 %; (c) 1. TsCl, KI,  $\text{Ag}_2\text{O}$ ,  $\text{CH}_2\text{Cl}_2$ ,  $0\text{ }^\circ\text{C} \rightarrow \text{rt}$ , 16 h, 2. *m*CPBA,  $\text{CH}_2\text{Cl}_2$ ,  $-40\text{ }^\circ\text{C}$ , 1 h, 48 % (over two steps); (d)  $\text{NaN}_3$ , TBAB, toluene/ $\text{H}_2\text{O}$ ,  $140\text{ }^\circ\text{C}$ , 16 h; (e)  $\text{TMSN}_3$ ,  $\text{BF}_3 \cdot \text{Et}_2\text{O}$ ,  $\text{CH}_2\text{Cl}_2$ , 2 h.

After these unsuccessful attempts of the nucleophilic opening of different Černý epoxides, it was concluded that for the regio- and stereoselective synthesis of 2,4-diamino xylosides another approach was required.

## 4.2 Starting from L-arabinose – the glycal approach

The next synthetic pathway en route to 2,4-diamino xylosides, no longer started from D-xylose (**52**), but from its C-4 epimer L-arabinose (**85**) (Figure 4.5).

For the introduction of the two amino functionalities at the 2- and 4- position different reaction methods were utilized. The introduction of the 2-amino moiety was planned by an azidonitration reaction (1. step), which is a radical addition of an azido radical to the double bond of a glycal. Hence, L-arabinal **86** was the key intermediate in this synthetic route. Glycals, 1,2-unsaturated sugar derivatives, serve as powerful building blocks in organic synthesis,<sup>[184]</sup> owing to the ease with which they can be transformed into many other derivatives (e.g. C-glycosides,<sup>[185]</sup> epoxides<sup>[186]</sup> or for the electrophilic and radical additions to the double bond). Once the arabinal **86** is functionalized with the 2-azido moiety it had to be converted into the corresponding arabinosyl donor **87**, which will be further used for the glycosylation of 4-bromophenol (2. step). As described for the glycosylation with thioglycosides, also this

reaction had to be optimized in order to yield high  $\beta$ -stereospecificity. Finally, for the introduction of the 4-amino functionality, an  $S_N2$  reaction of the 4-OH group was employed, which gave the respective 2,4-diamino D-xyloside (Figure 4.5).

Since the synthetic route of 2,4-diamino xylosides starting from L-arabinose is dependent on the azidonitration, it was started with the synthesis of L-arabinal **86**.

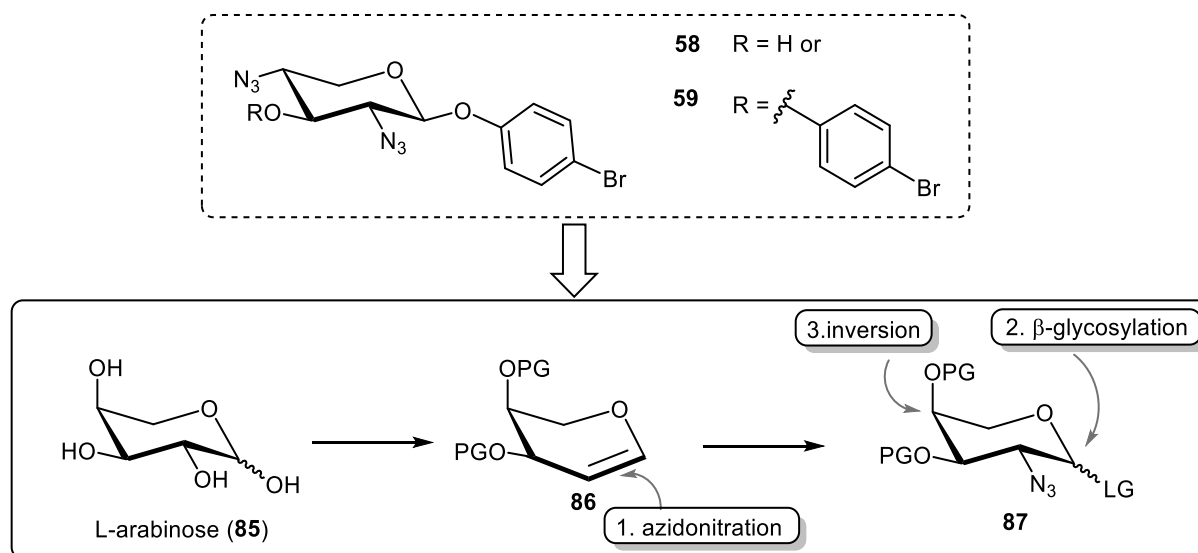
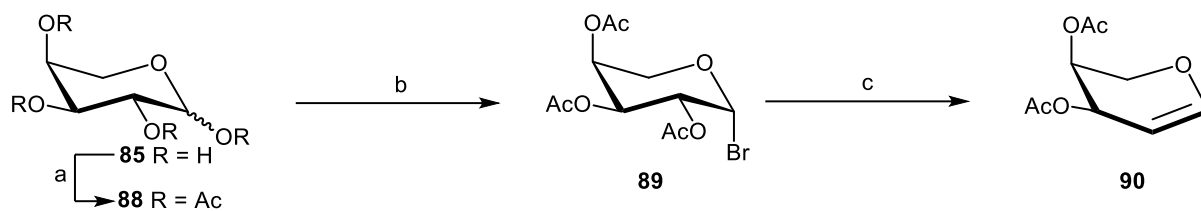


**Figure 4.5.** Synthesis of azide masked 2,4-diamino xylosides **58/59** with the azidonitration as the key reaction. Thus, L-arabinal (**86**) is synthesized from L-arabinose (**85**). After azidonitration the anomeric position of **87** is converted into a glycosyl donor for further glycosylation of an aromatic aglycone. An inversion of the 4-position yields D-xyloside derivative **58**. LG: leaving group; PG: protecting group.

The synthesis of glycal **86** was started from the pentose L-arabinose (**85**) and first of all, the hydroxyl groups were acetylated. According to a procedure of Gehrke et al., **85** was acetylated with acetic anhydride in pyridine, which gave the literature-known peracetate **88**<sup>[187]</sup> in a yield of 80 %. By treatment of **88** with hydrogen bromide (HBr) in acetic acid the arabinosyl bromide **89** was obtained, which was subjected to the glycal synthesis step without any further purification (Scheme 4.4).

The synthesis of glycals from their corresponding glycosyl bromides is a reductive elimination reaction and has been introduced by Fischer and Zach in 1913.<sup>[188]</sup> The fact that zinc can donate two electrons to the glycosyl halide, enables the formation of an unsaturated carbohydrate derivative. Over the years, the synthesis of glycals has been investigated extensively.<sup>[189]</sup> According to a procedure of Zhang and co-workers,<sup>[190]</sup> the bromide **89** was treated with zinc dust in an ammonium chloride-buffered system at 40 °C. The corresponding arabinal **90**<sup>[187]</sup> was isolated after column chromatography in a yield of 33 % over two steps (Scheme 4.4).



**Scheme 4.4.** Synthesis of arabinal **90** starting from peracetylated L-arabinose (**85**). (a)  $\text{Ac}_2\text{O}$ , pyridine, rt, 4 h, 80 %; (b) HBr, AcOH,  $\text{CH}_2\text{Cl}_2$ , 0 °C, 4 h; (c) Zn,  $\text{NH}_4\text{Cl}$ , MeCN, 40 °C, 3.5 h, 33 % (over 2 steps).

With the arabinal **90** in hand, the introduction of the equatorial 2-amino function became the focus of the next step. A well-known method to synthesize aminosugars from glycols is the azidonitration procedure. This reaction has been introduced by Lemieux and Ratcliffe and describes the radical addition of an azide to the glycol double bond and proceeds regioselectivity to yield anti-Markovnikov products.<sup>[191]</sup> The reaction takes place in the presence of ceric(IV) ammonium nitrate (CAN). In a first single electron transfer step, an azide anion is oxidized, and the corresponding azido radical can attack glycol **91**. By a second single electron transfer, **91a** is transferred into a carbocation, which can react with nucleophiles e.g., nitrate to an anomeric mixture **91b**. Since the radical addition to the double bond is not stereoselective, an axial derivative can be formed in addition to an equatorial azide at the C-2. It must be mentioned that the substituents and their configuration at the C-3 and C-4 position have an influence on the stereoselectivity. While axial C-4 substituents (as in galactal) favor the formation of an equatorial azido function, equatorial substituents (as in glucal) can increase the amount of the axial side product (Figure 4.6).<sup>[192]</sup>

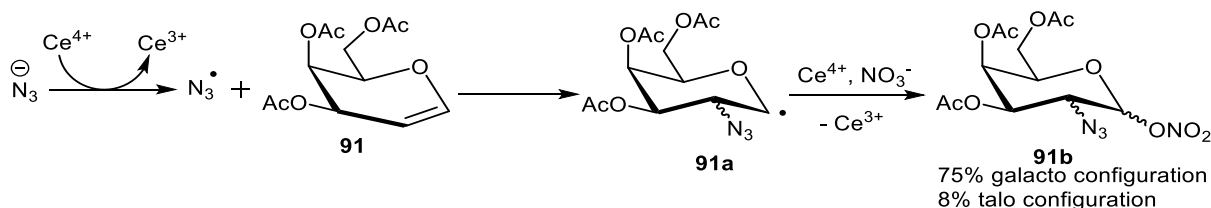
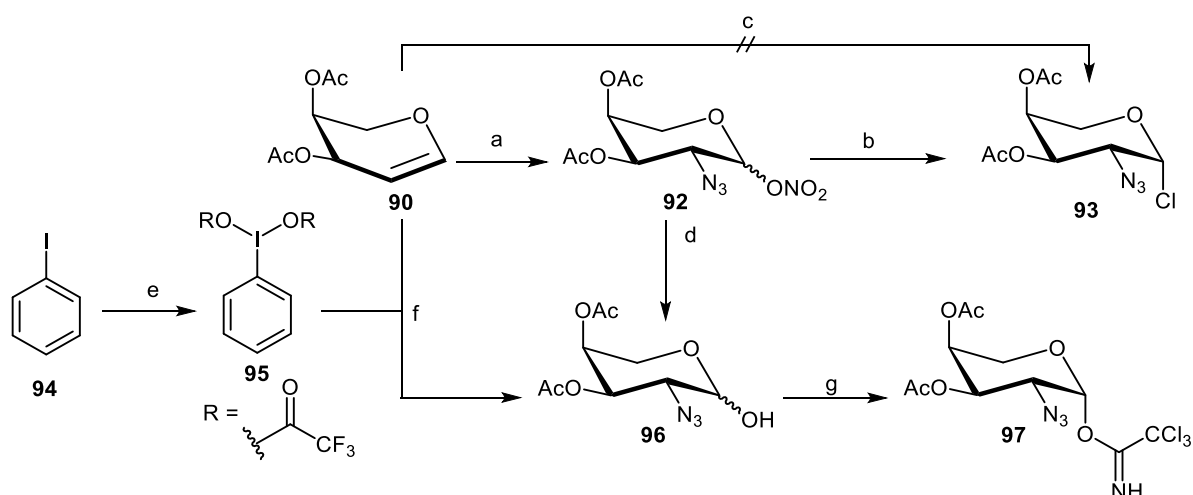


**Figure 4.6.** Mechanism of the radical azidonitration reaction to glycols.<sup>[193]</sup>

With the arabinal **90** in hand, first the synthesis of a respective glycosyl chloride **93**, a Koenigs-Knorr-type glycosyl donor was tackled. Thus, in a classical azidonitration according to a procedure of Yoshimura et al.,<sup>[194]</sup> the arabinal **90** was treated with CAN and  $\text{NaN}_3$  in acetonitrile to give the literature-known arabinosyl nitrate **92**,<sup>[194]</sup> which was subsequently used for the chlorination without purification. Thus, **92** was treated with tetraethylammonium chloride (TEACl) and the desired arabinose chloride **93**<sup>[194]</sup> was obtained in a yield of 30 % over two steps. The attempt to convert the arabinal **90** directly into the corresponding chloride **93** by an azidochlorination<sup>[195]</sup> with  $\text{FeCl}_3$ ,  $\text{NaN}_3$  and  $\text{H}_2\text{O}_2$  was not successful (Scheme 4.5).

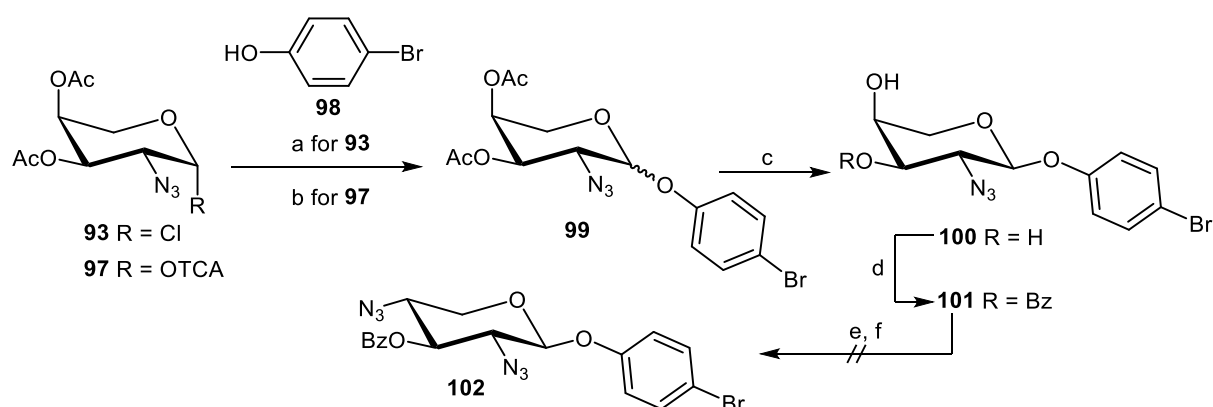
As an alternative glycosyl donor, the trichloroacetimidate **97** was synthesized. The required hemiacetal **96** can be achieved either directly by hydration of the nitrate **92** or by an azido-hydratization reaction with the arabinal **90**. For the anomeric denitration reaction, two different procedures were followed. On the one hand, according to Dean and co-workers<sup>[196]</sup> the nitrate **92** was treated with hydrazinium acetate in DMF, but no conversion of the starting material could be observed. Thus, in another approach following a procedure of Gauffeny et al.,<sup>[197]</sup> the nitrate **92** was reacted with thiophenol and DIPEA in acetonitrile. Thus, **96** was obtained from **90** in 25 % yield over two steps after column chromatography (Scheme 4.5). To increase the yield of hemiacetal **96**, an azido-hydratization was performed, as it has been introduced by the group of Vankar in 2018 as a regio- and stereoselective reaction under mild reaction conditions.<sup>[198]</sup> One reagent required for the derivatization of a glycal, is [bis(trifluoroacetoxy)iodo]benzene (**95**, PIFA), which had to be prepared. Thus, treatment of iodobenzene (**94**) with oxone in the presence of trifluoroacetic acid (TFA) gave **95** in a yield of 70 %.<sup>[199]</sup> With **95** in hand, the procedure of Vankar and co-workers was followed. Since the azido-hydratization is a radical reaction, **95** in the presence of TMSN<sub>3</sub> and the catalyst TEMPO forms an intermediate radical, which can react with the arabinal **90**. In the presence of water, the hemiacetal **96** can be formed, which was isolated after column chromatography in a yield of 51 %. Formation of the lyxo-configured side product was not observed in this case (Scheme 4.5). Accordingly, for the preparation of the trichloroacetimidate **97**, the anomeric hydroxyl group of the arabinose derivative **96** was deprotonated by DBU and the addition of the resulting anomeric oxyanion upon the triple bond of trichloroacetonitrile furnished the O-glycosyl trichloroacetimidate **97** in a yield of 50 %.



**Scheme 4.5.** Synthesis of arabinosyl donors **93** and **97** by azidonitration of arabinal **90**. (a) CAN, NaN<sub>3</sub>, dry MeCN, -30 °C, 5 h; (b) TEACl, MeCN, rt, 16 h, 30 % (over 2 steps); (c) FeCl<sub>3</sub>, NaN<sub>3</sub>, H<sub>2</sub>O<sub>2</sub>, MeCN, 0 °C, 6 h; (d) PhSH, DIPEA, MeCN, 0 °C, 45 min, 25 %; (e) TFA, Oxone, CH<sub>2</sub>Cl<sub>2</sub>, rt, 3 h, 70 %; (f) TMSN<sub>3</sub>, TEMPO, Bu<sub>4</sub>NHSO<sub>4</sub>, CH<sub>2</sub>Cl<sub>2</sub>/H<sub>2</sub>O, 0 °C, 1.5 h, 51 %; (g) Cl<sub>3</sub>CCN, DBU, CH<sub>2</sub>Cl<sub>2</sub>, 0 °C, 2 h, 50 %.

With the glycosyl donors **93** and **97** in hand, the anomeric position was functionalized in a glycosylation reaction with 4-bromophenol (**98**). In a first approach, chloride **93** was employed and according to a procedure of Van der Marel and colleagues<sup>[200]</sup> **98** was treated with CsOH in CH<sub>2</sub>Cl<sub>2</sub> in the presence of tetrabutylammonium bromide before arabinosyl chloride **93** was added. The targeted  $\alpha$ -L-arabinoside **99** was isolated in a yield of 21 % ( $\alpha$ : $\beta$  = 3:1) (Scheme 4.6). To increase the yield for this glycosylation reaction, the glycosyl donor **97** was employed. In order to avoid an anomeric mixture, the reaction had to be carried out in acetonitrile, which exerts a coordinating effect leading to the formation of  $\alpha$ -L-arabinosides. Accordingly, donor **97** and acceptor **98** were treated with BF<sub>3</sub>·Et<sub>2</sub>O in acetonitrile at -40 °C to yield arabinoside **99** in a good yield of 90 % ( $\alpha$ / $\beta$  = 1:1). Attempts to perform the reaction at higher temperatures (-10 °C, rt) increased the amount of the  $\beta$ -L-arabinoside side product. Also, the utilization of TMSOTf as a promoter did not increase the formation of the  $\alpha$ -L-arabinoside **99** (Scheme 4.6).

For the functionalization of the 4-position of **99**, a regioselective protecting group chemistry had to be applied, which required cleaving of the acetyl protecting groups first. Thus, **99** was treated under mild conditions with K<sub>2</sub>CO<sub>3</sub> in MeOH and the unprotected  $\alpha$ -L-arabinoside **100** was achieved in a yield of 50 % starting from the anomeric mixture ( $\alpha$ / $\beta$  = 1:1) of **99**. Next, the 3-OH group was selectively protected because it is known, that the equatorial 3-OH group is more acidic and selective acylation is thermodynamic favored.<sup>[201]</sup> According to a procedure of Thiem and co-workers,<sup>[202]</sup> **100** was treated with 1.0 equivalent of BzCl in pyridine and the targeted product **101** was obtained in a yield of 40 %. Then in a last step towards 2,4-diazidoxylosides, an equatorial azido group had to be introduced at the 4-position by a S<sub>N</sub>2 reaction with NaN<sub>3</sub> as the nucleophile. Thus, according to the work of Elchert et al.,<sup>[203]</sup> **101** was treated with Tf<sub>2</sub>O in pyridine at -35 °C, but the corresponding triflate was not stable and it was not possible to proceed with the nucleophilic substitution reaction (Scheme 4.6).

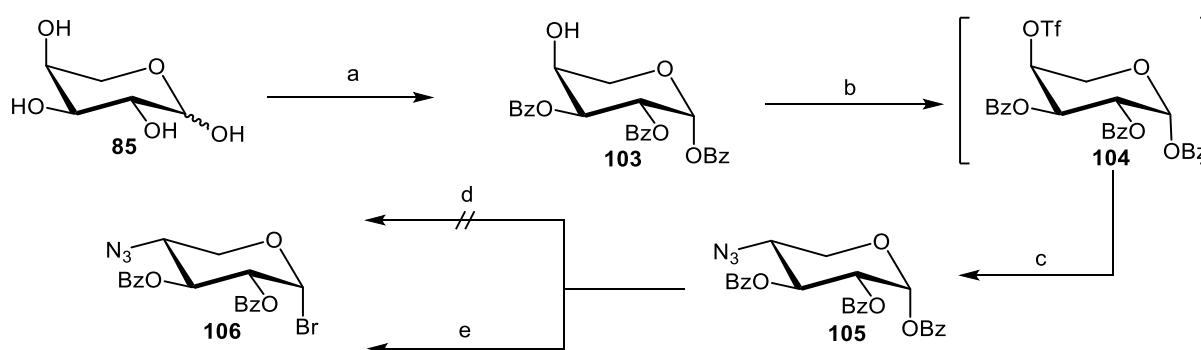


**Scheme 4.6.** Synthesis of 2,4-diazidoxyloside **58** by glycosylation of 4-bromophenol (**98**). (a) BF<sub>3</sub>·Et<sub>2</sub>O, dry MeCN, -40 °C, 1 h, 90 % ( $\alpha$ / $\beta$  = 1:1); (b) CsOH, TBAB, CH<sub>2</sub>Cl<sub>2</sub>, rt, 16 h, 21 % ( $\alpha$ / $\beta$  = 3:1); (c) K<sub>2</sub>CO<sub>3</sub>, MeOH, rt, 2 h, 50 %; (d) BzCl (1 equ.), pyridine, CH<sub>2</sub>Cl<sub>2</sub>, -35 °C, 2 h, 40 %; (e) Tf<sub>2</sub>O, pyridine, CH<sub>2</sub>Cl<sub>2</sub>; (f) NaN<sub>3</sub>, DMF; (g) NaOMe, MeOH. Abbr.: OTCA: O-trichloroacetimidate.

Since the yields for the functionalization of the glycal **90** to the corresponding glycosyl donors **93** and **97** (Scheme 4.5) were not satisfying and the substitution of the 4-OH group was not successful (Scheme 4.6), the synthetic strategy had to be changed. To this end, the functionalization sequence of the ring positions was changed, first addressing inversion of the 4-position of L-arabinose and then form the glycal and proceed with azidonitration.

In order to first functionalize the 4-position by an inversion reaction, a suitable protecting group pattern had to be implemented.<sup>[204]</sup> Starting from L-arabinose (**85**), the literature-known 1,2,3-tri-*O*-benzoylated L-arabinose derivative **103**<sup>[205]</sup> was synthesized. Thus, according to Beahm et al.,<sup>[205]</sup> L-arabinose (**85**) was treated with 3.0 equivalents of BzCl in a mixture of pyridine and CH<sub>2</sub>Cl<sub>2</sub> at -30 °C and the targeted **103** was isolated after column chromatography in a yield of 45 %. For the following nucleophilic substitution reaction, the free 4-OH group was activated employing a procedure of Beahm and colleagues.<sup>[205]</sup> Hence, the alcohol **103** was reacted with Tf<sub>2</sub>O in pyridine and the corresponding triflate intermediate **104** was subsequently dissolved in DMF and NaN<sub>3</sub> was added. The S<sub>N</sub>2 reaction yielded the desired azido-D-xylose derivative **105**<sup>[205]</sup> in 57 % over two steps after column chromatography (Scheme 4.7).

For the synthesis of the required xylal, the xylosyl bromide **106** had to be formed first. Hence, **105** was treated with HBr in acetic acid but unfortunately, these reaction conditions lead to decomposition of the starting. Since the group of Meier reported similar problems along the synthesis of azido-functionalized glycosyl bromides,<sup>[206]</sup> anomeric bromination was carried out under milder conditions. Indeed, the glycosyl bromide **106** could be obtained in 72 % yield after treatment with titanium bromide (TiBr<sub>4</sub>) according to a procedure of Jon and co-workers (Scheme 4.7).<sup>[207]</sup>



**Scheme 4.7.** Synthesis of xylosyl bromide **106** starting from L-arabinose (**85**). (a) BzCl (3 equ.), pyridine, dry CH<sub>2</sub>Cl<sub>2</sub>, -30 °C, 2 h, 45 %; (b) Tf<sub>2</sub>O, pyridine, dry CH<sub>2</sub>Cl<sub>2</sub>, -20 °C, 2 h; (c) NaN<sub>3</sub>, dry DMF, rt, 16 h, 57 % (over 2 steps); (d) HBr, AcOH, CH<sub>2</sub>Cl<sub>2</sub>, 0 °C, 2 h; (e) TiBr<sub>4</sub>, CH<sub>2</sub>Cl<sub>2</sub>/EE, 40 °C, MW, 1 h, 72 %.

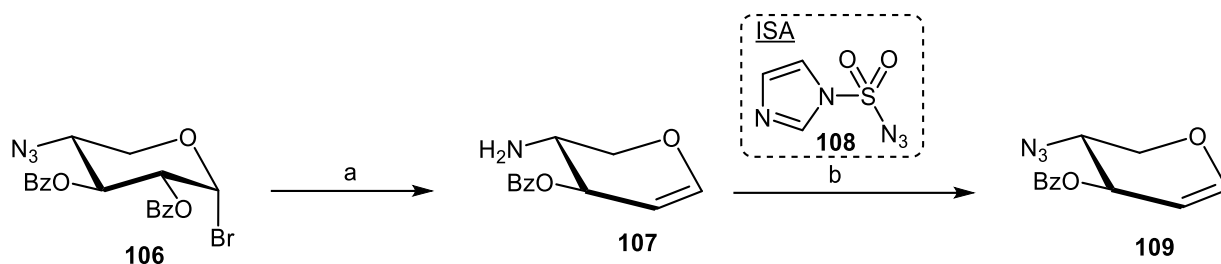
The xylosyl bromide **106** served as the starting material for the synthesis of the corresponding xylal **109**. Even if azides can be potentially reduced under the conditions of the reductive elimination, the synthesis of primary azide containing glycols is literature-known.<sup>[208]</sup> Thus,

according to the procedure of Zhang and co-workers,<sup>[208c]</sup> **106** was treated with zinc dust in a buffered (NH<sub>4</sub>Cl) suspension of acetonitrile at 40 °C for 3.5 h, but the targeted xylal **109** was not obtained. Hence, the reaction time was decreased, and the reaction carried out at 40 °C for 30 min (Table 4.1). Unfortunately, under these conditions only the respective amino xylal **107** (37 %) was isolated as confirmed by NMR and mass analysis. When the reaction was performed at lower temperatures (rt, 0 °C), no conversion was observed. In another attempt the buffering system of the reaction was changed and following a procedure of Shao and co-workers,<sup>[208a]</sup> **106** was treated with zinc in the presence of sodium dihydrogen phosphate, which gave again the amino xylal **107** in a yield of 38 % (Table 4.1). In order to reduce the risk of azide reduction during the xylal formation, the reaction was performed with titanocene chloride (Cp<sub>2</sub>TiCl) in the presence of a smaller amount of zinc powder (2.0 equ.).<sup>[209]</sup> However, these conditions resulted in the decomposition of the starting material **106**. Also, the attempt to use 1-methylimidazol as an additive and run the reaction under inert conditions as described by Németh and co-workers,<sup>[210]</sup> was not successful.

**Table 4.1.** Reaction conditions for the reductive elimination of xylosyl bromide **106** to synthesize xylals as shown in Scheme 4.8.

Entry	Reagents	Solvent	Temp.	Time	Yield of amino xylal <b>107</b>
1	Zn, NH <sub>4</sub> Cl	MeCN	40 °C	3.5 h	-
2	Zn, NH <sub>4</sub> Cl	MeCN	40 °C	30 min	37 %
3	Zn, NH <sub>4</sub> Cl	MeCN	rt	8 h	-
4	Zn, NH <sub>4</sub> Cl	MeCN	0 °C	8 h	-
5	Zn, NaH <sub>2</sub> PO <sub>4</sub>	acetone	rt	1 h	36 %
6	Zn, Cp <sub>2</sub> TiCl	THF	rt	1 h	-
7	Zn, 1-methylimidazol	ethyl acetate	rt	1 h	-

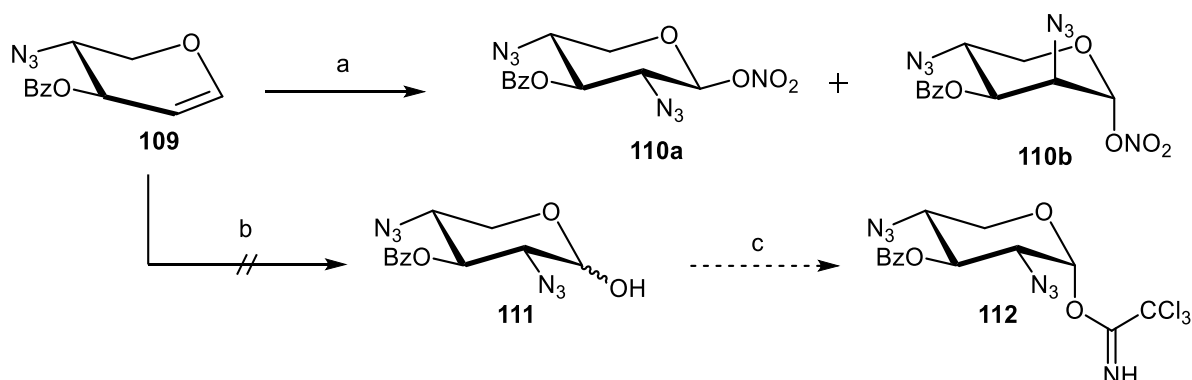
As the envisaged reaction pathway cannot be continued with a free amino function, in order to save the synthetic plan, it was tried to reverse the 4-amino group into an azide group. Hence, in a next effort to reach the xylal **109**, the xylal **107** was subjected to a copper-catalyzed diazotransfer reaction<sup>[211]</sup> using the diazo donor imidazole-1-sulfonyl azide (**108**, ISA) in methanol. This reaction indeed gave the desired azide **109** in almost 50 % (Scheme 4.8).



**Scheme 4.8.** Synthesis of azido xylal **109** starting from xylosyl bromide **106**. (a) Zn (detailed conditions in Table 4.1); (b) ISA,  $\text{K}_2\text{CO}_3$ ,  $\text{CuSO}_4$ , MeOH, rt, 16 h, 49 %.

With the azido xylal **109** in hand, the second amino function at the 2-position was introduced by an azidonitration reaction. Thus, according to the work of Yoshimura,<sup>[194]</sup> the xylal **109** was treated with CAN and  $\text{NaN}_3$  in acetonitrile at  $-30\text{ }^\circ\text{C}$ , which gave a stereoisomeric mixture of 2-azido xylosyl nitrate **110a** and 2-azido lyxosyl nitrate **110b** in a poor overall yield of 28 % (xylo:lyxo ratio of 1:2) (Scheme 4.9). The configuration of the two products was determined by NMR spectroscopy. Unfortunately, the two stereoisomers could not be separated by column chromatography. Attempts to increase the yield and the stereospecificity of the reaction by changing the temperature ( $0\text{ }^\circ\text{C}$  and rt) or the solvent ( $\text{CH}_2\text{Cl}_2$  instead of MeCN) were not successful.

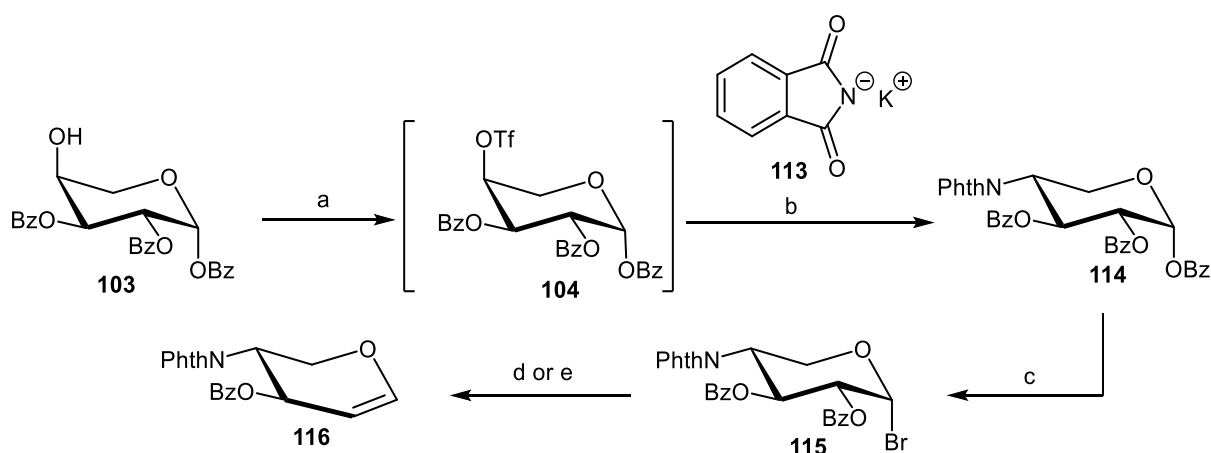
In an alternative approach, the direct synthesis of the glycosyl donor **112** was attempted and accordingly the azido-xylal **109** subjected to an azidohydration according to Vankar et al.<sup>[198]</sup> However, when **109** was treated with  $\text{TMSN}_3$ , PIFA (**95**), TEMPO and  $\text{Bu}_4\text{NHSO}_4$  in a mixture of  $\text{CH}_2\text{Cl}_2$  and water, the desired reducing xylose **111** was not obtained. Because of this failure, also the xylosyl trichloroacetimidate derivative **112** cannot be obtained along this route (Scheme 4.9).



**Scheme 4.9.** Azidonitration and azidohydration of xylal **109**. (a) CAN,  $\text{NaN}_3$ , dry MeCN,  $-30\text{ }^\circ\text{C}$ , 5 h, 28 % (ratio **110a** : **110b** in 1:2); (b)  $\text{TMSN}_3$ , PIFA (**95**), TEMPO,  $\text{Bu}_4\text{NHSO}_4$ ,  $\text{CH}_2\text{Cl}_2/\text{H}_2\text{O}$ ,  $0\text{ }^\circ\text{C}$ , 1.5 h; (c)  $\text{Cl}_3\text{CCN}$ , DBU,  $\text{CH}_2\text{Cl}_2$ ,  $0\text{ }^\circ\text{C}$ , 2 h.

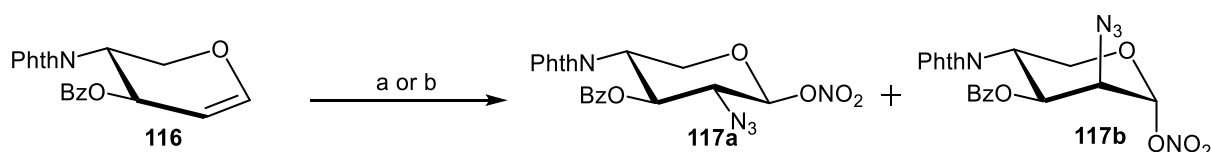
At this point it was decided to not continue with the reaction pathway based on the azidonitration of the azido-functionalized xylal **109** for two reasons. First, the synthesis of the 4-azido-functionalized xylal **109** hardly is a high-yielding reaction due to the concomitant reduction of the azido group during xylal formation. Second, the introduction of a 2-azido functionality by azidonitration comes along with low yields and lacking stereospecificity. As a consequence of these difficulties, in the next synthetic plan, the 4-azido group masking an amino function, was replaced by a protected amino function, where the protecting group is stable under reductive conditions (e.g., a phthaloyl protecting group).

Again, the synthesis started with the regioselective benzylation of L-arabinose to achieve the tri-benzoylated L-arabinose **103** (cf. Scheme 4.7).<sup>[205]</sup> Then, the triflate **104** was formed as before and in turn reacted with potassium phthalimide (**113**) in DMF yielding the desired D-xylo-configured epimer **114** in yields around 60 % over two steps (Scheme 4.10). Addition of 18-crown-6<sup>[212]</sup> increases the nucleophilicity of the naked phthalimide anion and improves the yield of the reaction to 78 %. In the next step, **114** was converted into the xylosyl bromide **115** with HBr in acetic acid in an excellent yield of 93 % after column chromatography. The xylosyl bromide **115** served as the starting material for the xylal synthesis under known conditions using zinc powder and NH<sub>4</sub>Cl<sup>[208a]</sup> to obtain the 4-phthalimido-protected xylal **116** in a yield of 42 %. When a catalytical system of zinc and vitamin B<sub>12</sub> as reported by Franck and co-workers was employed, the yield of the reaction was increased to over 80 % and the reaction time reduced to 1 h.<sup>[213]</sup> Vitamin B<sub>12</sub> is known as a catalyst in reductive elimination reactions to cleave β-chloroethyl-ester protecting groups or the synthesis of glycols.<sup>[214]</sup> In this type of reactions, the Co(III) of vitamin B<sub>12</sub> is reduced in the presence of zinc dust to Co(I). This reactive species can insert into the C-bromide bond of **115** in an oxidative addition and followed by a reductive elimination the corresponding glycol **116** is formed.



**Scheme 4.10.** Synthesis of xylal **116** starting from tri-benzoylated L-arabinose **103**. (a) Tf<sub>2</sub>O, pyridine, CH<sub>2</sub>Cl<sub>2</sub>, -20 °C, 2 h; (b) 18-crown-6, DMF, rt, 16 h, 78 % (over 2 steps); (c) HBr, AcOH, CH<sub>2</sub>Cl<sub>2</sub>, rt, 2 h, 93 %; (d) Zn, NH<sub>4</sub>Cl, MeCN, rt, 16 h, 42 %; (e) Zn, NH<sub>4</sub>Cl, Vit-B<sub>12</sub>, CH<sub>2</sub>Cl<sub>2</sub>, MeOH, rt, 1 h, 83 %.

Next, the 4-Phth-xylal **116** was subjected to an azidonitration employing CAN and NaN<sub>3</sub> in acetonitrile at -30 °C. Again, the isolated product displayed a stereoisomeric mixture of the *xylo*- (**117a**) and *lyxo*-configured (**117b**) azido glycosyl nitrates in a ratio of 2:1 (*xylo* : *lyxo*) (Scheme 4.11). Separation of the stereoisomers by column chromatography was unsuccessful. Because it was shown earlier for glucals that azidonitrations at higher temperatures are more stereoselective in the *gluco* series than in with mannosyl nitrates,<sup>[215]</sup> the azidonitration for **116** was also carried out at room temperature, but this decreased the overall yield and the ratio of the obtained stereoisomers remained unchanged.



**Scheme 4.11.** Azidonitration of xylal **116** yields a stereoisomeric mixture. (a) CAN, NaN<sub>3</sub>, dry MeCN, -30 °C, 5 h, 50 % (ratio **117a** : **117b**, 2:1); (b) CAN, NaN<sub>3</sub>, dry MeCN, rt, 5 h, 33 % (ratio **117a** : **117b**, 2:1).

During the azidonitration reaction, an azido radical is added to the glycal and the stereochemical outcome is influenced by different parameters. While solvents or temperatures can be optimized, the structure of the glycal and its substituents is harder to achieve. For the sterical outcome of the reaction especially the stabilization of the radical intermediate **91a** (Figure 4.6) is important. While carbohydrates with an axial C-4 group (e.g. arabinol) favor the equatorial addition of an azide, for equatorial C-4 groups (e.g. xylal) the amount of the axial side product increases.<sup>[193]</sup> In addition, pentoses have no methylene hydroxyl group, which can also have a directing sterically influence. Another factor influencing the reaction is the structure of the substituents. In case of azido xylal **109** the axial addition of an azido radical dominated and thus particularly the *lyxo*-configured side product was formed. On the other side, in case of phthaloyl xylal **116** the presence of two electron withdrawing protecting groups improved the stereoselectivity and the amount of *xylo*-configured product was increased, but not satisfying.

In conclusion, the azidonitration of xylals does not serve as a robust and stereoselective method for the functionalization towards 2,4-diamino xylosides. The addition of azido radicals is regio- but not stereoselective and once they are formed, they still must be converted into the respective glycosyl donors for further glycosylation. In fact, however, the synthesis of the xylal **116** was optimized and serves as a powerful building block in the next approach.

### 4.3 Following the glycal approach via iodosulfonamidation

The synthesis of 2-amino-2-deoxy saccharides is an important field of carbohydrate chemistry since these monosaccharides are subunits of many glycoconjugates such as glycoproteins or heparin.<sup>[216]</sup> Thus, many elegant methods have been employed to synthesize 2-amino-2-deoxy carbohydrates and often glycals serve as powerful building blocks. A promising method for the conversion of glycals is the iodosulfonamidoglycosylation introduced by Danishefsky et al., which was first described in 1990.<sup>[217]</sup> This reaction provides 2-amino-2-deoxy  $\beta$ -glycosides with a high stereo- and regioselectivity and thus Danishefsky and co-workers established this method over the years in the context of the synthesis of complex oligosaccharides.<sup>[218]</sup>

According to the reaction mechanism of the iodosulfonamidation the iodosulfonamide **119** serves as the key intermediate of this reaction pathway. In addition to the control of the stereochemistry the iodosulfonamidation also allows the introduction of various aglycons. While it was first focused on the synthesis of *O*-xyloside **120**, the intermediate **119** can also be rearranged resulting in xylosyl azides, respectively. However, once the 2,4-diamino xyloside **120** is synthesized, finally the derivatization of the 3-position can be targeted (Figure 4.7).

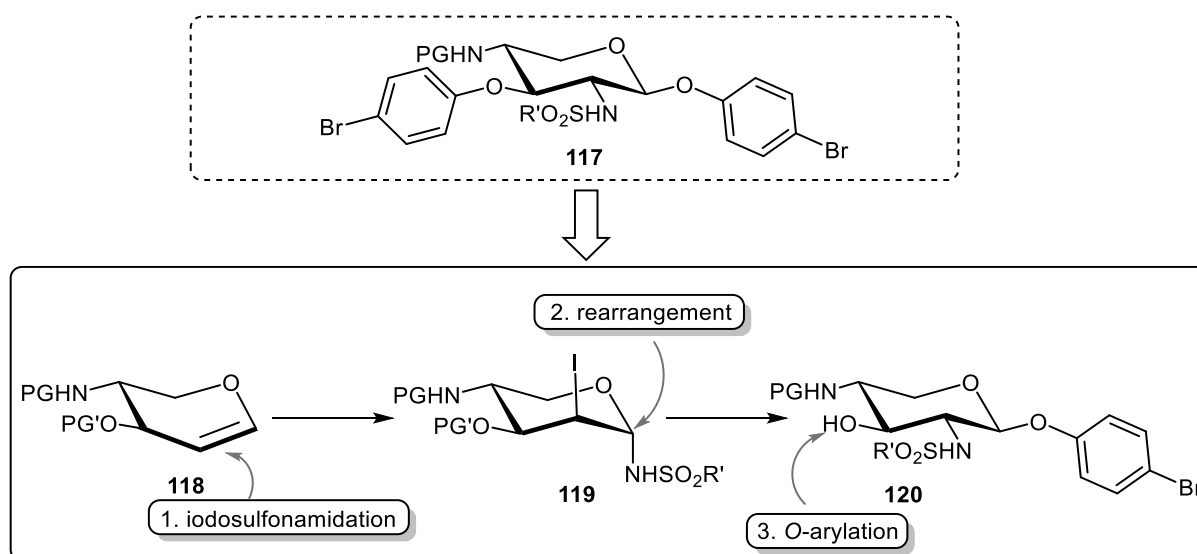
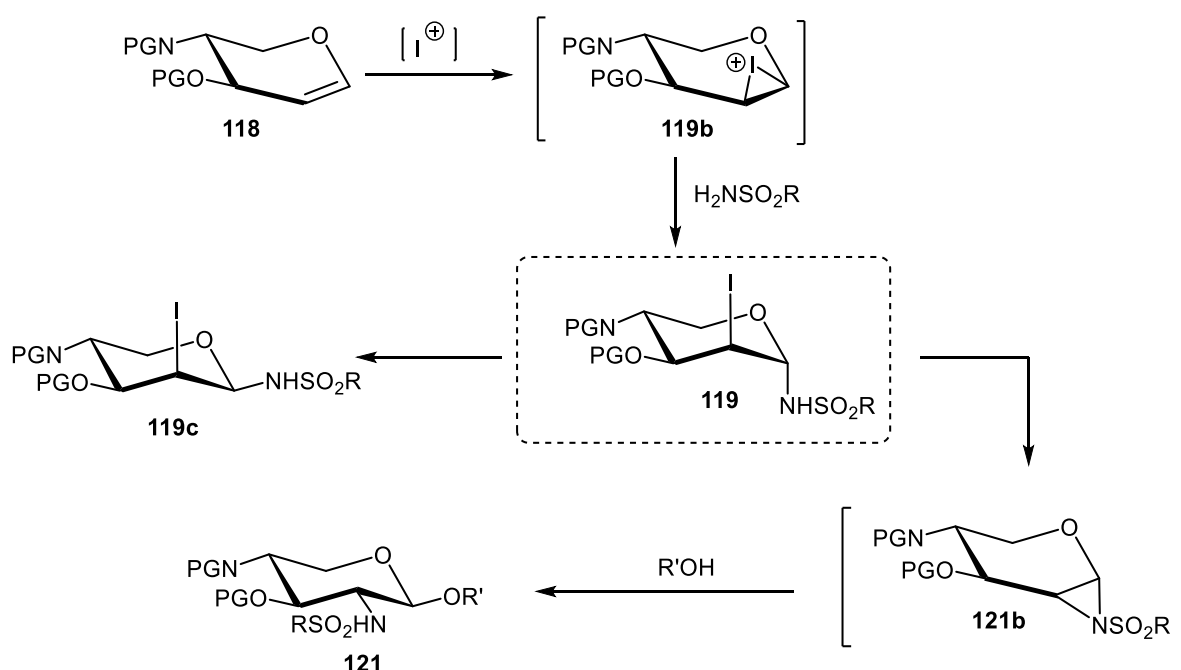


**Figure 4.7.** Synthesis of 2,4-diamino xyloside **117** by iodosulfonamidation of the xylal **118** as the key reaction step. After an iodosulfonamidation a rearrangement reaction of **119** gives 2,4-diamino xyloside **120**, which is further derivatized in an *O*-arylation reaction to yield **117**. PG: protecting group.

The key reaction step of this synthetic account is the iodosulfonamidation of xylal **118**. For the correct stereochemical outcome of this reaction the electrophilic addition of iodonium ( $I^+$ ) to the cyclic vinyl ether **118** is a crucial step. Iodonium is attacking the  $\beta$ -face of **118** leading to a cyclic iodonium ion **119b** (Scheme 4.12). This addition is stereospecific because the  $\beta$ -face iodonium is stabilized due to the *p*-orbitals of the endocyclic ring oxygen, which was shown by

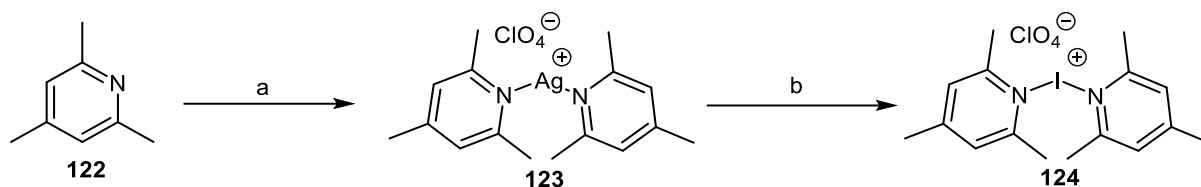
Fraser-Reid and Lemieux earlier.<sup>[219]</sup> Once **119b** is formed, it can be opened regioselectively by a nucleophile at the anomeric carbon assisted by the anomeric effect, for example a sulfonamide ( $\text{H}_2\text{NSO}_2\text{R}$ ) leading to trans-diaxial addition product **119**.<sup>[220]</sup> Next, due to the nucleophilic character of the *N*-sulfonamide and the iodine leaving group a cyclic aziridine **121b** is formed. Because of the instability of aziridine **121b**, this can be opened in the presence of a nucleophile (e.g., alcohol or azide) in order to give the 2-amino  $\beta$ -D-glycoside **121** with a high regio- and stereospecificity. Nevertheless, in the presence of electron-withdrawing protecting groups in glycals an unwanted anomerization of the iodosulfonamide **119** can occur. This 1,2-cis addition product **119c** cannot undergo an aziridine rearrangement and thus not be further derivatized.<sup>[221]</sup>



**Scheme 4.12.** Mechanism for the iodosulfonamidation of glycals via iodonium intermediate **119b** and aziridine **121b**.

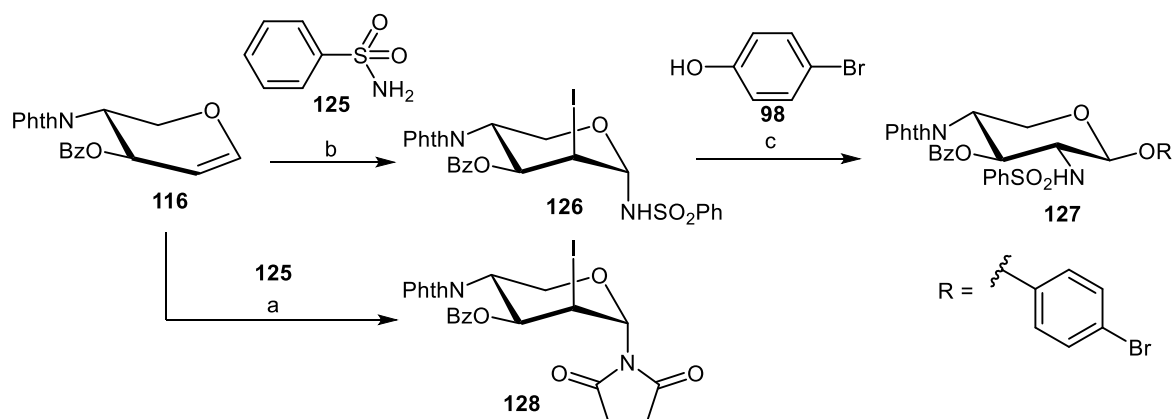
For the success of an iodosulfonamidation reaction, next to the configuration of the glycal also the iodonium source is a crucial factor. In most approaches, either *N*-iodosuccinimide (NIS) or iodonium di-*sym*-collidine perchlorate (IDCP) are used. While NIS is a commercially available chemical, IDCP has to be synthesized freshly.

To apply the iodosulfonamidation to the glycal **116** first of all the literature-known IDCP (**124**)<sup>[222]</sup> had to be prepared (Scheme 4.13). Thus, following the synthesis procedure of Lemieux and Morgan,<sup>[223]</sup> *sym*-collidine (**122**) was treated with sodium perchlorate and silver nitrate in water. Silver di-*sym*-collidine perchlorate (**123**) was precipitated and directly subjected to the next step by treatment with iodine in  $\text{CH}_2\text{Cl}_2$  gave the targeted IDCP **124** in a yield of 96 % after recrystallization from diethyl ether.



**Scheme 4.13.** Synthesis of IDCP **124** started from *sym*-collidine. (a) AgNO<sub>3</sub>, NaClO<sub>4</sub>, H<sub>2</sub>O, rt, 15 min; (b) I<sub>2</sub>, CH<sub>2</sub>Cl<sub>2</sub>, rt, 15 min, 96 %.

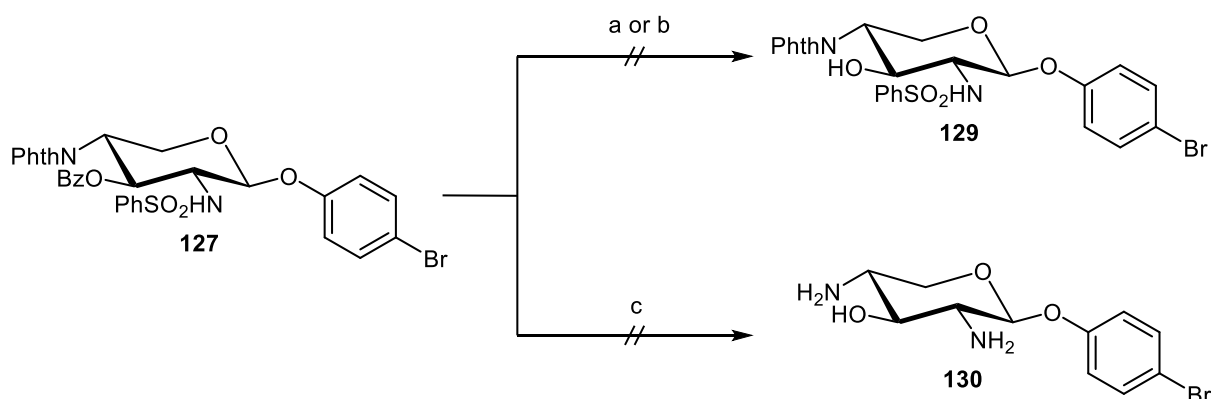
For the derivatization of xylal **116** by iodosulfonamidation with benzene sulfonamide (**125**) it was first tried to use NIS as the iodonium source. Following a procedure of Gautier et al.,<sup>[221]</sup> **116** was treated with NIS and iodine in the presence of **125** at -10 °C in CH<sub>2</sub>Cl<sub>2</sub>. It turned out however, that the succinimide was the stronger nucleophile and opened the iodonium intermediate, as it was described by Thiem and colleagues,<sup>[224]</sup> forming the *trans* addition product **128**, which was not able to undergo a rearrangement reaction via an aziridine (Scheme 4.14). In a second attempt, the iodonium source was changed to IDCP and according to the work of Danishefsky and co-workers,<sup>[218c]</sup> **116** was treated with IDCP in the presence of **125** in CH<sub>2</sub>Cl<sub>2</sub> and the corresponding iodosulfonamide **126** was obtained in a yield of 62 % (Scheme 4.14). Other than the azidonitration, the iodosulfonamidation gave stereospecifically the 1,2-*trans* addition product in the *lyxo*-configuration, as it was confirmed by <sup>1</sup>H NMR spectroscopy. Then, subsequently **126** was used in a rearrangement reaction and iodosulfonamide **126** and 4-bromophenol **98** were treated with lithium hexamethyldisilazane (LiHMDS) in THF at -78 °C. The presence of this base had two advantages. On the one hand, the nucleophilic lithium phenolate of **98** could be formed while on the other hand the formation of the aziridine intermediate (cf. Scheme 4.12) is preferred in a basic medium. In addition, silver triflate (AgOTf) was added to the reaction to abstract the produced iodide. The targeted 2,4-diamino β-D-xyloside **127** was isolated in a fair yield of 69 % and with excellent β-stereospecificity and a high regioselectivity of the sulfonamide at the 2-position (Scheme 4.14).



**Scheme 4.14.** Synthesis of diamino xyloside **127** starting from xylal **116**. (a) NIS, I<sub>2</sub>, CH<sub>2</sub>Cl<sub>2</sub>, -10 °C, 2 h, 61 %; (b) IDCP, CH<sub>2</sub>Cl<sub>2</sub>, 0 °C, 30 min, 62 %; (c) LiHMDS, AgOTf, THF, -78 °C→rt, 16 h, 69 %.

With xyloside **127** in hand, in an ultimate step the 3-position of the xyloside had to be functionalized in order to reach the targeted xyloside **117**. Thus, removal of the 3-O-benzoyl protecting group was required to subject the xyloside to an O-arylation reaction. It is known that benzoyl ester groups in the neighbourhood of phthalimido groups can be chemoselectively cleaved under Zemplén transesterification reaction conditions.<sup>[225]</sup> Thus, **127** was treated with sodium methoxide in methanol at room temperature, but the desired product **129** could not be obtained under these conditions. Lower reaction temperatures (0 °C or -10 °C) did not change the outcome of the reaction. In a second attempt it was tried to cleave the benzoyl protecting group under milder conditions by treating **127** with K<sub>2</sub>CO<sub>3</sub> in methanol at -30 °C. Unfortunately, also these conditions showed no conversion to the targeted **129** (Scheme 4.15).

At this point, it was decided to try a global deprotection of **127** and cleave the protecting groups of both amines and the 3-OH group at the same time. Thus, Birch conditions were applied according to Danishefsky and co-workers<sup>[218d]</sup> and **127** was treated with sodium in the presence of liquid ammonia in THF at -78 °C for 40 min. However, under these reaction conditions decomposition of the starting material was observed (Scheme 4.15).



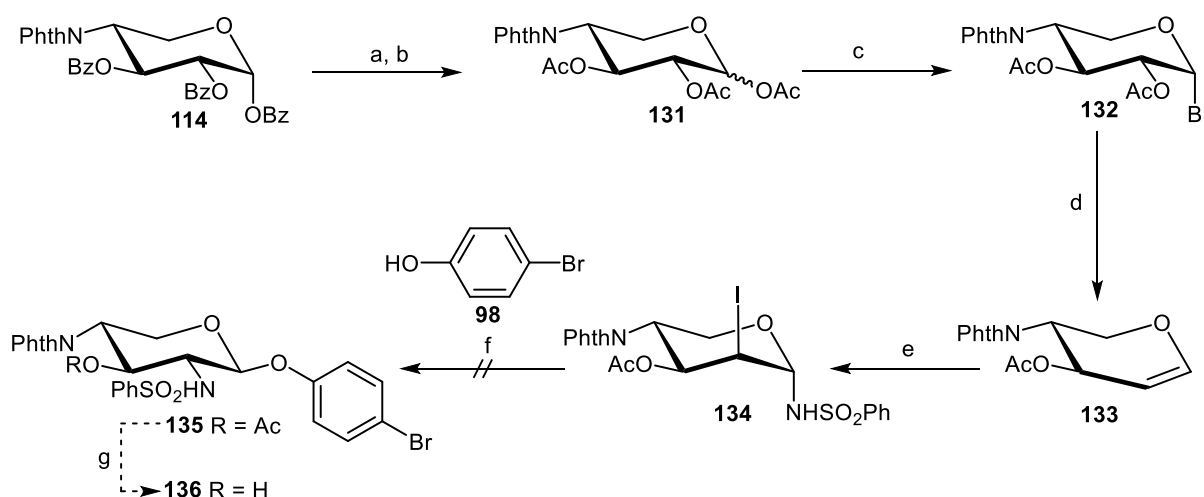
**Scheme 4.15.** Deprotection of 2,4-diamino xyloside **127**. (a) NaOMe, MeOH, rt, 2 h; (b) K<sub>2</sub>CO<sub>3</sub>, MeOH, -30 °C, 5 h; (c) Na, NH<sub>3</sub>, THF, -78 °C, 40 min.

Facing the unsatisfying situation of the deprotection of **127**, two main problems were figured out. On the one hand, the removal of the benzene sulfonamide group had to be optimized, since birch conditions were not compatible with **127**. On the other hand, a strategy for the chemoselective deprotection of the 3-position had to be sought. While benzoyl ester protecting groups are labile under basic conditions, acetyl esters can be cleaved under acidic conditions keeping the phthalimide intact.<sup>[226]</sup> Thus it was decided to change the protecting group at the 3-position of **127** into an acetyl protecting group.

For the synthesis pathway with acetyl protecting groups, the benzoyl protecting groups of **114** were cleaved under Zemplén conditions and the unprotected intermediate was subsequently

acetylated with acetic anhydride and pyridine to obtain **131** over two steps in an excellent yield of 96 % (Scheme 4.16). Bromination of the anomeric position with HBr in acetic acid gave the corresponding bromide **132** in high yields and in a reductive elimination reaction with zinc, NH<sub>4</sub>Cl and vitamin B<sub>12</sub>, the acetylated xylal **133** was reached in a yield of 83 %. With **133** in hand, the xylal double bond could be addressed by an iodosulfonamidation reaction and **133** was treated with benzene sulfonamide and IDCP in CH<sub>2</sub>Cl<sub>2</sub>. The corresponding iodosulfonamide **134** was isolated in a good yield of 88 % (Scheme 4.16), which proved again that the iodosulfonamidation serves as a stereoselective functionalization method for xylals.

Consequently, **134** was subjected to the aziridine rearrangement and glycosylation reaction to provide xyloside **135**. Hence, **134** was treated with LiHMDS and AgOTf in the presence of 4-bromophenol **98** at -78 °C. However, the desired **135** could not be isolated and the reaction conditions led to decomposition of the iodosulfonamide **134**, which can be assigned to the lability of the acetyl protecting group under the strong basic environment. Nevertheless, the rearrangement of iodosulfonamides requires lithium or potassium alkoxides. An alternative could be the use of stannyl alkoxides, which was described by Danishefsky et al. for the case of tributyltin benzyloxyde.<sup>[227]</sup> Since the use of stannyl phenolates in rearrangement reactions of iodosulfonamides is not intensively discussed, it was decided to not continue with the acetyl protecting group pathway. Instead, the deprotection of the sulfonamide group became the focus of further optimizations.

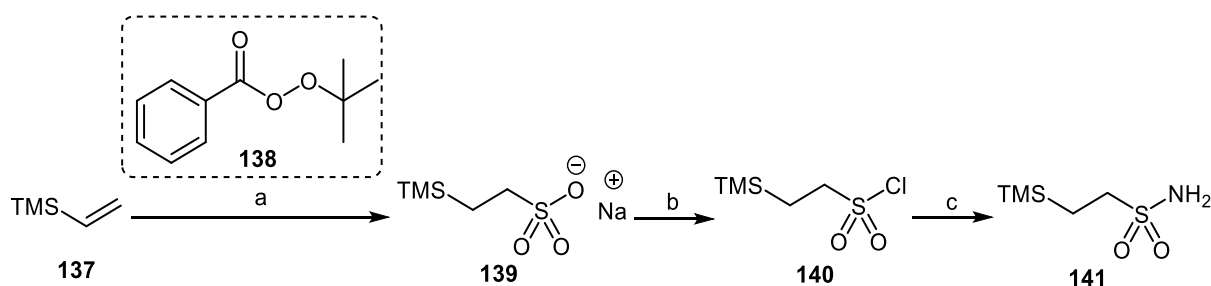


**Scheme 4.16.** Synthesis of acetylated 2,4-diamino xyloside **135** starting from xylose derivative **114**. (a) NaOMe, MeOH, rt, 1 h; (b) Ac<sub>2</sub>O, pyridine, rt, 2.5 h, 96 % (over 2 steps); (c) HBr, AcOH, CH<sub>2</sub>Cl<sub>2</sub>, rt, 2 h, 93 %; (d) Zn, NH<sub>4</sub>Cl, Vit-B<sub>12</sub>, CH<sub>2</sub>Cl<sub>2</sub>, MeOH, rt, 1 h, 83 %; (e) H<sub>2</sub>NSO<sub>2</sub>Ph, IDCP, CH<sub>2</sub>Cl<sub>2</sub>, 0 °C, 30 min, 88 %; (f) LiHMDS, AgOTf, THF, -78 °C→rt, 16 h; (g) AcCl, MeOH.

For iodosulfonamidation reactions different sulfonamide reagents (H<sub>2</sub>NSO<sub>2</sub>R) are known, which have to meet two main requirements in this synthetic approach. First, it has to be

nucleophilic enough to open the iodonium intermediate, formed by the addition of IDCP to the glycal. Second, in most cases the sulfonamide represents a protecting group, and its removal must be guaranteed. Next to the benzene sulfonamide several other aromatic sulfonamides (para-nitrobenzene sulfonamide<sup>[228]</sup> or para-toluene sulfonamide<sup>[229]</sup>) are used in iodosulfonamidation reactions of glycals. They all have in common that its cleavage requires harsh conditions, since aromatic sulfonamides are stable functional groups. An alternative is the 2-(trimethylsilyl)ethanesulfonamide (**141**, NSES).<sup>[230]</sup> This sulfonyl protecting group is cleaved under mild conditions using fluoride ions. For the introduction of this protecting group several methods exist. While free amines can be protected by the respective sulfonyl chloride **140** (SESCl),<sup>[231]</sup> SES protected amines can also be used in nucleophilic substitution or Mitsunobu reactions due to their strong nucleophilicity.<sup>[232]</sup> This makes the SESNH<sub>2</sub> **141** also suitable as an amine source for the iodosulfonamidation.<sup>[233]</sup>

The synthesis of 2-(trimethylsilyl)ethanesulfonamide (**141**, H<sub>2</sub>NSES) was started from vinyltrimethylsilane (**137**) according to the work of Weinreb et al. (Scheme 4.17).<sup>[230]</sup> In a radical addition to the vinyl group **137** was treated with *tert*-butyl perbenzoate (**138**) in the presence of sodium bisulfite (NaHSO<sub>3</sub>) in MeOH and the corresponding sodium sulfonate salt **139** was obtained in a yield of 54 %. Subsequently, **139** was converted into the sulfonyl chloride **140** by treatment with phosphorous pentachloride (PCl<sub>5</sub>) in CH<sub>2</sub>Cl<sub>2</sub> in an excellent yield of 96 %. In a final step according to Lamaty and co-workers,<sup>[234]</sup> the sulfonamide **141** was formed by treatment of **140** with gaseous ammonia, which gave the targeted H<sub>2</sub>NSES **141** after recrystallization in a good yield of 67 % (Scheme 4.17).



**Scheme 4.17.** Synthesis of trimethylsilyl ethylene sulfonamide (**141**, H<sub>2</sub>NSES) starting from vinyltrimethylsilane (**137**). (a) NaHSO<sub>3</sub>, MeOH, 80 °C, 72 h, 54 %; (b) PCl<sub>5</sub>, CH<sub>2</sub>Cl<sub>2</sub>, 0 °C→rt, 4 h, 96 %; (c) NH<sub>3</sub>, CH<sub>2</sub>Cl<sub>2</sub>, 0 °C, 3 h, 67 %.

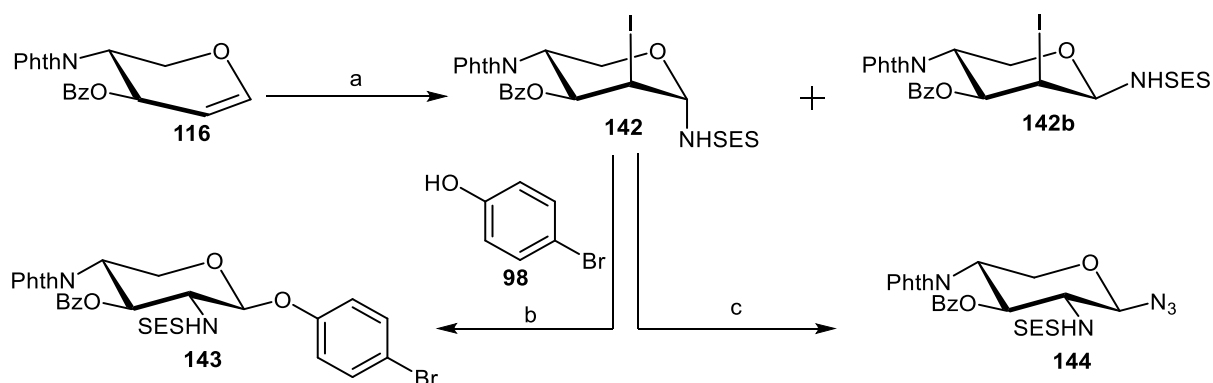
With the H<sub>2</sub>NSES **141** in hand, the iodosulfonamidation of xylal **116** was performed following a procedure of André and colleagues.<sup>[235]</sup> The xylal was reacted with **141** in the presence of IDCP at 0 °C for 1 h (Scheme 4.18). Unfortunately, the *cis*-addition product **142b** was formed in a yield of almost 80 % instead of the desired *trans*-addition product **142** as confirmed by <sup>1</sup>H NMR. Since the opening of the iodonium intermediate can only take place from the α-face

of the sugar ring (leading to **142**) the *cis*-product must be an epimerization product of **142** (cf. Scheme 4.12). In fact, it is known that epimerization of the anomeric sulfonamide can occur especially for armed glycals, which was described by Petillo and co-workers.<sup>[228]</sup> To avoid the formation of the  $\beta$ -lyxose product **142b**, first of all the temperature was decreased, and the reaction carried out at -20 °C for 1 h (Table 4.2). In fact, under these reaction conditions, the amount of formed  $\beta$ -lyxose **142b** was decreased and a mixture of both anomers (1.5:1) was isolated. Next, the reaction time was decreased<sup>[221]</sup> and **116** treated with H<sub>2</sub>NSES/IDCP at 0 °C for 30 min, which increased the selectivity for **142** significantly. Under these conditions, the targeted **142** was isolated in a yield of 85 % as the pure  $\alpha$ -lyxose anomer. Further decreasing of the reaction time led to lower yields (cf. Table 4.2). With **142** in hand, the glycosylation of 4-bromophenol was addressed next and in a rearrangement reaction iodosulfonamide **142** and 4-bromophenol **98** were treated with LiHMDS and AgOTf at -78 °C. The targeted diamino  $\beta$ -xyloside **143** was obtained in a high yield of 87 % and with an excellent  $\beta$ -stereospecificity and high regioselectivity of the amino function (Scheme 4.18).

**Table 4.2.** Optimization of the reaction conditions for the iodosulfonamidation of xylal **116** with H<sub>2</sub>NSES as depicted in Scheme 4.18. All reactions were carried out in dry CH<sub>2</sub>Cl<sub>2</sub> and 4 Å MS was added.

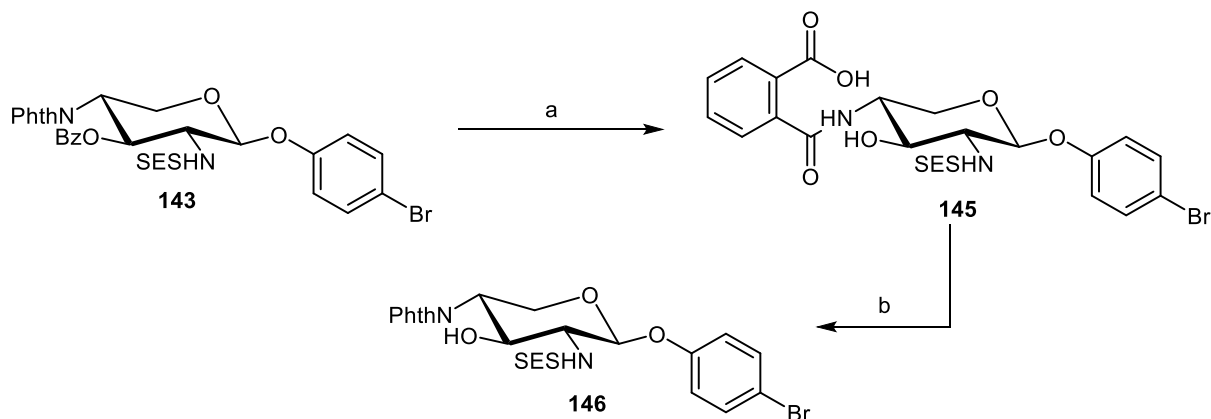
Entry	I <sup>+</sup> -source	Time	Temperature	Yield	$\alpha$ : $\beta$
1	IDCP	1 h	-20 °C	63 %	1.5 : 1
2	IDCP	1 h	0 °C	78 %	only $\beta$
3	IDCP	30 min	0 °C	85 %	only $\alpha$
4	IDCP	15 min	0 °C	55 %	only $\alpha$
5	NIS	30 min	0 °C	-	-

In addition to the  $\beta$ -selective glycosylation the iodosulfonamide **142** offered another synthetic advantage. According to Danishefsky's established iodosulfonazidation method, it was possible to introduce a third orthogonal amino function masked as an azide. Thus, **142** was treated with sodium azide in DMF and the triamine-xyloside **144** was obtained in a fair yield of 58 % (Scheme 4.18). This xylose scaffold offers the possibility to address each position chemoselectively to build up heteromultivalent glycoclusters, for example. In addition, the azido function can be used in CuAAC or Staudinger ligation chemistry for immobilization on surfaces, for instance.



**Scheme 4.18.** Synthesis of diamino xyloside **143** starting from xylal **116** (a)  $\text{H}_2\text{NSES}$ , IDCP,  $\text{CH}_2\text{Cl}_2$ ,  $0\text{ }^\circ\text{C}$ , 30 min, 85 %; (b) LiHMDS, AgOTf, THF,  $-78\text{ }^\circ\text{C}\rightarrow\text{rt}$ , 6 h, 87 %; (c)  $\text{NaN}_3$ , DMF, rt, 16 h, 58 %.

With xyloside **143** in hand, it was again tried to selectively deprotect the 3-O-benzoyl protecting group for further functionalizations. Thus, xyloside **143** was subjected to a transesterification reaction under Zemplén reaction conditions by treatment with sodium methoxide in methanol. Unfortunately, the phthaloyl protecting group was unstable under these conditions and the corresponding xyloside **145** was isolated in a high yield of 92 % (Scheme 4.19). To reinstall the phthaloyl by an intramolecular cyclization, **145** was treated with diisopropylcarbodiimide (DIC) and DMAP and the derivative **146** reached in a yield of 57 %.

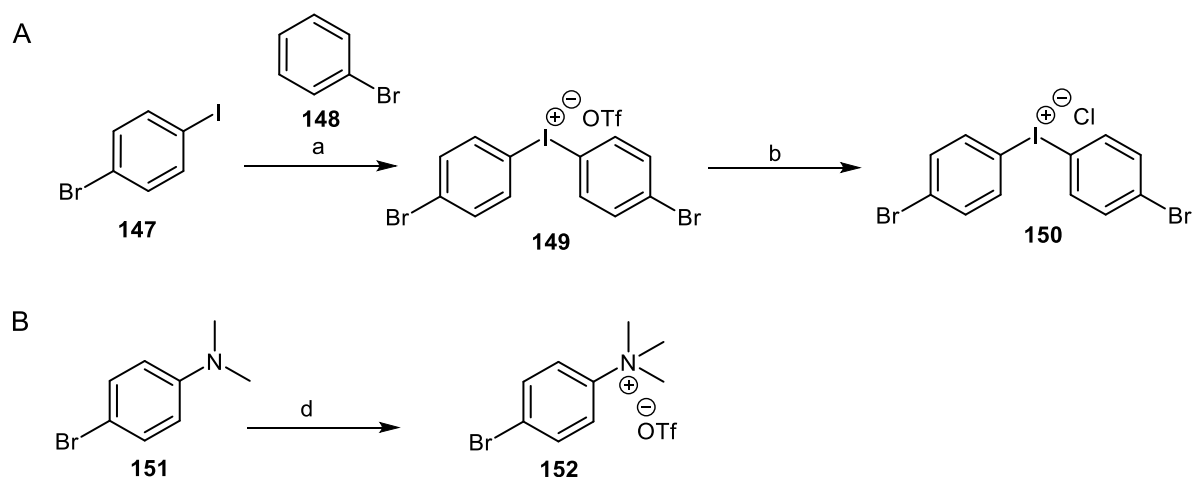


**Scheme 4.19.** Synthesis of xyloside **146** by debenzoylation and subsequent intramolecular ring closure of **143**. (a) NaOMe, MeOH, rt, 2 h, 92 %; (b) DIC, DMAP,  $\text{CH}_2\text{Cl}_2$ ,  $0\text{ }^\circ\text{C}$ , 16 h, 57 %.

With the xyloside **146** in hand, 3-OH group was addressed next in different functionalization reactions. The respective functional group at the 3-position had to fulfill two different aspects. On the one hand, an aromatic structure was envisaged, to support the conformational switch and stabilize the  ${}^1\text{C}_4$  conformation by  $\pi$ - $\pi$  interactions between the linkers at the 1- and 3-positions. Thus, like at the anomeric position an aromatic bromo derivative had to be implemented to build up enlarged aromatic biphenyl systems by Suzuki-Miyaura cross-coupling. On the other hand, it was planned to transfer the motion of the conformational xylosyl

hinge to the arms at the 1- and 3-position and it was decided to limit the degrees of freedom and arylate the 3-hydroxyl group with a 4-bromo phenyl residue. The *O*-arylation of carbohydrates is a challenging task in the aspects of regioselectivity, stereoselectivity and efficiency.<sup>[236]</sup> Often, the introduction of a phenyl ether to carbohydrates requires S<sub>N</sub>2 replacement, epoxide opening or Mitsunobu reactions, which leads to an inversion of the stereocenter.<sup>[237]</sup> Another approach is represented by the direct construction of the C(sp<sup>2</sup>)-O bond, which has the advantage to employ the sugar substrate without any further activation and gives the opportunity of a higher stereocontrolled functionalization. For these reactions a class of reactive electrophilic arylating reagents is needed. One class is represented by hypervalent iodine compounds. First Olofsson and co-workers showed that *O*-arylation of carbohydrate hydroxyl groups with hypervalent iodonium salts showed excellent stereochemistry (no inversion) and promising yields.<sup>[238]</sup> In addition, the basic arylation conditions are compatible with a range of functional groups and the arylating reagents are simple available.<sup>[239]</sup> In addition to the work of Olofsson the group of Niu showed that regioselective *O*-arylation of unprotected carbohydrates with hypervalent iodonium salts can be controlled by the addition of copper triflate (Cu(OTf)<sub>2</sub>).<sup>[240]</sup> Next to the class of hypervalent iodonium salts, another arylating reagent is represented by aryl ammonium salts. The group of Uchiyama showed that these reagents can arylate alcohols with a high stereo- and regioselectivity.<sup>[241]</sup> With the iodine and the ammonia salts two possibilities for the *O*-arylation of the 3-OH group of **146** were taken into account.

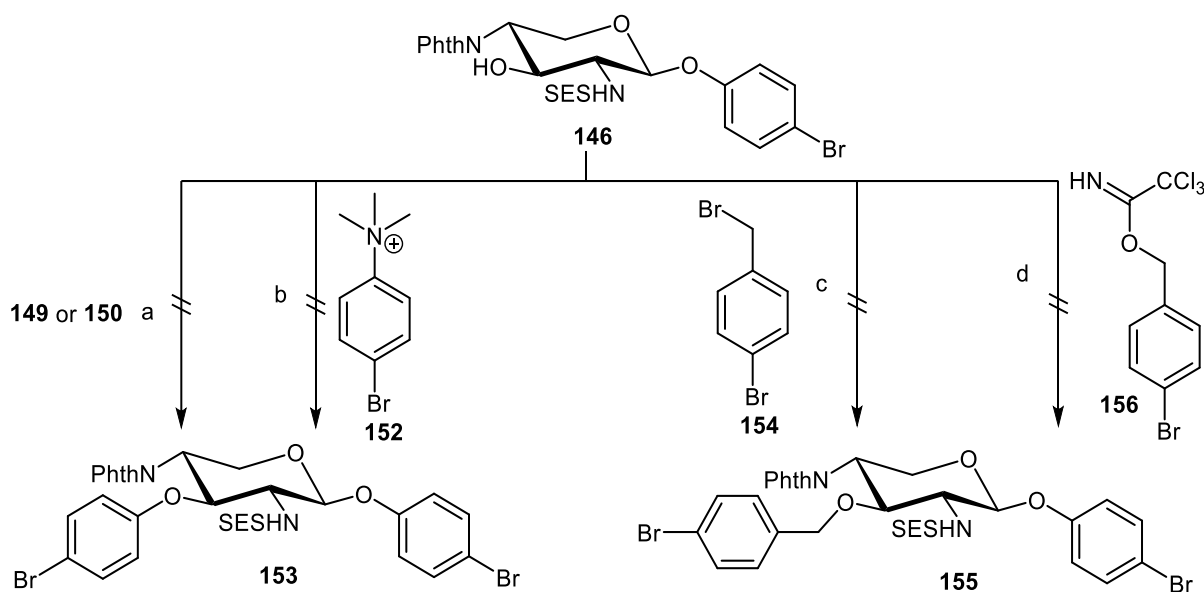
The synthesis of the iodonium salts was performed according to a procedure of Olofsson and co-workers starting from 4-iodo-bromobenzene (**147**).<sup>[242]</sup> In an oxidation reaction, **147** was reacted with bromobenzene **148** in the presence of *meta*-chloroperbenzoic acid (*m*CPBA), which gave oxidation to an iodine(III) species. By the addition of triflic acid (TfOH), **149** was precipitated as the iodonium triflate **149** in a yield of 70 %. As a second arylating reagent, the chloride salt **150** was synthesized. Thus, **149** was dissolved in acetonitrile and by the addition of an aqueous solution of ammonium chloride **150** was precipitated in a yield of 86 % (Scheme 4.20, A). For the arylation with ammonium salts, the trimethyl ammonium salt **152** was synthesized as a reagent. Following the procedure of Pees et al.,<sup>[243]</sup> 4-bromo-*N,N*-dimethylaniline (**151**) was treated with methyl trifluoromethane sulfonate (MeOTf) in CH<sub>2</sub>Cl<sub>2</sub> and **152** was obtained in a yield of 90 % (Scheme 4.20, B). With **149**, **150** and **152**, three reagents for the further arylation of **146** were available and had to be tested, respectively.



**Scheme 4.20.** Synthesis of arylating reagents **149**, **150** and **152**. (a) *m*CPBA, TfOH,  $\text{CH}_2\text{Cl}_2$ , rt, 1 h, 70 %; (b)  $\text{NH}_4\text{Cl}$ , MeCN, rt, 1 h, 86 %; (c) KBr, MeCN, rt, 1 h; (d) MeOTf,  $\text{CH}_2\text{Cl}_2$ , 0 °C, 1 h, 90 %.

For the arylation of the 3-OH group of xyloside **146**, first the hypervalent iodine reagents were tested. According to a procedure of Olofsson and co-workers,<sup>[238]</sup> **146** was treated with iodonium triflate **149** in the presence of  $\text{KO}^t\text{Bu}$  in toluene (Scheme 4.21). Unfortunately, under these conditions the targeted **153** was not formed but the formation of the *ortho*-carboxy amide **145** was observed. Also changing the counterion of the iodonium salt, by using **150**, did not change the outcome of this arylation reaction and **153** could not be achieved. Hence, according to a procedure of Wang et al., it was tried to functionalize the 3-OH group by treatment with trimethylammonium salt **152** in the presence of KHMDS. This reaction again, did not form **153** but instead a ring opening of the 4-phthaloyl group took place. It seemed that by deprotonation of the 3-OH group with a base, the corresponding alkoxide attacked the carbonyl function of the phthalimide leading to a transesterification and opening of the cyclic imide, respectively. To prove this, **146** was reacted in a Williamson etherification to install a benzyl group under basic conditions. Thus, **146** was treated with 4-bromo-benzyl bromide (**154**) and  $\text{K}_2\text{CO}_3$ . Nevertheless, also for this reaction no formation of xyloside **155** was observed, rather intramolecular phthalimide opening occurred.

In a last attempt, basic reaction conditions were avoided, and the etherification was performed with a trichloroacetimidate requiring acidic conditions. According to a procedure of Kinjo et al.,<sup>[244]</sup> **146** was treated with the literature-known trichloroacetimidate **156**<sup>[244]</sup>, which was activated by the addition of 0.3 equ. TfOH, but no conversion of the starting material **146** was observed. Equally, attempts to perform the reaction at higher temperatures or to activate the trichloroacetimidate **156** with TMSOTf did not lead to **155** (Scheme 4.21).

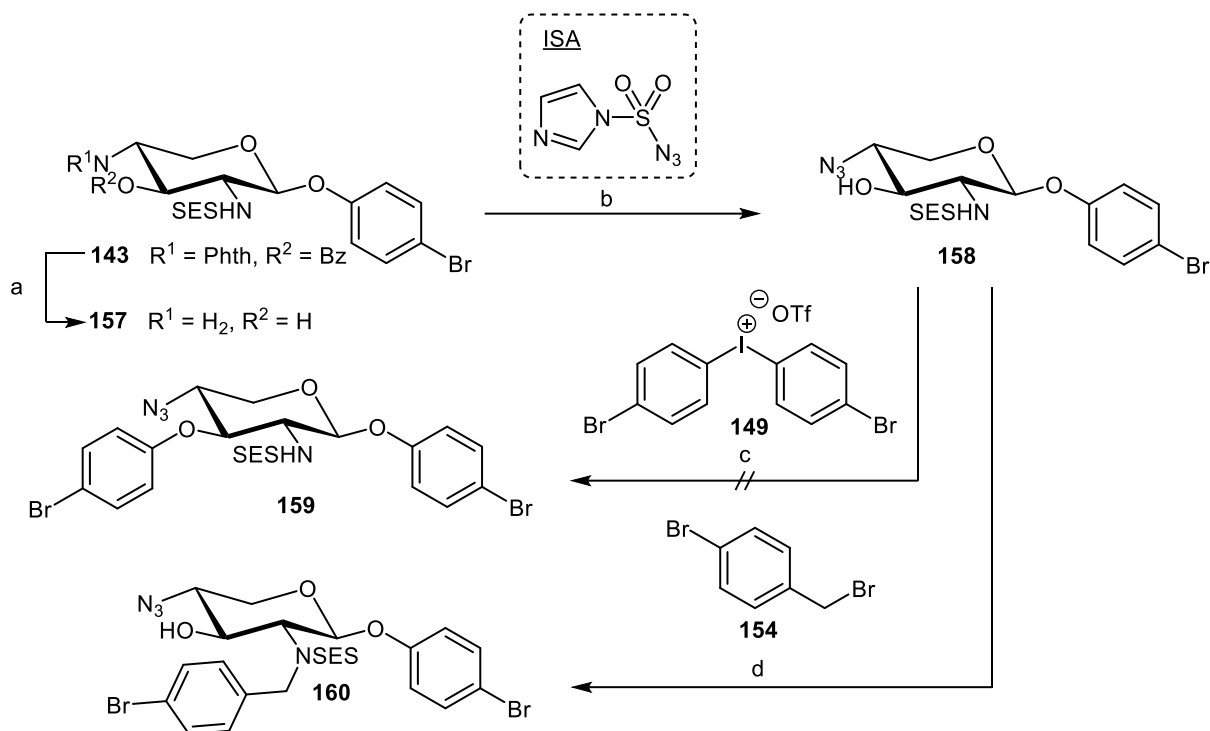


**Scheme 4.21.** Attempts to functionalize the 3-OH group of xyloside **146**. (a) KO<sup>t</sup>Bu, toluene, rt, 6 h; (b) KHMDS, THF, rt, 5 h; (c) K<sub>2</sub>CO<sub>3</sub>, DMF, 60 °C, 5 h; (d) TfOH, THF, 0 °C, 2 h.

To avoid the intramolecular opening of the phthalimido group, it was decided to remove the phthalimide protecting group and mask the corresponding free amine as an azide. Accordingly, the 3-*O*-benzoyl ester and the phthaloyl protecting group were removed by treatment of **143** with ethylenediamine (EDA) in EtOH at 70 °C and the unprotected xyloside **157** was obtained after column chromatography in an excellent yield of 90 % (Scheme 4.22). Subsequently treatment of **157** with ISA in the presence of K<sub>2</sub>CO<sub>3</sub> and catalytical amounts of CuSO<sub>4</sub> in MeOH gave the targeted azide **158** in a fair yield of 74 %. With this molecule in hand, further functionalization of the 3-position was tested keeping in mind to avoid intramolecular side reactions. First, *O*-arylation of the 3-OH group was performed with hypervalent iodine salts. When **158** was treated with the iodonium salt **149** in the presence of KO<sup>t</sup>Bu in toluene,<sup>[238]</sup> the arylated product **159** was not obtained. When the reaction was performed at higher temperatures (50 °C) or with an excess of the base (5 equivalents), no conversion was observed. In a second approach, *O*-arylation with aryl ammonium salt **152** was performed. But the reaction of **158** with aryl ammonium salt **152** in the presence of KO<sup>t</sup>Bu showed no formation of **159**. Also changing the base to KHMDS did not give the desired product (Scheme 4.22).

Furthermore, it was checked if either the functionalization of the 3-position under basic conditions prohibited, or if the problem lies in the arylation conditions. Accordingly, **158** was subjected to a Williamson etherification with the benzyl bromide derivative **154** in DMF in the presence of K<sub>2</sub>CO<sub>3</sub> at 60 °C and the formation of a product was observed. It turned out, that in this reaction not the 3-OH group was benzylated, but the sulfonamide was functionalized. The SES-*N*-bromobenzylated xyloside **160** was the only isolated product obtained in a high yield

of 86 % (Scheme 4.22). This result suggests that the NH-sulfonamide is the stronger nucleophile than the 3-OH group.



**Scheme 4.22.** Synthesis and functionalization of azidoxyloside **158** starting from xyloside **143**. (a) ethylenediamine, EtOH, 70 °C, 1.5 h, 90 %; (b) ISA, CuSO<sub>4</sub>, K<sub>2</sub>CO<sub>3</sub>, MeOH, rt, 16 h, 74 %; (c) KO<sup>t</sup>Bu, toluene, rt, 6 h; (d) K<sub>2</sub>CO<sub>3</sub>, DMF, 60 °C, 5 h, 86 %.

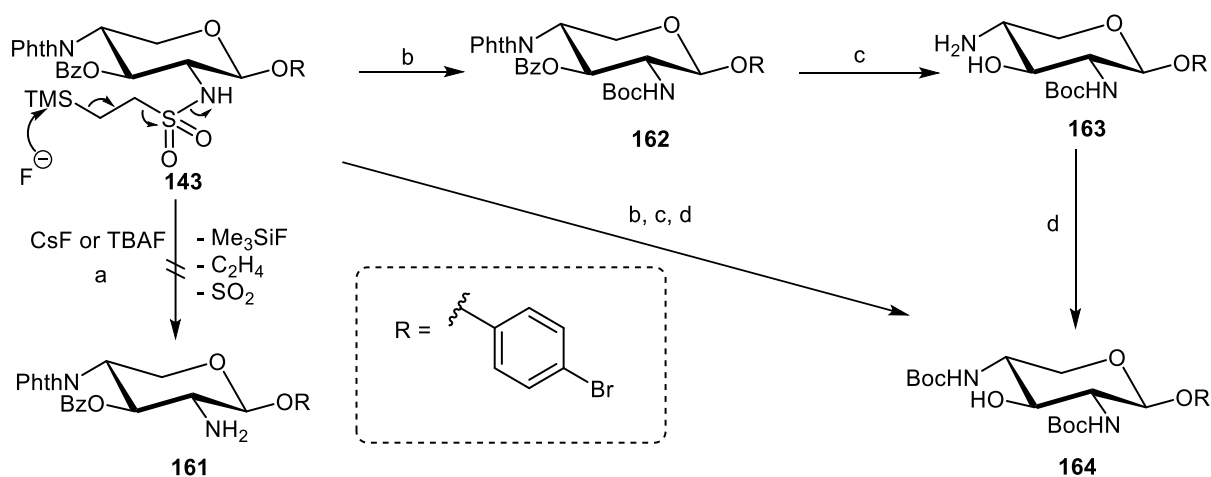
Owing to the fact that the 2-sulfonamide group is more nucleophilic than the 3-OH group, an alternative strategy for the removal of the SES-protecting group of **143** was sought. Furthermore, the respective free amine had to be protected with a protecting group, which is stable under basic modification conditions. Next, the 3-OH group had to be deprotected and the 4-phthalimide protecting group had to be exchanged in order to avoid intramolecular ring opening as described in Scheme 4.19.

In contrast to other sulfonamides the 2-(trimethylsilyl)ethanesulfonamide represents a protecting group, which can be cleaved with fluorides. Cleavage with fluorides produces volatile side products, namely fluorotrimethylsilane, ethylene and sulfur dioxide, which gives the free amine without any further workup. Fluoride attacks the fluorophilic silicon initiating  $\beta$ -elimination and producing the three gaseous side products (cf. Scheme 4.23).

The deprotection of **143** was performed according to a procedure of Danishefsky and co-workers,<sup>[218d]</sup> and **143** was treated with cesium fluoride in DMF at 90 °C in order to reach the free amine **161**. Unfortunately, this led to decomposition of the starting material and the formed side products could not be isolated. Attempts to carry the reaction out at 70 °C or 50 °C gave

the same results. In an approach to treat **143** with TBAF in THF at 70 °C again decomposition took place while at room temperature no conversion was observed (Scheme 4.23).

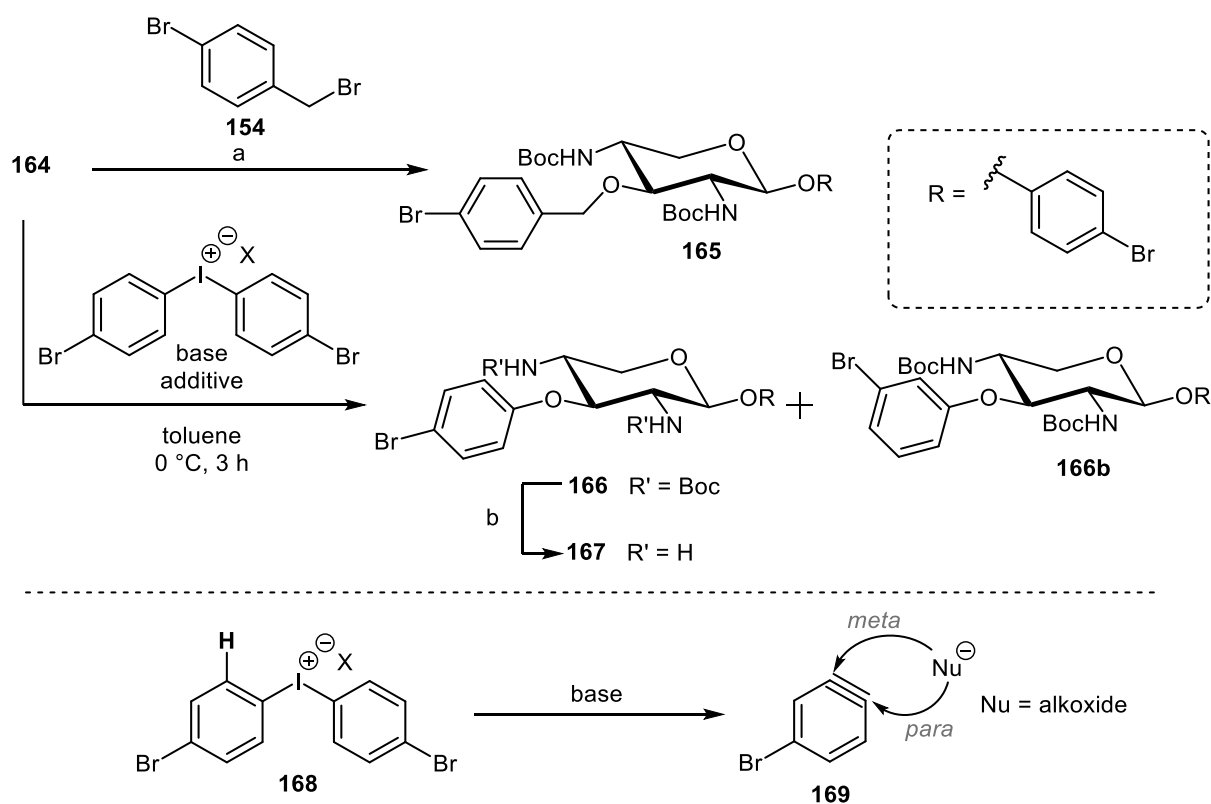
It is known that SES-protected primary amines show differences of reactivity during the deprotection step.<sup>[245]</sup> Especially the acylation of the SES-protected amine increases the reactivity for the deprotection step. The group of Kurt showed that neighbouring group-active ester functionalities can lead to unwanted side products but this can be avoided by derivatization with Boc protecting groups, which activate the SES-deprotection as well.<sup>[246]</sup> According to Kurt and co-workers, the deprotection of **143** was accomplished by treatment with  $\text{Boc}_2\text{O}$  and TBAF in THF (Scheme 4.23). This reaction gave the Boc-protected amino xyloside **162** in an excellent yield of 96 %. With this derivative in hand, next the 3-benzoyl and the 4-phthaloyl protecting groups were concomitantly cleaved by treating **143** with hydrazinium hydrate to achieve the unprotected xyloside **163** in a fair yield of 57 %. In a final step, the 4-amino group of **163** was protected with a protecting group, which is stable under basic conditions providing a uniform protecting group pattern of the xyloside. Thus, treatment of **163** with  $\text{Boc}_2\text{O}$  in the presence of triethylamine gave selective Boc protection of the 4-amino group in an excellent yield of 96 %. It has to be mentioned that the three steps leading from **143** to **164** can be carried out without any intermediate purification steps. Following this procedure **164** was synthesized from **143** in a yield of 86 % over three steps (Scheme 4.23).



**Scheme 4.23.** Synthesis of xyloside **164** starting from xyloside **143**. (a) Fluorides, dry  $\text{CH}_2\text{Cl}_2$ , rt, 16 h; (b)  $\text{Boc}_2\text{O}$ , TBAF, THF, rt, 2 h, 96 %; (c)  $\text{N}_2\text{H}_4 \cdot \text{H}_2\text{O}$ , EtOH, 70 °C, 2 h, 57 %; (d)  $\text{Boc}_2\text{O}$ , Et<sub>3</sub>N, THF,  $\text{H}_2\text{O}$ , rt, 2 h, 96 %; from **143** to **164** without isolation of the intermediates 86 % over 3 steps.

In order to validate if **164** is stable under basic conditions an etherification was performed. Thus, **164** was treated with the benzyl bromide **154** in the presence of NaH in DMF and the corresponding benzylated xyloside **165** was isolated after column chromatography in a moderate yield of 44 %. Nevertheless, this result proved that a general functionalization of the 3-position under basic conditions was possible (Scheme 4.24).

Accordingly, the *O*-arylation of xyloside **164** was performed with iodonium triflate **149** in the presence of  $\text{KO}t\text{Bu}$  in toluene at  $0\text{ }^\circ\text{C}$  giving the arylated product **166** in a fair yield of 53%. However, NMR spectroscopy showed that the product was a mixture of regioisomers. In addition to the *para*-bromo-arylated product **166**, also the *meta*-product **166b** (*para:meta* ratio 96:4) was formed and it was not possible to separate the regioisomers by column chromatography (Scheme 4.24). The formation of the *meta*-arylation product is known as a side reaction for *O*-arylation reactions.<sup>[239d]</sup> The fact that the proton next to the iodine in **168** is slightly acidic, favors an elimination reaction leading to the aryne **169** as a reactive intermediate.<sup>[247]</sup> This aryne can be attacked by a nucleophile (e.g. carbohydrate alkoxide) with a poor regioselectivity either at the *para*- or the *meta*-position, respectively (Scheme 4.24).



**Scheme 4.24.** Functionalization of the 3-position of **164** by benzylation or *O*-arylation. Aryne formation can take place as a side reaction giving regioisomeric mixtures (bottom). Acidic deprotection of the Boc-protecting groups gives diamino xyloside **167**. (a)  $\text{NaH}$ , DMF,  $0\text{ }^\circ\text{C} \rightarrow \text{rt}$ , 2 h, 44 %; (b) TFA,  $\text{CH}_2\text{Cl}_2$ , rt, 16 h, 92 %.

In order to regioselectively achieve the xyloside **166** and avoid aryne formation, the reaction was optimized. First, the arylation was carried out with iodonium chloride **150** as the arylating source to increase the reactivity of the arylating reagent (Table 4.3, entry 2). However, again a regioisomeric mixture of **166** and **166b** (*para:meta* ratio 92:8) was isolated in a yield of 61%. Next, the choice of the base was investigated (Table 4.3, entry 3-5), but the arylation of **164** with iodonium triflate **149** in the presence of sodium hexamethyldisilazane ( $\text{NaHMDS}$ ) or

$K_2CO_3$  was not successful and no conversion to **166** was observed. An additional attempt with iodonium chloride **150** and  $K_2CO_3$  gave again a regioisomeric mixture (*para:meta* ratio 93:7) in a yield of 41 %. Since the optimization of the base or the arylating reagent did not show an improvement for the arylation of **164**, it was tried to trap the formed aryne intermediate before a *meta*-arylation can take place. Hence, an additive in form of an aryne scavenger was added to the reaction mixture. It is known that amines are potential scavengers because they react with arynes but are not easily arylated.<sup>[248]</sup> Accordingly piperidine was added in sub-stoichiometric amounts and KOtBu was used as the base. Indeed, the formation of **166b** was inhibited and the *para*-substituted **166** was formed as the sole regioisomer and isolated in good yield of 58 % after column chromatography (Table 4.3, entry 6).

**Table 4.3.** Optimization of the reaction conditions for the *O*-arylation of the 3-position of **164** to reach **166** as depicted in Scheme 4.24. All reactions were carried out in toluene at 0 °C. The ratio between *para* and *meta* substituted product was determined by NMR-spectroscopy.

Entry	X <sup>-</sup>	Base	Additive	<i>para:meta</i> (166:166b)	Yield
1	OTf	KOtBu	-	96 : 4	53 %
2	Cl	KOtBu	-	92 : 8	61 %
3	OTf	NaHMDS	-	-	-
4	OTf	$K_2CO_3$	-	-	-
5	Cl	$K_2CO_3$	-	93 : 7	41 %
6	OTf	KOtBu	piperidine	100 : 0	58 %

Interestingly, the <sup>1</sup>H NMR spectra of the bis-Boc-protected xylosides **164**, **165**, and **166** suggested the presence of a conformational equilibrium by signal line broadening in various solvents. According to the fact that xylose is a conformationally flexible molecule, it was of interest to study the conformational features and dynamics of xylosides **164**, **165**, and **166**. This work is described in chapter 5.

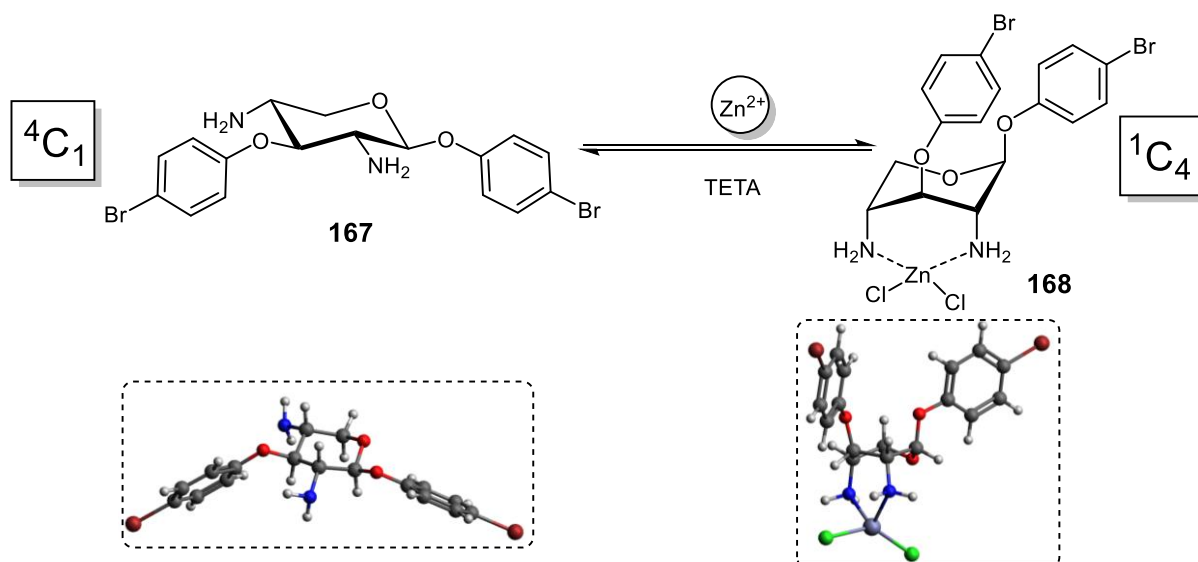
In a final step towards 2,4-diamino xylosides, the Boc protecting groups had to be removed. Thus, **166** was treated with TFA in  $CH_2Cl_2$  and in order to gain free amino groups the reaction solution was neutralized with ion exchange resin Amberlyst 21,<sup>[249]</sup> and the diamino xyloside **167** was purified by column chromatography and isolated in a yield of 72 % (Scheme 4.24).

Finally, after extensive investigations, the 2,4-diamino xyloside **167** was successfully obtained. In this synthesis, xylal derivatives serve as perfect key intermediates. The described synthetic

route starting from L-arabinose (**85**) comprises 9 steps delivering the unprotected diamino xyloside **167** in an overall yield of 9 %. Here, iodosulfonamidation of functionalized xylosides serves as the method of choice for the synthesis of 2,4-diamino xylosides. The beauty of this synthetic pathway lies in its convincing stereo- and regiochemistry and satisfying yields and it shows tolerance to a wide range of functional groups.

#### 4.4 2,4-Diamino xylosides as conformational switches

With the 2,4-diamino xyloside **167** in hand, it was of interest whether it is conformational switchable in a reversible fashion and thus suitable as a molecular switch. As described before, 2,4-diamino xylosides serve as ligands for either metal(II) ions or can complex protons.<sup>[90, 92b]</sup> In both cases a conformational ring flip from the thermodynamically more stable  ${}^4C_1$  to the less stable  ${}^1C_4$  conformer occurs and the orientation of all substituents changes from equatorial to axial. The formation of metal-xylose complexes using various metal cations was studied by NMR spectroscopy in different solvents (Scheme 4.25). Additionally, the association energy of the xyloside ligand **167** with zinc chloride ( $ZnCl_2$ ) was calculated at a B3LYP-D3/def2-TZVPP level of theory (computational experiments were performed by Prof. Dr. Alexander A. Auer (MPI Mülheim)) which confirmed that the complexation is exothermic by more than 90 kJ/mol. This result predicted the formation of complex **168** in high yields and with a short reaction time.



**Scheme 4.25.** Conformational switching of **167** by the addition of an external stimulus (zinc). The xylose ligand **167** undergoes a conformational transition from  ${}^4C_1$  to  ${}^1C_4$ , which is reversible. Complexation:  $ZnCl_2$ ,  $MeCN-d_3$ , rt; Backswitching: TETA,  $MeCN-d_3$ , rt. TETA: triethylenetetramine. Optimized conformations of **167** and **168** (B3LYP-D3/def2-TZVPP, see computational details for protocol using CREST<sup>[250]</sup> conformational search protocol) and rendered using Avogadro color code: dark grey: carbon; red: oxygen; blue: nitrogen; white: hydrogen; dark red: bromine; green: chloride; grey: zinc.

First, zinc(II) complexes were formed. Zinc(II) cations can exist with a tetragonal complexation geometry and are known as metal ions which are complexed by diamino xylosides. When to a solution of **167** in acetone- $d_6$  0.5 equiv. of zinc chloride ( $ZnCl_2$ ) were added, the conformational change was initiated as followed by  $^1H$  NMR spectroscopy at room temperature (Figure 4.8). It was observed that immediately in addition to the signal set of **167** a second set of pyranose protons occurred in a 1:1 ratio. For the new set of signals, small coupling constants were observed leading to singlets, which is an indication for the  $^1C_4$  structure. All new signals could be assigned to the corresponding ring protons, and it was shown that by complexation of zinc a downfield shift of all signals took place. By the addition of further 0.5 equiv. of  $ZnCl_2$  to the solution full conversion of the  $^4C_1$  conformer **167** to the  $^1C_4$  complex **168** proceeded. In order to test the system for reversibility an excess of triethylenetetramine (TETA) was added, which is a stronger chelating ligand and the zinc precipitated as the Zn-TETA complex. Furthermore, the xyloside ligand **167** was liberated with inverted  $^4C_1$  conformation. Besides the two species **167** and **168**, various other small signals (at 5.5 ppm and 4.4 ppm) were detected in the NMR spectrum, which can be assigned to the fact that free amines in acetone can form imines as side products. Accordingly, to get more information about the structure of the complexed xylose ligand the formation of **168** had to be observed in different solvents.

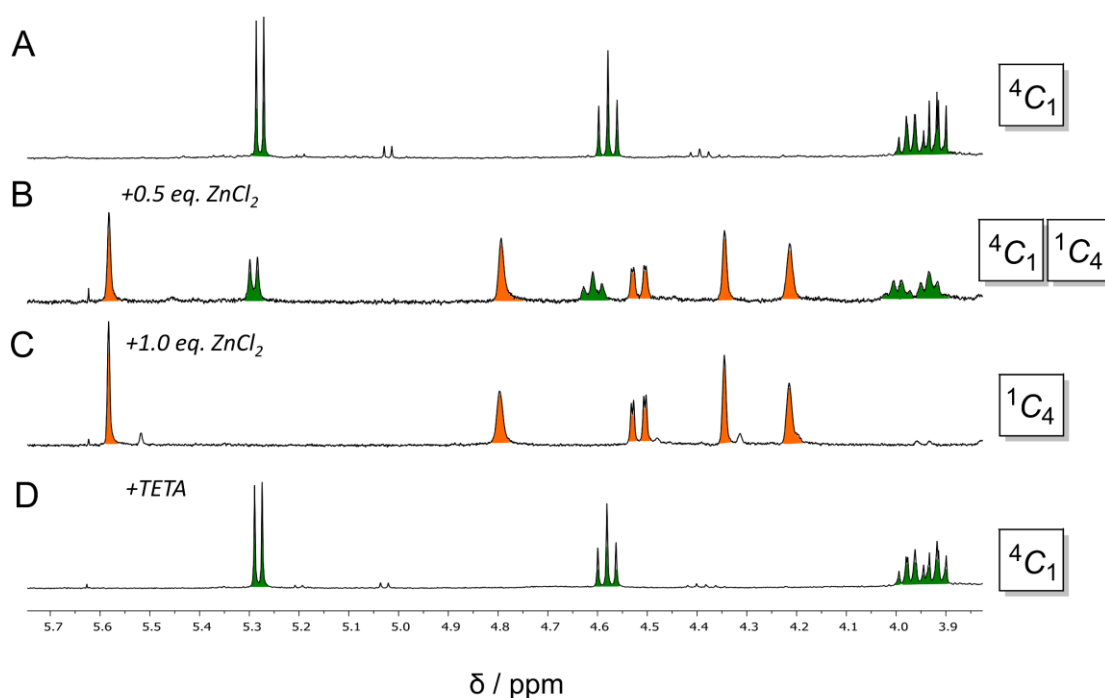


**Figure 4.8.** Switching ability of **167** by the addition of  $ZnCl_2$  in acetone. The free ligand **167** proved  $^4C_1$  conformation (A). By addition of 0.5 equiv. of  $ZnCl_2$  complex **168** was formed (B), which was the only species after addition of 1.0 equiv. of  $ZnCl_2$  (C). Backswitching was achieved by addition of TETA (D).  $^1H$  NMR spectra (acetone- $d_6$ , 500 MHz, 298 K, 0.01 M). Protons were assigned by COSY and HSQC. Color code: green: signal set of **167**; orange: signal set of **168**.

The complexation of zinc with **167** was further proceeded in deuterated acetonitrile (MeCN- $d_3$ ). Thus, **167** was dissolved in MeCN- $d_3$  and  $^1\text{H}$  NMR spectroscopy revealed that no imine side products were formed. Next, 1 equiv. of  $\text{ZnCl}_2$  was added to the solution and it was observed that the conformation of the xyloside ligand changed into the  $^1\text{C}_4$  conformer **168**. In accordance with the calculated association energy the complex was formed fast (less than 1 min). NMR spectroscopy for **168** indicated a  $^1\text{C}_4$  conformation due to small coupling constants (almost singlet signals) because all ring protons are equatorial orientated. Furthermore, the spectrum showed a slight downfield shift for all ring protons (Figure 4.9). In addition, the presence of **168** with two chloride ligands for the zinc ion was confirmed by ESI mass spectrometry. However, with **168** in hand the reversible backreaction was targeted to prove the switching ability of **167**. Thus, by the addition of TETA zinc precipitated, and the free xylose ligand **167** underwent a ring flip to the  $^4\text{C}_1$  conformation, respectively. Both reactions, the complexation and the backswitching, proceeded in quantitative yields, which makes **167** a suitable candidate as a molecular switch.

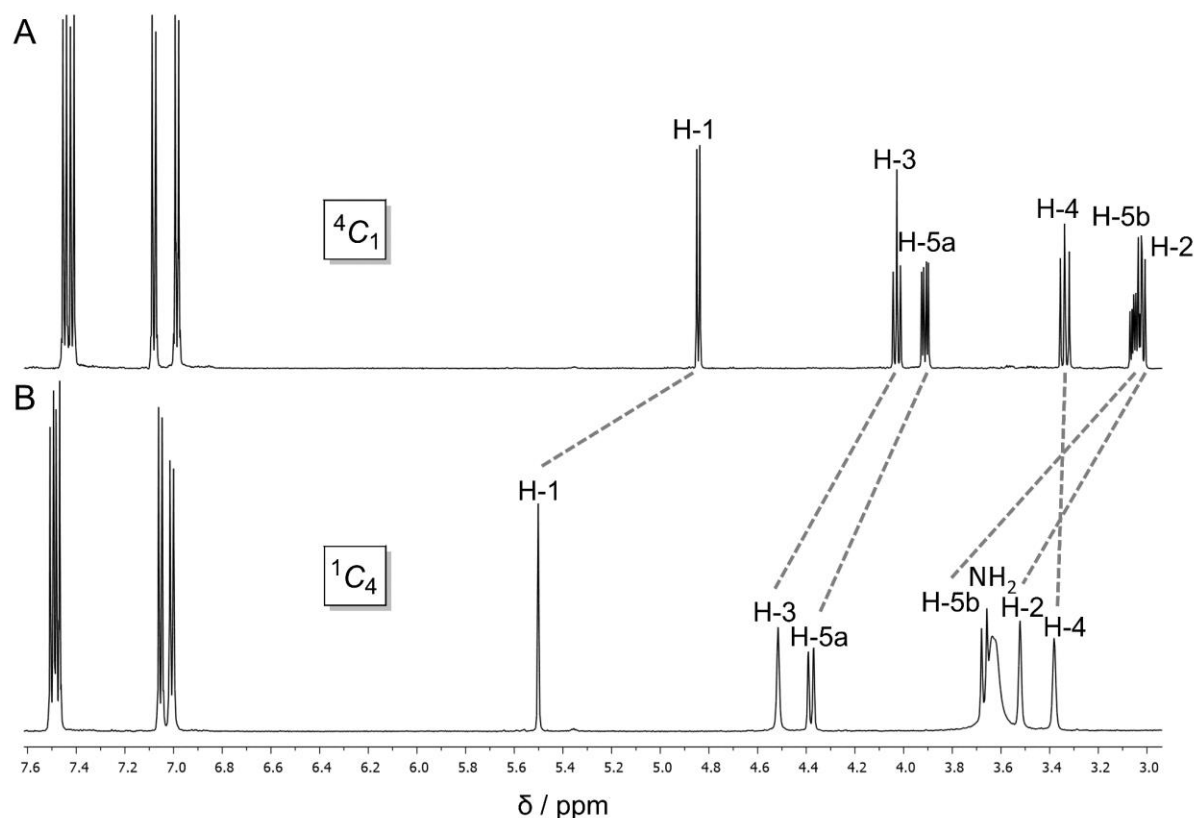
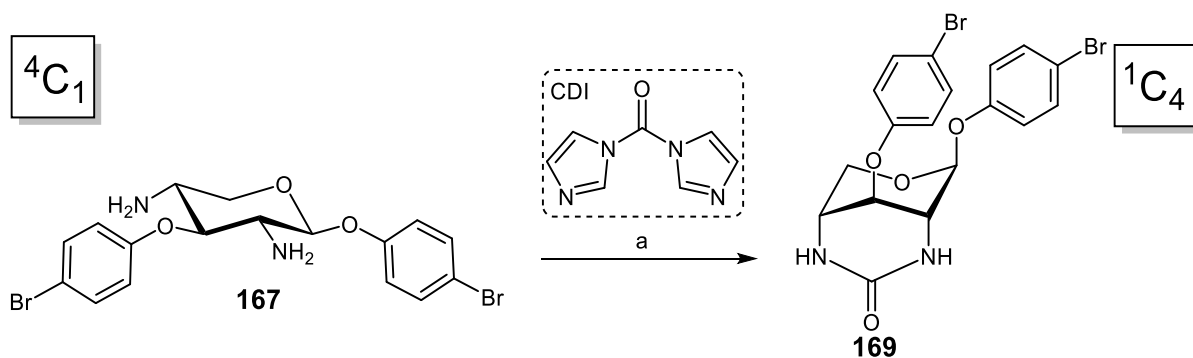


**Figure 4.9.** Conformational switching of **167** by the addition of  $\text{ZnCl}_2$  in MeCN. The free ligand **167** proved  $^4\text{C}_1$  conformation (A). By addition of 1.0 equiv. of  $\text{ZnCl}_2$  complex **168** was formed (B)  $^1\text{H}$  NMR spectrum (MeCN- $d_3$ , 500 MHz, 298 K, 0.01 M). Protons were assigned by COSY and HSQC. The signals of the  $\text{NH}_2$  groups in **167** (spectrum A) are buried under the solvent signal (water in  $\text{CD}_3\text{CN}$  at  $\sim 2.17$  ppm, not shown).

Besides  $\text{ZnCl}_2$  the switching ability of **167** was also tested with other zinc salts. However, the addition of zinc acetate ( $\text{Zn}(\text{OAc})_2$ ) or zinc triflimide ( $\text{Zn}(\text{N}(\text{Tf})_2)_2$ ) to solutions of **167** in  $\text{MeCN-d}_3$  were not leading to a ring flip induced by complexation of the metal. Also, other diamagnetic metal ions were tested for conformational switching. However, complexation of manganese perchlorate ( $\text{Mn}(\text{ClO}_4)_2$ ) or mercury acetate ( $\text{Hg}(\text{OAc})_2$ ) was not successfully at room temperature. Yuasa and Hashimoto describe the complexation process for these metal cations as relatively slow and with low yields and complexes could only be formed at higher temperatures.<sup>[90-91]</sup> Thus, experiments with manganese and mercury ions were performed at higher temperatures (328 K) but a ring flip of the xyloside ligand **167** could not be observed and thus these metals seem not to be suited for conformational switching.

In addition to the prove as a molecular switch the zinc complex **168** served also as a stable  $^1\text{C}_4$  conformer and defined conformation to study conformational dynamics of xylosides. To get more insights about different conformations of xylosides and their behavior of transition into each other it was necessary to synthesize additional xylose derivatives with defined conformation. Thus, in order to decrease the degrees of freedom diamino xyloside **167** was fixed into its  $^1\text{C}_4$  conformation by an intramolecular crosslinking of the diamino groups of the xyloside. Following a procedure of Fröhlich and co-workers,<sup>[251]</sup> **167** was treated with 1,1'-carbonyldiimidazol (CDI) in the presence of triethylamine in DMF to yield the desired bicyclic urea xyloside **169** in a good yield of 81 % (Scheme 4.26).



**Scheme 4.26.** Locking of the  $^1\text{C}_4$  conformation of **169** by cyclic urea formation. (a) CDI,  $\text{Et}_3\text{N}$ , DMF, rt, 16 h, 81 %. Abbreviation: CDI: carbonyldiimidazole.

The  $^1\text{C}_4$  conformation of **169** was confirmed by  $^1\text{H}$  NMR spectroscopy due to the small coupling constants of the ring protons (2-3 Hz, almost singlets). The conformational ring flip also induced a downfield shift of the ring protons, which was especially high for the ring protons next to the urea function (H-2, H-3, and H-4 by  $\sim 0.7$  ppm) (Figure 4.10). By comparison of the NMR spectra of **168** and **169**, similarities in the change of coupling constants and the chemical shift were observed. Thus, both compounds served as benchmarking molecules for a structural investigation of xyloside conformers.

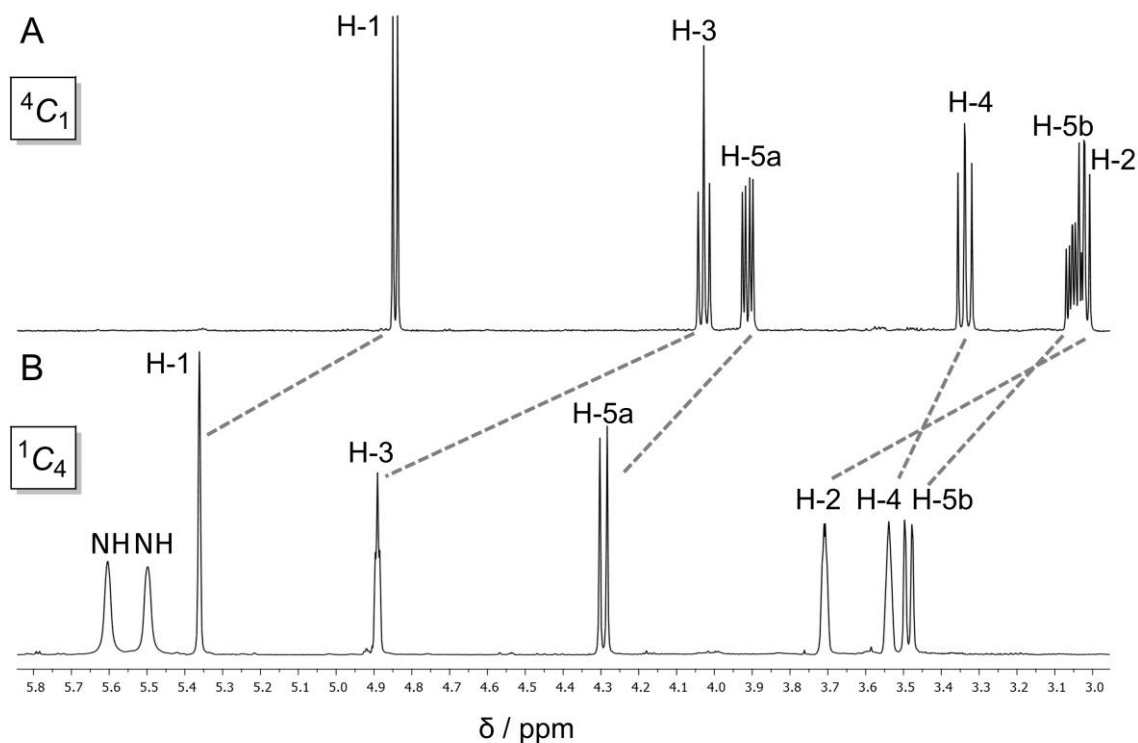


**Figure 4.10.** Conformational locking of the diamine **167** (A) by a bicyclic urea formation to yield the urea derivative **169** (B), where the  ${}^1C_4$  conformation was locked.  ${}^1H$  NMR spectrum (MeCN- $d_3$ , 500 MHz, 298 K, 0.01 M). Protons were assigned by COSY and HSQC. The signals of the  $NH_2$  groups in **167** (spectrum A) are buried under the solvent signal (water in  $CD_3CN$  at  $\sim 2.17$  ppm, not shown).

## 4.5 Conclusion

In conclusion of this subproject a new synthetic approach for the synthesis of 2,4-diamino xylosides was introduced. While previous synthetic accounts via a tandem ring opening of Černý epoxides are limited owing to their regio- and stereochemical outcome, xylals turned out as the intermediate of choice. Starting from L-arabinose, 4-amino-functionalized D-xylose derivatives such as **114** can readily be accessed and turned into difunctional xylals as **116**. Iodosulfonamidation and the following rearrangement of the 2-iodo lyxosyl sulfonamide **142** provide access to a wide range of orthogonally protected 2,4-diamino xylosides with a high regio- and stereospecificity. Furthermore, the number of reaction steps was decreased compared to previous pathways and the reaction conditions are tolerant to a wide range of protecting groups.

In addition, a surprising conformational dynamic was observed with the bis-Boc-protected diaminoxylosides **164**, **165** and **166**.  ${}^1H$  NMR spectra suggested a conformational equilibrium owing to the observed signal line broadening. On the other hand, the unprotected 2,4-diamino xyloside **167** proved to exist in the  ${}^4C_1$  conformation only and by complexation of zinc cations

a conformational switch from the  ${}^4C_1$  to the  ${}^1C_4$  conformation occurred. This ring flip is reversible by precipitation of the zinc, which makes **167** an ideal target for the use as a molecular switch.

The xylosides **167**, **168**, and **169** were presenting defined conformations and can be utilized as benchmarking molecules in following experiments to analyze the conformational equilibrium of the bis-Boc protected **166**.

## 5 Solvent-dependent conformational equilibria and their analysis

The synthetic bis-*N*-Boc protected xylosides **164**, **165**, and **166** (cf. chapter 4) apparently exist as dynamic equilibria between several conformations, as suggested by NMR analysis. In particular, the  $^1\text{H}$  NMR spectra of **166** are strongly dependent on the solvent in which they are conducted (Figure 5.1). The conformational dynamic of functionalized diamino xylosides hence depends on the environment (solvent). However, determination of the precise distribution for conformers of **166** in solution was not possible for two reasons: (i) the missing knowledge about the nature of conformers occurring in solution and (ii) the missing information about the coupling constants of the pure conformers (Figure 5.1).

However, the fact that the conformations of 2,4-diamino xylosides are in addition by the complexation with metal ions controllable by solvent parameters was of significant interest. Thus, for the investigation of the conformational behavior of **166** in solution a toolbox for conformational analysis had to be set up (Figure 5.1). Thus, in addition to NMR spectroscopy, the conformational analysis was assisted by computational methods. They offer the potential to predict the occurrence of conformers in solution and furthermore coupling constants can be computed to analyse conformational equilibria. This work was performed in a collaboration with Prof. Dr. Alexander A. Auer (MPI, Mülheim).

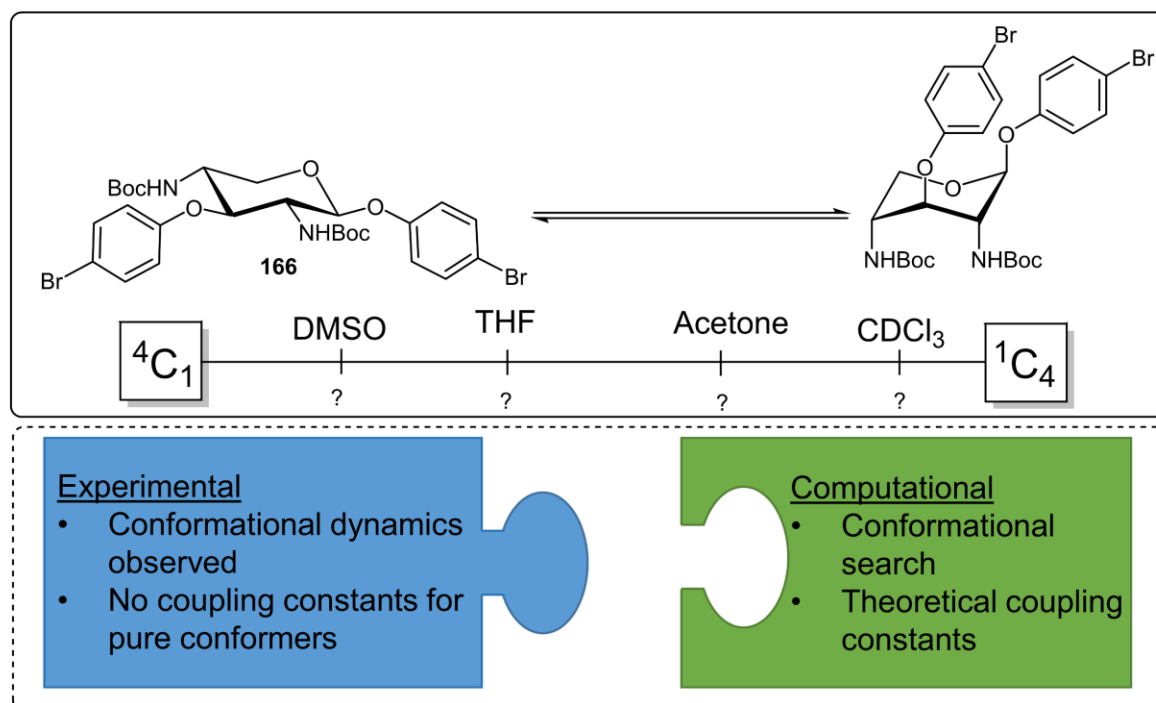


**Figure 5.1.** Diamino xyloside **166** occurs in a conformational equilibrium in various solvents. For the further investigation of the conformational behavior in different environments an analytical toolbox is needed, which combines experimental and computational approaches.

Before it was possible to study conformational equilibria of xylosides in solution, benchmarking data were required. On the one hand, coupling constants of defined conformations had to be determined by NMR spectroscopy in order to know the NMR data of occurring conformers. On the other hand, a theoretical approach was required to predict coupling constants of unknown conformers which cannot be isolated in pure form.

### 5.1 Determination of coupling constants to describe conformations

The conformational shape (pucker) of pyranosides parallels with the size of  $^3J_{H,H}$  coupling constants of the ring protons of the sugar ring. While the xyloside **166** suggested the presence of a conformational equilibrium in different solvents, the diamino xylosides **167**, **168**, and **169** explicitly exist as one conformer only. Whereas the diamine **167** exists in the  $^4C_1$  conformation, the xylosides **168** and **169** are locked in the  $^1C_4$  conformation either by zinc complexation or as cyclic urea derivative.

For the detailed structure analysis of the three compounds **167**, **168**, and **169**, it was necessary to determine the ring proton coupling constants. Several NMR techniques are available for the determination of coupling constants. In addition to  $^1H$  NMR spectroscopy also correlated NMR experiments can measure vicinal or geminal proton couplings. In  $^1H$ - $^1H$ -COSY spectroscopy, cross peaks give information about spin-spin couplings between protons or other nuclei. However, precise coupling constants cannot be determined this way, whereas this is different in double quantum filtered COSY spectroscopy (DQF-COSY), which is a phase sensitive method.<sup>[252]</sup> By employing a third pulse in a DQF-COSY experiment, a selection takes place, which selects only singlet signals that existed as double-quantum coherence between the first pulses. All other signals are canceled, and as a consequence the overlay of diagonal peaks is decreased and from the cross peaks coupling constants can be determined.<sup>[253]</sup>

For the xylosides **168** and **169** coupling constants could not be measured by  $^1H$  NMR spectroscopy. DQF-COSY experiments were employed to determine coupling constants from the cross peaks to provide a full characterization of the  $^1C_4$  conformers (Figure 5.2 for the example of **169**).

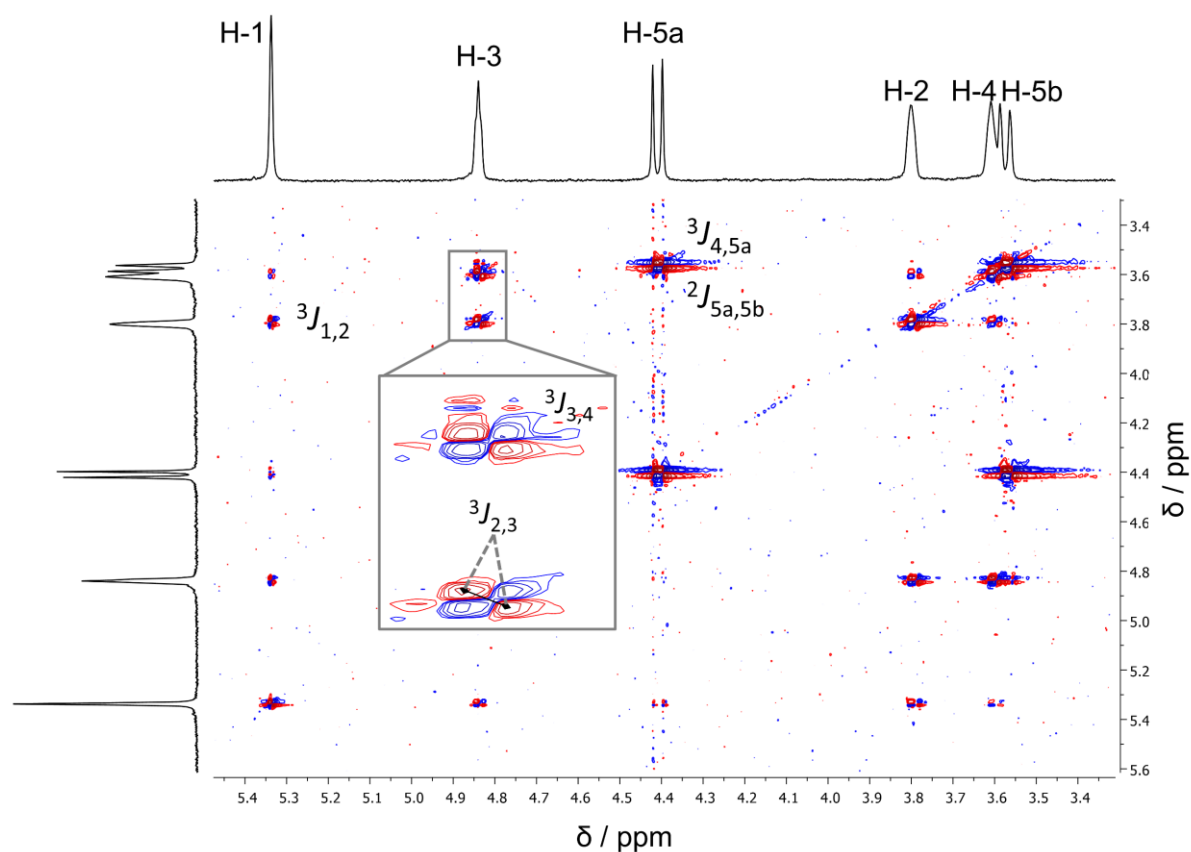


**Figure 5.2.** Determination of coupling constants of <sup>1</sup>C<sub>4</sub> xyloside **169** by DQF-COSY spectroscopy (500 MHz, MeCN-d<sub>4</sub>, 298 K). Signals with a positive sign are red; negative signs are blue.

The determined coupling constants of **168** and **169** are collected in Table 5.1 and show once again that <sup>3</sup>J coupling constants of the <sup>1</sup>C<sub>4</sub> xylosides are relatively small (1.6-3.9 Hz). Only the <sup>2</sup>J coupling constant for the CH<sub>2</sub> group is high (12-13 Hz) as expected. Additionally, for compound **167** coupling constants were determined by <sup>1</sup>H NMR spectroscopy (Table 5.1). Measurements in different solvents proved the conformational stability (variation of coupling constants less than 1 Hz) and coupling constants typical for a <sup>4</sup>C<sub>1</sub> conformation were measured.

**Table 5.1.** NMR-experiments for xylosides **167**, **168** and **169**. were measured in different solvents. For the determination of the coupling constants (in Hz)  $^1\text{NMR}$  or COSY-DQF experiments at different temperatures were performed.

Xyloside	Solvent	$J_{1,2}$	$J_{2,3}$	$J_{3,4}$	$J_{4,5a}$	$J_{4,5b}$	$J_{5a,5b}$
<b>167</b>	DMSO- $d_6$	7.44	8.93	8.93	5.00	10.73	11.54
<b>167</b>	acetone- $d_6$	7.64	9.20	9.20	n.d	n.d	n.d
<b>167</b>	$\text{CDCl}_3$	7.60	9.05	9.05	4.76	9.79	11.38
<b>167</b>	MeCN- $d_3$	7.52	9.06	9.06	5.03	10.22	11.66
<b>168</b>	MeCN- $d_3$	2.80	3.89	3.18	1.67	1.90	12.0
<b>169</b>	MeCN- $d_3$ (328 K)	2.18	3.54	3.90	2.24	2.83	13.0

With the determination of coupling constants of xylosides **167**, **168** and **169**, a sufficient basis to benchmark computational results against measured spin-spin coupling constants was available. Next, a computational method was employed to describe conformers of xylosides reliably. For the computation of the spin-spin coupling constants of **167**, **168** and **169**, various DFT functionals were tested for their accordance with the experimental results. For the investigation, the generalized gradient approximation (GGA) functionals PBE<sup>[254]</sup> and TPSS<sup>[255]</sup> were taken into account, as well as the hybrid functionals TPSSH,<sup>[256]</sup> PBE0<sup>[254, 257]</sup> and B3LYP.<sup>[258]</sup> First, coupling constants of **167** were calculated by employing the different functionals on a DFT/pc-J3 level of theory. Calculations with PBE revealed a good accordance with the experimental results (RMSD = 0.33). Coupling constants calculated with TPSS and TPSSH gave to high values for  $^3J$  couplings and too low values for the  $^2J_{5a,5b}$  coupling. The hybrid functionals PBE0 or B3LYP did not show a more precise accordance than PBE and hence cannot describe the  $^4C_1$  conformation of **167** satisfactory (Table 5.2).

**Table 5.2.** Computational and experimental spin-spin coupling constants (computed at the DFT/pc-J3 level of theory) for **167**. All values given in Hz.

	Exp. (DMSO-d <sub>6</sub> )	PBE	PBE0	TPSS	TPSSH	B3LYP
$J_{1,2}$	7.44	7.48	7.90	9.63	9.71	8.24
$J_{2,3}$	8.93	9.38	9.80	12.00	12.06	10.30
$J_{3,4}$	8.93	9.01	9.54	11.54	11.66	10.00
$J_{4,5a}$	5.00	5.61	5.79	5.73	5.85	6.09
$J_{4,5b}$	10.73	10.71	11.24	13.31	13.44	11.80
$J_{5a,5b}$	11.54	11.27	13.20	8.53	9.73	12.81
<b>RMSD exp/calc.</b>		0.33	0.91	2.49	2.37	1.13

For the calculation of the coupling constants of **169** all functionals showed for the coupling constants lower values than the experimental results. Also, the PBE functional was not in a good but still acceptable accordance with the experiment (RMSD = 1.48). In this case, it can be seen that small coupling constants were predicted systematically to small (Table 5.3).

**Table 5.3.** Computational and experimental spin-spin coupling constants (computed at the DFT/pc-J3 level of theory) for **169**. All values given in Hz.

	Exp. (MeCN-d <sub>3</sub> )	PBE	PBE0	TPSSH	B3LYP
$J_{1,2}$	2.18	0.07	0.99	0.40	1.03
$J_{2,3}$	3.54	1.60	1.72	1.28	1.76
$J_{3,4}$	3.90	2.55	2.67	2.31	2.78
$J_{4,5a}$	2.24	2.89	2.98	2.64	3.19
$J_{4,5b}$	2.83	1.33	1.53	1.04	1.62
$J_{5a,5b}$	13.0	12.35	14.42	11.28	14.06
<b>RMSD exp/calc.</b>		1.48	1.32	1.69	1.24

The calculation of coupling constants of the zinc complex **168** was in better agreement with the experiment. The functionals PBE, PBE0 and B3LYP correlated well with the small coupling constants. Only the calculation with TPSS and TPSSH were not satisfying and not in acceptable accordance with the NMR experiment (Table 5.4).

**Table 5.4.** Computational and experimental spin-spin coupling constants (computed at the DFT/pc-J3 level of theory) for **168**. All values given in Hz.

	Exp. (MeCN-d <sub>3</sub> )	PBE	PBE0	TPSS	TPSSH	B3LYP
$J_{1,2}$	2.80	1.87	2.01	1.39	1.50	2.14
$J_{2,3}$	3.89	3.44	3.56	3.38	3.46	3.72
$J_{3,4}$	3.18	4.34	4.48	4.36	4.45	4.71
$J_{4,5a}$	1.67	1.13	1.24	0.57	0.67	1.32
$J_{4,5b}$	1.90	2.23	2.40	1.81	1.94	2.56
$J_{5a,5b}$	12.00	10.97	12.87	7.91	9.14	12.39
<b>RMSD exp/calc.</b>		0.81	0.78	1.90	1.45	0.76

In summary, the results for calculated spin-spin coupling constants using the functionals TPSS and TPSSH was not in good agreement with the experimental values. But the results with PBE, PBE0 and B3LYP all showed promising results with a maximum deviation from the experimental data of approximately 1 Hz. Moreover, the PBE/pc-J3 level of theory revealed the best accordance with the experiment and offers superior cost-efficiency. In addition, by comparing the <sup>4</sup>C<sub>1</sub> conformation (**167**) with the <sup>1</sup>C<sub>4</sub> conformation (**168** and **169**), it is noticeable that coupling constants of the <sup>4</sup>C<sub>1</sub> chair ( $J_{1,2}$ ,  $J_{2,3}$ ,  $J_{3,4}$ , and  $J_{4,5b}$ ) are reduced by more than 6 Hz in comparison to those of the <sup>1</sup>C<sub>4</sub> conformer. Thus, the accuracy of the calculated spin-spin coupling constants can be regarded as satisfactory for predicting trends in conformational changes. For all further investigations the PBE/pc-J3 level of theory was employed to calculate spin-spin coupling constants.<sup>[259]</sup>

For the analysis of ring conformations of xylosides, the spin-spin coupling constants are of particular interest. Nevertheless, to prove the results of the computed electronic structures also the chemical shielding of the compounds had to be investigated and agree with the experimental data. Hence, in addition to the coupling constants also the chemical shift for <sup>13</sup>C and <sup>1</sup>H were calculated on a DLPNO-MP2/pcSseg-3 level of theory.<sup>[260]</sup> The theoretical and

experimental data are collected in Table 5.5 and Table 5.6. Since the chemical shift is dependent on the solvent, all experiments were carried out in MeCN-d<sub>3</sub>.

In summary, the theoretical chemical shifts for the ring protons of xylosides **167**, **168** and **169** were in good agreement with the experimental values. The maximum deviation of 0.74 ppm was observed for H-3 of **168**. The RMSD of 0.27 ppm on the other hand, suggested a fairly good accordance between experiment and theory (Table 5.5). In addition to the ring protons, also the chemical shifts for protons of the substituent were calculated (Table 8.5). Here an average RMSD of 0.44 ppm indicated that the calculation is less precise than for the ring proton chemical shifts. This is due to the conformational degrees of freedom of the free substituents. It has to be mentioned that the calculations were performed without solvents. Substituents (especially amino groups in **167**) can undergo interactions with the solvent, which affects the chemical shift of the corresponding proton.

**Table 5.5.** NMR data for the chemical shift (in ppm) of the pyranose ring protons (H-1 to H-5b) of xylosides **167**, **168** and **169** in MeCN-d<sub>3</sub> (298 K) and comparison to the calculated data. Calculated values were obtained at the DLPNO-MP2/pcSseg-3 level of theory and are displayed in grey columns.

Proton	167 (exp)	167 (calc.)	168 (exp)	168 (calc.)	169 (exp)	169 (calc.)
1	4.84	4.83	5.50	5.26	5.36	5.11
2	3.02	3.31	3.51	3.30	3.71	3.75
3	4.03	3.60	4.52	5.26	4.89	5.08
4	3.05	3.00	3.37	3.22	3.54	3.33
5a	3.91	4.17	4.36	4.55	4.29	4.63
5b	3.34	3.20	3.65	3.56	3.49	3.58

Next, the chemical shifts of the <sup>13</sup>C nuclei were calculated and compared to the experimental values. It was found that the theoretical shifts for <sup>13</sup>C were less good than for the protons. For this calculation it became even more apparent that the substituents are more affected by solvents than the xyloside ring carbons (Table 5.6). For the carbons of the carbohydrate ring an acceptable agreement between experiment and theory could be determined (RMSD = 8.52 ppm). However, for the substituents the deviation was higher (RMSD = 14.85 ppm) (Table 8.6). Here another effect is responsible for a low accuracy. The calculations were carried out without relativistic effects. Thus, carbons in the *ortho*- and *meta*-position to the bromine

substituents show a wrong trend and cannot be calculated correctly due to the absence of relativistic effects in this account.<sup>[261]</sup>

**Table 5.6.** NMR-data for the chemical shift (in ppm) of the pyranose ring carbons (C-1 to C-5) of xylosides **167**, **168** and **169** in MeCN-d<sub>3</sub> and comparison to the calculated data. Calculated values have been obtained at the DLPNO-MP2/pcSseg-3 level of theory and are displayed in grey columns.

Carbon	167 (exp.)	167 (calc.)	168 (exp.)	168 (calc.)	169 (exp.)	169 (calc.)
1	103.42	112.44	97.00	107.16	99.13	110.12
2	57.99	64.68	49.44	54.14	47.18	54.36
3	86.34	103.05	72.21	74.79	68.57	75.29
4	53.48	61.03	48.34	55.43	48.13	57.32
5	67.76	74.42	59.07	65.71	62.01	69.34

With the results for the calculation and experimental NMR data of the spin-spin coupling constants and the chemical shifts in hand, a solid toolbox for the conformational analysis of xylosides was set up. These tools could now be tested in the analysis of the conformational equilibrium of xyloside **166**.

## 5.2 Which conformers occur in solution?

Carbohydrates with a low energy barrier between two conformers can occur in a conformational equilibrium of these two species. The transition between conformers is relatively fast (100 ns) and thus NMR spectroscopy cannot resolve an equilibrium of conformers resulting in an average signals reflecting the dynamic process. However, to investigate conformational equilibria and predict coupling constants with computational methods it is necessary to know which conformers of a pyranoside occur in solution. At this stage, two different approaches can be followed. Either by low temperature NMR spectroscopy the signals of all occurring conformers can be resolved and characterized, or a computational conformational search is performed in order to predict the occurring pyranoside conformers.

Since the xylosides **168** and **169** are locked in the <sup>1</sup>C<sub>4</sub> conformation a conformational search was not necessary. But for **167** it was of interest if a conformational search supports the NMR results and defines the <sup>4</sup>C<sub>1</sub> conformation. By employing the CREST protocol<sup>[250]</sup> in combination with optimizations at the B3LYP-D3/def2-TZVPP level of theory an extensive conformational

search for **167** was carried out. The computational search yielded three energetically favored conformers. Next to the chair conformers  ${}^4C_1$  and  ${}^1C_4$ , an additional minimum corresponding to the skew conformation  ${}^1S_5$  was detected (Figure 5.3, A). For the three conformers single point energies were determined by employing DLPNO-CCSD(T)/cc-pVTZ level of theory to assess, whether relative energies can be used to identify stable conformers without taking solvent interactions and flexible substituents into account.<sup>[262]</sup> The calculations suggested an equilibrium between the two chair conformations  ${}^4C_1$  (0.80 kJ/mol) and  ${}^1C_4$  (0.00 kJ/mol). The skew conformation was predicted as unfavored with a single point energy of 23.4 kJ/mol. Note conformers found and the range of energies observed were in accordance with what has been found for other glycosides.<sup>[74, 263]</sup> At this stage it has to be mentioned that a better agreement would require methods that allow for extensive sampling of solvent-solute interactions (ab-initio molecular dynamics). As experimental data revealed that the  ${}^4C_1$  conformation is favored, we not only trusted in single point energies to assign the observed conformers. Spin-spin coupling constants were computed for the three suggested conformers by employing a PBE/pc-J3 level of theory. The spin-spin coupling constants of the conformers of **167** are shown in (Figure 5.3, B) and significant differences and trends can be observed. First, the calculated coupling constants of  ${}^4C_1$  are in good agreement with the experimental determined ones. Thus, it was concluded that in the presence of a solvent the equilibrium of conformers is trended to the  ${}^4C_1$  conformer. It was demonstrated that the coupling constants of the three conformers differ characteristically from each other. On the one hand, the  ${}^1C_4$  showed low spin-spin coupling constants, on the other hand, for the  ${}^4C_1$  conformer all coupling constants are 3-4 Hz larger than for the  ${}^1C_4$  conformer. Additionally, the  ${}^1S_5$  conformation showed a quite different coupling pattern with no clear trend in the coupling constants (Figure 5.3, B).

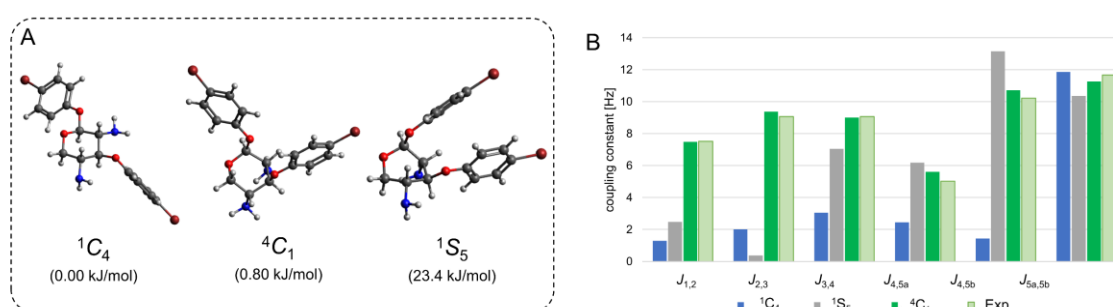


**Figure 5.3.** Optimized geometries of the lowest energy conformers for xyloside **167** (A) and relative free energies (in kJ/mol referenced to the lowest energy conformer) were obtained from conformational sampling. No solvent effects have been considered, geometries, frequencies and enthalpy corrections have been obtained at the B3LYP-D3/def2-TZVPP level of theory, energies have been obtained at the DLPNO-CCSD(T1)/cc-pVTZ level of theory. The spin-spin coupling constants (PBE/pc-J3) for all conformers obtained for compound **167** (B). The experimental coupling constants (light green) agree with the computed coupling constants of the  ${}^4C_1$  conformation (dark green).

With these results in hand, it was next aimed at a conformational search for the bis-*N*-Boc-protected xyloside **166** since it was of interest to study the existing conformational equilibrium. Again, by employing the CREST protocol in combination with optimizations at the B3LYP-D3/def2-TZVPP level of theory an extensive conformational search for **166** was carried out and three lowest energies conformers were obtained (Figure 5.4, A). As the most stable conformation the  ${}^1C_4$  conformation was suggested. Additionally, the  ${}^4C_1$  and the  ${}^2S_0$  conformers were assigned. Accordingly, for the three conformers single point energies were calculated by employing a DLPNO-CCSD(T)/cc-pVTZ level of theory. For **166** it was shown that the energies did not differ by more than 7 kJ/mol, which suggested a conformational equilibrium of the three conformers. However, as demonstrated for **166**, it was necessary to use computed coupling constants of the conformational assignment in addition to energies. Thus, the spin-spin coupling constants of the three conformers were calculated by employing a PBE/pcJ-3 level of theory. Again, it was shown that for the  ${}^1C_4$  low coupling constants are characteristic, while the  ${}^4C_1$  conformation coupling constants are systematically higher by 4-6 Hz. Furthermore, the  ${}^2S_0$  conformer showed a coupling pattern with alternating constants (Figure 5.4, B).

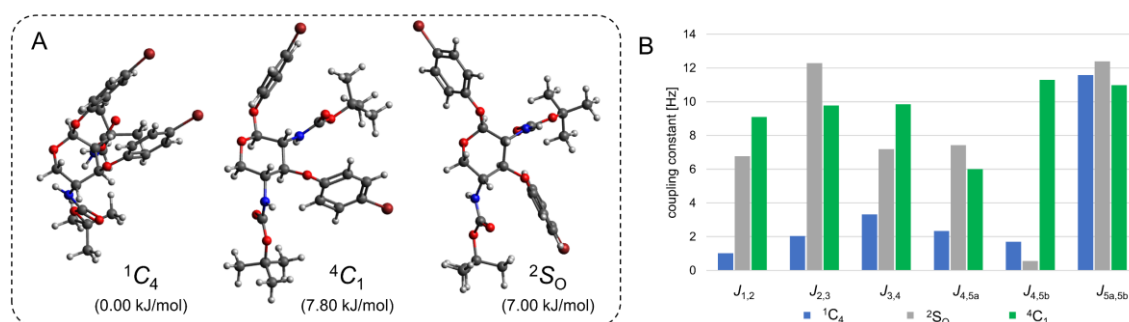


**Figure 5.4.** Optimized geometries of the lowest energy conformers for xyloside **166** (A) and relative free energies (in kJ/mol referenced to the lowest energy conformer) were obtained from conformational sampling. No solvent effects have been considered, geometries, frequencies and enthalpy corrections have been obtained at the B3LYP-D3/def2-TZVPP level of theory, energies have been obtained at the DLPNO-CCSD(T1)/cc-pVTZ level of theory. The spin-spin coupling constants (PBE/pcJ-3) for all conformers obtained for compound **166** (B).

With this conformational search, it was demonstrated that computed gas-phase energies alone are not sufficient for the interpretation of a conformational equilibrium. The effect of solvents on the conformational behavior of pyranosides is crucial and has to be considered. Widmalm and co-workers showed that the conformation of xylosides is influenced by solvent parameters.<sup>[78]</sup> But the computed energies indicate that different conformers are occurring in a conformational equilibrium and the size of energy differences gives a hint, which conformation

might dominate the equilibrium and which can be excluded. Thus, for investigation of the conformational equilibrium of **166** in solution, the computed conformers have to be considered.

### 5.3 Solvent-dependent conformational equilibria

As described in chapter 4.4 the bis-*N*-Boc-protected diaminoxyloside **166** exists as a conformational equilibrium as shown in  $^1\text{H}$  NMR experiments (line broadening of the ring proton peaks). In fact, the conformational equilibrium of pyranosides is influenced by solvation and intermolecular interactions.<sup>[73c, 263c]</sup> In order to gain more information about the conformational equilibrium of **166** in  $\text{CDCl}_3$ , a temperature dependent NMR experiment was carried out (Figure 5.5) with the aim in mind to separate the average signal set into single conformer signal sets and to determine their ratio. It was observed that between 278 K and 318 K the peaks for the ring protons were broadened. In this range the coalescence temperature is assumed, which was not further determined. It was demonstrated that by further increasing the temperature the signals became sharper and average coupling constants of all conformers in the equilibrium could be determined. On the other hand, decreasing the temperature did not lead to a separation of the signals into two (or more) signal sets.

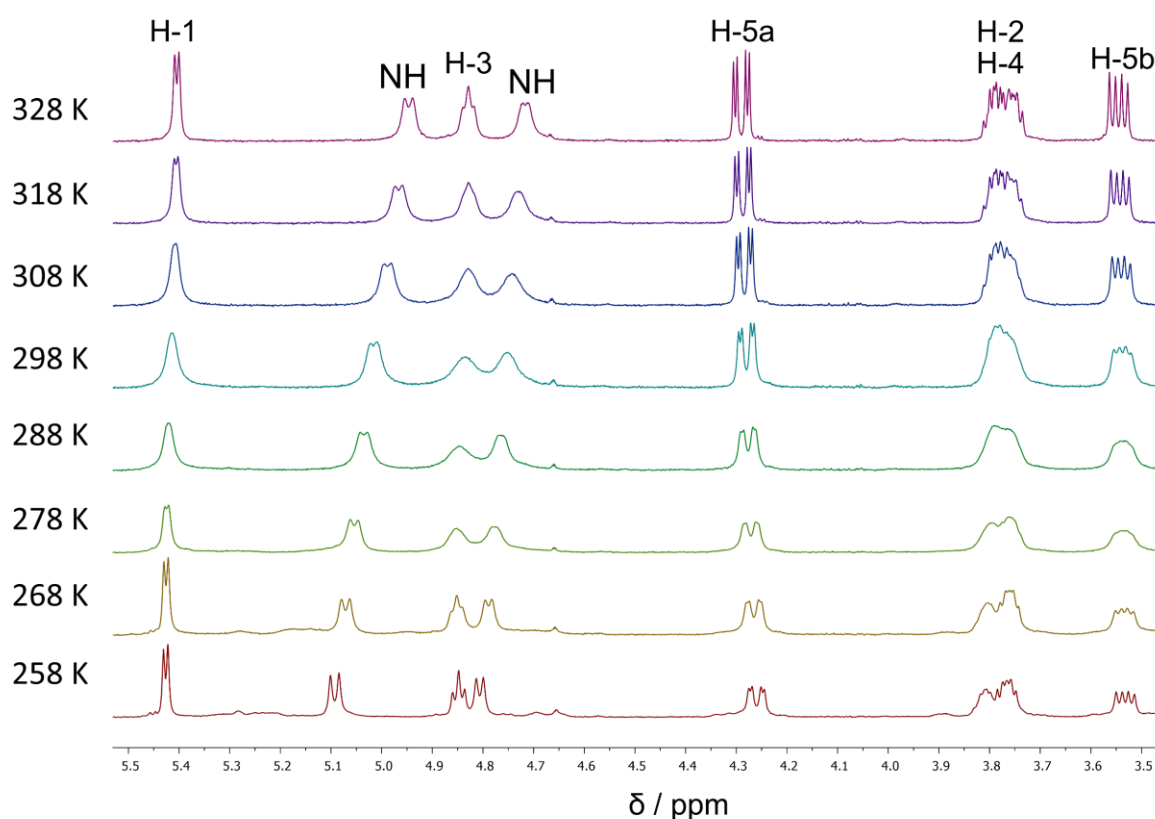


**Figure 5.5.** Temperature-dependent NMR spectroscopy to study the conformational equilibrium of **166**.  $^1\text{H}$  NMR spectra ( $\text{CDCl}_3$ , 500 MHz, 0.02 M). Protons were assigned by COSY and HSQC.

Therefore, another method for the analysis of the conformational equilibrium of **166** was required. Since the coupling constants of the pure conformers could not be determined, the composition of the conformational equilibrium had to be determined by a combination of experimental and computational analysis. First, average coupling constants (of all conformers in the equilibrium) were determined by NMR spectroscopy in ten different deuterated solvents. These experiments revealed that the coupling constants were highly dependent on the solvent. The solvents exhibited different characteristics ranging from polar (DMSO- $d_6$  or DMF- $d_7$ ) to non-polar solvents (benzene- $d_6$  or  $CDCl_3$ ) (Table 5.7). In addition to the  $^1H$  NMR experiments at different temperatures also 2D NMR experiments (DQF-COSY) were conducted, because they were valuable for the determination of xyloside coupling constants. In polar solvents it was observed that the coupling constants of the pyranoside protons were higher ( $^3J$  coupling constants between 5-10 Hz), indicating a favored  $^4C_1$  conformation. On the other hand, in less polar solvents it was seen that at 298 K the  $^1H$  NMR spectra showed broad signal indicative for a dynamic equilibrium between two conformers. Thus, the temperature was increased in order to determine coupling constants of the mixtures of conformers, and this led to sharper signals. Furthermore, for non-polar solvents with lower dielectric constants a systematic decrease of the coupling constants was observed ( $^3J$  coupling constants between 3-5 Hz). This trend was also observed for the experimental and computed coupling constants of **168** and **169** (Table 5.1).

With the results for the various conformational equilibria of **166** in hand, a trend for the different solvents was figured out and once again it was shown that the conformational behavior of pyranosides is dependent on solvent-solute interactions. This observation might be interpreted such that solvents function as different external stimuli to overcome the energy barrier between the conformers and change the distribution of conformers. Note that the conformational equilibria are highly dependent on polarity of the solvent. The observed trend is in accordance with the computed coupling constants of **166** and **167** (Figure 5.3 and Figure 5.4). The decrease of the coupling constants in less polar solvents is a convincing argument for the assumption of a conformational equilibrium between the two chair conformations  $^4C_1$  and  $^1C_4$ .

**Table 5.7.** NMR-experiments for xyloside **166** were measured in different solvents. For the determination of the coupling constants (given in Hz)  $^1\text{NMR}$  or DQF-COSY experiments were used. Theoretical coupling constants are colored in grey and were computed at the PBE/pc-J3 level of theory.

Solvent	$J_{1,2}$	$J_{2,3}$	$J_{3,4}$	$J_{4,5a}$	$J_{4,5b}$	$J_{5a,5b}$
$^4\text{C}_1$ (PBE)	9.09	9.77	9.84	6.00	11.30	10.98
DMSO- $\text{d}_6$ <sup>a</sup>	8.03	9.66	9.66	5.15	11.37	11.37
DMF- $\text{d}_7$ <sup>a</sup>	8.33	9.76	9.76	5.27	10.94	10.94
acetone- $\text{d}_6$ <sup>a</sup>	7.55	8.46	8.46	4.88	11.88	11.05
MeOD- $\text{d}_3$ <sup>a</sup>	7.41	8.73	9.38	5.12	9.61	11.92
pyridine- $\text{d}_5$ <sup>a</sup>	6.77	8.34	8.34	4.69	9.89	11.51
THF- $\text{d}_8$ <sup>a</sup>	5.87	7.89	7.89	4.49	9.18	11.84
toluene- $\text{d}_8$ <sup>b</sup>	4.38	6.10	6.10	3.87	6.58	11.83
benzene- $\text{d}_6$ <sup>b</sup>	n.d.	5.63	5.63	3.81	6.55	11.87
$\text{CDCl}_3$ <sup>b</sup>	4.17	5.53	5.53	3.70	5.97	12.04
chlorobenzene- $\text{d}_5$ <sup>b</sup>	4.21	5.42	5.42	3.47	5.50	12.00
$^1\text{C}_4$ (PBE)	1.02	2.04	3.33	2.34	1.70	11.57

<sup>a</sup> Spectra measured at 298 K

<sup>b</sup> Spectra measured at 328 K.

The coupling constants determined for **166** in various solvents reflect average values of a mixture of conformers of unknown distribution. Unfortunately, the spin-spin coupling constants of the pure conformers comprising the mixture could not be determined experimentally and thus the population of different conformers could not be assigned. On the other hand, we have demonstrated that coupling constants of single conformers can be computed with an accuracy of  $\sim 1$  Hz. In addition, the conformational search (chapter 5.3) revealed for **166** that three conformers are favored, namely the  $^4\text{C}_1$ ,  $^1\text{C}_4$  and the  $^2\text{S}_0$  conformer. With this information in hand, the coupling constants of all three conformers were calculated on a DFT/pc-J3 level of theory for the functionals PBE, PBE0 and B3LYP (cf. experimental section, Table 8.7).

Knowing the computational results of the coupling constants of the  ${}^4C_1$  and the  ${}^1C_4$  conformers, a least squares fit of the observed experimental coupling constants in a specific solvent was performed, leading to the  ${}^1C_4:{}_4C_1$  distribution in every employed solvent (Table 5.8). It was shown that the fitted ratios were stable regardless of the functional, which was used for the calculation. Again, the results obtained with the PBE functional were in best accordance with the experimental data and showed the lowest RMSD. It was seen that in polar solvents the  ${}^4C_1$  conformation was dominating (95 % for DMF or DMSO) and in less polar solvents the amount of  ${}^1C_4$  conformer increased significantly (up to 60 %).

Since the conformational search revealed that three conformers have to be considered in the dynamic conformation mixture of **166**, the least squares fit was also proceeded for a three-component average including the  ${}^2S_0$  conformation. As the population of the skew conformation was never above 2 %, it was excluded of the further investigations.

**Table 5.8.** The  ${}^1C_4:{}_4C_1$  distribution of conformers in conformational equilibria of **166** in various solvents was determined by a least squares fit of the type  $J_{\text{exp}}(\text{solvent}) = a * J_{\text{calc}}({}^1C_4) + * J_{\text{calc}}({}^4C_1)$  for different levels of theory.

Solvent	PBE		PBE0		B3LYP	
	${}^1C_4:{}_4C_1$	RMSD	${}^1C_4:{}_4C_1$	RMSD	${}^1C_4:{}_4C_1$	RMSD
DMF-d <sub>7</sub>	5:95	0.3	10:90	0.9	16:84	0.8
DMSO-d <sub>6</sub>	5:95	0.5	10:90	0.9	16:84	0.7
acetone-d <sub>6</sub>	11:89	0.8	16:84	1.2	22:78	1.2
MeOD-d <sub>3</sub>	16:84	0.5	21:79	0.6	27:73	0.4
pyridine-d <sub>5</sub>	21:79	0.5	26:74	0.8	31:69	0.7
THF-d <sub>8</sub>	29:71	0.6	33:67	0.8	38:62	0.7
toluene-d <sub>8</sub>	53:47	0.4	56:44	0.7	60:40	0.6
benzene-d <sub>6</sub>	55:45	0.5	58:42	0.8	62:38	0.7
CDCl <sub>3</sub>	59:41	0.4	62:38	0.6	65:35	0.5
chlorobenzene-d <sub>5</sub>	61:39	0.4	64:36	0.6	68:32	0.5

For a better understanding of how the solvent affects the conformational distribution the fitted ratios for the population of the  ${}^4C_1$  conformer at the PBE/pc-J3 level of theory were plotted against the experimental coupling constants measured in the respective solvents (Figure 5.6). It can be seen that the coupling constants followed the trend of the computational predicted values and ( $J_{1,2}$ ,  $J_{2,3}$ ,  $J_{3,4}$ ,  $J_{4,5a}$  and  $J_{4,5b}$  decreasing from  ${}^4C_1$  to  ${}^1C_4$  and  $J_{5a,5b}$  increasing). Thus, for each coupling constant a linear regression was performed and extrapolated for the values of 0 % and 100 % of  ${}^4C_1$  to forecast the coupling constants of the pure conformers from the experimental values.

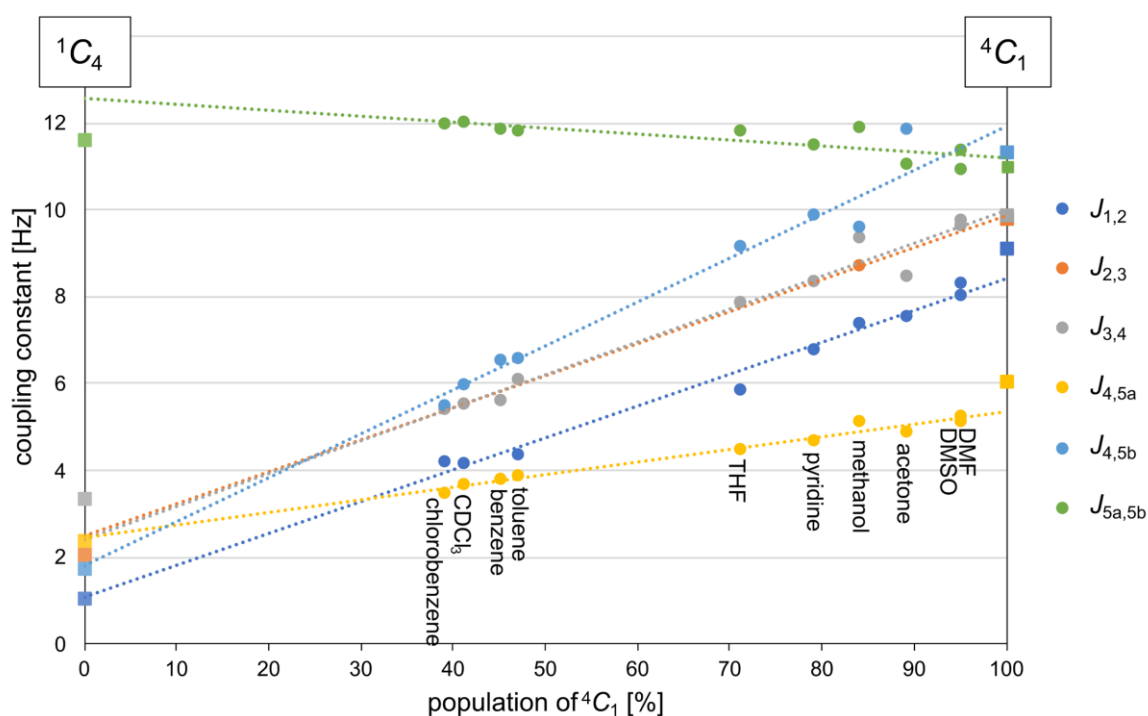


**Figure 5.6.** Dependence of experimental spin-spin coupling constants on the fitted ratio between the  ${}^4C_1$  and  ${}^1C_4$  conformers of **166** in different solvents. For each of the couplings in each solvent, a least squares fit has been carried out including  $J_{1,2}$ ,  $J_{2,3}$ ,  $J_{3,4}$ ,  $J_{4,5a}$ ,  $J_{4,5b}$ , and  $J_{5a,5b}$  to obtain the optimal  ${}^1C_4$ : ${}^4C_1$  ratio as % of  ${}^4C_1$  on the x-axis. Dotted lines illustrate a linear regression of the experimental values and computed ratios. Squares show the computed coupling constants of the  ${}^1C_4$  conformer at 0 % and the  ${}^4C_1$  conformer at 100 %, respectively.

The coupling constants from the extrapolation and the PBE-computed ones were compared to see that they are in excellent accordance (Table 5.9). The  ${}^3J$  couplings showed satisfying values in a range less than 1.00 Hz deviation and only the  ${}^2J_{5a,5b}$  coupling was less good predicted (deviation by 1.00 Hz). Nevertheless, these results demonstrated that the combination of experimental and computational methods have the potential to reveal information about equilibria of sugars, which are otherwise not available.

**Table 5.9.** Interpolated coupling constants of compound **166** using the experimental spin-spin coupling constants obtained in various solvents and the  ${}^1C_4:{}_4C_1$  ratios obtained from a least-squares-fit of the computed values to the experimental ones. All values given in Hz.

	${}^1C_4$ extrapolated	${}^1C_4$ (PBE)	Deviation	${}_4C_1$ extrapolated	${}_4C_1$ (PBE)	Deviation
$J_{1,2}$	1.10	1.02	0.08	8.41	9.09	-0.68
$J_{2,3}$	2.51	2.04	0.47	9.88	9.77	0.11
$J_{3,4}$	2.43	3.33	-0.90	10.01	9.84	0.17
$J_{4,5a}$	2.47	2.34	0.13	5.36	6.00	-0.64
$J_{4,5b}$	1.81	1.70	0.11	11.94	11.30	0.64
$J_{5a,5b}$	12.57	11.57	1.00	11.21	10.98	0.23

## 5.4 Conclusion

This subproject was dedicated to the analysis of the dynamic conformational equilibrium of the xyloside **166** in solution. The xylosides **167**, **168**, and **169**, existing in defined conformations, served as benchmarks for a conformational analysis based on combined experimental and computational approaches. The structures of all three xylosides were clarified by NMR experiments and coupling constants confirmed the pyranoside conformations. The experimental data were supported by computational studies.

With this toolbox the conformational equilibrium of the bis-*N*-Boc-protected xyloside **166** in various solvents was studied. A conformational search suggested three lowest energy conformers, namely  ${}_4C_1$ ,  ${}^1C_4$ , and  ${}^2S_0$  and the distribution of the conformers in solution was determined. It could be shown that in polar solvent (DMSO, DMF) the  ${}_4C_1$  conformation is dominating, while with decreasing solvent polarity the population of the  ${}^1C_4$  conformer increases.

In addition to metal complexation, the conformational flip or equilibrium, respectively, of xylosides can be influenced by solvent effects. The combination of computational and experimental approaches forms a useful toolbox to analyse conformational equilibria in different solvents.

## 6 Biphenyl xyloside clusters to control spatial ligand presentation

The synthesized 2,4-diamino xyloside **167** holds the potential of controlling the amplitude of glycoligand presentation by switching of the xylose chair conformation. Accordingly, bivalent mannoside clusters **170** and **171** based on a conformational switchable xylose scaffold were prepared (Figure 6.1). The functionalization of **167** with  $\alpha$ -D-mannoside ligands was targeted by Suzuki-Miyaura cross-coupling in order to form rigid biphenyl linkages. These linkers on one the hand, directly transfer the xylose ring-flip motion in order to control the amplitude of ligand presentation. On the other hand, the biphenyl moieties stabilize the  ${}^1C_4$  conformation by  $\pi$ - $\pi$  interactions and furthermore the biphenyl aglycones increase the binding affinity towards FimH. The conformational ring flip is afforded covalently by the formation of a bicyclic urea derivative. With both conformers in hand, they were evaluated for their binding abilities towards the lectin FimH.

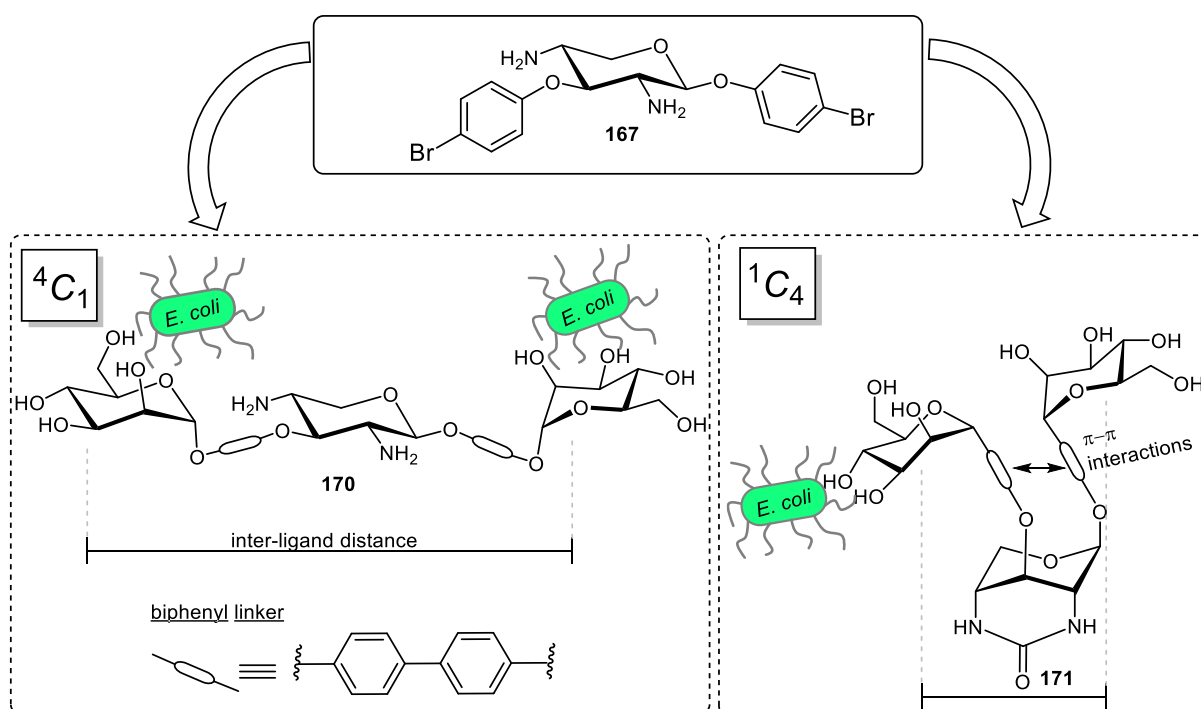


**Figure 6.1.** The control of ligand presentation based on scaffolding on the conformational switchable xyloside **167**. The structure of the bis-mannoside glycoclusters **170** ( ${}^4C_1$ ) and **171** ( ${}^1C_4$ ) is affected by the conformational ring flip and the mannoside ligands come closer to each other. Aromatic biphenyl linker moieties support the conformational ring flip by  $\pi$ - $\pi$  interactions.

Biphenyl  $\alpha$ -D-mannosides show high inhibitory potencies towards the lectin FimH relying on the strong  $\pi$ - $\pi$  interactions between the aromatic aglycone moiety and the tyrosine gate (Tyr48 and Tyr137).<sup>[154a]</sup> Over the years, several mannosides and oligomannosides were designed as potential antagonists of type 1 fimbriae-mediated bacterial adhesion.<sup>[36, 264]</sup> It turned out that

antagonists with a biphenyl aglycone show a high affinity (in the nanomolar range) and by specific further functionalization or tuning of the aglycone, the affinity can be further increased.<sup>[265]</sup> Thus, it is important that the terminal phenyl moiety is electrostatic complementary to the electron-rich Tyr48 residue, which results in a particularly strong electrostatic attraction (distance  $\sim 4$  Å) (Figure 6.2).<sup>[266]</sup>

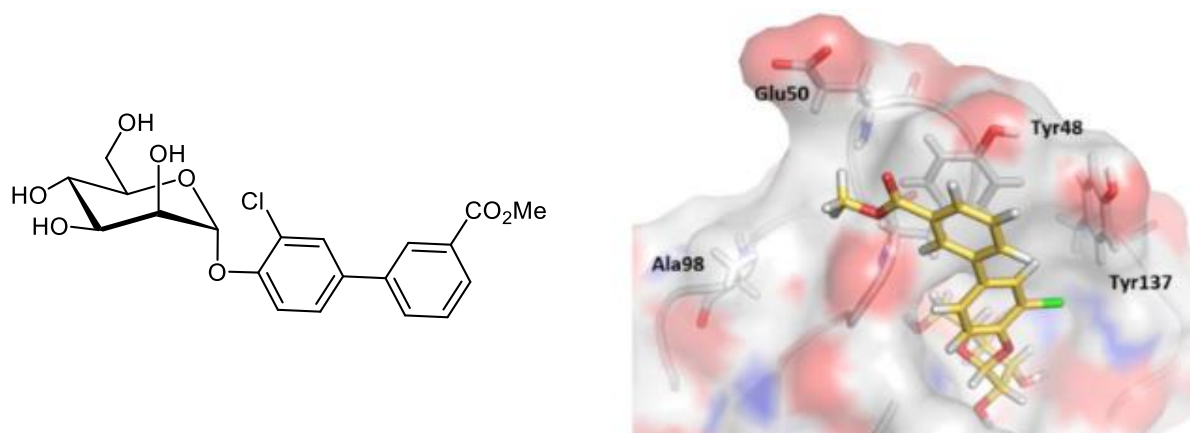


**Figure 6.2.** Binding mode of biphenyl  $\alpha$ -D-mannosides. The biphenyl aglycone is interacting by  $\pi$ - $\pi$  interactions with the tyrosine gate, especially Tyr48. Additionally, further functional groups can interact with the CRD periphery by non-covalent interactions.<sup>[37d]</sup>

According to the “sub-site-assisted aglycone binding” it is of interest to investigate biphenyl mannosides as ligands for FimH. Next to their strong binding affinity also their rigid structure is of interest, since the spatial ligand presentation can be influenced by the defined molecular geometry of bivalent glycoclusters.<sup>[267]</sup> The group of Roy studied the influence of carbohydrate assembly together with imparting conformational restriction. Thus, by applying cross-coupling reactions they built up glycoclusters with galactosides or mannosides as carbohydrate ligands, comprising rigid biphenyl or aryl-alkyne linkages as scaffold moieties, so-called “sugar rods” (Figure 6.3).<sup>[268]</sup> For bivalent glycoclusters, the group used the regiochemistry of the phenyl units of the scaffolds in order to vary inter-saccharide distances and test their effect in multivalent lectin binding interactions. By an aryl-alkyne cross-coupling, they prepared *ortho*- and *para*-substituted bis-mannosides. The rigidity of the scaffold provides a short distance between the carbohydrate ligands for the *ortho*-derivative and a maximum distance for the *para*-derivative.<sup>[269]</sup> Additionally, the group prepared a hexameric mannoside cluster with rigid biphenyl linkages. The divalent and hexavalent clusters were tested by turbidimetry for their cross-linking ability with the lectin ConA, which is known to form cross-linked lattices with multiantennary glycans.<sup>[270]</sup> In this assay, the results obtained with the hexameric cluster reflect the effects of cross-linking due to its highly multivalent character. Moreover, clusters with a long inter-mannoside distance (*para*-derivative) showed a higher preference to form cross-linked lattices, compared to the relatively short distanced *ortho*-derivative.

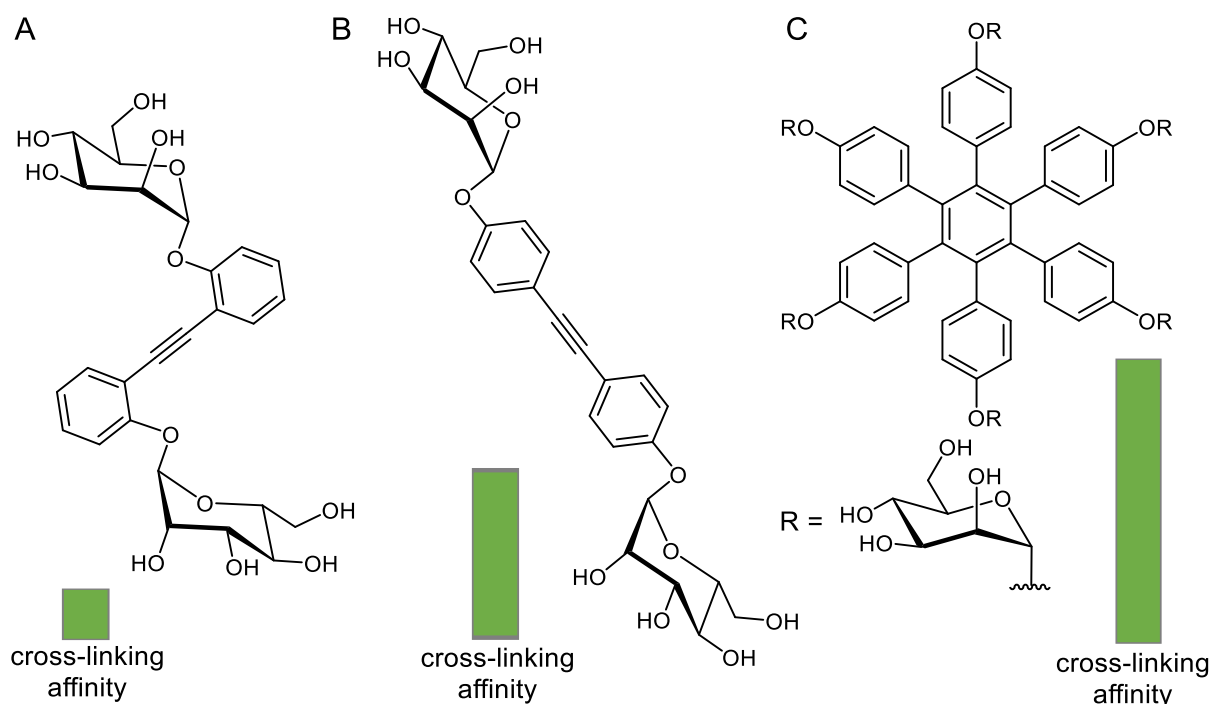


**Figure 6.3.** The given structure of a rigid scaffold molecule affects the cross-linking ability of mannose ligands towards tetrameric ConA. Additionally, multivalent glycocluster increase the binding ability.<sup>[269]</sup>

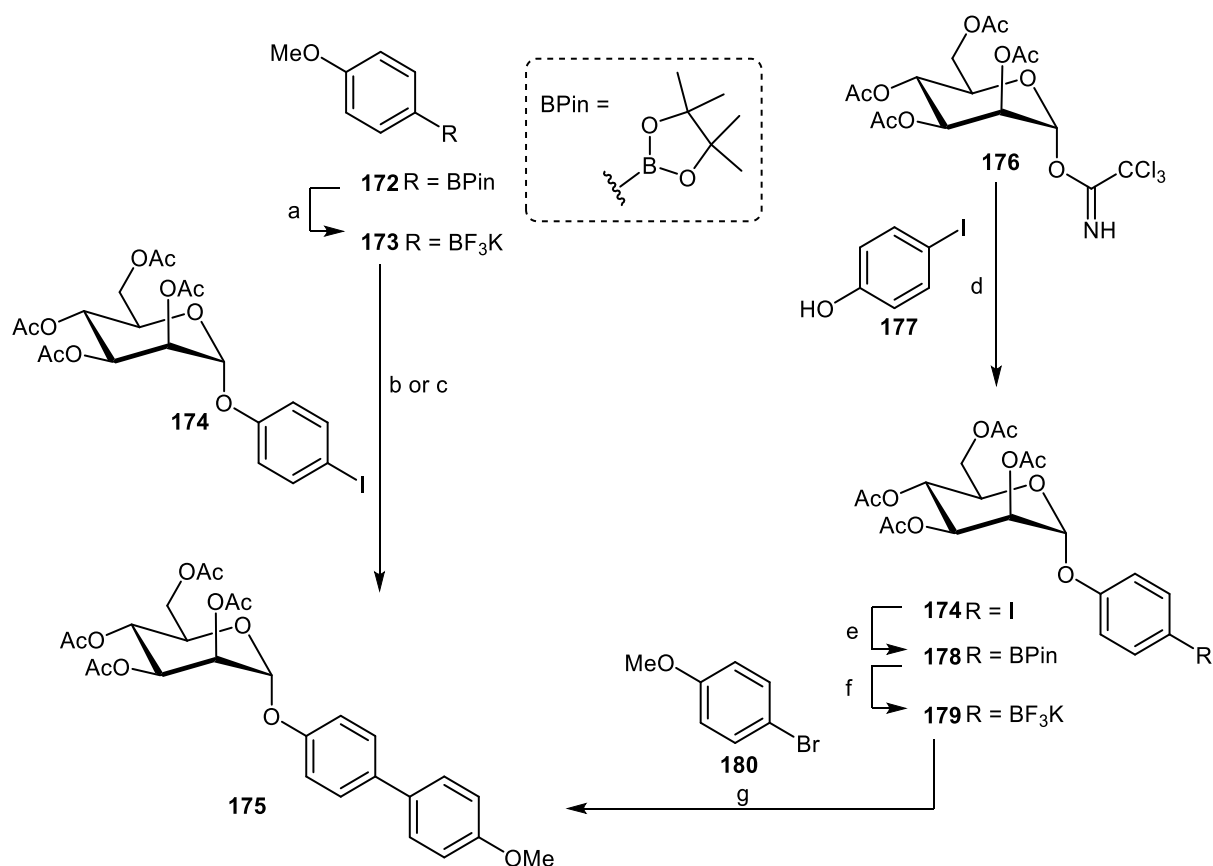
In order to investigate the xylose-based bivalent glycoclusters **170** and **171** as structurally varied ligands of the bacterial lectin FimH, the Suzuki-Miyaura cross-coupling reaction was employed for their preparation.

### 6.1 Synthesis of bis-biphenyl xyloside glycoclusters

The Suzuki-Miyaura cross-coupling is a reaction, which requires the optimization of many parameters. Besides the reaction partners, the base, the Pd-catalyst, the solvent, temperature, time and further additives can be varied.<sup>[271]</sup> In order to optimize the reaction conditions for the current xyloside substrate, the synthesis of the biphenyl mannoside **175** was employed as an inexpensive model system.

First of all the organoboron nucleophile (e.g. boronic acids or pinacol boronic esters) was chosen, which show differences in nucleophilicity.<sup>[272]</sup> In addition to pinacol boronic esters, potassium trifluoroborates serve also as C-nucleophiles and show a three times higher nucleophilicity.<sup>[272]</sup> Potassium trifluoroborates can be prepared from organoboronic acids or esters, respectively, by treatment with potassium bifluoride ( $\text{KHF}_2$ ) in aqueous solution.<sup>[273]</sup> Thus, in addition to the synthesis of pinacol boronic esters **172** and **178** also the trifluoroborates **173** and **179** were synthesized and tested in Suzuki reactions.

In one approach potassium 4-anisyl trifluoroborate (**173**)<sup>[274]</sup> was synthesized, according to a procedure of Molander et al. by treatment of the boron ester **172** with  $\text{KHF}_2$  giving **173** in high yield. Next, Suzuki-Miyaura cross-coupling with 4-iodophenyl mannoside **174** and the two boron derivatives **172**, respectively **173**, was performed. Adapting the conditions of Cutolo et al.,<sup>[275]</sup> boronic ester **172** and mannoside **174** were reacted in the presence of  $\text{Pd}(\text{PPh}_3)_4$  and  $\text{Cs}_2\text{CO}_3$  in dioxane to obtain the biphenyl derivative **175** in a yield of 37 %. On the other hand, the reaction of the trifluoroborate **173** with mannoside **174** according to a procedure of Sliman et al.<sup>[276]</sup> in the presence of  $\text{Pd}(\text{dppf})\text{Cl}_2$  and DIPEA gave the same product (**175**) in a higher yield of 57 % (Scheme 6.1).

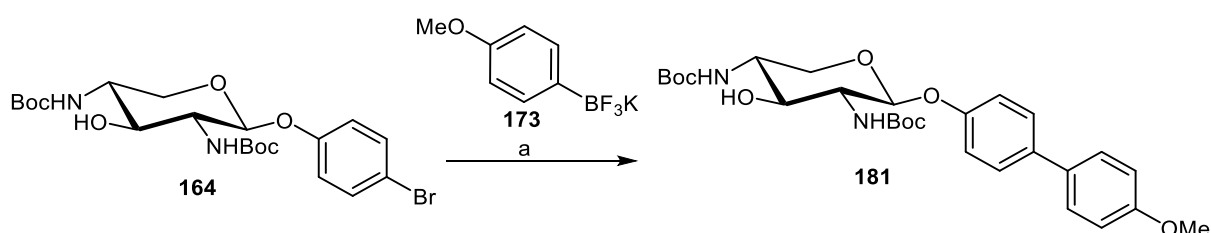


**Scheme 6.1.** Test reactions for the synthesis of biphenyl mannoside **175** and synthesis of  $\alpha$ -D-mannoside ligands **178** and **179** as precursors for Suzuki-Miyaura cross-coupling reactions. (a)  $\text{KHF}_2$ , MeOH, rt, 1 h, 86 %; (b)  $\text{Pd}(\text{PPh}_3)_4$ ,  $\text{Cs}_2\text{CO}_3$ , dioxane, 80 °C, 2 h, 37 % from **172**; (c) DIPEA,  $\text{Pd}(\text{dppf})\text{Cl}_2$ , MeOH, 70 °C, 2 h, 57 % from **173**; (d)  $\text{BF}_3 \cdot \text{Et}_2\text{O}$ , dry  $\text{CH}_2\text{Cl}_2$ , 0 °C  $\rightarrow$  rt, 16 h, 39 %; (e)  $(\text{BPin})_2$ , KOAc,  $\text{Pd}(\text{dppf})\text{Cl}_2 \cdot \text{CH}_2\text{Cl}_2$ , DMSO, 80 °C, 2.5 h, 60 %; (f)  $\text{KHF}_2$ , MeOH, rt, 1 h, 91 %; (g) DIPEA,  $\text{Pd}(\text{dppf})\text{Cl}_2$ , MeOH, 70 °C, 54 %.

Next, two different organoboronic mannosides were synthesized, namely the pinacol boronic ester **178** and the trifluoroborate **179** (Scheme 6.1). The synthesis of **178** was started from the trichloroacetimidate **176** and in a  $\text{BF}_3 \cdot \text{Et}_2\text{O}$ -promoted glycosylation reaction 4-iodo phenol (**177**) was glycosylated in a yield of 39%.<sup>[277]</sup> Subsequently, according to a procedure of

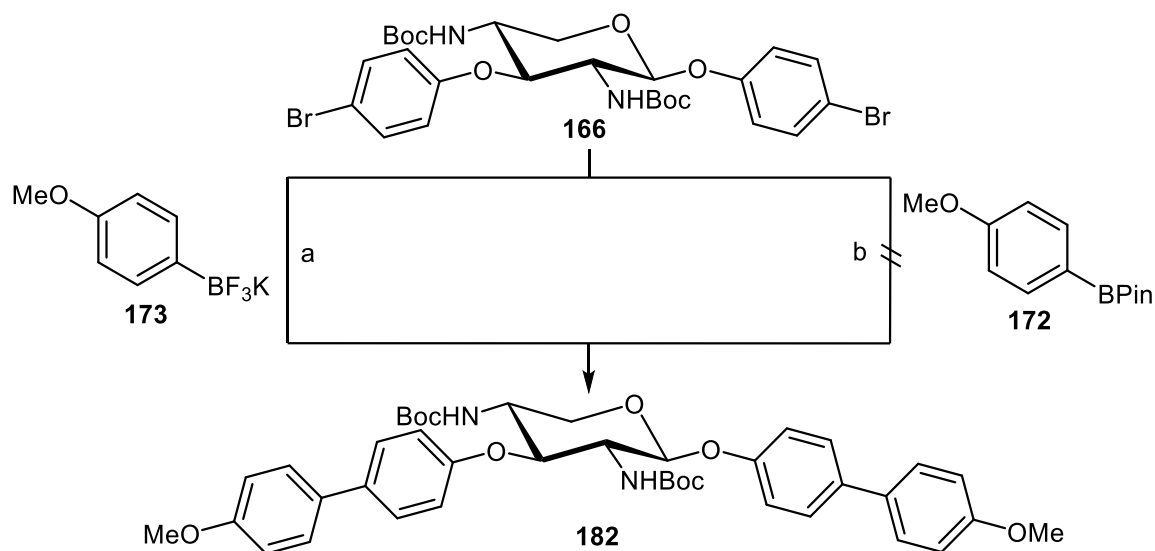
Janetka and co-workers,<sup>[278]</sup> **178** was treated with bis(pinacolato)diboron and KOAc in the presence of the catalyst Pd(dppf)Cl<sub>2</sub>, which gave the pinacol boronic ester **178** in a yield of 60 %. In order to prepare the trifluoroborate **179**, a procedure of Hutton and co-workers was followed.<sup>[274b]</sup> Hence, the pinacol boron ester **178** was treated with KHF<sub>2</sub> to achieve the targeted trifluoroborate salt **179** in a yield of 91 %. Finally, in a Suzuki-Miyaura cross-coupling reaction, trifluoroborate **179** and 4-bromoanisole (**180**) were treated with DIPEA and Pd(dppf)Cl<sub>2</sub> in MeOH at 70 °C and the corresponding biphenyl mannoside **175** was obtained in a moderate yield of 54 % after column chromatography (Scheme 6.1). In conclusion of these experiments, the trifluoroborates **173** and **179** can be regarded as suitable reagents for Suzuki reactions with peracetylated mannosides.

With the organoboron reagents **173** and **179** in hand, the derivatization of 2,4-diamino xylosides by Suzuki-Miyaura cross-coupling reactions was commenced, which required optimization of the reaction conditions for the xylosides **164** and **166**, respectively. First, the xyloside **164** and the trifluoroborate **173** were treated with DIPEA and Pd(dppf)Cl<sub>2</sub> in MeOH at 70 °C according to Molander et al.<sup>[273]</sup> to yield the biphenyl xyloside **181** in a yield of 85 % (Scheme 6.2). This reaction proved that the cross-coupling of trifluoroborates with Boc-protected-2,4-diamino xylosides is possible in promising yields.



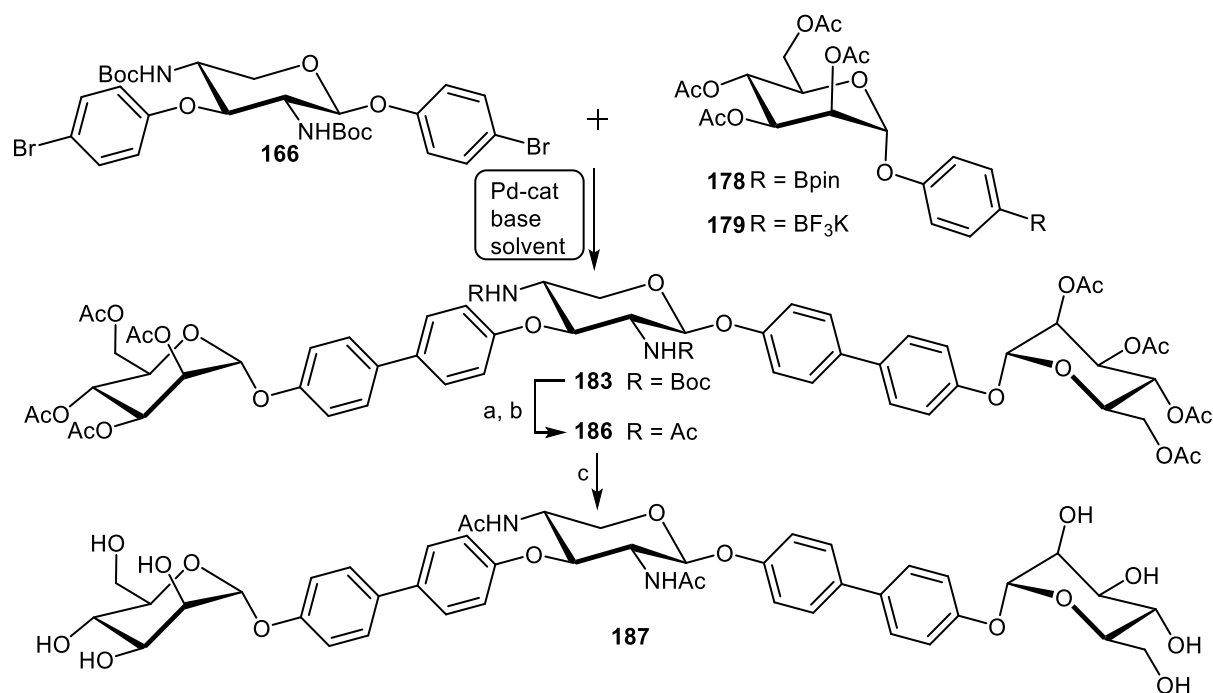
**Scheme 6.2.** Synthesis of biphenyl xyloside **181** by a Suzuki-Miyaura coupling with the trifluoro borate **173**. (a) DIPEA, Pd(dppf)Cl<sub>2</sub>·CH<sub>2</sub>Cl<sub>2</sub>, MeOH, 70 °C, 2 h, 85 %.

Next, the optimized reaction conditions were applied to the 1,3-disubstituted xyloside **166**. First, xyloside **166** was reacted with two equivalents of the trifluoroborate **173** in the presence of DIPEA and Pd(dppf)Cl<sub>2</sub> in MeOH for 2 h to isolate the desired bis-functionalized derivative **182** in a moderate yield of 37 % (Scheme 6.3). In order to improve the yield, **166** was reacted with pinacol boronic ester **172** in the presence of Pd(dppf)Cl<sub>2</sub> and potassium phosphate,<sup>[279]</sup> but the desired product **182** was not formed. However, the results of the test reactions of the trifluoroborate **173** with the xylosides **164** and **166** indicated that trifluoroborate derivatives are the reagents of choice for the Suzuki reaction with diamino xylosides.



**Scheme 6.3.** Synthesis of the bis-biphenyl xyloside **182** by a Suzuki-Miyaura coupling with trifluoroborate **173** or pinacol boronic ester **172** (a) DIPEA, Pd(dppf)Cl<sub>2</sub>·CH<sub>2</sub>Cl<sub>2</sub>, MeOH, 70 °C, 2 h, 37 %; (b) Pd(dppf)Cl<sub>2</sub>·CH<sub>2</sub>Cl<sub>2</sub>, K<sub>3</sub>PO<sub>4</sub>, DMF, 80 °C, 16 h.

Based on the experiences made in the preparation of **182**, the synthesis of bis-biphenyl glycocluster **183** was targeted (Scheme 6.4). However, when **166** was subjected to a cross-coupling reaction with the mannosyl trifluoroborate **179** in the presence of DIPEA and Pd(dppf)Cl<sub>2</sub> in MeOH, the desired cluster **183** could not be isolated (Table 6.1, entry 1). In order to exclude a negative influence of the solvent (e.g., transesterification of the acetyl protecting groups), dioxane was used instead of MeOH, but again the biphenyl cluster **183** did not form (Table 6.1, entry 2). In another approach, xyloside **166** was reacted with the boron pinacol ester **178** following a procedure of Cutolo et al. (Table 6.1, entry 3).<sup>[275]</sup> When **166** was treated with **178** in the presence of Pd(PPh<sub>3</sub>)<sub>4</sub> and Cs<sub>2</sub>CO<sub>3</sub> in a mixture of water and dioxane again the desired cluster **183** did not form. Equally, all approaches to perform the reaction under dry conditions and at higher temperature were not successful (Table 6.1, entry 4). Up to this point, all experiments showed that the starting material **166** reacted with the catalyst, proving that the oxidative addition was effective, but the transmetallation and reductive elimination did not take place. For these latter reaction steps, the base is important. It is known that fluorides are potent bases for Suzuki-Miyaura reactions due to the fluorophilicity of the organoboranes.<sup>[280]</sup> Thus, cesium fluoride (CsF) was utilized and according to the work of Kagechika and co-workers,<sup>[281]</sup> **166** and **178** were treated with CsF and Pd(dppf)Cl<sub>2</sub> in THF for 8 h. In fact, under these conditions the cluster **183** was obtained in a moderate yield of 40 %. By increasing the reaction time to 16 h the yield of **183** was almost doubled. With the optimization of the cross-coupling reaction the cluster **187** could be synthesized in a high yield (79 %). In addition, it was shown that CsF is perfectly suited as a base for Suzuki-Miyaura reactions with acetyl-protected glycosides.



**Scheme 6.4.** Synthesis of the bis-biphenyl glycocluster **183** by Suzuki-Miyaura cross-coupling between xyloside **166** and organoboronic derivatives **178/179**. (Reaction details are given in Table 6.1) Deprotection and acetylation of **183** gave the  $^4C_1$  glycocluster **187**. (a) TFA,  $\text{CH}_2\text{Cl}_2$ , rt, 2 h; (b)  $\text{Ac}_2\text{O}$ , pyridine, rt, 5 h, 87 % (over 2 steps); (c)  $\text{K}_2\text{CO}_3$ , MeOH, rt, 5 h, 95 %.

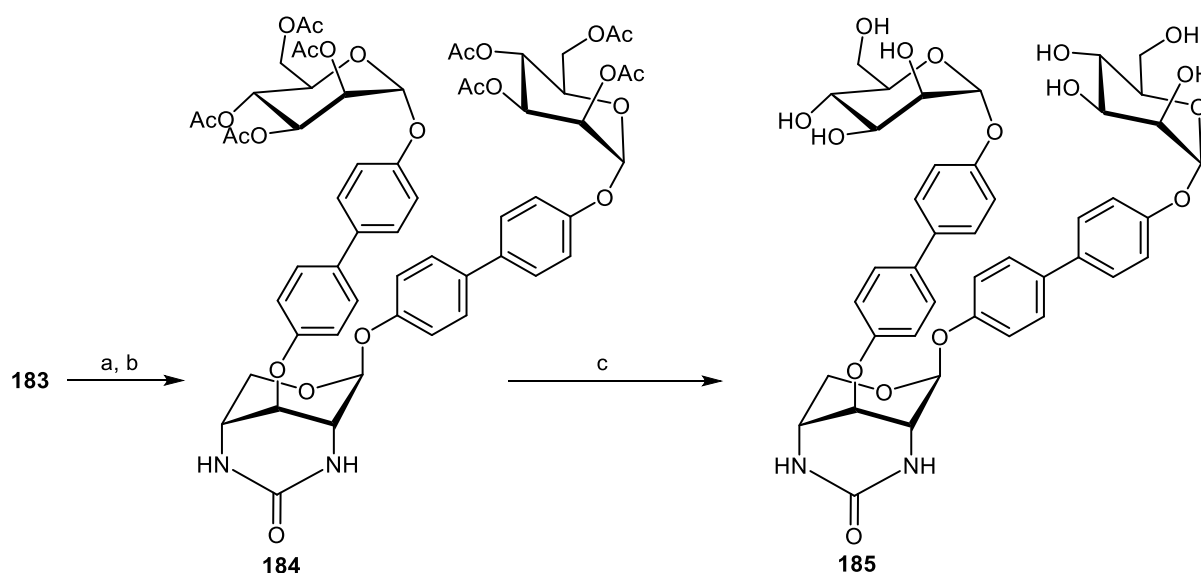
**Table 6.1.** Optimization of the reaction conditions for the Suzuki-Miyaura cross-coupling reaction of xyloside **166** with organoboron derivatives as depicted in Scheme 6.4.

Entry	Reactants	Pd-cat	Base	Solvent	Conditions	Yield
1	<b>179</b> - $\text{BF}_3$	$\text{Pd}(\text{dppf})\text{Cl}_2$	DIPEA	MeOH	80 °C, 2 h	-
2	<b>179</b> - $\text{BF}_3$	$\text{Pd}(\text{dppf})\text{Cl}_2$	DIPEA	dioxane	80 °C, 2 h	-
3	<b>178</b> -BPin	$\text{Pd}(\text{PPh}_3)_4$	$\text{Cs}_2\text{CO}_3$	dioxane/ $\text{H}_2\text{O}$	80 °C, 1 h	-
4	<b>178</b> -BPin	$\text{Pd}(\text{PPh}_3)_4$	$\text{Cs}_2\text{CO}_3$	dioxane	120 °C, 2.5 h	-
5	<b>178</b> -BPin	$\text{Pd}(\text{dppf})\text{Cl}_2$	CsF	THF	60 °C, 8 h	40 %
6	<b>178</b> -BPin	$\text{Pd}(\text{dppf})\text{Cl}_2$	CsF	THF	80 °C, 16 h	79 %

NMR spectroscopy proved that the bis-biphenyl glycocluster **183** exists in a conformational equilibrium in solution, as described above for its precursor **166**. In order to investigate the influence on bacterial adhesion of the conformation of the xylose hinge it was necessary to synthesize two defined conformers; on the one hand, a  $^4C_1$  conformer, and on the other hand,

a  ${}^1C_4$  conformer which is locked in its inverted chair conformation. For the  ${}^4C_1$  conformer, free amino groups ought to be avoided as in biological testing they can cause side effects which cannot be interpreted. Therefore, the 2,4-diamino xyloside **183** was converted into its NHAc derivative **186**. Accordingly, the Boc protecting groups of **183** were cleaved with TFA in  $\text{CH}_2\text{Cl}_2$  (Scheme 6.4). The crude product was acetylated with  $\text{Ac}_2\text{O}$  in pyridine and the corresponding *N*-acetylated xylose-based glycocluster **186** was isolated in a yield of 87 % over two steps. The  ${}^1\text{H}$  NMR spectrum of **186** showed no conformational dynamic. Then, the *O*-acetyl protecting groups were removed under Zemplén transesterification conditions to achieve the unprotected bivalent xylose-based cluster **187** in  ${}^4C_1$  conformation in a yield of 95 %.

The  ${}^1C_4$  conformer was realized by the synthesis of a cyclic urea derivative **184** (Scheme 6.5). This reaction is irreversible and hence, the xylose can no longer be considered a molecular switch. On the other hand, cyclic urea formation guarantees the defined  ${}^1C_4$  conformation in biological testings. Starting from the biphenyl xylose-based glycocluster **183**, first the Boc-protecting groups were cleaved with TFA and the unprotected intermediate was subjected to an intramolecular cyclization reaction with CDI in the presence of  $\text{Et}_3\text{N}$  in DMF according to Chen and co-workers.<sup>[251]</sup> The bicyclic urea derivative **184** was obtained in a good yield of 74 % over two steps. In a final step, the *O*-acetyl protecting groups were removed under Zemplén conditions, which gave the unprotected  ${}^1C_4$  glycocluster **185** in a yield of 74 %.



**Scheme 6.5.** Synthesis of the  ${}^1C_4$  locked glycocluster **185** by intramolecular urea formation of **183**. (a) TFA,  $\text{CH}_2\text{Cl}_2$ , rt, 16 h; (b) CDI,  $\text{Et}_3\text{N}$ , DMF, rt, 16 h, 74 % (over 2 steps); (c)  $\text{K}_2\text{CO}_3$ , MeOH, rt, 4 h, 74 %.

With the two xylose-based clusters **185** and **187** in hand, a pair of conformers was synthesized, which were tested as inhibitors of the adhesion of type1-fimbriae-mediated *E. coli* bacteria. Here, it was of interest to test the effect of varying ligand distances as provided by the conformers **185** and **187** on carbohydrate recognition.

## 6.2 Biological testing

The glycoclusters **185** and **187** were evaluated as inhibitors in a standard adhesion-inhibition assay with GFP-transfected *E. coli* (pPKL1162) in serial dilutions (experimental details in chapter 3.3 and chapter 8.3).<sup>[146]</sup> Because biological experiments with live bacteria can vary significantly between independent experiments, methyl  $\alpha$ -D-mannopyranoside (MeMan) and phenyl  $\alpha$ -D-mannopyranoside (PheMan) were utilized as reference ligands in each experiment in parallel to the tested ligands. Since the clusters **185** and **187** are bearing hydrophobic units in form of two biphenyls, the solubility of the clusters in water is limited. As it was assumed that both clusters show a high affinity to FimH due to their aromatic aglycone moieties, serial dilutions were started with a 0.4 mM solution. However, 5 % DMSO had to be added to the aqueous buffer in order to dissolve the glycocluster at this concentration.

The results of the inhibition assay are depicted in Figure 6.4 (cf. Experimental section, Figure 8.4). For each inhibitor dose-response inhibition curves were obtained to determine  $IC_{50}$  values. Testing of **185** and **187** on the same plate revealed that both clusters have a much higher inhibitory potency than the standard inhibitor MeMan and even higher than phenyl  $\alpha$ -D-mannopyranoside (PheMan). Furthermore, a difference between **185** and **187** was observed. The  ${}^4C_1$  conformer **187** turned out to be a more potent inhibitor than the  ${}^1C_4$  conformer **185**.

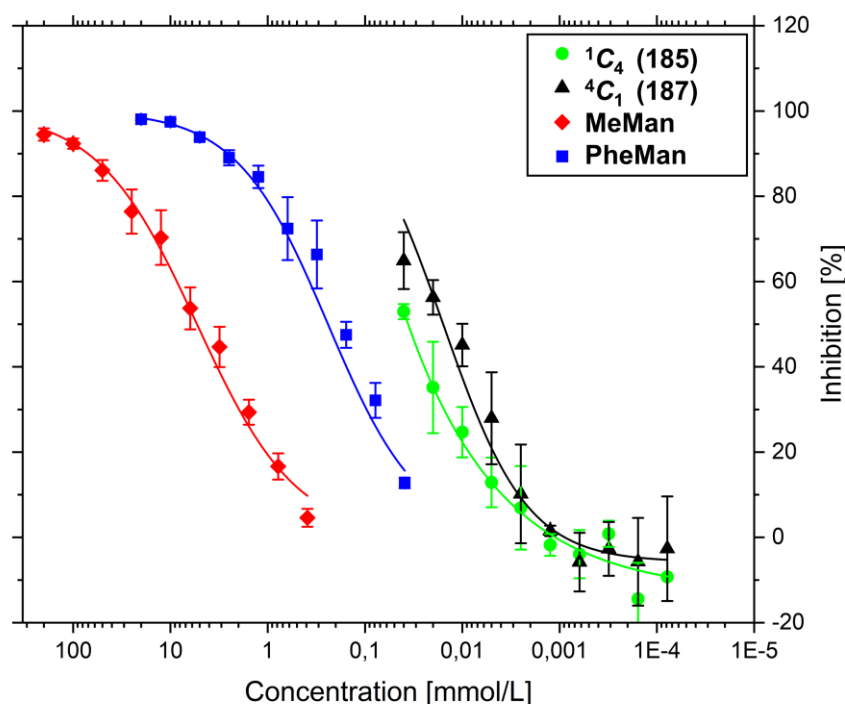


**Figure 6.4.** Inhibition curves obtained for clusters **185** and **187** as inhibitors for type 1 fimbriae-mediated bacterial adhesion. Sigmoidal concentration-response curves were fitted by non-linear regression. Error bars are standard deviations from triplicate values on one plate.

In order to compare independent experiments, for each plate relative inhibitory potency values (RIP) were deduced, relative to the reference ligand MeMan tested on the same plate (inhibitory potency of MeMan = 1), which are shown in Table 6.2. A reason for the high inhibitory potency of **185** and **187** in comparison to MeMan lies in the effect of the biphenyl aglycon units. For the conformationally locked  ${}^1C_4$  cluster **185** a RIP value of 157.05 was observed. On the other hand, the RIP value of the  ${}^4C_1$  conformer **187** is 2.6-fold higher (RIP = 410.46). This difference can be attributed to the different spatial orientations of the two mannoside ligands which is defined by the conformation of the xylose scaffold.

**Table 6.2.** Inhibitory potencies of the xyloside-based glycoclusters **185**, and **187** as determined in adhesion-inhibition assays with type 1 fimbriated *E. coli* (pPKL1162).

Cluster	IC <sub>50</sub> <sup>a</sup> [mmol]	IC <sub>50</sub> MeMan <sup>b</sup> [mmol]	RIP <sup>c</sup>	Average RIP <sup>d</sup>
${}^4C_1$ cluster <b>187</b>	0.0152 (±0.0015)	7.0789 (±0.4414)	466.33 (±76.08)	410.46 (±67.87)
	0.0157 (±0.0013)	5.3370 (±0.4837)	339.29 (±59.65)	
${}^1C_4$ cluster <b>185</b>	0.0639 (±0.0141)	7.0789 (±0.4414)	110.79 (±31.43)	157.05 (±45.44)
	0.0360 (±0.0111)	5.3370 (±0.4837)	148.17 (±59.46)	

<sup>a</sup> IC<sub>50</sub> values are average values of duplicate or triplicate results on one plate.

<sup>b</sup> IC<sub>50</sub> (MeMan) values are average values of triplicate results on the same plate.

<sup>c</sup> RIP values are based on the inhibitory potency of MeMan tested on the same microplate IP (MeMan) ≡ 1); RIP(glycocluster) = IC<sub>50</sub>(MeMan)/IC<sub>50</sub>(glycocluster).

<sup>d</sup> RIP mean values of two independent experiments with error propagation.

In order to explain the different inhibitory potencies of the two conformers **185** and **187**, molecular modelling studies were performed.

### 6.3 Molecular modelling

In order to explain the differences between **185** and **187** as inhibitors of mannose-specific bacterial binding, the three-dimensional structure of both biphenyl mannoside clusters has to be inspected. Especially the distance of the  $\alpha$ -D-mannoside ligands to each other and the spatial influence of the xylosyl hinge unit on the inter-ligand distances are of interest. Molecular dynamics (MD) simulations were performed employing the program *Desmond*<sup>[156]</sup> as implemented in the Schrödinger *Maestro* software package,<sup>[150]</sup> to provide occurrence of atomic distances and angles of the two conformers. The MD simulations, which are based on classical mechanics (Newton's equation of motion), were performed with *Desmond*, and were carried out in explicit water (SPC model) at 300 K for 200 ns (cf. Experimental section, chapter 8.4.1). The results of the MD simulations gave the trajectories of the MD trajectories of the two respective glycoclusters.

For **187** the  ${}^4C_1$  conformer was the dominant conformation over the simulation period and no other conformers were observed which is in accordance with the results obtained for the diamino xyloside **166** in polar solvents. On the other hand, the bicyclic urea derivative **185** exists to 100 % in the  ${}^1C_4$  conformation and the results of the MD simulations showed the influence of the conformational switching on the geometry of the respective clusters. The trajectories were analyzed by using the "Simulation Event Analysis" tool<sup>[156]</sup> in order to monitor the distances between the mannoside rings and the angles of the xylosyl hinge (Figure 6.5). The distance between the mannosyl residues of **185** and **187** (Figure 6.5, A) is controlled by the xyloside conformation. While for **187** the distance is oscillating from 20 Å to 27 Å, the respective  ${}^1C_4$  conformer **185** showed a distance from approximately 15 Å to 20 Å. In addition, it was observed for **185** that various events showed a relatively small distance (5 Å to 8 Å). The distance between the mannosyl residues parallels with the distance between the two biphenyl moieties. In order to determine if either the conformation of the xyloside scaffold or the general orientation of the biphenyl linkers has an influence on the mannosyl distance, the angle between the linker units was measured (Figure 6.5, B) (angle between biphenyl carbons and C-2 of the xylosyl). While for **187** this angle remained relatively constant ( $\sim 140^\circ$ ), the glycocluster **185** showed two different angles ( $\sim 90^\circ$  and  $\sim 30^\circ$ ).

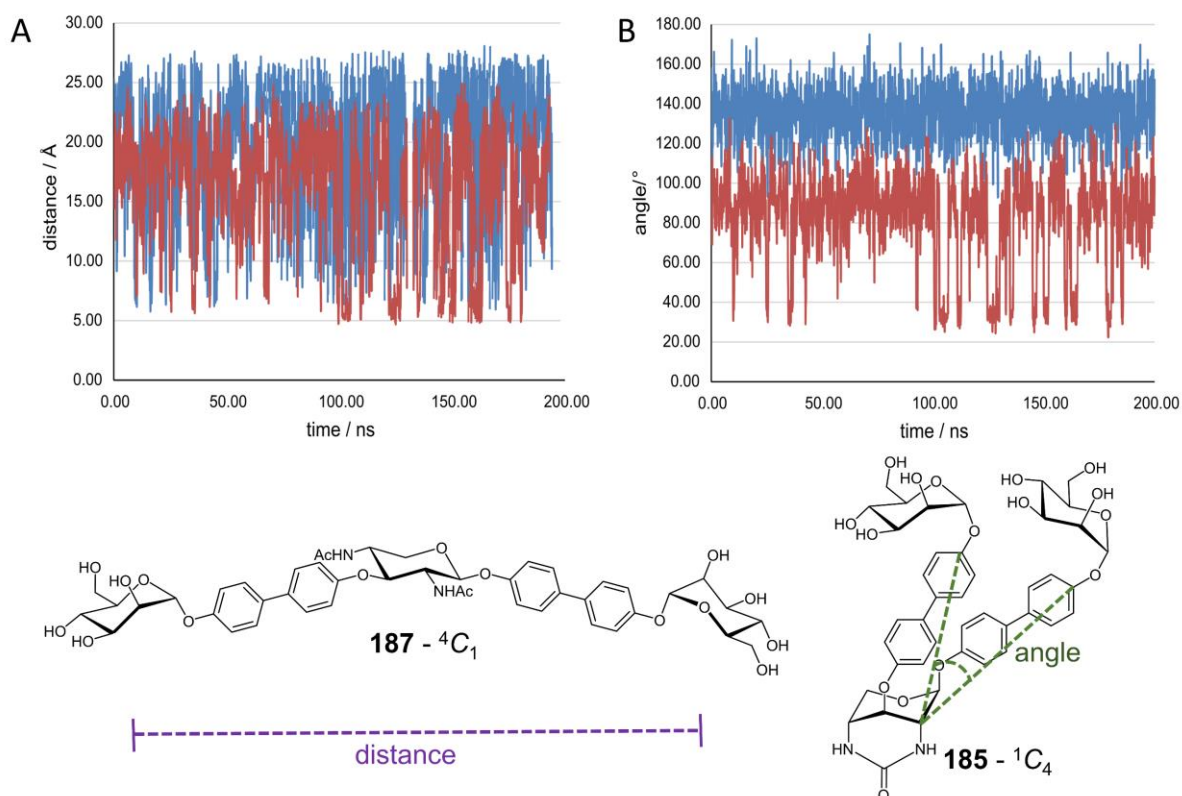


**Figure 6.5.** Distances (A) between the mannosyl residues and angles (B) between the biphenyl linker units are given as a function of the simulation time (in ns). Distances are measured between the two mannosyl rings. Angles are measured between the biphenyls related to the xylosyl C-2. Distances and angles for the  ${}^4C_1$  conformer **187** are given in blue and for the  ${}^1C_4$  conformer **185** in red.

For the distance between the mannosyl residues the distribution occurrence of the corresponding glycoclusters was plotted (Figure 6.6). This plot indicates that the change of the conformation from  ${}^4C_1$  to  ${}^1C_4$  has two consequences. First, the structure of **187** showed that the mannosyl residues were separated as far as possible from each other. The most frequently occurring distance was  $\sim 25$  Å. For structures C (Figure 6.6), the rigid biphenyl units separate the mannoside ligands and stretch the amplitude to its maximum (25.33 Å). This is different for **185**, which showed two main distances between the mannosides. On the one hand, switching the xyloside scaffold from  ${}^4C_1$  to  ${}^1C_4$ , brought the two arms of the cluster closer to each other (structures B, Figure 6.6), resulting in an occurring distance of  $\sim 19$  Å. On the other hand,  $\pi$ - $\pi$  interactions between the biphenyl moieties for structures A, as it was also observed for related xylosides published by Yuasa and colleagues,<sup>[92a]</sup> resulted in a relatively short distance of  $\sim 6$  Å (Figure 6.6).

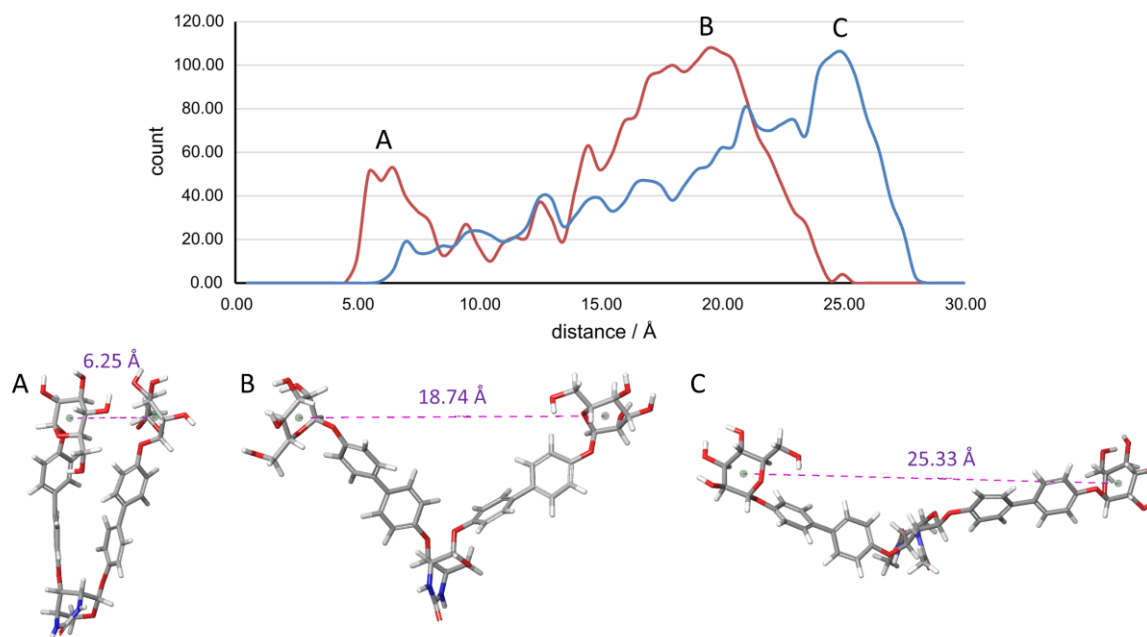


**Figure 6.6.** Intramolecular distance and their occurrence as determined for the two glycoclusters **187** (blue) and **185** (red). Distances are measured between the two mannose pyranosyl rings. Structures A, B and C show the influence of the conformational change and the  $\pi$ - $\pi$  interactions on the geometry of the glycoclusters. Structures rendered with Schrödinger. Color code for the structures: carbons (grey), nitrogens (blue), oxygen (red).

The xylose conformation and biphenyl  $\pi$ - $\pi$  interactions together contribute to the observed distribution occurrence of the angles between the biphenyl moieties. For **187** it was observed that the biphenyl units were strictly separated from each other, resulting in a most frequent angle of  $\sim 140^\circ$ , which was different for cluster **185**. Here, the change from  ${}^4C_1$  to  ${}^1C_4$  results in a general decrease of the angle between the biphenyls ( $\sim 89^\circ$ ), describing the most frequent occurring geometry (structures B). In this case, however, the two mannoside branches are relatively flexible. When the two biphenyl linkers can exert  $\pi$ - $\pi$  interactions, the flexibility is restricted and the two branches are positioned almost parallel to each other, resulting in a small angle the biphenyl units and xylosyl C-2 of  $\sim 32^\circ$  (cf. Figure 6.7).

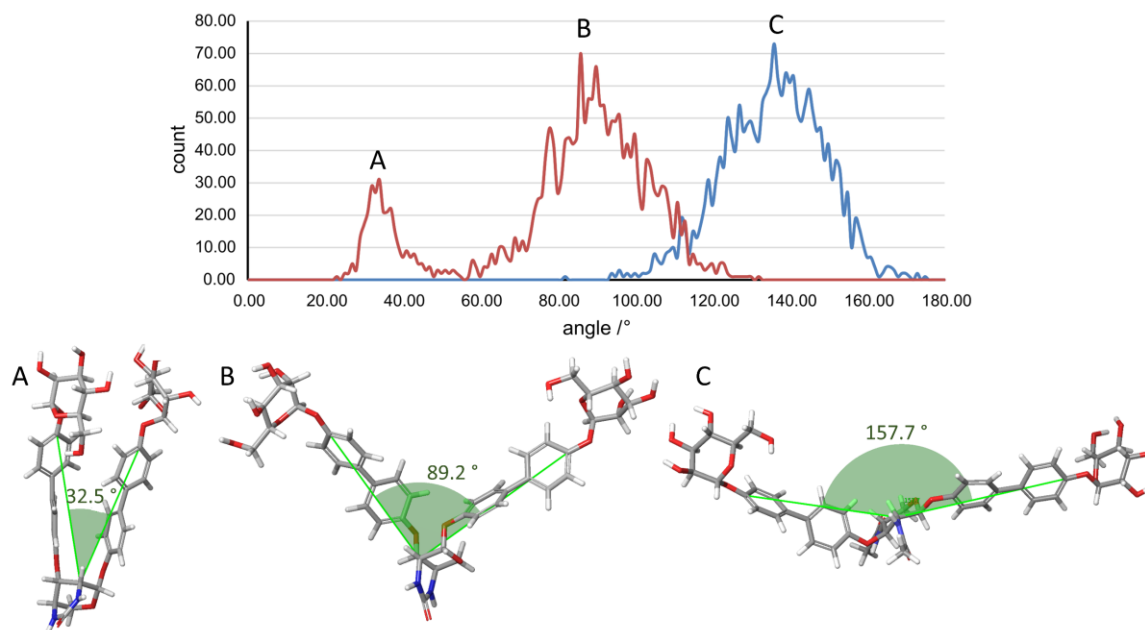


**Figure 6.7.** Intramolecular angles and their occurrence as determined for the two glycoclusters **187** (blue) and **185** (red). Angles are measured between the biphenyls related to the xylosyl C-2. Structures A, B and C show the influence of the conformational change and the  $\pi$ - $\pi$  interactions on the geometry of the glycoclusters. Structures rendered with Schrödinger. Color code for the structures: carbons (grey), nitrogens (blue), oxygen (red).

In conclusion, two events lead to basic changes in the geometry of the structures of **185** and **187**. On the one hand, the conformational change from  ${}^4C_1$  to  ${}^1C_4$  arranges the two mannoside branches closer to each other (from 25 Å to 19 Å). On the other hand,  $\pi$ - $\pi$  interactions between the biphenyl linkers stabilize the population of conformers where the mannosides were separated by 6 Å.

For the investigation of the detailed binding process of the biphenyl glycoclusters **185** and **187** and the lectin FimH, docking studies using *Glide* as implemented in the Schrödinger package were performed.<sup>[149]</sup> The glycocluster ligands were prepared by using *Maestro*<sup>[150]</sup> and then minimized by using *LigPrep*.<sup>[151]</sup>

Since it is known that carbohydrate-FimH complexes with aromatic aglycone moieties are stabilized by  $\pi$ - $\pi$  interactions with the tyrosine gate in the open gate conformation, the theoretical experiments were performed with the open gate conformation of FimH. Thus, a crystal structure (PDB code 6G2S)<sup>[266]</sup> bearing a biphenyl  $\alpha$ -D-mannoside as a ligand was utilized in order to achieve good accordance for the biphenyl clusters **185** and **187**. For the docking, the protein conformer was prepared with the implemented *Protein Preparation Wizard* in *Maestro*. In this case, due to the size of the xylose-based glycoclusters **185** and **187**, it was necessary to enlarge the grid box of the protein binding domain to 36 Å which enables more

ligand flexibility during the conformational search. Next, docking was performed in an extra precision mode, which fixed the lectin in a rigid conformation whereas the ligand is flexible during the docking process (for more details see experimental part). The top glide scoring results, which were obtained from the docking experiments of both conformers were then submitted to a MM-GBSA calculation<sup>[153]</sup> (molecular mechanics energies combined with generalized born and surface area continuum solvation) with the OPLS3e force field (Table 6.3).

**Table 6.3.** Computed results from molecular modelling studies with the synthetic ligands **185** and **187** and the open gate conformer of FimH (PDB code 6G2S).<sup>[266]</sup> The best docking scores and corresponding binding energies (MM-GBSA) using Glide are listed. Lower values suggest tighter FimH binding. RIP values (higher values relating to stronger FimH binding) are shown for comparison.

Glycocluster (RIP)	Glide score	Binding energy [kcal mol <sup>-1</sup> ] <sup>a</sup>
<sup>4</sup> C <sub>1</sub> cluster <b>187</b> (410.46 ±67.87)	-9.075	-73.53
<sup>1</sup> C <sub>4</sub> cluster <b>185</b> (157.05 ±45.44)	-8.998	-89.97

<sup>a</sup> best binding poses were used for the MM-GBSA calculations.

The docking experiment revealed that the binding of the two clusters is almost in the same range (comparison of the glide scores). The <sup>4</sup>C<sub>1</sub> cluster **187** (-9.075) had a better docking score than the respective <sup>1</sup>C<sub>4</sub> cluster **185** (-8.998), which is in accordance with the results from the biological testing. This changes unexpectedly, when the calculated binding energies for the two conformers are compared as cluster **185** binds stronger to the lectin FimH (-89.97 kcal mol<sup>-1</sup>) than the respective **187** (-73.53 kcal mol<sup>-1</sup>). However, binding energies were still in the same range. Because these findings were not in accordance with the results of the biological tests, the simulated structures of the protein-carbohydrate complexes were investigated in greater detail and the results are shown in Figure 6.8. Both structures revealed that the α-D-mannosyl ligand, bound to the 3-position of the xylose unit, is buried within the CRD of FimH and complexed by the typical hydrogen bond network with the CRD.<sup>[37b]</sup> Additionally, both structures showed explicit π-π interactions of the biphenyl aglycone with the tyrosine residue Tyr48 (light blue dotted lines). These interactions were responsible for a preorientation of the rest of the cluster to the backside of the lectin. In both cases the xylose unit is not interacting with the protein surface. The differences in binding affinity are assigned to the second mannosyl ligand of the clusters. For **185** the non-binding mannoside ligand is orientated towards the protein surface and can undergo secondary non-covalent interactions to the

periphery of the CRD of FimH (Figure 6.8, B). On the other hand, the non-binding mannoside ligand of **187** is pointing away from the lectin and is thus more flexible.

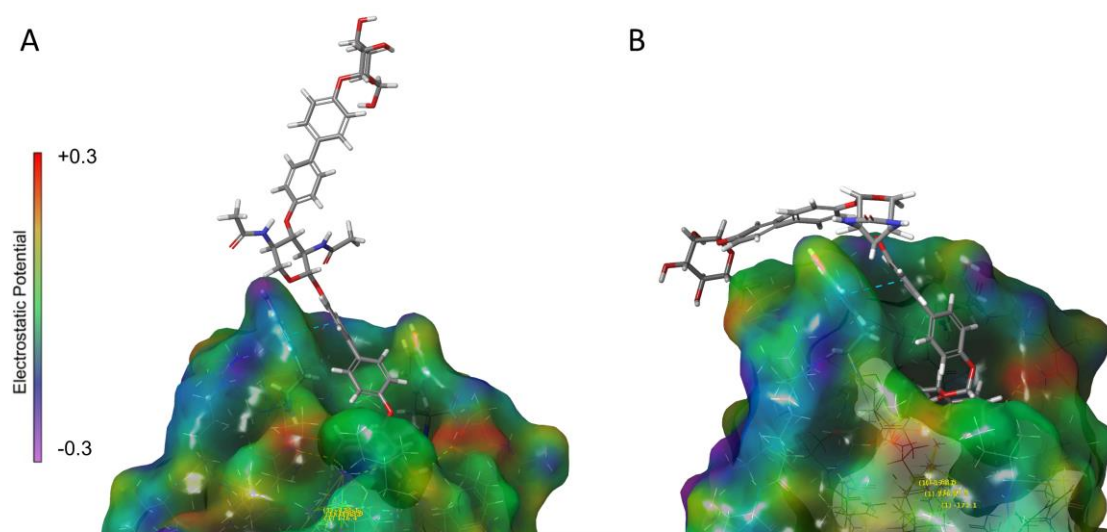


**Figure 6.8.** Connolly surface representations of selected FimH-glycocluster complexes as derived molecular docking using the open gate conformation of FimH (pdb: 6G2S).<sup>[266]</sup> The xylose-based glycoclusters **187** (A), and **185** (B) are depicted as stick models. Protein coloring represents the electrostatic potential of the surface (positive charges in purple, neutral in green, negative charges in red, cf. depicted color bar). Hydrogen bonds and  $\pi$ - $\pi$  interactions are indicated as dashed lines.

In docking studies only one binding event is investigated, and multivalent binding cannot be observed. The binding energy for a complex of one lectin and one carbohydrate ligand is dominated by the binding event in the CRD (hydrogen bonds) and the interaction with the tyrosine gate ( $\pi$ - $\pi$  interactions). Secondary interactions between cluster and protein have also an impact on the binding energy. However, the structures of the two clusters **185** and **187** differ only in the conformation of the xylose scaffold, which leads to a different orientation of the mannoside ligands (see above). The higher binding energy for **185** can be explained on the one hand by secondary interactions and on the other hand by a more flexible structure of **187**. Nevertheless, the orientation of the second mannoside ligand of **187** into the surroundings of the lectin allows further binding to a second lectin, resulting in a higher binding affinity due to a multivalent cluster effect as it was described for cross-linking processes by Roy et al.<sup>[269]</sup> Otherwise, for **185** the second ligand is orientated towards the protein and lectin binding is sterically not preferred. Thus, the binding energy of **185** for one binding event is higher, but when a second binding event is considered, this should change significantly.

## 6.4 The potential of orthogonal switchable glycoconjugates

As it was demonstrated that the conformation of carbohydrate clusters and the inter-ligand distance has an influence on carbohydrate recognition processes. With the 2,4-diamino xyloside **167** in hand, a molecular switch driven by the complexation of metal ions and an induced conformational ring flip was introduced. A strategy to enlarge the complexity of molecular motility is to incorporate multiple active parts in a single molecule to follow various movements, respectively.<sup>[282]</sup> Thus, further investigation of a multistimuli-responsive molecular switch based on 2,4-diamino xylosides might come into focus by adding an additional switchable unit.

One external stimulus orthogonal to the chemical addressable diamino xylosides is light. Among other stimuli, light has multiple advantages: i) it is energy efficient and generates no side products; ii) it imbues spatiotemporal control; iii) it can be controlled by different wavelength or polarization; iv) it is orthogonal to other stimuli. One possible molecular switch, which can be addressed by light is the photoswitchable azobenzene.<sup>[283]</sup> This molecule can be photoisomerized from its natural occurring and thermodynamical stable *E*-isomer by light (~365 nm) to the respective *Z*-isomer. The back isomerization can be facilitated either by light (~435 nm) or thermally. Furthermore, the isomerization of azobenzene leads to a structural change and an end-to-end distance decreasing between the *para*-carbons of about 4 Å.<sup>[284]</sup>

Accordingly, a multiple and orthogonal switchable glycoconjugate can be envisaged. Next to the 2,4-diamino functionalization the xyloside **164** was elongated with an azobenzene unit. By Suzuki-Miyaura cross-coupling an azobenzene moiety was attached to the aglycone moiety leading to xyloside **188** (Figure 6.9). This orthogonal switch can assume four different states. Starting from the thermodynamical favored  ${}^4C_1$ -*E* state by complexation of a metal ion (e.g.,  $Zn^{2+}$ ) the ring flip takes place, and the pyranose substituents are all axial orientated in the  ${}^1C_4$ -*E* state. Following by irradiation with light (~365 nm) the azobenzene moiety can be isomerized leading to the  ${}^1C_4$ -*Z* state. By addition of a stronger ligand (e.g., TETA) the xylose ring conformation can be switched back giving the  ${}^4C_1$ -*Z* state, which finally can be targeted by irradiation with a second wavelength or thermally to switch back the azobenzene unit and yield the original state again (Figure 6.9).

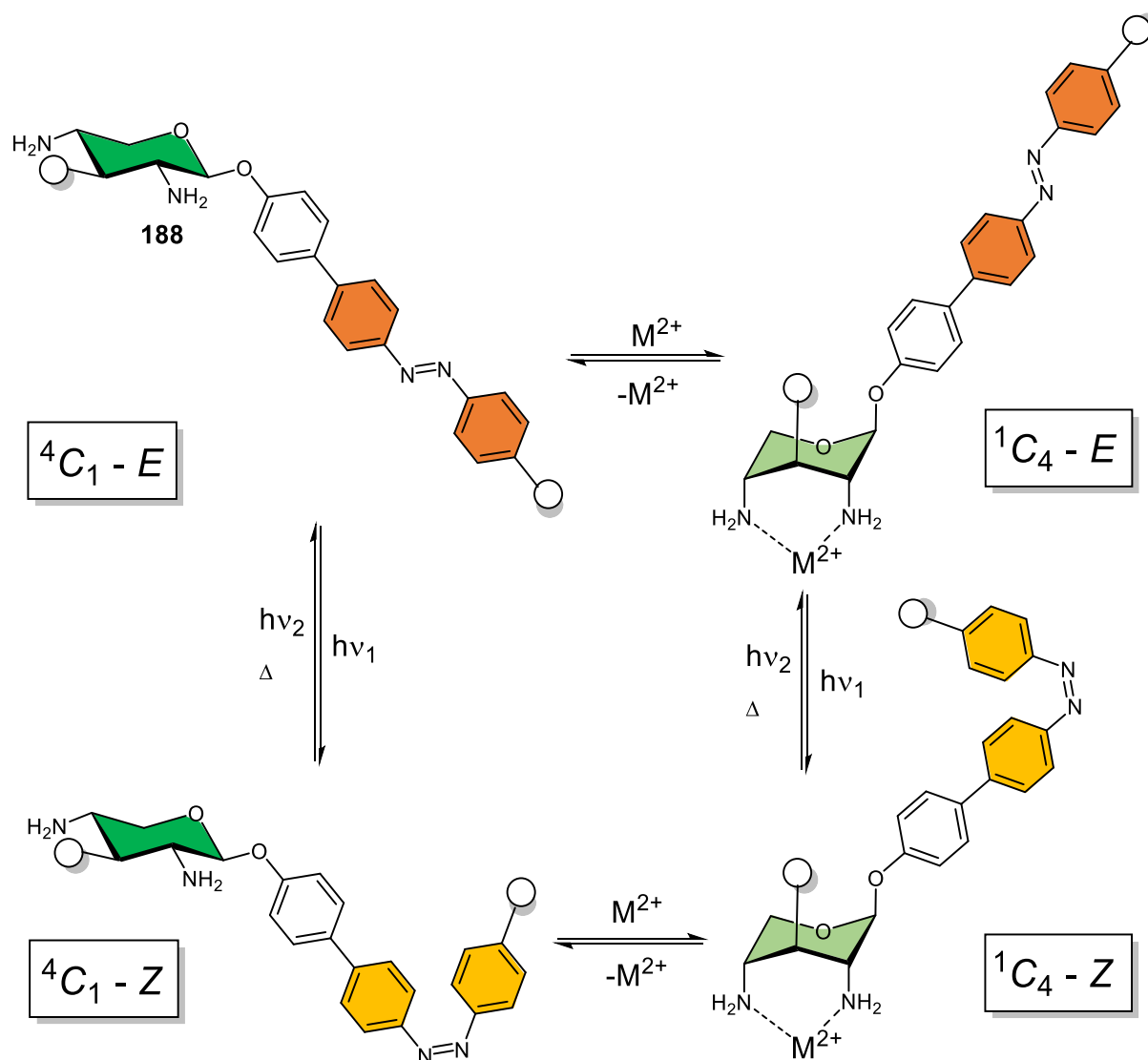
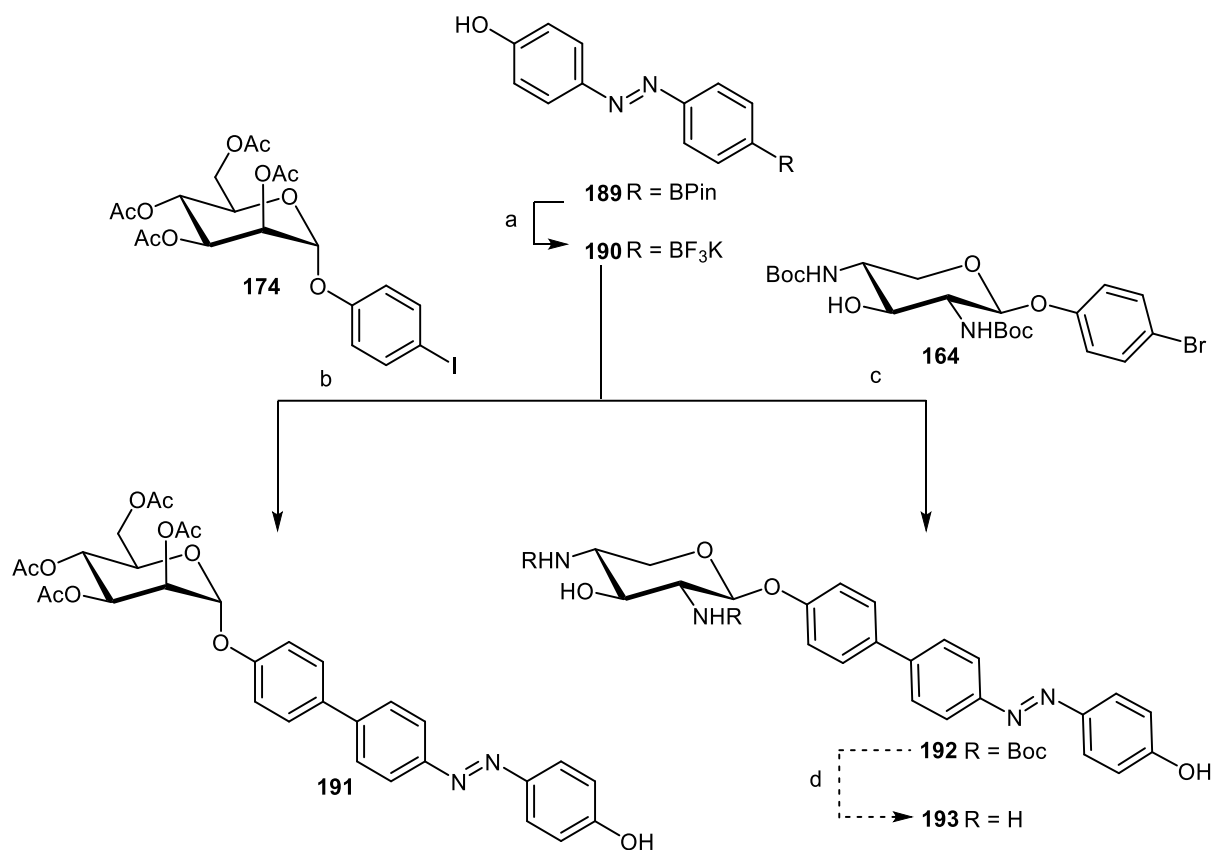


**Figure 6.9.** Schematic representation of a multistimuli-responsive switch based on a xyloside. The orthogonal switchable functional groups of **188** can be addressed either by light or the complexation of metal ions.

The synthesis of the multistimuli-responsive switch **188** required Suzuki reaction conditions with azobenzenes and the group of Trauner showed that azobenzene trifluoroborates serve ideal in cross-coupling reactions.<sup>[285]</sup> Thus, starting from the known azobenzene pinacol boronic ester **189**<sup>[286]</sup> first of all the corresponding potassium trifluoroborate **190** was synthesized by treatment of **189** with  $\text{KHF}_2$  in MeOH to yield **190** in an excellent yield of 86 % (Scheme 6.6). In order to test Suzuki reaction conditions with **190**, it was reacted with 4-iodophenyl  $\alpha$ -D-mannoside **174** under the approved conditions in the presence of DIPEA and  $\text{Pd}(\text{dppf})\text{Cl}_2$  in MeOH and the required biphenylazobenzene derivative **191** was isolated in a fair yield of 54 %.

Following this approach, xyloside **164** and **190** were reacted with DIPEA and  $\text{Pd}(\text{dppf})\text{Cl}_2$  in MeOH and the biphenylazobenzene derivative **192** was isolated in a poor yield of 24 %

(Scheme 6.6). Unfortunately, it was not possible to optimize the reaction conditions at this stage.



**Scheme 6.6.** Synthesis of a potential orthogonal switchable xyloside **193**, which is addressable by light or metal ions, respectively. (a)  $\text{KHF}_2$ , MeOH, rt, 1 h, 86 % (b) DIPEA,  $\text{Pd}(\text{dppf})\text{Cl}_2 \cdot \text{CH}_2\text{Cl}_2$ , MeOH,  $70^\circ\text{C}$ , 54 %; (c) DIPEA,  $\text{Pd}(\text{dppf})\text{Cl}_2 \cdot \text{CH}_2\text{Cl}_2$ , MeOH,  $70^\circ\text{C}$ , 24 %; (d) TFA,  $\text{CH}_2\text{Cl}_2$ .

In a future step **192** has to be deprotected by treatment with TFA and following the switching abilities of **193** have to be evaluated. Nevertheless, it could be shown that xyloside **192** represents a valuable intermediate, which can further be derivatized by Suzuki-Miyaura cross-coupling reactions. Furthermore, it is of interest to investigate orthogonal switches based on the conformational flexibility of xylose derivatives.

## 6.5 Conclusion

In the course of this subproject the effect of spatial ligand presentation by conformational switching was studied. Thus, the xyloside scaffold **166** was used successfully as a scaffold molecule for the synthesis of divalent glycoclusters by functionalization under Suzuki-Miyaura cross-coupling reaction conditions. Accordingly, a  ${}^4C_1$  and a  ${}^1C_4$  conformer were prepared. The two derivatives were tested in a well-established adhesion-inhibition assay and the  ${}^4C_1$  conformer showed higher inhibitory potency than the corresponding  ${}^1C_4$  conformer. These findings were underlined by molecular modelling studies and the structures of the two glycoclusters were further investigated to show that the relative inter-ligand distance is highly dependent on the conformation of the xylosyl unit. A  ${}^4C_1$  xylosyl moiety separates the mannoside ligands to a maximum length, whereas for the  ${}^1C_4$  derivative the distance decreases which is traced back to  $\pi$ - $\pi$  interactions between the biphenyl linkers.

Furthermore, the potential of an orthogonal switchable molecule was exemplified. By the attachment of a light-responsive azobenzene moiety, a second switch was installed and the glycoconjugate **192** promises interesting switching characteristics in the field of multistimuli-responsive materials.



Furthermore, the multifunctionality of the maltose-based scaffolds allows further modification by addressing the anomeric propargyl function, which gives the opportunity of immobilization to study bacterial adhesion to surfaces.

### Conformational switchable xylosides: Synthesis and conformational analysis

In the second subproject of this thesis, the synthesis of conformational switchable xylosides was targeted in order to study the effect of ligand presentation by conformational switches. In requirement of aspects of selective stereo- and regiochemistry it turned out that starting the synthetic route from L-arabinose gave access to 4-amino-functionalized xylals, serving as an intermediate. The reaction of choice for the introduction of the 2-amino function the iododisulfonamidation and its following rearrangement was established to provide a wide range of orthogonally protected 2,4-diamino xylosides with a high precision in stereo- and regiochemistry (Figure 7.2) and a decreased number of reaction steps.

Furthermore, 2,4-diamino xyloside **167** was investigated as a conformational switch by the complexation of  $\text{ZnCl}_2$  to achieve the conformational ring flip from the  ${}^4\text{C}_1$  to the  ${}^1\text{C}_4$ . The switching efficiency was followed by NMR spectroscopy, and it was shown that the switching process was reversible. With the new synthesis approach for diamino xylosides a robust method was established to prepare conformational switchable xylosides.

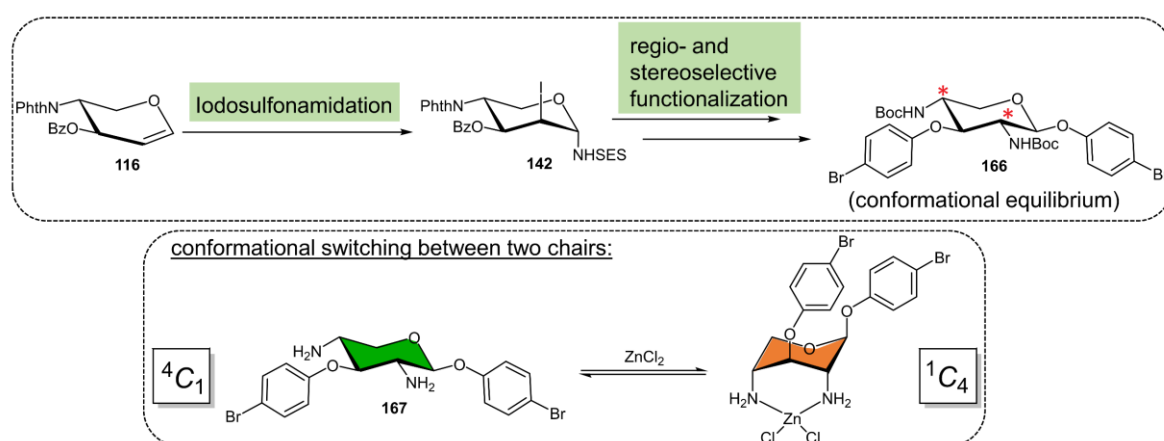


**Figure 7.2.** The regio- and stereoselective synthesis of 2,4-diamino xylosides is achieved by the functionalization of difunctional xylals by iododisulfonamidation and following rearrangement. By the complexation of Zn ions 2,4-diamino xylosides serve ideal switches.

Furthermore, for the synthesis of 2,4-diamino xylosides it turned out surprisingly that 2,4-bis-Boc protected xylosides occur in solution in a dynamic conformational equilibrium. Thus, a toolbox of a combination of experimental and computational methods was set up to analyze these conformational equilibria (Figure 7.3).

Hence, experimental NMR data for coupling constants of xylosides (**167**, **168**, **169**) with a defined conformation could benchmark computational methods. For xyloside **166** coupling constants were computed (PBE/pc-J3 level of theory) and in a computational conformer search the puckering behavior was investigated (three lowest energy conformers, namely  ${}^4C_1$ ,  ${}^1C_4$ , and  ${}^2S_0$ ). With the combined results the conformational equilibrium of **166** in different solvents was studied and the distribution of the conformers showed that in polar solvents the  ${}^4C_1$  conformation was dominating, while in less-polar solvents the population of the  ${}^1C_4$  conformation increased.

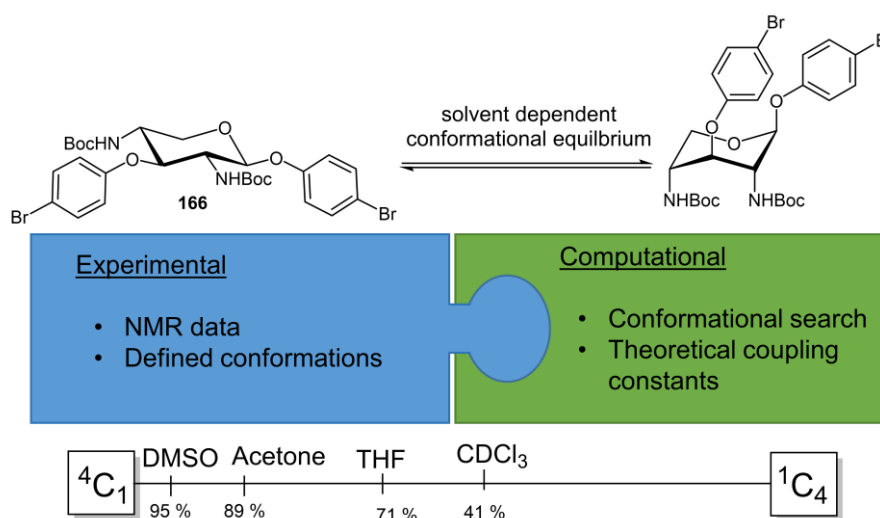


**Figure 7.3.** Investigation of the solvent-dependent conformational equilibrium of xyloside **166** in solution by a combined toolbox of experimental and computational methods.

In conclusion, the conformation of 2,4-diamino xylosides can be triggered by the carbohydrate environment in form of metal ions or the surrounding solvent.

### Conformational switchable xylosides: Control of biological function

In a final project conformational switchable xylosides were utilized in order to control ligand presentation in carbohydrate recognition processes. Thus, biphenyl mannoside ligands were attached to xyloside scaffold **166** in a Suzuki-Miyaura reaction to obtain homobivalent glycoclusters. In addition to the  ${}^4C_1$  conformer, the corresponding  ${}^1C_4$  conformer was synthesized by an intramolecular urea cyclization and testing in an adhesion-inhibition assay employing mannose-specific *E. coli* bacteria showed differences in the inhibition potency of the glycoclusters (Figure 7.4). Molecular modelling revealed that the relative inter-ligand distance of the Man ligands is dependent on the conformation of the xylosyl unit. In the  ${}^4C_1$  conformer the ligand amplitude showed a maximum length, whereas in the  ${}^1C_4$  derivative the distance decreased due to  $\pi$ - $\pi$  interactions between the biphenyl linker moieties.

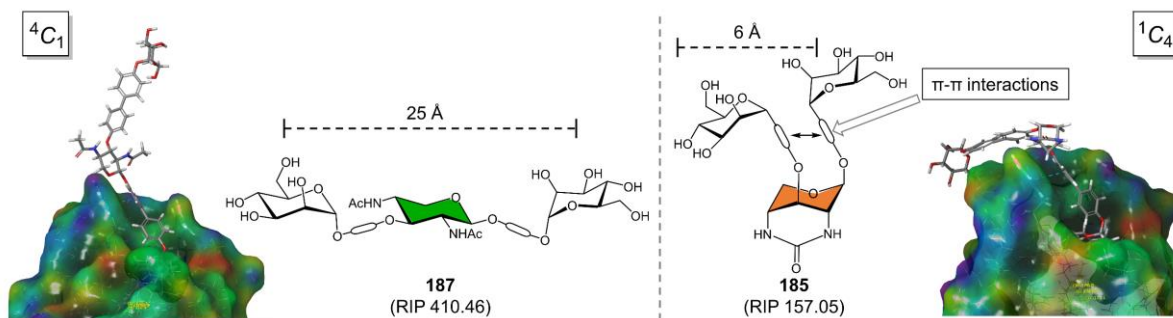


**Figure 7.4.** Conformational switchable xylosides affect the structural behavior of bivalent glycoclusters **185** and **187**. The decreasing of the ligand amplitude by  $\pi$ - $\pi$  interactions prevents multivalent binding events and thus influences carbohydrate recognition processes.

The results of this thesis showed that the spatial ligand presentation is an essential aspect in carbohydrate recognition processes. In two different approaches the control of ligand presentation was achieved either by regioisomeric placement on maltose-based scaffolds or by xylose-based conformational switches. Both cases demonstrated that the inhibitory potency is dependent on the relative ligand orientation which is also the case for natural occurring glycans in the glycocalyx. Furthermore, the ligand presentation by conformational switchable glycoclusters is a new tool which has to be further explored in order to control and analyze the conformational equilibria.

## 8 Experimental section

### 8.1 Materials and methods

All reactions were carried out under atmospheric conditions (unless otherwise stated). Moisture-sensitive reactions were carried out under a nitrogen atmosphere in reaction vessels that were baked out before use.

#### Solvents and chemicals

All chemicals were purchased from abcr, Acros, Alfa Aesar, Merck, Sigma-Aldrich, or TCI and used without any further purification. For extractions and column chromatography, technical grade solvents were used, which were purified by distillation before use. Dry solvents were either directly purchased from the manufacturer or dried by an Inert PureSolv MD5 solvent purification system.

Acetonitrile	over calcium hydride
Methanol	over magnesium

#### Thin layer chromatography (TLC)

TLC was performed on silica gel plates (GF 254, Merck) backed with aluminum. The detection of UV-active substances was achieved by a CAMAG UV lamp (wavelength  $\lambda = 254$  nm). In addition, substances were detected by coloring reagents. Therefore TLC-plates were wetted with following reagents followed by heating at  $\sim 500$  °C.

10 % sulfuric acid in EtOH

Vanillin staining reagent (3.0 g vanillin and 0.5 mL H<sub>2</sub>SO<sub>4</sub> in 100 mL EtOH)

Ninhydrin staining reagent (1.5 g ninhydrin and 15 mL acetic acid in 500 mL EtOH)

#### Flash chromatography

Flash chromatography was carried out on silica gel 60 (Merck, 230-400 mesh, particle size 0.040-0.063 mm) or by using an Interchim puriFlash<sub>R</sub>450 chromatography system with distilled solvents.

#### Nuclear magnetic resonance spectroscopy (NMR)

The <sup>1</sup>H and <sup>13</sup>C spectra were recorded on following spectrometers at 298 K:

Bruker AC 200	$^1\text{H}$ NMR (200 MHz)	$^{13}\text{C}$ NMR (50 MHz)
Bruker DRX 500	$^1\text{H}$ NMR (500 MHz)	$^{13}\text{C}$ NMR (125 MHz)
Bruker AV 600	$^1\text{H}$ NMR (600 MHz)	$^{13}\text{C}$ NMR (125 MHz)

Chemical shifts are referenced to the residual proton or the carbon signal of the used deuterated solvent.

$\text{CDCl}_3$	$^1\text{H}$ 7.26 ppm (s)	$^{13}\text{C}$ 77.2 ppm (t)
$\text{MeOD-d}_3$	$^1\text{H}$ 3.31 ppm (quint)	$^{13}\text{C}$ 49.0 ppm (sept)
$\text{DMSO-d}_6$	$^1\text{H}$ 2.50 ppm (quint)	$^{13}\text{C}$ 39.5 ppm (sept)
$\text{DMF-d}_7$	$^1\text{H}$ 8.03 ppm (s)	$^{13}\text{C}$ 163.2 ppm (t)
	$^1\text{H}$ 2.92 ppm (quint)	$^{13}\text{C}$ 34.9 ppm (sept)
	$^1\text{H}$ 2.75 ppm (quint)	$^{13}\text{C}$ 29.8 ppm (sept)
pyridine- $\text{d}_5$	$^1\text{H}$ 8.74 ppm (s)	$^{13}\text{C}$ 150.4 ppm (t)
	$^1\text{H}$ 7.58 ppm (s)	$^{13}\text{C}$ 135.9 ppm (t)
	$^1\text{H}$ 7.22 ppm (s)	$^{13}\text{C}$ 123.9 ppm (t)
benzene- $\text{d}_6$	$^1\text{H}$ 7.16 ppm (quint)	$^{13}\text{C}$ 128.1 ppm (t)
$\text{CD}_2\text{Cl}_2$	$^1\text{H}$ 5.32 ppm (quint)	$^{13}\text{C}$ 54.0 ppm (quint)
acetone- $\text{d}_6$	$^1\text{H}$ 2.05 ppm (s)	$^{13}\text{C}$ 29.8 ppm
$\text{MeCN-d}_3$	$^1\text{H}$ 1.94 ppm (s)	$^{13}\text{C}$ 1.32 ppm
$\text{D}_2\text{O}$	$^1\text{H}$ 4.79 ppm (s)	
toluene- $\text{d}_8$	$^1\text{H}$ 7.09 ppm (m)	$^{13}\text{C}$ 137.9 ppm (s)
	$^1\text{H}$ 7.00 ppm (quint)	$^{13}\text{C}$ 129.2 ppm (t)
	$^1\text{H}$ 6.98 ppm (quint)	$^{13}\text{C}$ 128.3 ppm (t)
	$^1\text{H}$ 2.09 ppm (s)	$^{13}\text{C}$ 125.5 ppm (t)
		$^{13}\text{C}$ 20.4 ppm (sept)

Data is presented in the following format: chemical shift ( $\delta$ ) (multiplicity: s for singlet, d for doublet, dd for doublet of doublets, t for triplet, q for quartet, m for multiplet; coupling constant in Hertz (Hz), integration, assignment).

### **Mass spectrometry (MS)**

ESI mass spectra were recorded on a Bruker Daltonics Esquire-LC instrument. EI mass spectra were recorded on a Jeol AccuTOF 4GCV instrument.

### **Infrared (IR) spectroscopy**

IR spectra were recorded on a PerkinElmer FT-IR Paragon 1000 (ATR) spectrometer. The absorption bands are presented in  $\text{cm}^{-1}$ .

### **Optical rotations**

Optical rotations were measured on a PerkinElmer 241 polarimeter (sodium D-line: 589 nm, cell length: 1 dm) in the solvents indicated. The specific rotation values  $[\alpha]_D^{23}$  are given in  $[\text{°}\cdot\text{mL}\cdot\text{g}^{-1}\cdot\text{dm}^{-1}]$  and the concentration  $c$  in  $[\text{mol}/\text{mL}]$ .

### **Melting points (m.p.)**

Melting points were determined on a BÜCHI Melting Point M-560 apparatus.

### **Purity of compounds**

The purity of synthesized compounds was ensured by validation of the corresponding  $^1\text{H}$  and  $^{13}\text{C}$  NMR spectra in combination with the respective ESI-MS spectra.

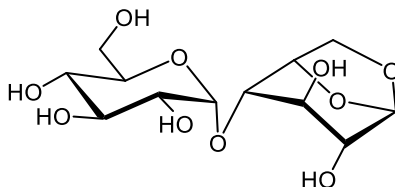
### **ELISA reader**

Fluorescence was measured on a Tecan infinite® 200 multifunction microplate reader. A bandpass filter was used with 485 nm for excitation and 535 nm for emission.

## 8.2 Individual synthetic procedures

### 8.2.1 Synthetic procedures for chapter 3

#### Maltosan (**6**)<sup>[113]</sup>



Maltose (**4**, 10.0 g, 27.8 mmol) was dissolved in H<sub>2</sub>O (400 mL) and, at 0 °C, 2-chlorodimethyl imidazolium chloride (**5**, 14.1 g, 83.3 mmol) and Et<sub>3</sub>N (34.7 mL, 250 mmol) were added. While stirring for 2 h the reaction mixture was allowed to warm to room temperature. The mixture was washed with CH<sub>2</sub>Cl<sub>2</sub> and the aqu. layer was concentrated and coevaporated with toluene under reduced pressure. The white residue was dissolved in pyridine (100 mL) and Ac<sub>2</sub>O (35.0 mL, 371 mmol) was added. The mixture was stirred for 2.5 h before the solvent was removed under reduced pressure. The residue was dissolved in ethyl acetate and washed with 1M HCl and H<sub>2</sub>O. The aqu. layer was extracted with ethyl acetate and the combined org. phases were washed with brine, dried over MgSO<sub>4</sub>, filtered and the solvents were removed. The residue was dissolved in dry MeOH (50 mL) and 5.4M sodium methoxide solution (2.00 mL, 10.8 mmol) was added dropwise. The mixture was stirred for 1 h and then neutralized by adding Amberlite IR 120. The resin was filtered off, washed with MeOH and the solvent was removed to afford **6** as a colorless solid. Analytical data correspond to the literature.<sup>[113]</sup>

**Yield:** 8.51 g (26.2 mmol, 94 %), (lit.:<sup>[113]</sup> 89 %);

**R<sub>f</sub>:** (MeCN/ H<sub>2</sub>O, 4:1): R<sub>f</sub> = 0.30;

**[α]<sub>D</sub><sup>23</sup>:** +41.7 (c = 0.02, H<sub>2</sub>O);

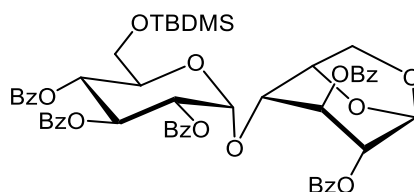
**IR (ATR):**  $\tilde{\nu}$  = 3359, 2909, 1148, 1075, 1032 cm<sup>-1</sup>;

**<sup>1</sup>H NMR:** (500 MHz, CDCl<sub>3</sub>, 300 K, TMS):  $\delta$  = 5.50 (s, 1H, H-1), 5.16 (d, <sup>3</sup>J<sub>1,2</sub> = 3.9 Hz, 1H, H-1'), 4.86-4.79 (m, 1H, H-5), 4.16 (dd, <sup>3</sup>J<sub>1,2</sub> = 7.8 Hz, <sup>3</sup>J<sub>2,3</sub> = 0.9 Hz, 1H, H-6a), 3.94-3.73 (m, 7H, H-3, H-4, H-6b, H-3', H-5', H-6a', H-6b'), 3.63-3.55 (m, 2H, H-2, H-2'), 3.45 (t, <sup>3</sup>J<sub>4,5</sub> = 8.86 Hz, <sup>3</sup>J<sub>3,4</sub> = 8.86 Hz, 1H, H-4') ppm;

**<sup>13</sup>C NMR:** (125 MHz, CDCl<sub>3</sub>, 300 K, TMS):  $\delta$  = 101.1 (C-1), 97.7 (C-1'), 75.6 (C-4), 75.3 (C-5), 72.9 (C-3'), 72.4 (C-5'), 71.4 (C-2'), 69.6 (3C, C-2, C-3, C-4'), 65.2 (C-6), 60.6 (C-6') ppm;

**ESI-MS:** *m/z* = 347.3 [M+Na]<sup>+</sup> (calculated *m/z* = 347.1 for [M+Na]<sup>+</sup>).

**2,3-Di-O-benzoyl-1,6-anhydro-4-O-(2',3',4'-tri-O-benzoyl-6'-tert-butyldimethylsilyl)- $\alpha$ -D-glucopyranosyl)- $\beta$ -D-glucopyranose (7)**



Maltosan (**6**, 4.00 g, 12.3 mmol) was dissolved in dry pyridine (24 mL) and *tert*-butyldimethylsilyl chloride (2.78 g, 18.5 mmol) and DMAP (300 mg, 2.46 mmol) were added. After stirring at room temperature for 4 h, a further portion of *tert*-butyldimethylsilyl chloride (927 mg, 6.15 mmol) was added and stirring was continued for 1 h. To the mixture was added, at 0 °C, benzoyl chloride (8.57 mL, 73.8 mmol) and the mixture was stirred for 1 h, at room temperature. MeOH was added and it was stirred for 15 min. The solvents were removed, and the crude product was dissolved in ethyl acetate and washed with 1N HCl. The combined aqu. layers were extracted with ethyl acetate and the combined org. phases were washed with brine, dried over MgSO<sub>4</sub>, filtered and the solvent was removed. Purification by column chromatography on silica gel (cyclohexane → cyclohexane/ethyl acetate, 4:1) yielded **7** as a colorless foam.

**Yield:** 9.08 g (9.47 mmol, 77 %);

**R<sub>f</sub>** (cyclohexane/ethyl acetate, 3:1): R<sub>f</sub> = 0.41;

**[ $\alpha$ ]<sub>D</sub><sup>23</sup>:** +41.0 (c = 0.02, CH<sub>2</sub>Cl<sub>2</sub>);

**IR (ATR):**  $\tilde{\nu}$  = 2927, 1722, 1451, 1249, 1092, 1025, 836, 706 cm<sup>-1</sup>;

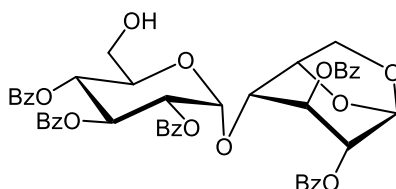
**<sup>1</sup>H NMR:** (500 MHz, CDCl<sub>3</sub>, 300 K):  $\delta$  = 8.35-8.28 (m, 2H, Bz-CH<sub>ortho</sub>), 8.01-7.96 (m, 2H, 2 Bz-CH<sub>ortho</sub>), 7.96-7.85 (m, 6H, 6 Bz-CH<sub>ortho</sub>), 7.63-7.54 (m, 4H, 4 Bz-CH<sub>meta</sub>), 7.54-7.40 (m, 4H, 4 Bz-CH<sub>meta</sub>), 7.36-7.28 (m, 5H, 5 Bz-CH<sub>para</sub>), 7.11-7.03 (m, 2H, 2 Bz-CH<sub>meta</sub>), 6.36 (t, <sup>3</sup>J<sub>2,3</sub> = 10.0 Hz, <sup>3</sup>J<sub>3,4</sub> = 10.0 Hz, 1H, H-3'), 5.72 (s, 1H, H-1), 5.67 (d, <sup>3</sup>J<sub>1,2</sub> = 3.8 Hz, 1H, H-1'), 5.58 (t, <sup>3</sup>J<sub>3,4</sub> = 10.0 Hz, <sup>3</sup>J<sub>4,5</sub> = 10.0 Hz, 1H, H-4'), 5.39 (dd, <sup>3</sup>J<sub>2,3</sub> = 10.3 Hz, <sup>3</sup>J<sub>1,2</sub> = 3.8 Hz, 1H H-2'), 5.17-5.12 (m, 1H, H-3), 5.06 (d, <sup>3</sup>J<sub>5,6b</sub> = 5.4 Hz, 1H, H-5), 5.04 (s, 1H, H-2), 4.61 (ddd, <sup>3</sup>J<sub>4,5</sub> = 10.2 Hz, <sup>3</sup>J<sub>5,6a</sub> = 4.8 Hz, <sup>3</sup>J<sub>5,6b</sub> = 3.6 Hz, 1H, H-5'), 4.15 (d, <sup>3</sup>J<sub>6a,6b</sub> = 7.2 Hz, 1H, H-6a), 3.89 (dd, <sup>3</sup>J<sub>6a,6b</sub> = 7.6 Hz, <sup>3</sup>J<sub>5,6b</sub> = 5.8 Hz, 1H, H-6b), 3.85-3.81 (m, 2H, H-6a', H-6b'), 3.76 (s, 1H, H-4), 0.84 (s, 9H, Si-*t*-Bu), -0.01 (s, 3H, Si-CH<sub>3</sub>), -0.02 (s, 3H, -Si-CH<sub>3</sub>) ppm;

**<sup>13</sup>C NMR:** (125 MHz, CDCl<sub>3</sub>, 300 K):  $\delta$  = 166.1, 165.8, 165.6, 165.5, 164.8 (5 C(O)Ph), 133.7, 133.7, 133.4, 133.3, 133.2 (5 Bz-CH<sub>para</sub>), 130.5, 130.1, 130.0, 129.9, 129.9 (10 Bz-CH<sub>ortho(a,b)</sub>), 129.5, 129.4, 129.3, 129.2, 128.9 (5 Bz-C<sub>quart</sub>), 129.1, 128.7, 128.5, 128.4, 128.3 (10 Bz-CH<sub>meta(a,b)</sub>), 99.2 (C-1), 98.8 (C-1'), 77.2 (C-3), 75.0 (C-5), 71.9 (2 C-2, C-5'), 71.7 (C-2'),

70.8 (C-3'), 69.5 (C-4'), 69.0 (C-2), 65.3 (C-6), 62.8 (C-6'), 26.0 (3 CH, Si-*t*-Bu), 18.5 (C<sub>q</sub>), -5.4 (2 Si-CH<sub>3</sub>) ppm;

**ESI-MS:**  $m/z = 982.0$  [M+Na]<sup>+</sup> (calculated  $m/z = 982.1$  for [M+Na]<sup>+</sup>).

**2,3-Di-O-benzoyl-1,6-anhydro-4-O-(2',3',4'-tri-O-benzoyl- $\alpha$ -D-glucopyranosyl)- $\beta$ -D-glucopyranose (8)**



The maltose derivative **7** (2.79 g, 2.91 mmol) was dissolved in dry THF (20 mL) and at 0 °C AcOH (886  $\mu$ L, 15.5 mmol) and tetra-*n*-butylammonium fluoride (1 M solution in THF) (7.73 mL, 7.73 mmol) were sequentially added. While stirring, the mixture was allowed to warm to room temperature and stirring was continued for 16 h. The mixture was diluted with ethyl acetate and washed with H<sub>2</sub>O, sat. sodium bicarbonate solution and brine. The aqu. layer was extracted with CH<sub>2</sub>Cl<sub>2</sub> and ethyl acetate, and the combined org. layers were dried over MgSO<sub>4</sub>, filtered and the solvent was removed under reduced pressure. The crude product was purified by flash chromatography (cyclohexane/ethyl acetate, 3:2→1:1) to afford **8** as a colorless foam.

**Yield:** 2.25 g (2.66 mmol, 92 %);

**R<sub>f</sub>** (cyclohexane/ethyl acetate, 3:1): R<sub>f</sub> = 0.11;

[ $\alpha$ ]<sub>D</sub><sup>23</sup>: +41.8 (c = 0.01, CH<sub>2</sub>Cl<sub>2</sub>);

**IR (ATR):**  $\tilde{\nu} = 2925, 1723, 1451, 1256, 1092, 1025, 706$  cm<sup>-1</sup>;

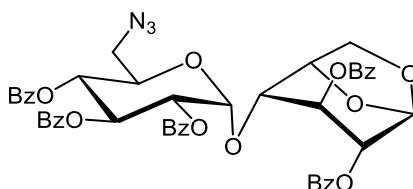
**<sup>1</sup>H NMR:** (500 MHz, CDCl<sub>3</sub>, 300 K):  $\delta = 8.36$ -8.28 (m, 2H, 2 Bz-CH<sub>ortho</sub>), 8.02-7.84 (m, 8H, 8 Bz-CH<sub>ortho</sub>), 7.68-7.29 (m, 13H, 4 Bz-CH<sub>meta, para</sub>), 7.28-7.22 (m, 2H, 2 Bz-CH<sub>meta, para</sub>), 6.45 (t, <sup>3</sup>J<sub>2,3</sub> = 10.0 Hz, <sup>3</sup>J<sub>3,4</sub> = 10.0 Hz, 1H, H-3'), 5.73 (s, 1H, H-1), 5.71 (d, <sup>3</sup>J<sub>1,2</sub> = 3.8 Hz, 1H, H-1'), 5.57 (t, <sup>3</sup>J<sub>3,4</sub> = 10.0 Hz, <sup>3</sup>J<sub>4,5</sub> = 10.0 Hz, 1H, H-4'), 5.44 (dd, <sup>3</sup>J<sub>2,3</sub> = 10.3 Hz, <sup>3</sup>J<sub>1,2</sub> = 3.8 Hz, 1H H-2'), 5.28-5.19 (m, 1H, H-3), 5.03 (s, 1H, H-2), 5.01 (d, <sup>3</sup>J<sub>5,6b</sub> = 5.4 Hz, 1H, H-5), 4.56 (ddd, <sup>3</sup>J<sub>4,5</sub> = 10.3 Hz, <sup>3</sup>J<sub>5,6a</sub> = 3.9 Hz, <sup>3</sup>J<sub>5,6b</sub> = 2.2 Hz, 1H, H-5'), 4.19 (d, <sup>3</sup>J<sub>6a,6b</sub> = 7.7 Hz, 1H, H-6a), 3.92 (dd, <sup>3</sup>J<sub>6a,6b</sub> = 7.6 Hz, <sup>3</sup>J<sub>5,6b</sub> = 5.9 Hz, 1H, H-6b), 3.83 (dd, <sup>3</sup>J<sub>6a',6b'</sub> = 13.0 Hz, <sup>3</sup>J<sub>5,6a'</sub> = 2.1 Hz, 1H, H-6a'), 3.79 (s, 1H, H-4), 3.75 (dd, <sup>3</sup>J<sub>6a',6b'</sub> = 13.0 Hz, <sup>3</sup>J<sub>5,6b'</sub> = 4.0 Hz, 1H, H-6b') ppm;

**<sup>13</sup>C NMR:** (125 MHz, CDCl<sub>3</sub>, 300 K):  $\delta = 166.6, 166.1, 165.8, 165.6, 164.8$  (5 C(O)Ph), 133.8, 133.7, 133.7, 133.4, 133.3 (5 Bz-CH<sub>para</sub>), 130.4, 130.2, 130.0, 129.9, 129.9 (10 Bz-CH<sub>ortho(a,b)</sub>), 129.4, 129.4, 129.2, 128.9, 128.6 (5 Bz-C<sub>quart</sub>), 128.7, 128.6, 128.5, 128.4, 128.4 (10

Bz-CH<sub>meta(a,b)</sub>, 99.2 (C-1), 98.4 (C-1'), 77.2 (C-3), 74.8 (C-5), 71.7 (C-2'), 71.4 (C-2), 71.1 (C-5'), 70.2 (C-3'), 69.6 (C-4'), 69.1 (C-2), 65.1 (C-6), 61.2 (C-6') ppm;

**ESI-MS:**  $m/z = 867.2258$  [M+Na]<sup>+</sup> (calcd  $m/z = 867.2265$  for [M+Na]<sup>+</sup>).

**2,3-Di-O-benzoyl-1,6-anhydro-4-O-(6'-azido-2',3',4'-tri-O-benzoyl-6'-deoxy- $\alpha$ -D-glucopyranosyl)- $\beta$ -D-glucopyranose (10)**



The maltose derivative **8** (2.00 g, 2.37 mmol) and PPh<sub>3</sub> (931 mg, 3.55 mmol) were dissolved in dry THF (10.0 mL), and the mixture was cooled to -15 °C. Then DIAD (1.16 mL, 5.92 mmol) was added dropwise, and the mixture was stirred at -15 °C for 15 min. Afterwards the mixture was allowed to warm to room temperature and DPPA (**26**, 765  $\mu$ L, 3.55 mmol) was added dropwise and stirring was continued for 16 h. The volatiles were removed under reduced pressure and purification by column chromatography on silica gel (cyclohexane/ethyl acetate, 4:1 $\rightarrow$ 3:1) yielded **10** as a colorless solid.

**Yield:** 1.49 g (1.71 mmol, 72 %);

**R<sub>f</sub>:** (cyclohexane/ethyl acetate, 3:2): R<sub>f</sub> = 0.77;

**[ $\alpha$ ]<sub>D</sub><sup>23</sup>:** +50.1 (c = 0.01, CH<sub>2</sub>Cl<sub>2</sub>);

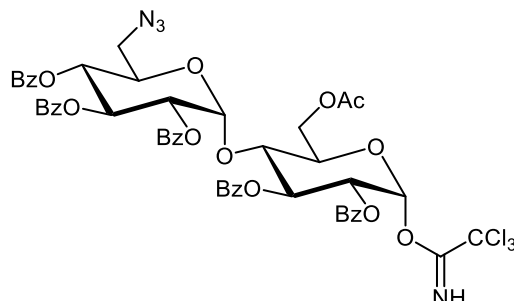
**IR (ATR):**  $\tilde{\nu} = 2097, 1715, 1450, 1255, 1093, 1024, 878, 706$  cm<sup>-1</sup>;

**<sup>1</sup>H NMR:** (500 MHz, CDCl<sub>3</sub>, 300 K):  $\delta = 8.36$ - $8.26$  (m, 2H, 2 Bz-CH<sub>ortho</sub>),  $8.01$ - $7.82$  (m, 8H, 8 Bz-CH<sub>ortho</sub>),  $7.66$ - $7.29$  (m, 13H, 4 Bz-CH<sub>meta, para</sub>),  $7.21$ - $7.05$  (m, 2H, 2 Bz-CH<sub>meta, para</sub>), 6.38 (t, <sup>3</sup>J<sub>2',3'</sub> = 10.0 Hz, <sup>3</sup>J<sub>3',4'</sub> = 10.0 Hz, 1H, H-3'), 5.75 (s, 1H, H-1), 5.70 (d, <sup>3</sup>J<sub>1',2'</sub> = 3.7 Hz, 1H, H-1'), 5.60 (t, <sup>3</sup>J<sub>3',4'</sub> = 9.9 Hz, <sup>3</sup>J<sub>4',5'</sub> = 9.9 Hz, 1H, H-4'), 5.43 (dd, <sup>3</sup>J<sub>2',3'</sub> = 10.4 Hz, <sup>3</sup>J<sub>1',2'</sub> = 3.7 Hz, 1H H-2'), 5.23-5.17 (m, 1H, H-3), 5.05 (s, 1H, H-2), 5.02 (d, <sup>3</sup>J<sub>5,6b</sub> = 5.2 Hz, 1H, H-5), 4.73-4.68 (m, 1H, H-5'), 4.20 (d, <sup>3</sup>J<sub>6a,6b</sub> = 7.2 Hz, 1H, H-6a), 3.92 (dd, <sup>3</sup>J<sub>6a,6b</sub> = 7.7 Hz, <sup>3</sup>J<sub>5,6b</sub> = 5.9 Hz, 1H, H-6b), 3.80 (s, 1H, H-4), 3.55-3.45 (m, 2H, H-6a', H-6b') ppm;

**<sup>13</sup>C NMR:** (125 MHz, CDCl<sub>3</sub>, 300 K, TMS):  $\delta = 166.3, 166.01, 165.8, 165.8, 165.05$  (5 C(O)Ph), 134.0, 134.0, 133.9, 133.7, 133.6 (5 Bz-CH<sub>para</sub>), 130.7, 130.4, 130.3, 130.2, 130.1 (10 Bz-CH<sub>ortho(a,b)</sub>), 129.7, 129.6, 129.4, 129.0, 128.9 (5 Bz-C<sub>quart</sub>), 129.3, 129.0, 128.8, 128.8, 128.6 (10 Bz-CH<sub>ortho(a,b)</sub>), 99.5 (C-1), 98.8 (C-1'), 77.8 (C-3), 75.2 (C-5), 71.9 (C-2'), 71.8 (C-2), 70.4 (C-5'), 70.3 (C-3'), 69.4 (C-4'), 65.5 (C-6), 51.7 (C-6') ppm;

**ESI-MS:**  $m/z = 892.3$   $[M+Na]^+$  (calculated  $m/z = 892.3$  for  $[M+Na]^+$ ).

**O-[6-O-acetyl-2,3-di-O-benzoyl-4-O-(6'-azido-2',3',4'-tri-O-benzoyl-6'-deoxy- $\alpha$ -D-glucopyranosyl)- $\alpha$ -D-glucopyranosyl] 2,2,2-trichloroacetimidate (13)**



The maltose derivative **10** (1.50 g, 1.72 mmol) was dissolved in a mixture of  $Ac_2O$  and  $AcOH$  (24.0 mL, 7:3) and  $H_2SO_4$  (300  $\mu$ L) was added. The mixture was stirred at room temperature for 1 h and then diluted with ethyl acetate. Afterwards the mixture was given into an ice-cold sodium bicarbonate solution poured dropwise and was stirred for 2 h at 0 °C. The aqu. layer was extracted with ethyl acetate and the combined org. layers were washed with brine. The solvent was removed, and it was coevaporated with toluene. The crude product was dissolved in DMF (12 mL), and the mixture was heated to 55 °C before  $N_2H_4 \cdot AcOH$  (266 mg) was added and stirring was continued for 2 h. The mixture was diluted with ethyl acetate and washed with brine, then concentrated to dryness. The crude product was dissolved in dry  $CH_2Cl_2$  (3.5 mL) and, at 0 °C, DBU (33  $\mu$ L) and  $Cl_3CCN$  (1.67 mL) were added. It was stirred for 20 min at 0 °C and then allowed to warm to room temperature while stirring was continued for 2 h. Afterwards the solvent was removed and purification by column chromatography on silica gel (cyclohexane/ethyl acetate, 3:1 $\rightarrow$ 7:3) yielded **13** as a colorless foam.

**Yield:** 1.25 g (1.16 mmol, 68 %);

**R<sub>f</sub>:** (cyclohexane/ethyl acetate, 3:2):  $R_f = 0.77$ ;

**$[\alpha]_D^{23}$ :** +67.2 ( $c = 0.01$ ,  $CH_2Cl_2$ );

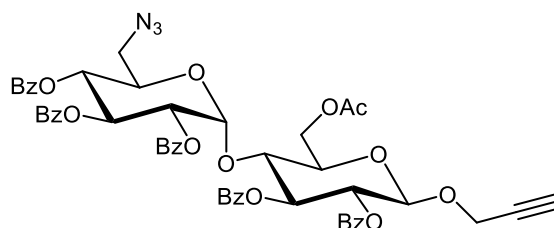
**IR (ATR):**  $\tilde{\nu} = 2104, 1726, 1677, 1451, 1258, 1091, 1025, 794, 704$   $cm^{-1}$ ;

**$^1H$  NMR:** (600 MHz,  $CDCl_3$ , 300 K):  $\delta = 8.58$  (s, 1H, NH), 7.97-7.64 (m, 10H, 10 Bz- $CH_{ortho}$ ), 7.55-7.26 (m, 15H, 10 Bz- $CH_{meta}$ , 5 Bz- $CH_{para}$ ), 6.69 (d,  $^3J_{1,2} = 3.5$  Hz, 1H, H-1), 6.12 (dd,  $^3J_{2,3} = 9.9$  Hz,  $^3J_{3,4} = 8.6$  Hz, 1H, H-3), 6.02 (dd,  $^3J_{2',3'} = 10.0$  Hz,  $^3J_{3',4'} = 10.0$  Hz, 1H, H-3'), 5.76 (d,  $^3J_{1,2} = 3.9$  Hz, 1H, H-1'), 5.49 (t,  $^3J_{3',4'} = 9.8$  Hz,  $^3J_{4',5'} = 9.8$  Hz, 1H, H-4'), 5.37 (dd,  $^3J_{2,3} = 10.0$  Hz,  $^3J_{1,2} = 3.5$  Hz, 1H H-2), 5.28 (dd,  $^3J_{2,3} = 10.5$  Hz,  $^3J_{1,2} = 3.9$  Hz, 1H H-2'), 4.65 (d,  $^2J_{6a,6b} = 10.4$  Hz, 1H, H-6a), 4.49 (m, 3H, H-4, H-5, H-6b), 4.24 (ddd,  $^3J_{4',5'} = 9.9$  Hz,  $^3J_{5',6a'} = 5.1$  Hz,  $^3J_{5',6b'} = 2.9$  Hz, 1H, H-5'), 3.45 (m, 2H, H-6a', H-6b'), 2.19 (s, 3H, C(O)CH<sub>3</sub>) ppm;

**$^{13}\text{C}$  NMR:** (125 MHz,  $\text{CDCl}_3$ , 300 K):  $\delta = 170.9, 165.8, 165.6, 165.6, 165.4$  (5  $\text{C}(\text{O})\text{Ph}$ ), 133.8, 133.6, 133.4, 133.3, 133.2 (4  $\text{Bz-CH}_{\text{para}}$ ), 130.1, 130.1, 130.1, 130.0, 130.0 (10  $\text{Bz-CH}_{\text{ortho}(a,b)}$ ), 129.2, 129.0 (2  $\text{Bz-C}_{\text{quart}}$ ), 128.7, 128.5, 128.5, 128.3, 128.3 (10  $\text{Bz-CH}_{\text{ortho}(a,b)}$ ), 96.6 (C-1), 93.1 (C-1'), 77.2 ( $\text{CCl}_3$ ), 73.1 (C-4), 71.9 (C-3), 71.1 (C-5), 71.1 (C-2), 70.8 (C-2'), 70.7 (C-5'), 69.9 (C-4'), 69.8 (C-3'), 62.7 (C-6), 51.2 (C-6'), 21.0 ( $\text{C}(\text{O})\underline{\text{C}}\text{H}_3$ ) ppm;

**ESI-MS:**  $m/z = 1095.1$  [ $\text{M}+\text{Na}$ ] $^+$  (calculated  $m/z = 1095.2$  for [ $\text{M}+\text{Na}$ ] $^+$ ).

**(2-Propargyl) 6-O-acetyl-2,3-di-O-benzoyl-4-O-(6'-azido-2',3',4'-tri-O-benzoyl-6'-deoxy- $\alpha$ -D-glucopyranosyl)- $\beta$ -D-glucopyranoside (15)**



The maltose trichloroacetimidate **13** (500 mg, 465  $\mu\text{mol}$ ) and propargyl alcohol (29.6 mL, 512  $\mu\text{mol}$ ) were dissolved in dry  $\text{CH}_2\text{Cl}_2$  (1.00 mL) and 3 Å molecular sieve (500 mg) was added. The mixture was stirred for 15 min at room temperature and then cooled to 0 °C and trimethylsilyl triflate (8.40  $\mu\text{L}$ , 46.5  $\mu\text{mol}$ ) was added. The reaction was allowed to warm to room temperature while stirring was continued for 16 h. Afterwards the mixture was diluted with  $\text{CH}_2\text{Cl}_2$  (10 mL) and filtrated over celite. The solvent was removed and purification by column chromatography on silica gel (cyclohexane/ethyl acetate, 3:1 $\rightarrow$ 7:3) gave **15** as a colorless solid.

**Yield:** 417 mg (431  $\mu\text{mol}$ , 93 %);

**R<sub>f</sub>:** (cyclohexane/ethyl acetate, 3:2):  $R_f = 0.33$ ;

**$[\alpha]_{\text{D}}^{23}$ :** +19.4 ( $c = 0.01$ ,  $\text{CH}_2\text{Cl}_2$ );

**IR (ATR):**  $\tilde{\nu} = 2105, 1725, 1451, 1251, 1091, 1025, 706$   $\text{cm}^{-1}$ ;

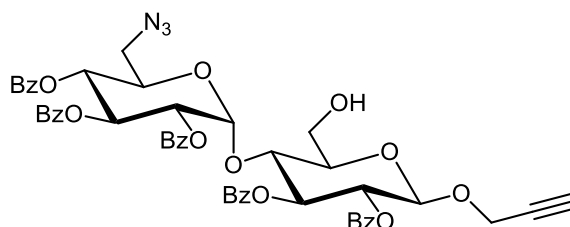
**$^1\text{H}$  NMR:** (500 MHz,  $\text{CDCl}_3$ , 300 K):  $\delta = 7.97\text{-}7.61$  (m, 10H, 10  $\text{Bz-CH}_{\text{ortho}}$ ), 7.56-7.16 (m, 15H, 10  $\text{Bz-CH}_{\text{meta}}$ , 5  $\text{Bz-CH}_{\text{para}}$ ), 6.00 (dd,  $^3J_{2,3'} = 10.4$  Hz,  $^3J_{3',4'} = 9.7$  Hz, 1H, H-3'), 5.72 (t,  $^3J_{2,3} = 9.3$  Hz,  $^3J_{3,4} = 9.3$  Hz, 1H, H-3), 5.70 (d,  $^3J_{1,2} = 3.8$  Hz, 1H, H-1'), 5.49 (t,  $^3J_{3',4'} = 9.8$  Hz,  $^3J_{4',5'}$  = 9.8 Hz, 1H, H-4'), 5.31 (dd,  $^3J_{2,3} = 9.3$  Hz,  $^3J_{1,2} = 7.6$  Hz, 1H H-2), 5.22 (dd,  $^3J_{2,3} = 10.5$  Hz,  $^3J_{1,2} = 3.9$  Hz, 1H H-2'), 5.05 (d,  $^3J_{1,2} = 7.5$  Hz, 1H, H-1), 4.71 (dd,  $^2J_{6a,6b} = 12.1$  Hz,  $^3J_{5,6b} = 2.7$  Hz, 1H, H-6b), 4.45-4.39 (m, 2H, H-4, H-6a), 4.39-4.33 (m, 2H,  $\text{OCH}_2$ ), 4.25 (ddd,  $^4,5' = 10.6$  Hz,  $^3J_{5',6a'} = 5.2$  Hz,  $^3J_{5',6b'} = 2.5$  Hz, 1H, H-5'), 4.00 (ddd,  $^3J_{4,5} = 9.4$  Hz,  $^3J_{5,6a} = 4.3$  Hz,  $^3J_{5,6b} = 2.8$  Hz, 1H, H-5), 3.50 (dd,  $^2J_{6a',6b'} = 13.4$  Hz,  $^3J_{5',6b'} = 2.9$  Hz, 1H, H-6b'), 3.45 (dd,  $^2J_{6a',6b'}$

= 13.4 Hz,  $^3J_{5',6a'} = 5.4$  Hz, 1H, H-6a'), 2.40 (t,  $^4J_{OCH',C\equiv CH} = 2.4$  Hz,  $^4J_{OCH,C\equiv CH} = 2.4$  Hz, 1H, C $\equiv$ CH), 2.21 (s, 3H, C(O)CH<sub>3</sub>) ppm;

**$^{13}\text{C}$  NMR:** (125 MHz, CDCl<sub>3</sub>, 300 K):  $\delta = 170.9, 165.8, 165.6, 165.4, 165.1$  (5 C(O)Ph), 133.8, 133.4, 133.4, 133.3, 133.2 (5 Bz-CH<sub>para</sub>), 130.1, 130.1, 130.0, 129.9, 129.7 (10 Bz-CH<sub>ortho(a,b)</sub>), 128.7, 128.4, 128.4, 128.3, 128.2 (10 Bz-CH<sub>ortho(a,b)</sub>), 129.3, 129.0, 128.9, 128.7, 128.6 (5 Bz-C<sub>quart</sub>), 98.0 (C-1'), 96.6 (C-1), 78.1 (OCH<sub>2</sub>C $\equiv$ CH), 75.0 (C-3), 73.4 (C-4), 72.8 (C-5), 72.0 (C-2), 70.8 (C-2'), 70.5 (C-5'), 69.7 (C-4'), 69.6 (C-3'), 63.0 (C-6), 55.8 (OCH<sub>2</sub>C $\equiv$ CH) 51.2 (C-6'), 21.0 (C(O)CH<sub>3</sub>) ppm;

**ESI-MS:**  $m/z = 990.2$  [M+Na]<sup>+</sup> (calculated  $m/z = 990.3$  for [M+Na]<sup>+</sup>).

**(2-Propargyl) 2,3-di-O-benzoyl-4-O-(6'-azido-2',3',4'-tri-O-benzoyl-6'-deoxy- $\alpha$ -D-glucopyranosyl)- $\beta$ -D-glucopyranoside (16)**



The maltoside **15** (142 mg, 147  $\mu\text{mol}$ ) was dissolved in a mixture of CH<sub>2</sub>Cl<sub>2</sub> and MeOH (3 mL, 1:1). Then AcCl (94.2  $\mu\text{L}$ , 1.32 mmol) was added dropwise, at 0 °C, and the mixture was stirred for 16 h at room temperature. Afterwards the reaction was neutralized by adding trimethylamine and the volatiles were removed. The solid residue was suspended in ethyl acetate (10 mL) and the insoluble solid was filtered off. The filtrate was concentrated and purified by column chromatography on silica gel (cyclohexane/ethyl acetate, 3:1→7:3) to afford **16** as a colorless solid.

**Yield:** 67.0 mg (72.4  $\mu\text{mol}$ , 49 %);

**R<sub>f</sub>:** (cyclohexane/ ethyl acetate, 3:2): R<sub>f</sub> = 0.31;

**$[\alpha]_D^{23}$ :** +18.6 (c = 0.01, CH<sub>2</sub>Cl<sub>2</sub>);

**IR (ATR):**  $\tilde{\nu} = 2923, 2105, 1725, 1451, 1263, 1091, 1025, 706, 685$  cm<sup>-1</sup>;

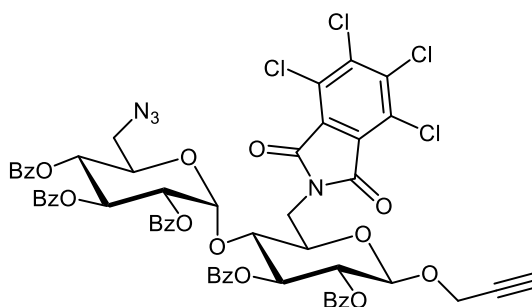
**$^1\text{H}$  NMR:** (600 MHz, CDCl<sub>3</sub>, 300 K):  $\delta = 7.97\text{-}7.63$  (m, 10H, 10 Bz-CH<sub>ortho</sub>), 7.56-7.18 (m, 15H, 10 Bz-CH<sub>meta</sub>, 5 Bz-CH<sub>para</sub>), 6.01 (t,  $^3J_{2',3'} = 10.1$  Hz,  $^3J_{3',4'} = 10.1$  Hz, 1H, H-3'), 5.76 (t,  $^3J_{2,3} = 9.5$  Hz,  $^3J_{3,4} = 9.5$  Hz, 1H, H-3), 5.73 (d,  $^3J_{1,2} = 4.0$  Hz, 1H, H-1'), 5.49 (t,  $^3J_{3',4'} = 9.8$  Hz,  $^3J_{4',5'} = 9.8$  Hz, 1H, H-4'), 5.32 (dd,  $^3J_{2,3} = 9.7$  Hz,  $^3J_{1,2} = 7.8$  Hz, 1H H-2), 5.20 (dd,  $^3J_{2,3} = 10.5$  Hz,  $^3J_{1,2} = 4.0$  Hz, 1H H-2'), 5.05 (d,  $^3J_{1,2} = 7.8$  Hz, 1H, H-1), 4.51 (t,  $^3J_{3,4} = 9.3$  Hz,  $^3J_{4,5} = 9.3$  Hz,

$^1\text{H}$ , H-4), 4.43 (dd,  $^2J_{\text{OCH},\text{OCH}'} = 16.0$  Hz,  $^4J_{\text{OCH},\text{C}\equiv\text{CH}} = 2.4$  Hz, 1H,  $\text{OCH}_2$ ), 4.35 (dd,  $^2J_{\text{OCH},\text{OCH}'} = 16.0$  Hz,  $^4J_{\text{OCH},\text{C}\equiv\text{CH}} = 2.4$  Hz, 1H,  $\text{OCH}_2$ ), 4.30 (ddd,  $^3J_{4',5'} = 10.0$  Hz,  $^3J_{5',6a'} = 5.3$  Hz,  $^3J_{5',6b'} = 2.7$  Hz, 1H, H-5'), 4.14 (dd,  $^2J_{6a,6b} = 12.3$  Hz,  $^3J_{5,6b} = 2.0$  Hz, 1H, H-6b), 4.08 (dd,  $^2J_{6a,6b} = 12.3$  Hz,  $^3J_{5,6a} = 3.4$  Hz, 1H, H-6a), 3.85-3.79 (m, 1H, H-5), 3.59 (dd,  $^2J_{6a',6b'} = 13.4$  Hz,  $^3J_{5',6b'} = 2.7$  Hz, 1H, H-6b'), 3.48 (dd,  $^2J_{6a',6b'} = 13.4$  Hz,  $^3J_{5',6a'} = 5.4$  Hz, 1H, H-6a'), 2.40 (t,  $^4J_{\text{OCH}',\text{C}\equiv\text{CH}} = 2.4$  Hz,  $^4J_{\text{OCH},\text{C}\equiv\text{CH}} = 2.4$  Hz, 1H,  $\text{C}\equiv\text{CH}$ ) ppm;

$^{13}\text{C}$  NMR: (125 MHz,  $\text{CDCl}_3$ , 300 K):  $\delta = 165.8, 165.4, 165.4, 165.3$  (4 C(O)Ph), 133.7, 133.4, 133.4, 133.3, 133.2 (5 Bz- $\text{CH}_{\text{para}}$ ), 130.1, 130.0, 130.0, 129.9, 129.7 (10 Bz- $\text{CH}_{\text{ortho}(a,b)}$ ), 129.3, 129.0, 128.9, 128.8, 128.7 (5 Bz- $\text{C}_{\text{quart}}$ ), 128.6, 128.4, 128.4, 128.3, 128.2 (10 Bz- $\text{CH}_{\text{ortho}(a,b)}$ ), 98.7 (C-1'), 96.1 (C-1), 78.5 ( $\text{OCH}_2\equiv\text{CH}$ ), 75.7 (C-5), 75.2 (C-3), 72.1 (C-2), 71.3 (C-4), 70.9 (C-2'), 70.2 (C-5'), 70.0 (C-4'), 70.0 (C-3'), 61.6 (C-6), 56.4 ( $\text{OCH}_2\equiv\text{CH}$ ), 51.3 (C-6') ppm;

ESI-MS:  $m/z = 948.3$   $[\text{M}+\text{Na}]^+$  (calculated  $m/z = 948.3$  for  $[\text{M}+\text{Na}]^+$ ).

**(2-Propargyl) 6-deoxy-2,3-di-O-benzoyl-6-(3,4,5,6-tetra-chlorophthalimido)-4-O-(6'-azido-2',3',4'-tri-O-benzoyl-6'-deoxy- $\alpha$ -D-glucopyranosyl)- $\beta$ -D-glucopyranoside (20)**



The maltoside **16** (600 mg, 648  $\mu\text{mol}$ ) and  $\text{PPh}_3$  (679 mg, 2.59 mmol) were dissolved in dry THF (30 mL) then 3,4,5,6-tetrachlorophthalimide (554 mg, 1.94 mmol) was added. The solution was cooled to 0  $^\circ\text{C}$  and DIAD (558  $\mu\text{L}$ , 2.59 mmol) was added dropwise. Stirring was continued for 16 h before the solvent was removed. The crude product was purified by column chromatography on silica gel (cyclohexane/ethyl acetate, 4:1) to give **20** as a colorless solid.

**Yield:** 612 mg (513  $\mu\text{mol}$ , 79 %);

**R<sub>f</sub>:** (cyclohexane/ ethyl acetate, 3:2):  $R_f = 0.49$ ;

$[\alpha]_{\text{D}}^{23}$ : +28.0 ( $c = 0.01$ ,  $\text{CH}_2\text{Cl}_2$ );

**IR (ATR):**  $\tilde{\nu} = 2103, 1721, 1602, 1451, 1370, 1315, 1248, 1177, 1090, 1068, 1025, 739, 705$   $\text{cm}^{-1}$ ;

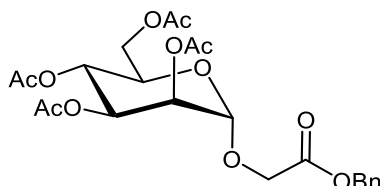
**$^1\text{H}$  NMR:** (500 MHz,  $\text{CDCl}_3$ , 300 K):  $\delta = 8.02$ -7.95 (m, 2H, 2 Bz- $\text{CH}_{\text{ortho}}$ ), 7.86-7.82 (m, 2H, 2 Bz- $\text{CH}_{\text{ortho}}$ ), 7.74-7.69 (m, 2H, 2 Bz- $\text{CH}_{\text{ortho}}$ ), 7.66-7.62 (m, 2H, 2 Bz- $\text{CH}_{\text{ortho}}$ ), 7.61-7.58 (m, 2H,

2 Bz-CH<sub>ortho</sub>), 7.55-7.23 (m, 15H, 10 Bz-CH<sub>meta</sub>, 5 Bz-CH<sub>para</sub>), 6.08 (dd,  $^3J_{2',3'} = 10.3$  Hz,  $^3J_{3',4'} = 9.5$  Hz, 1H, H-3'), 5.74-5.68 (m, 2H, H-3, H-1'), 5.49 (t,  $^3J_{3',4'} = 9.7$  Hz,  $^3J_{4',5'} = 9.7$  Hz, 1H, H-4'), 5.34-5.28 (m, 2H, H-2, H-2'), 4.97 (d,  $^3J_{1,2} = 7.3$  Hz, 1H, H-1), 4.56 (ddd,  $^4J_{5',6a'} = 9.7$  Hz,  $^3J_{5',6a'} = 6.2$  Hz,  $^3J_{5',6b'} = 2.7$  Hz, 1H, H-5'), 4.36 (dd,  $^2J_{6a',6b'} = 13.6$  Hz,  $^3J_{5',6b'} = 2.8$  Hz, 1H, H-6b), 4.33-4.19 (m, 5H, H-4, H-5, H-6b, OCH<sub>2</sub>), 3.56 (dd,  $^2J_{6a',6b'} = 13.3$  Hz,  $^3J_{5',6b'} = 2.7$  Hz, 1H, H-6b'), 3.51 (dd,  $^2J_{6a',6b'} = 13.4$  Hz,  $^3J_{5',6a'} = 6.1$  Hz, 1H, H-6a'), 2.27 (t,  $^4J_{OCH_2, C\equiv CH} = 2.4$  Hz,  $^4J_{OCH, C\equiv CH} = 2.4$  Hz, 1H, C≡CH) ppm;

**<sup>13</sup>C NMR:** (125 MHz, CDCl<sub>3</sub>, 300 K): δ = 165.61 (C(O)Ph), 165.59 (C(O)Ph), 165.44 (C(O)Ph), 165.27 (C(O)Ph), 165.06 (C(O)Ph), 163.50 (2 C(O)TCP), 140.46 (2 TCP-C<sub>Cl</sub>), 138.02 (2 TCP-C<sub>quart.</sub>) 133.78, 133.32, 133.28, 133.22, 133.22 (5C, Bz-CH<sub>para</sub>), 130.17, 130.06, 130.00, 129.80, 129.69 (10C, Bz-CH<sub>ortho(a,b)</sub>), 129.25, 129.18, 129.00, 128.77, 128.71 (5C, Bz-C<sub>quart.</sub>), 128.62, 128.37, 128.34, 128.32, 128.15 (10C, Bz-CH<sub>ortho(a,b)</sub>), 127.68 (2 TCP-C<sub>Cl</sub>), 97.52 (C-1), 97.47 (C-1'), 77.58 (C-4), 75.65 (OCH<sub>2</sub>≡CH), 74.89 (C-3), 72.18 (C-2), 71.77 (C-5), 70.90 (C-2'), 70.63 (C-5'), 70.02 (C-4'), 69.82 (C-3'), 55.49 (OCH<sub>2</sub>≡CH), 51.57 (C-6'), 40.67 (C-6) ppm;

**ESI-MS:** *m/z* = 1213.1243.1 [M+Na]<sup>+</sup> (calculated *m/z* = 1213.1242 for [M+Na]<sup>+</sup>).

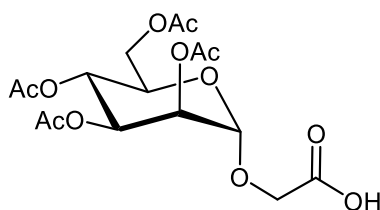
**(Benzyloxycarbonyl)methyl 2,3,4,6-tetra-O-acetyl-α-D-mannopyranoside (24)**<sup>[129]</sup>



Mannose pentaacetate (**22**, 2.50 g, 6.41 mmol) was dissolved in dry CH<sub>2</sub>Cl<sub>2</sub> (50 mL) and benzyl glycolate (**23**, 2.73 mL, 19.2 mmol) was added. Then 3 ÅMS was added and it was stirred for 15 min. at room temperature. Afterwards the reaction mixture was cooled to 0 °C and BF<sub>3</sub>·Et<sub>2</sub>O (1.62 mL, 12.8 mmol) was added dropwise. It was allowed to warm to room temperature and stirring was continued for 16 h. The mixture was diluted with CH<sub>2</sub>Cl<sub>2</sub> and filtered over celite. The org. layer was washed with sodium bicarbonate and brine, dried over MgSO<sub>4</sub>, filtered of and concentrated. Purification by flash column chromatography on silica (cyclohexane/ ethyl acetate, 3:2) led to **24** as a colorless solid.

**Yield:** 1.51 g (3.04 mmol, 47 %);

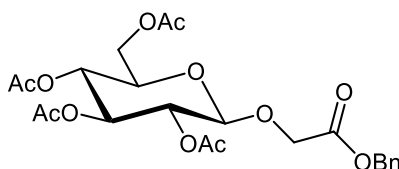
Analytical data corresponds to the literature.<sup>[129]</sup>

**Carboxy-methyl 2,3,4,6-tetra-O-acetyl- $\alpha$ -D-mannopyranoside (25)**<sup>[129]</sup>

The mannoside **24** (1.47 g, 2.96 mmol) was dissolved in ethyl acetate (50.0 mL) and a catalytic amount of Pd/C was added. The reaction mixture was stirred under a H<sub>2</sub>-atmosphere for 2 h. It was filtered over celite, and evaporation gave the title compound **25** as a colorless syrup.

**Yield:** 1.22 g (quant.);

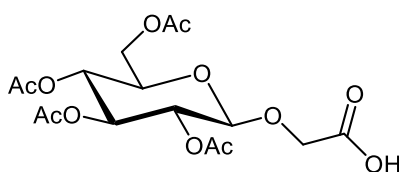
Analytical data corresponds to the literature.<sup>[129]</sup>

**(Benzyloxycarbonyl)methyl 2,3,4,6-tetra-O-acetyl- $\beta$ -D-glucopyranoside (27)**<sup>[130]</sup>

Glucose trichloroacetimidate **26** (2.00 g, 5.13 mmol) was dissolved in dry CH<sub>2</sub>Cl<sub>2</sub> (40 mL) and benzyl glycolate (**23**, 2.18 mL, 15.4 mmol) and 3 ÅMS were added and it was stirred for 15 min at room temperature. The mixture was cooled to 0 °C and BF<sub>3</sub>·Et<sub>2</sub>O (1.62 mL, 12.8 mmol) was added. It was allowed to warm to room temperature and stirred for 16 h. The mixture was diluted with CH<sub>2</sub>Cl<sub>2</sub> and filtered over celite. The org. layer was washed with sodium bicarbonate and brine, dried over MgSO<sub>4</sub>, filtered of and concentrated. Purification by flash column chromatography on silica (cyclohexane/ ethyl acetate, 7:3) led to **27** as a colorless solid.

**Yield:** 1.51 g (3.04 mmol, 59 %);

Analytical data corresponds to the literature.<sup>[130]</sup>

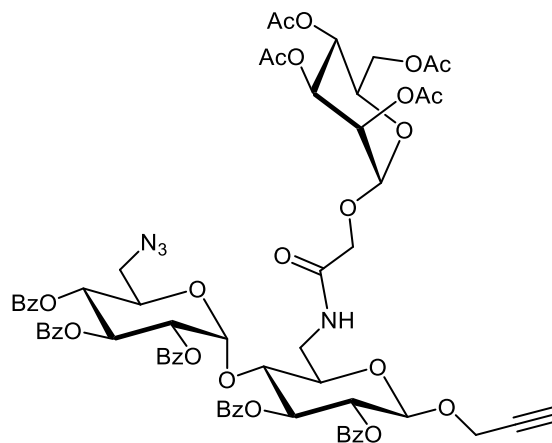
**Carboxymethyl 2,3,4,6-tetra-O-acetyl- $\beta$ -D-glucopyranoside (28)**<sup>[130]</sup>

Glucoside **27** (1.50 g, 3.02 mmol) was dissolved in ethyl acetate (100 mL) and a catalytic amount of Pd/C was added. The reaction mixture was stirred under a H<sub>2</sub>-atmosphere for 3 h. It was filtered over celite, and evaporation gave compound **28** as a colorless syrup.

**Yield:** 1.21 g (2.98 mmol, 99 %);

Analytical data corresponds to the literature.<sup>[130]</sup>

**(2-Propargyl) 2,3-di-O-benzoyl-6-deoxy-6-[[[(2,3,4,6-tetra-O-acetyl- $\alpha$ -D-mannoopyranosyl)oxy]acetyl]amino]-4-O-(6'-azido-2',3',4'-tri-O-benzoyl-6'-deoxy- $\alpha$ -D-glucopyranosyl)- $\beta$ -D-glucopyranoside (**29**)**



The maltoside **20** (500 mg, 419  $\mu$ mol) was dissolved in a mixture of MeCN/THF (4:1, 6.4 mL) and ethylenediamine (56.0  $\mu$ L, 838  $\mu$ mol) was added and stirred for 3 h at 55  $^{\circ}$ C. The volatiles were removed, and the crude product was taken up in ethyl acetate and washed with H<sub>2</sub>O. The aqu. layer was extracted with ethyl acetate and the combined org. layers were dried over MgSO<sub>4</sub>, filtered, and concentrated. The crude product was dissolved in dry DMSO (7.0 mL) and DIPEA (356  $\mu$ L, 2.10 mmol) was added. Afterwards a solution of activated carboxylic acid **25** (341 mg, 838  $\mu$ mol) in dry DMSO (7.0 mL) was added. The mixture was stirred at room temperature for 16 h. It was diluted with ethyl acetate and washed with 1M HCl and H<sub>2</sub>O. The org. layer was dried over MgSO<sub>4</sub>, filtered, and concentrated. Purification by column chromatography on silica gel (cyclohexane/ethyl acetate, 1:1) gave **29** as a colorless solid.

**Yield:** 330 mg (251  $\mu$ mol, 60 %);

**R<sub>f</sub>**: (cyclohexane/ ethyl acetate, 2:3): R<sub>f</sub> = 0.40;

**[ $\alpha$ ]<sub>D</sub><sup>23</sup>**: +35.4 (c = 0.01, CH<sub>2</sub>Cl<sub>2</sub>);

**IR (ATR)**:  $\tilde{\nu}$  = 3330, 2105, 1732, 1676, 1537, 1451, 1369, 1246, 1090, 1067, 1025, 707 cm<sup>-1</sup>;

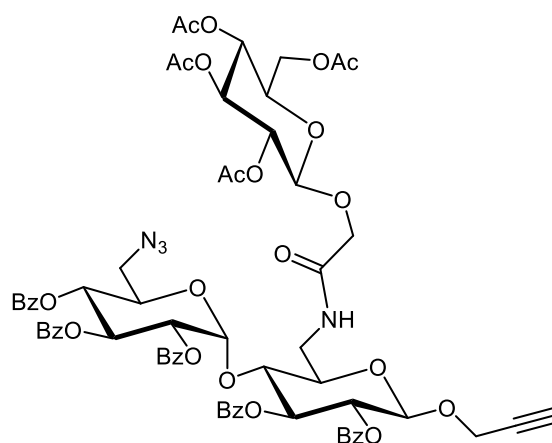
**<sup>1</sup>H NMR**: (500 MHz, CDCl<sub>3</sub>, 300 K):  $\delta$  = 7.98-7.94 (m, 2H, Bz<sub>ortho</sub>), 7.86-7.81 (m, 2H, Bz<sub>ortho</sub>), 7.71-7.66 (m, 2H, Bz<sub>ortho</sub>), 7.63-7.59 (m, 2H, Bz<sub>ortho</sub>), 7.55-7.49 (m, 3H, Bz<sub>ortho</sub>, Bz<sub>para</sub>), 7.47-7.28 (m, 8H, Bz<sub>meta</sub>, Bz<sub>para</sub>), 7.24-7.15 (m, 6H, Bz<sub>meta</sub>), 7.03 (dd, <sup>3</sup>J<sub>NH,6a</sub> = 7.7 Hz, <sup>3</sup>J<sub>NH,6b</sub> = 3.7 Hz, 1H, NH), 6.01 (dd, <sup>3</sup>J<sub>2',3'</sub> = 10.4 Hz, <sup>3</sup>J<sub>3',4'</sub> = 9.6 Hz, 1H, H-3'), 5.75-5.68 (m, 2H, H-1', H-3), 5.51 (t, <sup>3</sup>J<sub>3',4'</sub> = 9.8 Hz, <sup>3</sup>J<sub>4',5'</sub> = 9.8 Hz, 1H, H-4'), 5.40-5.27 (m, 5H, H-2<sub>Man</sub>, H-2, H-2', H-4<sub>Man</sub>, H-3<sub>Man</sub>),

5.08 (d,  ${}^3J_{1,2} = 7.7$  Hz, 1H, H-1), 4.95 (d,  ${}^3J_{1,2} = 1.2$  Hz, 1H, H-1<sub>Man</sub>), 4.47-4.40 (m, 2H, H-5', OCH<sub>2</sub>), 4.40-4.23 (m, 4H, OCH<sub>2</sub>, H-6b H-6a<sub>Man</sub>, Man-OCH<sub>2</sub>), 4.23-4.11 (m, 3H, H-4, H-6b<sub>Man</sub>, Man-OCH<sub>2</sub>), 4.04-4.00 (m, 1H, H-5<sub>Man</sub>), 3.99-3.94 (m, 1H, H-5), 3.66 (dd,  ${}^2J_{6a',6b'} = 13.4$  Hz,  ${}^3J_{5',6b'} = 2.5$  Hz, 1H, H-6b'), 3.54 (dd,  ${}^2J_{6a',6b'} = 13.5$  Hz,  ${}^3J_{5',6a'} = 5.7$  Hz, 1H, H-6a'), 3.48 (ddd,  ${}^2J_{6a,6b} = 13.8$  Hz,  ${}^3J_{NH,6a} = 7.5$  Hz,  ${}^3J_{5,6a} = 4.1$  Hz, 1H, H-6a), 2.44 (t,  ${}^4J_{OCH',C\equiv CH} = 2.4$  Hz,  ${}^4J_{OCH,C\equiv CH} = 2.4$  Hz, 1H, C≡CH), 2.20, 2.11, 2.06, 2.02, (each s, 12H, 4 C(O)CH<sub>3</sub>) ppm;

**<sup>13</sup>C NMR:** (125 MHz, CDCl<sub>3</sub>, 300 K): δ = 170.60, 170.11, 169.85, 169.69 (4C, C(O)-Ac), 168.10 (NH-C(O)), 165.51, 165.33, 165.30, 165.17, 164.92 (5C, C(O)Ph), 133.54, 133.13, 133.07, 133.01, 133.01 (5C, Bz-CH<sub>para</sub>), 130.01, 129.94, 129.82, 129.62, 129.51 (10C, Bz-CH<sub>ortho(a,b)</sub>), 129.21, 128.83, 128.60, 128.59, 128.24 (5C, Bz-C<sub>quat</sub>), 128.46, 128.14, 128.11, 128.11, 127.93 (10C, Bz-CH<sub>ortho(a,b)</sub>), 98.10 (C-1), 97.55 (C-1'), 97.44 (C-1<sub>Man</sub>), 78.68 (OCH<sub>2</sub>C≡CH), 76.04 (C-4), 75.32 (OCH<sub>2</sub>C≡CH), 74.78 (C-3), 73.38 (C-5), 71.98 (C-2'), 70.55 (C-2), 70.41 (C-5'), 69.75 (C-3'), 69.63 (C-4'), 69.38 (C5<sub>Man</sub>), 69.22 (C-2<sub>Man</sub>), 68.75 (C-3<sub>Man</sub>), 66.73 (Man-OCH<sub>2</sub>), 65.74 (C-4<sub>Man</sub>), 62.32 (C-6<sub>Man</sub>), 56.22 (OCH<sub>2</sub>C≡CH), 51.13 (C-6'), 40.20 (C-6), 20.84, 20.73, 20.66, 20.65 (4C, OAc) ppm;

**ESI-MS:**  $m/z = 1335.3747$  [M+Na]<sup>+</sup> (calculated  $m/z = 1335.3751$  for [M+Na]<sup>+</sup>).

**(2-Propargyl) 2,3-di-O-benzoyl-6-deoxy-6-[[[(2,3,4,6-tetra-O-acetyl-β-D-glucopyranosyl)oxy]acetyl]amino]-4-O-(6'-azido-2',3',4'-tri-O-benzoyl-6'-deoxy-α-D-glucopyranosyl)-β-D-glucopyranoside (30)**



The maltoside **20** (250 mg, 210 μmol) was dissolved in a mixture of MeCN/THF (4:1, 3.2 mL) and ethylenediamine (30.8 μL, 420 μmol) was added. It was stirred for 3 h at 55 °C. The solvent was removed, and the crude product was taken up in ethyl acetate and was washed with H<sub>2</sub>O. The aqu. layer was extracted with ethyl acetate and the combined org. layers were dried over MgSO<sub>4</sub>, filtered, and concentrated. The crude product was dissolved in dry DMSO (3.2 mL) and DIPEA (179 μL, 1.05 mmol) was added. Afterwards a solution of activated carboxylic acid **28** (171 mg, 420 μmol) in dry DMSO (3.2 mL) was added. The mixture was

stirred at room temperature for 16 h. It was diluted with ethyl acetate and washed with 1M HCl and H<sub>2</sub>O. The org. layer was dried over MgSO<sub>4</sub>, filtered, and concentrated. Purification by column chromatography on silica gel (cyclohexane/ethyl acetate, 1:1) gave **30** as a colorless solid.

**Yield:** 176 mg (134 μmol, 64 %);

**R<sub>f</sub>:** (cyclohexane/ ethyl acetate, 2:3): R<sub>f</sub> = 0.31;

**[α]<sub>D</sub><sup>23</sup>:** +12.1 (c = 0.01, CH<sub>2</sub>Cl<sub>2</sub>);

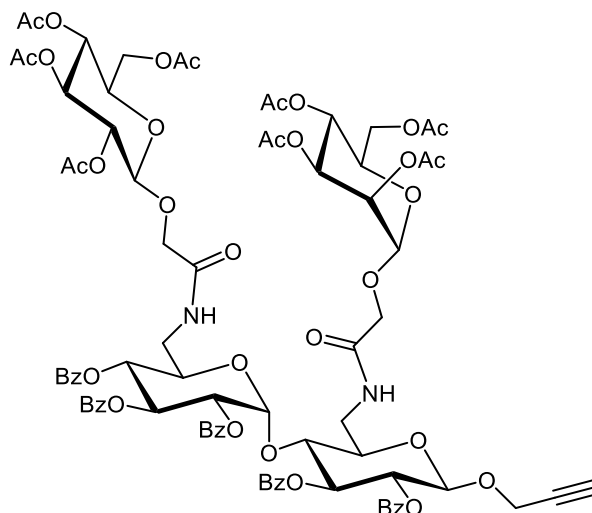
**IR (ATR):**  $\tilde{\nu}$  = 2103, 1732, 1683, 1602, 1532, 1451, 1368, 1247, 1218, 1177, 1091, 1067, 1026, 706 cm<sup>-1</sup>;

**<sup>1</sup>H NMR:** (500 MHz, CDCl<sub>3</sub>, 300 K):  $\delta$  = 7.99-7.96 (m, 2H, Bz<sub>ortho</sub>), 7.86-7.81 (m, 2H, Bz<sub>ortho</sub>), 7.73-7.69 (m, 2H, Bz<sub>ortho</sub>), 7.68-7.64 (m, 2H, Bz<sub>ortho</sub>), 7.58-7.54 (m, 2H, Bz<sub>ortho</sub>), 7.53-7.28 (m, 9H, Bz<sub>meta</sub>, Bz<sub>para</sub>), 7.25-7.15 (m, 6H, Bz<sub>meta</sub>), 7.03 (t, <sup>3</sup>J<sub>NH,6a</sub> = 5.6 Hz, <sup>3</sup>J<sub>NH,6b</sub> = 5.6 Hz, 1H, NH), 6.01 (dd, <sup>3</sup>J<sub>2,3</sub> = 10.1 Hz, <sup>3</sup>J<sub>3,4</sub> = 9.7 Hz, 1H, H-3'), 5.72 (t, <sup>3</sup>J<sub>2,3</sub> = 9.3 Hz, <sup>3</sup>J<sub>3,4</sub> = 9.3 Hz, 1H, H-3), 5.68 (d, <sup>3</sup>J<sub>1,2</sub> = 4.0 Hz, 1H, H-1'), 5.50 (t, <sup>3</sup>J<sub>3,4</sub> = 9.8 Hz, <sup>3</sup>J<sub>4,5</sub> = 9.8 Hz, 1H, H-4'), 5.43 (dd, <sup>3</sup>J<sub>2,3</sub> = 9.6 Hz, <sup>3</sup>J<sub>1,2</sub> = 7.8 Hz, 1H, H-2), 5.28 (t, <sup>3</sup>J<sub>2,3</sub> = 9.6 Hz, <sup>3</sup>J<sub>3,4</sub> = 9.6 Hz, 1H, H-3<sub>Glc</sub>), 5.22 (dd, <sup>3</sup>J<sub>2,3</sub> = 10.5 Hz, <sup>3</sup>J<sub>1,2</sub> = 4.0 Hz, 1H, H-2'), 5.13-5.04 (m, 3H, H-1, H-2<sub>Glc</sub>, H-4<sub>Glc</sub>), 4.58 (d, <sup>3</sup>J<sub>1,2</sub> = 7.9 Hz, 1H, H-1<sub>Glc</sub>), 4.51 (dd, <sup>2</sup>J<sub>OCH, OCH</sub> = 16.1 Hz, <sup>4</sup>J<sub>OCH, C≡CH</sub> = 2.4 Hz, 1H, OCH<sub>2</sub>), 4.44-4.37 (m, 3H, H-5', OCH<sub>2</sub>, Glc-OCH<sub>2</sub>), 4.34 (dd, <sup>2</sup>J<sub>6a,6b</sub> = 12.4 Hz, <sup>3</sup>J<sub>5,6a</sub> = 5.0 Hz, 1H, H-6a<sub>Glc</sub>), 4.19 (t, <sup>3</sup>J<sub>3,4</sub> = 9.2 Hz, <sup>3</sup>J<sub>4,5</sub> = 9.2 Hz, 1H, H-4), 4.16-4.04 (m, 3H, H-6b, H-6b<sub>Glc</sub>, Glc-OCH<sub>2</sub>), 3.98-3.91 (m, 1H, H-5), 3.79-3.74 (m, 1H, H-5<sub>Glc</sub>), 3.68 (dt, <sup>2</sup>J<sub>6a,6b</sub> = 13.6 Hz, <sup>3</sup>J<sub>NH,6a</sub> = 5.9 Hz, <sup>3</sup>J<sub>5,6a</sub> = 5.9 Hz, 1H, H-6a), 3.59 (dd, <sup>2</sup>J<sub>6a',6b'</sub> = 13.6 Hz, <sup>3</sup>J<sub>5',6b'</sub> = 2.5 Hz, 1H, H-6b'), 3.47 (dd, <sup>2</sup>J<sub>6a',6b'</sub> = 13.4 Hz, <sup>3</sup>J<sub>5',6a'</sub> = 5.5 Hz, 1H, H-6a'), 2.50 (t, <sup>4</sup>J<sub>OCH', C≡CH</sub> = 2.4 Hz, <sup>4</sup>J<sub>OCH, C≡CH</sub> = 2.4 Hz, 1H, C≡CH), 2.17, 2.12, 2.04, 2.03, (each s, 12H, 4 C(O)CH<sub>3</sub>) ppm;

**<sup>13</sup>C NMR:** (125 MHz, CDCl<sub>3</sub>, 300 K):  $\delta$  = 170.57, 170.14, 169.61, 169.42 (4C, C(O)-Ac), 168.56 (NH-C(O)), 165.51, 165.41, 165.32, 165.32, 164.94 (5C, C(O)Ph), 133.51, 133.16, 133.12, 133.02, 133.01 (5C, Bz-CH<sub>para</sub>), 130.04, 129.94, 129.81, 129.58, 129.53 (10C, Bz-CH<sub>ortho(a,b)</sub>), 129.21, 128.89, 128.73, 128.62, 128.39 (5C, Bz-C<sub>quart</sub>), 128.45, 128.16, 128.15, 128.13, 128.00 (10C, Bz-CH<sub>ortho(a,b)</sub>), 100.47 (C-1<sub>Glc</sub>), 98.13 (C-1), 96.85 (C-1'), 78.42 (OCH<sub>2</sub>C≡CH), 75.80 (OCH<sub>2</sub>C≡CH), 75.12 (C-3), 76.64 (C-4), 73.13 (C-5), 72.23 (C5<sub>Glc</sub>), 72.15 (C-3<sub>Glc</sub>), 71.77 (C-2), 71.19 (C-2<sub>Glc</sub>), 70.83 (C-2'), 70.19 (C-5'), 69.64 (C-3'), 69.55 (C-4'), 68.48 (Glc-OCH<sub>2</sub>), 68.25 (C-4<sub>Glc</sub>), 61.71 (C-6<sub>Glc</sub>), 56.17 (OCH<sub>2</sub>C≡CH), 51.17 (C-6'), 40.04 (C-6), 20.75, 20.75, 20.62, 20.57 (4C, OAc) ppm;

**ESI-MS:** *m/z* = 1335.3745 [M+Na]<sup>+</sup> (calculated *m/z* = 1335.3751 for [M+Na]<sup>+</sup>).

**(2-Propargyl) 2,3-di-O-benzoyl-6-deoxy-6-[[[(2,3,4,6-tetra-O-acetyl- $\alpha$ -D-mannopyranosyl)oxy]acetyl]amino]-4-O-(2',3',4'-tri-O-benzoyl-6'-deoxy-6'-[[[(2,3,4,6-tetra-O-acetyl- $\beta$ -D-glucopyranosyl)oxy]acetyl]amino]- $\alpha$ -D-glucopyranosyl)- $\beta$ -D-glucopyranoside (32)**



The carboxylic acid **28** (61.9 mg, 152  $\mu$ mol) was dissolved in dry THF (5 mL) and NHS (26.3 mg, 228  $\mu$ mol) and EDC-HCl (43.7 mg, 228  $\mu$ mol) were added. It was stirred for 2 h at room temperature. Then maltoside **29** (100 mg, 76.1  $\mu$ mol) was added and the reaction mixture was cooled to 0  $^{\circ}$ C. To the mixture  $\text{PMe}_3$  (1M in THF, 381  $\mu$ L) was added dropwise. It was allowed to warm to room temperature and stirring was continued for 16 h. Then  $\text{H}_2\text{O}$  was added and the aqu. layer was extracted with ethyl acetate. The combined org. layers were dried over  $\text{MgSO}_4$ , filtered of, and concentrated. Purification by column chromatography on silica gel (cyclohexane/ethyl acetate, 1:4) gave **32** as a colorless solid.

**Yield:** 82.9 mg (49.5  $\mu$ mol, 65 %);

**R<sub>f</sub>:** (cyclohexane/ ethyl acetate, 1:4): R<sub>f</sub> = 0.20;

**[ $\alpha$ ]<sub>D</sub><sup>23</sup>:** +22.5 (c = 0.01,  $\text{CH}_2\text{Cl}_2$ );

**IR (ATR):**  $\tilde{\nu}$  = 3196, 1732, 1687, 1529, 1451, 1368, 1218, 1090, 1026, 707  $\text{cm}^{-1}$ ;

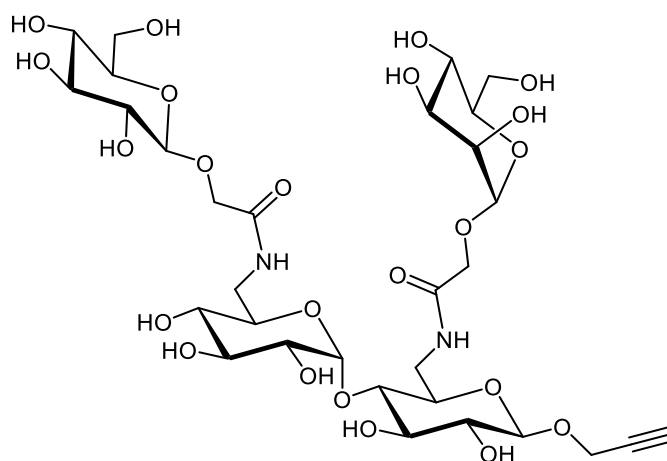
**<sup>1</sup>H NMR:** (600 MHz,  $\text{CDCl}_3$ , 300 K):  $\delta$  = 7.96-7.92 (m, 2H, Bz<sub>ortho</sub>), 7.85-7.82 (m, 2H, Bz<sub>ortho</sub>), 7.67-7.64 (m, 2H, Bz<sub>ortho</sub>), 7.62-7.58 (m, 2H, Bz<sub>ortho</sub>), 7.52-7.49 (m, 2H, Bz<sub>ortho</sub>), 7.47-7.28 (m, 9H, Bz<sub>meta</sub>, Bz<sub>para</sub>), 7.23-7.12 (m, 6H, Bz<sub>meta</sub>), 7.09 (t,  $^3J_{\text{NH},6a}$  = 5.9 Hz,  $^3J_{\text{NH},6b}$  = 5.9 Hz, 1H, NH), 7.03 (dd,  $^3J_{\text{NH},6a}$  = 7.7 Hz,  $^3J_{\text{NH},6b}$  = 3.5 Hz, 1H, NH), 6.01 (t,  $^3J_{2',3'}$  = 10.1 Hz,  $^3J_{3',4'}$  = 10.1 Hz, 1H, H-3'), 6.01 (t,  $^3J_{2,3}$  = 9.1 Hz,  $^3J_{3,4}$  = 9.1 Hz, 1H, H-3), 5.08 (d,  $^3J_{1',2'}$  = 4.1 Hz, 1H, H-1'), 5.44-5.26 (m, 7H, H-2<sub>Man</sub>, H-2, H-2', H-4', H-3<sub>Glc</sub>, H-4<sub>Man</sub>, H-3<sub>Man</sub>), 5.13-5.07 (m, 3H, H-1, H-2<sub>Glc</sub>, H-4<sub>Glc</sub>), 4.95 (d,  $^3J_{1,2}$  = 0.9 Hz, 1H, H-1<sub>Man</sub>), 4.62 (d,  $^3J_{1,2}$  = 7.9 Hz, 1H, H-1<sub>Glc</sub>), 4.52 (ddd,  $^3J_{4',5'}$  = 9.7 Hz,  $^3J_{5',6a'}$  = 4.6 Hz,  $^3J_{5',6b'}$  = 3.4 Hz, 1H, H-5'), 4.45-4.27 (m, 7H, H-6a, OCH<sub>2</sub>, OCH<sub>2</sub>, H-

$6a_{\text{Man}}$ ,  $\text{Man-OCH}_2$ ,  $\text{H-6a}_{\text{Glc}}$ ,  $\text{Glc-OCH}_2$ , 4.22-4.08 (m, 5H, H-4,  $\text{Glc-OCH}_2$ ,  $\text{Man-OCH}_2$ ,  $\text{H-6b}_{\text{Man}}$ ,  $\text{H-6b}_{\text{Glc}}$ ), 4.07-4.03 (m, 1H,  $\text{H-5}_{\text{Man}}$ ), 3.99-3.95 (m, 1H, H-5), 3.77 (ddd,  $^3J_{4,5} = 10.1$  Hz,  $^3J_{5,6a} = 5.2$  Hz,  $^3J_{5,6b} = 2.3$  Hz, 1H,  $\text{H-5}_{\text{Glc}}$ ), 3.75-3.69 (m, 1H,  $\text{H-6a}'$ ), 3.68-3.62 (m, 1H,  $\text{H-6b}'$ ), 3.41-3.34 (m, 1H, H-6b), 2.46 (t,  $^4J_{\text{OCH}'\text{C}\equiv\text{CH}} = 2.3$  Hz,  $^4J_{\text{OCH,C}\equiv\text{CH}} = 2.3$  Hz, 1H,  $\text{C}\equiv\text{CH}$ ), 2.20, 2.14, 2.11, 2.07, 2.05, 2.03, 2.03, 2.00 (each s, 24H, 8  $\text{C(O)CH}_3$ ) ppm;

$^{13}\text{C}$  NMR: (125 MHz,  $\text{CDCl}_3$ , 300 K):  $\delta = 170.66, 170.66, 170.21, 170.11, 169.90, 169.83, 169.70, 169.44$  (8C,  $\text{C(O)-Ac}$ ), 168.50, 168.18 (2  $\text{NH-C(O)}$ ), 165.60, 166.57, 165.44, 165.17, 164.91 (5C,  $\text{C(O)Ph}$ ), 133.38, 133.09, 132.98, 132.98, 132.92 (5C,  $\text{Bz-CH}_{\text{para}}$ ), 129.99, 129.95, 129.83, 129.65, 129.46 (10C,  $\text{Bz-CH}_{\text{ortho}(a,b)}$ ), 129.26, 129.00, 128.85, 128.70, 128.32 (5C,  $\text{Bz-C}_{\text{quat}}$ ), 128.40, 128.15, 128.07, 128.05, 127.91 (10C,  $\text{Bz-CH}_{\text{ortho}(a,b)}$ ), 100.29 ( $\text{C-1}_{\text{Glc}}$ ), 98.21 ( $\text{C-1}$ ), 97.97 ( $\text{C-1}'$ ), 97.52 ( $\text{C-1}_{\text{Man}}$ ), 78.80 ( $\text{OCH}_2\text{C}\equiv\text{CH}$ ), 76.72 ( $\text{C-4}$ ), 75.35 ( $\text{OCH}_2\text{C}\equiv\text{CH}$ ), 74.87 ( $\text{C-3}$ ), 73.57 ( $\text{C-5}$ ), 72.26 ( $\text{C5}_{\text{Glc}}$ ), 72.18 ( $\text{C-2}'$ ), 72.03 ( $\text{C-2}$ ), 71.16 ( $\text{C-2}_{\text{Glc}}$ ), 70.65 ( $\text{C-3}_{\text{Glc}}$ ), 70.15 ( $\text{C-3}'$ ), 69.61 ( $\text{C-5}'$ ), 69.39 ( $\text{C-4}'$ ), 69.31 ( $\text{C5}_{\text{Man}}$ ), 69.23 ( $\text{C-2}_{\text{Man}}$ ), 68.81 ( $\text{C-3}_{\text{Man}}$ ), 68.46 ( $\text{C-4}_{\text{Glc}}$ ), 68.30 ( $\text{C-6}_{\text{Man}}$ ), 66.71 ( $\text{C-6}_{\text{Glc}}$ ), 65.77 ( $\text{C-4}_{\text{Man}}$ ), 62.29 ( $\text{Glc-OCH}_2$ ), 61.88 ( $\text{Man-OCH}_2$ ), 56.32 ( $\text{OCH}_2\text{C}\equiv\text{CH}$ ), 40.76 ( $\text{C-6}$ ), 38.74 ( $\text{C-6}'$ ), 20.87, 20.79, 20.78, 20.73, 20.67, 20.66, 20.62, 20.61 (8C,  $\text{OAc}$ ) ppm;

ESI-MS:  $m/z = 1675.5038$   $[\text{M}+\text{H}]^+$  (calculated  $m/z = 1675.5033$  for  $[\text{M}+\text{H}]^+$ ).

**(2-Propargyl) 6-deoxy-6-[[ $(\alpha$ -D-mannopyranosyloxy)acetyl]amino]-4-O-(6'-deoxy-6'-[[ $(\beta$ -D-glucopyranosyloxy)acetyl]amino]- $\alpha$ -D-glucopyranosyl)- $\beta$ -D-glucopyranoside (2)**



The maltoside **32** (58.0 mg, 34.6  $\mu\text{mol}$ ) was dissolved in dry MeOH and a catalytical amount of a sodium methoxide solution (5.4M) was added. It was stirred at room temperature for 16 h and then neutralized with Amberlite IR120. The reaction mixture was filtered, and the solvent was removed under reduced pressure. The crude product was taken up in  $\text{H}_2\text{O}$  and washed with  $\text{Et}_2\text{O}$  (3 x). The aqu. layer was concentrated to dryness. Purification by size exclusion chromatography on Sephadex GP10 ( $\text{H}_2\text{O}$ ) gave the product as a colorless solid.

**Yield:** 25.0 mg (30.5  $\mu\text{mol}$ , 88 %);

**R<sub>f</sub>:** (CH<sub>2</sub>Cl<sub>2</sub>/MeOH, 8:2): R<sub>f</sub> = 0.05;

**[ $\alpha$ ]<sub>D</sub><sup>23</sup>:** -55.2 (c = 0.01, H<sub>2</sub>O);

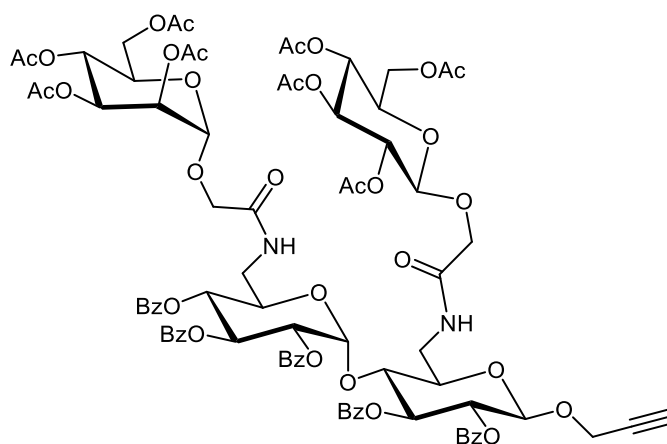
**IR (ATR):**  $\tilde{\nu}$  = 3291, 2923, 1648, 1546, 1358, 1034, 813 cm<sup>-1</sup>;

**<sup>1</sup>H NMR:** (600 MHz, D<sub>2</sub>O, 300 K):  $\delta$  = 5.38 (d, <sup>3</sup>J<sub>1,2'</sub> = 3.9 Hz, 1H, H-1'), 4.92 (d, <sup>3</sup>J<sub>1,2</sub> = 1.1 Hz, 1H, H-1<sub>Man</sub>), 4.63 (d, <sup>3</sup>J<sub>1,2</sub> = 8.0 Hz, 1H, H-1), 4.49 (d, <sup>3</sup>J<sub>1,2</sub> = 7.9 Hz, 1H, H-1<sub>Glc</sub>), 4.43 (s, 2H, OCH<sub>2</sub>), 4.35 (d, <sup>2</sup>J<sub>OCH,OCH</sub> = 15.9 Hz, 1H, Glc-OCH<sub>2</sub>), 4.30-4.23 (m, 2H, Glc-OCH<sub>2</sub>, Man-OCH<sub>2</sub>), 4.15 (d, <sup>2</sup>J<sub>OCH,OCH</sub> = 15.3 Hz, 1H, Man-OCH<sub>2</sub>), 4.07 (dd, <sup>3</sup>J<sub>2,3</sub> = 3.3 Hz, <sup>3</sup>J<sub>1,2</sub> = 1.7 Hz, 1H, H-2<sub>Man</sub>), 3.97-3.59 (m, 14H, H-2', H-3<sub>Man</sub>, H-6a<sub>Man</sub>, H-6a<sub>Glc</sub>, H-6b<sub>Man</sub>, H-6b<sub>Glc</sub>, H-6b, H-6b', H-5<sub>Man</sub>, H-3', H-5, H-5', H-4<sub>Man</sub>, H-4<sub>Glc</sub>), 3.54-3.28 (m, 9H, H-6a, H-6a', H-5<sub>Glc</sub>, H-3<sub>Glc</sub>, H-3, H-4, H-2, H-2<sub>Glc</sub>, H-4'), 2.94 (t, <sup>4</sup>J<sub>OCH',C $\equiv$ CH</sub> = 2.3 Hz, <sup>4</sup>J<sub>OCH,C $\equiv$ CH</sub> = 2.3 Hz, 1H, C $\equiv$ CH) ppm;

**<sup>13</sup>C NMR:** (125 MHz, D<sub>2</sub>O, 300 K):  $\delta$  = 171.91 (NH-C(O)-Glc), 171.62 (NH-C(O)-Man), 102.49 (C-1<sub>Glc</sub>), 100.16 (C-1), 99.98 (C-1'), 99.94 (C-1<sub>Man</sub>), 79.36 (C-4), 78.51 (OCH<sub>2</sub>C $\equiv$ CH), 76.57 (OCH<sub>2</sub>C $\equiv$ CH), 76.06 (C-4<sub>Glc</sub>), 76.03 (C-3), 75.59 (C-3<sub>Glc</sub>), 73.21 (C-2'), 72.93 (C-2<sub>Glc</sub>), 72.79 (C-3'), 72.71 (C-2), 72.46 (C-5), 71.55 (C-5'), 71.26 (C-5<sub>Man</sub>), 71.10 (C-4'), 70.38 (C-3<sub>Man</sub>), 69.69 (C-2<sub>Man</sub>), 69.45 (C-5<sub>Glc</sub>), 68.04 (Glc-OCH<sub>2</sub>), 66.54 (C-4<sub>Man</sub>), 65.71 (Man-OCH<sub>2</sub>), 60.82 (C-6<sub>Glc</sub>), 60.64 (C-6<sub>Man</sub>), 56.36 (OCH<sub>2</sub>C $\equiv$ CH), 40.18 (C-6), 39.73 (C-6')

**ESI-MS:**  $m/z$  = 841.2676 [M+Na]<sup>+</sup> (calculated  $m/z$  = 841.2696 for [M+Na]<sup>+</sup>).

**(2-Propargyl) 2,3-di-O-benzoyl-6-deoxy-6-[[[(2,3,4,6-tetra-O-acetyl- $\beta$ -D-glucopyranosyl)oxy]acetyl]amino]-4-O-(2',3',4'-tri-O-benzoyl-6'-deoxy-6'-[[[(2,3,4,6-tetra-O-acetyl- $\alpha$ -D-mannopyranosyl)oxy]acetyl]amino]- $\alpha$ -D-glucopyranosyl)- $\beta$ -D-glucopyranoside (31)**



The carboxylic acid **25** (61.9 mg, 152  $\mu\text{mol}$ ) was dissolved in dry THF (5 mL) and NHS (26.3 mg, 228  $\mu\text{mol}$ ) and EDC·HCl (43.7 mg, 228  $\mu\text{mol}$ ) were added. It was stirred for 2 h at

room temperature. Then maltoside **30** (100 mg, 76.1  $\mu\text{mol}$ ) was added and the reaction mixture was cooled to 0 °C. To the mixture  $\text{PMe}_3$  (1M in THF, 381  $\mu\text{L}$ ) was added dropwise. It was allowed to warm to room temperature and stirring was continued for 16 h. Then  $\text{H}_2\text{O}$  was added and the aqu. layer was extracted with ethyl acetate. The combined org. layers were dried over  $\text{MgSO}_4$ , filtered of, and concentrated. Purification by column chromatography on silica gel (cyclohexane/ethyl acetate, 1:4) gave **31** as a colorless solid.

**Yield:** 86.6 mg (51.7  $\mu\text{mol}$ , 68 %);

**R<sub>f</sub>:** (cyclohexane/ ethyl acetate, 1:4):  $R_f = 0.15$ ;

**$[\alpha]_D^{23}$ :** +22.6 (c = 0.01,  $\text{CH}_2\text{Cl}_2$ );

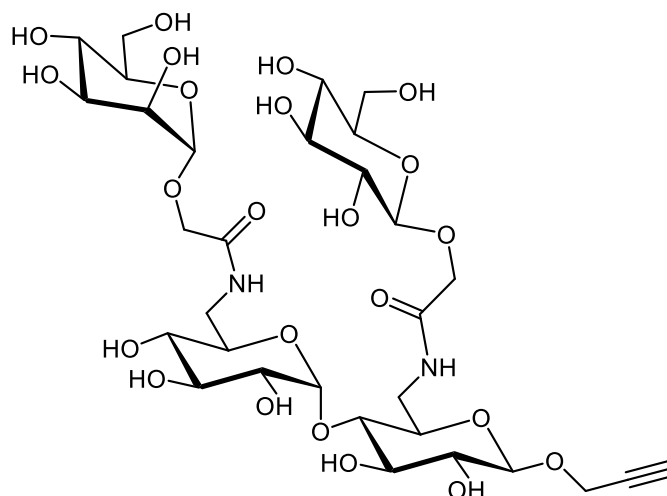
**IR (ATR):**  $\tilde{\nu} = 3289, 1733, 1531, 1451, 1368, 1218, 1090, 926, 750, 707 \text{ cm}^{-1}$ ;

**$^1\text{H NMR}$ :** (500 MHz,  $\text{CDCl}_3$ , 300 K):  $\delta = 8.01\text{-}7.92$  (m, 2H,  $\text{Bz}_{\text{ortho}}$ ), 7.83-7.78 (m, 2H,  $\text{Bz}_{\text{ortho}}$ ), 7.71-7.67 (m, 2H,  $\text{Bz}_{\text{ortho}}$ ), 7.65-7.59 (m, 2H,  $\text{Bz}_{\text{ortho}}$ ), 7.59-7.27 (m, 12H,  $\text{Bz}_{\text{ortho}}$ ,  $\text{Bz}_{\text{meta}}$ ,  $\text{Bz}_{\text{para}}$ ,  $\text{NH}$ ), 7.26-7.12 (m, 6H,  $\text{Bz}_{\text{meta}}$ ), 7.03 (t,  $^3J_{\text{NH},6a} = 5.2 \text{ Hz}$ ,  $^3J_{\text{NH},6b} = 5.2 \text{ Hz}$ , 1H,  $\text{NH}$ ), 6.02 (t,  $^3J_{2',3'} = 10.1 \text{ Hz}$ ,  $^3J_{3',4'} = 10.1 \text{ Hz}$ , 1H, H-3'), 5.72 (t,  $^3J_{2,3} = 3.5 \text{ Hz}$ ,  $^3J_{3,4} = 10.1 \text{ Hz}$ , 1H, H-3), 5.63 (d,  $^3J_{1',2'} = 4.1 \text{ Hz}$ , 1H, H-1'), 5.54 (dd,  $^3J_{2,3} = 9.3 \text{ Hz}$ ,  $^3J_{3,4} = 9.3 \text{ Hz}$ , 1H, H-3<sub>Man</sub>), 5.47-5.25 (m, 6H, H-2<sub>Man</sub>, H-2, H-2', H-4', H-3<sub>Glc</sub>, H-4<sub>Man</sub>), 5.14-5.07 (m, 2H, H-2<sub>Glc</sub>, H-4<sub>Glc</sub>), 5.05 (d,  $^3J_{1,2} = 7.8 \text{ Hz}$ , 1H, H-1), 4.95 (d,  $^3J_{1,2} = 1.5 \text{ Hz}$ , 1H, H-1<sub>Man</sub>), 4.61 (d,  $^3J_{1,2} = 7.9 \text{ Hz}$ , 1H, H-1<sub>Glc</sub>), 4.50 (dd,  $^2J_{\text{OCH},\text{OCH}} = 16.0 \text{ Hz}$ ,  $^4J_{\text{OCH},\text{C}\equiv\text{CH}} = 2.4 \text{ Hz}$ , 1H,  $\text{OCH}_2$ ), 4.47-4.31 (m, 5H,  $\text{OCH}_2$ , H-6a<sub>Glc</sub>, H-6a<sub>Man</sub>,  $\text{Glc-OCH}_2$ , H-5'), 4.29-3.91 (m, 10H, H-6b<sub>Man</sub>, H-6b<sub>Glc</sub>, H-4, H-6a, H-6a', H-5<sub>Man</sub>, H-5,  $\text{Man-OCH}_2$ ,  $\text{Glc-OCH}_2$ ,  $\text{Man-OCH}_2$ ), 3.77 (ddd,  $^3J_{4,5} = 9.8 \text{ Hz}$ ,  $^3J_{5,6a} = 5.0 \text{ Hz}$ ,  $^3J_{5,6b} = 2.3 \text{ Hz}$ , 1H, H-5<sub>Glc</sub>), 3.68-3.57 (m, 1H, H-6b'), 3.39-3.27 (m, 1H, H-6b), 2.49 (t,  $^4J_{\text{OCH},\text{C}\equiv\text{CH}} = 2.4 \text{ Hz}$ ,  $^4J_{\text{OCH},\text{C}\equiv\text{CH}} = 2.4 \text{ Hz}$ , 1H,  $\text{C}\equiv\text{CH}$ ), 2.17, 2.16, 2.12, 2.04, 1.91, 1.90 (each s, 24H, 8  $\text{C}(\text{O})\text{CH}_3$ ) ppm;

**$^{13}\text{C NMR}$ :** (125 MHz,  $\text{CDCl}_3$ , 300 K):  $\delta = 170.83, 170.74, 170.29, 170.07, 169.90, 169.90, 169.89, 169.59$  (8C,  $\underline{\text{C}}(\text{O})\text{-Ac}$ ), 168.97, 168.35 (2  $\text{NH}\text{-}\underline{\text{C}}(\text{O})$ ), 166.16, 165.76, 165.42, 165.42, 165.04 (5C,  $\underline{\text{C}}(\text{O})\text{Ph}$ ), 133.66, 133.24, 133.12, 133.11, 133.10 (5C,  $\text{Bz}\text{-}\underline{\text{C}}\text{H}_{\text{para}}$ ), 130.26, 130.07, 129.95, 129.75, 129.71 (10C,  $\text{Bz}\text{-}\underline{\text{C}}\text{H}_{\text{ortho}(a,b)}}$ ), 129.41, 129.14, 128.87, 128.82, 128.55 (5C,  $\text{Bz}\text{-}\text{C}_{\text{quat}}$ ), 128.53, 128.27, 128.22, 128.20, 128.07 (10C,  $\text{Bz}\text{-}\underline{\text{C}}\text{H}_{\text{ortho}(a,b)}}$ ), 100.68 (C-1<sub>Glc</sub>), 98.26 (C-1), 97.92 (C-1'), 97.32 (C-1<sub>Man</sub>), 78.66 ( $\text{OCH}_2\text{C}\equiv\text{CH}$ ), 75.87 ( $\text{OCH}_2\text{C}\equiv\text{CH}$ ), 75.49 (C-4), 75.36 (C-3), 73.28 (C-5), 72.35 (C5<sub>Glc</sub>), 72.32 (C-2'), 72.00 (C-2), 71.33 (C-2<sub>Glc</sub>), 70.89 (C-3<sub>Glc</sub>), 70.22 (C-3'), 69.89 (C-5'), 69.60 (C-4'), 69.55 (C5<sub>Man</sub>), 69.45 (C-2<sub>Man</sub>), 68.91 (C-3<sub>Man</sub>), 68.58 (C-4<sub>Glc</sub>), 68.44 (C-6<sub>Man</sub>), 66.42 (C-6<sub>Glc</sub>), 65.99 (C-4<sub>Man</sub>), 62.43 ( $\text{Glc-OCH}_2$ ), 61.85 ( $\text{Man-OCH}_2$ ), 56.24 ( $\text{OCH}_2\text{C}\equiv\text{CH}$ ), 40.52 (C-6), 38.52 (C-6'), 20.99, 20.97, 20.94, 20.91, 20.80, 20.74, 20.73, 20.72 (8C,  $\text{OAc}$ ) ppm;

**ESI-HRMS:**  $m/z = 1675.5049$   $[\text{M}+\text{H}]^+$  (calculated  $m/z = 1675.5033$  for  $[\text{M}+\text{H}]^+$ ).

**(2-Propargyl) 6-deoxy-6-[[[β-D-glucopyranosyloxy)acetyl]amino]-4-O-(6'-deoxy-6'-[[[α-D-mannopyranosyloxy)acetyl]amino]-α-D-glucopyranosyl)-β-D-glucopyranoside (1)**



The maltoside **31** (40.0 mg, 23.9  $\mu\text{mol}$ ) was dissolved in dry MeOH and a catalytical amount of a sodium methoxide solution was added. It was stirred at room temperature for 2 h and then neutralized with Amberlite IR120. The reaction mixture was filtered, and the solvent was removed under reduced pressure. The crude product was taken up in  $\text{H}_2\text{O}$  and washed with  $\text{Et}_2\text{O}$  (3 x). The aqu. layer was concentrated to dryness. Purification by size exclusion chromatography on Sephadex GP10 ( $\text{H}_2\text{O}$ ) gave the product as a colorless solid.

**Yield:** 16.0 mg (19.5  $\mu\text{mol}$ , 82 %);

**R<sub>f</sub>:** ( $\text{CH}_2\text{Cl}_2/\text{MeOH}$ , 8:2):  $R_f = 0.05$ ;

**$[\alpha]_{\text{D}}^{23}$ :** -221 ( $c = 0.01$ ,  $\text{H}_2\text{O}$ );

**IR (ATR):**  $\tilde{\nu} = 3285, 2923, 1648, 1546, 1357, 1034, 813 \text{ cm}^{-1}$ ;

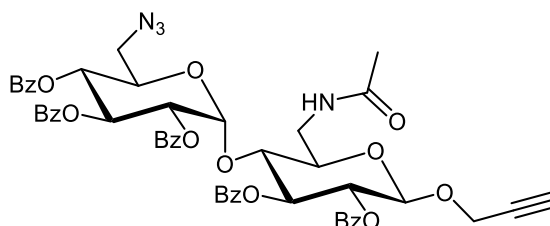
**$^1\text{H NMR}$ :** (600 MHz,  $\text{D}_2\text{O}$ , 300 K):  $\delta = 5.28$  (d,  $^3J_{1,2'} = 3.9 \text{ Hz}$ , 1H, H-1'), 4.79 (d,  $^3J_{1,2} = 1.0 \text{ Hz}$ , 1H, H-1<sub>Man</sub>), 4.52 (d,  $^3J_{1,2} = 8.0 \text{ Hz}$ , 1H, H-1), 4.41 (d,  $^3J_{1,2} = 7.9 \text{ Hz}$ , 1H, H-1<sub>Glc</sub>), 4.36-4.32 (m, 3H,  $\text{OCH}_2$ ,  $\text{OCH}_2$ ,  $\text{Glc-OCH}_2$ ), 4.20 (d,  $^2J_{\text{OCH}_2\text{OCH}} = 15.7 \text{ Hz}$ , 1H,  $\text{Glc-OCH}_2$ ), 4.14 (d,  $^2J_{\text{OCH}_2\text{OCH}} = 15.4 \text{ Hz}$ , 1H,  $\text{Man-OCH}_2$ ), 3.98 (d,  $^2J_{\text{OCH}_2\text{OCH}} = 15.4 \text{ Hz}$ , 1H,  $\text{Man-OCH}_2$ ), 3.94 (dd,  $^3J_{2,3} = 3.2 \text{ Hz}$ ,  $^3J_{1,2} = 1.6 \text{ Hz}$ , 1H, H-2<sub>Man</sub>), 3.84-3.74 (m, 3H, H-3<sub>Man</sub>, H-6a<sub>Man</sub>, H-6a<sub>Glc</sub>), 3.73-3.47 (m, 11H, H-2', H-3', H-5, H-6b, H-6b', H-5', H-4<sub>Man</sub>, H-5<sub>Man</sub>, H-6b<sub>Man</sub>, H-4<sub>Glc</sub>, H-6b<sub>Glc</sub>), 3.45-3.35 (m, 3H, H-3<sub>Glc</sub>, H-3, H-4), 3.34-3.23 (m, 5H, H-6a, H-6a', H-2, H-2<sub>Glc</sub>, H-5<sub>Glc</sub>), 3.19 (t,  $^3J_{3',4'} = 9.6 \text{ Hz}$ ,  $^3J_{4',5'} = 9.6 \text{ Hz}$ , 1H, H-4'), 2.85 (t,  $^4J_{\text{OCH}_2\text{C}\equiv\text{CH}} = 2.3 \text{ Hz}$ ,  $^4J_{\text{OCH}_2\text{C}\equiv\text{CH}} = 2.3 \text{ Hz}$ , 1H,  $\text{C}\equiv\text{CH}$ ) ppm;

**$^{13}\text{C NMR}$ :** (125 MHz,  $\text{CDCl}_3$ , 300 K):  $\delta = 171.90$  (NH-C(O)-Glc), 171.67 (NH-C(O)-Man), 102.43 (C-1<sub>Glc</sub>), 100.39 (C-1), 100.04 (C-1'), 99.86 (C-1<sub>Man</sub>), 79.39 (C-4), 78.27 ( $\text{OCH}_2\text{C}\equiv\text{CH}$ ), 76.51 ( $\text{OCH}_2\text{C}\equiv\text{CH}$ ), 76.10 (C-4<sub>Glc</sub>), 75.99 (C-3), 75.56 (C-3<sub>Glc</sub>), 73.23 (C-2'), 72.94 (C-2<sub>Glc</sub>),

72.76 (C-3'), 72.64 (C-2), 72.41 (C-5), 71.56 (C-5'), 71.36 (C-5<sub>Man</sub>), 71.25 (C-4'), 70.35 (C-3<sub>Man</sub>), 69.68 (C-2<sub>Man</sub>), 69.52 (C5<sub>Glc</sub>), 68.00 (Glc-OCH<sub>2</sub>), 66.53 (C-4<sub>Man</sub>), 65.64 (Man-OCH<sub>2</sub>), 60.81 (C-6<sub>Glc</sub>), 60.65 (C-6<sub>Man</sub>), 56.54 (OCH<sub>2</sub>C≡CH), 40.11 (C-6), 39.80 (C-6') ppm;

**ESI-MS:**  $m/z = 841.2681$  [M+Na]<sup>+</sup> (calculated  $m/z = 841.2696$  for [M+Na]<sup>+</sup>).

**(2-Propargyl) 6-acetamido-2,3-di-O-benzoyl-6-deoxy-4-O-(6'-azido-2',3',4'-tri-O-benzoyl-6'-deoxy- $\alpha$ -D-glucopyranosyl)- $\beta$ -D-glucopyranose (33)**



The maltoside **20** (200 mg, 168  $\mu$ mol) was dissolved in mixture of MeCN/THF (4:1, 2.5 mL) and ethylenediamine (22.0  $\mu$ L, 336  $\mu$ mol) was added. It was stirred for 3 h at 55 °C. The solvent was removed, and it was coevaporated with toluene. The crude product was dissolved in pyridine (3.00 mL) and Ac<sub>2</sub>O (1.5 mL) was added. It was stirred at room temperature for 16 h. The mixture was diluted with ethyl acetate and washed with 1M HCl, sodium bicarbonate and brine. The org. layer was dried over MgSO<sub>4</sub>, filtered, and concentrated. Purification by column chromatography on silica gel (cyclohexane/ethyl acetate, 1:1) gave **33** as a colorless solid.

**Yield:** 88.0 mg (91.0  $\mu$ mol, 54 %);

**R<sub>f</sub>:** (cyclohexane/ ethyl acetate, 1:1): R<sub>f</sub> = 0.44;

**[ $\alpha$ ]<sub>D</sub><sup>23</sup>:** +35.1 (c = 0.01, CH<sub>2</sub>Cl<sub>2</sub>);

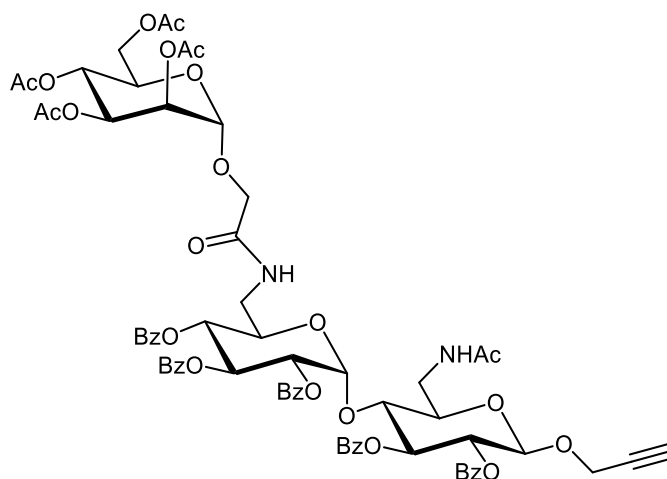
**IR (ATR):**  $\tilde{\nu} = 2105, 1728, 1451, 1259, 1091, 1067, 1025, 705$  cm<sup>-1</sup>;

**<sup>1</sup>H NMR:** (600 MHz, CDCl<sub>3</sub>, 300 K):  $\delta = 8.01$ -7.94 (m, 2H, Bz<sub>ortho</sub>), 7.87-7.82 (m, 2H, Bz<sub>ortho</sub>), 7.73-7.64 (m, 4H, Bz<sub>ortho</sub>), 7.61-7.55 (m, 2H, Bz<sub>ortho</sub>), 7.54-7.19 (m, 15H, Bz<sub>meta</sub>, Bz<sub>para</sub>), 6.05-5.98 (m, 2H, NHAc, H-3'), 5.71 (t, <sup>3</sup>J<sub>2,3</sub> = 9.2 Hz, <sup>3</sup>J<sub>3,4</sub> = 9.2 Hz, 1H, H-3), 5.682 (d, <sup>3</sup>J<sub>1,2'</sub> = 4.0 Hz, 1H, H-1'), 5.53 (t, <sup>3</sup>J<sub>3',4'</sub> = 9.8 Hz, <sup>3</sup>J<sub>4',5'</sub> = 9.8 Hz, 1H, H-4'), 5.29 (dd, <sup>3</sup>J<sub>2,3</sub> = 9.6 Hz, <sup>3</sup>J<sub>1,2</sub> = 7.8 Hz, 1H, H-2), 5.24 (dd, <sup>3</sup>J<sub>2',3'</sub> = 10.5 Hz, <sup>3</sup>J<sub>1',2'</sub> = 4.0 Hz, 1H, H-2'), 5.02 (d, <sup>3</sup>J<sub>1,2</sub> = 7.7 Hz, 1H, H-1), 4.47-4.39 (m, 2H, H-5', OCH<sub>2</sub>), 4.35 (dd, <sup>2</sup>J<sub>OCH',OCH</sub> = 16.0 Hz, <sup>4</sup>J<sub>OCH,C≡CH</sub> = 2.4 Hz, 1H, OCH<sub>2</sub>), 4.19 (t, <sup>3</sup>J<sub>3,4</sub> = 9.1 Hz, <sup>3</sup>J<sub>4,5</sub> = 9.1 Hz, 1H, H-4), 4.04 (ddd, <sup>2</sup>J<sub>6a,6b</sub> = 13.9 Hz, <sup>3</sup>J<sub>5,6a</sub> = 5.3 Hz, <sup>3</sup>J<sub>NH,6a</sub> = 3.4 Hz, 1H, H-6a), 3.93 (ddd, <sup>3</sup>J<sub>4,5</sub> = 9.3 Hz, <sup>3</sup>J<sub>5,6a</sub> = 5.9 Hz, <sup>3</sup>J<sub>5,6b</sub> = 3.3 Hz, 1H, H-5), 3.69-3.61 (m, 2H, H-6b, H-6a'), 3.49 (dd, <sup>2</sup>J<sub>6a',6b'</sub> = 13.5 Hz, <sup>3</sup>J<sub>5',6b'</sub> = 5.16 Hz, 1H, H-6b'), 2.44 (t, <sup>4</sup>J<sub>OCH',C≡CH</sub> = 2.4 Hz, <sup>4</sup>J<sub>OCH,C≡CH</sub> = 2.4 Hz, 1H, C≡CH), 2.09 (s, 3H, NHAc) ppm;

**$^{13}\text{C}$  NMR:** (125 MHz,  $\text{CDCl}_3$ , 300 K):  $\delta$  = 170.49 (NHAc-C(O)), 165.71, 165.50, 165.45, 165.41, 165.06 (5C,  $\underline{\text{C}}(\text{O})\text{Ph}$ ), 133.66, 133.33, 133.31, 133.26, 133.17 (5C, Bz- $\underline{\text{C}}\text{H}_{\text{para}}$ ), 130.18, 130.10, 129.98, 129.77, 129.69 (10C, Bz- $\underline{\text{C}}\text{H}_{\text{ortho}(a,b)}$ ), 129.21, 129.04, 128.77, 128.76, 128.55 (5C, Bz- $\text{C}_{\text{quat}}$ ), 128.60, 128.37, 128.34, 128.29, 128.15 (10C, Bz- $\underline{\text{C}}\text{H}_{\text{ortho}(a,b)}$ ), 98.72 (C-1), 97.03 (C-1'), 78.54 ( $\text{OCH}_2\underline{\text{C}}\equiv\text{CH}$ ), 75.69 ( $\text{OCH}_2\underline{\text{C}}\equiv\text{CH}$ ), 74.99 (C-3), 74.79 (C-4), 73.44 (C-5), 71.97 (C-2), 70.94 (C-2'), 70.37 (C-5'), 69.85 (C-3'), 69.58 (C-4'), 56.63 ( $\text{OCH}_2\underline{\text{C}}\equiv\text{CH}$ ), 51.20 (C-6'), 40.58 (C-6), 23.54 (NHAc) ppm;

**ESI-MS:**  $m/z$  = 967.3029  $[\text{M}+\text{H}]^+$  (calculated  $m/z$  = 967.3032 for  $[\text{M}+\text{H}]^+$ ).

**(2-Propargyl) 6-acetamido-2,3-di-O-benzoyl-6-deoxy-4-O-(2',3',4'-tri-O-benzoyl-6'-deoxy-6'-[[[(2,3,4,6-tetra-O-acetyl- $\alpha$ -D-mannopyranosyl)oxy]acetyl]amino]- $\alpha$ -D-glucopyranosyl)- $\beta$ -D-glucopyranoside (34)**



The carboxylic acid **25** (67.0 mg, 165  $\mu\text{mol}$ ) was dissolved in dry THF (5.5 mL) and NHS (28.5 mg, 248  $\mu\text{mol}$ ) and EDC·HCl (47.5 mg, 248  $\mu\text{mol}$ ) were added. It was stirred for 2 h at room temperature. Then maltoside **33** (80 mg, 82.7  $\mu\text{mol}$ ) was added and the reaction mixture was cooled to 0  $^{\circ}\text{C}$ . To the mixture  $\text{PMe}_3$  (1M in THF, 414  $\mu\text{L}$ ) was added dropwise. It was allowed to warm to room temperature and stirring was continued for 16 h. Then  $\text{H}_2\text{O}$  was added and the aqu. layer was extracted with ethyl acetate. The combined org. layers were dried over  $\text{MgSO}_4$ , filtered of, and concentrated. Purification by column chromatography on silica gel (cyclohexane/ethyl acetate, 1:9) gave **34** as a colorless solid.

**Yield:** 50.0.0 mg (37.6  $\mu\text{mol}$ , 45 %);

**$R_f$ :** (cyclohexane/ ethyl acetate, 1:9):  $R_f$  = 0.24;

**$[\alpha]_{\text{D}}^{23}$ :** 59.6 ( $c$  = 0.01,  $\text{CH}_2\text{Cl}_2$ );

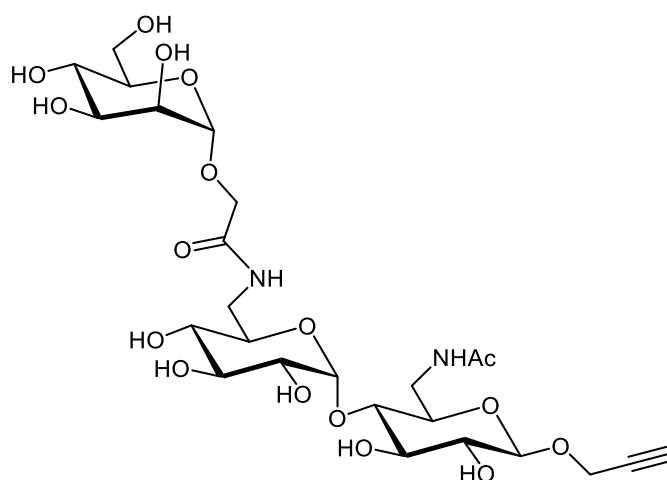
**IR (ATR):**  $\tilde{\nu}$  = 3324, 2929, 2850, 1733, 1625, 1573, 1451, 1369, 1244, 1088, 1069, 1026, 707  $\text{cm}^{-1}$ ;

**<sup>1</sup>H NMR:** (600 MHz, CDCl<sub>3</sub>, 300 K): δ = 7.99-7.92 (m, 2H, Bz<sub>ortho</sub>), 7.86-7.80 (m, 2H, Bz<sub>ortho</sub>), 7.71-7.64 (m, 2H, Bz<sub>ortho</sub>), 7.63-7.55 (m, 3H, Bz<sub>para</sub>, Bz<sub>ortho</sub>), 7.53-7.28 (m, 11H, Bz<sub>ortho</sub>, Bz<sub>meta</sub>, Bz<sub>para</sub>, NH), 7.23-7.11 (m, 6H, Bz<sub>meta</sub>), 6.34 (dd, <sup>3</sup>J<sub>NH,6a</sub> = 5.8 Hz, <sup>3</sup>J<sub>NH,6b</sub> = 5.1 Hz, 1H, NH), 6.00 (t, <sup>3</sup>J<sub>2',3'</sub> = 10.1 Hz, <sup>3</sup>J<sub>3',4'</sub> = 10.1 Hz, 1H, H-3'), 5.69 (t, <sup>3</sup>J<sub>2,3</sub> = 9.2 Hz, <sup>3</sup>J<sub>3,4</sub> = 9.2 Hz, 1H, H-3), 5.62 (d, <sup>3</sup>J<sub>1',2'</sub> = 4.1 Hz, 1H, H-1'), 5.51 (dd, <sup>3</sup>J<sub>2,3</sub> = 3.4 Hz, <sup>3</sup>J<sub>3,4</sub> = 10.1 Hz, 1H, H-3<sub>Man</sub>), 5.43-5.37 (m, 2H, H-4', H-2<sub>Man</sub>), 5.37-5.27 (m, 3H, H-2, H-2', H-4<sub>Man</sub>), 5.00 (d, <sup>3</sup>J<sub>1,2</sub> = 7.7 Hz, 1H, H-1), 4.89 (d, <sup>3</sup>J<sub>1,2</sub> = 0.9 Hz, 1H, H-1<sub>Man</sub>), 4.49-4.38 (m, 2H, H-5', OCH<sub>2</sub>), 4.38-4.30 (m, 2H, H-6a<sub>Man</sub>, OCH<sub>2</sub>), 4.26-4.06 (m, 5H, H-4, H-6a, H-5<sub>Man</sub>, H-6b<sub>Man</sub>, Man-OCH<sub>2</sub>), 3.97-3.87 (m, 3H, H-5, H-6a', Man-OCH<sub>2</sub>), 3.56-3.41 (m, 2H, H-6b, H-6b'), 2.46 (t, <sup>4</sup>J<sub>OCH',C≡CH</sub> = 2.4 Hz, <sup>4</sup>J<sub>OCH,C≡CH</sub> = 2.4 Hz, 1H, C≡CH), 2.17, 2.12, 2.09, 1.96, 1.96 (each s, 15H, 4 Oac, NHAc) ppm;

**<sup>13</sup>C NMR:** (125 MHz, CDCl<sub>3</sub>, 300 K): δ = 170.97, 170.83, 170.27, 170.16 (4C, C(O)-Ac), 169.90, 168.17 (2 NH-C(O)), 165.98, 165.77, 165.36, 165.36, 164.97 (5C, C(O)Ph), 133.63, 133.23, 133.19, 133.18, 133.10 (5C, Bz-CH<sub>para</sub>), 130.23, 130.09, 129.97, 129.75, 129.69 (10C, Bz-CH<sub>ortho(a,b)</sub>), 129.31, 129.07, 128.85, 128.69, 128.44 (5C, Bz-C<sub>quat</sub>), 128.54, 128.31, 128.22, 128.20, 128.02 (10C, Bz-CH<sub>ortho(a,b)</sub>), 98.61 (C-1), 98.23 (C-1'), 97.47 (C-1<sub>Man</sub>), 78.60 (OCH<sub>2</sub>C≡CH), 76.37 (OCH<sub>2</sub>C≡CH), 75.65 (C-4), 75.03 (C-3), 73.45 (C-5), 72.09 (C-2'), 70.72 (C-2), 70.54 (C-3'), 69.95 (C-5'), 69.91 (C-4'), 69.61 (C5<sub>Man</sub>), 69.37 (C-2<sub>Man</sub>), 68.90 (C-3<sub>Man</sub>), 66.78 (C-6<sub>Man</sub>), 65.97 (C-4<sub>Man</sub>), 62.42 (Man-OCH<sub>2</sub>), 56.42 (OCH<sub>2</sub>C≡CH), 41.27 (C-6), 39.11 (C-6'), 23.36 (NHAc), 21.02, 20.93, 20.78, 20.78 (4C, OAc) ppm;

**ESI-MS:** *m/z* = 1351.3948 [M+Na]<sup>+</sup> (calculated *m/z* = 1351.3952 for [M+Na]<sup>+</sup>).

**(2-Propargyl) 6-acetamido-6-deoxy-4-O-(6'-deoxy-6'-[[α-D-mannopyranosyloxy]acetyl]amino]-α-D-glucopyranosyl)-β-D-glucopyranoside (35)**



The maltoside **34** (70.0 mg, 52.7 μmol) was dissolved in dry MeOH and a catalytical amount of a sodium methoxide solution (5.4M) was added. It was stirred at room temperature for 16 h and then neutralized with Amberlite IR120. The reaction mixture was filtered, and the solvent

was removed under reduced pressure. The crude product was taken up in H<sub>2</sub>O and washed with Et<sub>2</sub>O. The aqu. layer was concentrated to dryness. Purification by size exclusion chromatography on Sephadex GP10 (H<sub>2</sub>O) gave the product as a colorless solid.

**Yield:** 28.0 mg (43.7 μmol, 83 %);

**R<sub>f</sub>:** (CH<sub>2</sub>Cl<sub>2</sub>/MeOH, 8:2): R<sub>f</sub> = 0.05;

**[α]<sub>D</sub><sup>23</sup>:** -42.1 (c = 0.01, H<sub>2</sub>O);

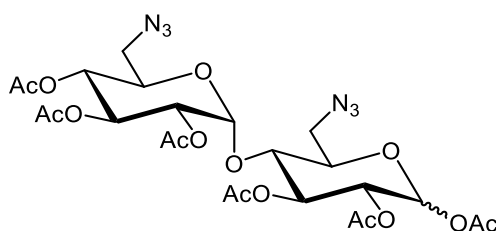
**IR (ATR):**  $\tilde{\nu}$  = 3286, 2004, 1648, 1541, 1364, 1044, 673 cm<sup>-1</sup>;

**<sup>1</sup>H NMR:** (600 MHz, D<sub>2</sub>O, 300 K):  $\delta$  = 5.37 (d, <sup>3</sup>J<sub>1,2'</sub> = 3.9 Hz, 1H, H-1'), 4.88 (d, <sup>3</sup>J<sub>1,2</sub> = 1.1 Hz, 1H, H-1<sub>Man</sub>), 4.62 (d, <sup>3</sup>J<sub>1,2</sub> = 8.0 Hz, 1H, H-1), 4.49-4.40 (m, 2H, OCH<sub>2</sub>), 4.24 (d, <sup>2</sup>J<sub>OCH<sub>2</sub>OCH</sub> = 15.4 Hz, 1H, Man-OCH<sub>2</sub>), 4.07 (d, <sup>2</sup>J<sub>OCH<sub>2</sub>OCH</sub> = 15.4 Hz, 1H, Man-OCH<sub>2</sub>), 4.04 (dd, <sup>3</sup>J<sub>2,3</sub> = 3.3 Hz, <sup>3</sup>J<sub>1,2</sub> = 1.7 Hz, 1H, H-2<sub>Man</sub>), 3.90-3.84 (m, 2H, H-6a<sub>Man</sub>, H-3<sub>Man</sub>), 3.83-3.65 (m, 7H, H-3, H-6a, H-3', H-5', H-6a', H-4<sub>Man</sub>, H-6b<sub>Man</sub>), 3.63-3.58 (m, 3H, H-2', H-5, H-5<sub>Man</sub>), 3.47 (t, <sup>3</sup>J<sub>3,4</sub> = 9.2 Hz, <sup>3</sup>J<sub>4,5</sub> = 9.2 Hz, 1H, H-4), 3.42 (dd, <sup>2</sup>J<sub>6a',6b'</sub> = 14.1 Hz, <sup>3</sup>J<sub>5',6b'</sub> = 7.4 Hz, H-6b'), 3.34 (dd, <sup>3</sup>J<sub>2,3</sub> = 9.4 Hz, <sup>3</sup>J<sub>1,2</sub> = 8.1 Hz, H-2), 3.28 (t, <sup>3</sup>J<sub>3',4'</sub> = 9.6 Hz, <sup>3</sup>J<sub>4',5'</sub> = 9.6 Hz, 1H, H-4'), 3.19 (dd, <sup>2</sup>J<sub>6a,6b</sub> = 14.1 Hz, <sup>3</sup>J<sub>5,6b</sub> = 8.6 Hz, H-6b), 2.93 (t, <sup>4</sup>J<sub>OCH',C≡CH</sub> = 2.4 Hz, <sup>4</sup>J<sub>OCH,C≡CH</sub> = 2.4 Hz, 1H, C≡CH), 2.03 (s, 3H, NHAc) ppm;

**<sup>13</sup>C NMR:** (125 MHz, D<sub>2</sub>O, 300 K):  $\delta$  = 174.06 (NHAc-C(O)), 171.64 (NH-C(O)-Man), 100.26 (C-1), 99.89 (C-1'), 99.86 (C-1<sub>Man</sub>), 79.18 (C-4), 76.04 (C-3), 73.22 (C-2'), 72.83 (C-3'), 72.67 (C-2), 72.42 (C-5), 71.57 (C-5'), 71.31 (C-5<sub>Man</sub>), 71.22 (C-4'), 70.35 (C-3<sub>Man</sub>), 69.68 (C-2<sub>Man</sub>), 66.52 (C-4<sub>Man</sub>), 65.63 (Man-OCH<sub>2</sub>), 60.80 (C-6<sub>Man</sub>), 56.44 (OCH<sub>2</sub>C≡CH), 40.52 (C-6), 39.72 (C-6'), 21.85 (NHAc) ppm;

**ESI-MS:** *m/z* = 641.2396 [M+H]<sup>+</sup> (calculated *m/z* = 641.2399 for [M+H]<sup>+</sup>).

**1,2,3-Tri-O-acetyl-6-azido-6-deoxy-4-O-(6'-azido-2',3',4'-tri-O-acetyl-6'-deoxy- $\alpha$ -D-glucopyranosyl)- $\beta$ -D-glucopyranose (39)<sup>[287]</sup>**



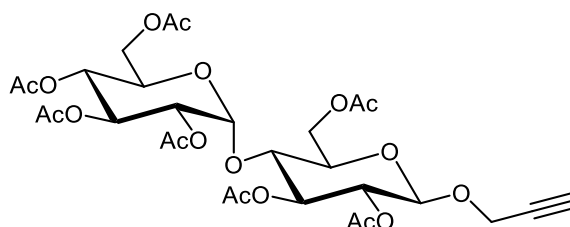
Maltose (**4**, 2.00 g, 5.55 mmol) and NaN<sub>3</sub> (3.61 g, 55.5 mmol) were dissolved in DMF (30.0 mL) and PPh<sub>3</sub> (2.91 g, 11.1 mmol) and CBr<sub>4</sub> (3.68 g, 11.1 mmol, dissolved in 8.00 mL DMF) were added. The mixture was stirred for 16 h before MeOH was added and the solution was filtered

and concentrated. To the residue H<sub>2</sub>O, toluene and ethyl acetate were added, it was extracted with H<sub>2</sub>O and the combined aqu. Layers were concentrated. The crude product was dissolved in pyridine (6.00 mL) and Ac<sub>2</sub>O (3.00 mL) and it was stirred for 16 h. Then the volatiles were removed and the residue was taken up in ethyl acetate and washed with 1N HCl, sodium bicarbonate, dried over MgSO<sub>4</sub>, filtered of and concentrated. Purification by column chromatography on silica gel (cyclohexane/ethyl acetate, 1:1) yielded **39** as a colorless solid.

**Yield:** 1.28 g (1.99 mmol, 36 %);

Analytical data corresponds to the literature.<sup>[287]</sup>

**(2-Propargyl) 2,3,6,2',3',4',6'-hept-O-acetyl-β-D-maltoside (42)**<sup>[142]</sup>



Maltose octaacetate **41** (25.0 g, 36.8 mmol) and propargyl alcohol (3.19 mL, 55.3 mmol) were dissolved in dry CH<sub>2</sub>Cl<sub>2</sub> (250 mL) and 3 Å molecular sieve was added. The mixture was stirred 15 min at room temperature and then cooled to 0 °C before BF<sub>3</sub>.Et<sub>2</sub>O (9.24 mL, 73.6 mmol) was added. The reaction was allowed to warm to room temperature while stirring for 16 h. The mixture was diluted with CH<sub>2</sub>Cl<sub>2</sub> and filtrated over celite. The org. layer was washed with sodium bicarbonate and brine. Then the combined org. layers were dried over MgSO<sub>4</sub>, filtered of, and concentrated. Purification by flash column chromatography on silica gel (cyclohexane/ethyl acetate, 3:2) gave **42** as a colorless solid.

**Yield:** 13.8 g (20.5 mmol, 56 %);

**R<sub>f</sub>:** (cyclohexane/ ethyl acetate, 1:1): R<sub>f</sub> = 0.60;

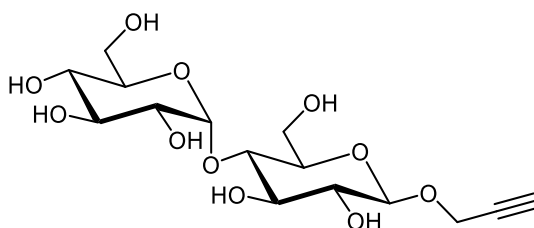
**IR (ATR):**  $\tilde{\nu}$  = 1741, 1367, 1216, 1029, 899 cm<sup>-1</sup>;

**<sup>1</sup>H NMR:** (500 MHz, CDCl<sub>3</sub>, 300 K):  $\delta$  = 5.42 (d, <sup>3</sup>J<sub>1,2</sub> = 4.0 Hz, 1H, H-1'), 5.36 (dd, <sup>3</sup>J<sub>2',3'</sub> = 10.2 Hz, <sup>3</sup>J<sub>3',4'</sub> = 9.9 Hz, 1H, H-3'), 5.29 (t, <sup>3</sup>J<sub>2,3</sub> = 9.0 Hz, <sup>3</sup>J<sub>3,4</sub> = 9.0 Hz, 1H, H-3), 5.06 (t, <sup>3</sup>J<sub>3',4'</sub> = 9.9 Hz, <sup>3</sup>J<sub>4',5'</sub> = 9.9 Hz, 1H, H-4'), 4.88-4.83 (m, 2H, H-2, H-2'), 4.80 (d, <sup>3</sup>J<sub>1,2</sub> = 7.9 Hz, 1H, H-1), 4.50 (dd, <sup>2</sup>J<sub>6a,6b</sub> = 12.2 Hz, <sup>3</sup>J<sub>5,6a</sub> = 2.7 Hz, 1H, H-6a), 4.35 (d, <sup>4</sup>J<sub>OCH,C≡CH</sub> = 2.4 Hz, 2H, OCH<sub>2</sub>), 4.29-4.21 (m, 2H, H-6a', H-6b), 4.08-4.00 (m, 2H, H-4, H-6b'), 3.95 (ddd, <sup>4',5'</sup> = 10.3 Hz, <sup>3</sup>J<sub>5',6a'</sub> = 3.6 Hz, <sup>3</sup>J<sub>5',6b'</sub> = 2.5 Hz, 1H, H-5'), 3.72 (ddd, <sup>4,5</sup> = 9.6 Hz, <sup>3</sup>J<sub>5,6a</sub> = 4.2 Hz, <sup>3</sup>J<sub>5,6b</sub> = 2.8 Hz, 1H, H-5), 2.47 (t, <sup>4</sup>J<sub>OCH',C≡CH</sub> = 2.4 Hz, <sup>4</sup>J<sub>OCH,C≡CH</sub> = 2.4 Hz, 1H, C≡CH), 2.15, 2.10, 2.05, 2.04, 2.03, 2.01, 2.00 (each s, 21H, 7 C(O)CH<sub>3</sub>) ppm;

**<sup>13</sup>C NMR:** (125 MHz, CDCl<sub>3</sub>, 300 K): δ = 170.69 (C=O), 170.67 (C=O), 170.59 (C=O), 170.35 (C=O), 170.08 (C=O), 169.87 (C=O), 169.56 (C=O), 97.75 (C-1), 95.66 (C-1'), 75.66 (OCH<sub>2</sub>≡CH), 75.47 (C-3), 72.70 (C-4), 72.39 (C-5), 71.91 (C-2), 70.14 (C-2'), 69.45 (C-3'), 68.64 (C-5'), 68.14 (C-4'), 62.76 (C-6), 61.62 (C-6'), 56.02 (OCH<sub>2</sub>≡CH), 21.04 (C(O)CH<sub>3</sub>), 20.97 (C(O)CH<sub>3</sub>), 20.82 (C(O)CH<sub>3</sub>), 20.82 (C(O)CH<sub>3</sub>), 20.74 (C(O)CH<sub>3</sub>), 20.72 (C(O)CH<sub>3</sub>), 20.71 (C(O)CH<sub>3</sub>) ppm;

**ESI-MS:** *m/z* = 697.1945 [M+H]<sup>+</sup> (calculated *m/z* = 697.1950 [M+H]<sup>+</sup>).

**(2-Propargyl) β-D-maltoside (43)**<sup>[142]</sup>



The maltoside **42** (13.7 g, 20.3 mmol) was dissolved in dry MeOH (50.0 mL) and sodium methoxide (5.4M, 2.00 mL) was added. The mixture was stirred at room temperature for 16 h. Then it was neutralized by adding Amberlite IR120. It was filtered and the solvent was removed under reduced pressure. It was coevaporated with toluene, which gave **43** as a colorless solid.

**Yield:** 9.51 g (quant.);

**R<sub>f</sub>:** (cyclohexane/ ethyl acetate, 3:1): R<sub>f</sub> = 0.01;

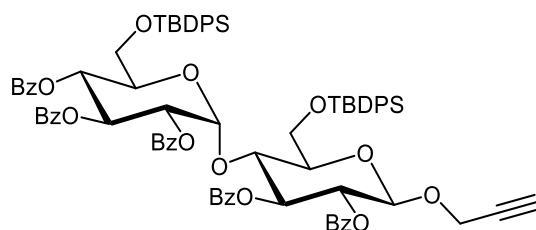
**IR (ATR):**  $\tilde{\nu}$  = 3281, 2925, 1637, 1359, 1069, 1017, 912 cm<sup>-1</sup>;

**<sup>1</sup>H NMR:** (600 MHz, MeOD, 300 K): δ = 5.18 (d, <sup>3</sup>J<sub>1,2'</sub> = 3.7 Hz, 1H, H-1'), 4.49 (d, <sup>3</sup>J<sub>1,2</sub> = 7.8 Hz, 1H, H-1), 4.42 (qd, <sup>2</sup>J<sub>OCH, OCH</sub> = 15.7 Hz, <sup>4</sup>J<sub>OCH, C≡CH</sub> = 2.3 Hz, 2H, OCH<sub>2</sub>), 3.90 (dd, <sup>2</sup>J<sub>6a,6b</sub> = 12.1 Hz, <sup>3</sup>J<sub>5,6b</sub> = 1.5 Hz, 1H, H-6b), 3.85-3.77 (m, 2H, H-6a, H-6b'), 3.73-3.58 (m, 4H, H-3, H-3', H-4', H-6a'), 3.55 (t, <sup>3</sup>J<sub>3,4</sub> = 9.3 Hz, <sup>3</sup>J<sub>4,5</sub> = 9.3 Hz, 1H, H-4), 3.46 (dd, <sup>3</sup>J<sub>2',3'</sub> = 9.7 Hz, <sup>3</sup>J<sub>1',2'</sub> = 3.7 Hz, 1H, H-2'), 3.40 (ddd, <sup>3</sup>J<sub>4,5</sub> = 9.5 Hz, <sup>3</sup>J<sub>5,6a</sub> = 4.5 Hz, <sup>3</sup>J<sub>5,6b</sub> = 1.6 Hz, 1H, H-5), 3.31-3.23 (m, 2H, H-5', H-2), 2.87 (t, <sup>4</sup>J<sub>OCH', C≡CH</sub> = 2.3 Hz, <sup>4</sup>J<sub>OCH, C≡CH</sub> = 2.3 Hz, 1H, C≡CH) ppm;

**<sup>13</sup>C NMR:** (125 MHz, CDCl<sub>3</sub>, 300 K): δ = 102.75 (C-1'), 102.00 (C-1), 80.98 (C-4), 79.94 (OCH<sub>2</sub>C≡CH), 77.70 (C-3), 76.63 (C-5), 76.39 (OCH<sub>2</sub>C≡CH), 74.98 (C-3'), 74.69 (C-4'), 74.39 (C-2), 74.04 (C-2'), 71.38 (C-5'), 62.63 (C-6'), 62.08 (C-6), 56.69 (OCH<sub>2</sub>C≡CH) ppm;

**ESI-MS:** *m/z* = 403.1210 [M+Na]<sup>+</sup> (calculated *m/z* = 403.1210 for [M+Na]<sup>+</sup>).

**(2-Propargyl) 2,3-di-O-benzoyl-6-*tert*-butyldimethylsilyl-4-O-(2',3',4'-tri-O-benzoyl-6'-*tert*-butyldimethylsilyl- $\alpha$ -D-glucopyranosyl)- $\beta$ -D-glucopyranoside (44)**



The maltoside **43** (282 mg, 741  $\mu$ mol) was dissolved in dry pyridine (5.00 mL) and the mixture was cooled to 0 °C before TBDPSCI (946  $\mu$ L, 3.71 mmol) was added. It was allowed to warm to room temperature and stirring was continued for 2 h. Then at 0 °C BzCl (689  $\mu$ L, 5.93 mmol) was added, it was allowed to warm to room temperature and stirring was continued for 6 h. Then MeOH was added, and it was stirred for further 15 min before the solvent was removed. The crude product was taken up in ethyl acetate and washed with 1N HCl, sodium bicarbonate and brine, dried over MgSO<sub>4</sub>, filtered of, and concentrated. Purification by flash column chromatography on silica gel (cyclohexane/ethyl acetate, 9:1) gave **44** as a colorless solid.

**Yield:** 758 mg (550  $\mu$ mol, 74 %);

**R<sub>f</sub>:** (cyclohexane/ ethyl acetate, 3:1): R<sub>f</sub> = 0.56;

**[ $\alpha$ ]<sub>D</sub><sup>23</sup>:** +31.0 (c = 0.02, CH<sub>2</sub>Cl<sub>2</sub>);

**IR (ATR):**  $\tilde{\nu}$  = 2937, 1726, 1351, 1249, 1082, 1028, 836 cm<sup>-1</sup>;

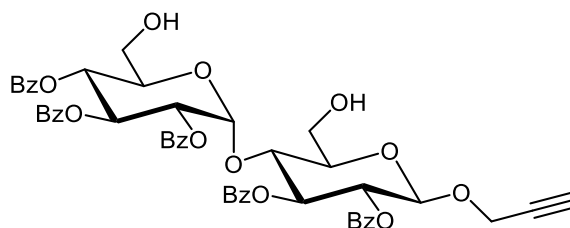
**<sup>1</sup>H NMR:** (500 MHz, CDCl<sub>3</sub>, 300 K):  $\delta$  = 7.88-7.81 (m, 4H, Bz<sub>ortho</sub>), 7.80-7.74 (m, 2H, Bz<sub>ortho</sub>), 7.72-7.68 (m, 4H, Bz<sub>ortho</sub>), 7.67-7.27 (m, 21H, Bz<sub>meta</sub>, Bz<sub>para</sub>, Si-Ph), 7.25-7.10 (m, 14H, Bz<sub>meta</sub>, Si-Ph), 5.96 (dd, <sup>3</sup>J<sub>2',3'</sub> = 10.1 Hz, <sup>3</sup>J<sub>3',4'</sub> = 9.81 Hz, 1H, H-3'), 5.75-5.69 (m, 2H, H-3, H-4'), 5.68 (d, <sup>3</sup>J<sub>1',2'</sub> = 3.9 Hz, 1H, H-1'), 5.29 (dd, <sup>3</sup>J<sub>2,3</sub> = 9.7 Hz, <sup>3</sup>J<sub>1,2</sub> = 7.8 Hz, 1H, H-2), 5.19 (dd, <sup>3</sup>J<sub>2',3'</sub> = 10.4 Hz, <sup>3</sup>J<sub>1',2'</sub> = 3.9 Hz, 1H, H-2'), 4.97 (d, <sup>3</sup>J<sub>1,2</sub> = 7.8 Hz, 1H, H-1), 4.33-4.28 (m, 2H, OCH<sub>2</sub>), 4.26 (t, <sup>3</sup>J<sub>3,4</sub> = 9.2 Hz, <sup>3</sup>J<sub>4,5</sub> = 9.2 Hz, H-4), 4.14-4.02 (m, 3H, H-5', H-6b, H-6a), 3.74 (ddd, <sup>4</sup>J<sub>4,5</sub> = 9.4 Hz, <sup>3</sup>J<sub>5,6a</sub> = 4.8 Hz, <sup>3</sup>J<sub>5,6b</sub> = 2.5 Hz, 1H, H-5), 3.54 (dd, <sup>2</sup>J<sub>6a',6b'</sub> = 11.9 Hz, <sup>3</sup>J<sub>5',6b'</sub> = 1.5 Hz, 1H, H-6b'), 3.40 (dd, <sup>2</sup>J<sub>6a',6b'</sub> = 11.7 Hz, <sup>3</sup>J<sub>5',6a'</sub> = 3.2 Hz, 1H, H-6a'), 2.37 (t, <sup>4</sup>J<sub>OCH<sub>2</sub>,C $\equiv$ CH</sub> = 2.4 Hz, <sup>4</sup>J<sub>OCH<sub>2</sub>,C $\equiv$ CH</sub> = 2.4 Hz, 1H, C $\equiv$ CH), 1.02, 0.99 (each s, 18H, 2 Si-*t*-Bu), ppm;

**<sup>13</sup>C NMR:** (125 MHz, CDCl<sub>3</sub>, 300 K):  $\delta$  = 165.72, 165.48, 165.42, 165.27, 164.80 (5C, C(O)Ph), 135.75, 135.66, 135.56, 135.34 (8C, Si-Ph) 133.37, 133.10, 133.01, 133.01, 132.89 (5C, Bz-CH<sub>para</sub>), 129.90, 129.82, 129.82, 129.79, 129.74 (10C, Bz-CH<sub>ortho(a,b)</sub>), 129.65, 129.61, 129.61, 129.51 (4C, Si-Ph), 129.40, 129.36, 129.27, 129.10, 128.75 (5C, Bz-C<sub>quat</sub>), 128.29, 128.14, 128.13, 128.13, 128.02 (10C, Bz-CH<sub>ortho(a,b)</sub>), 127.65, 127.65, 127.62, 127.51 (8C, Si-Ph), 97.70 (C-1), 96.20 (C-1'), 78.27 (OCH<sub>2</sub>C $\equiv$ CH), 75.77 (C-5), 75.35 (OCH<sub>2</sub>C $\equiv$ CH), 75.19 (C-3),

73.05 (C-4), 72.03 (C-2), 71.34 (C-5'), 71.31 (C-2'), 70.56 (C-3'), 68.43 (C-4'), 63.34 (C-6), 61.60 (C-6'), 55.46 (OCH<sub>2</sub>C≡CH) ppm;

**ESI-MS:**  $m/z = 1399.4842$  [M+Na]<sup>+</sup> (calculated  $m/z = 1399.4883$  for [M+Na]<sup>+</sup>).

**(2-Propargyl) 2,3-di-O-benzoyl-4-O-(2',3',4'-tri-O-benzoyl- $\alpha$ -D-glucopyranosyl)- $\beta$ -D-glucopyranoside (45)**



The maltoside **44** (700 mg, 508  $\mu$ mol) was dissolved in dry THF (7.00 mL) and the mixture was cooled to 0 °C before AcOH (349  $\mu$ L, 6.10 mmol) and TBAF (1M in THF, 797  $\mu$ L, 3.05 mmol) were added. It was allowed to warm to room temperature and stirring was continued for 16 h. It was diluted with ethyl acetate and washed with H<sub>2</sub>O, sodium bicarbonate and brine, dried over MgSO<sub>4</sub>, filtered of, and concentrated. Purification by flash column chromatography on silica gel (cyclohexane/ethyl acetate, 2:3) gave **45** as a colorless solid.

**Yield:** 399 mg (443  $\mu$ mol, 87 %);

**R<sub>f</sub>:** (cyclohexane/ ethyl acetate, 3:1): R<sub>f</sub> = 0.10;

**IR (ATR):**  $\tilde{\nu} = 3483, 1723, 1694, 1602, 1451, 1262, 1067, 1026, 845$  cm<sup>-1</sup>;

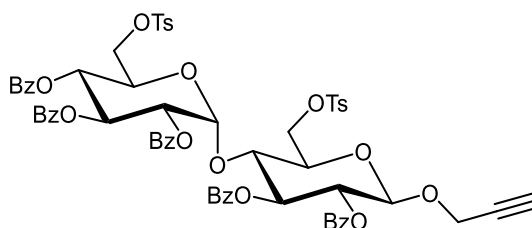
**<sup>1</sup>H NMR:** (500 MHz, CDCl<sub>3</sub>, 300 K):  $\delta = 7.98$ -7.92 (m, 2H, Bz<sub>ortho</sub>), 7.88-7.81 (m, 2H, Bz<sub>ortho</sub>), 7.78-7.71 (m, 4H, Bz<sub>ortho</sub>), 7.65-7.60 (m, 2H, Bz<sub>ortho</sub>), 7.58-7.18 (m, 15H, Bz<sub>meta</sub>, Bz<sub>para</sub>), 6.05 (t, <sup>3</sup>J<sub>2',3'</sub> = 9.9 Hz, <sup>3</sup>J<sub>3',4'</sub> = 9.9 Hz, 1H, H-3'), 5.78-5.72 (m, 2H, H-1', H-3), 5.37 (t, <sup>3</sup>J<sub>3',4'</sub> = 9.9 Hz, <sup>3</sup>J<sub>4',5'</sub> = 9.9 Hz, 1H, H-4'), 5.29 (dd, <sup>3</sup>J<sub>2,3</sub> = 9.7 Hz, <sup>3</sup>J<sub>1,2</sub> = 7.8 Hz, 1H, H-2), 5.23 (dd, <sup>3</sup>J<sub>2',3'</sub> = 10.4 Hz, <sup>3</sup>J<sub>1',2'</sub> = 4.1 Hz, 1H, H-2'), 5.05 (d, <sup>3</sup>J<sub>1,2</sub> = 7.8 Hz, 1H, H-1), 4.55 (t, <sup>3</sup>J<sub>3,4</sub> = 9.4 Hz, <sup>3</sup>J<sub>4,5</sub> = 9.4 Hz, H-4), 4.42 (dd, <sup>2</sup>J<sub>OCH<sub>2</sub>OCH</sub> = 16.0 Hz, <sup>4</sup>J<sub>OCH<sub>2</sub>C≡CH</sub> = 2.4 Hz, 1H, OCH<sub>2</sub>), 4.34 (dd, <sup>2</sup>J<sub>OCH<sub>2</sub>OCH</sub> = 16.0 Hz, <sup>4</sup>J<sub>OCH<sub>2</sub>C≡CH</sub> = 2.4 Hz, 1H, OCH<sub>2</sub>), 4.14 (ddd, <sup>3</sup>J<sub>4',5'</sub> = 10.0 Hz, <sup>3</sup>J<sub>5',6a'</sub> = 5.2 Hz, <sup>3</sup>J<sub>5',6b'</sub> = 1.7 Hz, 1H, H-5'), 4.10 (m, 2H, H-6b, H-6a), 3.86 (ddd, <sup>2</sup>J<sub>6a',6b'</sub> = 12.4 Hz, <sup>3</sup>J<sub>OH',6b'</sub> = 6.6 Hz, <sup>3</sup>J<sub>5',6b'</sub> = 1.8 Hz, 1H, H-6b'), 3.80 (dt, <sup>3</sup>J<sub>4,5</sub> = 9.4 Hz, <sup>3</sup>J<sub>5,6a</sub> = 2.3 Hz, <sup>3</sup>J<sub>5,6b</sub> = 2.4 Hz, 1H, H-5), 3.74 (dt, <sup>2</sup>J<sub>6a',6b'</sub> = 12.5 Hz, <sup>3</sup>J<sub>OH',6a'</sub> = 6.6 Hz, <sup>3</sup>J<sub>5',6a'</sub> = 5.6 Hz, 1H, H-6a'), 2.96 (t, <sup>3</sup>J<sub>OH',6a'</sub> = 6.6 Hz, <sup>3</sup>J<sub>OH',6b'</sub> = 6.6 Hz, 1H, OH'), 2.47 (t, <sup>3</sup>J<sub>OH,6a</sub> = 7.0 Hz, <sup>3</sup>J<sub>OH,6b</sub> = 7.0 Hz, 1H, OH), 2.39 (t, <sup>4</sup>J<sub>OCH',C≡CH</sub> = 2.4 Hz, <sup>4</sup>J<sub>OCH<sub>2</sub>C≡CH</sub> = 2.4 Hz, 1H, C≡CH) ppm;

**<sup>13</sup>C NMR:** (125 MHz, CDCl<sub>3</sub>, 300 K):  $\delta = 166.25, 165.91, 165.39, 165.31, 165.19$  (5C, C(O)Ph), 133.86, 133.37, 133.37, 133.29, 133.16 (5C, Bz-C<sub>para</sub>), 130.12, 130.10, 129.96, 129.83,

129.70 (10C, Bz-CH<sub>ortho(a,b)</sub>), 129.34, 129.18, 129.04, 128.87, 128.73 (5C, Bz-C<sub>qart</sub>), 128.65, 128.36, 128.35, 128.30, 128.21 (10C, Bz-CH<sub>ortho(a,b)</sub>), 98.60 (C-1), 96.50 (C-1'), 78.42 (OCH<sub>2</sub>C≡CH), 75.68 (OCH<sub>2</sub>C≡CH), 75.24 (C-3), 75.04 (C-5), 72.11 (C-2), 71.69 (C-5'), 71.00 (C-4), 70.74 (C-2'), 70.04 (C-3'), 69.73 (C-4'), 61.59 (C-6'), 61.20 (C-6), 56.33 (OCH<sub>2</sub>C≡CH) ppm;

**ESI-MS:**  $m/z = 923.2514$  [M+Na]<sup>+</sup> (calculated  $m/z = 923.2521$  for [M+Na]<sup>+</sup>).

**(2-Propargyl) 2,3-di-O-benzoyl-6-tosylate-4-O-(2',3',4'-tri-O-benzoyl-6'-tosylate- $\alpha$ -D-glucopyranosyl)- $\beta$ -D-glucopyranoside (47)**



The maltoside **43** (9.20 g, 25.0 mmol) was dissolved in dry pyridine (80.0 mL), and was cooled to 0 °C. Then TsCl (15.2 g, 79.9 mmol) was added portion wise. It was stirred for 2 h. Then at 0 °C BzCl (23.2 mL, 200 mmol) was added dropwise. It was allowed to warm to room temperature and stirring was continued for 16 h. MeOH was added to the reaction mixture, and it was stirred for 15 min before the solvent was removed. The crude product was taken up in ethyl acetate and it was washed with 1N HCl, sodium bicarbonate and brine. The org. layer was dried over MgSO<sub>4</sub>, filtered of, and concentrated. Purification by flash column chromatography on silica (cyclohexane/ ethyl acetate, 3:1) led to a colorless solid.

**Yield:** 19.1 g (16.6 mmol, 67 %);

**R<sub>f</sub>:** (cyclohexane/ ethyl acetate, 3:2): R<sub>f</sub> = 0.30;

**[ $\alpha$ ]<sub>D</sub><sup>23</sup>:** +6.67 (c = 0.01, CH<sub>2</sub>Cl<sub>2</sub>);

**IR (ATR):**  $\tilde{\nu} = 2925, 1731, 1600, 1451, 1362, 1265, 1176, 1091, 1068, 1026, 995, 514$  cm<sup>-1</sup>;

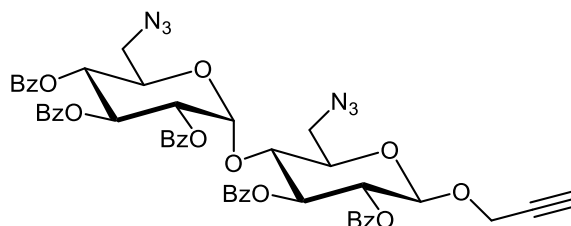
**<sup>1</sup>H NMR:** (500 MHz, CDCl<sub>3</sub>, 300 K):  $\delta = 7.92$ -7.65 (m, 14H, Ts<sub>ortho</sub>, Bz<sub>ortho</sub>), 7.55-7.17 (19H, Ts<sub>meta</sub>, Bz<sub>meta</sub>, Bz<sub>para</sub>), 5.93 (dd, <sup>3</sup>J<sub>2',3'</sub> = 10.3 Hz, <sup>3</sup>J<sub>3',4'</sub> = 9.7 Hz, 1H, H-3'), 5.62-5.57 (m, 2H, H-1', H-3), 5.47 (t, <sup>3</sup>J<sub>3',4'</sub> = 9.9 Hz, <sup>3</sup>J<sub>4',5'</sub> = 9.9 Hz, 1H, H-4'), 5.13 (dd, <sup>3</sup>J<sub>2,3</sub> = 9.3 Hz, <sup>3</sup>J<sub>1,2</sub> = 7.5 Hz, 1H, H-2), 5.05 (dd, <sup>3</sup>J<sub>2',3'</sub> = 10.4 Hz, <sup>3</sup>J<sub>1',2'</sub> = 3.9 Hz, 1H, H-2'), 4.90 (d, <sup>3</sup>J<sub>1,2</sub> = 7.5 Hz, 1H, H-1), 4.53 (dd, <sup>2</sup>J<sub>6a,6b</sub> = 11.3 Hz, <sup>3</sup>J<sub>5,6b</sub> = 3.9 Hz, 1H, H-6b), 4.49 (dd, <sup>2</sup>J<sub>6a,6b</sub> = 11.4 Hz, <sup>3</sup>J<sub>5,6a</sub> = 2.4 Hz, 1H, H-6a), 4.43 (ddd, <sup>2</sup>J<sub>6a',6b'</sub> = 11.4 Hz, <sup>3</sup>J<sub>5',6b'</sub> = 1.9 Hz, 1H, H-6b'), 4.36 (ddd, <sup>3</sup>J<sub>4',5'</sub> = 10.0 Hz, <sup>3</sup>J<sub>5',6a'</sub> = 3.7 Hz, <sup>3</sup>J<sub>5',6b'</sub> = 1.7 Hz, 1H, H-5'), 4.26-4.13 (m, 4H, OCH<sub>2</sub>, H-4, H-6a'), 3.860 (dd, <sup>3</sup>J<sub>4,5</sub>

= 9.6 Hz,  $^3J_{5,6a} = 3.7$  Hz,  $^3J_{5,6b} = 2.4$  Hz, 1H, H-5), 2.45 (s, 1H, Ts-CH<sub>3</sub>), 2.38 (t,  $^4J_{\text{OCH},\text{C}\equiv\text{CH}} = 2.4$  Hz,  $^4J_{\text{OCH},\text{C}\equiv\text{CH}} = 2.4$  Hz, 1H, C≡CH), 2.30 (s, 1H, Ts-CH<sub>3</sub>), ppm;

**<sup>13</sup>C NMR:** (125 MHz, CDCl<sub>3</sub>, 300 K): δ = 165.59, 165.19, 165.08, 164.99, 164.74 (5C, C(O)Ph), 145.33, 144.87 (2 Ts), 133.40, 133.30, 133.19, 133.11, 133.07 (5C, Bz-CH<sub>para</sub>), 132.54, 132.36 (2 Ts), 129.98, 129.87, 129.78, 129.75, 129.73 (10C, Bz-CH<sub>ortho(a,b)</sub>), 129.61, 129.58 (4C, Ts), 129.08, 128.89, 128.69, 128.66, 128.49 (5C, Bz-C<sub>quat</sub>), 128.38, 128.27, 128.23, 128.21, 128.17, 128.13, 128.07 (14C, Ts, Bz-CH<sub>ortho(a,b)</sub>), 97.60 (C-1), 96.02 (C-1'), 77.99 (OCH<sub>2</sub>C≡CH), 75.61 (OCH<sub>2</sub>C≡CH), 74.64 (C-3), 72.48 (C-5), 71.81 (C-4), 71.51 (C-2), 70.64 (C-2'), 69.84 (C-3'), 68.73 (C-5'), 68.14 (C-4'), 68.13 (C-6'), 67.43 (C-6), 55.57 (OCH<sub>2</sub>C≡CH), 21.70, 21.59 (2 Ts-CH<sub>3</sub>) ppm;

**ESI-MS:** *m/z* = 1231.2668.1 [M+Na]<sup>+</sup> (calculated *m/z* = 1231.2698 for [M+Na]<sup>+</sup>).

**(2-Propargyl) 6-azido-2,3-di-O-benzoyl-6-deoxy-4-O-(6'-azido-2',3',4'-tri-O-benzoyl-6'-deoxy-α-D-glucopyranosyl)-β-D-glucopyranose (46)**



The maltoside **47** (19.0 g, 16.6 mmol) was dissolved in DMF (500 mL), and NaN<sub>3</sub> (25.8 g, 397 mmol) was added. The mixture was heated to 80 °C for 16 h. After cooling down to room temperature the solvent was removed, and the crude product was diluted with CH<sub>2</sub>Cl<sub>2</sub> and washed with brine. The org. layer was dried over MgSO<sub>4</sub>, filtered of, and concentrated. Purification by flash column chromatography on silica (cyclohexane/ ethyl acetate, 4:1 → 3:1) led to **46** as a colorless solid.

**Yield:** 13.3 g (13.9 mmol, 84 %);

**R<sub>f</sub>:** (cyclohexane/ ethyl acetate, 3:1): R<sub>f</sub> = 0.44;

**[α]<sub>D</sub><sup>23</sup>:** +35.4 (c = 0.01, CH<sub>2</sub>Cl<sub>2</sub>);

**IR (ATR):**  $\tilde{\nu}$  = 2102, 1725, 1601, 1492, 1451, 1263, 1178, 1090, 1067, 1025, 849, 705, 685 cm<sup>-1</sup>;

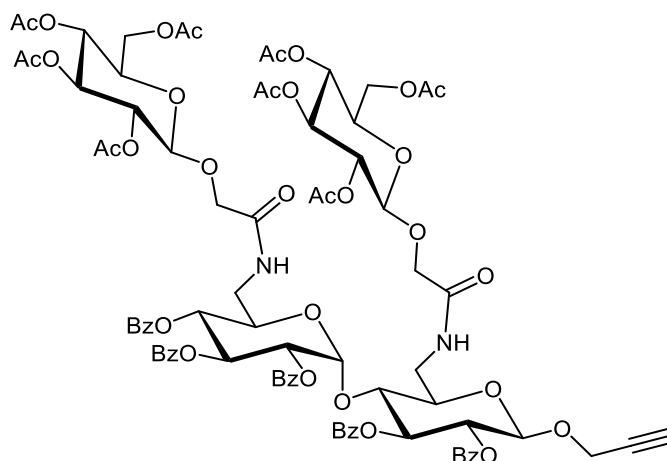
**<sup>1</sup>H NMR:** (600 MHz, CDCl<sub>3</sub>, 300 K): δ = 7.96-7.89 (m, 2H, Bz<sub>ortho</sub>), 7.86-7.80 (m, 2H, Bz<sub>ortho</sub>), 7.76-7.70 (m, 4H, Bz<sub>ortho</sub>), 7.69-7.63 (m, 2H, Bz<sub>ortho</sub>), 7.57-7.23 (m, 15H, Bz<sub>meta</sub>, Bz<sub>para</sub>), 5.97 (dd,  $^3J_{2,3'} = 10.0$  Hz,  $^3J_{3',4'} = 10.0$  Hz, 1H, H-3'), 5.76-5.69 (m, 2H, H-1', H-3), 5.46 (t,  $^3J_{3',4'} =$

9.8 Hz,  ${}^3J_{4',5'} = 9.8$  Hz, 1H, H-4'), 5.35 (dd,  ${}^3J_{2,3} = 9.5$  Hz,  ${}^3J_{1,2} = 7.8$  Hz, 1H, H-2), 5.19 (dd,  ${}^3J_{2',3'} = 10.5$  Hz,  ${}^3J_{1',2'} = 4.0$  Hz, 1H, H-2'), 5.09 (d,  ${}^3J_{1,2} = 7.7$  Hz, 1H, H-1), 4.18 (ddd,  ${}^4J_{5',6a'} = 8.8$  Hz,  ${}^3J_{5',6a'} = 5.5$  Hz,  ${}^3J_{5',6b'} = 2.6$  Hz, 1H, H-5'), 3.98 (ddd,  ${}^4J_{4,5} = 9.2$  Hz,  ${}^3J_{5,6a} = 5.2$  Hz,  ${}^3J_{5,6b} = 2.4$  Hz, 1H, H-5), 4.49-4.34 (m, 3H,  $\text{OCH}_2$ , H-4), 3.81 (dd,  ${}^2J_{6a,6b} = 13.2$  Hz,  ${}^3J_{5,6b} = 2.3$  Hz, 1H, H-6b), 3.72 (dd,  ${}^2J_{6a,6b} = 13.2$  Hz,  ${}^3J_{5,6a} = 5.3$  Hz, 1H, H-6a), 3.56 (dd,  ${}^2J_{6a',6b'} = 13.4$  Hz,  ${}^3J_{5',6b'} = 2.6$  Hz, 1H, H-6b'), 3.48 (dd,  ${}^2J_{6a',6b'} = 13.4$  Hz,  ${}^3J_{5',6a'} = 5.6$  Hz, 1H, H-6a'), 2.42 (t,  ${}^4J_{\text{OCH}',\text{C}\equiv\text{CH}} = 2.3$  Hz,  ${}^4J_{\text{OCH},\text{C}\equiv\text{CH}} = 2.3$  Hz, 1H,  $\text{C}\equiv\text{CH}$ ) ppm;

${}^{13}\text{C}$  NMR: (125 MHz,  $\text{CDCl}_3$ , 300 K):  $\delta = 165.80, 165.43, 165.37, 165.34, 165.19$  (5C,  $\text{C}(\text{O})\text{Ph}$ ), 133.80, 133.43, 133.43, 133.33, 133.20 (5C,  $\text{Bz-CH}_{\text{para}}$ ), 130.07, 130.05, 129.97, 129.87, 129.71 (10C,  $\text{Bz-CH}_{\text{ortho}(a,b)}$ ), 129.28, 128.93, 128.82, 128.69, 128.59 (5C,  $\text{Bz-C}_{\text{qart}}$ ), 128.65, 128.41, 128.37, 128.31, 128.25 (10C,  $\text{Bz-CH}_{\text{ortho}(a,b)}$ ), 97.96 (C-1), 96.18 (C-1'), 78.17 ( $\text{OCH}_2\text{C}\equiv\text{CH}$ ), 75.83 ( $\text{OCH}_2\text{C}\equiv\text{CH}$ ), 74.93 (C-3), 74.60 (C-5), 73.10 (C-4), 71.97 (C-2), 70.82 (C-2'), 70.44 (C-5'), 69.90 (C-4'), 69.71 (C-3'), 55.91 ( $\text{OCH}_2\text{C}\equiv\text{CH}$ ), 51.58 (C-6), 51.34 (C-6') ppm;

ESI-MS:  $m/z = 951.2830$   $[\text{M}+\text{H}]^+$  (calculated  $m/z = 951.2831$  for  $[\text{M}+\text{H}]^+$ ).

**(2-Propargyl) 2,3-di-O-benzoyl-6-deoxy-6-[[[(2,3,4,6-tetra-O-acetyl- $\beta$ -D-glucopyranosyl)oxy]acetyl]amino]-4-O-(2',3',4'-tri-O-benzoyl-6'-deoxy-6'-[[[(2,3,4,6-tetra-O-acetyl- $\beta$ -D-glucopyranosyl)oxy]acetyl]amino]- $\alpha$ -D-glucopyranosyl)- $\beta$ -D-glucopyranoside (49)**



The carboxylic acid **28** (214 mg, 526  $\mu\text{mol}$ ) was dissolved in dry THF (10 mL) and NHS (72.6 mg, 631  $\mu\text{mol}$ ) and EDC·HCl (121 mg, 631  $\mu\text{mol}$ ) were added. It was stirred for 2 h at room temperature. Then maltoside **46** (200 mg, 210  $\mu\text{mol}$ ) was added and the reaction mixture was cooled to 0 °C before  $\text{PMe}_3$  (1M in THF, 1.68 mL) was added dropwise. It was allowed to warm to room temperature and stirring was continued for 16 h. Then  $\text{H}_2\text{O}$  was added and the aqu. layer was extracted with ethyl acetate. The combined org. layers were dried over  $\text{MgSO}_4$ ,

filtered of, and concentrated to dryness. Purification by column chromatography on silica gel (cyclohexane/ethyl acetate, 1:4) gave **49** as a colorless solid.

**Yield:** 229 mg (137  $\mu$ mol, 65 %);

**R<sub>f</sub>** (cyclohexane/ ethyl acetate, 1:4): R<sub>f</sub> = 0.18;

**[ $\alpha$ ]<sub>D</sub><sup>23</sup>:** +38.6 (c = 0.01, CH<sub>2</sub>Cl<sub>2</sub>);

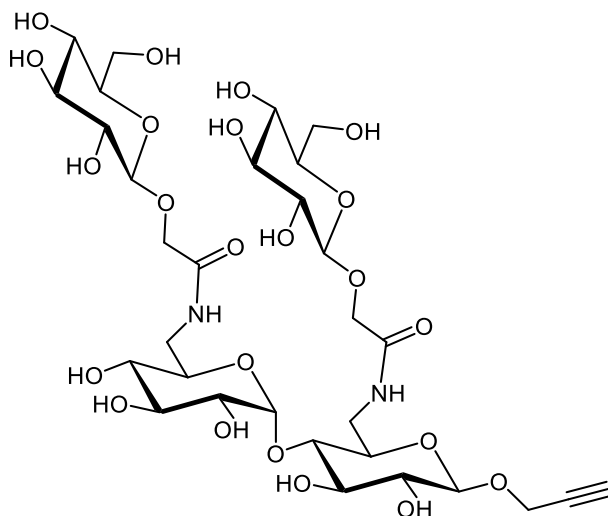
**IR (ATR):**  $\tilde{\nu}$  = 2864, 1756, 1611, 1542, 1421, 1377, 1217, 1151, 1100, 1032, 806, 710 cm<sup>-1</sup>;

**<sup>1</sup>H NMR:** (500 MHz, CDCl<sub>3</sub>, 300 K):  $\delta$  = 7.97-7.91 (m, 2H, Bz<sub>ortho</sub>), 7.86-7.81 (m, 2H, Bz<sub>ortho</sub>), 7.71-7.66 (m, 2H, Bz<sub>ortho</sub>), 7.65-7.62 (m, 2H, Bz<sub>ortho</sub>), 7.56-7.52 (m, 2H, Bz<sub>ortho</sub>), 7.50-7.28 (m, 9H, Bz<sub>meta</sub>, Bz<sub>para</sub>), 7.24-7.14 (m, 6H, Bz<sub>meta</sub>), 7.08-7.02 (m, 1H, NH), 6.97 (t, <sup>3</sup>J<sub>NH,6a</sub> = 5.5 Hz, <sup>3</sup>J<sub>NH,6b</sub> = 5.5 Hz, 1H, NH), 6.01 (t, <sup>3</sup>J<sub>2',3'</sub> = 10.1 Hz, <sup>3</sup>J<sub>3',4'</sub> = 10.1 Hz, 1H, H-3'), 5.72 (t, <sup>3</sup>J<sub>2,3</sub> = 9.2 Hz, <sup>3</sup>J<sub>3,4</sub> = 9.2 Hz, 1H, H-3), 5.67 (d, <sup>3</sup>J<sub>1,2'</sub> = 4.0 Hz, 1H, H-1'), 5.43-5.35 (m, 3H, H-2, H-2', H-4'), 5.30-5.25 (m, 2H, H-3<sub>Glc</sub>, H-3<sub>Glc'</sub>), 5.14-5.07 (m, 4H, H-2<sub>Glc'</sub>, H-2<sub>Glc</sub>, H-4<sub>Glc</sub>, H-4<sub>Glc'</sub>), 5.05 (d, <sup>3</sup>J<sub>1,2</sub> = 7.8 Hz, 1H, H-1), 4.63 (d, <sup>3</sup>J<sub>1,2</sub> = 7.9 Hz, 1H, H-1<sub>Glc'</sub>), 4.61 (d, <sup>3</sup>J<sub>1,2</sub> = 8.0 Hz, 1H, H-1<sub>Glc</sub>), 4.50 (dd, <sup>2</sup>J<sub>OCH',OCH</sub> = 16.1 Hz, <sup>4</sup>J<sub>OCH,C $\equiv$ CH</sub> = 2.4 Hz, 1H, OCH<sub>2</sub>), 4.46-4.28 (m, 6H, H-5', OCH<sub>2</sub>, H-6a<sub>Glc</sub>, H-6a<sub>Glc'</sub>, Glc-OCH<sub>2</sub>, Glc'-OCH<sub>2</sub>), 4.23 (t, <sup>3</sup>J<sub>3,4</sub> = 9.2 Hz, <sup>3</sup>J<sub>4,5</sub> = 9.3 Hz, 1H, H-4), 4.19-4.05 (m, 5H, H-6a, H-6b<sub>Glc'</sub>, H-6b<sub>Glc</sub>, Glc-OCH<sub>2</sub>, Glc'-OCH<sub>2</sub>), 3.93-3.90 (m, 1H, H-5), 3.81-3.75 (m, 2H, H-5<sub>Glc'</sub>, H-5<sub>Glc</sub>), 3.69-3.62 (m, 1H, H-6a'), 3.61-3.53 (m, 2H, H-6b', H-6b), 2.51 (t, <sup>4</sup>J<sub>OCH',C $\equiv$ CH</sub> = 2.4 Hz, <sup>4</sup>J<sub>OCH,C $\equiv$ CH</sub> = 2.4 Hz, 1H, C $\equiv$ CH), 2.16, 2.12, 2.10, 2.08, 2.04, 2.03, 2.03 (each s, 24H, 8 OAc) ppm;

**<sup>13</sup>C NMR:** (125 MHz, CDCl<sub>3</sub>, 300 K):  $\delta$  = 170.78, 170.75, 170.30, 170.28, 169.93, 169.82, 169.58, 169.58 (8C, C(O)-Ac), 168.70, 168.55 (2 NH-C(O)), 165.79, 165.71, 165.64, 165.43, 165.08 (5C, C(O)Ph), 133.51, 133.25, 133.14, 133.14, 133.07 (5C, Bz-CH<sub>para</sub>), 130.14, 130.08, 129.96, 129.78, 129.61 (10C, Bz-CH<sub>ortho(a,b)</sub>), 129.40, 129.20, 129.00, 128.97, 128.59 (5C, Bz-C<sub>quat</sub>), 128.54, 128.30, 128.23, 128.23, 128.11 (10C, Bz-CH<sub>ortho(a,b)</sub>), 100.66 (C-1<sub>Glc</sub>), 100.33 (C-1<sub>Glc'</sub>), 98.34 (C-1), 97.58 (C-1'), 78.66 (OCH<sub>2</sub>C $\equiv$ CH), 75.94 (OCH<sub>2</sub>C $\equiv$ CH), 75.42 (C-4), 75.28 (C-3), 73.41 (C-5), 72.41 (C-3<sub>Glc</sub>), 72.39 (C-3<sub>Glc'</sub>), 72.36 (C5<sub>Glc</sub>), 72.29 (C-5<sub>Glc'</sub>), 72.02 (C-2'), 71.36 (C-2<sub>Glc</sub>), 71.35 (C-2<sub>Glc'</sub>), 70.96 (C-2), 70.27 (C-3'), 69.46 (C-5'), 69.12 (C-4'), 68.66 (C-6<sub>Glc'</sub>), 68.55 (C-4<sub>Glc</sub>), 68.40 (C-4<sub>Glc'</sub>), 68.26 (C-6<sub>Glc</sub>), 62.01 (Glc-OCH<sub>2</sub>), 61.84 (Glc'-OCH<sub>2</sub>), 56.35 (OCH<sub>2</sub>C $\equiv$ CH), 40.50 (C-6), 38.49 (C-6'), 20.95, 20.92, 20.89, 20.87, 20.78, 20.77, 20.75, 20.73 (8C, OAc) ppm;

**ESI-MS:** *m/z* = 1675.5018 [M+Na]<sup>+</sup> (calculated *m/z* = 1675.5033 for [M+H]<sup>+</sup>).

**(2-Propargyl) 6-deoxy-6-[[[ $\beta$ -D-glucopyranosyloxy)acetyl]amino]-4-O-(6'-deoxy-6'-[[[ $\beta$ -D-glucopyranosyloxy)acetyl]amino]- $\alpha$ -D-glucopyranosyl)- $\beta$ -D-glucopyranoside (**50**)**



The maltoside **49** (60.0 mg, 35.8  $\mu$ mol) was dissolved in dry MeOH and a catalytical amount of a sodium methoxide solution (5.4M) was added. It was stirred at room temperature for 16 h and then neutralized with Amberlite IR120. The reaction mixture was filtered, and the solvent was removed under reduced pressure. The crude product was taken up in H<sub>2</sub>O and washed with Et<sub>2</sub>O. The aqu. layer was concentrated to dryness. Purification by size exclusion chromatography on Sephadex GP10 (H<sub>2</sub>O) gave the product **50** as a colorless solid.

**Yield:** 24.0 mg (29.3  $\mu$ mol, 79 %);

**R<sub>f</sub>:** (CH<sub>2</sub>Cl<sub>2</sub>/MeOH, 9:1): R<sub>f</sub> = 0.05;

**[ $\alpha$ ]<sub>D</sub><sup>23</sup>:** -19.3 (c = 0.01, H<sub>2</sub>O);

**IR (ATR):**  $\tilde{\nu}$  = 3293, 2931, 1655, 1552, 1436, 1042, 1018, 975, 815 cm<sup>-1</sup>;

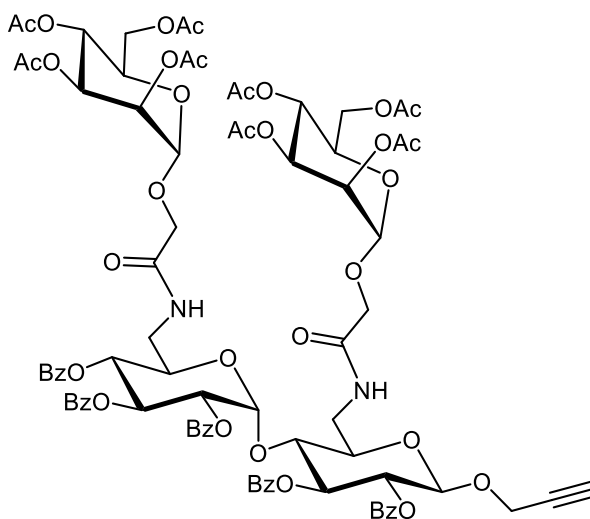
**<sup>1</sup>H NMR:** (600 MHz, D<sub>2</sub>O, 300 K):  $\delta$  = 5.37 (d, <sup>3</sup>J<sub>1,2'</sub> = 3.9 Hz, 1H, H-1'), 4.61 (d, <sup>3</sup>J<sub>1,2</sub> = 8.0 Hz, 1H, H-1), 4.49 (d, <sup>3</sup>J<sub>1,2</sub> = 8.0 Hz, 1H, H-1<sub>Glc</sub>), 4.48 (d, <sup>3</sup>J<sub>1,2</sub> = 8.0 Hz, 1H, H-1<sub>Glc'</sub>), 4.47-4.39 (m, 3H, OCH<sub>2</sub>, OCH<sub>2</sub>, Glc'-OCH<sub>2</sub>), 4.35 (d, <sup>2</sup>J<sub>OCH, OCH</sub> = 15.9 Hz, 1H, Glc-OCH<sub>2</sub>), 4.31-4.22 (m, 2H, Glc-OCH<sub>2</sub>, Glc'-OCH<sub>2</sub>), 3.94-3.88 (m, 2H, H-6a<sub>Glc</sub>, H-6a<sub>Glc'</sub>), 3.85-3.59 (m, 9H, H-2', H-6b<sub>Glc</sub>, H-6b<sub>Glc'</sub>, H-6b, H-6b', H-5', H-5, H-3', H-3), 3.54-3.28 (m, 13H, H-2, H-4, H-2<sub>Glc</sub>, H-2<sub>Glc'</sub>, H-3<sub>Glc</sub>, H-3<sub>Glc'</sub>, H-4<sub>Glc</sub>, H-4<sub>Glc'</sub>, H-5<sub>Glc</sub>, H-5<sub>Glc'</sub>, H-6a, H-6a', H-4'), 2.94 (t, <sup>4</sup>J<sub>OCH', C≡CH</sub> = 2.4 Hz, <sup>4</sup>J<sub>OCH, C≡CH</sub> = 2.4 Hz, 1H, C≡CH) ppm;

**<sup>13</sup>C NMR:** (125 MHz, D<sub>2</sub>O, 300 K):  $\delta$  = 172.01 (NH-C(O)-Glc'), 171.96 (NH-C(O)-Glc), 102.50 (C-1<sub>Glc'</sub>), 102.44 (C-1<sub>Glc</sub>), 100.39 (C-1), 100.03 (C-1'), 79.27 (C-4), 78.28 (OCH<sub>2</sub>C≡CH), 76.50 (OCH<sub>2</sub>C≡CH), 76.11 (C-3<sub>Glc</sub>), 76.04 (C-3<sub>Glc'</sub>), 75.98 (C-3), 75.60 (C-4<sub>Glc</sub>), 75.55 (C-4<sub>Glc'</sub>), 72.95 (C-2<sub>Glc</sub>), 72.93 (C-2<sub>Glc'</sub>), 72.75 (C-2'), 72.68 (C-2), 72.44 (C-3'), 71.55 (C-5), 71.26 (C-5'), 71.08

(C-4'), 69.55 (C-5<sub>Glc</sub>), 69.44 (C-5<sub>Glc'</sub>), 68.05 (Glc-OCH<sub>2</sub>), 68.00 (Glc'-OCH<sub>2</sub>), 60.66 (C-6<sub>Glc</sub>), 60.64 (C-6<sub>Glc'</sub>), 56.53 (OCH<sub>2</sub>C≡CH), 40.13 (C-6), 39.75 (C-6') ppm;

**ESI-MS:**  $m/z = 841.2683$  [M+Na]<sup>+</sup> (calculated  $m/z = 841.2696$  for [M+Na]<sup>+</sup>).

**(2-Propargyl) 2,3-di-O-benzoyl-6-deoxy-6-[[[(2,3,4,6-tetra-O-acetyl- $\alpha$ -D-mannopyranosyl)oxy]acetyl]amino]-4-O-(2',3',4'-tri-O-benzoyl-6'-deoxy-6'-[[[(2,3,4,6-tetra-O-acetyl- $\alpha$ -D-mannopyranosyl)oxy]acetyl]amino]- $\alpha$ -D-glucopyranosyl)- $\beta$ -D-glucopyranoside (**48**)**



The carboxylic acid **25** (427 mg, 1.05 mmol) was dissolved in dry THF (20 mL) and NHS (145 mg, 1.20 mmol) and EDC·HCl (242 mg, 1.20 mmol) were added. It was stirred for 2 h at room temperature. Then maltoside **46** (400 mg, 420  $\mu$ mol) was added and the reaction mixture was cooled to 0 °C before PMe<sub>3</sub> (1M in THF, 3.36 mL) was added dropwise. It was allowed to warm to room temperature and stirring was continued for 16 h. Then H<sub>2</sub>O was added and the aqu. layer was extracted with ethyl acetate. The combined org. layers were dried over MgSO<sub>4</sub>, filtered of, and concentrated. Purification by column chromatography on silica gel (cyclohexane/ethyl acetate, 1:4) gave **48** as a colorless solid.

**Yield:** 394 mg (23.5  $\mu$ mol, 56 %);

**R<sub>f</sub>:** (cyclohexane/ ethyl acetate, 1:4): R<sub>f</sub> = 0.32;

**[ $\alpha$ ]<sub>D</sub><sup>23</sup>:** +48.6 (c = 0.01, CH<sub>2</sub>Cl<sub>2</sub>);

**IR (ATR):**  $\tilde{\nu} = 2924, 1733, 1602, 1535, 1451, 1369, 1220, 1141, 1089, 1068, 1026, 801, 707$  cm<sup>-1</sup>;

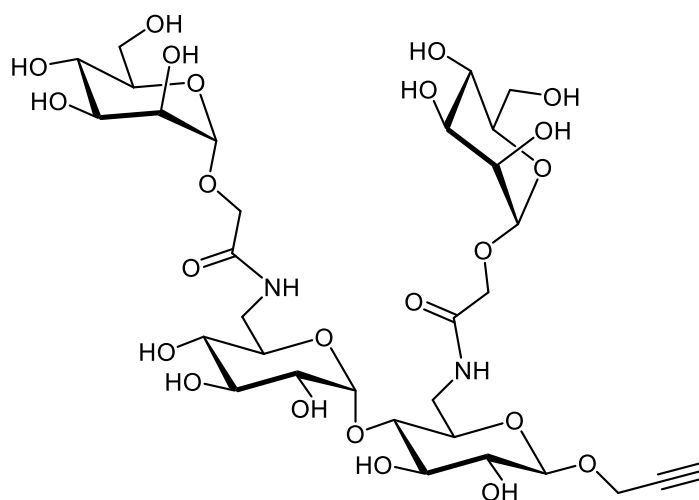
**<sup>1</sup>H NMR:** (500 MHz, CDCl<sub>3</sub>, 300 K):  $\delta = 7.98$ -7.92 (m, 2H, Bz<sub>ortho</sub>), 7.84-7.80 (m, 2H, Bz<sub>ortho</sub>), 7.67-7.63 (m, 2H, Bz<sub>ortho</sub>), 7.55-7.27 (m, 15H, 4 Bz<sub>ortho</sub>, 6 Bz<sub>meta</sub>, 5 Bz<sub>para</sub>), 7.20-7.10 (m, 6H, 4

Bz<sub>meta</sub>, 2 NH), 6.01 (t,  $^3J_{2',3'} = 10.1$  Hz,  $^3J_{3',4'} = 10.1$  Hz, 1H, H-3'), 5.71 (t,  $^3J_{2,3} = 9.2$  Hz,  $^3J_{3,4} = 9.2$  Hz, 1H, H-3), 5.62 (d,  $^3J_{1',2'} = 4.2$  Hz, 1H, H-1'), 5.49 (dd,  $^3J_{3,4} = 10.1$  Hz,  $^3J_{2,3} = 3.3$  Hz, 1H, H-3<sub>Man</sub>), 5.42 (t,  $^3J_{3,4} = 9.8$  Hz,  $^3J_{4,5} = 9.8$  Hz, 1H, H-4<sub>Man'</sub>), 5.39-5.28 (m, 7H, H-2', H-4', H-2, H-2<sub>Man</sub>, H-2<sub>Man'</sub>, H-3<sub>Man'</sub>, H-4<sub>Man</sub>), 5.08 (d,  $^3J_{1,2} = 7.8$  Hz, 1H, H-1), 4.96 (d,  $^3J_{1,2} = 1.3$  Hz, 1H, H-1<sub>Man</sub>), 4.95 (d,  $^3J_{1,2} = 1.4$  Hz, 1H, H-1<sub>Man'</sub>), 4.51-4.39 (m, 2H, OCH<sub>2</sub>, H-5'), 4.37-4.00 (m, 13H, H-6a, H-5<sub>Man'</sub>, OCH<sub>2</sub>, 2 Man'-OCH<sub>2</sub>, 2 Man-OCH<sub>2</sub>, H-6a<sub>Man</sub>, H-6a<sub>Man'</sub>, H-4, H-6b<sub>Man</sub>, H-6b<sub>Man'</sub>, H-5<sub>Man</sub>), 3.99-3.89 (m, 2H, H-6a', H-5), 3.57-3.49 (m, 1H, H-6b'), 3.47-3.38 (m, 1H, H-6b), 2.46 (t,  $^4J_{OCH',C\equiv CH} = 2.4$  Hz,  $^4J_{OCH,C\equiv CH} = 2.4$  Hz, 1H, C≡CH), 2.20, 2.17, 2.12, 2.11, 2.04, 1.99, 1.98, 1.96 (each s, 24H, 8 C(O)CH<sub>3</sub>) ppm;

**<sup>13</sup>C NMR:** (125 MHz, CDCl<sub>3</sub>, 300 K): δ = 170.82, 170.78, 170.28, 170.22, 170.22, 169.94, 169.91, 169.82 (8C, C(O)-Ac), 168.68, 168.28 (2 NH-C(O)), 165.97, 165.74, 165.34, 165.33, 164.98 (5C, C(O)Ph), 133.63, 133.21, 133.12, 133.09, 133.09 (5C, Bz-CH<sub>para</sub>), 130.21, 130.09, 129.96, 129.74, 129.66 (10C, Bz-CH<sub>ortho(a,b)</sub>), 129.43, 129.06, 128.71, 128.54, 128.36 (5C, Bz-C<sub>quat</sub>), 128.54, 128.28, 128.18, 128.18, 127.98 (10C, Bz-CH<sub>ortho(a,b)</sub>), 98.64 (C-1'), 98.16 (C-1), 97.70 (C-1<sub>Man'</sub>), 97.41 (C-1<sub>Man</sub>), 78.94 (OCH<sub>2</sub>C≡CH), 75.46 (C-4), 75.05 (OCH<sub>2</sub>C≡CH), 73.52 (C-3), 72.22 (C-5), 70.65 (C-5<sub>Man'</sub>), 70.44 (C-2'), 70.02 (C-2), 69.93 (C-3'), 69.57 (C-5'), 69.44 (C-4'), 69.42 (2 C-3<sub>Man'</sub>, C-3<sub>Man</sub>), 68.93 (C-5<sub>Man</sub>), 68.88 (2 C-2<sub>Man</sub>, C-2<sub>Man'</sub>), 65.98 (2 C-6<sub>Man</sub>, C-6<sub>Man'</sub>), 65.88 (2 C-4<sub>Man</sub>, C-4<sub>Man'</sub>), 62.43 (Man'-OCH<sub>2</sub>), 62.43 (Man-OCH<sub>2</sub>), 56.25 (OCH<sub>2</sub>C≡CH), 41.20 (C-6), 38.88 (C-6'), 21.03, 20.95, 20.93, 20.90, 20.81, 20.79, 20.77, 20.76 (8C, OAc) ppm;

**ESI-MS:**  $m/z = 1675.5030$  [M+H]<sup>+</sup> (calculated  $m/z = 1675.5033$  for [M+H]<sup>+</sup>).

**(2-Propargyl) 6-deoxy-6-[[ $\alpha$ -D-mannopyranosyloxy]acetyl]amino]-4-O-(6'-deoxy-6'-[[ $\alpha$ -D-mannopyranosyloxy]acetyl]amino]- $\alpha$ -D-glucopyranosyl)- $\beta$ -D-glucopyranoside (36)**



The maltoside **48** (146 mg, 87.2  $\mu$ mol) was dissolved in dry MeOH and a catalytical amount of a sodium methoxide solution was added. It was stirred at room temperature for 16 h and then

neutralized with Amberlite IR120. The reaction mixture was filtered, and the solvent was removed under reduced pressure. The crude product was taken up in H<sub>2</sub>O and washed with Et<sub>2</sub>O (3 x). The aqu. layer was concentrated to dryness. Purification by size exclusion chromatography on Sephadex GP10 (H<sub>2</sub>O) gave the product as a colorless solid.

**Yield:** 55.0 mg (67.2 μmol, 77 %);

**R<sub>f</sub>:** (CH<sub>2</sub>Cl<sub>2</sub>/MeOH, 8:2): R<sub>f</sub> = 0.05;

**[α]<sub>D</sub><sup>23</sup>:** -16.9 (c = 0.01, H<sub>2</sub>O);

**IR (ATR):**  $\tilde{\nu}$  = 3286, 2923, 1651, 1548, 1435, 1139, 1044, 1008, 965, 812 cm<sup>-1</sup>;

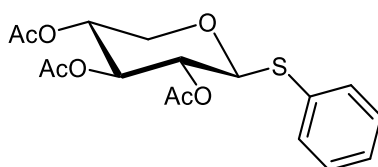
**<sup>1</sup>H NMR:** (600 MHz, D<sub>2</sub>O, 300 K): δ = 5.38 (d, <sup>3</sup>J<sub>1',2'</sub> = 3.9 Hz, 1H, H-1'), 4.79 (d, <sup>3</sup>J<sub>1,2</sub> = 0.9 Hz, 1H, H-1<sub>Man</sub>), 4.41 (d, <sup>3</sup>J<sub>1,2</sub> = 1.0 Hz, 1H, H-1<sub>Man'</sub>), 4.64 (d, <sup>3</sup>J<sub>1,2</sub> = 8.0 Hz, 1H, H-1), 4.43 (s, 2H, OCH<sub>2</sub>), 4.29-4.22 (m, 2H, Man-OCH<sub>2</sub>, Man'-OCH<sub>2</sub>), 4.15 (d, <sup>2</sup>J<sub>OCH<sub>2</sub>OCH</sub> = 15.3 Hz, 1H, Man-OCH<sub>2</sub>), 4.08-4.03 (m, 3H, H-2<sub>Man</sub>, H-2<sub>Man'</sub>, Man'-OCH<sub>2</sub>), 3.91-3.73 (m, 10H, H-5', H-6b, H-6b', H-6a<sub>Man</sub>, H-6a<sub>Man'</sub>, H-6b<sub>Man</sub>, H-6b<sub>Man'</sub>, H-3<sub>Man</sub>, H-3<sub>Man'</sub>, H-3), 3.72-3.58 (m, 7H, H-4<sub>Man</sub>, H-4<sub>Man'</sub>, H-2', H-5<sub>Man</sub>, H-5<sub>Man'</sub>, H-2, H-5), 3.48 (t, <sup>3</sup>J<sub>3,4</sub> = 9.2 Hz, <sup>3</sup>J<sub>4,5</sub> = 9.2 Hz, 1H, H-4), 3.43-3.27 (m, 4H, H-3', H-4', H-6a, H-6a'), 2.95 (t, <sup>4</sup>J<sub>OCH<sub>2</sub>C≡CH</sub> = 2.3 Hz, <sup>4</sup>J<sub>OCH<sub>2</sub>C≡CH</sub> = 2.3 Hz, 1H, C≡CH) ppm;

**<sup>13</sup>C NMR:** (125 MHz, D<sub>2</sub>O, 300 K): δ = 171.57 (NH-C(O)-Man'), 171.57 (NH-C(O)-Man), 100.179 (C-1), 99.98 (C-1'), 99.96 (C-1<sub>Man'</sub>), 99.87 (C-1<sub>Man</sub>), 79.45 (C-4), 78.51 (OCH<sub>2</sub>C≡CH), 76.52 (OCH<sub>2</sub>C≡CH), 76.03 (C-3), 73.23 (2 C-4<sub>Man</sub>, C-4<sub>Man'</sub>), 72.81 (C-2'), 72.67 (C-3'), 72.41 (C-2), 71.55 (C-5), 71.33 (C-5'), 71.27 (C-4'), 70.36 (2 C-3<sub>Man</sub>, C-3<sub>Man'</sub>), 69.99 (2 C-2<sub>Man</sub>, C-2<sub>Man'</sub>), 66.55 (C-5<sub>Man</sub>), 66.51 (C-5<sub>Man'</sub>), 65.76 (Man-OCH<sub>2</sub>), 65.64 (Man'-OCH<sub>2</sub>), 60.82 (C-6<sub>Man'</sub>), 60.80 (C-6<sub>Man</sub>), 56.38 (OCH<sub>2</sub>C≡CH), 40.14 (C-6), 39.79 (C-6') ppm;

**ESI-MS:** *m/z* = 841.2676 [M+Na]<sup>+</sup> (calculated *m/z* = 841.2696 for [M+Na]<sup>+</sup>).

## 8.2.2 Synthetic procedures for chapter 4.1

### Phenyl 2,3,4-tri-O-acetyl-β-D-thioxylopyranoside (**64**)<sup>[164]</sup>



D-Xylose tetraacetate **62** (7.60 g, 23.9 mmol) was dissolved in dry CH<sub>2</sub>Cl<sub>2</sub> (70 mL) and thiophenol (**63**, 6.09 mL, 59.7 mmol) was added. Then the mixture was cooled to 0 °C and BF<sub>3</sub>·Et<sub>2</sub>O (7.03 mL, 59.7 mmol) was added dropwise. The reaction mixture was allowed to

warm to room temperature and stirring was continued for 16 h. The mixture was diluted with  $\text{CH}_2\text{Cl}_2$  and washed with sodium bicarbonate and  $\text{H}_2\text{O}$ . The org. layer was dried over  $\text{MgSO}_4$ , filtered, and concentrated. Purification by column chromatography on silica (cyclohexane/ ethyl acetate, 7:3→5:3) gave **64** as a colorless solid.

**Yield:** 4.59 g (12.4 mmol, 52 %);

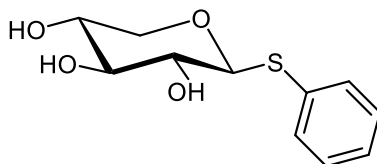
**R<sub>f</sub>:** (cyclohexane/ethyl acetate, 1:1):  $R_f = 0.54$ ;

**<sup>1</sup>H NMR:** (600 MHz,  $\text{CDCl}_3$ , 300 K, TMS):  $\delta = 7.52\text{--}7.45$  (m, 2H, 2 SPh-CH<sub>ortho</sub>), 7.37–7.29 (m, 3H, SPh-CH<sub>para</sub>, SPh-CH<sub>meta</sub>), 5.18 (t,  $^3J_{3,4} = 8.2$  Hz,  $^3J_{2,3} = 8.2$  Hz, 1H, H-3), 4.98–4.89 (m, 2H, H-2, H-4), 4.81 (d,  $^3J_{1,2} = 8.3$  Hz, 1H, H-1), 4.28 (dd,  $^2J_{5a,5b} = 11.8$  Hz,  $^3J_{5a,4} = 4.9$  Hz, 1H, H-5a), 3.43 (dd,  $^2J_{5a,5b} = 11.8$  Hz,  $^3J_{5b,4} = 8.7$  Hz, 1H, H-5b), 2.09, 2.05, 2.04 (each s, each 3H, OAc) ppm;

**<sup>13</sup>C NMR:** (125 MHz,  $\text{CDCl}_3$ , 300 K, TMS):  $\delta = 169.92, 169.79, 169.33$  (3 C(O)CH<sub>3</sub>), 132.75 (2 SPh-CH<sub>ortho</sub>), 132.23 (SPh-C<sub>quart</sub>), 129.04 (2 SPh-CH<sub>meta</sub>), 128.24 (SPh-CH<sub>para</sub>), 86.25 (C-1), 72.01 (C-3), 69.82 (C-4), 68.41 (C-2), 65.21 (C-5), 20.80, 20.74, 20.72 (3 C(O)CH<sub>3</sub>) ppm;

**ESI-MS:**  $m/z = 391.0818$  [M+Na]<sup>+</sup> (calculated  $m/z = 391.0821$  for [M+Na]<sup>+</sup>).

### Phenyl β-D-thioxylopyranoside (**65**)<sup>[165]</sup>



The thioxyloside **64** (3.45 g, 9.36 mmol) was dissolved in dry MeOH (20 mL) and sodium methoxide (5.4 M in MeOH, 320  $\mu\text{L}$ , 1.73 mmol) was added. The mixture was stirred at room temperature for 2 h. It was neutralized by Amberlite IR 120 ion exchange resin. The resin was filtered off and the filtrate concentrated to afford **65** as a colorless solid.

**Yield:** 2.18 g (9.00 mmol, 96 %);

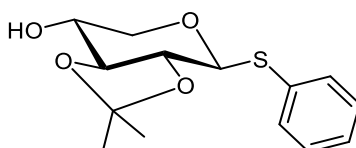
**R<sub>f</sub>:** ( $\text{CH}_2\text{Cl}_2/\text{MeOH}$ , 9:1):  $R_f = 0.15$ ;

**<sup>1</sup>H NMR:** (600 MHz,  $\text{CDCl}_3$ , 300 K, TMS):  $\delta = 7.54\text{--}7.48$  (m, 2H, 2 SPh-CH<sub>ortho</sub>), 7.36–7.24 (m, 3H, SPh-CH<sub>para</sub>, SPh-CH<sub>meta</sub>), 4.55 (d,  $^3J_{1,2} = 9.3$  Hz, 1H, H-1), 3.94 (dd,  $^2J_{5a,5b} = 11.3$  Hz,  $^3J_{5a,4} = 5.2$  Hz, 1H, H-5a), 3.47 (dd,  $^3J_{4,5b} = 10.0$  Hz,  $^3J_{4,3} = 8.9$  Hz,  $^3J_{4,5a} = 5.2$  Hz, 1H, H-4), 3.34 (t,  $^3J_{3,4} = 8.6$  Hz,  $^3J_{2,3} = 8.6$  Hz, 1H, H-3), 3.27–3.17 (m, 2H, H-2, H-5b) ppm;

**$^{13}\text{C}$  NMR:** (125 MHz,  $\text{CDCl}_3$ , 300 K, TMS):  $\delta$  = 134.88 (SPh- $\text{C}_{\text{quart}}$ ), 133.15 (2 SPh- $\text{CH}_{\text{ortho}}$ ), 129.88 (2 SPh- $\text{CH}_{\text{meta}}$ ), 128.54 (SPh- $\text{CH}_{\text{para}}$ ), 90.10 (C-1), 79.22 (C-3), 73.71 (C-2), 70.90 (C-4), 70.42 (C-5) ppm;

**ESI-MS:**  $m/z$  = 265.0503  $[\text{M}+\text{Na}]^+$  (calculated  $m/z$  = 265.0510 for  $[\text{M}+\text{Na}]^+$ ).

**Phenyl 2,3-O-isopropylidene- $\beta$ -D-thioxylopyranoside (67)<sup>[164]</sup>**



The thioxyloside **65** (1.00 g, 4.13 mmol) was dissolved in dry DMF (7.50 mL) and D(+)-camphor sulfonic acid (145 mg, 619  $\mu\text{mol}$ ) was added. Then 2-Methoxypropene (593  $\mu\text{L}$ , 6.19 mmol) was added dropwise. The reaction mixture was stirred at room temperature for 4 h, before it was neutralized by adding triethylamine. Then the solvent was removed under reduced pressure. Purification by column chromatography on silica (cyclohexane/ ethyl acetate, 7:3 $\rightarrow$ 3:2) yielded **67** as a colorless solid.

**Yield:** 660 mg (2.34 mmol, 57 %);

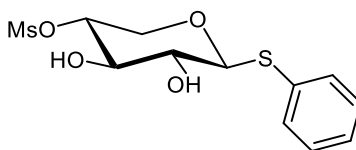
**R<sub>f</sub>:** (cyclohexane/ethyl acetate, 1:1): R<sub>f</sub> = 0.44;

**$^1\text{H}$  NMR:** (500 MHz,  $\text{CDCl}_3$ , 300 K, TMS):  $\delta$  = 7.59–7.54 (m, 2H, 2 SPh- $\text{CH}_{\text{ortho}}$ ), 7.35–7.29 (m, 3H, SPh- $\text{CH}_{\text{para}}$ , SPh- $\text{CH}_{\text{meta}}$ ), 4.79 (d,  $^3J_{1,2}$  = 9.5 Hz, 1H, H-1), 4.51 (dd,  $^2J_{5a,5b}$  = 11.7 Hz,  $^3J_{5a,4}$  = 5.3 Hz, 1H, H-5a), 3.97 (td,  $^3J_{4,5a}$  = 9.2 Hz,  $^3J_{4,3}$  = 9.2 Hz,  $^3J_{4,5b}$  = 5.3 Hz, 1H, H-4), 3.53 (t,  $^3J_{3,4}$  = 9.2 Hz,  $^3J_{2,3}$  = 9.2 Hz, 1H, H-3), 3.29-3.18 (m, 2H, H-2, H-5b), 2.67 (s, 1H, OH), 1.49, 1.44 (each s, each 3H,  $\text{CH}_3$ ) ppm;

**$^{13}\text{C}$  NMR:** (125 MHz,  $\text{CDCl}_3$ , 300 K, TMS):  $\delta$  = 132.88 (2 SPh- $\text{CH}_{\text{ortho}}$ ), 131.82 (SPh- $\text{C}_{\text{quart}}$ ), 128.89 (2 SPh- $\text{CH}_{\text{meta}}$ ), 128.15 (SPh- $\text{CH}_{\text{para}}$ ), 85.40 (C-1), 82.85 (C-3), 75.12 (C-2), 69.90 (C-5), 68.92 (C-4), 26.90 ( $\text{C}(\text{CH}_3)_2$ ), 26.65 ( $\text{C}(\text{CH}_3)_2$ ), 26.51 ( $\text{C}(\text{CH}_3)_2$ ) ppm;

**ESI-MS:**  $m/z$  = 305.0815  $[\text{M}+\text{Na}]^+$  (calculated  $m/z$  = 305.0818 for  $[\text{M}+\text{Na}]^+$ ).

**Phenyl 4-O-mesyl- $\beta$ -D-thioxylopyranoside (68)**



The thioxyloside **65** (650 mg, 2.30 mmol) was dissolved in dry pyridine (5.00 mL) and MsCl (267  $\mu\text{L}$ , 3.45 mmol) was added slowly. It was stirred for 16 h at room temperature before  $\text{H}_2\text{O}$

was added to the solution. It was extracted with  $\text{CH}_2\text{Cl}_2$ , and the combined org. layers were dried over  $\text{MgSO}_4$ , filtered of, and concentrated to dryness. The crude product was dissolved in AcOH (88 %, 100 mL). The reaction mixture was heated to 60 °C and stirring was continued for 4 h. Afterwards the solution was concentrated to dryness. Purification by column chromatography on silica (cyclohexane/ ethyl acetate, 1:2) gave **68** as a colorless solid.

**Yield:** 530 mg (1.65 mmol, 72 %);

**R<sub>f</sub>** (cyclohexane/ethyl acetate, 1:2): R<sub>f</sub> = 0.30;

**[ $\alpha$ ]<sub>D</sub><sup>23</sup>:** -5.08 (c = 0.01,  $\text{CH}_2\text{Cl}_2$ )

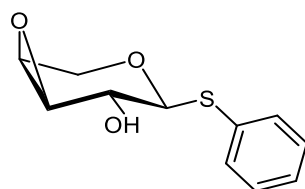
**IR (ATR):**  $\tilde{\nu}$  = 3434, 2865, 1597, 1479, 1439, 1358, 1189, 1173, 1063, 1025, 960, 810, 667  $\text{cm}^{-1}$ ;

**<sup>1</sup>H NMR:** (500 MHz,  $\text{CDCl}_3$ , 300 K, TMS):  $\delta$  = 7.55–7.50 (m, 2H, 2 SPh-CH<sub>ortho</sub>), 7.37–7.30 (m, 3H, SPh-CH<sub>para</sub>, SPh-CH<sub>meta</sub>), 4.46 (d, <sup>3</sup>J<sub>1,2</sub> = 9.6 Hz, 1H, H-1), 4.23 (dd, <sup>2</sup>J<sub>5a,5b</sub> = 11.5 Hz, <sup>3</sup>J<sub>5a,4</sub> = 5.6 Hz, 1H, H-5a), 4.49 (ddd, <sup>3</sup>J<sub>4,5a</sub> = 10.4 Hz, <sup>3</sup>J<sub>4,3</sub> = 9.2 Hz, <sup>3</sup>J<sub>4,5b</sub> = 5.7 Hz, 1H, H-4), 3.75 (t, <sup>3</sup>J<sub>3,4</sub> = 8.9 Hz, <sup>3</sup>J<sub>2,3</sub> = 8.9 Hz, 1H, H-3), 3.44 (dd, <sup>2</sup>J<sub>5a,5b</sub> = 11.5 Hz, <sup>3</sup>J<sub>5b,4</sub> = 10.4 Hz, 1H, H-5b), 3.35 (dd, <sup>3</sup>J<sub>1,2</sub> = 9.6 Hz, <sup>3</sup>J<sub>2,3</sub> = 8.9 Hz, 1H, H-2), 3.31 (s, 1H, OH), 3.12 (s, 3H, CH<sub>3</sub>), 2.91 (s, 1H, OH) ppm;

**<sup>13</sup>C NMR:** (125 MHz,  $\text{CDCl}_3$ , 300 K, TMS):  $\delta$  = 133.44 (2 SPh-CH<sub>ortho</sub>), 130.83 (SPh-C<sub>quart</sub>), 129.35 (2 SPh-CH<sub>meta</sub>), 128.81 (SPh-CH<sub>para</sub>), 88.45 (C-1), 77.26 (C-4), 75.21 (C-3), 72.31 (C-2), 67.53 (C-5), 38.40 (CH<sub>3</sub>) ppm;

**ESI-MS:**  $m/z$  = 343.0279 [M+Na]<sup>+</sup> (calculated  $m/z$  = 343.0280 for [M+Na]<sup>+</sup>).

### Phenyl 3,4-anhydro- $\alpha$ -L-thioarabinopyranoside (**70**)



The thioxyloside **68** (520 mg, 1.62 mmol) was dissolved in dry MeOH (7 mL) and at 0 °C a solution of sodium methoxide (5.4 M in MeOH, 330  $\mu\text{L}$ , 1.79 mmol) was added dropwise. The mixture was allowed to warm to room temperature, and it was stirred for 2 h. Subsequently it was neutralized by adding AcOH (800  $\mu\text{L}$ ) and then concentrated under reduced pressure. Purification by column chromatography on silica (cyclohexane/ethyl acetate, 1:1) gave **70** as a colorless solid.

**Yield:** 342 mg (1.52 mmol, 94 %);

**R<sub>f</sub>**: (cyclohexane/ethyl acetate, 1:2): R<sub>f</sub> = 0.55;

**[α]<sub>D</sub><sup>23</sup>**: -7.47 (c = 0.01, CH<sub>2</sub>Cl<sub>2</sub>);

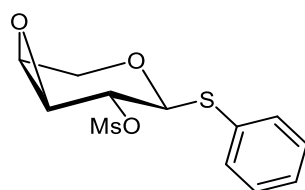
**IR (ATR)**:  $\tilde{\nu}$  = 3414, 2915, 1735, 1583, 1475, 1439, 1239, 1049, 1023, 809, 742, 690 cm<sup>-1</sup>;

**<sup>1</sup>H NMR**: (500 MHz, CDCl<sub>3</sub>, 300 K, TMS): δ = 7.51–7.47 (m, 2H, 2 SPh-CH<sub>ortho</sub>), 7.34–7.27 (m, 3H, SPh-CH<sub>para</sub>, SPh-CH<sub>meta</sub>), 4.48 (d, <sup>3</sup>J<sub>1,2</sub> = 7.4 Hz, 1H, H-1), 4.37 (d, <sup>2</sup>J<sub>5a,5b</sub> = 13.6 Hz, <sup>3</sup>J<sub>5a,4</sub> = 13.6 Hz, 1H, H-5a), 3.97 (dd, <sup>2</sup>J<sub>5a,5b</sub> = 13.5 Hz, <sup>3</sup>J<sub>5b,4</sub> = 1.6 Hz, 1H, H-5b), 3.86 (dd, <sup>3</sup>J<sub>1,2</sub> = 7.4 Hz, <sup>3</sup>J<sub>2,OH</sub> = 4.8 Hz, 1H, H-2), 3.41–3.39 (m, 1H, H-3), 3.25–3.22 (m, 1H, H-4), 2.34 (d, <sup>3</sup>J<sub>2,OH</sub> = 4.8 Hz, 1H, OH) ppm;

**<sup>13</sup>C NMR**: (125 MHz, CDCl<sub>3</sub>, 300 K, TMS): δ = 133.13 (SPh-C<sub>quart</sub>), 131.98 (2 SPh-CH<sub>ortho</sub>), 129.08 (2 SPh-CH<sub>meta</sub>), 127.85 (SPh-CH<sub>para</sub>), 87.75 (C-1), 65.70 (C-2), 63.86 (C-5), 53.63 (C-3), 49.71 (C-4) ppm;

**ESI-MS**: *m/z* = 247.0402 [M+Na]<sup>+</sup> (calculated *m/z* = 247.0405 for [M+Na]<sup>+</sup>).

### Phenyl 3,4-anhydro-2-O-mesyl-α-L-thioarabinopyranoside (**71**)



The thioxyloside **70** (50.0 mg, 223 μmol) was dissolved in dry CH<sub>2</sub>Cl<sub>2</sub> (2.50 mL) and subsequently pyridine (76.0 μL, 941 μmol) and MsCl (39.7 μL, 513 μmol) were added. The reaction mixture was stirred for 1 h. Then sodium bicarbonate solution (1.00 mL) was added, and it was stirred for 30 min. The layers were separated and the aqu. layer was extracted with CH<sub>2</sub>Cl<sub>2</sub>. The combined org. layers were washed with brine, dried over MgSO<sub>4</sub>, filtered and the solvent was removed under reduced pressure to obtain **71** as a colorless solid.

**Yield**: 60.0 mg (198 μmol, 89 %);

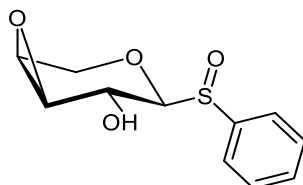
**R<sub>f</sub>**: (cyclohexane/ethyl acetate, 1:2): R<sub>f</sub> = 0.77;

**<sup>1</sup>H NMR**: (500 MHz, CDCl<sub>3</sub>, 300 K, TMS): δ = 7.49–7.45 (m, 2H, 2 SPh-CH<sub>ortho</sub>), 7.36–7.30 (m, 3H, SPh-CH<sub>para</sub>, SPh-CH<sub>meta</sub>), 4.88 (d, <sup>3</sup>J<sub>1,2</sub> = 5.9 Hz, 1H, H-2), 4.80 (d, <sup>3</sup>J<sub>1,2</sub> = 5.9 Hz, 1H, H-1), 4.47 (d, <sup>2</sup>J<sub>5a,5b</sub> = 13.7, 1H, H-5a), 4.03 (dd, <sup>2</sup>J<sub>5a,5b</sub> = 13.7 Hz, <sup>3</sup>J<sub>5b,4</sub> = 2.1 Hz, 1H, H-5b), 3.57 (d, <sup>3</sup>J<sub>3,4</sub> = 3.8 Hz, 1H, H-3), 3.35–3.31 (m, 1H, H-4), 3.16 (s, 3H, CH<sub>3</sub>) ppm;

**<sup>13</sup>C NMR:** (125 MHz, CDCl<sub>3</sub>, 300 K, TMS):  $\delta$  = 133.31 (SPh-C<sub>quart</sub>), 131.98 (2 SPh-CH<sub>ortho</sub>), 129.35 (2 SPh-CH<sub>meta</sub>), 128.17 (SPh-CH<sub>para</sub>), 84.43 (C-1), 72.67 (C-2), 62.52 (C-5), 51.59 (C-3), 49.80 (C-4), 38.92 (CH<sub>3</sub>) ppm;

**ESI-MS:**  $m/z$  = 325.0176 [M+Na]<sup>+</sup> (calculated  $m/z$  = 325.0180 for [M+Na]<sup>+</sup>).

### Phenyl 3,4-anhydro-1-thio- $\alpha$ -L-arabinopyranoside S-oxide (**81**)



The thioxyloside **70** (100 mg, 446  $\mu$ mol) was dissolved in CH<sub>2</sub>Cl<sub>2</sub> (2.50 ml) and at -20 °C 3-chloroperbenzoic acid (121 mg, 491  $\mu$ mol) was added. The reaction mixture was stirred for 1.5 h before sodium bicarbonate was added. The aqu. layer was extracted with CH<sub>2</sub>Cl<sub>2</sub>, and the combined org layers were washed with brine, then dried over MgSO<sub>4</sub>, filtered off and the solvent was removed under reduced pressure. Purification by column chromatography on silica (cyclohexane/ethyl acetate, 3:7→1:4) yielded **81** as a colorless solid.

**Yield:** 57.0 mg (237  $\mu$ mol, 53 %);

**R<sub>f</sub>:** (cyclohexane/ethyl acetate, 2:1): R<sub>f</sub> = 0.10;

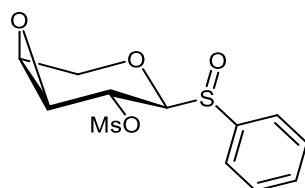
**[ $\alpha$ ]<sub>D</sub><sup>23</sup>:** +25.57 (c = 0.02, CH<sub>2</sub>Cl<sub>2</sub>);

**IR (ATR):**  $\tilde{\nu}$  = 3339, 2937, 2111, 1439, 1340, 1172, 1028, 958, 825 cm<sup>-1</sup>;

**<sup>1</sup>H NMR:** (500 MHz, CDCl<sub>3</sub>, 300 K, TMS):  $\delta$  = 7.76–7.66 (m, 2H, 2 S(O)Ph-CH<sub>ortho</sub>), 7.60–7.50 (m, 3H, S(O)Ph-CH<sub>para</sub>, S(O)Ph-CH<sub>meta</sub>), 4.48 (dd, <sup>3</sup>J<sub>1,2</sub> = 8.8 Hz, <sup>3</sup>J<sub>2,OH</sub> = 1.6 Hz, 1H, H-2), 4.23 (d, <sup>2</sup>J<sub>5a,5b</sub> = 13.3 Hz, 1H, H-5a), 3.98 (d, <sup>3</sup>J<sub>2,OH</sub> = 1.8 Hz, 1H, OH), 3.69 (dd, <sup>2</sup>J<sub>5a,5b</sub> = 13.3 Hz, <sup>3</sup>J<sub>5b,4</sub> = 0.8 Hz, 1H, H-5b), 3.67 (d, <sup>3</sup>J<sub>1,2</sub> = 8.8 Hz, 1H, H-1), 3.38 (d, <sup>3</sup>J<sub>3,4</sub> = 3.8 Hz, 1H, H-3), 3.19 (dd, <sup>3</sup>J<sub>4,3</sub> = 3.8 Hz, <sup>3</sup>J<sub>4,5b</sub> = 0.8 Hz, 1H, H-4) ppm;

**<sup>13</sup>C NMR:** (125 MHz, CDCl<sub>3</sub>, 300 K, TMS):  $\delta$  = 141.93 (S(O)Ph-C<sub>quart</sub>), 132.08 (S(O)Ph-CH<sub>para</sub>), 129.46 (2 S(O)Ph-CH<sub>ortho</sub>), 124.52 (2 S(O)Ph-CH<sub>meta</sub>), 93.88 (C-1), 65.55 (C-5), 66.29 (C-2), 54.43 (C-3), 49.20 (C-4) ppm;

**ESI-MS:**  $m/z$  = 263.0345 [M+Na]<sup>+</sup> (calculated  $m/z$  = 263.0348 for [M+Na]<sup>+</sup>).

**Phenyl 3,4-anhydro-2-O-mesyl-1-thio- $\alpha$ -L-arabinopyranoside S-oxide (82)**

The xylosyl sulfoxide **81** (25.0 mg, 104  $\mu$ mol) was dissolved in dry pyridine (1.00 mL) and at 0 °C MsCl (18.5  $\mu$ L, 239  $\mu$ mol) was added dropwise. The reaction mixture was stirred for 16 h. Afterwards it was diluted with ethyl acetate and the org. layer was washed with 1N HCl and H<sub>2</sub>O, it was dried over MgSO<sub>4</sub>, filtered, and concentrated to dryness. Purification by column chromatography on silica (cyclohexane/ethyl acetate, 1:2) yielded **82** as a colorless solid.

**Yield:** 25.0 mg (78.5  $\mu$ mol, 76 %);

**R<sub>f</sub>:** (cyclohexane/ethyl acetate, 1:2): R<sub>f</sub> = 0.20;

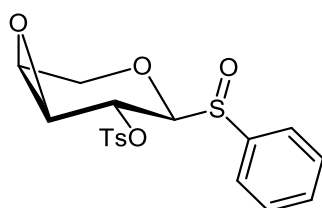
**[ $\alpha$ ]<sub>D</sub><sup>23</sup>:** +36.45 (c = 0.01, CH<sub>2</sub>Cl<sub>2</sub>);

**IR (ATR):**  $\tilde{\nu}$  = 2936, 2349, 1633, 1438, 1330, 1169, 1034, 957, 830, 522 cm<sup>-1</sup>;

**<sup>1</sup>H NMR:** (500 MHz, CDCl<sub>3</sub>, 300 K, TMS):  $\delta$  = 7.72–7.65 (m, 2H, 2 S(O)Ph-CH<sub>ortho</sub>), 7.58–7.49 (m, 3H, S(O)Ph-CH<sub>para</sub>, S(O)Ph-CH<sub>meta</sub>), 5.36 (d, <sup>3</sup>J<sub>1,2</sub> = 5.3 Hz, 1H, H-2), 4.31 (d, <sup>2</sup>J<sub>5a,5b</sub> = 13.5, 1H, H-5a), 4.21 (d, <sup>3</sup>J<sub>1,2</sub> = 5.2 Hz, 1H, H-1), 4.02 (dd, <sup>2</sup>J<sub>5a,5b</sub> = 13.5 Hz, <sup>3</sup>J<sub>5b,4</sub> = 1.7 Hz, 1H, H-5b), 3.71 (d, <sup>3</sup>J<sub>3,4</sub> = 3.8 Hz, 1H, H-3), 3.39–3.36 (m, 1H, H-4), 3.18 (s, 3H, CH<sub>3</sub>) ppm;

**<sup>13</sup>C NMR:** (125 MHz, CDCl<sub>3</sub>, 300 K, TMS):  $\delta$  = 141.96 (S(O)Ph-C<sub>quart</sub>), 132.03 (S(O)Ph-CH<sub>para</sub>), 129.44 (2 S(O)Ph-CH<sub>ortho</sub>), 124.96 (2 S(O)Ph-CH<sub>meta</sub>), 92.54 (C-1), 68.80 (C-2), 63.67 (C-5), 50.93 (C-3), 49.36 (C-4), 38.99 (CH<sub>3</sub>) ppm;

**ESI-MS:**  $m/z$  = 341.0125 [M+Na]<sup>+</sup> (calculated  $m/z$  = 341.0129 for [M+Na]<sup>+</sup>).

**Phenyl-3,4-anhydro-2-O-tosyl-1-thio- $\alpha$ -L-arabinopyranoside S-oxide (83)**

The thioxyloside **81** (500 mg, 2.23 mmol) was dissolved in dry CH<sub>2</sub>Cl<sub>2</sub> (15.0 mL) and KI (740 mg, 4.46 mmol) and Ag<sub>2</sub>O (1.03 g, 4.46 mmol) were added. The suspension was cooled to 0 °C and TsCl (637 mg, 3.34 mmol) was added. The reaction mixture was allowed to warm to room temperature and stirring was continued for 16 h. It was diluted with CH<sub>2</sub>Cl<sub>2</sub>, filtered

over a pad of celite and the org. layer was washed H<sub>2</sub>O, it was dried over MgSO<sub>4</sub>, filtered off and concentrated two the half volume. The org. layer was cooled to -20 °C and 3-chloroperbenzoic acid (423 mg, 2.45 mmol) was added. The reaction mixture was stirred for 1 h before sodium bicarbonate was added. The aqu. layer was extracted with CH<sub>2</sub>Cl<sub>2</sub>, and the combined org layers were washed with brine, dried over MgSO<sub>4</sub>, filtered off and the solvent was removed. The crude product was purified by column chromatography on silica (cyclohexane/ethyl acetate, 2:1) to obtain **83** as a colorless solid.

**Yield:** 420 mg (1.06 mmol, 48 %);

**R<sub>f</sub>:** (cyclohexane/ethyl acetate, 2:1): R<sub>f</sub> = 0.16;

**[α]<sub>D</sub><sup>23</sup>:** +26.33 (c = 0.02, CH<sub>2</sub>Cl<sub>2</sub>);

**IR (ATR):**  $\tilde{\nu}$  = 3417, 2925, 1736, 1596, 1441, 1365, 1190, 1174, 1094, 1009, 664, 551 cm<sup>-1</sup>;

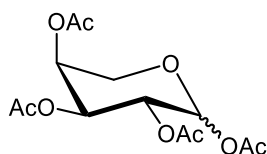
**<sup>1</sup>H NMR:** (500 MHz, CDCl<sub>3</sub>, 300 K, TMS):  $\delta$  = 7.98–7.94 (m, 2H, Tos-CH<sub>ortho</sub>), 7.81–7.76 (m, 2H, 2 S(O)Ph-CH<sub>ortho</sub>), 7.71–7.64 (m, 1H, S(O)Ph-CH<sub>para</sub>), 7.56–7.50 (m, 2H, S(O)Ph-CH<sub>meta</sub>), 7.45–7.38 (m, 2H, Tos-CH<sub>meta</sub>), 4.98 (d, <sup>3</sup>J<sub>1,2</sub> = 7.5 Hz, 1H, H-2), 4.30 (d, <sup>2</sup>J<sub>5a,5b</sub> = 13.5, 1H, H-5a), 4.20 (d, <sup>3</sup>J<sub>1,2</sub> = 7.5 Hz, 1H, H-1), 3.91 (dd, <sup>2</sup>J<sub>5a,5b</sub> = 13.5 Hz, <sup>3</sup>J<sub>5b,4</sub> = 1.0 Hz, 1H, H-5b), 3.61 (d, <sup>3</sup>J<sub>3,4</sub> = 3.8 Hz, 1H, H-3), 3.23–3.19 (m, 1H, H-4), 2.48 (s, 3H, CH<sub>3</sub>) ppm;

**<sup>13</sup>C NMR:** (125 MHz, CDCl<sub>3</sub>, 300 K, TMS):  $\delta$  = 145.97 (Tos-C<sub>quart</sub>), 135.69 (S(O)Ph-C<sub>quart</sub>), 134.61 (S(O)Ph-CH<sub>para</sub>), 132.49 (Tos-C<sub>quart</sub>), 130.39 (2 Tos-CH<sub>meta</sub>), 130.09 (2 S(O)Ph-CH<sub>ortho</sub>), 129.18 (2 S(O)Ph-CH<sub>meta</sub>), 128.97 (2 Tos-CH<sub>ortho</sub>), 88.46 (C-1), 67.38 (C-2), 64.69 (C-5), 51.45 (C-3), 48.49 (C-4), 21.96 (CH<sub>3</sub>) ppm;

**ESI-MS:**  $m/z$  = 395.0612 [M+Na]<sup>+</sup> (calculated  $m/z$  = 395.0617 for [M+Na]<sup>+</sup>).

### 8.2.3 Synthetic procedures for chapter 4.2

#### 1,2,3,4-Tetra-O-acetyl- $\alpha/\beta$ -L-arabinopyranose (**88**)<sup>[187]</sup>

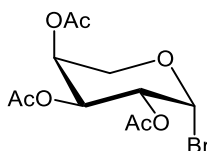


L-arabinose (**85**, 15.0 g, 100 mmol) was dissolved in dry pyridine (100 mL) and Ac<sub>2</sub>O (75.5 mL, 800 mmol) was added dropwise. The reaction mixture was stirred for 4 h. Then the solvent was removed, and the crude product was taken up in ethyl acetate. The org. phase was washed with 1N HCl and brine. The combined org. layers were dried over MgSO<sub>4</sub>, filtered and it was concentrated to dryness to yield **88**.

**Yield:** 32.3 g (96.7 mmol, 80 %,  $\alpha:\beta = 1:3$ );

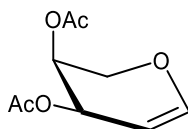
Analytical data correspond to the literature<sup>[187]</sup>

**2,3,4-Tri-O-acetyl- $\alpha$ -L-arabinosylbromide (89)<sup>[187]</sup>**



The arabinose tetraacetate **88** (10.0 g, 33.4 mmol) was dissolved in  $\text{CH}_2\text{Cl}_2$  (10.0 mL) and the solution was cooled down to 0 °C. Then HBr in AcOH (33 % w/w, 172 mL, 334 mmol) was added dropwise and it was stirred for 4 h. The mixture was diluted with  $\text{CH}_2\text{Cl}_2$ , and the org. layer was washed with  $\text{H}_2\text{O}$ , dried over  $\text{MgSO}_4$ , filtered, and concentrated to dryness. The product was used in further reaction steps without further purification.

**3,4-Di-O-acetyl-arabinal (90)<sup>[288]</sup>**



The arabinosyl bromide **89** was dissolved in MeCN (40 mL) and zinc (15.4 g, 233 mmol) and  $\text{NH}_4\text{Cl}$  (12.6 g, 233 mmol) was added. The reaction mixture was stirred at room temperature for 72 h and was filtered over celite<sup>®</sup>. The solvent was removed, and purification by column chromatography on silica (cyclohexane/ethyl acetate, 3:1) gave **90** as a colorless solid.

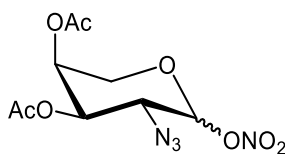
**Yield:** 2.87 g (11.2 mmol, 33 % over 2 steps);

**R<sub>f</sub>:** (cyclohexane/ethyl acetate, 3:1):  $R_f = 0.35$ ;

**<sup>1</sup>H NMR:** (500 MHz,  $\text{CDCl}_3$ , 300 K, TMS):  $\delta = 6.51$  (d,  $^3J_{1,2} = 6.0$  Hz, 1H, H-1), 5.45 (t,  $^3J_{3,2} = 4.5$  Hz,  $^3J_{3,4} = 4.5$  Hz, 1H, H-3), 5.19 (dt,  $^3J_{3,4} = 4.1$  Hz,  $^3J_{5a,4} = 4.1$  Hz,  $^3J_{5b,4} = 9.4$  Hz, 1H, H-4), 4.85 (dd,  $^3J_{1,2} = 6.0$  Hz,  $^3J_{2,3} = 5.1$  Hz, 1H, H-2), 4.03 (dd,  $^2J_{5a,5b} = 10.7$  Hz,  $^3J_{5a,4} = 4.1$  Hz, 1H, H-5a), 3.99 (dd,  $^2J_{5a,5b} = 10.7$  Hz,  $^3J_{5b,4} = 9.5$  Hz, 1H, H-5b), 2.08, 2.08 (each s, each 3H, OAc) ppm;

**<sup>13</sup>C NMR:** (125 MHz,  $\text{CDCl}_3$ , 300 K, TMS):  $\delta = 170.46$ , 169.86 (2  $\text{C}(\text{O})\text{CH}_3$ ), 147.8 (C-1), 97.5 (C-2), 65.95 (C-4), 62.87 (C-5), 62.86 (C-3), 21.06, 20.79 (2  $\text{C}(\text{O})\text{CH}_3$ ) ppm;

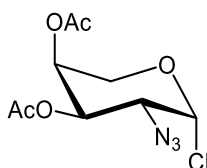
**ESI-MS:**  $m/z = 223.0575$   $[\text{M}+\text{Na}]^+$  (calculated  $m/z = 223.0582$  for  $[\text{M}+\text{Na}]^+$ ).

**3,4-Di-O-acetyl-2-azido-2-deoxy-L-arabinopyranosyl nitrate (92)**<sup>[194]</sup>

Arabinal **90** (2.81 g, 14.1 mmol) was dissolved in CH<sub>2</sub>Cl<sub>2</sub> (100 mL), and the solution was cooled down to -20 °C. Then NaN<sub>3</sub> (1.37 g, 21.1 mmol) and CAN (23.1 g, 42.3 mmol) were added. The reaction mixture was stirred for 6 h. Then the suspension was diluted with Et<sub>2</sub>O and washed with H<sub>2</sub>O. The org. layer was dried over MgSO<sub>4</sub>, filtered, and concentrated to dryness. The product was used in further steps without further purification.

**Yield:** 2.14 g (7.05 mmol, 50 %);

**R<sub>f</sub>:** (cyclohexane/ethyl acetate, 3:1): R<sub>f</sub> = 0.40;

**3,4-Di-O-acetyl-2-azido-2-deoxy-β-L-arabinopyranosyl chloride (93)**<sup>[194]</sup>

The arabinosyl nitrate **92** (2.14 g, 7.05 mmol) was dissolved in MeCN (60.0 mL) and tetraethylammonium chloride (11.7 g, 70.5 mmol) was added. The reaction mixture was stirred for 16 h at room temperature. Then it was diluted with CH<sub>2</sub>Cl<sub>2</sub>, and the org. layer was washed with H<sub>2</sub>O, dried over MgSO<sub>4</sub>, filtered, and concentrated to dryness. Purification by column chromatography on silica (cyclohexane/ethyl acetate, 4:1) yielded **93** as a colorless solid.

**Yield:** 1.17 g (4.23 mmol, 30 % over 2 steps);

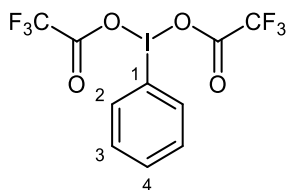
**R<sub>f</sub>:** (cyclohexane/ethyl acetate, 4:1): R<sub>f</sub> = 0.35;

**IR (ATR):**  $\tilde{\nu}$  = 2111.8, 1736.8, 1215.6, 1096.6 cm<sup>-1</sup>;

**<sup>1</sup>H NMR:** (500 MHz, CDCl<sub>3</sub>, 300 K, TMS):  $\delta$  = 6.18 (d, <sup>3</sup>J<sub>1,2</sub> = 3.8 Hz, 1H, H-1), 5.40 (dt, <sup>3</sup>J<sub>3,4</sub> = 3.2 Hz, <sup>3</sup>J<sub>5a,4</sub> = 1.7 Hz, <sup>3</sup>J<sub>5b,4</sub> = 1.7 Hz, 1H, H-4), 5.37 (dd, <sup>3</sup>J<sub>3,2</sub> = 10.5 Hz, <sup>3</sup>J<sub>3,4</sub> = 3.3 Hz, 1H, H-3), 4.26 (d, <sup>2</sup>J<sub>5a,5b</sub> = 13.2 Hz, 1H, H-5a), 4.13 (dd, <sup>3</sup>J<sub>1,2</sub> = 3.7 Hz, <sup>3</sup>J<sub>2,3</sub> = 10.5 Hz, 1H, H-2), 3.91 (dd, <sup>2</sup>J<sub>5a,5b</sub> = 13.4 Hz, <sup>3</sup>J<sub>5b,4</sub> = 1.9 Hz, 1H, H-5b), 2.17, 2.09 (each s, each 3H, OAc) ppm;

**<sup>13</sup>C NMR:** (125 MHz, CDCl<sub>3</sub>, 300 K, TMS):  $\delta$  = 169.91, 169.60 (2 C(O)CH<sub>3</sub>), 93.55 (C-1), 68.33 (C-3), 67.60 (C-4), 63.41 (C-5), 58.81 (C-2), 20.85, 20.63 (2 C(O)CH<sub>3</sub>) ppm;

**ESI-MS:**  $m/z$  = 300.0353 [M+Na]<sup>+</sup> (calculated  $m/z$  = 300.0357 for [M+Na]<sup>+</sup>).

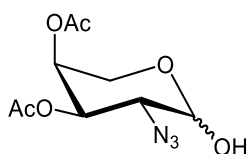
**[Bis(trifluoroacetoxy)iodo]benzene (PIFA) (95)<sup>[199]</sup>**

Iodobenzene (**94**, 1.10 mL, 10.0 mmol) was dissolved in CH<sub>2</sub>Cl<sub>2</sub> (10.0 mL) and TFA (30.0 mL, 88.9 mmol) was added followed by Oxone<sup>®</sup> (2.28 g, 15.0 mmol) and it was stirred for 3 h at room temperature. The solvent was removed under reduced pressure and the crude product was taken up in CH<sub>2</sub>Cl<sub>2</sub> and filtered. Recrystallization from cyclohexane gave the product **95** as a colorless solid.

**Yield:** 1.16 g (2.69 mmol, 27 %);

**<sup>1</sup>H NMR:** (500 MHz, CDCl<sub>3</sub>, 300 K, TMS): δ = 8.20 (dd, <sup>3</sup>J<sub>2,3</sub> = 8.5 Hz, <sup>4</sup>J<sub>2,4</sub> = 1.2 Hz, 2H, H-2), 7.75 (t, <sup>3</sup>J<sub>4,3</sub> = 7.4 Hz, <sup>4</sup>J<sub>4,2</sub> = 1.2 Hz, 1H, H-4), 7.75 (t, <sup>3</sup>J<sub>4,3</sub> = 7.6 Hz, <sup>3</sup>J<sub>3,2</sub> = 7.6 Hz, 1H, H-3) ppm;

**ESI-MS:** *m/z* = 452.9023 [M+Na]<sup>+</sup> (calculated *m/z* = 452.9034 for [M+Na]<sup>+</sup>).

**3,4-Di-O-acetyl-2-azido-2-deoxy-α/β-L-arabinopyranose (96)**

Arabinal **90** (50.0 mg, 250 μmol) was dissolved in CH<sub>2</sub>Cl<sub>2</sub> and TMSN<sub>3</sub> (99.5 μL, 750 μmol) was added. The mixture was cooled down to 0 °C and subsequently PIFA (**95**, 215 mg, 500 μmol), TEMPO (7.81 mg, 50.0 μmol), tetra-*n*-butyl ammonium hydrogen sulfate (17.0 mg, 50.0 μmol) and H<sub>2</sub>O were added. The mixture was stirred for 1 h. Then sodium bicarbonate solution was added and stirring was continued for further 15 min. The aqu. layer was extracted with CH<sub>2</sub>Cl<sub>2</sub>, and the combined org. layers were washed with H<sub>2</sub>O, dried over MgSO<sub>4</sub>, filtered, and concentrated. The crude product was purified by column chromatography on silica (cyclohexane/ ethyl acetate, 2:1) to obtain **96** as a colorless solid.

**Yield:** 33.0 mg (127 μmol, 51 %);

**R<sub>f</sub>:** (cyclohexane/ethyl acetate, 2:1): R<sub>f</sub> = 0.33;

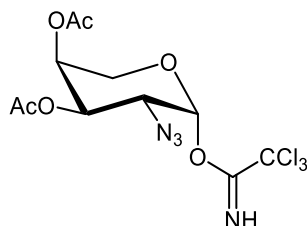
**IR (ATR):**  $\tilde{\nu}$  = 3358.28, 2113.8, 1741.0, 1224.83, 1069.65 cm<sup>-1</sup>;

**<sup>1</sup>H NMR:** (500 MHz, CDCl<sub>3</sub>, 300 K, TMS): β-anomer: δ = 5.43-5.40 (m, 1H, H-3), 5.39 (d, <sup>3</sup>J<sub>1,2</sub> = 3.4 Hz, 1H, H-1), 5.34 (dt, <sup>3</sup>J<sub>3,4</sub> = 3.4 Hz, <sup>3</sup>J<sub>5a,4</sub> = 1.8 Hz, <sup>3</sup>J<sub>5b,4</sub> = 1.8 Hz, 1H, H-4), 4.20 (dd, <sup>2</sup>J<sub>5a,5b</sub> = 13.1 Hz, <sup>3</sup>J<sub>5a,4</sub> = 1.2 Hz, 1H, H-5a), 3.80 (dd, <sup>3</sup>J<sub>1,2</sub> = 3.3 Hz, <sup>3</sup>J<sub>2,3</sub> = 10.8 Hz, 1H, H-2), 3.73 (dd, <sup>2</sup>J<sub>5a,5b</sub> = 13.1 Hz, <sup>3</sup>J<sub>5b,4</sub> = 2.1 Hz, 1H, H-5b), 2.15, 2.09 (each s, each 3H, OAc), 1.40 (s, 1H, OH) ppm; α-anomer: δ = 5.22 (dt, <sup>3</sup>J<sub>3,4</sub> = 3.5 Hz, <sup>3</sup>J<sub>5a,4</sub> = 1.8 Hz, <sup>3</sup>J<sub>5b,4</sub> = 1.8 Hz, 1H, H-4), 4.83 (dd, <sup>3</sup>J<sub>3,2</sub> = 10.7 Hz, <sup>3</sup>J<sub>3,4</sub> = 3.5 Hz, 1H, H-3), 4.63 (d, <sup>3</sup>J<sub>1,2</sub> = 7.9 Hz, 1H, H-1), 4.03 (dd, <sup>2</sup>J<sub>5a,5b</sub> = 13.5 Hz, <sup>3</sup>J<sub>5a,4</sub> = 2.1 Hz, 1H, H-5a), 3.68 (dd, <sup>3</sup>J<sub>1,2</sub> = 7.9 Hz, <sup>3</sup>J<sub>2,3</sub> = 10.6 Hz, 1H, H-2), 3.66 (dd, <sup>2</sup>J<sub>5a,5b</sub> = 13.5 Hz, <sup>3</sup>J<sub>5b,4</sub> = 1.2 Hz, 1H, H-5b), 2.18, 2.12 (each s, each 3H, OAc), 1.25 (s, 1H, OH) ppm;

**<sup>13</sup>C NMR:** (125 MHz, CDCl<sub>3</sub>, 300 K, TMS): β-anomer: δ = 169.91 (2 C(O)CH<sub>3</sub>), 92.61 (C-1), 68.54 (C-4), 67.94 (C-3), 60.76 (C-5), 58.41 (C-2), 20.93, 20.74 (2 C(O)CH<sub>3</sub>) ppm; α-anomer: δ = 170.23 (2 C(O)CH<sub>3</sub>), 96.80 (C-1), 70.93 (C-3), 67.40 (C-4), 64.50 (C-5), 62.34 (C-2), 20.89, 20.68 (2 C(O)CH<sub>3</sub>) ppm;

**ESI-MS:** *m/z* = 282.0694 [M+Na]<sup>+</sup> (calculated *m/z* = 282.0702 for [M+Na]<sup>+</sup>).

#### O-[3,4-Di-O-acetyl-2-azido-2-deoxy-β-L-arabinopyranosyl]-trichloroacetimidate (**97**)



The arabinose derivative **96** (259 mg, 1.00 mmol) was dissolved in dry CH<sub>2</sub>Cl<sub>2</sub> (10.0 mL) and the mixture was cooled down to 0 °C. Then DBU (44.0 μL, 300 μL) and Cl<sub>3</sub>CCN (1.00 mL, 10.0 mmol) were added. The reaction mixture was stirred for 3.5 h at 0 °C. Then the solvent was removed and purification by column chromatography on silica (cyclohexane/ ethyl acetate, 4:1) yielded **97** as a colorless solid.

**Yield:** 202 mg (500 μmol, 50 %);

**R<sub>f</sub>:** (cyclohexane/ethyl acetate, 4:1): R<sub>f</sub> = 0.42;

**[α]<sub>D</sub><sup>23</sup>:** +32.3 (c = 0.02, CH<sub>2</sub>Cl<sub>2</sub>);

**IR (ATR):**  $\tilde{\nu}$  = 3349.69, 2930.06, 2109.94, 1743.78, 1720.74, 1217.18, 1095.85 cm<sup>-1</sup>;

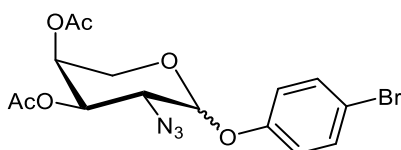
**<sup>1</sup>H NMR:** (500 MHz, CDCl<sub>3</sub>, 300 K, TMS): δ = 8.77 (s, 1H, NH), 6.47 (d, <sup>3</sup>J<sub>1,2</sub> = 3.5 Hz, 1H, H-1), 5.44 (dd, <sup>3</sup>J<sub>3,4</sub> = 4.0 Hz, <sup>3</sup>J<sub>5a,4</sub> = 1.0 Hz, <sup>3</sup>J<sub>5b,4</sub> = 1.0 Hz, 1H, H-4), 5.39 (dd, <sup>3</sup>J<sub>3,2</sub> = 11.0 Hz, <sup>3</sup>J<sub>3,4</sub> = 3.3 Hz, 1H, H-3), 4.15 (dd, <sup>2</sup>J<sub>5a,5b</sub> = 13.3 Hz, <sup>3</sup>J<sub>5a,4</sub> = 1.0 Hz, 1H, H-5a), 4.08 (dd, <sup>3</sup>J<sub>1,2</sub> =

3.5 Hz,  $^3J_{2,3} = 11.0$  Hz, 1H, H-2), 3.88 (dd,  $^2J_{5a,5b} = 13.3$  Hz,  $^3J_{5b,4} = 1.6$  Hz, 1H, H-5b), 2.17, 2.11 (each s, each 3H, OAc) ppm;

**$^{13}\text{C}$  NMR:** (125 MHz,  $\text{CDCl}_3$ , 300 K, TMS):  $\delta = 170.05$ , 169.74 (2  $\text{C}(\text{O})\text{CH}_3$ ), 160.82 ( $\text{C}\text{NH}$ ), 95.01 (C-1), 68.79 (C-3), 67.88 (C-4), 63.01 (C-5), 57.29 (C-2), 20.89, 20.71 (2  $\text{C}(\text{O})\text{CH}_3$ ) ppm;

**ESI-MS:**  $m/z = 424.9788$   $[\text{M}+\text{Na}]^+$  (calculated  $m/z = 424.9798$  for  $[\text{M}+\text{Na}]^+$ ).

#### 4-Bromophenyl 3,4-di-O-acetyl-2-azido-2-deoxy- $\alpha/\beta$ -L-arabinopyranoside (**99**)



##### Method A:

4-Bromophenole (**98**, 70.9 mg, 409  $\mu\text{mol}$ ) and TBAB (132 mg, 409  $\mu\text{mol}$ ) were dissolved in  $\text{CH}_2\text{Cl}_2$  (1.00 mL). Then a solution of CsOH (230 mg, 1.37 mmol) was added, and the mixture was stirred for 10 min at room temperature. Afterwards arabinosyl chloride **97** (76.0 mg, 273  $\mu\text{mol}$ ), dissolved in  $\text{CH}_2\text{Cl}_2$  (300  $\mu\text{L}$ ), was added dropwise. The reaction mixture was stirred for 1 h before it was diluted with  $\text{CH}_2\text{Cl}_2$ . The org. layer was washed with  $\text{H}_2\text{O}$  and brine, dried over  $\text{MgSO}_4$ , filtered of, and concentrated. Purification by column chromatography on silica (cyclohexane/ ethyl acetate, 3:1) gave **99** as a colorless solid.

**Yield:** 24.0 mg (57.9  $\mu\text{mol}$ , 21 %,  $\alpha:\beta = 3:1$ );

##### Method B:

The trichloroacetimidate **93** (300 mg, 747  $\mu\text{mol}$ ) and 4-bromophenole (**98**, 259 mg, 1.49 mmol) were dissolved in dry MeCN (5.00 mL) and the reaction mixture was cooled to  $-40$   $^\circ\text{C}$ . Then  $\text{BF}_3\cdot\text{Et}_2\text{O}$  (960  $\mu\text{L}$ , 7.07 mmol) was added and the reaction was stirred for 3 h. After full conversion sodium bicarbonate solution (12.0 mL) was added and it was filtered over celite<sup>®</sup>. The org. layer was washed with  $\text{H}_2\text{O}$ , sodium bicarbonate and brine, dried over  $\text{MgSO}_4$ , filtered of, and concentrated. Purification by column chromatography on silica (cyclohexane/ ethyl acetate, 3:1) yielded **99** as a colorless solid.

**Yield:** 279 mg (672  $\mu\text{mol}$ , 90 %,  $\alpha:\beta = 1:1$ );

**R<sub>f</sub>:** (cyclohexane/ethyl acetate, 1:1):  $R_f = 0.57$ ;

**$[\alpha]_D^{23}$ :** +6.43 ( $c = 0.02$ ,  $\text{CH}_2\text{Cl}_2$ );

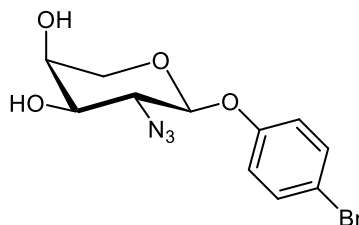
**IR (ATR):**  $\tilde{\nu} = 2822$ , 2111, 1732, 1220, 1094  $\text{cm}^{-1}$ ;

**<sup>1</sup>H NMR:** (500 MHz, CDCl<sub>3</sub>, 300 K, TMS): β-anomer: δ = 7.32 (d, <sup>3</sup>J = 9.0 Hz, 2H, OPhe-CH), 6.72 (d, <sup>3</sup>J = 9.0 Hz, 2H, OPhe-CH), 5.47 (d, <sup>3</sup>J<sub>1,2</sub> = 3.9 Hz, 1H, H-1), 5.36-5.32 (m, 1H, H-4), 5.20 (dd, <sup>3</sup>J<sub>3,2</sub> = 10.7 Hz, <sup>3</sup>J<sub>3,4</sub> = 3.3 Hz, 1H, H-3), 4.12-4.08 (m, 1H, H-5a), 3.95 (dd, <sup>3</sup>J<sub>1,2</sub> = 4.0 Hz, <sup>3</sup>J<sub>2,3</sub> = 10.7 Hz, 1H, H-2), 3.82 (dd, <sup>2</sup>J<sub>5a,5b</sub> = 13.3 Hz, <sup>3</sup>J<sub>5b,4</sub> = 2.2 Hz, 1H, H-5b), 2.17, 2.09 (each s, each 3H, OAc) ppm; α-anomer: δ = 7.43 (d, <sup>3</sup>J = 9.0 Hz, 2H, OPhe-CH), 6.97 (d, <sup>3</sup>J = 9.0 Hz, 2H, OPhe-CH), 5.30-5.27 (m, 1H, H-4), 4.87 (dd, <sup>3</sup>J<sub>3,2</sub> = 10.7 Hz, <sup>3</sup>J<sub>3,4</sub> = 3.4 Hz, 1H, H-3), 4.83 (d, <sup>3</sup>J<sub>1,2</sub> = 7.9 Hz, 1H, H-1), 4.11 (dd, <sup>2</sup>J<sub>5a,5b</sub> = 13.3 Hz, <sup>3</sup>J<sub>5a,4</sub> = 2.2 Hz, 1H, H-5a), 4.00 (dd, <sup>3</sup>J<sub>1,2</sub> = 7.9 Hz, <sup>3</sup>J<sub>2,3</sub> = 10.7 Hz, 1H, H-2), 3.73 (dd, <sup>2</sup>J<sub>5a,5b</sub> = 13.3 Hz, <sup>3</sup>J<sub>5b,4</sub> = 3.5 Hz, 1H, H-5b), 2.18, 2.11 (each s, each 3H, OAc) ppm;

**<sup>13</sup>C NMR:** (125 MHz, CDCl<sub>3</sub>, 300 K, TMS): β-anomer: δ = 171.32, 166.29 (2 C(O)CH<sub>3</sub>), 154.91 (OPhe-C<sub>quart</sub>), 132.56 (OPhe-CBr<sub>quart</sub>), 132.57 (2 OPhe-CH<sub>ortho</sub>), 118.59 (2 OPhe-CH<sub>meta</sub>), 88.66 (C-1), 68.35 (C-3), 67.97 (C-4), 62.56 (C-5), 60.07 (C-2), 20.88, 20.67 (2 C(O)CH<sub>3</sub>) ppm; α-anomer: δ = 175.62, 168.10 (2 C(O)CH<sub>3</sub>), 155.74 (OPhe-C<sub>quart</sub>), 132.43 (OPhe-CBr<sub>quart</sub>), 132.60 (2 OPhe-CH<sub>ortho</sub>), 118.91 (2 OPhe-CH<sub>meta</sub>), 101.13 (C-1), 70.55 (C-3), 67.97 (C-4), 62.56 (C-5), 60.07 (C-2), 20.88, 20.67 (2 C(O)CH<sub>3</sub>) ppm;

**ESI-MS:** *m/z* = 436.0111 [M+Na]<sup>+</sup> (calculated *m/z* = 436.0114 for [M+Na]<sup>+</sup>).

#### (4-Bromophenyl) 2-azido-2-deoxy-α-L-arabinopyranoside (**100**)



The α/β-arabinoside **99** (320 mg, 772 μmol) was dissolved in dry MeOH (15.0 mL) and at room temperature K<sub>2</sub>CO<sub>3</sub> (21.0 mg, 154 μmol) was added. The reaction mixture was stirred for 3 h before the solvent was removed under reduced pressure. Purification by column chromatography on silica (cyclohexane/ethyl acetate, 1:1) yielded **100** as a colorless solid.

**Yield:** 122 mg of the α-anomer (371 μmol, 48 %), 132 mg of the β-anomer (401 μmol, 52 %);

**R<sub>f</sub>:** (cyclohexane/ethyl acetate, 1:1): R<sub>f</sub> = 0.12;

**[α]<sub>D</sub><sup>23</sup>:** +32.5 (c = 0.02, CH<sub>2</sub>Cl<sub>2</sub>);

**IR (ATR):**  $\tilde{\nu}$  = 3294, 2922, 2857, 2108, 1720, 1259, 1078 cm<sup>-1</sup>;

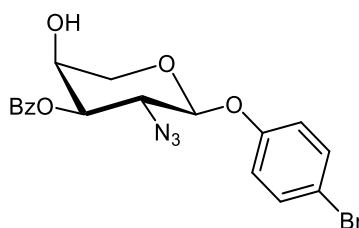
**<sup>1</sup>H NMR:** (500 MHz, CDCl<sub>3</sub>, 300 K, TMS): δ = 7.43 (d, <sup>3</sup>J = 9.0 Hz, 2H, OPhe-CH), 7.00 (d, <sup>3</sup>J = 9.0 Hz, 2H, OPhe-CH), 5.42-5.40 (m, 1H, H-4), 4.85 (d, <sup>3</sup>J<sub>1,2</sub> = 7.7 Hz, 1H, H-1), 4.29 (dd,

$^2J_{5a,5b} = 13.4$  Hz,  $^3J_{5a,4} = 2.2$  Hz, 1H, H-5a), 3.97 (dd,  $^3J_{1,2} = 7.7$  Hz,  $^3J_{2,3} = 10.1$  Hz, 1H, H-2), 3.84 (dd,  $^3J_{3,2} = 9.7$  Hz,  $^3J_{3,4} = 3.2$  Hz, 1H, H-3), 3.79 (dd,  $^2J_{5a,5b} = 13.4$  Hz,  $^3J_{5b,4} = 1.3$  Hz, 1H, H-5b), 2.25 (s, 1H, 3-OH), 1.26 (s, 1H, 4-OH) ppm;

$^{13}\text{C NMR}$ : (125 MHz,  $\text{CDCl}_3$ , 300 K, TMS):  $\delta = 155.83$  (OPhe- $\text{C}_{\text{quart}}$ ), 133.66 (Phe- $\text{CBr}_{\text{quart}}$ ), 132.58 (2 OPhe- $\text{CH}_{\text{ortho}}$ ), 118.87 (2 OPhe- $\text{CH}_{\text{meta}}$ ), 101.18 (C-1), 70.62 (C-3), 69.47 (C-4), 64.55 (C-5), 64.10 (C-2) ppm;

**ESI-MS**:  $m/z = 351.9899$   $[\text{M}+\text{Na}]^+$  (calculated  $m/z = 351.9903$  for  $[\text{M}+\text{Na}]^+$ ).

#### 4-Bromophenyl 2-azido-3-O-benzoyl-2-deoxy- $\alpha$ -L-arabinopyranoside (**101**)



The arabinoside **100** (52.0 mg, 158  $\mu\text{mol}$ ) was dissolved in dry pyridine (1.00 mL) and the mixture was cooled to  $-35$   $^{\circ}\text{C}$ . Then  $\text{BzCl}$  (18.2  $\mu\text{L}$ , 158  $\mu\text{mol}$ ) was added dropwise and it was allowed to warm to room temperature while stirring was continued for 2 h. Then the solvent was removed under reduced pressure and the crude product was taken up in  $\text{CH}_2\text{Cl}_2$  (10 mL). The org. layer was washed with 1N HCl, sodium bicarbonate solution and  $\text{H}_2\text{O}$ . The combined org. layers were dried over  $\text{MgSO}_4$ , filtered and the solvent was removed under reduced pressure. The crude product was purified by column chromatography on silica (cyclohexane/ethyl acetate, 2:1) to obtain **101** as a colorless solid.

**Yield**: 11.0 mg (25.3  $\mu\text{mol}$ , 17 %);

**R<sub>f</sub>**: (cyclohexane/ethyl acetate, 2:1):  $R_f = 0.45$ ;

$[\alpha]_{\text{D}}^{23}$ : +26.5 ( $c = 0.02$ ,  $\text{CH}_2\text{Cl}_2$ );

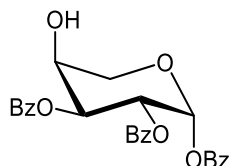
**IR (ATR)**:  $\tilde{\nu} = 3304, 2922, 2851, 2113, 1719, 1069$   $\text{cm}^{-1}$ ;

$^1\text{H NMR}$ : (500 MHz,  $\text{CDCl}_3$ , 300 K, TMS):  $\delta = 8.16$ – $8.12$  (m, 2H, 2 Bz- $\text{CH}_{\text{ortho}}$ ), 7.65–7.61 (m, 1H, Bz- $\text{CH}_{\text{para}}$ ), 7.52–7.47 (m, 2H, Bz- $\text{CH}_{\text{meta}}$ ), 7.43–7.39 (m, 2H, OPhe-CH), 7.02–6.98 (m, 2H, OPhe-CH), 5.06 (dd,  $^3J_{3,2} = 10.1$  Hz,  $^3J_{3,4} = 3.2$  Hz, 1H, H-3), 4.91 (d,  $^3J_{1,2} = 7.5$  Hz, 1H, H-1), 4.28–4.22 (m, 1H, H-4), 4.21 (dd,  $^3J_{1,2} = 7.5$  Hz,  $^3J_{2,3} = 10.1$  Hz, 1H, H-2), 4.15 (dd,  $^2J_{5a,5b} = 12.8$  Hz,  $^3J_{5a,4} = 2.8$  Hz, 1H, H-5a), 3.77 (dd,  $^2J_{5a,5b} = 12.8$  Hz,  $^3J_{5b,4} = 1.4$  Hz, 1H, H-5b), 2.25 (s, 1H, OH) ppm;

**$^{13}\text{C}$  NMR:** (125 MHz,  $\text{CDCl}_3$ , 300 K, TMS):  $\delta$  = 165.55 (C(O)Ph), 155.78 (OPhe- $\text{C}_{\text{quart}}$ ), 133.80 ( $\text{Bz-CH}_{\text{para}}$ ), 132.56 (OPhe- $\text{CH}_{\text{ortho}}$ ), 129.93 (2  $\text{Bz-CH}_{\text{ortho}}$ ), 129.01 ( $\text{Bz-C}_{\text{quart}}$ ), 128.65 (2  $\text{Bz-CH}_{\text{meta}}$ ), 118.99 (OPhe- $\text{CH}_{\text{meta}}$ ), 115.94 (Phe- $\text{CBr}_{\text{quart}}$ ), 100.94 (C-1), 73.41 (C-3), 66.03 (C-5), 65.99 (C-4), 60.91 (C-2) ppm;

**ESI-MS:**  $m/z$  = 456.0162  $[\text{M}+\text{Na}]^+$  (calculated  $m/z$  = 456.0171 for  $[\text{M}+\text{Na}]^+$ ).

### 1,2,3-Tri-O-benzoyl- $\beta$ -L-arabinopyranose (**103**)<sup>[205]</sup>

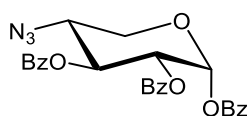


L-Arabinose (**85**, 20.0 g, 133 mmol) was dissolved in dry pyridine (650 mL), cooled down to  $-35\text{ }^\circ\text{C}$  and  $\text{BzCl}$  (48.3 mL, 399 mmol) was added dropwise to the solution. The reaction mixture was stirred for 16 h and it was allowed to warm to room temperature. Then, MeOH (40 mL) was added, and it was stirred for 15 min. The solvent was removed, and the crude product was taken up in ethyl acetate and it was washed with 1N HCl, sodium bicarbonate and brine. The combined org. layers were dried over  $\text{MgSO}_4$ , filtered, and concentrated. Purification by column chromatography on silica (cyclohexane:ethyl acetate, 3:1) yielded **103** as a colorless solid.

**Yield:** 27.7 g (59.9 mmol, 45 %);

The obtained analytical data are in agreement with reported literature.<sup>[205]</sup>

### 4-Azido-1,2,3-tri-O-benzoyl-4-deoxy- $\alpha$ -D-xylopyranose (**105**)<sup>[205]</sup>



The arabinose derivative **103** (13.8 g, 29.9 mmol) was dissolved in dry  $\text{CH}_2\text{Cl}_2$  (200 mL) and pyridine (4.50 mL) was added. Then at  $-35\text{ }^\circ\text{C}$   $\text{Tf}_2\text{O}$  (6.03 mL, 35.8 mmol) was added dropwise. The reaction mixture was stirred for 2 h. Then it was diluted with ethyl acetate and washed with 1N HCl, sodium bicarbonate and brine. It was dried over  $\text{MgSO}_4$ , filtered off and concentrated. The crude product was dissolved in dry DMF (140 mL), and  $\text{NaN}_3$  (7.78 g, 120 mmol) was added. The reaction mixture was stirred at room temperature for 2.5 h. Afterwards the solvent was removed under reduced pressure. The crude product was taken up in  $\text{CH}_2\text{Cl}_2$  and it was washed with  $\text{H}_2\text{O}$  and brine, dried over  $\text{MgSO}_4$ , filtered off and concentrated to dryness. Purification by flash column chromatography on silica (cyclohexane/ethyl acetate, 3:1) led to **105** as a colorless solid.

**Yield:** 9.86 g (20.2 mmol, 68 %);

**R<sub>f</sub>:** (cyclohexane/ethyl acetate, 3:1): R<sub>f</sub> = 0.44;

**[α]<sub>D</sub><sup>23</sup>:** +250.72 (c = 0.23, CH<sub>2</sub>Cl<sub>2</sub>);

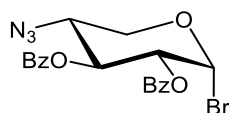
**IR (ATR):**  $\tilde{\nu}$  = 2109, 1726, 1601, 1452, 1257, 1085, 1067, 1018, 705, 686 cm<sup>-1</sup>;

**<sup>1</sup>H NMR:** (500 MHz, CDCl<sub>3</sub>, 300 K, TMS): δ = 8.18–7.81 (m, 6H, 6 Bz-CH<sub>ortho</sub>), 7.67–7.28 (m, 9H, 3 Bz-CH<sub>para</sub>, 6 Bz-CH<sub>meta</sub>), 6.69 (d, <sup>3</sup>J<sub>1,2</sub> = 3.6 Hz, 1H, H-1), 6.01 (t, <sup>3</sup>J<sub>2,3</sub> = 9.8 Hz, <sup>3</sup>J<sub>3,4</sub> = 9.8 Hz, 1H, H-3), 5.49 (dd, <sup>3</sup>J<sub>2,3</sub> = 10.1 Hz, <sup>3</sup>J<sub>1,2</sub> = 3.6 Hz, 1H, H-2), 4.13–4.00 (m, 2H, H-4, H-5a), 3.96–3.83 (m, 1H, H-5b), ppm;

**<sup>13</sup>C NMR:** (125 MHz, CDCl<sub>3</sub>, 300 K, TMS): δ = 165.69, 165.43, 164.52 (3 C(O)Ph), 133.91, 133.61, 133.52 (3 Bz-CH<sub>para</sub>), 129.95, 129.83, 129.82 (6 Bz-CH<sub>ortho</sub>), 128.88, 128.83 (2 Bz-C<sub>quart</sub>), 128.77, 128.54 (4 Bz-CH<sub>meta</sub>), 128.48 (Bz-C<sub>quart</sub>), 128.42 (2 Bz-CH<sub>meta</sub>), 90.20 (C-1), 71.02 (C-3), 70.38 (C-2), 61.96 (C-5), 59.48 (C-4) ppm;

**ESI-MS:** *m/z* = 510.1268 [M+Na]<sup>+</sup> (calculated *m/z* = 510.1271 for [M+Na]<sup>+</sup>).

#### 4-Azido-2,3-di-O-benzoyl-4-deoxy-α-D-xylopyranosyl bromide (106)



The xylose derivative **105** (2.00 g, 4.56 mmol) was dissolved in CH<sub>2</sub>Cl<sub>2</sub>/ ethyl acetate (100:1, 22.8 mL) and TiBr<sub>4</sub> (3.35 g, 9.12 mmol) was added. The reaction mixture was stirred for 16 h at room temperature. Then an excess of NaOAc was added, and it was stirred for 30 min. Afterwards it was diluted with CH<sub>2</sub>Cl<sub>2</sub>, and the org. layer was washed with H<sub>2</sub>O, it was dried over MgSO<sub>4</sub>, filtered off and concentrated. Purification by column chromatography on silica gel (cyclohexane/ethyl acetate, 5:1) gave the title compound as a colorless solid.

**Yield:** 970 mg (2.17 mmol, 48 %);

**R<sub>f</sub>:** (cyclohexane/ethyl acetate, 5:1): R<sub>f</sub> = 0.34;

**[α]<sub>D</sub><sup>23</sup>:** +132.27 (c = 0.2, CH<sub>2</sub>Cl<sub>2</sub>);

**IR (ATR):**  $\tilde{\nu}$  = 2927, 2109, 1725, 1451, 1247, 1091, 1025, 929, 704, 497 cm<sup>-1</sup>;

**<sup>1</sup>H NMR:** (500 MHz, CDCl<sub>3</sub>, 300 K, TMS): δ = 8.06–7.94 (m, 4H, 4 Bz-CH<sub>ortho</sub>), 7.59–7.51 (m, 2H, 2 Bz-CH<sub>para</sub>), 7.45–7.36 (m, 4H, 4 Bz-CH<sub>meta</sub>), 6.73 (d, <sup>3</sup>J<sub>1,2</sub> = 3.9 Hz, 1H, H-1), 5.95 (t, <sup>3</sup>J<sub>2,3</sub>

= 9.6 Hz,  ${}^3J_{3,4} = 9.6$  Hz, 1H, H-3), 5.15 (dd,  ${}^3J_{2,3} = 9.8$  Hz,  ${}^3J_{1,2} = 4.0$  Hz, 1H, H-2), 4.16–4.09 (m, 1H, H-5a), 4.04–3.95 (m, 2H, H-4, H-5b), ppm;

**${}^{13}\text{C}$  NMR:** (125 MHz,  $\text{CDCl}_3$ , 300 K, TMS):  $\delta = 166.36, 166.35$  (2 C(O)Ph), 133.81, 133.59 (2 Bz-CH<sub>para</sub>), 130.06, 129.82 (4 Bz-CH<sub>ortho</sub>), 128.80 (Bz-C<sub>quart</sub>), 128.56 (2 Bz-CH<sub>meta</sub>), 128.52 (2 Bz-CH<sub>meta</sub>), 128.31 (Bz-C<sub>quart</sub>), 87.61 (C-1), 71.36 (C-2), 71.12 (C-3), 63.76 (C-5), 58.84 (C-4) ppm;

**ESI-MS:**  $m/z = 468.0182$  [M+Na]<sup>+</sup> (calculated  $m/z = 468.0171$  for [M+Na]<sup>+</sup>).

#### 4-Amino-3-O-benzoyl-4-deoxy-D-xylal (**107**)



The xylosyl bromide **106** (501 mg, 1.12 mmol) was dissolved in dry MeCN (24 mL) and zinc (1.12 g, 17.1 mmol) and  $\text{NH}_4\text{Cl}$  (915 mg, 17.1 mmol) were added. The mixture was heated to 40 °C and stirred for 30 min. Then it was diluted with ethyl acetate and filtered over a pad of celite. The org. layer was washed with  $\text{H}_2\text{O}$ , dried over  $\text{MgSO}_4$ , filtered and the solvent was removed under reduced pressure. The crude product was purified by column chromatography (ethyl acetate/toluene/MeOH, 16:7:1) to give **107** as a colorless solid.

**Yield:** 90.8 mg (414  $\mu\text{mol}$ , 37 %);

**R<sub>f</sub>:** (ethyl acetate/toluene/MeOH, 16:7:1):  $R_f = 0.35$ ;

**$[\alpha]_D^{23}$ :** -223.73 ( $c = 0.24$ ,  $\text{CH}_2\text{Cl}_2$ );

**IR (ATR):**  $\tilde{\nu} = 2927, 1709, 1638, 1451, 1266, 1241, 1095, 1068, 943, 708, 499$   $\text{cm}^{-1}$ ;

**${}^1\text{H}$  NMR:** (500 MHz,  $\text{CDCl}_3$ , 300 K, TMS):  $\delta = 8.09$ – $8.00$  (m, 2H, 2 Bz-CH<sub>ortho</sub>), 7.63–7.54 (m, 1H, 1 Bz-CH<sub>para</sub>), 7.51–7.41 (m, 2H, 2 Bz-CH<sub>meta</sub>), 6.64 (d,  ${}^3J_{1,2} = 6.2$  Hz, 1H, H-1), 5.33 (t,  ${}^3J_{2,3} = 3.4$  Hz,  ${}^3J_{3,4} = 3.4$  Hz, 1H, H-3), 5.07 (ddd,  ${}^3J_{1,2} = 6.1$  Hz,  ${}^3J_{2,3} = 4.8$  Hz,  $J = 1.2$  Hz, 1H, H-2), 4.22 (ddd,  ${}^2J_{5a,5b} = 11.8$  Hz,  ${}^3J_{4,5a} = 4.1$  Hz,  $J = 1.4$  Hz, 1H, H-5a), 4.16 (dd,  ${}^2J_{5a,5b} = 11.9$  Hz,  ${}^3J_{4,5b} = 2.3$  Hz, 1H, H-5b), 3.90–3.80 (m, 1H, H-4), ppm;

**${}^{13}\text{C}$  NMR:** (125 MHz,  $\text{CDCl}_3$ , 300 K, TMS):  $\delta = 165.66$  (C(O)Ph), 148.32 (C-1), 133.54 (Bz-CH<sub>para</sub>), 129.81 (2 Bz-CH<sub>ortho</sub>), 129.72 (Bz-C<sub>quart</sub>), 128.64 (2 Bz-CH<sub>meta</sub>), 128.50 (Bz-C<sub>quart</sub>), 97.76 (C-2), 65.22 (C-3), 64.19 (C-5), 56.49 (C-4) ppm;

**ESI-MS:**  $m/z = 220.0967$  [M+H]<sup>+</sup> (calculated  $m/z = 220.0974$  for [M+H]<sup>+</sup>).

**4-Azido-3-O-benzoyl-4-deoxy-D-xylal (108)**

The amino xylal **107** (131 mg, 598  $\mu\text{mol}$ ) was dissolved in MeOH (4.0 mL) and  $\text{K}_2\text{CO}_3$  (179 mg, 1.30 mmol) and  $\text{CuSO}_4$  (2.00 mg, 8.01  $\mu\text{mol}$ ) were added followed by the addition of ISA (201 mg, 959  $\mu\text{mol}$ ). The reaction mixture was then stirred for 16 h at room temperature. Afterwards the solvent was removed under reduced pressure and the crude was taken up in ethyl acetate and washed with  $\text{H}_2\text{O}$ . The org. layer was dried over  $\text{MgSO}_4$ , filtered and the solvent was removed. The crude product was purified by column chromatography on silica (cyclohexane/ ethyl acetate, 9:1) to obtain **108** as a colorless solid.

**Yield:** 90.0 mg (367  $\mu\text{mol}$ , 49 %);

**R<sub>f</sub>**: (cyclohexane/ ethyl acetate, 3:1): R<sub>f</sub> = 0.45;

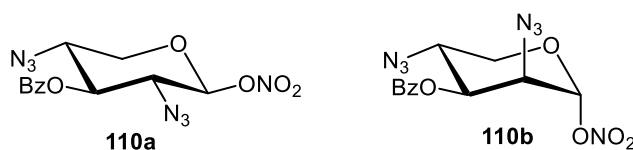
**[ $\alpha$ ]<sub>D</sub><sup>23</sup>:** -280.58 (c = 0.28,  $\text{CH}_2\text{Cl}_2$ );

**IR (ATR):**  $\tilde{\nu}$  = 2926, 2109, 1601, 1451, 1314, 1247, 1088, 1067, 706  $\text{cm}^{-1}$ ;

**<sup>1</sup>H NMR:** (500 MHz,  $\text{CDCl}_3$ , 300 K, TMS):  $\delta$  = 8.09–8.00 (m, 2H, 2 Bz-CH<sub>ortho</sub>), 7.63–7.54 (m, 1H, 1 Bz-CH<sub>para</sub>), 7.51–7.41 (m, 2H, 2 Bz-CH<sub>meta</sub>), 6.64 (d, <sup>3</sup>J<sub>1,2</sub> = 6.2 Hz, 1H, H-1), 5.33 (t, <sup>3</sup>J<sub>2,3</sub> = 3.4 Hz, <sup>3</sup>J<sub>3,4</sub> = 3.4 Hz, 1H, H-3), 5.07 (ddd, <sup>3</sup>J<sub>1,2</sub> = 6.1 Hz, <sup>3</sup>J<sub>2,3</sub> = 4.8 Hz, J = 1.2 Hz, 1H, H-2), 4.22 (ddd, <sup>2</sup>J<sub>5a,5b</sub> = 11.8 Hz, <sup>3</sup>J<sub>4,5a</sub> = 4.1 Hz, J = 1.4 Hz, 1H, H-5a), 4.16 (dd, <sup>2</sup>J<sub>5a,5b</sub> = 11.9 Hz, <sup>3</sup>J<sub>4,5b</sub> = 2.3 Hz, 1H, H-5b), 3.90–3.80 (m, 1H, H-4,) ppm;

**<sup>13</sup>C NMR:** (125 MHz,  $\text{CDCl}_3$ , 300 K, TMS):  $\delta$  = 165.66 (C(O)Ph), 148.32 (C-1), 133.54 (Bz-CH<sub>para</sub>), 129.81 (2 Bz-CH<sub>ortho</sub>), 129.72 (Bz-C<sub>quart</sub>), 128.64 (2 Bz-CH<sub>meta</sub>), 128.50 (Bz-C<sub>quart</sub>), 97.76 (C-2), 65.22 (C-3), 64.19 (C-5), 56.49 (C-4) ppm;

**ESI-MS:**  $m/z$  = 268.0688 [M+Na]<sup>+</sup> (calculated  $m/z$  = 268.0692 for [M+Na]<sup>+</sup>).

**3-O-benzoyl-2,4-diazido-2,4-dideoxy-D-xylopyranose nitrate (110a) and 3-O-benzoyl-2,4-diazido-2,4-dideoxy-D-lyxopyranose nitrate (110b)**

The glycal **109** (30.0 mg, 122  $\mu\text{mol}$ ) was dissolved in dry MeCN (1.50 mL) and at -20 °C CAN (201 mg, 367  $\mu\text{mol}$ ) and  $\text{NaN}_3$  (12.0 mg, 184  $\mu\text{mol}$ ) were added. The reaction mixture was stirred for 3 h. Then it was diluted with ethyl acetate and washed with  $\text{H}_2\text{O}$  and brine, dried

over  $\text{MgSO}_4$ , filtered, and concentrated to dryness. Purification by column chromatography on silica (cyclohexane/ethyl acetate, 9:1) gave the products as a colorless solid.

**Yield:** 12.0 mg (34.4  $\mu\text{mol}$ , 28 % ratio **110a**:**110b**: 1:2);

**R<sub>f</sub>:** (cyclohexane/ethyl acetate, 2:1):  $R_f = 0.66$ ;

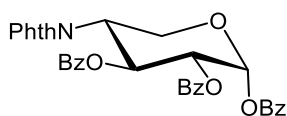
**IR (ATR):**  $\tilde{\nu} = 2921, 2109, 1727, 1656, 1451, 1261, 1090, 1069, 823, 708 \text{ cm}^{-1}$ ;

**<sup>1</sup>H NMR:** (500 MHz,  $\text{CDCl}_3$ , 300 K, TMS): **110a**:  $\delta = 8.06\text{--}8.01$  (m, 2H, 2 Bz- $\text{CH}_{\text{ortho}}$ ), 7.62–7.56 (m, 1H, Bz- $\text{CH}_{\text{para}}$ ), 7.49–7.43 (m, 2H, 2 Bz- $\text{CH}_{\text{meta}}$ ), 6.64 (d,  $^3J_{1,2} = 6.2 \text{ Hz}$ , 1H, H-1), 5.34–5.31 (m, 1H, H-3), 5.07 (dd,  $^3J_{2,3} = 9.6 \text{ Hz}$ ,  $^3J_{1,2} = 6.1 \text{ Hz}$ , 1H, H-2), 4.25–4.13 (m, 2H, H-5a, H-5b), 3.87–3.84 (m, 1H, H-4) ppm; **110b**:  $\delta = 8.14\text{--}8.08$  (m, 2H, 2 Bz- $\text{CH}_{\text{ortho}}$ ), 7.70–7.62 (m, 1H, Bz- $\text{CH}_{\text{para}}$ ), 7.53–7.49 (m, 2H, 2 Bz- $\text{CH}_{\text{meta}}$ ), 6.16 (d,  $^3J_{1,2} = 2.6 \text{ Hz}$ , 1H, H-1), 5.36 (dd,  $^3J_{2,3} = 3.7 \text{ Hz}$ ,  $^3J_{3,4} = 9.5 \text{ Hz}$ , 1H, H-3), 4.32 (dd,  $^3J_{2,3} = 3.5 \text{ Hz}$ ,  $^3J_{1,2} = 2.8 \text{ Hz}$ , 1H, H-2), 4.25–4.13 (m, 1H, H-4), 4.04 (dd,  $^3J_{4,5b} = 5.2 \text{ Hz}$ ,  $^2J_{5a,5b} = 11.9 \text{ Hz}$ , 1H, H-5b), 3.75 (dd,  $^3J_{4,5a} = 10.2 \text{ Hz}$ ,  $^2J_{5a,5b} = 11.9 \text{ Hz}$ , 1H, H-5a) ppm;

**<sup>13</sup>C NMR:** (125 MHz,  $\text{CDCl}_3$ , 300 K, TMS): **110a**:  $\delta = 165.50$  (C(O)Ph), 133.38 (Bz- $\text{CH}_{\text{para}}$ ), 129.66 (2 Bz- $\text{CH}_{\text{ortho}}$ ), 128.48 (2 Bz- $\text{CH}_{\text{meta}}$ ), 128.35 (Bz- $\text{C}_{\text{quart}}$ ), 97.61 (C-1), 65.08 (C-3), 64.04 (C-5), 56.34 (C-2), 55.74 (C-4) ppm; **110b**:  $\delta = 165.21$  (C(O)Ph), 134.10 (Bz- $\text{CH}_{\text{para}}$ ), 130.03 (2 Bz- $\text{CH}_{\text{ortho}}$ ), 128.76 (2 Bz- $\text{CH}_{\text{meta}}$ ), 128.20 (Bz- $\text{C}_{\text{quart}}$ ), 97.41 (C-1), 71.82 (C-3), 62.87 (C-5), 58.25 (C-2), 55.74 (C-4) ppm;

**ESI-MS:**  $m/z = 372.0647$  [ $\text{M}+\text{Na}$ ]<sup>+</sup> (calculated  $m/z = 372.0669$  for [ $\text{M}+\text{Na}$ ]<sup>+</sup>).

### 1,2,3-Tri-O-benzoyl-4-deoxy-4-phthalimido- $\alpha$ -D-xylopyranose (**114**)



The arabinose derivative **103** (11.5 g, 24.9 mmol) was dissolved in dry  $\text{CH}_2\text{Cl}_2$  (140 mL) and pyridine (3.50 mL) was added. It was cooled to  $-35 \text{ }^\circ\text{C}$  and  $\text{Tf}_2\text{O}$  (5.02 mL, 29.8 mmol) was added dropwise. The reaction mixture was stirred for 2 h and then diluted with ethyl acetate and washed with 1N HCl, sodium bicarbonate and brine. It was dried over  $\text{MgSO}_4$ , filtered and the solvent was removed. The crude product was dissolved in dry DMF (140 mL) and 18-crown-6 (13.2 g, 49.8 mmol) and potassium phthalimide (9.22 g, 49.8 mmol) were added. The reaction mixture was stirred at room temperature for 16 h. Afterwards, the solvent was removed. The crude product was taken up in  $\text{CH}_2\text{Cl}_2$  and it was washed with  $\text{H}_2\text{O}$  and brine, dried over  $\text{MgSO}_4$ , filtered, and concentrated. Purification by flash column chromatography on silica (cyclohexane/ ethyl acetate, 3:1) gave **114** as a colorless solid.

**Yield:** 11.5 g (19.4 mmol, 78 % over 2 steps);

**R<sub>f</sub>**: (cyclohexane/ethyl acetate, 2:1): R<sub>f</sub> = 0.49;

**[α]<sub>D</sub><sup>23</sup>**: +202.2 (c = 0.05, CH<sub>2</sub>Cl<sub>2</sub>);

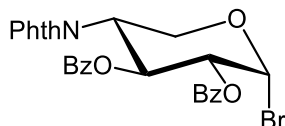
**IR (ATR)**:  $\tilde{\nu}$  = 3344, 2978, 1777, 1731, 1382, 1247, 1083, 1017, 704, 685, 641 cm<sup>-1</sup>;

**<sup>1</sup>H NMR**: (600 MHz, CDCl<sub>3</sub>, 300 K):  $\delta$  = 8.38–8.31 (m, 2H, 2 Bz-CH<sub>ortho</sub>), 7.90–7.79 (m, 6H, 2 NPhth-CH<sub>ortho</sub>, 2 NPhth-CH<sub>meta</sub>, 2 Bz-CH<sub>ortho</sub>), 7.73–7.69 (m, 2H, 2 Bz-CH<sub>ortho</sub>), 7.70–7.56 (m, 3H, 3 Bz-CH<sub>para</sub>), 7.48–7.26 (m, 6H, 6 Bz-CH<sub>meta</sub>), 6.80 (d, <sup>3</sup>J<sub>1,2</sub> = 3.5 Hz, 1H, H-1), 6.75 (t, <sup>3</sup>J<sub>2,3</sub> = 9.9 Hz, <sup>3</sup>J<sub>4,3</sub> = 9.9 Hz, 1H, H-3), 5.64 (dd, <sup>3</sup>J<sub>2,3</sub> = 9.8 Hz, <sup>3</sup>J<sub>1,2</sub> = 3.6 Hz, 1H, H-2), 5.01–4.86 (m, 2H, H-4, H-5a), 3.95–3.87 (m, 1H, H-5b) ppm;

**<sup>13</sup>C NMR**: (125 MHz, CDCl<sub>3</sub>, 300 K):  $\delta$  = 167.79 (2 C(O)Phth), 165.98, 165.60, 164.84 (3 C(O)Ph), 134.49 (2 Phth-CH<sub>meta</sub>), 133.97, 133.54, 133.48 (3 Bz-CH<sub>para</sub>), 130.43, 129.99, 129.90 (6 Bz-CH<sub>ortho</sub>), 129.20 (Bz-C<sub>quart</sub>), 128.97 (2 Bz-CH<sub>meta</sub>), 128.87, 128.84 (Bz-C<sub>quart</sub>), 128.51 (4 Bz-CH<sub>meta</sub>), 123.83 (2 Phth-CH<sub>ortho</sub>), 90.30 (C-1), 71.34 (C-2), 68.40 (C-3), 59.58 (C-5), 50.01 (C-4) ppm;

**ESI-MS**: *m/z* = 614.1417 [M+Na]<sup>+</sup> (calculated *m/z* = 614.1422 for [M+Na]<sup>+</sup>).

### 2,3-Di-O-benzoyl-4-deoxy-4-phthalimido- $\alpha$ -D-xylopyranosyl bromide (**115**)



The xylose derivative **114** (6.73 g, 11.4 mmol) was dissolved in dry CH<sub>2</sub>Cl<sub>2</sub> (30 mL) and at 0 °C HBr in AcOH (33 wt. %, 33.5 mL) was added dropwise. The reaction mixture was allowed to warm up to room temperature and stirring was continued for 2 h. Then it was diluted with CH<sub>2</sub>Cl<sub>2</sub> and washed successfully with sodium bicarbonate and brine. It was dried over MgSO<sub>4</sub>, filtered, and concentrated to dryness. Purification by flash column chromatography on silica (toluene/ ethyl acetate, 9:1) led to **115** as a colorless solid.

**Yield:** 5.82 g (10.6 mmol, 93 %);

**R<sub>f</sub>**: (toluene/ethyl acetate, 9:1): R<sub>f</sub> = 0.50;

**[α]<sub>D</sub><sup>23</sup>**: +38.46 (c = 0.05, CH<sub>2</sub>Cl<sub>2</sub>);

**IR (ATR)**:  $\tilde{\nu}$  = 2251, 1777, 1717, 1601, 1380, 1263, 1112, 1091, 1068, 707 cm<sup>-1</sup>;

**<sup>1</sup>H NMR:** (500 MHz, CDCl<sub>3</sub>, 298 K, TMS): δ = 7.98–7.89 (m, 4H, 4 Bz-CH<sub>ortho</sub>), 7.80–7.60 (m, 4H, 2 NPhth-CH<sub>ortho</sub>, 2 NPhth-CH<sub>meta</sub>), 7.54–7.20 (m, 6H, 2 Bz-CH<sub>para</sub>, 4 Bz-CH<sub>meta</sub>), 6.74 (d, <sup>3</sup>J<sub>1,2</sub> = 4.0 Hz, 1H, H-1), 6.54 (t, <sup>3</sup>J<sub>2,3</sub> = 9.9 Hz, <sup>3</sup>J<sub>3,4</sub> = 9.9 Hz, 1H, H-3), 5.25 (dd, <sup>3</sup>J<sub>2,3</sub> = 9.6 Hz, <sup>3</sup>J<sub>1,2</sub> = 4.0 Hz, 1H, H-2), 4.98 (t, <sup>2</sup>J<sub>5a,5b</sub> = 11.4 Hz, <sup>3</sup>J<sub>4,5a</sub> = 11.4 Hz, 1H, H-5a), 4.77 (ddd, <sup>3</sup>J<sub>4,5a</sub> = 11.8 Hz, <sup>3</sup>J<sub>4,3</sub> = 10.3 Hz, <sup>3</sup>J<sub>4,5b</sub> = 5.3 Hz, 1H, H-4), 3.90 (dd, <sup>2</sup>J<sub>5a,5b</sub> = 10.9 Hz, <sup>3</sup>J<sub>4,5b</sub> = 5.3 Hz, 1H, H-5b) ppm;

**<sup>13</sup>C NMR:** (125 MHz, CDCl<sub>3</sub>, 298 K, TMS): δ = 167.62 (2 C(O)Phth), 165.59, 165.52 (2 C(O)Ph), 134.55 (2 Phth-CH<sub>meta</sub>), 133.85, 133.48 (2 Bz-CH<sub>para</sub>), 131.50 (Bz-C<sub>quart</sub>), 130.22, 129.89 (4 Bz-CH<sub>ortho</sub>), 129.18 (Bz-C<sub>quart</sub>), 128.66, 128.50 (4 Bz-CH<sub>meta</sub>), 123.86 (2 Phth-CH<sub>ortho</sub>), 87.58 (C-1), 72.41 (C-2), 68.57 (C-3), 61.84 (C-5), 49.45 (C-4) ppm;

**ESI-MS:** *m/z* = 572.0317 [M+Na]<sup>+</sup> (calculated *m/z* = 572.0315 for [M+Na]<sup>+</sup>).

### 3-O-Benzoyl-4-deoxy-4-phthalimido-D-xylal (**116**)



Vitamine B-12 (97.3 mg, 71.8 μmol) was dissolved in dry MeOH (25 mL) and zinc (5.63 g, 86.2 mmol) and NH<sub>4</sub>Cl (2.89 g, 86.2 mmol) were added. The suspension was stirred vigorously for 45 min. Then, xylose bromide **115** (3.95 g, 7.18 mmol) was dissolved in dry CH<sub>2</sub>Cl<sub>2</sub> (10 mL) and added to the reaction mixture. Stirring at room temperature was continued for 20 min. The mixture was diluted with CH<sub>2</sub>Cl<sub>2</sub> and filtered over a pad of celite. The org. layer was washed with H<sub>2</sub>O, and it was extracted with CH<sub>2</sub>Cl<sub>2</sub>. The combined org. layers were dried over MgSO<sub>4</sub>, filtered, and concentrated. Purification by flash column chromatography on silica (cyclohexane/ethyl acetate, 3:1) gave **116** as a colorless solid.

**Yield:** 2.08 g (5.96 mmol, 83 %);

**R<sub>f</sub>:** (cyclohexane/ethyl acetate, 2:1): R<sub>f</sub> = 0.40;

**[α]<sub>D</sub><sup>23</sup>:** -207.82 (c = 0.05, CH<sub>2</sub>Cl<sub>2</sub>);

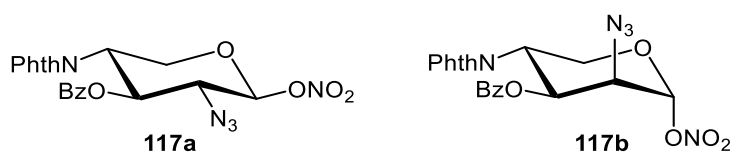
**IR (ATR):**  $\tilde{\nu}$  = 3061, 2249, 1778, 1708, 1645, 1379, 1268, 1069, 910, 711 cm<sup>-1</sup>;

**<sup>1</sup>H NMR:** (500 MHz, CDCl<sub>3</sub>, 298 K, TMS): δ = 7.95–7.92 (m, 2H, 2 Bz-CH<sub>ortho</sub>), 7.85–7.81 (m, 2H, 2 NPhth-CH<sub>ortho</sub>), 7.74–7.68 (m, 2H, 2 NPhth-CH<sub>meta</sub>), 7.54–7.49 (m, 1H, 2 Bz-CH<sub>para</sub>), 7.42–7.36 (m, 2H, 2 Bz-CH<sub>meta</sub>), 6.56 (dd, <sup>4</sup>J<sub>1,3</sub> = 6.1 Hz, <sup>3</sup>J<sub>1,2</sub> = 1.4 Hz, 1H, H-1), 6.32–6.27 (m, 1H, H-3), 4.99 (dd, <sup>3</sup>J<sub>2,3</sub> = 6.1 Hz, <sup>3</sup>J<sub>1,2</sub> = 1.4 Hz, 1H, H-2), 4.91 (ddd, <sup>3</sup>J<sub>4,5a</sub> = 12.0 Hz, <sup>3</sup>J<sub>4,3</sub> = 8.7 Hz, <sup>3</sup>J<sub>4,5b</sub> = 4.1 Hz, 1H, H-4), 4.81 (dd, <sup>3</sup>J<sub>5a,4</sub> = 12.0 Hz, <sup>2</sup>J<sub>5a,5b</sub> = 10.6 Hz, 1H, H-5a), 4.11 (dd, <sup>2</sup>J<sub>5a,5b</sub> = 10.6 Hz, <sup>3</sup>J<sub>5b,4</sub> = 4.1 Hz, 1H, H-5b) ppm;

**<sup>13</sup>C NMR:** (125 MHz, CDCl<sub>3</sub>, 298 K, TMS): δ = 167.78 (2 C(O)Phth), 166.23 (C(O)Ph), 146.79 (C-1), 134.25 (2 Phth-CH<sub>meta</sub>), 133.11 (Bz-CH<sub>para</sub>), 131.56 (Bz-C<sub>quart</sub>), 129.70 (2 Bz-CH<sub>ortho</sub>), 128.36 (2 Bz-CH<sub>meta</sub>), 123.56 (2 Phth-CH<sub>ortho</sub>), 100.47 (C-2), 67.66 (C-3), 65.04 (C-5), 49.02 (C-4) ppm;

**ESI-MS:** *m/z* = 372.0840 [M+Na]<sup>+</sup> (calculated *m/z* = 372.0842 for [M+Na]<sup>+</sup>).

**2-Azido-3-O-benzoyl-2-azido-2,4-dideoxy-4-phthalimido-D-xylopyranose nitrate (117a) and 2-Azido-3-O-benzoyl-2-azido-2,4-dideoxy-4-phthalimido-D-lyxopyranose nitrate (117b)**



Xylal **116** (20.0 mg, 57.3 μmol) was dissolved in dry MeCN (1.00 mL) and at -20 °C CAN (94.2 mg, 172 μmol) and NaN<sub>3</sub> (5.59 mg, 86.0 μmol) were added. The reaction mixture was stirred for 3 h. Then it was diluted with ethyl acetate and washed with H<sub>2</sub>O and brine, dried over MgSO<sub>4</sub>, filtered, and concentrated. Purification by column chromatography on silica (cyclohexane/ethyl acetate, 3:1) gave the products as a colorless solid.

**Yield:** 13.0 mg (28.7 μmol, 50 %, ratio **117a:117b**: 2:1);

**R<sub>f</sub>:** (cyclohexane/ethyl acetate, 2:1): R<sub>f</sub> = 0.26;

**IR (ATR):**  $\tilde{\nu}$  = 2112, 1776, 1716, 1451, 1386, 1266, 1111, 1070, 712, 530 cm<sup>-1</sup>;

**<sup>1</sup>H NMR:** (500 MHz, CDCl<sub>3</sub>, 300 K, TMS): **117a**: δ = 7.90–7.85 (m, 2H, 2 Bz-CH<sub>ortho</sub>), 7.83–7.79 (m, 2H, 2 NPhth-CH<sub>ortho</sub>), 7.73–7.68 (m, 2H, 2 NPhth-CH<sub>meta</sub>), 7.57–7.51 (m, 1H, Bz-CH<sub>para</sub>), 7.42–7.36 (m, 2H, 2 Bz-CH<sub>meta</sub>), 6.01 (t, <sup>3</sup>J<sub>2,3</sub> = 9.9 Hz, <sup>3</sup>J<sub>3,4</sub> = 9.9 Hz, 1H, H-3), 5.82 (d, <sup>3</sup>J<sub>1,2</sub> = 8.8 Hz, 1H, H-1), 4.76–4.64 (m, 1H, H-4), 4.58 (t, <sup>3</sup>J<sub>4,5a</sub> = 11.4 Hz, <sup>2</sup>J<sub>5a,5b</sub> = 11.4 Hz, 1H, H-5a), 4.04 (dd, <sup>3</sup>J<sub>4,5b</sub> = 5.3 Hz, <sup>2</sup>J<sub>5a,5b</sub> = 11.5 Hz, 1H, H-5b), 3.84 (dd, <sup>3</sup>J<sub>2,3</sub> = 9.6 Hz, <sup>3</sup>J<sub>1,2</sub> = 8.8 Hz, 1H, H-2) ppm; **117b**: δ = 7.95–7.91 (m, 2H, 2 Bz-CH<sub>ortho</sub>), 7.83–7.79 (m, 2H, 2 NPhth-CH<sub>ortho</sub>), 7.73–7.68 (m, 2H, 2 NPhth-CH<sub>meta</sub>), 7.57–7.51 (m, 1H, Bz-CH<sub>para</sub>), 7.42–7.36 (m, 2H, 2 Bz-CH<sub>meta</sub>), 6.28 (d, <sup>3</sup>J<sub>1,2</sub> = 2.0 Hz, 1H, H-1), 6.19 (t, <sup>3</sup>J<sub>2,3</sub> = 3.9 Hz, <sup>3</sup>J<sub>3,4</sub> = 10.6 Hz, 1H, H-3), 5.11–5.04 (m, 1H, H-4), 4.76–4.64 (m, 1H, H-5a), 4.52 (dd, <sup>3</sup>J<sub>2,3</sub> = 3.8 Hz, <sup>3</sup>J<sub>1,2</sub> = 2.0 Hz, 1H, H-2), 3.90 (dd, <sup>3</sup>J<sub>4,5b</sub> = 5.5 Hz, <sup>2</sup>J<sub>5a,5b</sub> = 11.2 Hz, 1H, H-5b) ppm;

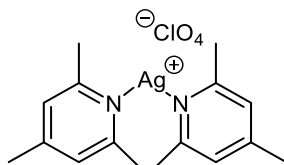
**<sup>13</sup>C NMR:** (125 MHz, CDCl<sub>3</sub>, 300 K, TMS): **117a**: 167.68 (2 C(O)Phth), 165.49 (C(O)Ph), 134.61 (2 Phth-CH<sub>meta</sub>), 133.88 (Bz-CH<sub>para</sub>), 131.39 (Bz-C<sub>quart</sub>), 130.01 (2 Bz-CH<sub>ortho</sub>), 129.19 (2 Bz-CH<sub>meta</sub>), 125.45 (2 Phth-CH<sub>ortho</sub>), 98.93 (C-1), 71.11 (C-3), 62.53 (C-5), 61.97 (C-2), 49.76 (C-4) ppm; **117b**: 167.68 (2 C(O)Phth), 165.49 (C(O)Ph), 134.61 (2 Phth-CH<sub>meta</sub>), 133.88 (Bz-

CH<sub>para</sub>), 131.39 (Bz-C<sub>quart</sub>), 130.01 (2 Bz-CH<sub>ortho</sub>), 129.19 (2 Bz-CH<sub>meta</sub>), 125.45 (2 Phth-CH<sub>ortho</sub>), 97.88 (C-1), 68.15 (C-3), 59.16 (C-2), 60.60 (C-5), 45.83 (C-4) ppm;

**ESI-MS:**  $m/z = 330.0551$  [M+Na]<sup>+</sup> (calculated  $m/z = 330.0576$  for [M+Na]<sup>+</sup>).

## 8.2.4 Synthetic procedures for chapter 4.3

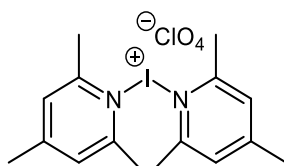
### Silver di-*sym*-collidine perchlorate (**123**)<sup>[223]</sup>



Sodium perchlorate (11.1 g, 91.0 mmol) and silver nitrate (9.03 g, 53.2 mmol) were dissolved in H<sub>2</sub>O (90 mL). Then *sym*-collidine (20.0 mL, 151 mmol) was added and the suspension was stirred for 5 min and was then filtrated and washed with H<sub>2</sub>O, EtOH, and Et<sub>2</sub>O. The crude product was not further purified and subsequently used in the next reaction.

Analytical data corresponds to the literature.<sup>[223]</sup>

### Iodonium di-*sym*-collidine perchlorate (**124**)<sup>[223]</sup>

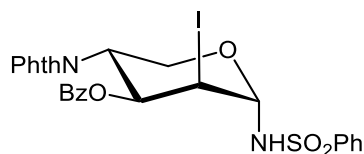


Silver di-*sym*-collidine perchlorate (**123**, 18.4 g, 40.9 mmol) was suspended in dry CH<sub>2</sub>Cl<sub>2</sub> (95.0 mL) and *sym*-collidine (2.00 mL) was added, followed by iodine (9.83 g) It was stirred for 15 min at room temperature and then filtered over a pad of celite. The targeted **124** crystallized from the filtrate (16 h, 6 °C). Then it was filtrated and dried under reduced pressure

**Yield:** 18.4 g (39.3 mmol, 96 %);

**Smp:** 126.9 °C.

### 3-O-Benzoyl-2-iodo-4-phthalimido-1,2,4-trideoxy- $\alpha$ -D-lyxopyranosyl benzenesulfonamide (**126**)



The xylal **116** (40.0 mg, 115  $\mu$ mol) and benzene sulfonamide (21.6 mg, 137  $\mu$ mol) were dissolved in dry  $\text{CH}_2\text{Cl}_2$  (1.5 mL) and 4 Å molecular sieve was added. It was stirred for 30 min at room temperature. Then at 0 °C IDCP (80.9 mg, 173  $\mu$ mol) was added. It was allowed to warm to room temperature and stirring was continued for 3 h. The reaction mixture was diluted with ethyl acetate and filtered over a pad of celite. Then the org. layer was washed with sodium thiosulfate, copper sulfate and brine, dried over  $\text{MgSO}_4$ , filtered, and concentrated to dryness. Purification by column chromatography on silica (cyclohexane/ethyl acetate, 7:3) gave the product **126** as a colorless solid.

**Yield:** 45.0 mg (71.2  $\mu$ mol, 62 %);

**R<sub>f</sub>:** (cyclohexane/ethyl acetate, 2:1): R<sub>f</sub> = 0.24;

**[ $\alpha$ ]<sub>D</sub><sup>23</sup>:** +5.25 (c = 0.01,  $\text{CH}_2\text{Cl}_2$ );

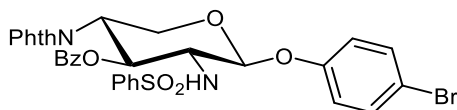
**IR (ATR):**  $\tilde{\nu}$  = 1713, 1449, 1384, 1263, 1070, 872, 711, 597  $\text{cm}^{-1}$ ;

**<sup>1</sup>H NMR:** (500 MHz,  $\text{CDCl}_3$ , 300 K, TMS):  $\delta$  = 7.96–7.90 (m, 4H, 2 Bz- $\text{CH}_{\text{ortho}}$ , 2  $\text{SO}_2\text{Ph-CH}_{\text{ortho}}$ ), 7.82–7.77 (m, 2H, 2 NPhth- $\text{CH}_{\text{ortho}}$ ), 7.71–7.67 (m, 2H, 2 NPhth- $\text{CH}_{\text{meta}}$ ), 7.56–7.50 (m, 4H, 2 Bz- $\text{CH}_{\text{meta}}$ , 2  $\text{SO}_2\text{Ph-CH}_{\text{meta}}$ ), 7.40–7.35 (m, 2H, Bz- $\text{CH}_{\text{para}}$ ,  $\text{SO}_2\text{Ph-CH}_{\text{para}}$ ), 5.56 (d,  $^3J_{\text{NH},1}$  = 10.6 Hz, 1H, NH), 5.41 (dd,  $^3J_{3,4}$  = 10.6 Hz,  $^3J_{2,3}$  = 4.1 Hz, 1H, H-3), 5.02 (dd,  $^3J_{2,3}$  = 4.2 Hz,  $^3J_{1,2}$  = 1.6 Hz, 1H, H-2), 4.92–4.85 (m, 1H, H-4), 4.43 (dd,  $^3J_{1,2}$  = 10.7 Hz,  $^3J_{\text{NH},1}$  = 1.6 Hz, 1H, H-1), 4.26 (t,  $^3J_{5a,4}$  = 11.5 Hz,  $^2J_{5a,5b}$  Hz, 1H, H-5a), 3.77 (dd,  $^2J_{5a,5b}$  = 11.5 Hz,  $^3J_{5b,4}$  = 5.6 Hz, 1H, H-5b) ppm;

**<sup>13</sup>C NMR:** (125 MHz,  $\text{CDCl}_3$ , 300 K, TMS):  $\delta$  = 164.65 (2 C(O)Phth), 140.92 (C(O)Ph), 134.44 (2 Phth- $\text{CH}_{\text{meta}}$ ), 133.62 ( $\text{SO}_2\text{Ph-C}_{\text{quart}}$ ), 133.15 (Bz- $\text{C}_{\text{quart}}$ ), 130.06 (2 Bz- $\text{CH}_{\text{ortho}}$ ), 129.06 (2  $\text{SO}_2\text{Ph-CH}_{\text{meta}}$ , 2 Bz- $\text{CH}_{\text{meta}}$ ), 128.25 ( $\text{SO}_2\text{Ph-CH}_{\text{para}}$ , Bz- $\text{CH}_{\text{para}}$ ), 127.05 (2  $\text{SO}_2\text{Ph-CH}_{\text{ortho}}$ ), 123.73 (2 Phth- $\text{CH}_{\text{ortho}}$ ), 80.59 (C-1), 68.51 (C-3), 63.80 (C-5), 47.86 (C-4), 40.74 (C-2) ppm;

**ESI-MS:**  $m/z$  = 654.9993 [ $\text{M}+\text{Na}$ ]<sup>+</sup> (calculated  $m/z$  = 655.0006 for [ $\text{M}+\text{Na}$ ]<sup>+</sup>).

#### 4-Bromophenyl 3-O-benzoyl-2,4-dideoxy-4-phthalimido-2-[phenylsulfonamido]- $\beta$ -D-xylopyranoside (**127**)



The iodosulfonamide **126** (15.0 mg, 23.7  $\mu$ mol) and 4-Bromophenole (6.15 mg, 35.6  $\mu$ mol) were dissolved in dry THF (500  $\mu$ L). Then at  $-78$   $^{\circ}$ C LiHMDS (1M in THF, 52.1  $\mu$ L, 52.1  $\mu$ mol) was added dropwise. It was stirred for 10 min before a solution of AgOTf (9.15 mg, 35.6  $\mu$ mol, in 50  $\mu$ L THF) was added to the reaction mixture. The flask was covered with foil, and it was allowed to warm to room temperature. The reaction was stirred for 16 h. Then an excess of  $\text{NH}_4\text{Cl}$  was added, and it was stirred for further 10 min before it was filtered over a pad of celite and concentrated to dryness. The crude product was purified by column chromatography on silica (cyclohexane/ethyl acetate, 2:1), which gave the title compound as a colorless solid.

**Yield:** 11.0 mg (16.2  $\mu$ mol, 69 %);

**R<sub>f</sub>:** (toluene/ethyl acetate, 85:15):  $R_f = 0.28$ ;

**$[\alpha]_D^{23}$ :** +21.5 ( $c = 0.02$ ,  $\text{CH}_2\text{Cl}_2$ );

**IR (ATR):**  $\tilde{\nu} = 2252, 1712, 1486, 1382, 1266, 1233, 1066, 986, 711, 686, 587$   $\text{cm}^{-1}$ ;

**$^1\text{H NMR}$ :** (500 MHz,  $\text{CDCl}_3$ , 300 K, TMS):  $\delta = 7.77\text{--}7.70$  (m, 2H, Bz- $\text{CH}_{\text{ortho}}$ ), 7.65-7.59 (m, 4H, NPhth-CH), 7.53-7.45 (m, 1H, Bz- $\text{CH}_{\text{para}}$ ), 7.35-7.24 (m, 6H, BrPh- $\text{CH}_{\text{ortho}}$ ,  $\text{SO}_2\text{Ph-CH}_{\text{ortho}}$ ,  $\text{SO}_2\text{Ph-CH}_{\text{meta}}$ ), 7.21-7.07 (m, 3H,  $\text{SO}_2\text{Ph-CH}_{\text{para}}$ , Bz- $\text{CH}_{\text{meta}}$ ), 6.77-6.68 (m, 2H, BrPh- $\text{CH}_{\text{meta}}$ ), 6.15 (t,  $^3J_{3,4} = 10.4$  Hz,  $^3J_{2,3} = 10.4$  Hz, 1H, H-3), 5.67 (d,  $^3J_{\text{NH},2} = 8.8$  Hz, 1H, NH), 5.27 (d,  $^3J_{1,2} = 8.0$  Hz, 1H, H-1), 4.78 (td,  $^3J_{3,4} = 10.7$  Hz,  $^3J_{5a,4} = 10.7$  Hz,  $^3J_{5b,4} = 5.3$  Hz, 1H, H-4), 4.56 (t,  $^3J_{5a,4} = 11.3$  Hz,  $^2J_{5a,5b} = 11.3$  Hz, 1H, H-5a), 4.15-4.01 (m, 2H, H-2, H-5b) ppm;

**$^{13}\text{C NMR}$ :** (125 MHz,  $\text{CDCl}_3$ , 300 K, TMS):  $\delta = 167.84, 166.88$  (2 C(O)Phth), 156.23 (C(O)Ph), 141.75 (BrPh- $\text{C}_{\text{quart}}$ ), 134.59 (2 Phth- $\text{CH}_{\text{meta}}$ ), 133.74 ( $\text{SO}_2\text{Ph-C}_{\text{quart}}$ ), 132.61 (Bz- $\text{C}_{\text{quart}}$ ), 132.40 (BrPh- $\text{CH}_{\text{ortho}}$ ), 132.09 (2 Bz- $\text{CH}_{\text{ortho}}$ ), 131.24 (2  $\text{SO}_2\text{Ph-CH}_{\text{meta}}$ ), 130.29 (2 Bz- $\text{CH}_{\text{meta}}$ ), 128.77 ( $\text{SO}_2\text{Ph-CH}_{\text{para}}$ ), 128.43 (Bz- $\text{CH}_{\text{para}}$ ), 126.82 (2  $\text{SO}_2\text{Ph-CH}_{\text{ortho}}$ ), 123.77 (2 Phth- $\text{CH}_{\text{ortho}}$ ), 119.24 (BrPh- $\text{CH}_{\text{meta}}$ ), 117.34 (BrPh- $\text{CH}_{\text{para}}$ ), 101.21 (C-1), 70.38 (C-3), 61.85 (C-5), 59.28 (C-2), 50.51 (C-4) ppm;

**ESI-MS:**  $m/z = 699.0392$   $[\text{M}+\text{Na}]^+$  (calculated  $m/z = 699.0407$  for  $[\text{M}+\text{Na}]^+$ ).

**1,2,3-Tri-O-acetyl-4-deoxy-4-phthalimido- $\alpha/\beta$ -D-xylopyranose (131)**

The xylose derivative **114** (190 mg, 321  $\mu$ mol) was dissolved in MeOH (4.00 mL) and sodium methoxide (5.4 M, 3.21  $\mu$ mol) was added. The reaction mixture was stirred for 1 h at room temperature. Then it was neutralized with Amberlite® IR120, filtered and concentrated to dryness. The crude product was dissolved in dry pyridine (2.00 mL) and Ac<sub>2</sub>O (1.00 mL) was added. The mixture was stirred at room temperature for 16 h. Then it was diluted with ethyl acetate and washed with 1N HCl, sodium bicarbonate and brine. The combined org. layers were dried over MgSO<sub>4</sub>, filtered, and concentrated to dryness. Purification by column chromatography on silica (cyclohexane/ethyl acetate, 2:1) gave **131** as a colorless solid.

**Yield:** 80.0 mg (197  $\mu$ mol, 61 %,  $\alpha$ : $\beta$  = 4:5);

**R<sub>f</sub>:** (cyclohexane/ethyl acetate, 1:1): R<sub>f</sub> = 0.38;

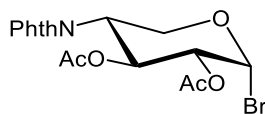
**[ $\alpha$ ]<sub>D</sub><sup>23</sup>:** +2.08 (c = 0.01, CH<sub>2</sub>Cl<sub>2</sub>);

**IR (ATR):**  $\tilde{\nu}$  = 1745, 1712, 1384, 1368, 1211, 1128, 1082, 946, 884 cm<sup>-1</sup>;

**<sup>1</sup>H NMR:** (600 MHz, CDCl<sub>3</sub>, 300 K, TMS):  $\alpha$ -anomer:  $\delta$  = 7.87–7.84 (m, 2H, 2 NPhth-CH<sub>ortho</sub>), 7.76–7.73 (m, 2H, 2 NPhth-CH<sub>meta</sub>), 6.33 (d, <sup>3</sup>J<sub>1,2</sub> = 3.6 Hz, 1H, H-1), 6.06 (t, <sup>3</sup>J<sub>3,2</sub> = 10.1 Hz, <sup>3</sup>J<sub>3,4</sub> = 10.1 Hz, 1H, H-3), 5.13 (dd, <sup>3</sup>J<sub>1,2</sub> = 3.7 Hz, <sup>3</sup>J<sub>2,3</sub> = 9.9 Hz, 1H, H-2), 4.71 (t, <sup>2</sup>J<sub>5a,5b</sub> = 11.4 Hz, <sup>3</sup>J<sub>5a,4</sub> = 11.4 Hz, 1H, H-5a), 4.60–4.54 (m, 1H, H-4), 3.73 (dd, <sup>2</sup>J<sub>5a,5b</sub> = 11.1 Hz, <sup>3</sup>J<sub>5b,4</sub> = 5.8 Hz, 1H, H-5b), 2.27, 2.03, 1.88 (each s, each 3H, OAc) ppm;  $\beta$ -anomer:  $\delta$  = 7.87–7.84 (m, 2H, 2 NPhth<sub>ortho</sub>), 7.76–7.73 (m, 2H, 2 NPhth<sub>meta</sub>), 5.87 (t, <sup>3</sup>J<sub>3,2</sub> = 9.8 Hz, <sup>3</sup>J<sub>3,4</sub> = 9.8 Hz, 1H, H-3), 5.80 (d, <sup>3</sup>J<sub>1,2</sub> = 8.4 Hz, 1H, H-1), 5.17 (dd, <sup>3</sup>J<sub>1,2</sub> = 8.8 Hz, <sup>3</sup>J<sub>2,3</sub> = 9.2 Hz, 1H, H-2), 4.60–4.54 (m, 1H, H-4), 4.48 (dd, <sup>2</sup>J<sub>5a,5b</sub> = 11.5 Hz, <sup>3</sup>J<sub>5a,4</sub> = 11.5 Hz, 1H, H-5a), 3.93 (dd, <sup>2</sup>J<sub>5a,5b</sub> = 11.4 Hz, <sup>3</sup>J<sub>5b,4</sub> = 5.5 Hz, 1H, H-5b), 2.13, 2.04, 1.87 (each s, each 3H, OAc) ppm;

**<sup>13</sup>C NMR:** (125 MHz, CDCl<sub>3</sub>, 300 K, TMS):  $\alpha$ -anomer:  $\delta$  = 170.37, 169.57, 169.51 (3 C(O)CH<sub>3</sub>), 167.70 (2 C(O)Phth), 134.60 (2 Phth-CH<sub>meta</sub>), 131.50 (2 Phth-C<sub>quart</sub>), 123.84 (2 Phth-CH<sub>ortho</sub>), 89.57 (C-1), 70.41 (C-2), 67.85 (C-3), 62.41 (C-5), 49.94 (C-4), 21.08, 20.69, 20.66 (3 C(O)CH<sub>3</sub>) ppm;  $\beta$ -anomer:  $\delta$  = 170.25, 169.96, 169.28 (3 C(O)CH<sub>3</sub>), 167.70 (2 C(O)Phth), 134.60 (2 Phth-CH<sub>meta</sub>), 131.50 (2 Phth-C<sub>quart</sub>), 123.77 (2 Phth-CH<sub>ortho</sub>), 92.74 (C-1), 70.17 (C-2), 70.45 (C-3), 59.25 (C-5), 50.02 (C-4), 20.98, 20.78, 20.60 (3 C(O)CH<sub>3</sub>) ppm;

**ESI-MS:**  $m/z$  = 282.0768 [M+Na]<sup>+</sup> (calculated  $m/z$  = 282.0715 for [M+Na]<sup>+</sup>).

**2,3-Di-O-acetyl-4-deoxy-4-phthalimido- $\alpha$ -D-xylopyranosyl bromide (132)**

The xylose derivative **131** (90.0 mg, 222  $\mu$ mol) was dissolved in dry  $\text{CH}_2\text{Cl}_2$  (1.00 mL) and at 0 °C HBr in AcOH (350  $\mu$ L) was added dropwise. The reaction mixture was allowed to warm to room temperature and stirring was continued for 1 h. Then it was diluted with  $\text{CH}_2\text{Cl}_2$  and washed successfully with sodium bicarbonate and brine. It was dried over  $\text{MgSO}_4$ , filtered off and concentrated to yield **132**.

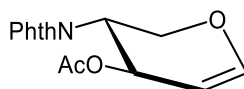
**Yield:** 90.0 mg (211  $\mu$ mol, 95 %);

**R<sub>f</sub>:** (cyclohexane/ethyl acetate, 1:1): R<sub>f</sub> = 0.66;

**<sup>1</sup>H NMR:** (500 MHz,  $\text{CDCl}_3$ , 300 K, TMS):  $\delta$  = 7.89–7.75 (m, 2H, 2 NPhth-CH<sub>ortho</sub>), 7.78–7.72 (m, 2H, 2 NPhth-CH<sub>meta</sub>), 6.65 (d, <sup>3</sup>J<sub>1,2</sub> = 4.0 Hz, 1H, H-1), 6.11 (t, <sup>3</sup>J<sub>3,4</sub> = 10.0 Hz, <sup>3</sup>J<sub>2,3</sub> = 10.0 Hz, 1H, H-3), 4.93 (t, <sup>2</sup>J<sub>5a,5b</sub> = 11.6 Hz, <sup>3</sup>J<sub>5a,4</sub> = 11.6 Hz, 1H, H-5a), 4.89 (t, <sup>3</sup>J<sub>1,2</sub> = 4.0 Hz, <sup>3</sup>J<sub>2,3</sub> = 9.6 Hz, 1H, H-2), 4.61–4.52 (m, 1H, H-4), 3.86 (dd, <sup>2</sup>J<sub>5a,5b</sub> = 11.4 Hz, <sup>3</sup>J<sub>4,5b</sub> = 5.8 Hz, 1H, H-5b), 2.11, 1.89 (each s, 6H, OAc) ppm;

**<sup>13</sup>C NMR:** (125 MHz,  $\text{CDCl}_3$ , 300 K, TMS):  $\delta$  = 170.07 (2 C(O)Phth), 134.63 (2 Phth-CH<sub>meta</sub>), 123.84 (2 Phth-CH<sub>ortho</sub>), 123.77 (2 Phth-C<sub>quart</sub>), 87.33 (C-1), 71.82 (C-2), 68.07 (C-3), 61.54 (C-5), 49.46 (C-4), 20.87, 20.60 (2 C(O)CH<sub>3</sub>) ppm;

**ESI-MS:**  $m/z$  = 301.9725 [M+Na]<sup>+</sup> (calculated  $m/z$  = 301.9766 for [M+Na]<sup>+</sup>).

**3-O-Acetyl-4-deoxy-4-phthalimido-D-xylal (133)**

Vitamine B-12 (1.75 mg, 1.29  $\mu$ mol) was dissolved in dry MeOH (500  $\mu$ L) and zinc (101 mg, 1.55 mmol) and  $\text{NH}_4\text{Cl}$  (51.9 g, 1.55 mmol) were added. The suspension was stirred vigorously for 45 min. Then, xylose bromide **132** (55.0 mg, 129  $\mu$ mol) was dissolved in dry  $\text{CH}_2\text{Cl}_2$  (500  $\mu$ L) and added to the reaction mixture. Stirring at room temperature was continued for 20 min. The mixture was diluted with  $\text{CH}_2\text{Cl}_2$  and filtered over a pad of celite. The solvent was removed, and the crude product was taken up in  $\text{CH}_2\text{Cl}_2$  and  $\text{H}_2\text{O}$ . It was extracted with  $\text{CH}_2\text{Cl}_2$ . The combined org. layers were dried over  $\text{MgSO}_4$ , filtered, and concentrated. Purification by flash column chromatography on silica (cyclohexane/ ethyl acetate, 2:1) led to **133** as a colorless solid.

**Yield:** 24.0 mg (83.6  $\mu$ mol, 64 %);

**R<sub>f</sub>**: (cyclohexane/ethyl acetate, 1:1): R<sub>f</sub> = 0.34;

[α]<sub>D</sub><sup>23</sup>: -6.0 (c = 0.01, CH<sub>2</sub>Cl<sub>2</sub>);

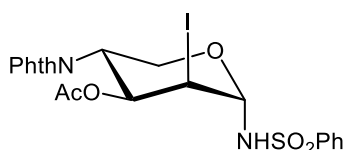
**IR (ATR)**:  $\tilde{\nu}$  = 3061, 2249, 1778, 1708, 1645, 1379, 1268, 1069, 910, 711 cm<sup>-1</sup>;

**<sup>1</sup>H NMR**: (600 MHz, CDCl<sub>3</sub>, 298 K, TMS): δ = 7.88–7.83 (m, 2H, 2 NPhth-CH<sub>ortho</sub>), 7.76–7.72 (m, 2H, 2 NPhth-CH<sub>meta</sub>), 6.52 (dd, <sup>4</sup>J<sub>1,3</sub> = 6.2 Hz, <sup>3</sup>J<sub>1,2</sub> = 1.2 Hz, 1H, H-1), 6.13–6.08 (m, 1H, H-3), 4.99 (dd, <sup>3</sup>J<sub>2,3</sub> = 6.2 Hz, <sup>3</sup>J<sub>1,2</sub> = 2.3 Hz, 1H, H-2), 4.75–4.66 (m, 2H, H-4, H-5a), 4.06–4.01 (m, 1H, H-5b), 1.95 (s, 3H, OAc) ppm;

**<sup>13</sup>C NMR**: (125 MHz, CDCl<sub>3</sub>, 298 K, TMS): δ = 171.06 (C(O)CH<sub>3</sub>), 168.02 (2 C(O)Phth), 146.91 (C-1), 134.44 (2 Phth-CH<sub>meta</sub>), 131.74 (2 Phth-C<sub>quart</sub>), 123.69 (2 Phth-CH<sub>ortho</sub>), 100.51 (C-2), 66.98 (C-3), 65.08 (C-5), 49.33 (C-4), 21.11 (C(O)CH<sub>3</sub>) ppm;

**ESI-MS**: *m/z* = 164.0413 [M+Na]<sup>+</sup> (calculated *m/z* = 164.0449 for [M+Na]<sup>+</sup>).

### 3-O-Acetyl-2-iodo-4-phthalimido-1,2,4-trideoxy-α-D-lyxopyranosyl benzenesulfonamide (134)



The xylal **133** (20.0 mg, 69.6 μmol) and benzene sulfonamide (15.3 mg, 97.5 μmol) were dissolved in dry CH<sub>2</sub>Cl<sub>2</sub> (800 μL) and 4 Å molecular sieve was added. It was stirred for 30 min at room temperature. Then at 0 °C IDCP (81.6 mg, 174 μmol) was added. It was allowed to warm to room temperature and stirring was continued for 3 h. The reaction mixture was diluted with ethyl acetate and filtered over celite. The org. layer was washed with sodium thiosulfate, copper sulfate and brine, dried over MgSO<sub>4</sub>, filtered, and concentrated. Purification by column chromatography on silica (cyclohexane/ethyl acetate, 2:1) gave **134** as a colorless solid.

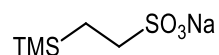
**Yield**: 35.0 mg (61.4 μmol, 88 %);

**R<sub>f</sub>**: (cyclohexane/ethyl acetate, 1:1): R<sub>f</sub> = 0.34;

**<sup>1</sup>H NMR**: (200 MHz, CDCl<sub>3</sub>, 300 K, TMS) δ = 7.97–7.92 (m, 2H, 2 SO<sub>2</sub>Ph-CH<sub>ortho</sub>), 7.97–7.72 (m, 4H, 2 NPhth-CH<sub>ortho</sub>, 2 NPhth-CH<sub>meta</sub>), 7.62–7.49 (m, 3H, 2 SO<sub>2</sub>Ph-CH<sub>meta</sub>, SO<sub>2</sub>Ph-CH<sub>para</sub>), 5.54 (d, <sup>3</sup>J<sub>NH,1</sub> = 10.7 Hz, 1H, NH), 5.19 (dd, <sup>3</sup>J<sub>3,4</sub> = 10.6 Hz, <sup>3</sup>J<sub>2,3</sub> = 4.2 Hz, 1H, H-3), 4.91 (dd, <sup>3</sup>J<sub>2,3</sub> = 4.1 Hz, <sup>3</sup>J<sub>1,2</sub> = 1.3 Hz, 1H, H-2), 4.85–4.73 (m, 1H, H-4), 4.35 (dd, <sup>3</sup>J<sub>1,2</sub> = 1.6 Hz, <sup>3</sup>J<sub>NH,1</sub> = 10.6 Hz, 1H, H-1), 4.10 (t, <sup>3</sup>J<sub>5a,4</sub> = 11.4 Hz, <sup>2</sup>J<sub>5a,5b</sub> = 11.4 Hz, 1H, H-5a), 3.70 (dd, <sup>2</sup>J<sub>5a,5b</sub> = 11.5 Hz, <sup>3</sup>J<sub>5b,4</sub> = 5.6 Hz, 1H, H-5b), 1.96 (s, 3H, OAc) ppm;

**ESI-MS:**  $m/z = 592.9836$   $[M+Na]^+$  (calculated  $m/z = 592.9849$  for  $[M+Na]^+$ ).

**2-(Trimethylsilyl)ethane sodium sulfonate (139)**<sup>[230]</sup>



Vinyltrimethylsilane (**137**, 8.00 g, 79.8 mmol) and *t*-butylperbenzoate (298  $\mu$ L, 1.60 mmol) were combined in MeOH (31 mL) at room temperature. Then a sodium bisulfite solution (39 % in H<sub>2</sub>O, 31.8 mL) was added, and the mixture was heated to reflux for 72 h. Afterwards the solvent was removed under reduced pressure, and it was coevaporated with toluene (3x). Then the solid was extracted with MeOH. Removing the solvent gave **139** as a colorless solid.

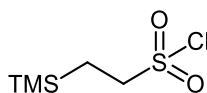
**Yield:** 8.86 g (43.4 mmol, 54 %);

**<sup>1</sup>H NMR:** (200 MHz, D<sub>2</sub>O, 300 K):  $\delta = 2.92$ – $2.61$  (m, 2H, CH<sub>2</sub>),  $0.97$ – $0.68$  (m, 2H, CH<sub>2</sub>),  $0.01$  (s, 9H, TMS) ppm;

**<sup>13</sup>C NMR:** (125 MHz, D<sub>2</sub>O, 298 K):  $\delta = 59.21$  (CH<sub>2</sub>),  $10.72$  (CH<sub>2</sub>),  $-2.81$  (Si(CH<sub>3</sub>)<sub>3</sub>) ppm;

Analytical data corresponds to the literature.<sup>[230]</sup>

**2-(Trimethylsilyl)ethane)sulfonyl chloride (140)**<sup>[230]</sup>



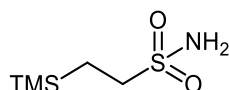
SESNa (**139**, 2.50 g, 12.3 mmol) was suspended in dry CH<sub>2</sub>Cl<sub>2</sub> (50 mL) and PCl<sub>5</sub> (3.88 g, 18.5 mmol) was added portionwise. The reaction mixture was stirred for 30 min at room temperature. It was diluted with CH<sub>2</sub>Cl<sub>2</sub> and successively washed with sodium bicarbonate and brine. The org. layer was dried over MgSO<sub>4</sub>, filtered off and the solvent was removed under reduced pressure to achieve **140** as a yellow oil.

**Yield:** 1.90 g (9.50 mmol, 77 %);

**<sup>1</sup>H NMR:** (200 MHz, CDCl<sub>3</sub>, 300 K, TMS):  $\delta = 3.65$ – $3.56$  (m, 2H, CH<sub>2</sub>),  $1.36$ – $1.27$  (m, 2H, CH<sub>2</sub>),  $0.11$  (s, 9H, TMS) ppm;

**<sup>13</sup>C NMR:** (125 MHz, CDCl<sub>3</sub>, 298 K):  $\delta = 63.21$  (CH<sub>2</sub>),  $11.84$  (CH<sub>2</sub>),  $-2.34$  (Si(CH<sub>3</sub>)<sub>3</sub>) ppm

Analytical data corresponds to the literature.<sup>[230]</sup>

**2-(Trimethylsilyl)ethanesulfonamide (141)**<sup>[234]</sup>

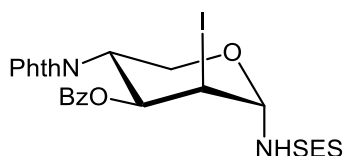
SES-Cl (**140**, 1.90 g, 9.50 mmol) was dissolved in dry  $\text{CH}_2\text{Cl}_2$  (100 mL) and cooled to 0 °C. Then gaseous ammonia (produced by warming a 25 % aqu. ammonia solution) was bubbled through the stirred solution for 6 h. Afterwards the mixture was diluted with  $\text{CH}_2\text{Cl}_2$  and filtered over celite. The org. layer was washed with  $\text{H}_2\text{O}$  and brine, dried over  $\text{MgSO}_4$ , and concentrated to give the title compound as a creamy crystalline solid.

**Yield:** 1.37 g (7.55 mmol, 79 %);

**$^1\text{H}$  NMR:** (200 MHz,  $\text{CDCl}_3$ , 300 K, TMS):  $\delta$  = 4.67 (s, 2H,  $\text{NH}_2$ ), 3.11–2.96 (m, 2H,  $\text{CH}_2$ ), 1.18–1.00 (m, 2H,  $\text{CH}_2$ ), 0.06 (s, 9H, TMS) ppm;

**$^{13}\text{C}$  NMR:** (125 MHz,  $\text{CDCl}_3$ , 298 K):  $\delta$  = 51.50 ( $\text{CH}_2$ ), 10.93 ( $\text{CH}_2$ ), -2.01 ( $\text{Si}(\text{CH}_3)_3$ ) ppm

Analytical data corresponds to the literature.<sup>[234]</sup>

**3-O-Benzoyl-2-iodo-4-phthalimido-1,2,4-trideoxy- $\alpha$ -D-lyxopyranosyl 2-(trimethylsilyl)ethanesulfonamide (142)**

The xylal **116** (50.0 mg, 143  $\mu\text{mol}$ ) and  $\text{SESNH}_2$  (104 mg, 572  $\mu\text{mol}$ ) were dissolved in dry  $\text{CH}_2\text{Cl}_2$  (1.00 mL) and 4 Å molecular sieve was added. It was stirred for 30 min at room temperature. The mixture was cooled down to 0 °C and IDCP (268 mg, 572  $\mu\text{mol}$ ) was added. It was stirred for 30 min at 0 °C. Then the reaction mixture was diluted with ethyl acetate and filtered over a pad of celite. The org. layer was washed with sodium thiosulfate, copper sulfate and brine, dried over  $\text{MgSO}_4$ , filtered, and concentrated to dryness. Purification by column chromatography on silica (toluene/ ethyl acetate, 9:1) gave **142** as a colorless solid.

**Yield:** 79.8 mg (122  $\mu\text{mol}$ , 85 %);

**R<sub>f</sub>:** (cyclohexane/ethyl acetate, 2:1):  $R_f$  = 0.40;

**$[\alpha]_D^{23}$ :** -18.64 ( $c$  = 0.05,  $\text{CH}_2\text{Cl}_2$ );

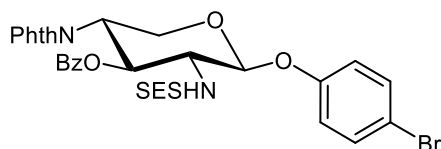
**IR (ATR):**  $\tilde{\nu}$  = 3304, 2953, 2253, 1774, 1714, 1383, 1263, 1022, 840, 709, 529  $\text{cm}^{-1}$ ;

**<sup>1</sup>H NMR:** (500 MHz, CDCl<sub>3</sub>, 298 K, TMS): δ = 7.97–7.91 (m, 2H, 2 Bz-CH<sub>ortho</sub>), 7.85–7.80 (m, 2H, 2 NPhth-CH<sub>ortho</sub>), 7.74–7.69 (m, 2H, 2 NPhth-CH<sub>meta</sub>), 7.57–7.51 (m, 1H, Bz-CH<sub>para</sub>), 7.42–7.37 (m, 2H, Bz-CH<sub>meta</sub>), 5.56 (d, <sup>3</sup>J<sub>NH,1</sub> = 8.3 Hz, 1H, NH), 5.65 (dd, <sup>3</sup>J<sub>NH,1</sub> = 8.5 Hz, <sup>3</sup>J<sub>1,2</sub> = 2.9 Hz, 1H, H-1), 5.35 (dd, <sup>3</sup>J<sub>3,4</sub> = 9.0 Hz, <sup>3</sup>J<sub>2,3</sub> = 4.1 Hz, 1H, H-3), 5.03–4.94 (m, 2H, H-2, H-4), 4.26 (dd, <sup>2</sup>J<sub>5a,5b</sub> = 11.7 Hz, <sup>3</sup>J<sub>5a,4</sub> = 10.1 Hz, 1H, H-5a), 3.93 (dd, <sup>2</sup>J<sub>5a,5b</sub> = 11.8 Hz, <sup>3</sup>J<sub>5b,4</sub> = 5.6 Hz, 1H, H-5b), 3.15–3.05 (m, 2H, CH<sub>2</sub>), 1.22–1.06 (m, 2H, CH<sub>2</sub>), 0.05 (s, 9H, TMS) ppm;

**<sup>13</sup>C NMR:** (125 MHz, CDCl<sub>3</sub>, 298 K, TMS): δ = 167.93 (2 C(O)Phth), 164.92 (C(O)Ph), 134.62 (2 Phth-CH<sub>meta</sub>), 133.81 (Bz-CH<sub>para</sub>), 131.27 (Bz-C<sub>quart</sub>), 130.11 (2 Bz-CH<sub>ortho</sub>), 128.51 (2 Bz-CH<sub>meta</sub>), 123.65 (2 Phth-CH<sub>ortho</sub>), 84.27 (C-1), 67.02 (C-3), 59.76 (C-5), 51.38 (CH<sub>2</sub>), 48.44 (C-4), 29.41 (C-2), 10.27 (CH<sub>2</sub>), -1.99 (3C, Si(CH<sub>3</sub>)<sub>3</sub>) ppm;

**ESI-MS:** *m/z* = 679.0396 [M+Na]<sup>+</sup> (calculated *m/z* = 679.0402 for [M+Na]<sup>+</sup>).

#### 4-Bromophenyl 3-O-benzoyl-2,4-dideoxy-4-phthalimido-2-[2-(trimethylsilyl)ethane-sulfonamido]-β-D-xylopyranoside (**143**)



The iodosulfonamide **142** (43.0 mg, 65.5 μmol) and 4-bromophenole (17.0 mg, 98.2 μmol) were dissolved in dry THF (720 μL). Then at -78 °C LiHMDS (1M in THF, 144 μL, 144 μmol) was added dropwise. It was stirred for 10 min before a solution of AgOTf (25.2 mg, 98.2 μmol, in 150 μL THF) was added to the reaction mixture. The flask was covered with foil, and it was allowed to warm to room temperature. The reaction was stirred for 5.5 h. Then an excess of ammonium chloride was added, and it was stirred for further 10 min before it was filtered over a pad of celite and concentrated to dryness. Purification by column chromatography on silica (cyclohexane/ ethyl acetate, 2:1) gave **143** as a colorless solid.

**Yield:** 40.0 mg (57.0 μmol, 87 %);

**R<sub>f</sub>:** (cyclohexane/ethyl acetate, 2:1): R<sub>f</sub> = 0.34;

**[α]<sub>D</sub><sup>23</sup>:** -12.3 (c = 0.1, CH<sub>2</sub>Cl<sub>2</sub>);

**IR (ATR):**  $\tilde{\nu}$  = 3314, 1779, 1715, 1487, 1384, 1331, 1235, 1068, 839, 712, 653 cm<sup>-1</sup>;

**<sup>1</sup>H NMR:** (500 MHz, CDCl<sub>3</sub>, 298 K, TMS): δ = 7.94–7.89 (m, 2H, 2 Bz-CH<sub>ortho</sub>), 7.75–7.70 (m, 2H, 2 NPhth-CH<sub>ortho</sub>), 7.69–7.65 (m, 2H, 2 NPhth-CH<sub>meta</sub>), 7.54–7.46 (m, 1H, Bz-CH<sub>para</sub>), 7.43–7.39 (m, 2H, OPhe-CH), 7.38–7.32 (m, 2H, Bz-CH<sub>meta</sub>), 7.02–6.98 (m, 2H, OPhe-CH), 6.11 (t, <sup>3</sup>J<sub>3,4</sub> = 10.4 Hz, <sup>3</sup>J<sub>2,3</sub> = 10.4 Hz, 1H, H-3), 5.26 (d, <sup>3</sup>J<sub>1,2</sub> = 8.1 Hz, 1H, H-1), 5.00 (d, <sup>3</sup>J<sub>NH,2</sub> =

8.6 Hz, 1H, NH), 4.80 (td,  $^3J_{4,5a} = 10.6$  Hz,  $^3J_{4,3} = 10.6$  Hz,  $^3J_{4,5b} = 5.3$  Hz, 1H, H-4), 4.51 (t,  $^2J_{5a,5b} = 11.7$  Hz,  $^3J_{5a,4} = 11.4$  Hz, 1H, H-5a), 4.11–4.02 (m, 2H, H-2, H-5b), 2.98–2.85 (m, 2H, CH<sub>2</sub>), 0.99–0.89 (m, 2H, CH<sub>2</sub>), -0.19 (s, 9H, TMS) ppm;

**<sup>13</sup>C NMR:** (125 MHz, CDCl<sub>3</sub>, 298 K, TMS):  $\delta = 167.76$  (2 C(O)Phth), 166.91 (C(O)Ph), 155.68 (OPhe-C<sub>quart</sub>), 134.47 (2 Phth-CH<sub>meta</sub>), 133.77 (Bz-CH<sub>para</sub>), 132.65 (2 OPhe-CH<sub>ortho</sub>), 131.19 (Bz-C<sub>quart</sub>), 130.05 (2 Bz-CH<sub>ortho</sub>), 128.61 (2 Bz-CH<sub>meta</sub>), 123.75 (2 Phth-CH<sub>ortho</sub>), 118.98 (2 OPhe-CH<sub>meta</sub>), 115.89 (Phe-CBr<sub>quart</sub>), 100.83 (C-1), 70.46 (C-3), 61.80 (C-5), 58.66 (C-2), 51.19 (CH<sub>2</sub>), 50.05 (C-4), 10.28 (CH<sub>2</sub>), -2.06 (3C, Si(CH<sub>3</sub>)<sub>3</sub>) ppm;

**ESI-MS:**  $m/z = 723.0807$  [M+Na]<sup>+</sup> (calculated  $m/z = 723.0803$  for [M+Na]<sup>+</sup>).

### 3-O-benzoyl-4-phthalimido-1,2,4-trideoxy-2-[2-(trimethylsilyl)ethanesulfonamido]- $\beta$ -D-xylopyranosyl azide (**144**)



To a solution of iodosulfonamide **142** (40.0 mg, 115  $\mu$ mol) in dry DMF (400  $\mu$ L) was added NaN<sub>3</sub> (15.0 mg, 230  $\mu$ mol) at 0 °C. The mixture was allowed to warm to room temperature and stirring was continued for 16 h. The reaction mixture was diluted with CH<sub>2</sub>Cl<sub>2</sub> and washed with sodium bicarbonate solution and brine, dried over MgSO<sub>4</sub>, filtered off and concentrated to dryness. Column chromatography on silica (cyclohexane/ ethyl acetate, 4:1) of the resulting residue provided **144** as a colorless solid.

**Yield:** 28.4 mg (66.7  $\mu$ mol, 58 %);

**R<sub>f</sub>:** (cyclohexane/ethyl acetate, 3:1): R<sub>f</sub> = 0.34;

**[ $\alpha$ ]<sub>D</sub><sup>23</sup>:** -98.64 (c = 0.04, CH<sub>2</sub>Cl<sub>2</sub>);

**IR (ATR):**  $\tilde{\nu} = 3286, 2954, 2116, 1712, 1383, 1261, 710$  cm<sup>-1</sup>;

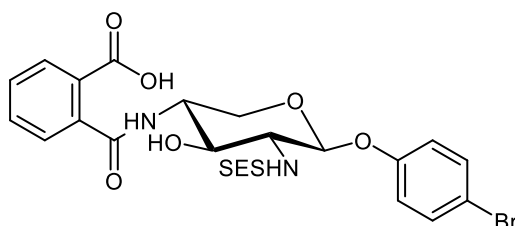
**<sup>1</sup>H NMR:** (500 MHz, CDCl<sub>3</sub>, 298 K, TMS):  $\delta = 7.93$ –7.88 (m, 2H, 2 Bz-CH<sub>ortho</sub>), 7.83–7.79 (m, 2H, 2 NPhth-CH<sub>ortho</sub>), 7.73–7.68 (m, 2H, 2 NPhth-CH<sub>meta</sub>), 7.51–7.45 (m, 1H, Bz-CH<sub>para</sub>), 7.36–7.31 (m, 2H, Bz-CH<sub>meta</sub>), 6.15 (t,  $^3J_{3,4} = 10.3$  Hz,  $^3J_{2,3} = 10.3$  Hz, 1H, H-3), 5.52 (d,  $^3J_{NH,2} = 9.2$  Hz, 1H, NH), 5.02 (d,  $^3J_{1,2} = 9.1$  Hz, 1H, H-1), 4.74 (td,  $^3J_{4,5a} = 10.8$  Hz,  $^3J_{4,3} = 10.8$  Hz,  $^3J_{4,5b} = 5.2$  Hz, 1H, H-4), 4.60 (t,  $^2J_{5a,5b} = 11.5$  Hz,  $^3J_{5a,4} = 11.5$  Hz, 1H, H-5a), 4.09 (dd,  $^2J_{5a,5b} = 11.5$  Hz,  $^3J_{5b,4} = 5.3$  Hz, 1H, H-5b), 3.85–3.74 (m, 1H, H-2), 2.98–2.83 (m, 2H, CH<sub>2</sub>), 0.95–0.88 (m, 2H, CH<sub>2</sub>), -0.18 (s, 9H, TMS) ppm;

**<sup>13</sup>C NMR:** (125 MHz, CDCl<sub>3</sub>, 298 K, TMS):  $\delta = 167.80$  (2C, C(O)Phth), 166.89 (C(O)Ph), 134.56 (2 Phth-CH<sub>meta</sub>), 133.79 (Bz-CH<sub>para</sub>), 131.17 (Bz-C<sub>quart</sub>), 130.11 (2 Bz-CH<sub>ortho</sub>), 128.59

(2 Bz-CH<sub>meta</sub>), 123.74 (2 Phth-CH<sub>ortho</sub>), 90.07 (C-1), 70.68 (C-3), 63.64 (C-5), 58.46 (C-2), 51.10 (CH<sub>2</sub>), 50.51 (C-4), 10.27 (CH<sub>2</sub>), -2.28 (3 Si(CH<sub>3</sub>)<sub>3</sub>) ppm;

**ESI-MS:**  $m/z = 594.1450$  [M+Na]<sup>+</sup> (calculated  $m/z = 594.1449$  for [M+Na]<sup>+</sup>).

#### 4-Bromophenyl 2,4-dideoxy-4-[2-carboxybenzamido]-2-[2-(trimethylsilyl)ethane-sulfonamido]-β-D-xylopyranoside (**145**)



The xyloside **143** (13.0 mg, 18.5 μmol) was dissolved in dry MeOH (1 mL, 1:1) and a solution of sodium methoxide (5.4M in MeOH) was added. It was stirred for 2 h at room temperature. Subsequently it was neutralized by adding Amberlite IR 120 ion exchange resin. The resin was filtered off and the filtrate concentrated under reduced pressure. Purification by column chromatography on silica (CH<sub>2</sub>Cl<sub>2</sub>/MeOH, 9:1) yielded **145** as a colorless solid.

**Yield:** 10.5 mg (17.0 μmol, 92 %);

**R<sub>f</sub>:** (CH<sub>2</sub>Cl<sub>2</sub>/MeOH, 9:1): R<sub>f</sub> = 0.26;

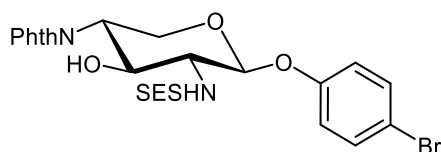
**[α]<sub>D</sub><sup>23</sup>:** +12.5 (c = 0.01, CH<sub>2</sub>Cl<sub>2</sub>);

**IR (ATR):**  $\tilde{\nu} = 2152, 1722, 1496, 1371, 1238, 1166, 876, 731, 666, 581$  cm<sup>-1</sup>;

**<sup>1</sup>H NMR:** (500 MHz, DMSO-d<sub>6</sub>, 300 K): δ = 8.68 (d, <sup>3</sup>J<sub>NH,4</sub> = 7.5 Hz, 1H, NHC(O)), 7.78–7.71 (m, 1H, NPhth-CH), 7.56–7.47 (m, 2H, OPhe-CH), 7.44–7.39 (m, 3H, NPhth-CH 7.36 (d, <sup>3</sup>J<sub>NH,2</sub> = 8.8 Hz, 1H, NH), 7.09–6.98 (m, 2H, OPhe-CH), 4.91 (d, <sup>3</sup>J<sub>1,2</sub> = 8.1 Hz, 1H, H-1), 3.93–3.85 (m, 2H, H-4, H-5a), 3.62 (t, <sup>3</sup>J<sub>3,4</sub> = 9.7 Hz, <sup>3</sup>J<sub>2,3</sub> = 9.7 Hz, 1H, H-3), 3.30–3.22 (m, 2H, H-5b, H-2), 3.11–2.94 (m, 2H, CH<sub>2</sub>), 1.16–0.83 (m, 2H, CH<sub>2</sub>), -0.02 (s, 9H, TMS) ppm;

**<sup>13</sup>C NMR:** (125 MHz, DMSO-d<sub>6</sub>, 300 K): δ = 169.99, 156.11 (2 C(O)Phth), 141.22 (OPhe-C<sub>quart</sub>), 129.10, 128.56, 127.27 (4C, 4 Phth-CH), 132.16 (OPhe-CH<sub>ortho</sub>), 122.99 (2C, 2 Phth-C<sub>quart</sub>), 118.74 (OPhe-CH<sub>meta</sub>), 113.75 (Phe-CBr<sub>quart</sub>), 99.84 (C-1), 71.84 (C-3), 63.41 (C-5), 59.50 (C-2), 52.20 (C-4), 49.63 (CH<sub>2</sub>), 9.99 (CH<sub>2</sub>), -2.03 (3C, Si(CH<sub>3</sub>)<sub>3</sub>) ppm;

**ESI-MS:**  $m/z = 653.0365$  [M+Na]<sup>+</sup> (calculated  $m/z = 653.0391$  for [M+K]<sup>+</sup>).

**4-Bromophenyl 2,4-dideoxy-4-phthalimido-2-[2-(trimethylsilyl)ethanesulfonamido]- $\beta$ -D-xylopyranoside (146)**

The xyloside **143** (20.0 mg, 32.5  $\mu$ mol) was dissolved in dry  $\text{CH}_2\text{Cl}_2$  (100  $\mu$ L) and DMAP (2.61 mg, 21.4  $\mu$ mol) and DIC (8.83 mg, 57.0  $\mu$ mol) were added at 0  $^\circ\text{C}$ . It was allowed to warm to room temperature and stirring was continued for 16 h. It was diluted with  $\text{CH}_2\text{Cl}_2$ , and it was filtered over a pad of celite. The solvent was removed and purification by column chromatography on silica (cyclohexane/ ethyl acetate, 1:1) gave **146** as a colorless solid.

**Yield:** 8.36 mg (18.5  $\mu$ mol, 57 %);

**R<sub>f</sub>**: (cyclohexane/ethyl acetate, 1:1): R<sub>f</sub> = 0.40;

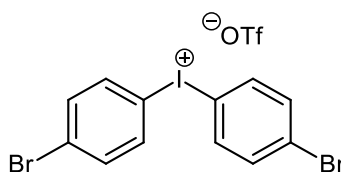
**[ $\alpha$ ]<sub>D</sub><sup>23</sup>**: +8.5 (c = 0.01, acetone);

**IR (ATR)**:  $\tilde{\nu}$  = 3308, 2924, 1709, 1487, 1386, 1326, 1106, 1054, 840, 720, 530  $\text{cm}^{-1}$ ;

**<sup>1</sup>H NMR**: (500 MHz,  $\text{CDCl}_3$ , 300 K, TMS):  $\delta$  = 7.84–7.79 (m, 2H, 2 NPhth-CH<sub>ortho</sub>), 7.74–7.69 (m, 2H, 2 NPhth-CH<sub>meta</sub>), 7.45–7.39 (m, 2H, OPhe-CH), 6.95–6.89 (m, 2H, OPhe-CH), 5.05 (d, <sup>3</sup>J<sub>1,2</sub> = 8.1 Hz, 1H, H-1), 5.02 (d, <sup>3</sup>J<sub>NH,2</sub> = 6.7 Hz, 1H, NH), 4.52 (t, <sup>3</sup>J<sub>3,4</sub> = 10.0 Hz, <sup>3</sup>J<sub>2,3</sub> = 10.0 Hz, 1H, H-3), 4.45 (td, <sup>3</sup>J<sub>4,5a</sub> = 10.8 Hz, <sup>3</sup>J<sub>4,3</sub> = 10.8 Hz, <sup>3</sup>J<sub>4,5b</sub> = 5.2 Hz, 1H, H-4), 4.21 (t, <sup>2</sup>J<sub>5a,5b</sub> = 11.2 Hz, <sup>3</sup>J<sub>5a,4</sub> = 11.2 Hz, 1H, H-5a), 3.92 (dd, <sup>2</sup>J<sub>5a,5b</sub> = 11.3 Hz, <sup>3</sup>J<sub>5b,4</sub> = 5.1 Hz, 1H, H-5b), 3.64–3.54 (m, 1H, H-2), 3.19–3.02 (m, 2H, CH<sub>2</sub>), 1.10–1.03 (m, 2H, CH<sub>2</sub>), -0.02 (s, 9H, TMS) ppm;

**<sup>13</sup>C NMR**: (125 MHz,  $\text{CDCl}_3$ , 300 K, TMS):  $\delta$  = 168.35 (2 C(O)Phth), 155.49 (OPhe-C<sub>quart</sub>), 134.49 (2 Phth-CH<sub>meta</sub>), 132.82 (OPhe-CH<sub>ortho</sub>), 131.71 (Phe-CBr<sub>quart</sub>), 123.73 (2 Phth-CH<sub>ortho</sub>), 118.89 (OPhe-CH<sub>meta</sub>), 100.02 (C-1), 69.58 (C-3), 62.23 (C-5), 61.19 (C-2), 52.61 (C-4), 50.47 (CH<sub>2</sub>), 10.43 (CH<sub>2</sub>), -1.85 (3C, Si(CH<sub>3</sub>)<sub>3</sub>) ppm;

**ESI-MS**:  $m/z$  = 473.0295 [M+Na]<sup>+</sup> (calculated  $m/z$  = 473.0304 for [M+Na]<sup>+</sup>).

**Bis(4-bromophenyl)iodonium triflate (149)<sup>[242]</sup>**

4-Iodobromobenzene (1.00 g, 3.53 mmol), bromobenzene (408  $\mu$ L, 3.89 mmol) and 3-chloroperbenzoic acid (617 mg, 3.89 mmol) were dissolved in dry  $\text{CH}_2\text{Cl}_2$  (64 mL). Then at

0 °C TfOH (935  $\mu$ L, 10.6 mmol) was added. It was stirred for 1 h before the solvent was removed under reduced pressure. The crude product was taken up in  $\text{CH}_2\text{Cl}_2$  (6 mL) and cold  $\text{Et}_2\text{O}$  (40 mL) was added slowly. The white precipitate was filtered off, washed with cool  $\text{Et}_2\text{O}$ , and dried under reduced pressure to give the title compound as a colorless solid.

**Yield:** 1.10 g (1.87 mmol, 53 %);

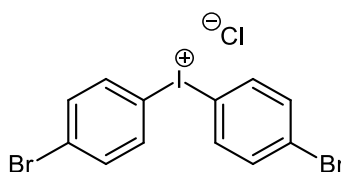
**$^1\text{H NMR}$ :** (200 MHz,  $\text{DMSO-d}_6$ , 300 K):  $\delta$  = 8.24–8.13 (m, 4H,  $\text{CH}_{\text{arom}}$ ), 7.82–7.71 (m, 4H,  $\text{CH}_{\text{arom}}$ ), ppm;

**$^{13}\text{C NMR}$ :** (125 MHz,  $\text{DMSO-d}_6$ , 300 K):  $\delta$  = 136.94 (4C,  $\text{CH}_{\text{arom}}$ ), 134.60 (2  $\text{CH}_{\text{quart}}$ ), 134.58 (4C,  $\text{CH}_{\text{arom}}$ ), 126.26 (2  $\text{CH}_{\text{quart}}$ ) ppm;

**ESI-MS:**  $m/z$  = 436.8027  $[\text{M}]^+$  (calculated  $m/z$  = 436.8037 for  $[\text{M}]^+$ ).

Analytical data corresponds to the literature.<sup>[242]</sup>

#### **Bis(4-bromophenyl)iodonium chloride (150)**<sup>[242]</sup>



The iodonium triflate **149** (200 mg, 340  $\mu$ mol) was dissolved in MeCN (3.5 mL) and it was heated to 60 °C. Then a solution of  $\text{NH}_4\text{Cl}$  (90.9 mg, 1.69 mmol in 6 mL  $\text{H}_2\text{O}$ ) was added dropwise. The suspension was stirred further for 1 h. Then it was filtered off and washed with  $\text{Et}_2\text{O}$  to give the title compound as colorless crystals.

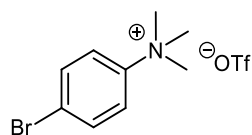
**Yield:** 137 mg (289  $\mu$ mol, 85 %);

**$^1\text{H NMR}$ :** (500 MHz,  $\text{DMSO-d}_6$ , 300 K):  $\delta$  = 8.12 (d,  $^3J_{2,3}$  = 8.6 Hz, 4H,  $\text{CH}_{\text{arom}}$ ), 7.71 (d,  $^3J_{2,3}$  = 8.6 Hz, 4H,  $\text{CH}_{\text{arom}}$ ), ppm;

**$^{13}\text{C NMR}$ :** (125 MHz,  $\text{DMSO-d}_6$ , 300 K):  $\delta$  = 136.76 (4C,  $\text{CH}_{\text{arom}}$ ), 134.63 (2  $\text{CH}_{\text{quart}}$ ), 134.23 (4C,  $\text{CH}_{\text{arom}}$ ), 125.57 (2  $\text{CH}_{\text{quart}}$ ) ppm;

**ESI-MS:**  $m/z$  = 436.8032  $[\text{M}]^+$  (calculated  $m/z$  = 436.8037 for  $[\text{M}+\text{Na}]^+$ ).

Analytical data corresponds to the literature.<sup>[242]</sup>

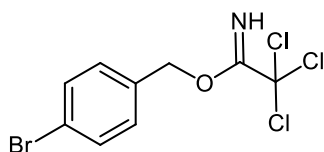
**4-Bromo-*N,N,N*-trimethyl-1,1,1-trifluoromethanesulfonate (152)**<sup>[243]</sup>

4-Bromo-*N,N*-dimethylaniline (200 mg, 1.00 mmol) was dissolved in dry CH<sub>2</sub>Cl<sub>2</sub> (1.00 mL) and MeOTf (124 μL, 1.10 mmol) was added dropwise. The reaction mixture was stirred for 1.5 h at room temperature. Then the solvent was removed under reduced pressure, and it was washed with Et<sub>2</sub>O. Drying under reduced pressure gave **152** as a colorless solid.

**Yield:** 327 mg (898 μmol, 90 %);

**<sup>1</sup>H NMR:** (200 MHz, DMSO-d<sub>6</sub>, 300 K, TMS): δ = 8.03-7.80 (m, 4H, CH<sub>arom</sub>), 3.59 (s, 9H, 3 CH<sub>3</sub>), ppm;

Analytical data corresponds to the literature.<sup>[243]</sup>

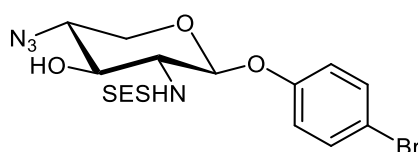
**O-[(4-Bromophenyl)methyl] 2,2,2-trichloroacetimidate (156)**<sup>[244]</sup>

Benzyl alcohol (3.00 g, 16.0 mmol) was dissolved in dry CH<sub>2</sub>Cl<sub>2</sub> (16 mL) and trichloro MeCN (16.1 mL, 160 mmol) and DBU (239 L, 1.60 mmol) were added. It was stirred at room temperature for 2 h before the solvent was removed. Purification by column chromatography on silica (cyclohexane/ethyl acetate, 4:1→3:2) gave the title compound as a colorless solid.

**Yield:** 5.33 g (16.0 mmol, quant.);

**<sup>1</sup>H NMR:** (200 MHz, CDCl<sub>3</sub>, 300 K, TMS): δ = 8.41 (s, 1H, NH), 7.59–7.46 (m, 2H, CH<sub>arom</sub>), 7.37–7.27 (m, 2H, CH<sub>arom</sub>), 5.29 (s, 2H, CH<sub>2</sub>), ppm;

Analytical data corresponds to the literature.<sup>[244]</sup>

**4-Bromophenyl 4-azido-2,4-dideoxy-2-[2-(trimethylsilyl)ethanesulfonamido]-β-D-xylopyranoside (158)**

The xyloside **143** (300 mg, 428 μmol) was dissolved in EtOH (10 mL) and ethylene diamine (85.8 μL, 1.28 mmol) was added. The mixture was heated to 70 °C and stirred for 7 h.

Afterwards the solvent was removed, and the crude product was filtered over a filter column of silica (CH<sub>2</sub>Cl<sub>2</sub>/MeOH, 9:1). The crude product was dissolved in MeOH (3.00 mL) and K<sub>2</sub>CO<sub>3</sub> (148 mg, 1,07 mmol) and CuSO<sub>4</sub> (1.00 mg, 4.28 μmol) were added followed by the addition of ISA (179 mg, 856 μmol). The reaction mixture was then stirred for 16 h at room temperature. Afterwards the solvent was removed under reduced pressure and the crude was taken up in ethyl acetate and washed with H<sub>2</sub>O. The org. layer was then dried over MgSO<sub>4</sub> and filtered. The solvent was removed, and the crude product was purified by column chromatography on silica (cyclohexane/ ethyl acetate, 3:2) to obtain **158** as a colorless solid.

**Yield:** 93.0 mg (188 μmol, 44 %);

**R<sub>f</sub>** (cyclohexane/ethyl acetate, 1:1): R<sub>f</sub> = 0.55;

**[α]<sub>D</sub><sup>23</sup>:** -14.07 (c = 0.2, CH<sub>2</sub>Cl<sub>2</sub>);

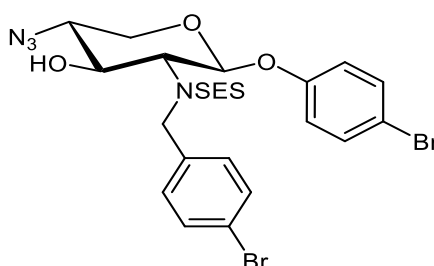
**IR (ATR):**  $\tilde{\nu}$  = 3264, 2954, 2112, 1638, 1487, 1316, 1231, 1142, 1108, 824, 696 cm<sup>-1</sup>;

**<sup>1</sup>H NMR:** (500 MHz, CDCl<sub>3</sub>, 300 K, TMS): δ = 7.45–7.39 (m, 2H, OPhe-CH), 6.92–6.84 (m, 2H, OPhe-CH), 5.42 (d, <sup>3</sup>J<sub>NH,2</sub> = 8.2 Hz, 1H, NH), 4.97 (d, <sup>3</sup>J<sub>1,2</sub> = 6.9 Hz, 1H, H-1), 4.07 (dd, <sup>2</sup>J<sub>5a,5b</sub> = 12.2 Hz, <sup>3</sup>J<sub>5a,4</sub> = 4.7 Hz, 1H, H-5a), 3.74 (t, <sup>3</sup>J<sub>3,4</sub> = 8.4 Hz, <sup>3</sup>J<sub>2,3</sub> = 8.4 Hz, 1H, H-3), 3.67 (td, <sup>3</sup>J<sub>4,5a</sub> = 8.6 Hz, <sup>3</sup>J<sub>4,3</sub> = 8.6 Hz, <sup>3</sup>J<sub>4,5b</sub> = 4.8 Hz, 1H, H-4), 3.60–3.54 (m, 1H, H-2), 3.34 (dd, <sup>2</sup>J<sub>5a,5b</sub> = 12.2 Hz, <sup>3</sup>J<sub>5b,4</sub> = 9.0 Hz, 1H, H-5b), 3.15–3.01 (m, 2H, CH<sub>2</sub>), 1.08–1.00 (m, 2H, CH<sub>2</sub>), -0.02 (s, 9H, TMS) ppm;

**<sup>13</sup>C NMR:** (125 MHz, CDCl<sub>3</sub>, 300 K, TMS): δ = 155.17 (OPhe-C<sub>quart</sub>), 132.72 (2 OPhe-CH<sub>ortho</sub>), 118.80 (2 OPhe-CH<sub>meta</sub>), 116.20 (Phe-C<sub>Br</sub><sub>quart</sub>), 99.79 (C-1), 73.44 (C-3), 61.19 (C-4), 62.86 (C-5), 58.56 (C-2), 50.79 (CH<sub>2</sub>), 10.47 (CH<sub>2</sub>), -1.87 (3 Si(CH<sub>3</sub>)<sub>3</sub>) ppm;

**ESI-MS:** 515.0388 [M+Na]<sup>+</sup> (calcd *m/z* = 515.0396 for [M+Na]<sup>+</sup>)

#### 4-Bromophenyl 4-azido-2,4-dideoxy-2-(4-bromobenzyl)-2-[2-(trimethylsilyl)ethane-sulfonamido]-β-D-xylopyranoside (**160**)



The xyloside **158** (20.0 mg, 40.5 μmol) was dissolved in dry DMF (500 μL), and 4-bromobenzyl bromide (11.1 mg, 44.6 μmol) was added, followed by K<sub>2</sub>CO<sub>3</sub> (8.40 mg, 60.8 μmol). The reaction mixture was heated to 60 °C and stirring was continued for 5 h. Then it was diluted

with ethyl acetate and washed with brine. The combined org. layers were dried over  $\text{MgSO}_4$ , filtered, and concentrated to dryness. The crude product was purified by column chromatography on silica (cyclohexane/ ethyl acetate, 7:2) to obtain **160** as a colorless solid.

**Yield:** 23.0 mg (34.7  $\mu\text{mol}$ , 86 %);

**R<sub>f</sub>:** (cyclohexane/ethyl acetate, 3:1):  $R_f = 0.32$ ;

**$[\alpha]_D^{23}$ :** +3.13 ( $c = 0.01$ ,  $\text{CH}_2\text{Cl}_2$ );

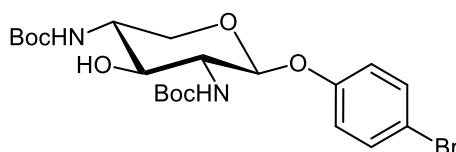
**IR (ATR):**  $\tilde{\nu} = 2926, 2111, 1699, 1486, 1325, 1231, 1140, 1107, 1010, 822, 697, 517 \text{ cm}^{-1}$ ;

**$^1\text{H NMR}$ :** (600 MHz,  $\text{CDCl}_3$ , 300 K, TMS):  $\delta = 7.44\text{--}7.39$  (m, 2H, OPhe-CH), 7.39–7.32 (m, 2H, Bn-CH), 7.25–7.20 (m, 2H, Bn-CH), 6.77–6.70 (m, 2H, OPhe-CH), 4.52 (d,  $^2J = 15.5 \text{ Hz}$ , 1H, Bn- $\text{CH}_2$ ), 4.43 (d,  $^2J = 15.5 \text{ Hz}$ , 1H, Bn- $\text{CH}_2$ ), 3.99 (dd,  $^2J_{5a,5b} = 11.8 \text{ Hz}$ ,  $^3J_{5a,4} = 5.3 \text{ Hz}$ , 1H, H-5a), 4.90 (br s, 1H, H-1), 3.70 (br s, 1H, H-3), 3.57-3.50 (m, 1H, H-4), 2.34 (t,  $^3J_{1,2} = 6.7 \text{ Hz}$ ,  $^3J_{2,3} = 6.7 \text{ Hz}$ , 1H, H-2), 3.16 (br s, 1H, H-5b), 3.10–2.83 (m, 2H,  $\text{CH}_2$ ), 1.06 (br s, 2H,  $\text{CH}_2$ ), -0.03 (s, 9H, TMS) ppm;

**$^{13}\text{C NMR}$ :** (125 MHz,  $\text{CDCl}_3$ , 300 K, TMS):  $\delta = 155.24$  (OPhe- $\text{C}_{\text{quart}}$ ), 135.51 (Bn- $\text{C}_{\text{quart}}$ ), 132.88 (2 OPhe- $\text{CH}_{\text{ortho}}$ ), 132.15 (2 Bn- $\text{CH}_{\text{ortho}}$ ), 130.45 (2 Bn- $\text{CH}_{\text{meta}}$ ), 122.67 (Bn- $\text{CH}_{\text{para}}$ ), 117.95 (2 OPhe- $\text{CH}_{\text{meta}}$ ), 115.98 (Phe- $\text{C}_{\text{Br}_{\text{quart}}}$ ), 98.07 (C-1), 63.99 (Bn- $\text{CH}_2$ ), 62.82 (C-3), 50.40 ( $\text{CH}_2$ ), 29.85 (C-4), 27.17 (C-5), 25.15 (C-2), 10.23 ( $\text{CH}_2$ ), -1.94 (3  $\text{Si}(\text{CH}_3)_3$ ) ppm;

**ESI-MS:**  $m/z = 698.9701$   $[\text{M}+\text{K}]^+$  (calculated  $m/z = 698.9710$  for  $[\text{M}+\text{K}]^+$ ).

#### 4-Bromophenyl 2,4-dideoxy-2,4-*N*-Boc- $\beta$ -D-xylopyranoside (**164**)



The xyloside **143** (268 mg, 382  $\mu\text{mol}$ ) was dissolved in dry THF (13.5 mL) and  $\text{Boc}_2\text{O}$  (2.45 mL, 11.5 mmol) was added. It was stirred at room temperature for 5 min before TBAF (1M in THF, 3.82 mL, 3.82 mmol) was added. The mixture was stirred at room temperature for 1 h. Then it was diluted with ethyl acetate and washed with  $\text{H}_2\text{O}$ , dried over  $\text{MgSO}_4$ , filtered and the solvent was removed under reduced pressure. The crude product was dissolved in EtOH (1.00 mL), and  $\text{N}_2\text{H}_4 \cdot \text{H}_2\text{O}$  (50.0  $\mu\text{L}$ ) was added. The mixture was heated to 70 °C and stirred for 1.5 h. Then the solvent was removed, and it was coevaporated with toluene. The crude product was dissolved in THF/ $\text{H}_2\text{O}$  (10 mL, 9:1) and trimethylamine (500  $\mu\text{L}$ ) and  $\text{Boc}_2\text{O}$  (100  $\mu\text{L}$ , 469  $\mu\text{mol}$ ) were added. The mixture was stirred for 16 h at room temperature. It was diluted with ethyl acetate and washed with  $\text{H}_2\text{O}$ . The org. layers were dried over  $\text{MgSO}_4$ , filtered, and

concentrated to dryness. The crude product was purified by column chromatography on silica (cyclohexane/ethyl acetate, 2:1), which gave **164** as a colorless solid.

**Yield:** 116 mg (230  $\mu\text{mol}$ , 86 %);

**R<sub>f</sub>:** (cyclohexane/ethyl acetate, 1:1): R<sub>f</sub> = 0.40;

**[ $\alpha$ ]<sub>D</sub><sup>23</sup>:** -6.00 (c = 0.1, CH<sub>2</sub>Cl<sub>2</sub>);

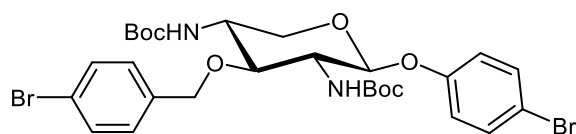
**IR (ATR):**  $\tilde{\nu}$  = 3307, 2980, 1682, 1538, 1487, 1237, 1169, 1035, 983, 658 cm<sup>-1</sup>;

**<sup>1</sup>H NMR:** (500 MHz, acetone-d<sub>6</sub>, 298 K, TMS):  $\delta$  = 7.47–7.42 (m, 2H, OPhe-CH), 7.00–6.95 (m, 2H, OPhe-CH), 6.20 (s, 1H, NHBoc), 6.03 (s, 1H, NHBoc), 5.07 (d, <sup>3</sup>J<sub>1,2</sub> = 8.0 Hz, 1H, H-1), 4.45 (d, <sup>3</sup>J<sub>3,OH</sub> = 4.8 Hz, 1H, OH), 4.02 (dd, <sup>2</sup>J<sub>5a,5b</sub> = 11.4 Hz, <sup>3</sup>J<sub>5a,4</sub> = 5.1 Hz, 1H, H-5a), 3.81–3.71 (m, 1H, H-3), 3.67–3.57 (m, 2H, H-2, H-4), 3.39 (t, <sup>2</sup>J<sub>5a,5b</sub> = 11.0 Hz, <sup>3</sup>J<sub>5a,4</sub> = 11.0 Hz, 1H, H-5b), 1.41 (s, 9H, C(CH<sub>3</sub>)<sub>3</sub>), 1.40 (s, 9H, C(CH<sub>3</sub>)<sub>3</sub>) ppm;

**<sup>13</sup>C NMR:** (125 MHz, acetone-d<sub>6</sub>, 298 K, TMS):  $\delta$  = 158.06 (OPhe-C<sub>quart</sub>), 156.75 (NH-C(O)), 156.71 (NH-C(O)), 133.12 (2 OPhe-CH<sub>ortho</sub>), 119.65 (2 OPhe-CH<sub>meta</sub>), 114.87 (Phe-CBr<sub>quart</sub>), 101.40 (C-1), 79.10 (C(CH<sub>3</sub>)<sub>3</sub>), 78.96 (C(CH<sub>3</sub>)<sub>3</sub>), 72.47 (C-3), 64.83 (C-5), 58.91 (C-2), 54.41 (C-4), 28.61 (3C, C(CH<sub>3</sub>)<sub>3</sub>), 28.57 (3C, C(CH<sub>3</sub>)<sub>3</sub>) ppm;

**ESI-MS:**  $m/z$  = 525.1213 [M+Na]<sup>+</sup> (calculated  $m/z$  = 525.1207 for [M+Na]<sup>+</sup>).

#### 4-Bromophenyl 2,4-dideoxy-2,4-N-Boc-3-O-(4-bromobenzyl)- $\beta$ -D-xylopyranoside (**165**)



The xyloside **164** (10.0 mg, 19.9  $\mu\text{mol}$ ) was dissolved in dry THF (300  $\mu\text{L}$ ) and the solution was cooled down to 0 °C. Then NaH (60 %, 1.19 mg, 29.9  $\mu\text{mol}$ ) was added and the reaction mixture was stirred for 30 min. Afterwards 4-bromobenzyl bromide (5.47 mg, 21.9  $\mu\text{mol}$ ) was added. It was allowed to warm to room temperature and stirring was continued for 2 h. Then MeOH was added, followed by H<sub>2</sub>O and it was extracted with ethyl acetate. The combined org. layers were dried over MgSO<sub>4</sub>, filtered, and concentrated. Column chromatography on silica (cyclohexane/ ethyl acetate, 4:1) of the resulting residue provided **165** as a colorless solid. **Yield:** 6.00 mg (8.92  $\mu\text{mol}$ , 44 %);

**R<sub>f</sub>:** (cyclohexane/ethyl acetate, 4:1): R<sub>f</sub> = 0.31;

**[ $\alpha$ ]<sub>D</sub><sup>23</sup>:** +3.11 (c = 0.01, CH<sub>2</sub>Cl<sub>2</sub>);

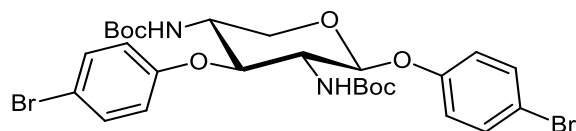
**IR (ATR):**  $\tilde{\nu}$  = 3338, 2927, 2309, 1682, 1525, 1467, 1298, 1233, 1166, 1062, 1010 820 cm<sup>-1</sup>;

**<sup>1</sup>H NMR:** (600 MHz, CDCl<sub>3</sub>, 298 K, TMS): δ = 7.48 (d, <sup>3</sup>J = 8.3 Hz, 2H, OBn-CH), 7.38 (d, <sup>3</sup>J = 8.9 Hz, 2H, OPhe-CH), 7.27-7.23 (m, 2H, OBn-CH), 6.89 (d, <sup>3</sup>J = 8.9 Hz, 2H, OPhe-CH), 5.30 (s, 1H, H-1), 4.97 (s, 1H, NH), 4.77-4.70 (m, 1H, CH<sub>2</sub>), 4.68-4.55 (m, 2H, NH, CH<sub>2</sub>), 4.22 (dd, <sup>2</sup>J<sub>5a,5b</sub> = 11.7 Hz, <sup>3</sup>J<sub>5a,4</sub> = 3.4 Hz, 1H, H-5a), 3.95 (s, 1H, H-3), 3.79-3.68 (m, 2H, H-2, H-4), 4.22 (dd, <sup>2</sup>J<sub>5a,5b</sub> = 10.3 Hz, <sup>3</sup>J<sub>5a,4</sub> = 6.4 Hz, 1H, H-5b), 1.45 (s, 9H, C(CH<sub>3</sub>)<sub>3</sub>), 1.44 (s, 9H, C(CH<sub>3</sub>)<sub>3</sub>) ppm;

**<sup>13</sup>C NMR:** (125 MHz, CDCl<sub>3</sub>, 298 K, TMS): δ = 156.12 (C2-NHC(O)), 155.30 (C4-NHC(O)), 137.17 (OPhe-C<sub>quart</sub>), 132.60 (OBn-C<sub>quart</sub>), 132.54 (2 OPhe-CH<sub>ortho</sub>), 131.70 (2 OPhe-CH<sub>ortho</sub>), 129.62 (2 OPhe-CH<sub>meta</sub>), 121.86 (Phe-CBr<sub>quart</sub>), 118.85 (2 OPhe-CH<sub>meta</sub>), 115.18 (Phe-CBr<sub>quart</sub>), 98.73 (C-1), 80.37 (2 C(CH<sub>3</sub>)<sub>3</sub>), 75.70 (C-3), 71.68 (CH<sub>2</sub>), 62.18 (C-5), 53.33 (C-2), 50.36 (C-4), 28.47 (6C, C(CH<sub>3</sub>)<sub>3</sub>) ppm;

**ESI-MS:** *m/z* = 693.0765 [M+Na]<sup>+</sup> (calculated *m/z* = 693.0787 for [M+Na]<sup>+</sup>).

#### 4-Bromophenyl 2,4-dideoxy-2,4-*N*-Boc-3-*O*-(4-bromophenyl)-β-*D*-xylopyranoside (**166**)



Potassium *tert*-butoxide (5.36 mg, 47.8 μmol) was suspended in dry toluene (160 μL) and the xyloside **164** (20.0 mg, 39.8 μmol) was added. The mixture was stirred for 15 min at room temperature. It was cooled down to 0 °C and piperidine (1.18 μL, 11.9 μmol) was added followed by bis(4-bromophenyl)iodonium triflate **149** (28.2 mg, 47.8 μmol). The mixture was allowed to warm to room temperature and stirring was continued for 3 h. Then sat. ammonium chloride solution was added, and it was extracted with CH<sub>2</sub>Cl<sub>2</sub>. The combined org. layers were dried over MgSO<sub>4</sub>, filtered, and concentrated. Purification by column chromatography on silica (cyclohexane/ ethyl acetate, 9:1 → 4:1) yielded **166** as a colorless solid.

**Yield:** 15.3 mg (23.2 μmol, 58 %);

**R<sub>f</sub>:** (cyclohexane/ethyl acetate, 3:1): R<sub>f</sub> = 0.42;

**[α]<sub>D</sub><sup>23</sup>:** -28.54 (c = 0.1, acetone);

**IR (ATR):**  $\tilde{\nu}$  = 3325, 2977, 1681, 1538, 1487, 1303, 1228, 1172, 1031, 818 cm<sup>-1</sup>;

**<sup>1</sup>H NMR:** (500 MHz, DMF-*d*<sub>7</sub>, 300 K): δ = 7.52 (d, <sup>3</sup>J = 8.9 Hz, 2H, H-6, H-6'), 7.43 (d, <sup>3</sup>J = 9.0 Hz, 2H, H-8, H-8'), 7.21–6.97 (m, 6H, NH, NH, H-9, H-9', H-7, H-7'), 5.27 (d, <sup>3</sup>J<sub>1,2</sub> = 8.33 Hz, 1H, H-1), 4.76 (t, <sup>3</sup>J<sub>3,4</sub> = 9.76 Hz, <sup>3</sup>J<sub>2,3</sub> = 9.76 Hz, 1H, H-3), 3.95 (dd, <sup>2</sup>J<sub>5a,5b</sub> = 10.94 Hz, <sup>3</sup>J<sub>5a,4</sub> = 5.27 Hz, 1H, H-5a), 3.88 (m, 1H, H-4), 3.82 (m, 1H, H-2), 3.66 (m, 2H, H-2, H-5b), 1.31 (s, 9H,

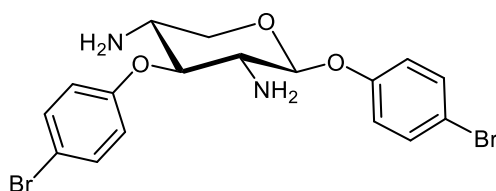
C(CH<sub>3</sub>)<sub>3</sub>, 1.28 (s, 9H, C(CH<sub>3</sub>)<sub>3</sub>) ppm; (500 MHz, DMSO-d<sub>6</sub>, 300 K):  $\delta$  = 7.49 (d, <sup>3</sup>J = 8.8 Hz, 2H, H-6, H-6'), 7.41 (d, <sup>3</sup>J = 8.8 Hz, 2H, H-8, H-8'), 7.09 (d, <sup>3</sup>J<sub>NH,2</sub> = 9.3 Hz, 1H, NH), 7.03 (d, <sup>3</sup>J<sub>NH,4</sub> = 9.2 Hz, 1H, NH), 6.97 (d, <sup>3</sup>J = 8.8 Hz, 2H, H-9, H-9'), 6.93 (d, <sup>3</sup>J = 8.8 Hz, 2H, H-7, H-7'), 5.04 (d, <sup>3</sup>J<sub>1,2</sub> = 8.03 Hz, 1H, H-1), 4.48 (t, <sup>3</sup>J<sub>3,4</sub> = 9.66 Hz, <sup>3</sup>J<sub>2,3</sub> = 9.66 Hz, 1H, H-3), 3.80 (dd, <sup>2</sup>J<sub>5a,5b</sub> = 11.37 Hz, <sup>3</sup>J<sub>5a,4</sub> = 5.15 Hz, 1H, H-5a), 3.68 (m, 1H, H-4), 3.60 (m, 1H, H-2), 3.43 (dd, <sup>2</sup>J<sub>5a,5b</sub> = 11.37 Hz, <sup>3</sup>J<sub>5b,4</sub> = 11.37 Hz, 1H, H-5b), 1.27 (s, 9H, C(CH<sub>3</sub>)<sub>3</sub>), 1.24 (s, 9H, C(CH<sub>3</sub>)<sub>3</sub>) ppm; (500 MHz, acetone-d<sub>6</sub>, 300 K):  $\delta$  = 7.47 (d, <sup>3</sup>J = 8.9 Hz, 2H, H-6, H-6'), 7.38 (d, <sup>3</sup>J = 8.9 Hz, 2H, H-8, H-8'), 7.07–6.98 (m, 4H, H-9, H-9', H-7, H-7'), 6.48 (d, <sup>3</sup>J<sub>NH,2</sub> = 9.0 Hz, 1H, NH), 6.32 (d, <sup>3</sup>J<sub>NH,4</sub> = 8.0 Hz, 1H, NH), 5.35 (d, <sup>3</sup>J<sub>1,2</sub> = 7.7 Hz, 1H, H-1), 4.88 (t, <sup>3</sup>J<sub>3,4</sub> = 9.1 Hz, <sup>3</sup>J<sub>2,3</sub> = 9.1 Hz, 1H, H-3), 3.99 (dd, <sup>2</sup>J<sub>5a,5b</sub> = 11.2 Hz, <sup>3</sup>J<sub>5a,4</sub> = 4.7 Hz, 1H, H-5a), 3.88 (m, 1H, H-4), 3.91–3.84 (m, 1H, H-2), 3.80–3.65 (m, 1H, H-5b), 1.32 (s, 9H, C(CH<sub>3</sub>)<sub>3</sub>), 1.30 (s, 9H, C(CH<sub>3</sub>)<sub>3</sub>) ppm; (500 MHz, MeOD-d<sub>3</sub>, 300 K):  $\delta$  = 7.41 (d, <sup>3</sup>J = 8.9 Hz, 2H, H-6, H-6'), 7.35 (d, <sup>3</sup>J = 9.0 Hz, 2H, H-8, H-8'), 6.99 (d, <sup>3</sup>J = 9.0 Hz, 2H, H-9, H-9'), 6.94 (d, <sup>3</sup>J = 8.8 Hz, 2H, H-7, H-7'), 5.14 (d, <sup>3</sup>J<sub>1,2</sub> = 7.41 Hz, 1H, H-1), 4.59 (t, <sup>3</sup>J<sub>3,4</sub> = 9.38 Hz, <sup>3</sup>J<sub>2,3</sub> = 8.73 Hz, 1H, H-3), 3.97 (dd, <sup>2</sup>J<sub>5a,5b</sub> = 11.92 Hz, <sup>3</sup>J<sub>5a,4</sub> = 5.12 Hz, 1H, H-5a), 3.80 (ddd, <sup>3</sup>J<sub>3,4</sub> = 9.38 Hz, <sup>3</sup>J<sub>4,5b</sub> = 9.61 Hz, <sup>3</sup>J<sub>4,5a</sub> = 5.12 Hz, 1H, H-4), 3.69 (dd, <sup>3</sup>J<sub>2,3</sub> = 8.73 Hz, <sup>3</sup>J<sub>1,2</sub> = 7.41 Hz, 1H, H-2), 3.52 (dd, <sup>3</sup>J<sub>4,5b</sub> = 9.61 Hz, <sup>2</sup>J<sub>5a,5b</sub> = 11.92 Hz, 1H, H-5b), 1.34 (s, 9H, C(CH<sub>3</sub>)<sub>3</sub>), 1.32 (s, 9H, C(CH<sub>3</sub>)<sub>3</sub>) ppm; (500 MHz, Pyridine-d<sub>5</sub>, 328 K):  $\delta$  = 7.35 (d, <sup>3</sup>J = 8.9 Hz, 2H, H-6, H-6'), 7.30 (d, <sup>3</sup>J = 8.9 Hz, 2H, H-8, H-8'), 7.15 (d, <sup>3</sup>J = 8.8 Hz, 2H, H-9, H-9'), 7.05 (d, <sup>3</sup>J = 8.8 Hz, 2H, H-7, H-7'), 5.78 (d, <sup>3</sup>J<sub>1,2</sub> = 6.77 Hz, 1H, H-1), 5.32 (t, <sup>3</sup>J<sub>3,4</sub> = 7.89 Hz, <sup>3</sup>J<sub>2,3</sub> = 7.89 Hz, 1H, H-3), 4.27 (dd, <sup>2</sup>J<sub>5a,5b</sub> = 11.51 Hz, <sup>3</sup>J<sub>5a,4</sub> = 4.69 Hz, 1H, H-5a), 4.22 (ddd, <sup>3</sup>J<sub>3,4</sub> = 8.34 Hz, <sup>3</sup>J<sub>4,5b</sub> = 9.89 Hz, <sup>3</sup>J<sub>4,5a</sub> = 4.69 Hz, 1H, H-4), 4.11 (dd, <sup>3</sup>J<sub>2,3</sub> = 8.34 Hz, <sup>3</sup>J<sub>1,2</sub> = 6.77 Hz, 1H, H-2), 3.88 (dd, <sup>3</sup>J<sub>4,5b</sub> = 9.89 Hz, <sup>2</sup>J<sub>5a,5b</sub> = 11.51 Hz, 1H, H-5b), 1.37 (s, 9H, C(CH<sub>3</sub>)<sub>3</sub>), 1.34 (s, 9H, C(CH<sub>3</sub>)<sub>3</sub>) ppm; (500 MHz, THF-d<sub>8</sub>, 300 K):  $\delta$  = 7.38 (d, <sup>3</sup>J = 8.7 Hz, 2H, H-6, H-6'), 7.33 (d, <sup>3</sup>J = 8.3 Hz, 2H, H-8, H-8'), 7.03 (d, <sup>3</sup>J = 8.0 Hz, 2H, H-9, H-9'), 6.95 (d, <sup>3</sup>J = 8.5 Hz, 2H, H-7, H-7'), 6.66 (d, <sup>3</sup>J<sub>NH,2</sub> = 7.6 Hz, 1H, NH), 6.40 (d, <sup>3</sup>J<sub>NH,4</sub> = 7.2 Hz, 1H, NH), 5.39 (d, <sup>3</sup>J<sub>1,2</sub> = 5.87 Hz, 1H, H-1), 4.82 (t, <sup>3</sup>J<sub>3,4</sub> = 7.89 Hz, <sup>3</sup>J<sub>2,3</sub> = 7.89 Hz, 1H, H-3), 4.01 (dd, <sup>2</sup>J<sub>5a,5b</sub> = 11.84 Hz, <sup>3</sup>J<sub>5a,4</sub> = 4.49 Hz, 1H, H-5a), 3.75 (ddd, <sup>3</sup>J<sub>3,4</sub> = 7.89 Hz, <sup>3</sup>J<sub>4,5b</sub> = 9.18 Hz, <sup>3</sup>J<sub>4,5a</sub> = 4.49 Hz, 1H, H-4), 3.55 (dd, <sup>3</sup>J<sub>2,3</sub> = 7.89 Hz, <sup>3</sup>J<sub>1,2</sub> = 5.87 Hz, 1H, H-2), 3.52 (dd, <sup>3</sup>J<sub>4,5b</sub> = 9.18 Hz, <sup>2</sup>J<sub>5a,5b</sub> = 11.84 Hz, 1H, H-5b), 1.35 (s, 9H, C(CH<sub>3</sub>)<sub>3</sub>), 1.32 (s, 9H, C(CH<sub>3</sub>)<sub>3</sub>) ppm; (500 MHz, toluene-d<sub>8</sub>, 328 K):  $\delta$  = 7.19 (d, <sup>3</sup>J = 8.9 Hz, 2H, H-6, H-6'), 7.13 (d, <sup>3</sup>J = 8.9 Hz, 2H, H-8, H-8'), 6.89 (d, <sup>3</sup>J = 8.9 Hz, 2H, H-9, H-9'), 6.71 (d, <sup>3</sup>J = 8.9 Hz, 2H, H-7, H-7'), 5.10 (d, <sup>3</sup>J<sub>1,2</sub> = 4.38 Hz, 1H, H-1), 4.76 (t, <sup>3</sup>J<sub>3,4</sub> = 6.10 Hz, <sup>3</sup>J<sub>2,3</sub> = 6.10 Hz, 1H, H-3), 4.42 (d, <sup>3</sup>J<sub>NH,2</sub> = 7.9 Hz, 1H, NH), 4.18 (d, <sup>3</sup>J<sub>NH,4</sub> = 3.5 Hz, 1H, NH), 3.89 (dd, <sup>2</sup>J<sub>5a,5b</sub> = 11.83 Hz, <sup>3</sup>J<sub>5a,4</sub> = 3.87 Hz, 1H, H-5a), 3.55 (ddd, <sup>3</sup>J<sub>3,4</sub> = 6.10 Hz, <sup>3</sup>J<sub>4,5b</sub> = 6.58 Hz, <sup>3</sup>J<sub>4,5a</sub> = 3.87 Hz, 1H, H-4), 3.49 (dd, <sup>3</sup>J<sub>2,3</sub> = 6.10 Hz, <sup>3</sup>J<sub>1,2</sub> = 4.38 Hz, 1H, H-2), 3.09 (dd, <sup>3</sup>J<sub>4,5b</sub> = 6.58 Hz, <sup>2</sup>J<sub>5a,5b</sub> = 11.83 Hz, 1H, H-5b), 1.36 (s, 9H, C(CH<sub>3</sub>)<sub>3</sub>), 1.32 (s, 9H, C(CH<sub>3</sub>)<sub>3</sub>) ppm; (500 MHz, benzene-d<sub>6</sub>, 328 K):  $\delta$  = 7.24 (d, <sup>3</sup>J = 8.8 Hz, 2H, H-6, H-6'), 7.18 (d, <sup>3</sup>J = 8.8 Hz, 2H, H-8, H-

8'), 6.94 (d,  $^3J = 8.8$  Hz, 2H, H-9, H-9'), 6.75 (d,  $^3J = 8.8$  Hz, 2H, H-7, H-7'), 5.18 (s, 1H, H-1), 4.85 (t,  $^3J_{3,4} = 5.63$  Hz,  $^3J_{2,3} = 5.63$  Hz, 1H, H-3), 4.50 (d,  $^3J_{\text{NH},2} = 7.9$  Hz, 1H, NH), 4.22 (s, 1H, NH), 3.92 (dd,  $^2J_{5a,5b} = 11.87$  Hz,  $^3J_{5a,4} = 3.81$  Hz, 1H, H-5a), 3.65 (ddd,  $^3J_{3,4} = 5.63$  Hz,  $^3J_{4,5b} = 6.55$  Hz,  $^3J_{4,5a} = 3.81$  Hz, 1H, H-4), 3.56 (dd,  $^3J_{2,3} = 5.63$  Hz, 1H, H-2), 3.11 (dd,  $^3J_{4,5b} = 6.55$  Hz,  $^2J_{5a,5b} = 11.87$  Hz, 1H, H-5b), 1.38 (s, 9H, C(CH<sub>3</sub>)<sub>3</sub>), 1.33 (s, 9H, C(CH<sub>3</sub>)<sub>3</sub>) ppm; (500 MHz, CDCl<sub>3</sub>, 328 K):  $\delta = 7.40\text{--}7.37$  (m, 4H, H-6, H-6', H-8, H-8'), 6.99 (d,  $^3J = 8.9$  Hz, 2H, H-9, H-9'), 6.91 (d,  $^3J = 9.0$  Hz, 2H, H-7, H-7'), 5.40 (d,  $^3J_{1,2} = 4.17$  Hz, 1H, H-1), 4.95 (d,  $^3J_{\text{NH},2} = 8.1$  Hz, 1H, NH), 4.83 (t,  $^3J_{3,4} = 5.53$  Hz,  $^3J_{2,3} = 5.53$  Hz, 1H, H-3), 4.72 (d,  $^3J_{\text{NH},4} = 4.6$  Hz, 1H, NH), 4.28 (dd,  $^2J_{5a,5b} = 12.04$  Hz,  $^3J_{5a,4} = 3.70$  Hz, 1H, H-5a), 3.79 (ddd,  $^3J_{3,4} = 5.53$  Hz,  $^3J_{4,5b} = 5.97$  Hz,  $^3J_{4,5a} = 3.70$  Hz, 1H, H-4), 3.75 (dd,  $^3J_{2,3} = 5.53$  Hz, 1H, H-2), 3.55 (dd,  $^3J_{4,5b} = 5.97$  Hz,  $^2J_{5a,5b} = 12.04$  Hz, 1H, H-5b), 1.43 (s, 9H, C(CH<sub>3</sub>)<sub>3</sub>), 1.40 (s, 9H, C(CH<sub>3</sub>)<sub>3</sub>) ppm; (500 MHz, Chlorobenzene-d<sub>5</sub>, 328 K):  $\delta = 7.00$  (d,  $^3J = 8.8$  Hz, 2H, H-6, H-6'), 6.98 (d,  $^3J = 8.9$  Hz, 2H, H-8, H-8'), 6.74 (d,  $^3J = 8.8$  Hz, 2H, H-9, H-9'), 6.56 (d,  $^3J = 8.8$  Hz, 2H, H-7, H-7'), 5.04 (d,  $^3J_{1,2} = 4.21$  Hz, 1H, H-1), 4.67 (t,  $^3J_{3,4} = 5.42$  Hz,  $^3J_{2,3} = 5.42$  Hz, 1H, H-3), 4.60 (d,  $^3J_{\text{NH},2} = 7.3$  Hz, 1H, NH), 4.38 (d,  $^3J_{\text{NH},4} = 5.9$  Hz, 1H, NH), 3.90 (dd,  $^2J_{5a,5b} = 12.00$  Hz,  $^3J_{5a,4} = 3.47$  Hz, 1H, H-5a), 3.58 (ddd,  $^3J_{3,4} = 5.42$  Hz,  $^3J_{4,5b} = 5.50$  Hz,  $^3J_{4,5a} = 3.47$  Hz, 1H, H-4), 3.45 (dd,  $^3J_{2,3} = 5.42$  Hz, 1H, H-2), 3.08 (dd,  $^3J_{4,5b} = 5.50$  Hz,  $^2J_{5a,5b} = 12.00$  Hz, 1H, H-5b), 1.19 (s, 9H, C(CH<sub>3</sub>)<sub>3</sub>), 1.15 (s, 9H, C(CH<sub>3</sub>)<sub>3</sub>) ppm;

**<sup>13</sup>C NMR:** (125 MHz, acetone-d<sub>6</sub>, 298 K, TMS):  $\delta = 160.13$  (C3-O-C<sub>quart</sub>), 157.84 (C1-O-C<sub>quart</sub>), 156.20 (C2-NH-C(O)), 156.12 (C4-NH-C(O)), 133.21 (2 OPhe-CH<sub>ortho</sub>), 132.80 (2 OPhe-CH<sub>ortho</sub>), 119.83 (2 OPhe-CH<sub>meta</sub>), 119.81 (2 OPhe-CH<sub>meta</sub>), 115.17 (Phe-CBr<sub>quart</sub>), 113.73 (Phe-CBr<sub>quart</sub>), 100.41 (C-1), 79.25 (2 C(CH<sub>3</sub>)<sub>3</sub>), 79.20 (C-3), 64.58 (C-5), 57.71 (C-2), 53.08 (C-4), 28.50 (6 C(CH<sub>3</sub>)<sub>3</sub>) ppm;

**ESI-MS:**  $m/z = 679.0629$  [M+Na]<sup>+</sup> (calculated  $m/z = 679.0625$  for [M+Na]<sup>+</sup>).

#### 4-Bromophenyl 2,4-diamino-2,4-dideoxy-3-O-(4-bromophenyl)- $\beta$ -D-xylopyranoside (167)



The xyloside **166** (39.0 mg, 382  $\mu$ mol) was dissolved in CH<sub>2</sub>Cl<sub>2</sub> (1.5 mL) and TFA (250  $\mu$ L) was added. It was stirred at room temperature for 16 h. Then the mixture was diluted with CH<sub>2</sub>Cl<sub>2</sub>, and it was neutralized by adding Amberlyst® A21. The mixture was filtered and concentrated and purification by column chromatography on silica (CH<sub>2</sub>Cl<sub>2</sub>/MeOH/NH<sub>3</sub>, 96:3:1) led to **167** as a colorless solid.

**Yield:** 25.0 mg (54.6  $\mu\text{mol}$ , 92 %);

**R<sub>f</sub>:** (CH<sub>2</sub>Cl<sub>2</sub>/MeOH/diethylamine, 96:3:1): R<sub>f</sub> = 0.40;

**[ $\alpha$ ]<sub>D</sub><sup>23</sup>:** -10.57 (c 0.08, CH<sub>2</sub>Cl<sub>2</sub>);

**IR (ATR):**  $\tilde{\nu}$  = 3304, 2922, 1578, 1484, 1226, 1068, 1004, 820, 659 cm<sup>-1</sup>;

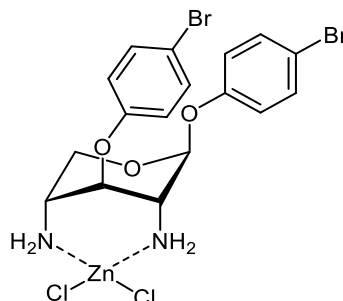
**<sup>1</sup>H NMR:** (600 MHz, acetone-d<sub>6</sub>, 298 K):  $\delta$  = 7.44 (d, <sup>3</sup>J = 9.0 Hz, 2H, H-6, H-6'), 7.33 (d, <sup>3</sup>J = 9.1 Hz, 2H, H-8, H-8'), 6.99 (d, <sup>3</sup>J = 9.0 Hz, 2H, H-9, H-9'), 6.93 (d, <sup>3</sup>J = 9.0 Hz, 2H, H-7, H-7'), 5.28 (d, <sup>3</sup>J<sub>1,2</sub> = 7.6 Hz, 1H, H-1), 4.58 (t, <sup>3</sup>J<sub>3,4</sub> = 9.2 Hz, <sup>3</sup>J<sub>2,3</sub> = 9.2 Hz, 1H, H-3), 4.00–3.94 (m, 1H, H-4), 3.91 (dd, <sup>3</sup>J<sub>2,3</sub> = 9.3 Hz, <sup>3</sup>J<sub>1,2</sub> = 7.6 Hz, 1H, H-2), 3.81–3.76 (m, 2H, H-5a, H-5b); (600 MHz, CDCl<sub>3</sub>, 298 K, TMS):  $\delta$  = 7.40 (d, <sup>3</sup>J = 8.9 Hz, 2H, H-6, H-6'), 7.39 (d, <sup>3</sup>J = 9.0 Hz, 2H, H-8, H-8'), 7.07 (d, <sup>3</sup>J = 9.0 Hz, 2H, H-9, H-9'), 7.01 (d, <sup>3</sup>J = 8.9 Hz, 2H, H-7, H-7'), 4.84 (d, <sup>3</sup>J<sub>1,2</sub> = 7.60 Hz, 1H, H-1), 4.05 (m, 1H, H-3), 4.03 (m, 1H, H-5a), 3.32 (1H, H-5b), 3.28 (1H, H-4), 3.26 (m, 1H, H-2) ppm; (600 MHz, MeCN-d<sub>3</sub>, 298 K):  $\delta$  = 7.45 (d, <sup>3</sup>J = 8.9 Hz, 2H, H-6, H-6'), 7.42 (d, <sup>3</sup>J = 9.0 Hz, 2H, H-8, H-8'), 7.08 (d, <sup>3</sup>J = 9.0 Hz, 2H, H-9, H-9'), 6.99 (d, <sup>3</sup>J = 8.9 Hz, 2H, H-7, H-7'), 4.84 (d, <sup>3</sup>J<sub>1,2</sub> = 7.52 Hz, 1H, H-1), 4.03 (t, <sup>3</sup>J<sub>3,4</sub> = 9.06 Hz, <sup>3</sup>J<sub>2,3</sub> = 9.06 Hz, 1H, H-3), 3.91 (dd, <sup>3</sup>J<sub>4,5a</sub> = 5.03 Hz, <sup>2</sup>J<sub>5a,5b</sub> = 11.66 Hz, 1H, H-5a), 3.34 (dd, <sup>3</sup>J<sub>4,5b</sub> = 10.22 Hz, <sup>2</sup>J<sub>5a,5b</sub> = 11.66 Hz, 1H, H-5b), 3.05 (ddd, <sup>3</sup>J<sub>3,4</sub> = 9.06 Hz, <sup>3</sup>J<sub>4,5b</sub> = 10.22 Hz, <sup>3</sup>J<sub>4,5a</sub> = 5.03 Hz, 1H, H-4), 3.02 (dd, <sup>3</sup>J<sub>2,3</sub> = 9.06 Hz, <sup>3</sup>J<sub>1,2</sub> = 7.52 Hz, 1H, H-2) ppm; (500 MHz, DMSO-d<sub>6</sub>, 298 K):  $\delta$  = 7.48 (d, <sup>3</sup>J = 8.9 Hz, 2H, H-6, H-6'), 7.42 (d, <sup>3</sup>J = 9.0 Hz, 2H, H-8, H-8'), 7.14 (d, <sup>3</sup>J = 9.0 Hz, 2H, H-9, H-9'), 7.01 (d, <sup>3</sup>J = 9.0 Hz, 2H, H-7, H-7'), 4.90 (d, <sup>3</sup>J<sub>1,2</sub> = 7.44 Hz, 1H, H-1), 4.07 (t, <sup>3</sup>J<sub>3,4</sub> = 8.93 Hz, <sup>3</sup>J<sub>2,3</sub> = 8.93 Hz, 1H, H-3), 3.84 (dd, <sup>3</sup>J<sub>4,5a</sub> = 5.00 Hz, <sup>2</sup>J<sub>5a,5b</sub> = 11.54 Hz, 1H, H-5a), 3.32 (dd, <sup>3</sup>J<sub>4,5b</sub> = 10.73 Hz, <sup>2</sup>J<sub>5a,5b</sub> = 11.54 Hz, 1H, H-5b), 2.92 (ddd, <sup>3</sup>J<sub>3,4</sub> = 8.93 Hz, <sup>3</sup>J<sub>4,5b</sub> = 10.73 Hz, <sup>3</sup>J<sub>4,5a</sub> = 5.00 Hz, 1H, H-4), 2.88 (dd, <sup>3</sup>J<sub>2,3</sub> = 8.93 Hz, <sup>3</sup>J<sub>1,2</sub> = 7.44 Hz, 1H, H-2), 1.67 (s, 4H, NH<sub>2</sub>) ppm;

**<sup>13</sup>C NMR:** (125 MHz, MeCN-d<sub>3</sub>, 298 K):  $\delta$  = 160.90 (C-12), 157.71 (C-10), 133.31 (2C, C-6, C-6'), 133.15 (2C, C-8, C-8'), 119.68 (2C, C-9, C-9'), 119.56 (2C, C-7, C-7'), 115.13 (C-11), 113.68 (C-13), 103.68 (C-1), 86.34 (C-3), 67.76 (C-5), 57.99 (C-2), 53.48 (C-4), ppm; (125 MHz, CDCl<sub>3</sub>, 298 K):  $\delta$  = 159.19 (C-12), 156.23 (C-10), 132.82 (2C, C-6, C-6'), 132.60 (2C, C-8, C-8'), 118.86 (2C, C-9, C-9'), 118.33 (2C, C-7, C-7'), 115.52 (C-11), 114.32 (C-13), 102.84 (C-1), 85.81 (C-3), 67.35 (C-5), 56.79 (C-2), 52.46 (C-4), ppm; ESI-HRMS:  $m/z$  = 456.9761 [M+Na]<sup>+</sup> (calcd  $m/z$  = 456.9757 for [M+Na]<sup>+</sup>).

**ESI-MS:**  $m/z$  = 456.9761 [M+Na]<sup>+</sup> (calculated  $m/z$  = 456.9757 for [M+Na]<sup>+</sup>).

## 8.2.5 Synthetic procedures for chapter 4.4

### Dichloro [4-Bromophenyl-2,4-*N*-carbonyl-2,4-diamino-2,4-dideoxy-3-*O*-(4-bromophenyl)- $\beta$ -D-xylopyranoside-*N,N'*] zinc (**168**)



The amino xyloside **167** (2.00 mg, 4.37  $\mu$ mol) was dissolved in MeCN- $d_3$  (600  $\mu$ L) and zinc chloride (595  $\mu$ g, 4.37  $\mu$ mol) was added. The formation of the complex **3** was observed in a quantitative yield (detected by  $^1\text{H}$  NMR).

$[\alpha]_{\text{D}}^{23}$ : -70.62 ( $c = 0.1$ , MeCN);

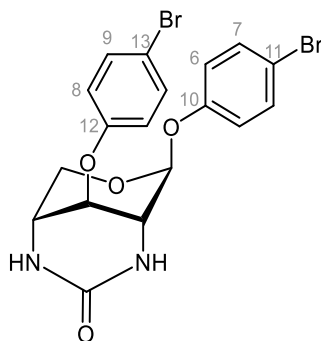
**IR (ATR)**:  $\tilde{\nu} = 2927, 1624, 1485, 1281, 1231, 1003, 825, 659 \text{ cm}^{-1}$ ;

**$^1\text{H}$  NMR**: (600 MHz, MeCN- $d_3$ , 328 K):  $\delta = 7.52$  (d,  $^3J = 8.8$  Hz, 2H, H-6, H-6'), 7.49 (d,  $^3J = 8.9$  Hz, 2H, H-8, H-8'), 7.07 (d,  $^3J = 8.9$  Hz, 2H, H-9, H-9'), 7.01 (d,  $^3J = 7.7$  Hz, 2H, H-7, H-7'), 5.50 (d,  $^3J_{1,2} = 2.18$  Hz, 1H, H-1), 4.52 (dd,  $^3J_{3,4} = 3.90$  Hz,  $^3J_{2,3} = 3.54$  Hz, 1H, H-3), 4.36 (dd,  $^3J_{4,5a} = 2.24$  Hz,  $^2J_{5a,5b} = 13.0$  Hz, 1H, H-5a), 3.65 (dd,  $^3J_{4,5b} = 2.83$  Hz,  $^2J_{5a,5b} = 13.0$  Hz, 1H, H-5b), 3.51 (dd,  $^3J_{2,3} = 3.54$  Hz,  $^3J_{1,2} = 2.18$  Hz, 1H, H-2), 3.37 (ddd,  $^3J_{3,4} = 3.90$  Hz,  $^3J_{4,5b} = 2.83$  Hz,  $^3J_{4,5a} = 2.24$  Hz, 1H, H-4), ppm;

**$^{13}\text{C}$  NMR**: (125 MHz, MeCN- $d_3$ , 298 K):  $\delta = 156.45$  (C-12), 156.22 (C-10), 133.53 (2C, C-6, C-6'), 133.45 (2C, C-8, C-8'), 119.82 (2C, C-9, C-9'), 119.66 (2C, C-7, C-7'), 115.05 (C-11), 115.03 (C-13), 97.00 (C-1), 72.21 (C-3), 59.07 (C-5), 49.44 (C-2), 48.34 (C-4) ppm;

**ESI-MS**:  $m/z = 590.8452$   $[\text{M}+\text{H}]^+$  (calculated  $m/z = 590.8431$  for  $[\text{M}+\text{H}]^+$ )

**4-Bromophenyl-2,4-*N*-carbonyl-2,4-diamino-2,4-dideoxy-3-*O*-(4-bromophenyl)- $\beta$ -D-xylopyranoside (**169**)**



The xyloside **167** (7.33 mg, 15.2  $\mu$ mol) was dissolved in DMF (100  $\mu$ L) and *N,N*-carbonyldiimidazole (3.00 mg, 18.2  $\mu$ mol) was added. Then trimethylamine (8.50  $\mu$ L, 60.8  $\mu$ mol) was added dropwise. The reaction mixture was stirred for 16 h at room temperature. Then it was diluted with ethyl acetate and washed with 1N HCl, sodium bicarbonate and brine. The combined org. layers were dried over  $\text{MgSO}_4$ , filtered, and concentrated. Purification by column chromatography on silica ( $\text{CH}_2\text{Cl}_2/\text{MeOH}$ , 95:5) gave **169** as a colorless solid.

**Yield:** 6.00 mg (12.3  $\mu$ mol, 81 %);

**R<sub>f</sub>:** ( $\text{CH}_2\text{Cl}_2/\text{MeOH}$ , 95:5):  $R_f = 0.40$ ;

**$[\alpha]_D^{23}$ :** -80.33 ( $c = 0.1$ ,  $\text{CH}_2\text{Cl}_2$ );

**IR (ATR):**  $\tilde{\nu} = 3242, 2927, 2262, 1671, 1589, 1485, 1216, 1066, 1003, 821, 640 \text{ cm}^{-1}$ ;

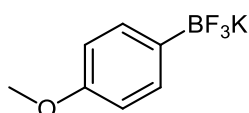
**$^1\text{H NMR}$ :** (600 MHz,  $\text{MeCN-d}_3$ , 298 K):  $\delta = 7.49$  (d,  $^3J = 9.0$  Hz, 2H, H-6, H-6'), 7.40 (d,  $^3J = 9.0$  Hz, 2H, H-8, H-8'), 7.04 (d,  $^3J = 9.0$  Hz, 2H, H-9, H-9'), 6.89 (d,  $^3J = 9.0$  Hz, 2H, H-7, H-7'), 5.60 (s, 1H, NH), 5.50 (s, 1H, NH), 5.36 (d,  $^3J_{1,2} = 2.80$  Hz, 1H, H-1), 4.89 (t,  $^3J_{3,4} = 3.18$  Hz,  $^3J_{2,3} = 3.89$  Hz, 1H, H-3), 4.29 (dd,  $^3J_{4,5a} = 1.67$  Hz,  $^2J_{5a,5b} = 12.0$  Hz, 1H, H-5a), 3.71 (dd,  $^3J_{2,3} = 3.89$  Hz,  $^3J_{1,2} = 2.80$  Hz, 1H, H-2), 3.54 (ddd,  $^3J_{3,4} = 3.18$  Hz,  $^3J_{4,5b} = 1.90$  Hz,  $^3J_{4,5a} = 1.67$  Hz, 1H, H-4), 3.49 (dd,  $^3J_{4,5b} = 1.90$  Hz,  $^2J_{5a,5b} = 12.0$  Hz, 1H, H-5b) ppm; (600 MHz,  $\text{CDCl}_3$ , 298 K):  $\delta = 7.46$  (d,  $^3J = 8.9$  Hz, 2H, H-6, H-6'), 7.35 (d,  $^3J = 8.9$  Hz, 2H, H-8, H-8'), 6.91 (d,  $^3J = 8.9$  Hz, 2H, H-9, H-9'), 6.83 (d,  $^3J = 8.9$  Hz, 2H, H-7, H-7'), 6.45 (s, 1H, NH), 6.15 (s, 1H, NH), 5.35 (d,  $^3J_{1,2} = 2.88$  Hz, 1H, H-1), 4.84 (t,  $^3J_{3,4} = 3.29$  Hz,  $^3J_{2,3} = 3.90$  Hz, 1H, H-3), 4.41 (dd,  $^3J_{4,5a} = 1.71$  Hz,  $^2J_{5a,5b} = 11.9$  Hz, 1H, H-5a), 3.80 (dd,  $^3J_{2,3} = 3.90$  Hz,  $^3J_{1,2} = 2.88$  Hz, 1H, H-2), 3.61 (ddd,  $^3J_{3,4} = 3.29$  Hz,  $^3J_{4,5b} = 2.00$  Hz,  $^3J_{4,5a} = 1.71$  Hz, 1H, H-4), 3.57 (dd,  $^3J_{4,5b} = 2.00$  Hz,  $^2J_{5a,5b} = 11.9$  Hz, 1H, H-5b) ppm;

**<sup>13</sup>C NMR:** (125 MHz, MeCN-d<sub>3</sub>, 298 K):  $\delta$  = 162.74 (C-14), 157.08 (C-12), 156.81 (C-10), 133.47 (2C, C-6, C-6'), 133.26 (2C, C-8, C-8'), 119.45 (2C, C-9, C-9'), 118.97 (2C, C-7, C-7'), 114.71 (C-11), 114.25 (C-13), 99.13 (C-1), 68.51 (C-3), 62.01 (C-5), 48.13 (C-4), 47.18 (C-2) ppm; (125 MHz, CDCl<sub>3</sub>, 298 K):  $\delta$  = 175.72 (C-14), 155.69 (C-12), 155.62 (C-10), 132.86 (2C, C-6, C-6'), 132.53 (2C, C-8, C-8'), 118.15 (2C, C-9, C-9'), 117.69 (2C, C-7, C-7'), 114.78 (C-11), 114.61 (C-13), 98.24 (C-1), 67.63 (C-3), 61.08 (C-5), 47.68 (C-4), 46.74 (C-2) ppm;

**ESI-MS:**  $m/z$  = 504.9369 [M+Na]<sup>+</sup> (calculated  $m/z$  = 504.9375 for [M+Na]<sup>+</sup>).

## 8.2.6 Synthetic procedures for chapter 6

### Potassium (4-Methoxyphenyl)trifluoroborate (**173**)<sup>[289]</sup>



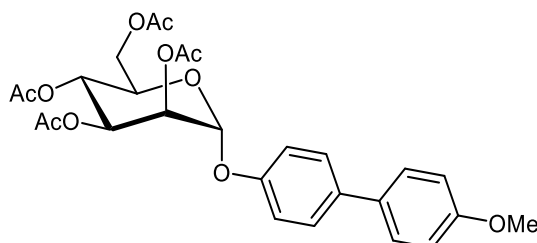
The boronic ester **172** (100 mg, 454  $\mu$ mol) was dissolved in MeOH (1.32 mL) and a KHF<sub>2</sub>-solution (4.5 M in H<sub>2</sub>O, 565  $\mu$ L, 2.54 mmol) was added. It was stirred for 1 h at room temperature. Then the solvent was removed, and the crude product was dissolved in hot acetone and filtered. The filtrate was concentrated, and it was recrystallized from a small amount of acetone and Et<sub>2</sub>O.

**Yield:** 69.0 mg (322  $\mu$ mol, 71 %);

**<sup>1</sup>H NMR:** (200 MHz, DMSO-d<sub>6</sub>, 300 K):  $\delta$  = 7.21 (d, <sup>3</sup>J = 8.4 Hz, 2H, CH<sub>arom</sub>), 6.66 (d, <sup>3</sup>J = 8.5 Hz, 2H, CH<sub>arom</sub>), 3.67 (s, 3H, OCH<sub>3</sub>), ppm;

Analytical data corresponds to the literature.<sup>[289]</sup>

### [4'-Methoxy-(1,1'-biphenyl)-4-yl] 2,3,4,6-tetra-O-acetyl- $\alpha$ -D-mannopyranoside (**175**)



The trifluoroborate **173** (30.0 mg, 140  $\mu$ mol) and mannoside **174** (58.0 mg, 105  $\mu$ mol) were dissolved in dry MeOH (1.00 mL). Then DIPEA (53.6  $\mu$ L, 315  $\mu$ mol) and Pd(dppf)Cl<sub>2</sub>·CH<sub>2</sub>Cl<sub>2</sub> (6.00 mg, 7.35  $\mu$ mol) were added. The reaction mixture was heated to 70 °C and stirred for 2 h. The volatiles were removed, and the crude product was taken up in ethyl acetate. It was

washed with H<sub>2</sub>O and the combined org. layers were dried over MgSO<sub>4</sub>, filtered, and concentrated. Purification by flash column chromatography on silica (cyclohexane/ ethyl acetate, 2:1) gave **175** as a colorless solid.

**Yield:** 30.0 mg (56.5 μmol, 54 %);

**R<sub>f</sub>:** (cyclohexane/ethyl acetate, 2:1): R<sub>f</sub> = 0.27;

**[α]<sub>D</sub><sup>23</sup>:** -19.8 (c = 0.02, CH<sub>2</sub>Cl<sub>2</sub>);

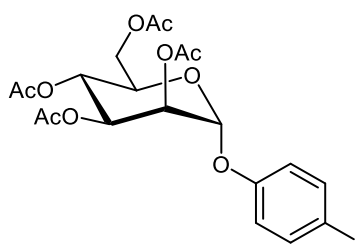
**IR (ATR):**  $\tilde{\nu}$  = 2251, 2112, 1754, 1699, 1539, 1369, 1210, 1036, 981, 823, 603 cm<sup>-1</sup>;

**<sup>1</sup>H NMR:** (600 MHz, CDCl<sub>3</sub>, 300 K, TMS): δ = 7.49-7.45 (m, 4H, H<sub>arom</sub>), 7.13 (d, <sup>3</sup>J = 8.7 Hz, 2H, H<sub>arom</sub>), 6.96 (d, <sup>3</sup>J = 8.7 Hz, 2H, CH<sub>arom</sub>), 5.59 (dd, <sup>3</sup>J<sub>3,4</sub> = 10.0 Hz, <sup>3</sup>J<sub>2,3</sub> = 3.5 Hz, 1H, H-3), 5.55 (d, <sup>3</sup>J<sub>1,2</sub> = 1.4 Hz, 1H, H-1), 5.47 (dd, <sup>3</sup>J<sub>2,3</sub> = 3.4 Hz, <sup>3</sup>J<sub>1,2</sub> = 1.8 Hz, 1H, H-2), 5.38 (dd~t, <sup>3</sup>J<sub>3,4</sub> = 10.1 Hz, <sup>3</sup>J<sub>4,5</sub> = 10.1 Hz, 1H, H-4), 4.29 (dd, <sup>2</sup>J<sub>6a,6b</sub> = 12.2 Hz, <sup>3</sup>J<sub>5,6a</sub> = 5.3 Hz, 1H, H-6a), 4.13 (ddd, <sup>3</sup>J<sub>4,5</sub> = 10.1 Hz, <sup>3</sup>J<sub>5,6a</sub> = 5.3 Hz, <sup>3</sup>J<sub>5,6b</sub> = 2.1 Hz, 1H, H-5), 4.09 (dd, <sup>2</sup>J<sub>6a,6b</sub> = 12.2 Hz, <sup>3</sup>J<sub>5,6b</sub> = 2.1 Hz, 1H, H-6b), 3.85 (s, 3H, OCH<sub>3</sub>), 2.21, 2.06, 2.05, 2.03 (s, each 3 H, 4 OAc) ppm;

**<sup>13</sup>C NMR:** (125 MHz, CDCl<sub>3</sub>, 300 K, TMS): δ = 170.71, 170.16, 170.12, 169.92 (4C, C(O)-Ac), 159.14 (1C<sub>quart</sub>), 154.77 (1C<sub>quart</sub>), 136.00 (1C<sub>quart</sub>), 133.12 (1C<sub>quart</sub>), 128.01 (2C), 127.99 (2C), 116.93 (2C), 114.38 (2C), 96.04 (C-1), 69.59 (C-2), 69.31 (C-5), 69.06 (C-3), 66.13 (C-4), 62.29 (C-6), 55.51 (OCH<sub>3</sub>), 21.05, 20.87, 20.86, 20.83 (4C, Ac-CH<sub>3</sub>) ppm;

**ESI-MS:** *m/z* = 553.1642 [M+Na]<sup>+</sup> (calculated *m/z* = 553.1686 for [M+Na]<sup>+</sup>).

#### 4-Iodophenyl 2,3,4,6-tetra-O-acetyl-α-D-mannopyranoside (**177**)<sup>[277]</sup>



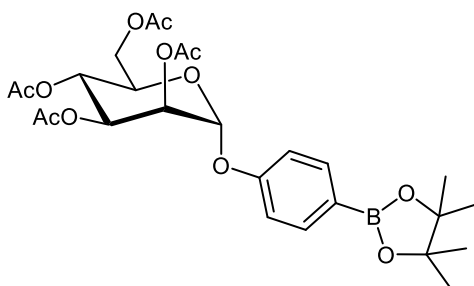
The mannosyl trichloroacetimidate **176** (1.43 g, 2.90 mmol) and 4-iodo phenol (1.28 g, 5.80 mmol) were dissolved in dry CH<sub>2</sub>Cl<sub>2</sub> (50.0 mL) and 4Å MS was added. The suspension was stirred for 30 min at room temperature. Then it was cooled down to 0 °C and BF<sub>3</sub>·Et<sub>2</sub>O (716 μL, 5.80 mmol) was added. The reaction mixture was allowed to warm to room temperature and stirring was continued for 16 h before a solution of NaHCO<sub>3</sub> was added. It was diluted with ethyl acetate and filtered over celite. The org. layer was washed with brine and H<sub>2</sub>O, dried over MgSO<sub>4</sub>, filtered, and concentrated. Purification by column chromatography on silica (toluene/ethyl acetate, 4:1) gave the title compound as a colorless solid.

**Yield:** 622 mg (1.13 mmol, 39 %);

**<sup>1</sup>H NMR:** (500 MHz, CDCl<sub>3</sub>, 300 K, TMS): δ = 7.60 (d, <sup>3</sup>J = 8.9 Hz, 2H, CH<sub>arom</sub>), 6.87 (d, <sup>3</sup>J = 8.9 Hz, 2H, CH<sub>arom</sub>), 5.45 (d, <sup>3</sup>J<sub>1,2</sub> = 1.7 Hz, 1H, H-1), 5.43 (dd, <sup>3</sup>J<sub>3,4</sub> = 10.0 Hz, <sup>3</sup>J<sub>3,2</sub> = 3.5 Hz, 1H, H-3), 5.40 (dd, <sup>3</sup>J<sub>2,3</sub> = 3.5 Hz, <sup>3</sup>J<sub>1,2</sub> = 1.8 Hz, 1H, H-2), 5.35 (dd~t, <sup>3</sup>J<sub>3,4</sub> = 10.2 Hz, <sup>3</sup>J<sub>4,5</sub> = 10.2 Hz, 1H, H-4), 4.26 (dd, <sup>2</sup>J<sub>6a,6b</sub> = 12.4 Hz, <sup>3</sup>J<sub>5,6a</sub> = 5.6 Hz, 1H, H-6a), 4.09-4.01 (m, 2H, H-5, H-6b), 2.20, 2.20, 2.06, 2.04 (s, each 3 H, 4 OAc) ppm;

Analytical data corresponds to the literature.<sup>[277]</sup>

**4-(4,4,5,5-Tetramethyl-1,3,2-dioxaborolan-2-yl)phenyl 2,3,4,6-tetra-O-acetyl-α-D-mannopyranoside (178)**<sup>[278]</sup>

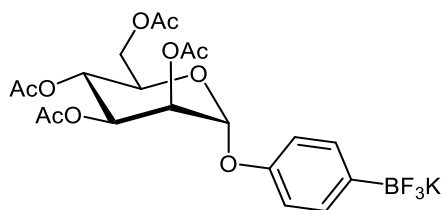


Under a nitrogen atmosphere 4-iodophenyl mannoside **176** (550 mg, 999 μmol), bis(pinacolato)diboron (280 mg, 1.10 mmol), KOAc (430 mg, 4.38 mmol) and Pd(dppf)Cl<sub>2</sub>·CH<sub>2</sub>Cl<sub>2</sub> (43.4 mg, 59.4 μmol) were suspended in dry DMF (10.0 mL). Then the reaction mixture was heated to 80 °C and stirred for 2.5 h. After cooling down to room temperature, the solvent was removed under reduced pressure. Purification by flash column chromatography on silica (cyclohexane/ ethyl acetate, 4:1) led to a colorless solid.

**Yield:** 330 mg (599 μmol, 60 %);

**<sup>1</sup>H NMR:** (500 MHz, CDCl<sub>3</sub>, 300 K, TMS): δ = 7.76 (d, <sup>3</sup>J = 8.7 Hz, 2H, CH<sub>arom</sub>), 7.08 (d, <sup>3</sup>J = 8.7 Hz, 2H, CH<sub>arom</sub>), 5.61-5.52 (m, 2H, H-1, H-3), 5.45 (dd, <sup>3</sup>J<sub>2,3</sub> = 3.4 Hz, <sup>3</sup>J<sub>1,2</sub> = 1.9 Hz, 1H, H-2), 5.36 (dd~t, <sup>3</sup>J<sub>3,4</sub> = 10.0 Hz, <sup>3</sup>J<sub>4,5</sub> = 10.0 Hz, 1H, H-4), 4.29 (dd, <sup>2</sup>J<sub>6a,6b</sub> = 11.9 Hz, <sup>3</sup>J<sub>5,6a</sub> = 5.0 Hz, 1H, H-6a), 4.12-3.98 (m, 2H, H-5, H-6b), 2.20, 2.05, 2.03, 2.03 (s, each 3 H, 4 OAc), 1.33 (s, 12H, 4 CH<sub>3</sub>) ppm;

Analytical data corresponds to the literature.<sup>[278]</sup>

**Potassium 4-trifluoroborate-phenyl 2,3,4,6-tetra-O-acetyl- $\alpha$ -D-mannopyranoside (179)**

The mannosyl boron ester **178** (100 mg, 454  $\mu$ mol) was dissolved in MeOH (1.32 mL) and a KHF<sub>2</sub>-solution (4.5 M in H<sub>2</sub>O, 565  $\mu$ L, 2.54 mmol) was added. It was stirred for 1 h at room temperature. Then the solvent was removed under reduced pressure. The crude product was dissolved in hot acetone and filtered. The filtrate was concentrated, and it was recrystallized from a small amount of acetone and Et<sub>2</sub>O.

**Yield:** 88.0 mg (166  $\mu$ mol, 91 %);

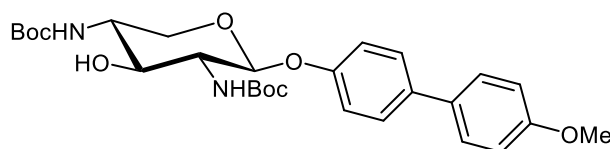
**[ $\alpha$ ]<sub>D</sub><sup>23</sup>:** -5.8 (c = 0.01, acetone);

**IR (ATR):**  $\tilde{\nu}$  = 1747, 1369, 1203, 1125, 1037, 952, 826, 601 cm<sup>-1</sup>;

**<sup>1</sup>H NMR:** (600 MHz, DMSO-d<sub>6</sub>, 300 K, TMS):  $\delta$  = 7.60 (d, <sup>3</sup>J = 8.1 Hz, 2H, H<sub>arom</sub>), 6.85 (d, <sup>3</sup>J = 7.9 Hz, 2H, CH<sub>arom</sub>), 5.56 (s, 1H, H-1), 5.37-5.29 (m, 2H, H-2, H-3), 5.16 (dd~t, <sup>3</sup>J<sub>3,4</sub> = 10.0 Hz, <sup>3</sup>J<sub>4,5</sub> = 10.0 Hz, 1H, H-4), 4.15 (dd, <sup>2</sup>J<sub>6a,6b</sub> = 12.1 Hz, <sup>3</sup>J<sub>5,6a</sub> = 5.6 Hz, 1H, H-6a), 4.08 (ddd, <sup>3</sup>J<sub>4,5</sub> = 9.4 Hz, <sup>3</sup>J<sub>5,6a</sub> = 5.5 Hz, <sup>3</sup>J<sub>5,6b</sub> = 1.8 Hz, 1H, H-5), 3.97 (dd, <sup>2</sup>J<sub>6a,6b</sub> = 12.1 Hz, <sup>3</sup>J<sub>5,6b</sub> = 1.6 Hz, 1H, H-6b), 2.14, 2.04, 1.98, 1.93 (s, each 3 H, 4 OAc) ppm;

**<sup>13</sup>C NMR:** (125 MHz, DMSO-d<sub>6</sub>, 300 K, TMS):  $\delta$  = 169.93, 169.66, 169.56 (4C, C(O)-Ac), 153.13 (1C<sub>quart</sub>), 132.35 (2C), 115.16 (2C), 95.55 (C-1), 68.66 (C-2), 68.59 (C-3), 68.50 (C-5), 65.37 (C-4), 61.77 (C-6), 20.67, 20.45 (4C, Ac-C<sub>H3</sub>) ppm;

**ESI-MS:**  $m/z$  = 531.0931 [M+H]<sup>+</sup> (calculated  $m/z$  = 531.0973 for [M+H]<sup>+</sup>).

**[4'-Methoxy(1,1'-biphenyl)-4-yl] 2,4-dideoxy-2,4-N-Boc- $\beta$ -D-xylopyranoside (181)**

The trifluoroborate **173** (5.70 mg, 26.4  $\mu$ mol) and xyloside **164** (10.0 mg, 19.9  $\mu$ mol) were dissolved in dry MeOH (200  $\mu$ L). To the mixture DIPEA (10.2  $\mu$ L, 60.0  $\mu$ mol) and Pd(dppf)Cl<sub>2</sub>·CH<sub>2</sub>Cl<sub>2</sub> (1.14 mg, 1.39  $\mu$ mol) were added. The reaction mixture was heated to 80 °C and it was stirred for 2 h. Then the volatiles were removed, and the crude product was taken up in ethyl acetate. It was washed with H<sub>2</sub>O and the combined org. layers were dried

over  $\text{MgSO}_4$ , filtered, and concentrated to dryness. Purification by flash column chromatography on silica (cyclohexane/ ethyl acetate, 2:1) gave **181** as a colorless solid.

**Yield:** 9.00 mg (17.0  $\mu\text{mol}$ , 85 %);

**R<sub>f</sub>:** (cyclohexane/ethyl acetate, 2:1):  $R_f = 0.30$ ;

$[\alpha]_D^{23}$ : +7.1 ( $c = 0.01$ ,  $\text{CH}_2\text{Cl}_2$ );

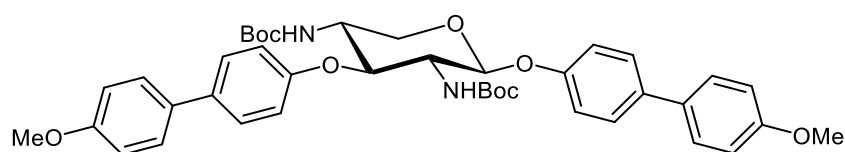
**IR (ATR):**  $\tilde{\nu} = 3751, 3323, 2970, 1681, 1536, 1497, 1293, 1235, 1169, 1042, 821, 611 \text{ cm}^{-1}$ ;

**$^1\text{H NMR}$ :** (600 MHz, acetone- $d_6$ , 298 K, TMS):  $\delta = 7.57\text{--}7.48$  (m, 4H,  $\text{H}_{\text{arom}}$ ), 7.06 (d,  $^3J = 8.6 \text{ Hz}$ , 2H,  $\text{H}_{\text{arom}}$ ), 6.99 (d,  $^3J = 8.8 \text{ Hz}$ , 2H,  $\text{H}_{\text{arom}}$ ), 6.22 (s, 1H,  $\text{NH}_{\text{Boc}}$ ), 6.02 (s, 1H,  $\text{NH}_{\text{Boc}}$ ), 5.10 (d,  $^3J_{1,2} = 7.9 \text{ Hz}$ , 1H, H-1), 4.42 (d,  $^3J_{3,\text{OH}} = 3.3 \text{ Hz}$ , 1H, OH), 4.04 (dd,  $^2J_{5a,5b} = 11.4 \text{ Hz}$ ,  $^3J_{5a,4} = 5.1 \text{ Hz}$ , 1H, H-5a), 3.82 (s, 3H,  $\text{OCH}_3$ ), 3.80–3.74 (m, 1H, H-3), 3.69–3.60 (m, 2H, H-2, H-4), 3.40 (t,  $^2J_{5a,5b} = 11.0 \text{ Hz}$ ,  $^3J_{5a,4} = 11.0 \text{ Hz}$ , 1H, H-5b), 1.41 (s, 18H, 2  $\text{C}(\text{CH}_3)_3$ ) ppm;

**$^{13}\text{C NMR}$ :** (125 MHz, acetone- $d_6$ , 298 K, TMS):  $\delta = 160.11$  (NH-C(O)), 158.05 (NH-C(O)), 136.80 ( $\text{C}_{\text{quart}}$ ), 135.88 ( $\text{C}_{\text{quart}}$ ), 133.93 ( $\text{C}_{\text{quart}}$ ), 128.55 (2  $\text{C}_{\text{H}_{\text{arom}}}$ ), 128.36 (2  $\text{C}_{\text{H}_{\text{arom}}}$ ), 118.03 (2  $\text{C}_{\text{H}_{\text{arom}}}$ ), 115.18 (2  $\text{C}_{\text{H}_{\text{arom}}}$ ), 113.95 ( $\text{C}_{\text{quart}}$ ), 101.62 (C-1), 79.18 ( $\text{C}(\text{CH}_3)_3$ ), 79.10 ( $\text{C}(\text{CH}_3)_3$ ), 72.88 (C-3), 64.23 (C-5), 59.12 (C-2), 55.69 ( $\text{OCH}_3$ ), 55.40 (C-4), 28.75 (3C,  $\text{C}(\text{CH}_3)_3$ ), 28.68 (3C,  $\text{C}(\text{CH}_3)_3$ ) ppm;

**ESI-MS:**  $m/z = 553.2513$  [ $\text{M}+\text{Na}$ ] $^+$  (calculated  $m/z = 553.2526$  for [ $\text{M}+\text{Na}$ ] $^+$ ).

**[4'-Methoxy(1,1'-biphenyl)-4-yl] 2,4-dideoxy-2,4-N-Boc-3-O-[4'-methoxy(1,1'-biphenyl)-4-yl]- $\beta$ -D-xylopyranoside (182)**



The trifluoroborate **173** (8.65 mg, 40.4  $\mu\text{mol}$ ) and xyloside **166** (10.0 mg, 15.2  $\mu\text{mol}$ ) were dissolved in dry MeOH (200  $\mu\text{L}$ ). To the mixture DIPEA (15.5  $\mu\text{L}$ , 91.2  $\mu\text{mol}$ ) and  $\text{Pd}(\text{dppf})\text{Cl}_2 \cdot \text{CH}_2\text{Cl}_2$  (1.74 mg, 2.13  $\mu\text{mol}$ ) were added. The reaction mixture was heated to 80  $^\circ\text{C}$  and it was stirred for 2 h. Then the volatiles were removed, and the crude product was taken up in ethyl acetate. It was washed with  $\text{H}_2\text{O}$  and the combined org. layers were dried over  $\text{MgSO}_4$ , filtered, and concentrated to dryness. Purification by flash column chromatography on silica (cyclohexane/ ethyl acetate, 3:1) gave **182** as a colorless solid.

**Yield:** 4.00 mg (5.61  $\mu\text{mol}$ , 37 %);

**R<sub>f</sub>:** (cyclohexane/ethyl acetate, 2:1):  $R_f = 0.40$ ;

$[\alpha]_D^{23}$ : +20.1 (c = 0.02, DMSO);

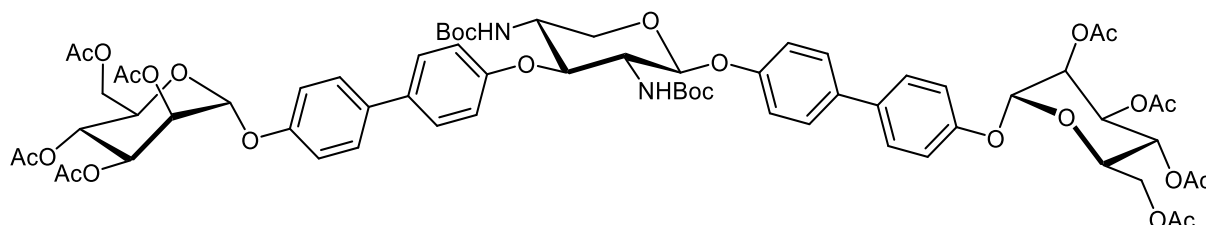
**IR (ATR):**  $\tilde{\nu}$  = 3761, 2975, 1701, 1533, 1477, 1296, 1287, 1163, 1062, 811, 607  $\text{cm}^{-1}$ ;

**$^1\text{H NMR}$ :** (600 MHz, DMSO- $d_6$ , 298 K, TMS):  $\delta$  = 7.58–7.45 (m, 8H, 8  $\text{H}_{\text{arom}}$ ), 7.18–6.97 (m, 10H, 2  $\text{NH Boc}$ , 8  $\text{H}_{\text{arom}}$ ), 5.11 (d,  $^3J_{1,2}$  = 7.7 Hz, 1H, H-1), 4.52 (d,  $^3J_{2,3}$  = 9.3 Hz,  $^3J_{3,4}$  = 9.3 Hz, 1H, H-3), 3.82 (dd,  $^2J_{5a,5b}$  = 11.2 Hz,  $^3J_{5a,4}$  = 4.8 Hz, 1H, H-5a), 3.79 (s, 3H,  $\text{OCH}_3$ ), 3.78 (s, 3H,  $\text{OCH}_3$ ), 3.76–3.70 (m, 1H, H-4), 3.67–3.61 (m, 1H, H-2), 3.45 (t,  $^2J_{5a,5b}$  = 11.0 Hz,  $^3J_{5a,4}$  = 11.0 Hz, 1H, H-5b), 1.28 (s, 9H,  $\text{C}(\text{CH}_3)_3$ ), 1.27 (s, 9H,  $\text{C}(\text{CH}_3)_3$ ) ppm;

**$^{13}\text{C NMR}$ :** (125 MHz, DMSO- $d_6$ , 298 K, TMS):  $\delta$  = 158.83 ( $\text{C}_{\text{quart}}$ ), 158.58 ( $\text{NH-C(O)}$ ), 158.40 ( $\text{NH-C(O)}$ ), 156.19 ( $\text{C}_{\text{quart}}$ ), 155.23 ( $\text{C}_{\text{quart}}$ ), 155.03 ( $\text{C}_{\text{quart}}$ ), 134.25 ( $\text{C}_{\text{quart}}$ ), 132.99 ( $\text{C}_{\text{quart}}$ ), 132.44 ( $\text{C}_{\text{quart}}$ ), 132.07 ( $\text{C}_{\text{quart}}$ ), 127.43 (2  $\text{C}_{\text{H}_{\text{arom}}}$ ), 127.36 (2  $\text{C}_{\text{H}_{\text{arom}}}$ ), 127.28 (2  $\text{C}_{\text{H}_{\text{arom}}}$ ), 126.79 (2  $\text{C}_{\text{H}_{\text{arom}}}$ ), 117.13 (2  $\text{C}_{\text{H}_{\text{arom}}}$ ), 116.91 (2  $\text{C}_{\text{H}_{\text{arom}}}$ ), 114.33 (2  $\text{C}_{\text{H}_{\text{arom}}}$ ), 114.31 (2  $\text{C}_{\text{H}_{\text{arom}}}$ ), 99.46 (C-1), 79.12 (C-3), 78.03 ( $\text{C}(\text{CH}_3)_3$ ), 77.87 ( $\text{C}(\text{CH}_3)_3$ ), 63.76 (C-5), 56.55 (C-2), 55.16 (2  $\text{OCH}_3$ ), 51.87 (C-4), 28.10 (6C,  $\text{C}(\text{CH}_3)_3$ ) ppm;

**ESI-MS:**  $m/z$  = 735.3255  $[\text{M}+\text{Na}]^+$  (calculated  $m/z$  = 735.3258 for  $[\text{M}+\text{Na}]^+$ ).

**4'-[(1,1'-Biphenyl)-2,3,4,6-tetra-O-acetyl- $\alpha$ -D-mannopyranoside]-4-yl 2,4-dideoxy-2,4-N-Boc-3-O-{4'-[(1,1'-biphenyl)-2,3,4,6-tetra-O-acetyl- $\alpha$ -D-mannopyranoside]-4-yl}- $\beta$ -D-xylopyranoside (183)**



The xyloside **166** (60.0 mg, 87.2  $\mu\text{mol}$ ), pinacol ester **178** (144 mg, 261  $\mu\text{mol}$ ), CsF (79.4 mg, 523  $\mu\text{mol}$ ) and  $\text{Pd}(\text{dppf})\text{Cl}_2 \cdot \text{CH}_2\text{Cl}_2$  (14.2 mg, 17.4  $\mu\text{mol}$ ) were dissolved in dry THF (6.00 mL). The reaction mixture was heated to 80  $^\circ\text{C}$  a stirring was continued for 32 h. Then it was diluted with ethyl acetate and the org layer was washed with  $\text{H}_2\text{O}$ . The combined org. layers were dried over  $\text{MgSO}_4$ , filtered, and concentrated. Purification by column chromatography on silica (cyclohexane/ethyl acetate, 1:1) gave **183** as a colorless solid.

**Yield:** 93.0 mg (69.1  $\mu\text{mol}$ , 79 %);

**R<sub>f</sub>:** (cyclohexane/ethyl acetate, 1:1):  $R_f$  = 0.22;

$[\alpha]_D^{23}$ : +31.2 (c = 0.02, acetone);

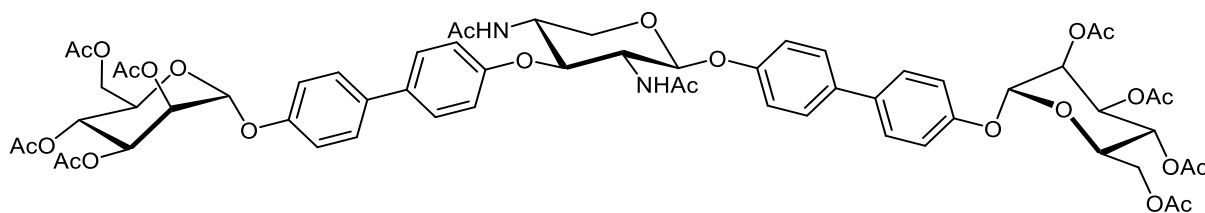
**IR (ATR):**  $\tilde{\nu}$  = 3309, 1750, 1683, 1497, 1367, 1220, 1039, 824, 601  $\text{cm}^{-1}$ ;

**<sup>1</sup>H NMR:** (600 MHz, acetone-d<sub>6</sub>, 298 K, TMS): δ = 7.63–7.57 (m, 6H, 6 H<sub>arom</sub>), 7.52 (d, <sup>3</sup>J = 8.7 Hz, 2H, H<sub>arom</sub>), 7.27-7.21 (m, 4H, 4 H<sub>arom</sub>), , 7.20-7.11 (m, 4H, 4 H<sub>arom</sub>), 6.50 (d, <sup>3</sup>J<sub>NH,2</sub> = 8.6 Hz, 1H, NH), 6.33 (d, <sup>3</sup>J<sub>NH,4</sub> = 7.9 Hz, 1H, NH), 5.71 (d, <sup>3</sup>J<sub>1,2</sub> = 1.1 Hz, 1H, H-1<sub>Man</sub>), 5.70 (d, <sup>3</sup>J<sub>1,2</sub> = 1.1 Hz, 1H, H-1<sub>Man</sub>), 5.51-5.46 (m, 4H, 2 H-2<sub>Man</sub>, 2 H-3<sub>Man</sub>), 5.43 (d, <sup>3</sup>J<sub>1,2</sub> = 7.2 Hz, 1H, H-1), 5.34 (dd-t, <sup>3</sup>J<sub>3,4</sub> = 9.9 Hz, <sup>3</sup>J<sub>4,5</sub> = 9.9 Hz, 2H, 2 H-4<sub>Man</sub>), 4.93 (t, <sup>3</sup>J<sub>3,4</sub> = 9.2 Hz, <sup>3</sup>J<sub>2,3</sub> = 9.2 Hz, 1H, H-3), 4.25 (dd, <sup>2</sup>J<sub>6a,6b</sub> = 12.0 Hz, <sup>3</sup>J<sub>5,6a</sub> = 5.9 Hz, 1H, H-6a<sub>Man</sub>), 4.24 (dd, <sup>2</sup>J<sub>6a,6b</sub> = 12.0 Hz, <sup>3</sup>J<sub>5,6a</sub> = 5.9 Hz, 1H, H-6a<sub>Man</sub>), 4.20-4.15 (m, 2H, 2 H-5<sub>Man</sub>), 4.10-4.07 (m, 2H, 2 H-6b<sub>Man</sub>), 4.03 (dd, <sup>2</sup>J<sub>5a,5b</sub> = 11.1 Hz, <sup>3</sup>J<sub>5a,4</sub> = 4.7 Hz, 1H, H-5a), 3.96-3.90 (m, 1H, H-4), 3.84–3.78 (m, 1H, H-2), 3.73 (t, <sup>2</sup>J<sub>5a,5b</sub> = 10.9 Hz, <sup>3</sup>J<sub>5a,4</sub> = 10.9 Hz, 1H, H-5b), 2.16 (s, 6H, 2 OAc), 2.06 (s, 6H, 2 OAc), 1.99 (s, 6H, 2 OAc), 1.95 (s, 3H, OAc), 1.94 (s, 3H, OAc), 1.33 (s, 9H, C(CH<sub>3</sub>)<sub>3</sub>), 1.31 (s, 9H, C(CH<sub>3</sub>)<sub>3</sub>) ppm;

**<sup>13</sup>C NMR:** (125 MHz, acetone-d<sub>6</sub>, 298 K, TMS): δ = 170.62, 170.40, 170.37, 170.28 (8C, C(O)-Ac), 160.33 (NH-C(O)), 158.03 (NH-C(O)), 155.91 (C<sub>quart</sub>), 155.75 (C<sub>quart</sub>), 138.50 (2 C<sub>quart</sub>), 136.50 (C<sub>quart</sub>), 136.54 (C<sub>quart</sub>), 136.27 (C<sub>quart</sub>), 135.53 (C<sub>quart</sub>), 128.61 (2 CH<sub>arom</sub>), 128.57 (2 CH<sub>arom</sub>), 128.47 (2 CH<sub>arom</sub>), 128.24 (2 CH<sub>arom</sub>), 118.24 (2 CH<sub>arom</sub>), 118.23 (2 CH<sub>arom</sub>), 118.15 (2 CH<sub>arom</sub>), 118.12 (2 CH<sub>arom</sub>), 100.54 (C-1), 96.97 (2 C-1<sub>Man</sub>), 79.06 (C-3), 70.28 (2 C-5<sub>Man</sub>), 69.88 (2 C-2<sub>Man</sub>), 69.80 (2 C-3<sub>Man</sub>), 66.61 (2 C-4<sub>Man</sub>), 64.64 (C-5), 62.94 (2 C-6<sub>Man</sub>), 57.89 (C-2), 53.26 (C-4), 28.55 (3C, C(CH<sub>3</sub>)<sub>3</sub>), 28.53 (3C, C(CH<sub>3</sub>)<sub>3</sub>), 21.71, 20.65, 20.61, 20.59 (8C, OAc-CH<sub>3</sub>) ppm;

**ESI-MS:** *m/z* = 1362.5278 [M+NH<sub>4</sub>]<sup>+</sup> (calculated *m/z* = 1362.5292 for [M+NH<sub>4</sub>]<sup>+</sup>).

**4'-[(1,1'-Biphenyl)-2,3,4,6-tetra-O-acetyl-α-D-mannopyranoside]-4-yl 2,4-dideoxy-2,4-N-acetyl-3-O-{4'-[(1,1'-biphenyl)-2,3,4,6-tetra-O-acetyl-α-D-mannopyranoside]-4-yl}-β-D-xylopyranoside (186)**



The xyloside cluster **183** (20.0 mg, 14.9 μmol) was dissolved in CH<sub>2</sub>Cl<sub>2</sub> (1.00 mL) and TFA (200 μL) was added. It was stirred for 2 h at room temperature. Then all volatiles were removed, and it was coevaporated with toluene (3 x). The crude product was dissolved in dry pyridine (2.00 mL) and Ac<sub>2</sub>O (500 μL) was added. The reaction mixture was stirred at room temperature for 5 h. Then it was diluted with ethyl acetate and the org. layer was washed with 1N HCl, sodium bicarbonate and brine. The combined org. layers were dried over MgSO<sub>4</sub>, filtered, and concentrated. Purification by column chromatography on silica (toluene/acetone, 1:1) gave the title compound **186** as a colorless solid.

**Yield:** 16.0 mg (13.0  $\mu\text{mol}$ , 87 %);

**R<sub>f</sub>:** (toluene/acetone, 1:1): R<sub>f</sub> = 0.32;

**[ $\alpha$ ]<sub>D</sub><sup>23</sup>:** +16.6 (c = 0.02, acetone);

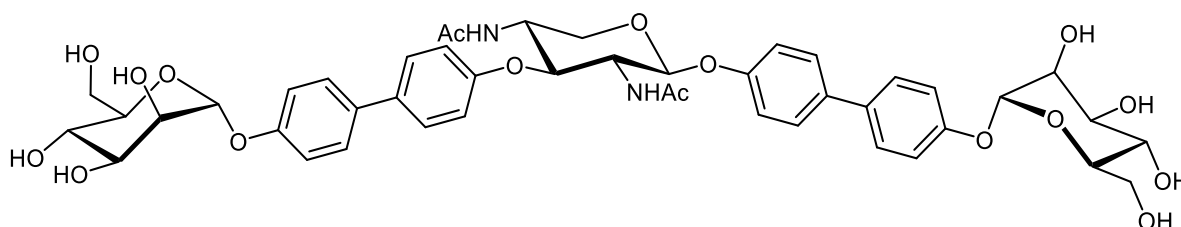
**IR (ATR):**  $\tilde{\nu}$  = 2298, 1750, 1662, 1496, 1370, 1221, 1039, 825, 600  $\text{cm}^{-1}$ ;

**<sup>1</sup>H NMR:** (500 MHz, acetone-d<sub>6</sub>, 298 K, TMS):  $\delta$  = 7.63–7.59 (m, 4H, 4 H<sub>arom</sub>), 7.58–7.54 (m, 4H, 4 H<sub>arom</sub>), 7.51 (d, <sup>3</sup>J<sub>NH,2</sub> = 8.6 Hz, 1H, NH), 7.36 (d, <sup>3</sup>J<sub>NH,4</sub> = 8.4 Hz, 1H, NH), 7.27–7.22 (m, 4H, 4 H<sub>arom</sub>), 7.19 (d, <sup>3</sup>J = 8.9 Hz, 2H, H<sub>arom</sub>), 7.11 (d, <sup>3</sup>J = 8.8 Hz, 2H, H<sub>arom</sub>), 5.71–5.69 (m, 2H, 2 H-1<sub>Man</sub>), 5.57 (d, <sup>3</sup>J<sub>1,2</sub> = 6.5 Hz, 1H, H-1), 5.50–5.46 (m, 4H, 2 H-2<sub>Man</sub>, 2 H-3<sub>Man</sub>), 5.33 (dd~t, <sup>3</sup>J<sub>3,4</sub> = 9.9 Hz, <sup>3</sup>J<sub>4,5</sub> = 9.9 Hz, 2H, 2 H-4<sub>Man</sub>), 4.99 (t, <sup>3</sup>J<sub>3,4</sub> = 7.9 Hz, <sup>3</sup>J<sub>2,3</sub> = 7.9 Hz, 1H, H-3), 4.23 (dd, <sup>2</sup>J<sub>6a,6b</sub> = 12.0 Hz, <sup>3</sup>J<sub>5,6a</sub> = 5.9 Hz, 2H, 2 H-6a<sub>Man</sub>), 4.21–4.10 (m, 4H, 2 H-5<sub>Man</sub>, H-5a, H-4), 4.08 (dd, <sup>2</sup>J<sub>6a,6b</sub> = 12.0 Hz, <sup>3</sup>J<sub>5,6b</sub> = 2.3 Hz, 2H, 2 H-6b<sub>Man</sub>), 4.05–3.99 (m, 1H, H-2), 3.73 (dd, <sup>2</sup>J<sub>5a,5b</sub> = 11.6 Hz, <sup>3</sup>J<sub>5a,4</sub> = 8.4 Hz, 1H, H-5b), 2.16 (s, 6H, 2 OAc), 2.05 (s, 6H, 2 OAc), 1.99 (s, 6H, 2 OAc), 1.94 (s, 6H, 2 OAc), 1.80 (s, 3H, NHAc), 1.75 (s, 3H, NHAc) ppm;

**<sup>13</sup>C NMR:** (125 MHz, acetone-d<sub>6</sub>, 298 K, TMS):  $\delta$  = 170.65, 170.43, 170.40, 170.31 (8C, C(O)-Ac), 170.54 (NH-C(O)), 170.34 (NH-C(O)), 159.70 (C<sub>quart</sub>), 159.62 (C<sub>quart</sub>), 155.94 (C<sub>quart</sub>), 155.80 (C<sub>quart</sub>), 136.45 (C<sub>quart</sub>), 136.31 (C<sub>quart</sub>), 134.33 (C<sub>quart</sub>), 128.63 (2 C<sub>Harom</sub>), 128.59 (2 C<sub>Harom</sub>), 128.49 (2 C<sub>Harom</sub>), 128.23 (2 C<sub>Harom</sub>), 118.28 (4C, C<sub>Harom</sub>), 118.10 (2 C<sub>Harom</sub>), 117.97 (2 C<sub>Harom</sub>), 99.43 (C-1), 97.01 (2 C-1<sub>Man</sub>), 77.09 (C-3), 70.31 (2 C-5<sub>Man</sub>), 69.92 (2 C-2<sub>Man</sub>), 69.83 (2 C-3<sub>Man</sub>), 66.64 (2 C-4<sub>Man</sub>), 63.38 (C-5), 62.97 (2 C-6<sub>Man</sub>), 55.57 (C-2), 50.93 (C-4), 23.09 (NHAc), 23.00 (NHAc), 21.74, 20.68, 20.64, 20.61 (8C, OAc-C<sub>H3</sub>) ppm;

**ESI-MS:**  $m/z$  = 1246.4428 [M+NH<sub>4</sub>]<sup>+</sup> (calculated  $m/z$  = 1246.4449 for [M+NH<sub>4</sub>]<sup>+</sup>).

**4'-[(1,1'-Biphenyl)- $\alpha$ -D-mannopyranosyloxy]-4-yl 2,4-dideoxy-2,4-N-acetyl-3-O-{4'-[(1,1'-biphenyl)- $\alpha$ -D-mannopyranosyloxy]-4-yl}- $\beta$ -D-xylopyranoside (**187**)**



The xylosecluster **186** (13.0 mg, 10.6  $\mu\text{mol}$ ) was dissolved in MeOH (1.00 mL) and K<sub>2</sub>CO<sub>3</sub> (414  $\mu\text{g}$ , 3.00  $\mu\text{mol}$ ) was added. It was stirred for 5 h at room temperature. It was neutralized with Amberlite® IR120, filtered and concentrated to dryness. Coevaporation with toluene and CH<sub>2</sub>Cl<sub>2</sub> gave **187** as a colorless solid.

**Yield:** 9.00 mg (10.1  $\mu\text{mol}$ , 95 %);

$[\alpha]_{\text{D}}^{23}$ : 26.3 ( $c = 0.02$ , MeOH);

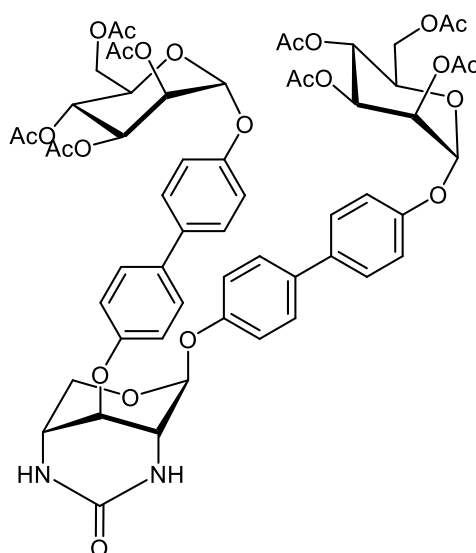
**IR (ATR):**  $\tilde{\nu} = 3364, 2467, 1494, 1220, 999, 824, 677, 575 \text{ cm}^{-1}$ ;

**$^1\text{H NMR}$ :** (600 MHz, MeOD- $d_3$ , 298 K, TMS):  $\delta = 7.53\text{--}7.47$  (m, 8H, 8  $\text{H}_{\text{arom}}$ ), 7.24–7.05 (m, 8H, 8  $\text{H}_{\text{arom}}$ ), 5.51 (s, 2H, 2 H-1 $_{\text{Man}}$ ), 5.35 (d,  $^3J_{1,2} = 7.7 \text{ Hz}$ , 1H, H-1), 4.85-4.82 (m, 1H, H-3), 4.24-4.18 (m, 1H, H-4), 4.06-4.00 (m, 4H, H-2, H-5a, 2 H-2 $_{\text{Man}}$ ), 3.92 (dd,  $^3J_{3,4} = 8.3 \text{ Hz}$ ,  $^3J_{2,3} = 4.0 \text{ Hz}$ , 2H, 2 H-3 $_{\text{Man}}$ ), 3.80-3.70 (m, 6H, 2 H-4 $_{\text{Man}}$ , 2 H-6a $_{\text{Man}}$ , 2 H-6b $_{\text{Man}}$ ), 3.66-3.59 (m, 3H, 2 H-5 $_{\text{Man}}$ , H-5b), 1.81 (s, 3H, NHAc), 1.76 (s, 3H, NHAc) ppm;

**$^{13}\text{C NMR}$ :** (125 MHz, MeOD- $d_3$ , 298 K, TMS):  $\delta = 173.68$  (NH-C(O)), 173.53 (NH-C(O)), 159.96 ( $\text{C}_{\text{quart}}$ ), 157.96 ( $\text{C}_{\text{quart}}$ ), 157.23 ( $\text{C}_{\text{quart}}$ ), 157.14 ( $\text{C}_{\text{quart}}$ ), 136.70 ( $\text{C}_{\text{quart}}$ ), 136.11 ( $\text{C}_{\text{quart}}$ ), 136.06 ( $\text{C}_{\text{quart}}$ ), 135.69 ( $\text{C}_{\text{quart}}$ ), 129.22 (2  $\text{CH}_{\text{arom}}$ ), 128.77 (2  $\text{CH}_{\text{arom}}$ ), 128.64 (2  $\text{CH}_{\text{arom}}$ ), 128.61 (2  $\text{CH}_{\text{arom}}$ ), 118.21 (4C,  $\text{CH}_{\text{arom}}$ ), 118.11 (4C,  $\text{CH}_{\text{arom}}$ ), 100.47 (C-1), 100.23 (2 C-1 $_{\text{Man}}$ ), 78.89 (C-3), 75.40 (2 C-5 $_{\text{Man}}$ ), 72.43 (2 C-2 $_{\text{Man}}$ ), 72.03 (2 C-3 $_{\text{Man}}$ ), 68.36 (2 C-4 $_{\text{Man}}$ ), 64.40 (C-5), 62.70 (2 C-6 $_{\text{Man}}$ ), 57.20 (C-2), 52.18 (C-4), 22.74 (NHAc), 22.66 (NHAc) ppm;

**ESI-MS:**  $m/z = 910.3593$  [ $\text{M}+\text{NH}_4$ ] $^+$  (calculated  $m/z = 910.3604$  for [ $\text{M}+\text{NH}_4$ ] $^+$ ).

**4'-[(1,1'-Biphenyl)-2,3,4,6-tetra-O-acetyl- $\alpha$ -D-mannopyranoside]-4-yl 2,4-N-carbonyl-2,4-dideoxy-3-O-{4'-[(1,1'-biphenyl)-2,3,4,6-tetra-O-acetyl- $\alpha$ -D-mannopyranoside]-4-yl}- $\beta$ -D-xylopyranoside (184)**



The xyloside cluster **183** (20.0 mg, 14.9  $\mu\text{mol}$ ) was dissolved in  $\text{CH}_2\text{Cl}_2$  (1.00 mL) and TFA (200  $\mu\text{L}$ ) was added. It was stirred for 2 h at room temperature. Then all volatiles were removed under reduced pressure, and it was coevaporated with toluene (3 x). The crude product was dissolved in DMF (150  $\mu\text{L}$ ) and *N,N*-carbonyldiimidazole (2.90 mg, 17.9  $\mu\text{mol}$ ) was added.

Then trimethylamine (10.4  $\mu\text{L}$ , 74.5  $\mu\text{mol}$ ) was added dropwise. The reaction mixture was stirred for 16 h at room temperature. Then it was diluted with ethyl acetate and washed with 1N HCl, sodium bicarbonate and brine. The combined org. layers were dried over  $\text{MgSO}_4$ , filtered, and concentrated. Purification by column chromatography on silica (toluene/acetone, 4:6) gave the title compound as a colorless solid.

**Yield:** 13.0 mg (11.1  $\mu\text{mol}$ , 74 %);

**R<sub>f</sub>:** (toluene/acetone, 4:6: R<sub>f</sub> = 0.15;

**[ $\alpha$ ]<sub>D</sub><sup>23</sup>:** -27.3 (c = 0.02, acetone);

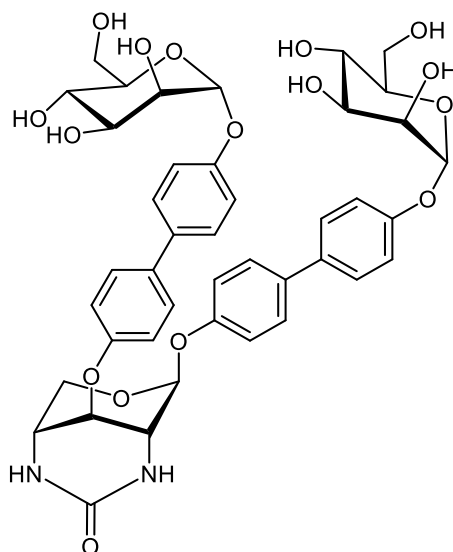
**IR (ATR):**  $\tilde{\nu}$  = 2925, 1749, 1607, 1496, 1369, 1217, 1039, 825, 598  $\text{cm}^{-1}$ ;

**<sup>1</sup>H NMR:** (600 MHz, acetone-d<sub>6</sub>, 298 K, TMS):  $\delta$  = 7.68 (d, <sup>3</sup>J = 8.7 Hz, 2H, 2 CH<sub>arom</sub>), 7.65 (d, <sup>3</sup>J = 8.7 Hz, 2H, 2 CH<sub>arom</sub>), 7.59 (d, <sup>3</sup>J = 8.7 Hz, 2H, 2 CH<sub>arom</sub>), 7.55 (d, <sup>3</sup>J = 8.7 Hz, 2H, 2 CH<sub>arom</sub>), 7.29 (d, <sup>3</sup>J = 8.7 Hz, 2H, 2 CH<sub>arom</sub>), 7.26 (d, <sup>3</sup>J = 8.7 Hz, 2H, 2 CH<sub>arom</sub>), 7.23 (d, <sup>3</sup>J = 8.7 Hz, 2H, 2 CH<sub>arom</sub>), 7.09 (d, <sup>3</sup>J = 8.7 Hz, 2H, 2 CH<sub>arom</sub>), 6.17 (d, <sup>3</sup>J<sub>NH,2</sub> = 4.2 Hz, 1H, NH), 6.07 (d, <sup>3</sup>J<sub>NH,4</sub> = 4.6 Hz, 1H, NH), 5.72-5.68 (m, 2H, 2 H-1<sub>Man</sub>), 5.52 (s, 1H, H-1), 5.51-5.45 (m, 4H, 2 H-2<sub>Man</sub>, 2 H-3<sub>Man</sub>), 5.33 (dd-t, <sup>3</sup>J<sub>3,4</sub> = 10.0 Hz, <sup>3</sup>J<sub>4,5</sub> = 10.0 Hz, 2H, 2 H-4<sub>Man</sub>), 5.06 (t, <sup>3</sup>J<sub>3,4</sub> = 3.1 Hz, <sup>3</sup>J<sub>2,3</sub> = 3.1 Hz, 1H, H-3), 4.45 (d, <sup>2</sup>J<sub>5a,5b</sub> = 11.4 Hz, 1H, H-5a), 4.23 (dd, <sup>2</sup>J<sub>6a,6b</sub> = 11.9 Hz, <sup>3</sup>J<sub>5,6a</sub> = 5.9 Hz, 2H, 2 H-6a<sub>Man</sub>), 4.20-4.14 (m, 2H, 2 H-5<sub>Man</sub>), 4.08 (dd, <sup>2</sup>J<sub>6a,6b</sub> = 12.0 Hz, <sup>3</sup>J<sub>5,6b</sub> = 2.2 Hz, 2H, 2 H-6b<sub>Man</sub>), 3.95 (s, 1H, H-4), 3.69 (s, 1H, H-2), 3.60 (d, <sup>2</sup>J<sub>5a,5b</sub> = 12.0 Hz, 1H, H-5b), 2.16, 2.16, 2.06, 2.04, 1.99, 1.99, 1.95, 1.93 (each s, each 3H, 8 OAc) ppm;

**<sup>13</sup>C NMR:** (125 MHz, acetone-d<sub>6</sub>, 298 K, TMS):  $\delta$  = 170.66, 170.43, 170.40, 170.31 (8 C(O)CH<sub>3</sub>), 157.37, 157.22, 155.86, 155.82, 136.35, 136.31, 134.81, 134.59 (8 C<sub>quart</sub>), 128.71, 128.53, 128.52, 128.49, 118.27, 118.23, 117.57, 117.32 (16 CH<sub>arom</sub>), 99.31 (C-1), 96.98, 96.96 (2 C-1<sub>Man</sub>), 70.26 (2 C-5<sub>Man</sub>), 69.88 (2 C-2<sub>Man</sub>), 69.80 (2 C-3<sub>Man</sub>), 68.88 (C-3), 66.60 (2 C-4<sub>Man</sub>), 62.94 (2 C-6<sub>Man</sub>), 61.98 (C-5), 48.57 (C-2), 47.85 (C-4), 21.71, 20.65, 20.61, 20.59 (8 C(O)CH<sub>3</sub>) ppm;

**ESI-MS:**  $m/z$  = 1188.4013 [M+NH<sub>4</sub>]<sup>+</sup> (calculated  $m/z$  = 1188.4031 for [M+NH<sub>4</sub>]<sup>+</sup>).

**4'-[(1,1'-Biphenyl)- $\alpha$ -D-mannopyranoside]-4-yl 2,4-N-carbonyl-2,4-dideoxy-3-O-{4'-[(1,1'-biphenyl)- $\alpha$ -D-mannopyranoside]-4-yl}- $\beta$ -D-xylopyranoside (**185**)**



The xylosecluster **184** (10.0 mg, 8.54  $\mu$ mol) was dissolved in MeOH (1.00 mL) and  $K_2CO_3$  (354  $\mu$ g, 2.56  $\mu$ mol) was added. It was stirred for 4 h at room temperature. It was neutralized with Amberlite® IR120, filtered and concentrated to dryness. Coevaporation with toluene and  $CH_2Cl_2$  gave **185** as a colorless solid.

**Yield:** 5.30 mg (6.35  $\mu$ mol, 74 %);

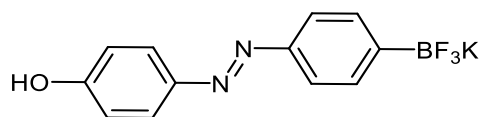
$[\alpha]_D^{23}$ : +36.2 (c = 0.02, MeOH);

**IR (ATR):**  $\tilde{\nu}$  = 3251, 2013, 1495, 1220, 999, 825, 674, 584  $cm^{-1}$ ;

**$^1H$  NMR:** (600 MHz, MeOD- $d_3$ , 298 K, TMS):  $\delta$  = 7.63–7.46 (m, 8H, 8  $H_{arom}$ ), 7.25–7.01 (m, 8H, 8  $H_{arom}$ ), 5.52 (s, 1H, H-1 $_{Man}$ ), 5.50 (s, 1H, H-1 $_{Man}$ ), 5.43 (s, 1H, H-1), 5.01 (t,  $^3J_{3,4}$  = 3.7 Hz,  $^3J_{2,3}$  = 3.7 Hz, 1H, H-3), 4.50 (dd,  $^2J_{5a,5b}$  = 11.5 Hz,  $^3J_{4,5a}$  = 11.5 Hz, H, H-5a), 4.04-4.01 (m, 2H, 2 H-2 $_{Man}$ ), 3.94-3.90 (m, 2H, 2 H-3 $_{Man}$ ), 3.89 (s, 1H, H-2), 3.80-3.57 (m, 10H, 2 H-4 $_{Man}$ , 2 H-5 $_{Man}$ , 2 H-6a $_{Man}$ , 2 H-6b $_{Man}$ , H-4, H-5b), ppm;

**$^{13}C$  NMR:** (125 MHz, MeOD- $d_3$ , 298 K, TMS):  $\delta$  = 160.15 (NH-C(O)-NH), 157.41 ( $C_{quart}$ ), 157.36 ( $C_{quart}$ ), 157.19 ( $C_{quart}$ ), 157.14 ( $C_{quart}$ ), 136.18 ( $C_{quart}$ ), 136.15 ( $C_{quart}$ ), 136.00 ( $C_{quart}$ ), 135.85 ( $C_{quart}$ ), 128.96 (2  $CH_{arom}$ ), 128.75 (2  $CH_{arom}$ ), 128.72 (2  $CH_{arom}$ ), 128.68 (2  $CH_{arom}$ ), 118.14 (2C,  $CH_{arom}$ ), 118.08 (2C,  $CH_{arom}$ ), 117.79 (2C,  $CH_{arom}$ ), 117.46 (2C,  $CH_{arom}$ ), 99.64 (C-1), 100.24 (2 C-1 $_{Man}$ ), 75.39 (2 C-5 $_{Man}$ ), 72.43 (2 C-3 $_{Man}$ ), 72.03 (2 C-2 $_{Man}$ ), 68.68 (C-3), 68.36 (2 C-4 $_{Man}$ ), 62.69 (2 C-6 $_{Man}$ ), 61.94 (C-5), 52.79 (C-4), 47.85 (C-2) ppm;

**ESI-MS:**  $m/z$  = 852.3178  $[M+NH_4]^+$  (calculated  $m/z$  = 852.3185 for  $[M+NH_4]^+$ ).

**Potassium 4-(4'-hydroxyphenyldiazenyl)-phenyl trifluoroborate (190)**

The boronic ester **189** (100 mg, 308  $\mu\text{mol}$ ) was dissolved in MeOH (800  $\mu\text{L}$ ) and a  $\text{KHF}_2$ -solution (4.5 M in  $\text{H}_2\text{O}$ , 384  $\mu\text{L}$ , 1.73 mmol) was added. It was stirred for 1.5 h at room temperature. The volatiles were removed, and the crude product was dissolved in hot acetone and filtered. The filtrate was concentrated, and it was recrystallized from a small amount of acetone and  $\text{Et}_2\text{O}$ .

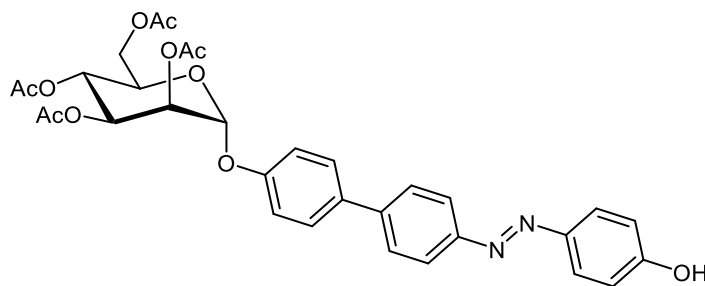
**Yield:** 67.0 mg (220  $\mu\text{mol}$ , 72 %);

**IR (ATR):**  $\tilde{\nu} = 3636, 3541, 1629, 1599, 1504, 1230, 1209, 1142, 952, 848, 573 \text{ cm}^{-1}$ ;

**$^1\text{H NMR}$ :** (600 MHz,  $\text{DMSO-d}_6$ , 300 K):  $\delta = 7.70$  (d,  $^3J = 8.8 \text{ Hz}$ , 2H,  $\text{CH}_{\text{arom}}$ ),  $7.55$  (d,  $^3J = 7.8 \text{ Hz}$ , 2H,  $\text{CH}_{\text{arom}}$ ),  $7.46$  (d,  $^3J = 8.1 \text{ Hz}$ , 2H,  $\text{CH}_{\text{arom}}$ ),  $6.82$  (d,  $^3J = 8.7 \text{ Hz}$ , 2H,  $\text{CH}_{\text{arom}}$ ) ppm;

**$^{13}\text{C NMR}$ :** (125 MHz,  $\text{DMSO-d}_6$ , 300 K, TMS):  $\delta = 150.50$  (2  $\text{C}_{\text{quart}}$ ),  $144.21$  (2  $\text{C}_{\text{quart}}$ ),  $131.93$  (2 C),  $124.46$  (2 C),  $120.22$  (2 C),  $116.22$  (2 C) ppm;

**ESI-MS:**  $m/z = 289.0718$   $[\text{M}+\text{H}]^+$  (calculated  $m/z = 289.0521$  for  $[\text{M}+\text{Na}]^+$ ).

**(E)-4-[4'-Hydroxybiphenylazo]phenyl 2,3,4,6-tetra-O-acetyl- $\alpha$ -D-mannopyranoside (191)**

4-Iodo-phenyl mannoside **174** (27.1 mg, 49.3  $\mu\text{mol}$ ), azobenzene trifluoroborate **190** (15.0 mg, 49.3  $\mu\text{mol}$ ) and  $\text{Pd}(\text{dppf})\text{Cl}_2 \cdot \text{CH}_2\text{Cl}_2$  (2.82 mg, 3.45  $\mu\text{mol}$ ) were dissolved in dry MeOH (1.00 mL). Then DIPEA (25.2  $\mu\text{L}$ , 148  $\mu\text{mol}$ ) was added and the reaction mixture was heated to 80  $^\circ\text{C}$  and stirred for 2 h. After cooling down to room temperature the solvent was removed under reduced pressure and the crude product was taken up in ethyl acetate. The org. layer was washed with  $\text{H}_2\text{O}$  then dried over  $\text{MgSO}_4$ , filtered, and concentrated to dryness. Purification by column chromatography on silica (cyclohexane/ethyl acetate, 2:1) gave the title compound **191** as an orange solid.

**Yield:** 8.00 mg (12.9  $\mu\text{mol}$ , 26 %);

**R<sub>f</sub>**: (cyclohexane/ethyl acetate, 1:1: R<sub>f</sub> = 0.50;

**[α]<sub>D</sub><sup>23</sup>**: +52.6 (c = 0.02, DMSO);

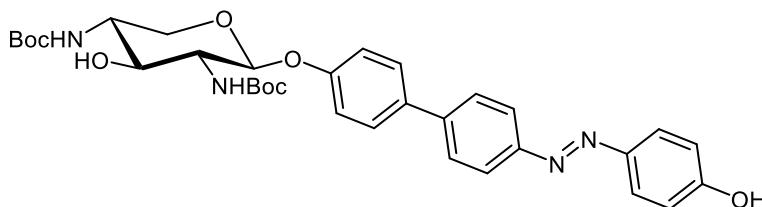
**IR (ATR)**:  $\tilde{\nu}$  = 3326, 2913, 2312, 1666, 1545, 1343, 1222, 1143, 1072, 847, 647 cm<sup>-1</sup>;

**<sup>1</sup>H NMR**: (500 MHz, DMSO-d<sub>6</sub>, 300 K, TMS): δ = 10.35 (s, 1H, OH), 7.96-7.72 (m, 8H, H<sub>arom</sub>), 7.30-7.24 (m, 2H, H<sub>arom</sub>), 6.99-6.92 (m, 2H, H<sub>arom</sub>), 5.83 (s, 1H, H-1), 5.39-5.33 (m, 2H, H-2, H-3), 5.20 (dd-t, <sup>3</sup>J<sub>3,4</sub> = 9.8 Hz, <sup>3</sup>J<sub>4,5</sub> = 9.8 Hz, 1H, H-4), 4.17 (dd, <sup>2</sup>J<sub>6a,6b</sub> = 12.2 Hz, <sup>3</sup>J<sub>5,6a</sub> = 5.5 Hz, 1H, H-6a), 4.09 (ddd, <sup>3</sup>J<sub>4,5</sub> = 8.2 Hz, <sup>3</sup>J<sub>5,6a</sub> = 5.3 Hz, <sup>3</sup>J<sub>5,6b</sub> = 2.5 Hz, 1H, H-5), 3.99 (dd, <sup>2</sup>J<sub>6a,6b</sub> = 12.1 Hz, <sup>3</sup>J<sub>5,6b</sub> = 2.3 Hz, 1H, H-6b), 2.16, 2.05, 1.99, 1.92 (s, each 3 H, 4 OAc) ppm;

**<sup>13</sup>C NMR**: (125 MHz, DMSO-d<sub>6</sub>, 300 K, TMS): δ = 169.97, 169.77, 169.68, 169.61 (4C, C(O)-Ac), 160.99 (1C<sub>quart</sub>), 155.02 (1C<sub>quart</sub>), 151.04 (1C<sub>quart</sub>), 145.39 (1C<sub>quart</sub>), 141.33 (1C<sub>quart</sub>), 133.86 (1C<sub>quart</sub>), 128.10 (2C), 127.23 (2C), 124.91 (2C), 122.83 (2C), 117.55 (2C), 116.02 (2C), 95.18 (C-1), 68.83 (C-5), 68.54 (C-2), 68.39 (C-3), 65.26 (C-4), 61.72 (C-6), 20.69, 20.49, 20.49, 20.45 (4C, Ac-C<sub>H</sub>3) ppm;

**ESI-MS**: *m/z* = 621.2001 [M+H]<sup>+</sup> (calculated *m/z* = 621.2006 for [M+H]<sup>+</sup>).

**(E)-4-[4'-Hydroxybiphenylazo]phenyl 2,4-dideoxy-2,4-N-Boc-β-D-xylopyranoside (192)**



The xyloside **164** (10.0 mg, 19.9 μmol), azobenzene trifluoroborate **190** (6.05 mg, 19.9 μmol) and Pd(dppf)Cl<sub>2</sub>·CH<sub>2</sub>Cl<sub>2</sub> (1.14 mg, 1.39 μmol) were dissolved in dry MeOH (500 μL). Then DIPEA (10.1 μL, 59.6 μmol) was added and the reaction mixture was heated to 80 °C and stirred for 2 h. After cooling down to room temperature the solvent was removed, and the crude product was taken up in ethyl acetate. The org. layer was washed with H<sub>2</sub>O then dried over MgSO<sub>4</sub>, filtered, and concentrated to dryness. Purification by column chromatography on silica (cyclohexane/ethyl acetate, 2:1) gave the title compound **192** as an orange solid.

**Yield**: 3.00 mg (4.83 μmol, 24 %);

**R<sub>f</sub>**: (cyclohexane/ethyl acetate, 2:3: R<sub>f</sub> = 0.34;

**[α]<sub>D</sub><sup>23</sup>**: +6.4 (c = 0.01, acetone);

**IR (ATR)**:  $\tilde{\nu}$  = 3337, 2928, 2358, 1687, 1519, 1367, 1238, 1166, 1044, 844, 637 cm<sup>-1</sup>;

**<sup>1</sup>H NMR:** (600 MHz, acetone-d<sub>6</sub>, 298 K, TMS): δ = 9.45 (s, 1H, OH), 7.93 (d, <sup>3</sup>J = 8.5 Hz, 2H, H<sub>arom</sub>), 7.86 (d, <sup>3</sup>J = 8.8 Hz, 2H, H<sub>arom</sub>), 7.81 (d, <sup>3</sup>J = 8.5 Hz, 2H, H<sub>arom</sub>), 7.70 (d, <sup>3</sup>J = 8.7 Hz, 2H, H<sub>arom</sub>), 7.13 (d, <sup>3</sup>J = 8.6 Hz, 2H, H<sub>arom</sub>), 7.02 (d, <sup>3</sup>J = 8.8 Hz, 2H, H<sub>arom</sub>), 6.26 (s, 1H, NHBoc), 6.07 (s, 1H, NHBoc), 5.15 (d, <sup>3</sup>J<sub>1,2</sub> = 8.0 Hz, 1H, H-1), 4.53 (d, <sup>3</sup>J<sub>3,OH</sub> = 4.4 Hz, 1H, OH), 4.06 (dd, <sup>2</sup>J<sub>5a,5b</sub> = 11.3 Hz, <sup>3</sup>J<sub>5a,4</sub> = 5.0 Hz, 1H, H-5a), 3.82–3.72 (m, 1H, H-3), 3.70–3.60 (m, 2H, H-2, H-4), 3.45–3.40 (m, 1H, H-5b), 1.42 (s, 18H, 2 C(CH<sub>3</sub>)<sub>3</sub>) ppm;

**<sup>13</sup>C NMR:** (125 MHz, acetone-d<sub>6</sub>, 298 K, TMS): δ = 161.51 (NH-C(O)), 158.61 (NH-C(O)), 152.20 (C<sub>quart</sub>), 146.93 (C<sub>quart</sub>), 142.99 (C<sub>quart</sub>), 134.63 (C<sub>quart</sub>), 128.76 (C<sub>quart</sub>), 128.68 (2 CH<sub>arom</sub>), 127.88 (C<sub>quart</sub>), 127.83 (2 CH<sub>arom</sub>), 125.49 (2 CH<sub>arom</sub>), 123.55 (2 CH<sub>arom</sub>), 117.76 (2 CH<sub>arom</sub>), 116.50 (2 CH<sub>arom</sub>), 101.11 (C-17), 72.49 (C-3), 71.16 (C(CH<sub>3</sub>)<sub>3</sub>), 70.86 (C(CH<sub>3</sub>)<sub>3</sub>), 65.14 (C-5), 61.75 (C-2), 54.22 (C-4), 28.41 (3C, C(CH<sub>3</sub>)<sub>3</sub>), 28.35 (3C, C(CH<sub>3</sub>)<sub>3</sub>) ppm;

**ESI-MS:** *m/z* = 621.2907 [M+H]<sup>+</sup> (calculated *m/z* = 621.2918 for [M+H]<sup>+</sup>).

## 8.3 Biological tests

### Equipment

The equipment was sterilized in an autoclave before usage. To determine the optical density of the bacterial suspension a Jenway Spectrophotometer Model 7305 was used.

### Buffer and bacteria

For the biological testing, the following buffers and media were used. All solutions were made with bidestilled water and were autoclaved before usage. The solutions were made by following procedures:

LB-Medium: Trypton (10.0 g), sodium chloride (10.0 g) and yeast extract (5.00 g) were dissolved in 1 L bidest. water and then adjusted to pH-Wert = 7.0. The solution was autoclaved and afterwards antibiotic (Ampicillin (100 mg), Chloramphenicol (50.0 mg)) were added.

PBS-buffer: Sodium chloride (8.00 g), potassium chloride (200 mg), sodium biphosphate (1.44 g) and potassium biphosphate (200 mg) were dissolved in 1 L bidest. water and the pH-value was adjusted to 7.2.

PBST-buffer: Tween<sup>®</sup>20 (0.05 % v/v) was added to PBS-buffer.

Carbonate buffer (pH 9.6): sodium carbonate (1.59 g) and sodium hydrogen carbonate (2.52 g) were dissolved in distilled deionized water (1.00 L).

### Bacteria

For the binding assays the GFP-expressing *E. coli* bacteria strain PKL1162, produced in the laboratory of Per Klemm, was used.<sup>[147]</sup> This *E. coli* strain PKL1162 was constructed by insertation of the plasmid pPKL1174 into the strain SAR18. The pPKL1174 plasmid contains the *fim* gene cluster, which is responsible for the expression of type 1 fimbriae. SAR18 includes the *gfp* gene in its genome, controlled by a constitutive promoter. The final bacterial strain PKL1162 expresses type 1 fimbriae as the only fimbriae type in addition to green fluorescence protein (GFP) allowing fluorescence read-out.

### Cultivation of bacteria

GFP-expressing *E.coli* bacteria (strainpPKL1162) were cultured in 5 mL LB-medium and incubated overnight at 37 °C and 100 rpm. Afterwards the mixture was centrifuged at 4 °C and

4000 rpm for 15 min. The bacteria pellet was washed twice with PBS buffer (2.00 mL) and then resuspended in PBS buffer. Finally, the suspension was adjusted to  $OD_{600} = 0.4$ .

### **Mannan coating of microtiter plates**

The published assay<sup>[146]</sup> was adapted and modified as follows: Black 96-well microtiter plates (Nunc™, Maxisorp®) were incubated with a solution of mannan from *Saccharomyces cerevisiae* (1.2 mg/mL in carbonate buffer, 120 µL/well) and desiccated overnight at 37 °C and 100 rpm. Then the plates were washed with PBST (3 x 150 µL/well) and blocked with polyvinyl alcohol (PVA) (1 % in PBS, 120 µL/well) at ambient temperature and 100 rpm for 2 h. Afterwards the microtiter plates were washed with PBST (2 x 150 µL/well) and PBS (150 µL/well).

### **Inhibition assay with GFP-PKL1162 *E.coli* bacteria**

Inhibitor solutions of the respective glycosides (20 mM in PBS buffer) as well as MeMan (200 mM in PBS buffer) were prepared, and serial dilutions of each solution added to the mannan coated microtiter plates (50 µL/well). In addition, the prepared bacterial suspension ( $OD_{400} = 0.4$ , 50 µL/well) was added and the microtiter plates were incubated at 37 °C and 100 rpm for 45 min. After washing the plates with PBS buffer (3 x 150 µL/well), the wells were filled with PBS (100 µL/well) and the fluorescence intensity (485 nm/ 535 nm) was determined. On each individual plate the standard inhibitor MeMan was tested simultaneously. Each compound was tested at least in triplicates.

Inhibition curves of adhesion-inhibition assay with GFP expressing *E. coli* bacteria.

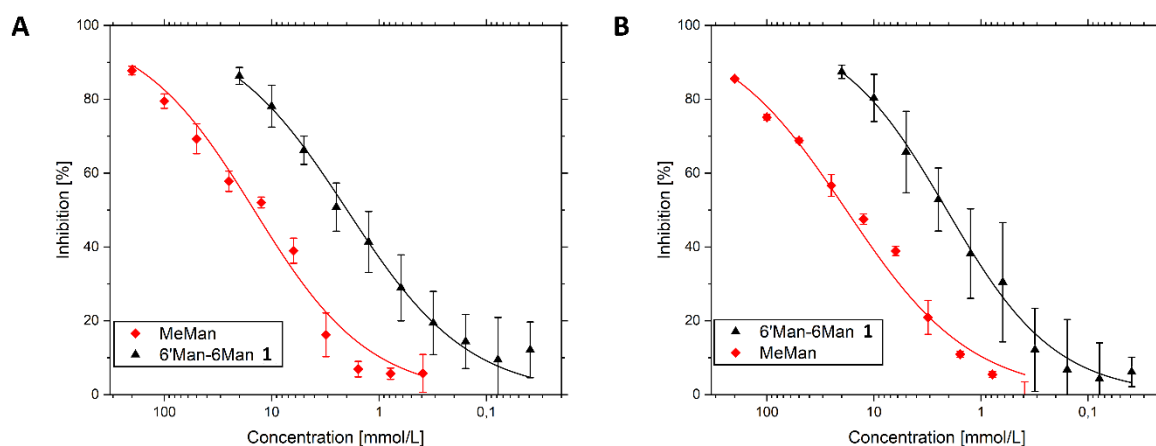


**Figure 8.1.** Inhibition curves obtained with maltoside **36** as inhibitor for type 1 fimbriae-mediated bacterial adhesion to mannan. MeMan was tested simultaneously on each plate. Sigmoidal concentration-response curves were fitted by non-linear regression. Error bars are standard deviations from triplicate values on one plate.

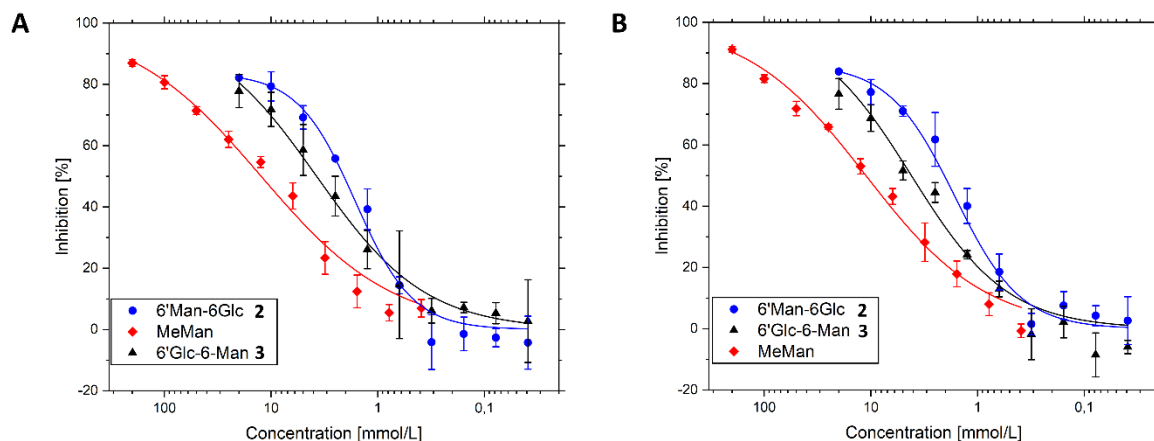
**Table 8.1.** IC<sub>50</sub> values as deduced from the inhibition curves obtained with MeMan, 6'Man-6Man (**36**) and corresponding RIP values.

Plate	Entry	MeMan	6'Man-6Man ( <b>36</b> )
A	IC <sub>50</sub> <sup>a</sup> [mmol]	14.57 (±1.58)	1.98 (±0.13)
	RIP <sup>b</sup>	1.00	7.34 (±1.28)
B	IC <sub>50</sub> <sup>a</sup> [mmol]	18.12 (±1.61)	2.08 (±0.15)
	RIP <sup>b</sup>	1.00	8.71 (±1.40)
	average RIP <sup>c</sup>	1.00	8.03 (±1.39)

<sup>a</sup> IC<sub>50</sub> values are average values from at least duplicate results. Note that IC<sub>50</sub> values can vary significantly in independent experiments as live bacteria are investigated.

<sup>b</sup> RIP values are based on the inhibitory potency of methyl-D-mannopyranoside (MeMan tested on the same microtiter plate (MeMan, IP = 1); RIP = IC<sub>50</sub>(MeMan)/IC<sub>50</sub>(tested compound). Errors are determined by error propagation; RIP(error) = [1/IC<sub>50</sub>(glycocluster)\*error(IC<sub>50</sub>(MeMan))] + [(IC<sub>50</sub>(MeMan)/IC<sub>50</sub>(glycocluster)<sup>2</sup>)\*error(IC<sub>50</sub>(glycocluster))].

<sup>c</sup> average RIP values of two independent experiments are given with error propagation; error = (error(IC<sub>50</sub>(MeMan)) + error(IC<sub>50</sub>(glycocluster)))/2



**Figure 8.2.** Inhibition curves obtained with maltosides **1** and **2** as inhibitors for type 1 fimbriae-mediated bacterial adhesion to mannan. MeMan was tested simultaneously on each plate. Sigmoidal concentration-response curves were fitted by non-linear regression. Error bars are standard deviations from triplicate values on one plate.

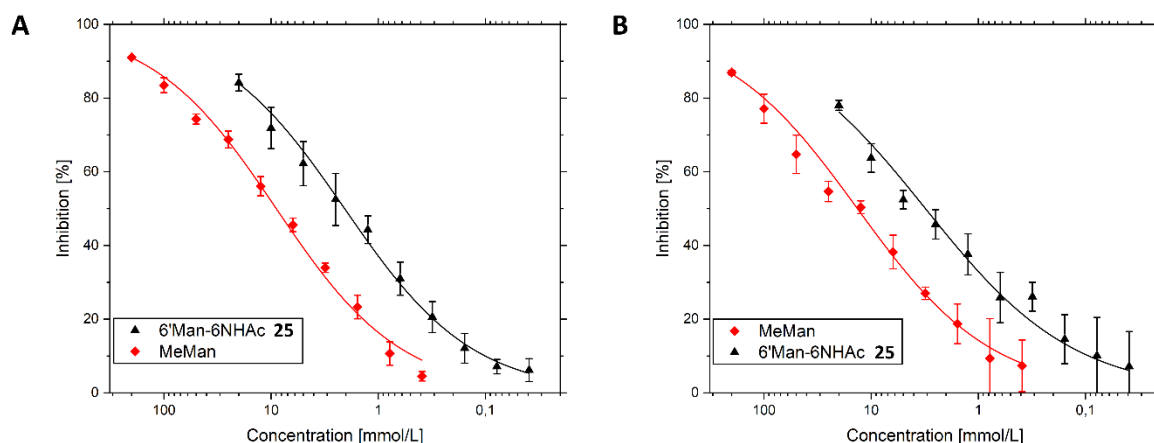
**Table 8.2.** IC<sub>50</sub> values as deduced from the inhibition curves obtained with MeMan, 6'Man-6Glc (**1**) and 6'Glc-6Man (**2**) and corresponding RIP values.

Plate	Entry	MeMan	6'Man-6Glc ( <b>1</b> )	6'Glc-6Man ( <b>2</b> )
<b>A</b>	IC <sub>50</sub> <sup>a</sup> [mmol]	12.39 (±1.19)	2.08 (±0.03)	3.74 (±0.31)
	RIP <sup>b</sup>	1.00	5.96 (±0.66)	3.31 (±0.59)
<b>B</b>	IC <sub>50</sub> <sup>a</sup> [mmol]	11.14 (±0.97)	2.05 (±0.15)	4.17 (±0.48)
	RIP <sup>b</sup>	1.00	5.44 (±0.87)	2.67 (±0.54)
	average RIP <sup>c</sup>	1.00	5.70 (±0.77)	2.99 (±0.57)

<sup>a</sup> IC<sub>50</sub> values are average values from at least duplicate results. Note that IC<sub>50</sub> values can vary significantly in independent experiments as live bacteria are investigated.

<sup>b</sup> RIP values are based on the inhibitory potency of methyl-D-mannopyranoside (MeMan tested on the same microtiter plate (MeMan, IP = 1);  $RIP = IC_{50}(MeMan)/IC_{50}(tested\ compound)$ ). Errors are determined by error propagation;  $RIP(error) = [1/IC_{50}(glycocluster) * error(IC_{50}(MeMan))] + [(IC_{50}(MeMan)/IC_{50}(glycocluster)^2) * error(IC_{50}(glycocluster))]$ .

<sup>c</sup> average RIP values of two independent experiments are given with error propagation;  $error = (error(IC_{50}(MeMan)) + error(IC_{50}(glycocluster)))/2$



**Figure 8.3.** Inhibition curves obtained with maltoside **35** as inhibitor for type 1 fimbriae-mediated bacterial adhesion to mannan. MeMan was tested simultaneously on each plate. Sigmoidal concentration-response curves were fitted by non-linear regression. Error bars are standard deviations from triplicate values on one plate.

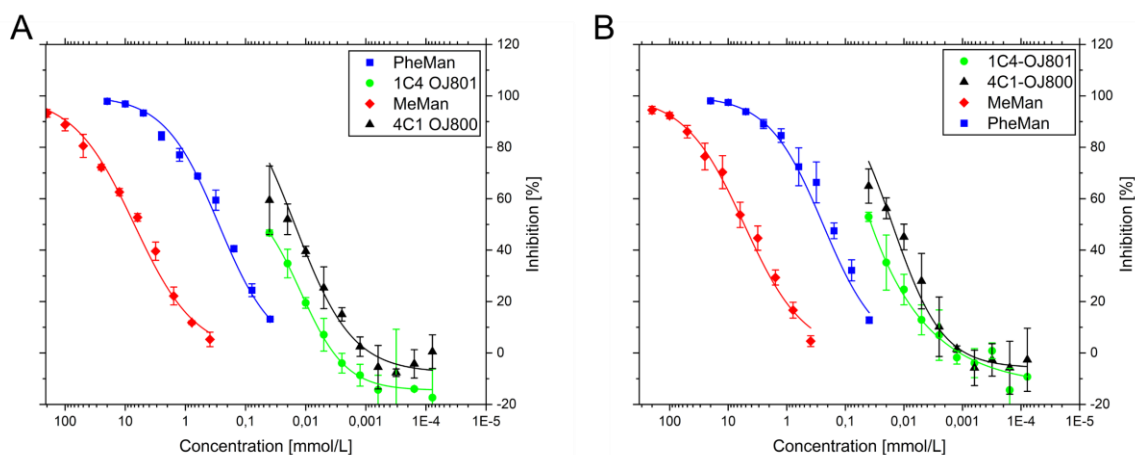
**Table 8.3.** IC<sub>50</sub> values as deduced from the inhibition curves obtained with MeMan, 6'Man-6NHAc (**35**) and corresponding RIP values.

Plate	Entry	MeMan	6'Man-6NHAc ( <b>35</b> )
A	IC <sub>50</sub> <sup>a</sup> [mmol]	13.43 (±0.77)	3.11 (±0.34)
	RIP <sup>b</sup>	1.00	4.32 (±0.72)
B	IC <sub>50</sub> <sup>a</sup> [mmol]	8.94 (±0.67)	2.06 (±0.12)
	RIP <sup>b</sup>	1.00	4.34 (±0.58)
	average RIP <sup>c</sup>	1.00	4.33 (±0.65)

<sup>a</sup> IC<sub>50</sub> values are average values from at least duplicate results. Note that IC<sub>50</sub> values can vary significantly in independent experiments as live bacteria are investigated.

<sup>b</sup> RIP values are based on the inhibitory potency of methyl-D-mannopyranoside (MeMan tested on the same microtiter plate (MeMan, IP = 1); RIP = IC<sub>50</sub>(MeMan)/IC<sub>50</sub>(tested compound). Errors are determined by error propagation; RIP(error) = [1/ IC<sub>50</sub>(glycocluster)\*error(IC<sub>50</sub>(MeMan))]+[(IC<sub>50</sub>(MeMan)/IC<sub>50</sub>(glycocluster)<sup>2</sup>)\*error(IC<sub>50</sub>(glycocluster))].

<sup>c</sup> average RIP values of two independent experiments are given with error propagation; error = (error(IC<sub>50</sub>(MeMan)+ error(IC<sub>50</sub>(glycocluster)))/2



**Figure 8.4.** Inhibition curves obtained with clusters **185** and **187** as inhibitors for type 1 fimbriae-mediated bacterial adhesion to mannan. MeMan was tested simultaneously on each plate. Sigmoidal concentration-response curves were fitted by non-linear regression. Error bars are standard deviations from triplicate values on one plate.

**Table 8.4.**  $IC_{50}$  values as deduced from the inhibition curves obtained with MeMan,  $^4C_1$  cluster **187** and  $^1C_4$  cluster **185** and corresponding RIP values.

Plate	Entry	MeMan	$^4C_1$ cluster ( <b>187</b> )	$^1C_4$ cluster ( <b>185</b> )
A	$IC_{50}^a$ [mmol]	7.0789 ( $\pm 0.4414$ )	0.0152 ( $\pm 0.0015$ )	0.0639 ( $\pm 0.0141$ )
	RIP <sup>b</sup>	1.00	466.33 ( $\pm 76.08$ )	110.79 ( $\pm 31.43$ )
B	$IC_{50}^a$ [mmol]	5.3370 ( $\pm 0.4837$ )	0.0157 ( $\pm 0.0013$ )	0.0360 ( $\pm 0.0111$ )
	RIP <sup>b</sup>	1.00	339.29 ( $\pm 59.65$ )	148.17 ( $\pm 59.46$ )
	average RIP <sup>c</sup>	1.00	410.46 ( $\pm 67.87$ )	157.05 ( $\pm 45.44$ )

<sup>a</sup>  $IC_{50}$  values are average values from at least duplicate results. Note that  $IC_{50}$  values can vary significantly in independent experiments as live bacteria are investigated.

<sup>b</sup> RIP values are based on the inhibitory potency of methyl-D-mannopyranoside (MeMan tested on the same microtiter plate (MeMan, IP = 1);  $RIP = IC_{50}(\text{MeMan})/IC_{50}(\text{tested compound})$ ). Errors are determined by error propagation;  $RIP(\text{error}) = [1/IC_{50}(\text{glycocluster}) * \text{error}(IC_{50}(\text{MeMan}))] + [(IC_{50}(\text{MeMan})/IC_{50}(\text{glycocluster})^2) * \text{error}(IC_{50}(\text{glycocluster}))]$ .

<sup>c</sup> average RIP values of two independent experiments are given with error propagation;  $\text{error} = (\text{error}(IC_{50}(\text{MeMan})) + \text{error}(IC_{50}(\text{glycocluster}))) / 2$

## 8.4 Computational methods

### 8.4.1 Molecular modelling with Schrödinger

For molecular modelling the Schrödinger software package implementing the Maestro interface was used.<sup>[150]</sup> All ligands were built using Maestro and prepared for docking using LigPrep and the OPLS3e force field.<sup>[151, 290]</sup> Crystal structures of FimH in its open gate form (pdb: 1KLF)<sup>[152]</sup> or closed gate conformation (pdb: 1UWF)<sup>[38a]</sup> conformation were constructed using the protein preparation wizard implemented in Maestro.

#### Glide docking

Receptor grids for docking were built using Glide,<sup>[149]</sup> by defining an outer box of 36 Å around the centroid of the ligand as complexed within the binding site of the respective FimH crystal structure. Hydroxy groups of Tyr48 and Tyr137 were set rotatable. Both receptor grids were built using the OPLS3e force field. Extra precision (XP) docking was carried out with Glide, setting the ligand sampling to flexible. Ring conformations (energy window 2.5 kcal mol<sup>-1</sup>) and nitrogen inversions were allowed during sampling. Epic state penalties were added to docking scores. At most, 20 poses were reported per ligand and a post-docking minimization was performed with a threshold for rejecting minimized poses of 0.50 kcal mol<sup>-1</sup>. Additionally, poses with a RMSD less than 0.5 Å and a maximum atomic displacement less than 1.3 Å were treated as duplicates and discarded.

Calculation of binding energies was performed by subjecting the top scoring binding poses from Glide docking to a MM-GBSA<sup>[153]</sup> (molecular mechanics generalized born surface area) calculation, giving the free binding energy  $\Delta G_{\text{Bind}}$  in kcal mol<sup>-1</sup>. The MM-GBSA calculations were performed using the VGSB solvation model and the OPLS3e force field.

#### Induced fit docking

Induced fit docking (IFD) was performed using the standard IFD protocol with the OPLS3e force field.<sup>[155]</sup> The receptor protein (FimH) was defined as an outer box of 36 Å around the centroid of the ligand as complexed within the binding site of FimH (pdb: 1UWF).<sup>[38a]</sup> Ligands were set flexible and sampled for ring conformations with an energy window of 2.5 kcal mol<sup>-1</sup>. Non-planar amide bonds were penalized. Glide redocking was performed with extra precision (XP) for structures within 30 kcal mol<sup>-1</sup> of the best structure, employing a maximum of 20 top-ranked structures. Docking poses found for glycoclusters **1** and **2** where the  $\beta$ -D-glucosyl residue was bound to the mannose binding pocket of FimH instead of the  $\alpha$ -D-mannosyl moiety were discarded.<sup>[291]</sup> The top five binding poses according to the IFD score ranking were

subjected to a binding pose metadynamics<sup>[292]</sup> simulation to determine the most stable protein-ligand complex. For each binding pose metadynamics simulations (10 trials of 10 ns) were performed and averaged. Then, the binding pose with the lowest metadynamics composite score was selected as the most stable one.

Calculation of binding energies was performed by subjecting the most stable binding poses from binding pose metadynamics simulations to a MM-GBSA<sup>[153]</sup> (molecular mechanics generalized born surface area) calculation, giving the free binding energy  $\Delta G_{\text{Bind}}$  in kcal mol<sup>-1</sup>. The MM-GBSA calculations were performed using the VGSB solvation model and the OPLS3e force field. These computed binding energies are correlated with results from biological testing.

### **Molecular dynamics**

Molecular modeling was performed by using the Schrödinger software package implementing the Maestro interface.<sup>[150]</sup> The structure of **185** and **187** were built by using Maestro. The resulting structures were minimized by use of MacroModel,<sup>[293]</sup> with the OPLS3 force field in implicit water (GB/SA continuum solvation model). Molecular dynamics in explicit water was carried out with the Desmond software, implemented in the Schrödinger package.<sup>[156]</sup> Firstly, an orthorhombic solvent box (SPC H<sub>2</sub>O molecules<sup>[294]</sup>), including **185** or **187**, with a buffering distance of 15 Å between the edges and the solute was generated. Each solvated system was then subjected to a molecular dynamics simulation at 300 K for 200 ns (time step=2 fs, energy=1.2, NPT conditions), with monitoring of the geometry every ps. The trajectories were analyzed by using the “Simulation Event Analysis” tool, implemented in the Desmond program,<sup>[156]</sup> in order to calculate the distances between the glycocluster mannoside residues and the dihedral angles.

### 8.4.2 DFT calculations

All calculations were carried out with a local development version of the ORCA 5.0 program package.<sup>[295]</sup> All geometries were obtained from geometry optimizations at the B3LYP-D3/def2-TZVPP level of theory (D3BJ correction, RI approximation with def2 aux basis sets and tight optimization and convergence criteria).<sup>[258, 296]</sup> Spin-spin coupling constants were computed at the DFT/pc-J3 level of theory (RI with Autoaux basis set and tight convergence criteria). The functionals applied were PBE, TPSS, TPSSH, PBE0 and B3LYP. Note that all contributions to the coupling constants (Fermi contact, paramagnetic and diamagnetic spin-orbit as well as spin-dipole) are included. NMR Chemical shifts were obtained at the DLPNO-MP2/pcSseg-3<sup>[260, 297]</sup> level of theory (no frozen core approximation, RIJCOSX approximation with def2/JK and cc-pwCVQZ/C aux basis set and very tight convergence criteria) using gauge including atomic orbitals. Single point energies were obtained at the DLPNO-CCSD(T1)/cc-pVTZ level of theory (RI approximation with the corresponding JK and C basis sets).

In order to find low energy conformer structures for compound **166** and **167**, several possible conformers were used as starting structures for the CREST protocol at the XTB level of theory.<sup>[250]</sup> The resulting 20 lowest energy conformers and some additional non <sup>1</sup>C<sub>4</sub> and <sup>4</sup>C<sub>1</sub> structures were then further optimized at the B3LYP-D3/def2-svp level of theory. From these, the lowest energy <sup>1</sup>C<sub>4</sub> and <sup>4</sup>C<sub>1</sub> structures and one additional conformer (denoted as “skew”) were then optimized at the B3LYP-D3/def2-tzvpp level of theory.

#### Association energy for compound **2** with ZnCl<sub>2</sub> to yield **3**

In order to assess the energy for the association of compound **167** with ZnCl<sub>2</sub> to constrain it to the <sup>1</sup>C<sub>4</sub> conformation, the geometries of **167**, the adduct **168** and ZnCl<sub>2</sub> were optimized at the B3LYP-D3BJ/def-TZVPP level of theory, and their relative energies and free energies were evaluated. The free energy difference for the reaction **167** + ZnCl<sub>2</sub> → **168** amounts to 94.7 kJ/mol (relative electronic energies 158.2 kJ/mol). Despite uncertainties in the DFT results this large exothermic free energy is a strong indication for a quantitative reaction in this case.

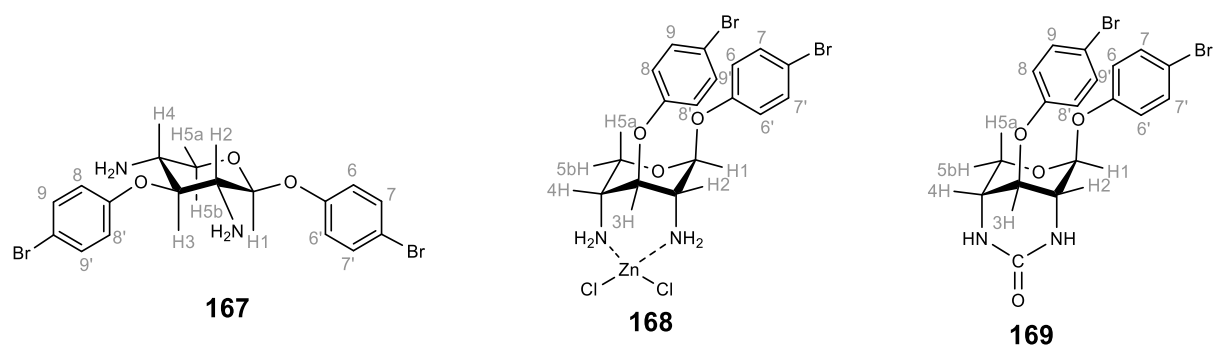
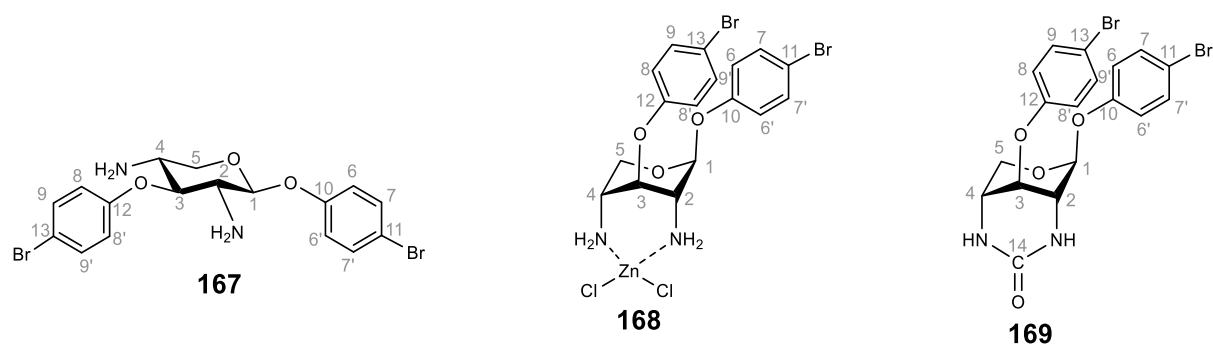


Figure 8.5. Numbering (grey) of the protons for the xylosides **167**, **168**, and **169**.

**Table 8.5.** NMR-data for the chemical shift (in ppm) of the protons of xylosides **167**, **168**, and **169** in MeCN-d<sub>3</sub> and comparison to the calculated data. Protons were assigned by 2D-NMR (COSY and HSQC). Calculated values have been obtained at the DLPNO-MP2/pcSseg-3 level of theory and are displayed in grey columns.

Proton	Int.	167 (exp)	167 (calc.)	168 (exp)	168 (calc.)	169 (exp)	169 (calc.)
2	1	3.02	3.31	3.51	3.30	3.71	3.75
4	1	3.05	3.00	3.37	3.22	3.54	3.33
5b	1	3.34	3.20	3.65	3.56	3.49	3.58
5a	1	3.91	4.17	4.36	4.55	4.29	4.63
3	1	4.03	3.60	4.52	5.26	4.89	5.08
1	1	4.84	4.83	5.50	5.26	5.36	5.11
7, 7'	2	6.99	7.62	7.01	7.60	6.89	7.42
9, 9'	2	7.08	7.58	7.07	7.74	7.04	7.75
8, 8'	2	7.41	7.63	7.49	7.47	7.41	7.44
6, 6'	2	7.45	7.35	7.52	7.51	7.49	7.26


 Figure 8.6. Numbering (grey) of the carbons for the xylosides **167**, **168**, and **169**.

**Table 8.6.** NMR-data for the chemical shift (in ppm) of the carbons of xylosides **167**, **168**, and **169** in MeCN-d<sub>3</sub> and comparison to the calculated data. Protons were assigned by 2D-NMR (COSY and HSQC). Calculated values have been obtained at the DLPNO-MP2/pcSseg-3 level of theory.

Carbon	Int.	167 (exp)	167 (calc.)	168 (exp)	168 (calc.)	169 (exp)	169 (calc.)
4	1	53.48	61.03	48.34	55.43	48.13	57.32
2	1	57.99	64.68	49.44	54.14	47.18	54.36
5	1	67.76	74.42	59.07	65.71	62.01	69.34
3	1	86.34	103.05	72.21	74.79	68.57	75.29
1	1	103.42	112.44	97.00	107.16	99.13	110.12
13	1	113.68	136.74	n.d.	138.14	114.25	137.03
11	1	115.13	136.51	n.d.	137.44	114.71	136.62
7, 7'	2	119.56	137.07	119.66	137.85	118.97	137.21
9, 9'	2	119.68	137.43	119.82	138.32	119.45	137.30
8, 8'	2	133.15	125.49	133.45	123.78	133.26	123.80
6, 6'	2	133.31	123.49	133.53	123.62	133.47	124.09
10	1	157.71	165.37	156.22	164.46	156.81	165.61
12	1	160.90	171.13	156.45	162.36	157.08	164.32
14	1	-	-	-	-	157.27	160.50

**Table 8.7.** Computed (DFT/pcJ-3 level of theory) spin-spin coupling constants of  $^1C_4$  and  $^4C_1$  conformers of **166**. All values given in Hz.

	$^1C_4$ conformer			$^4C_1$ conformer		
	PBE	PBE0	B3LYP	PBE	PBE0	B3LYP
$J_{1,2}$	1.02	1.15	1.19	9.09	9.64	10.16
$J_{2,3}$	2.04	2.23	2.29	9.77	10.28	10.90
$J_{3,4}$	3.33	3.43	3.57	9.84	10.31	10.86
$J_{4,5a}$	2.34	2.46	2.65	6.00	6.19	6.54
$J_{4,5b}$	1.70	1.90	2.01	11.30	11.75	12.40
$J_{5a,5b}$	11.57	13.63	13.15	10.98	13.05	12.61

## 8.5 NMR spectra of synthesized compounds

In this chapter NMR spectra of synthesized compounds are depicted which are not published to this end. Published compounds can be found in literature.<sup>[112, 162]</sup>

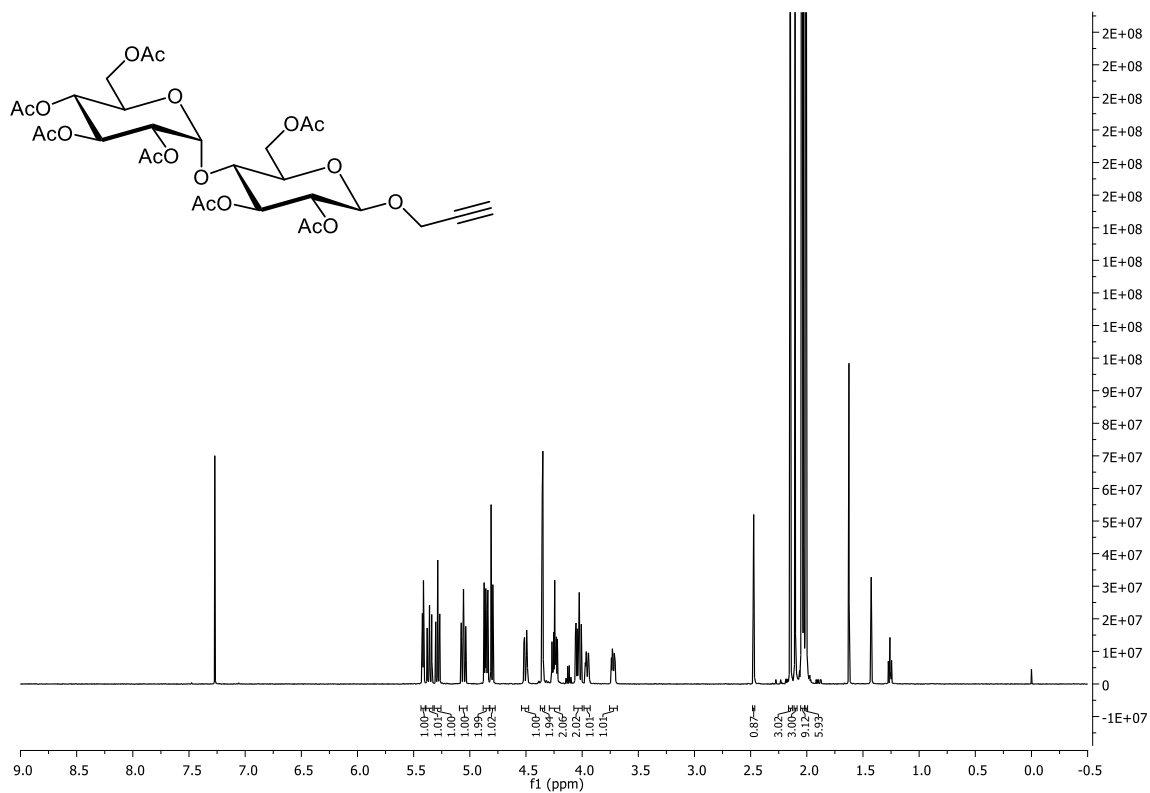


**Figure 8.7.** <sup>1</sup>H NMR spectrum of **42** (500 MHz, CDCl<sub>3</sub>, 298 K).

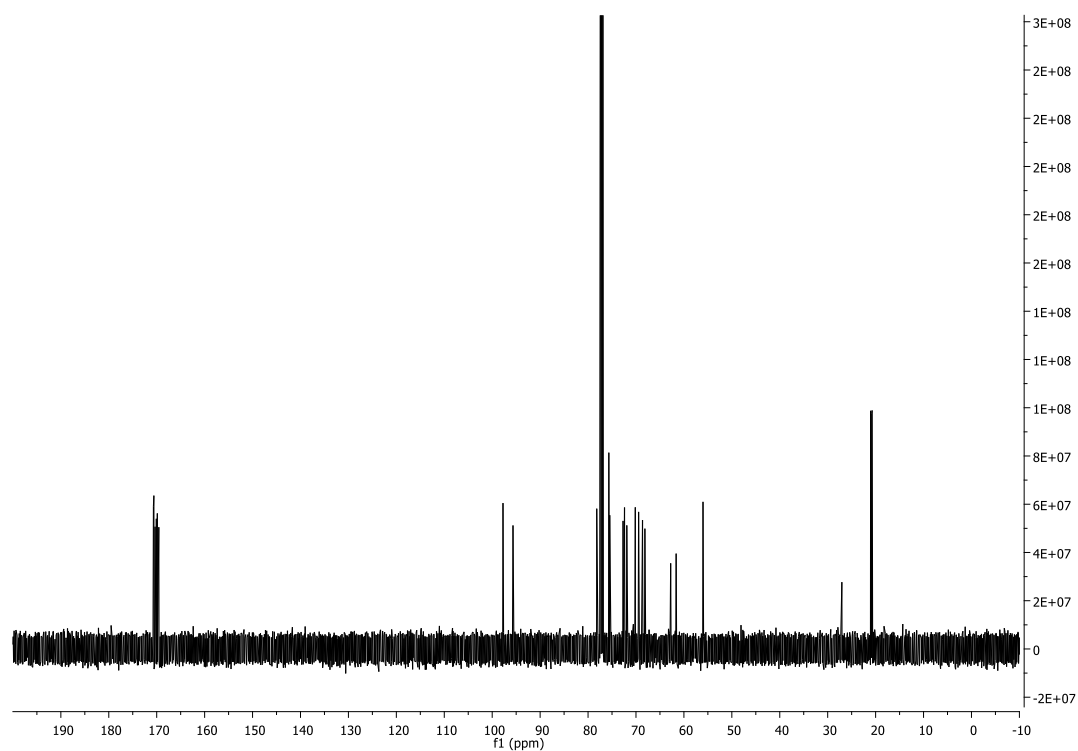


**Figure 8.8.** <sup>13</sup>C NMR spectrum of **42** (125 MHz, CDCl<sub>3</sub>, 298 K).

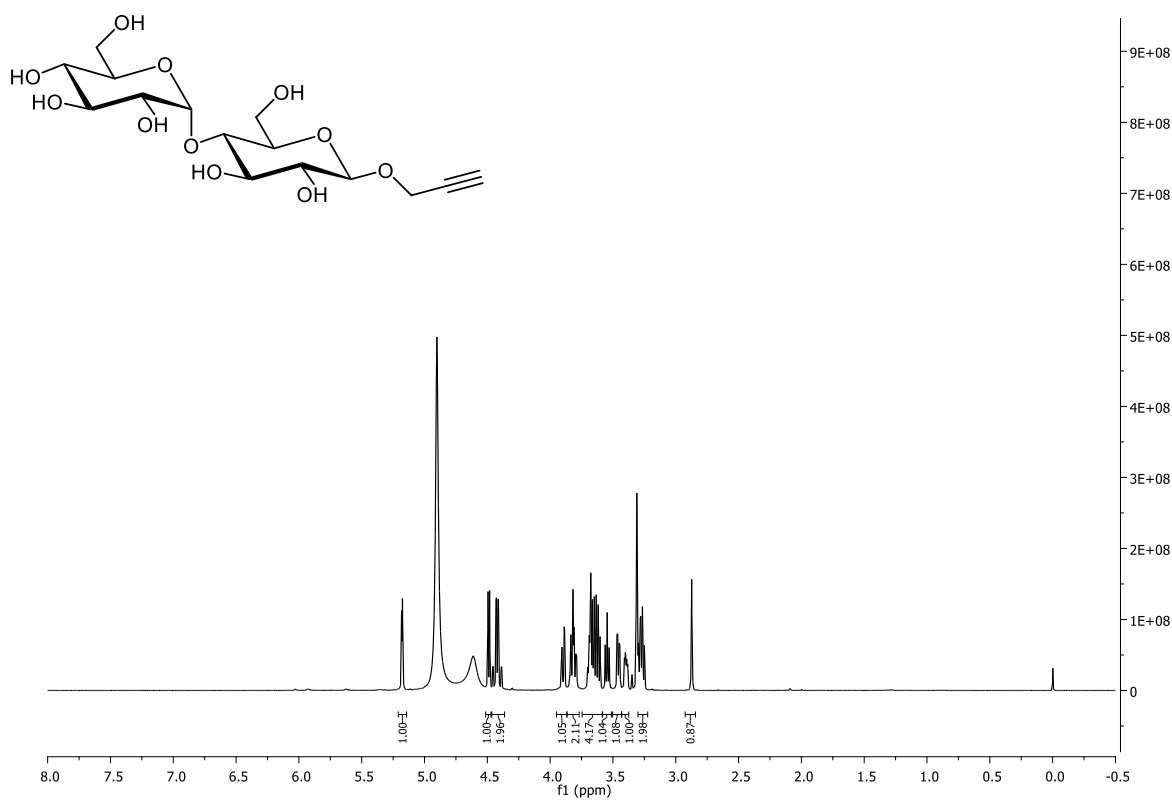


**Figure 8.9.** <sup>1</sup>H NMR spectrum of **43** (600 MHz, MeOD, 298 K).

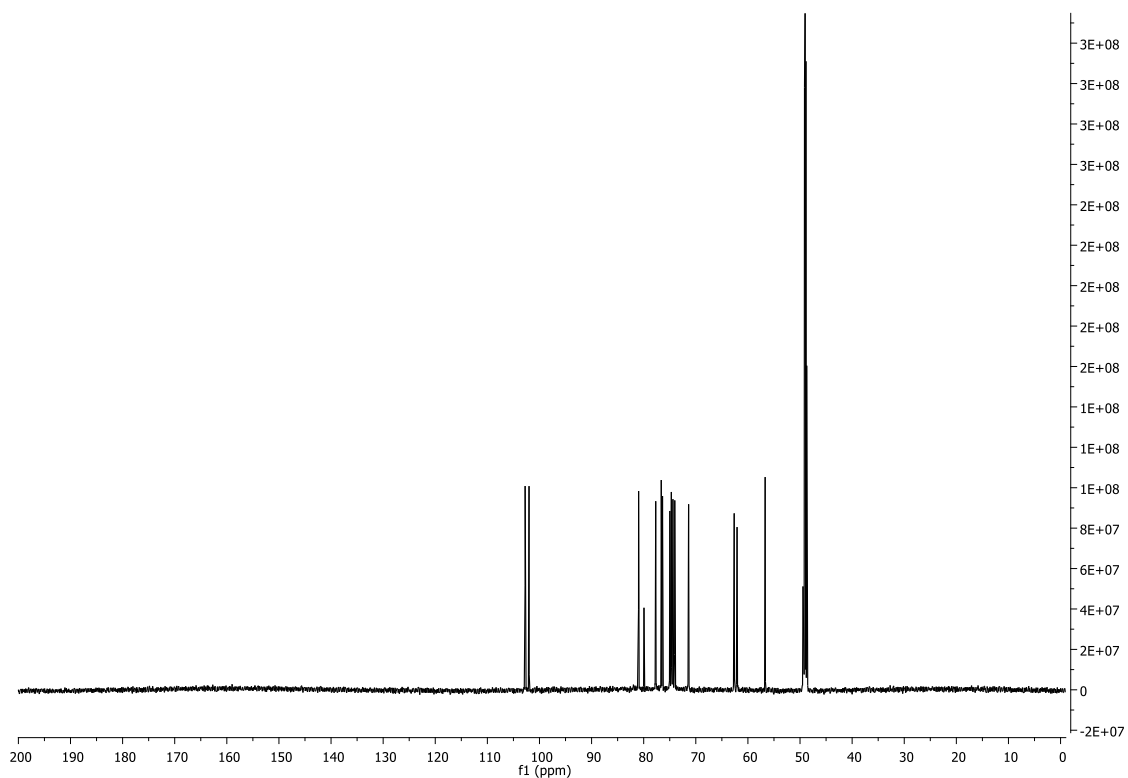


**Figure 8.10.** <sup>13</sup>C NMR spectrum of **43** (125 MHz, MeOD, 298 K).

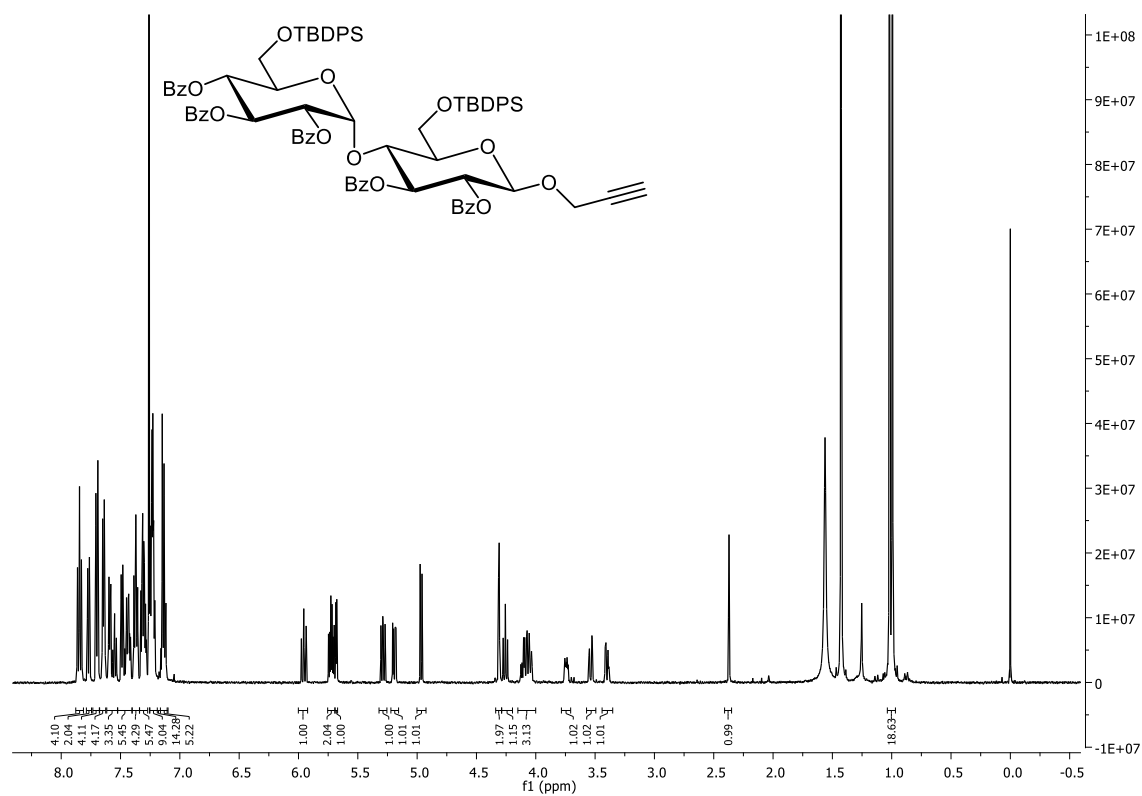


Figure 8.11. <sup>1</sup>H NMR spectrum of **44** (500 MHz, CDCl<sub>3</sub>, 298 K).

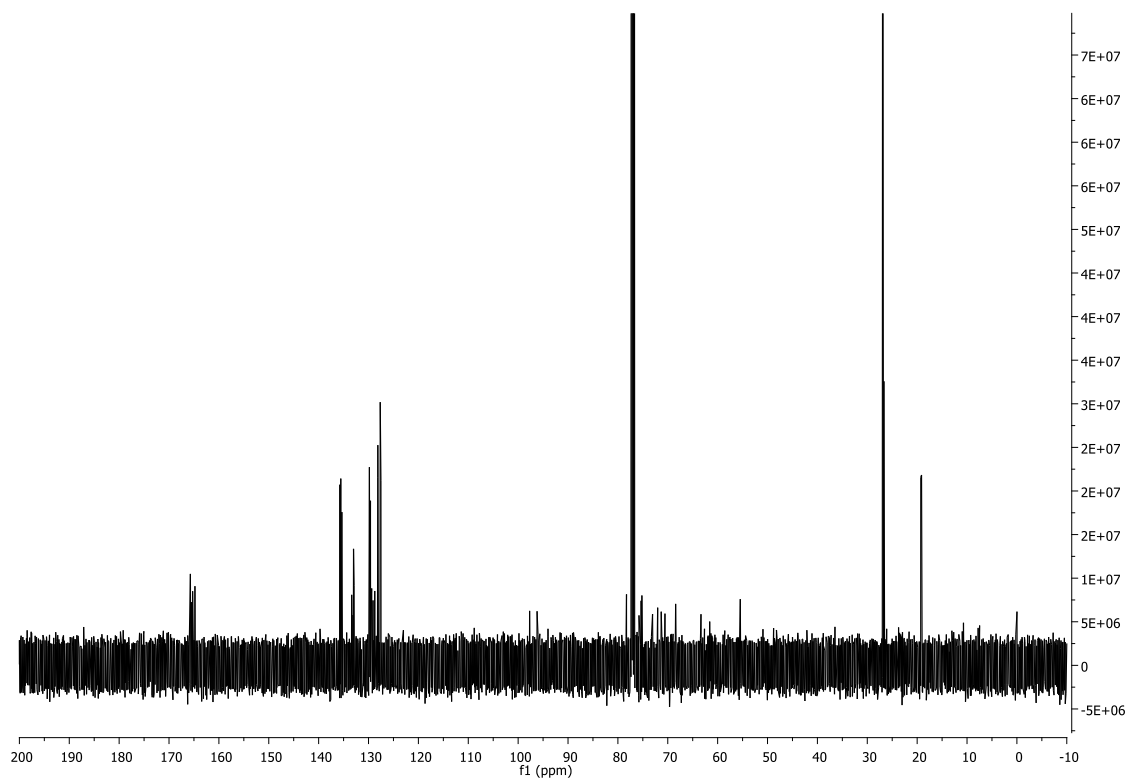


Figure 8.12. <sup>13</sup>C NMR spectrum of **44** (125 MHz, CDCl<sub>3</sub>, 298 K).

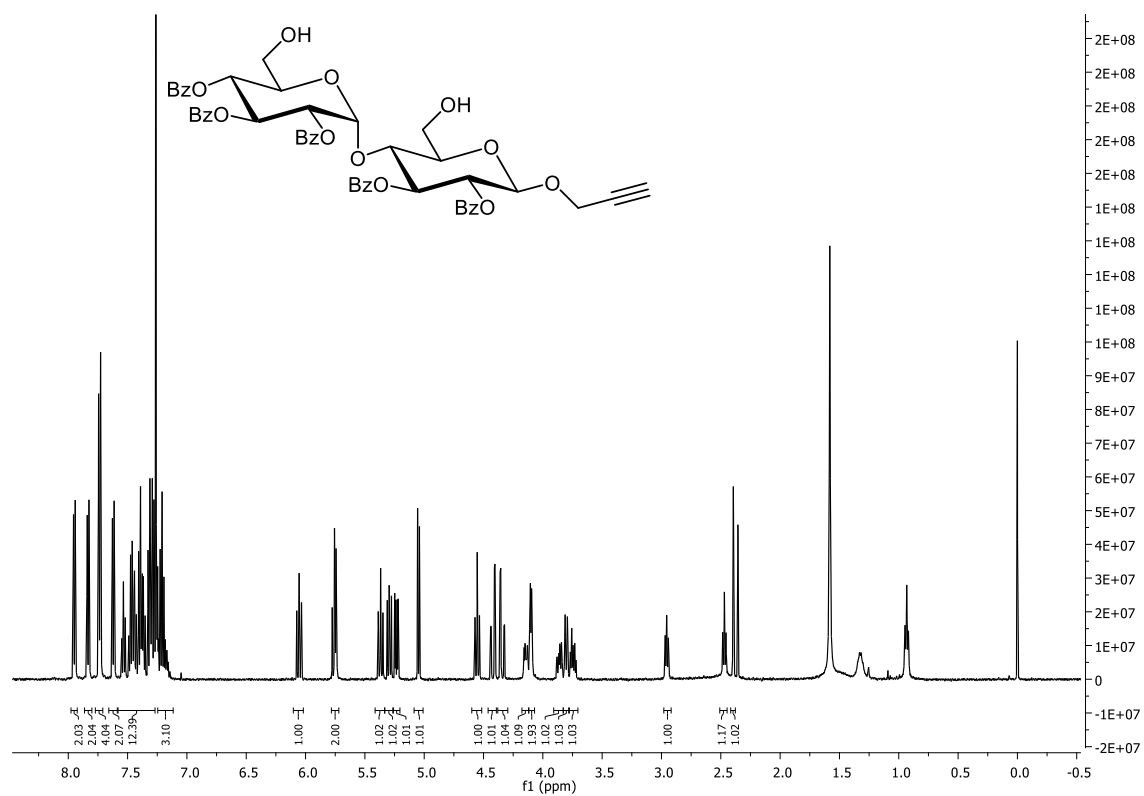


Figure 8.13. <sup>1</sup>H NMR spectrum of **45** (500 MHz, CDCl<sub>3</sub>, 298 K).

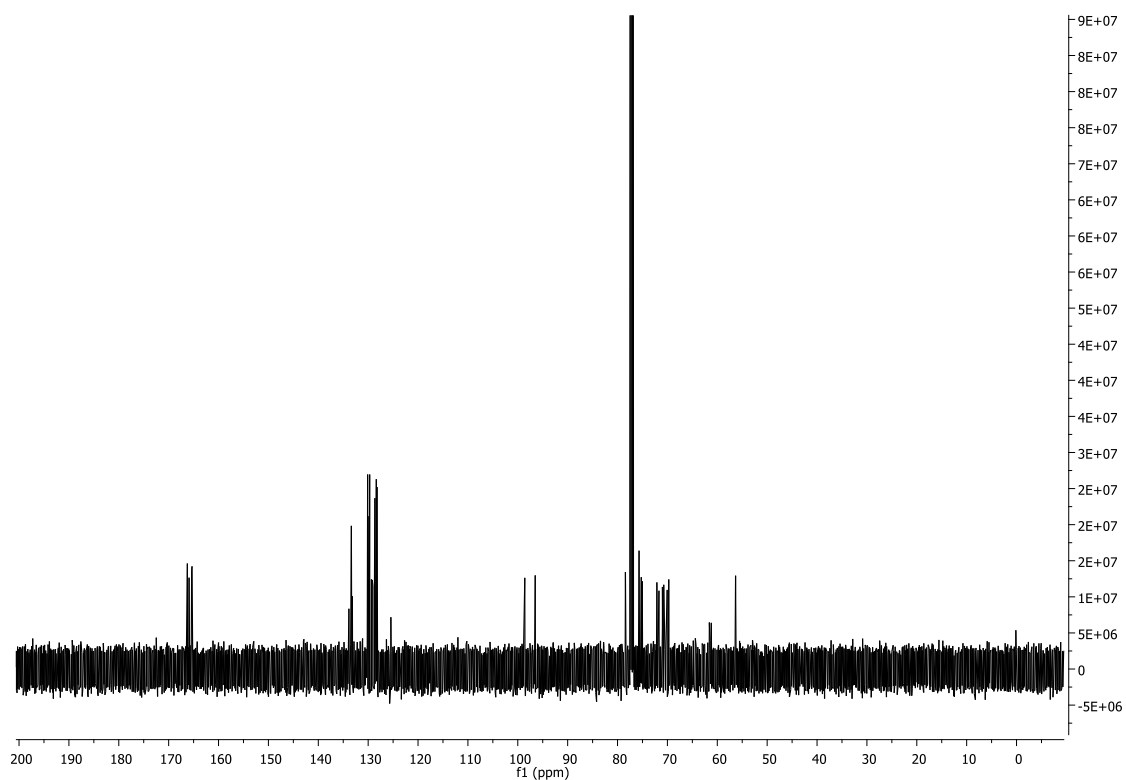


Figure 8.14. <sup>13</sup>C NMR spectrum of **45** (125 MHz, CDCl<sub>3</sub>, 298 K).

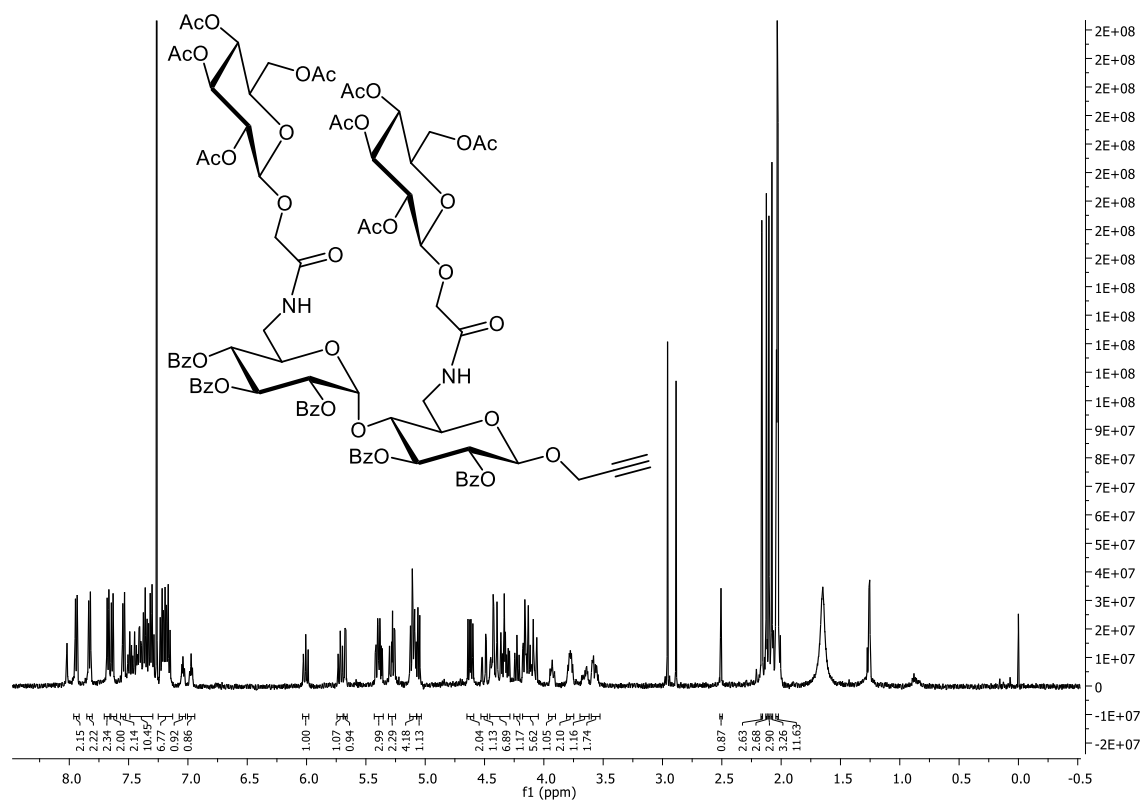


Figure 8.15. <sup>1</sup>H NMR spectrum of **49** (500 MHz, CDCl<sub>3</sub>, 298 K).

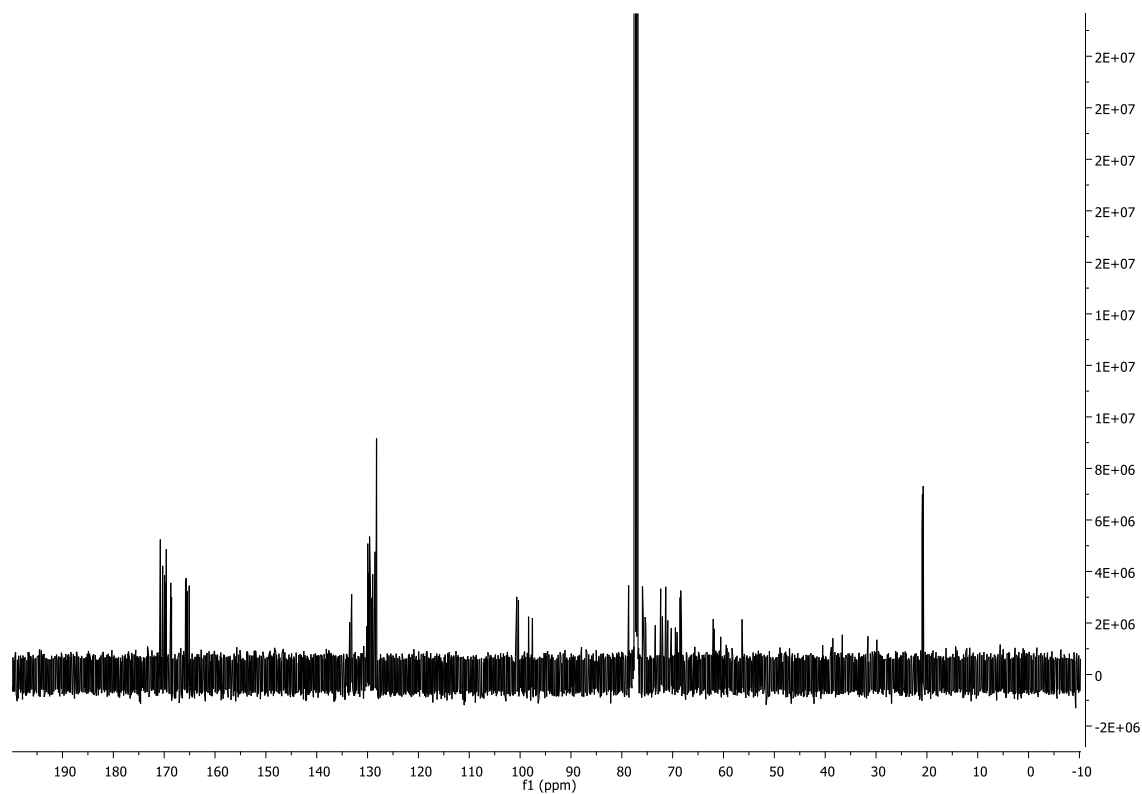
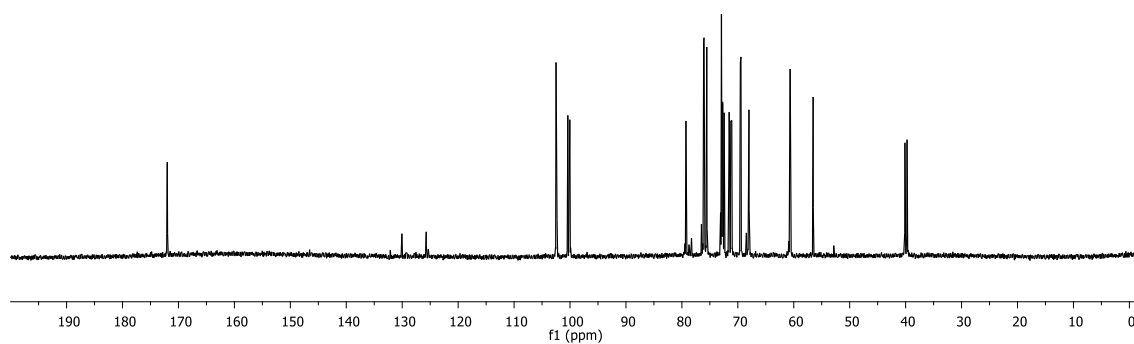
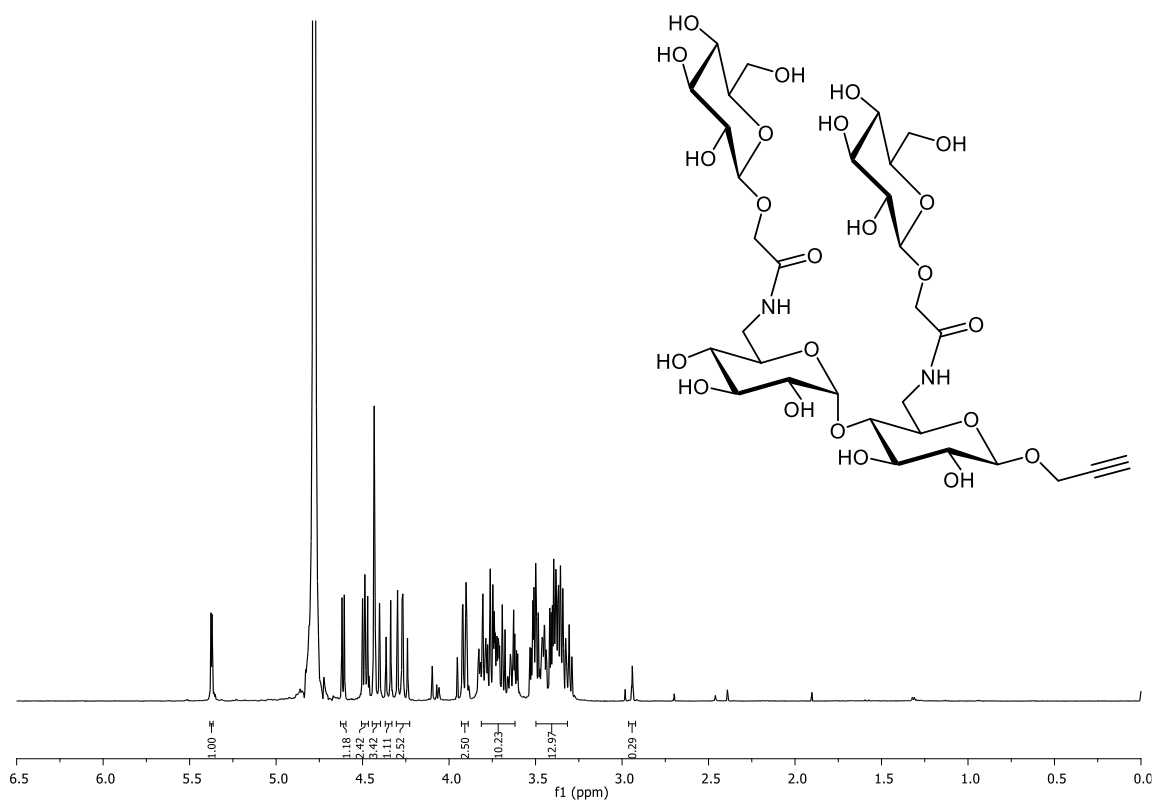


Figure 8.16. <sup>13</sup>C NMR spectrum of **49** (125 MHz, CDCl<sub>3</sub>, 298 K).



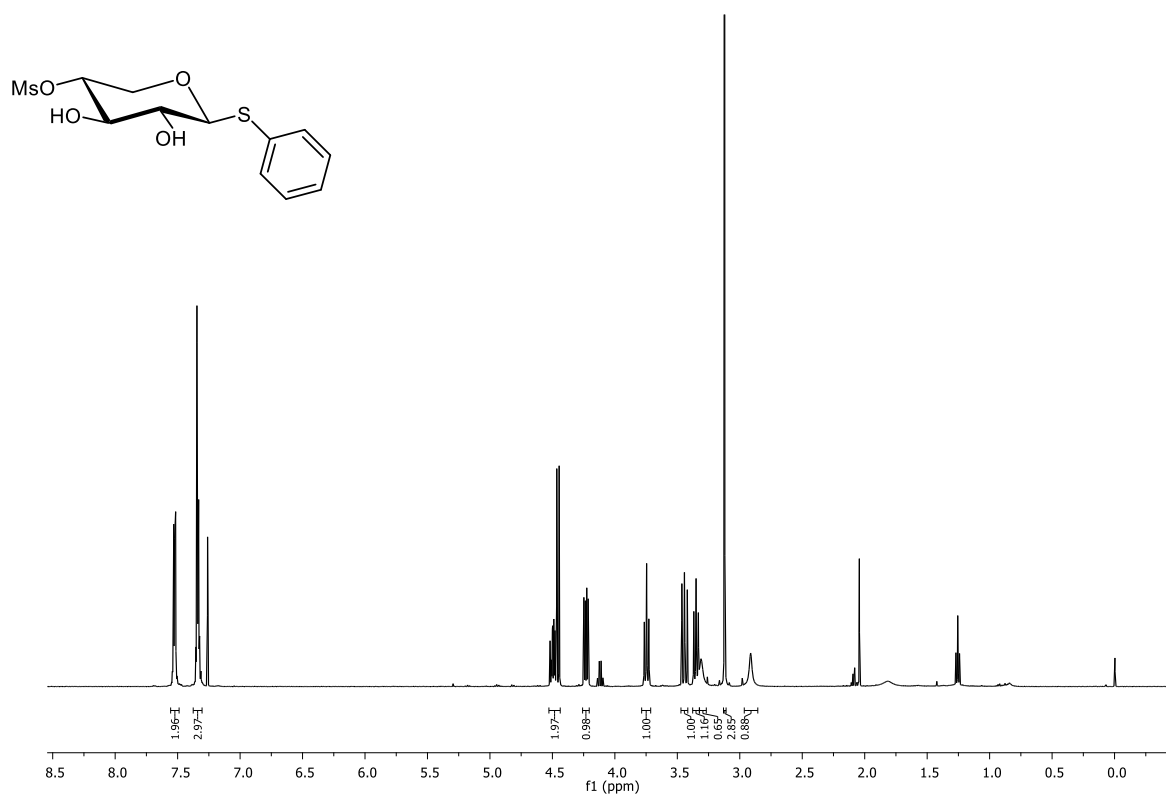


Figure 8.19. <sup>1</sup>H NMR spectrum of **68** (500 MHz, CDCl<sub>3</sub>, 298 K).

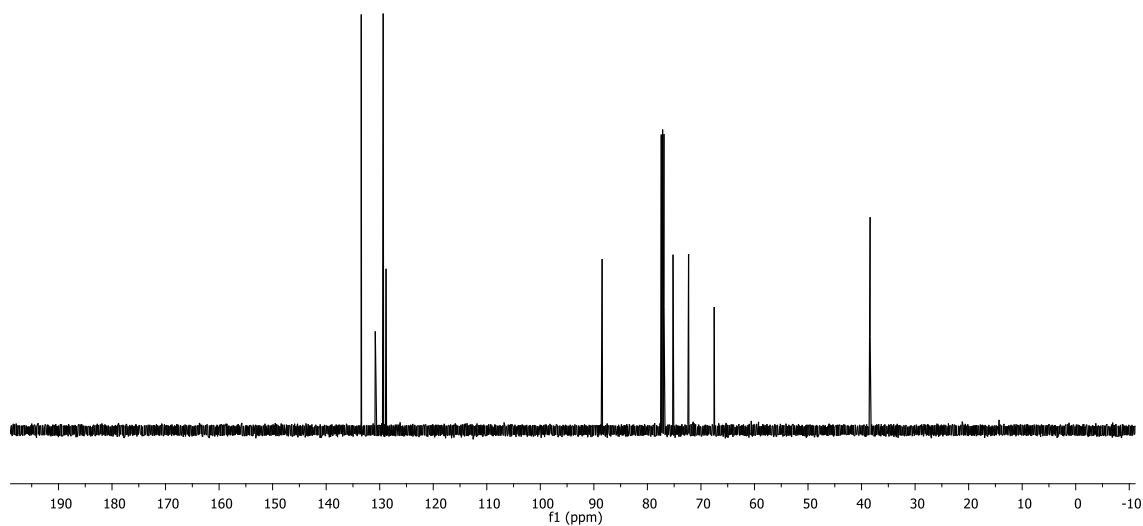


Figure 8.20. <sup>13</sup>C NMR spectrum of **68** (125 MHz, CDCl<sub>3</sub>, 298 K).

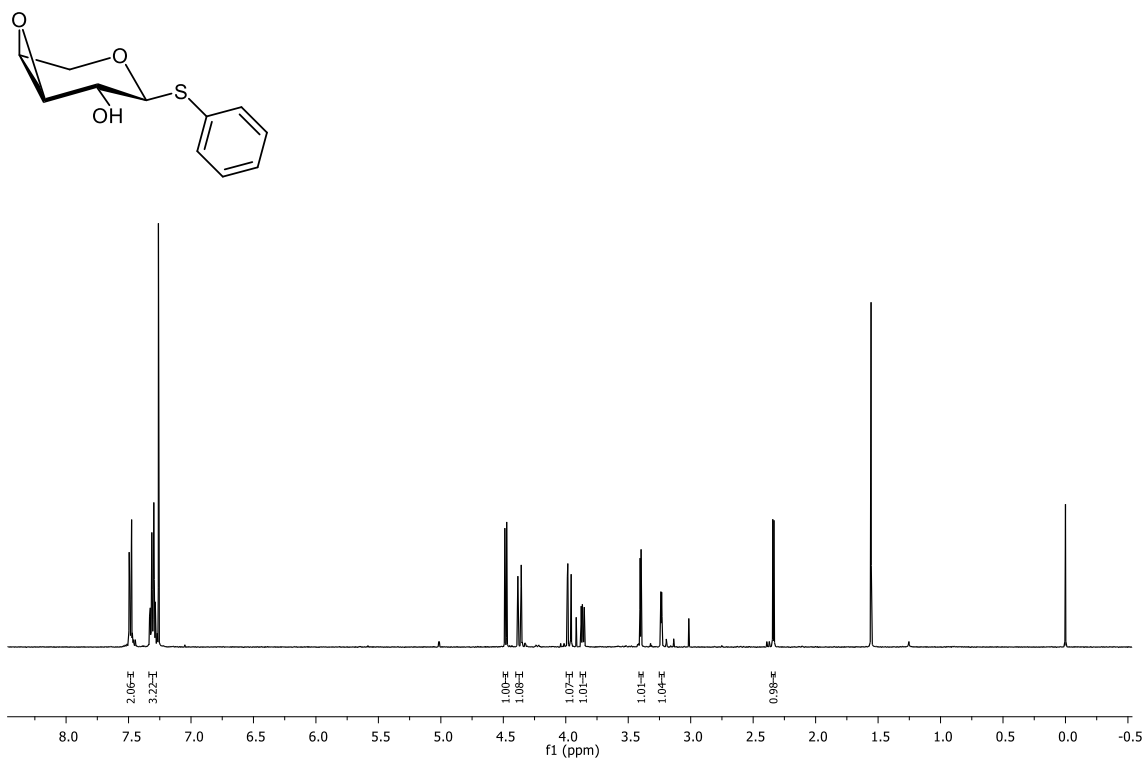


Figure 8.21.  $^1\text{H}$  NMR spectrum of **70** (500 MHz,  $\text{CDCl}_3$ , 298 K).

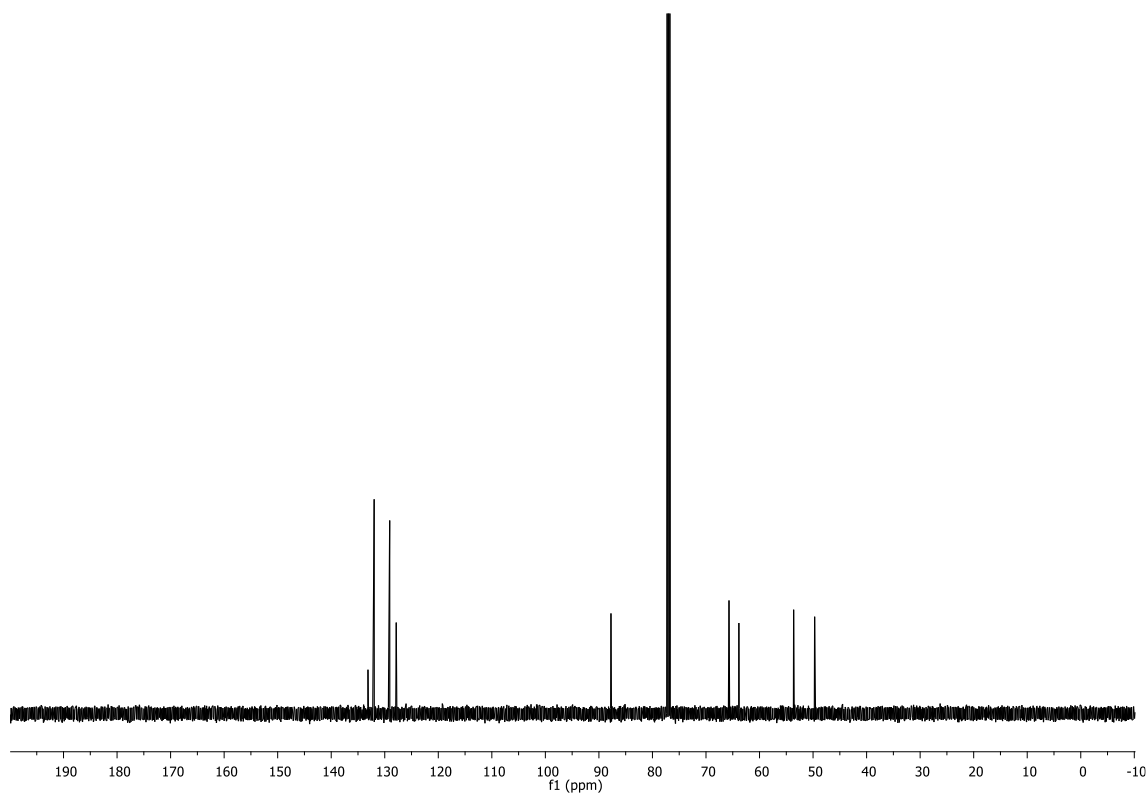
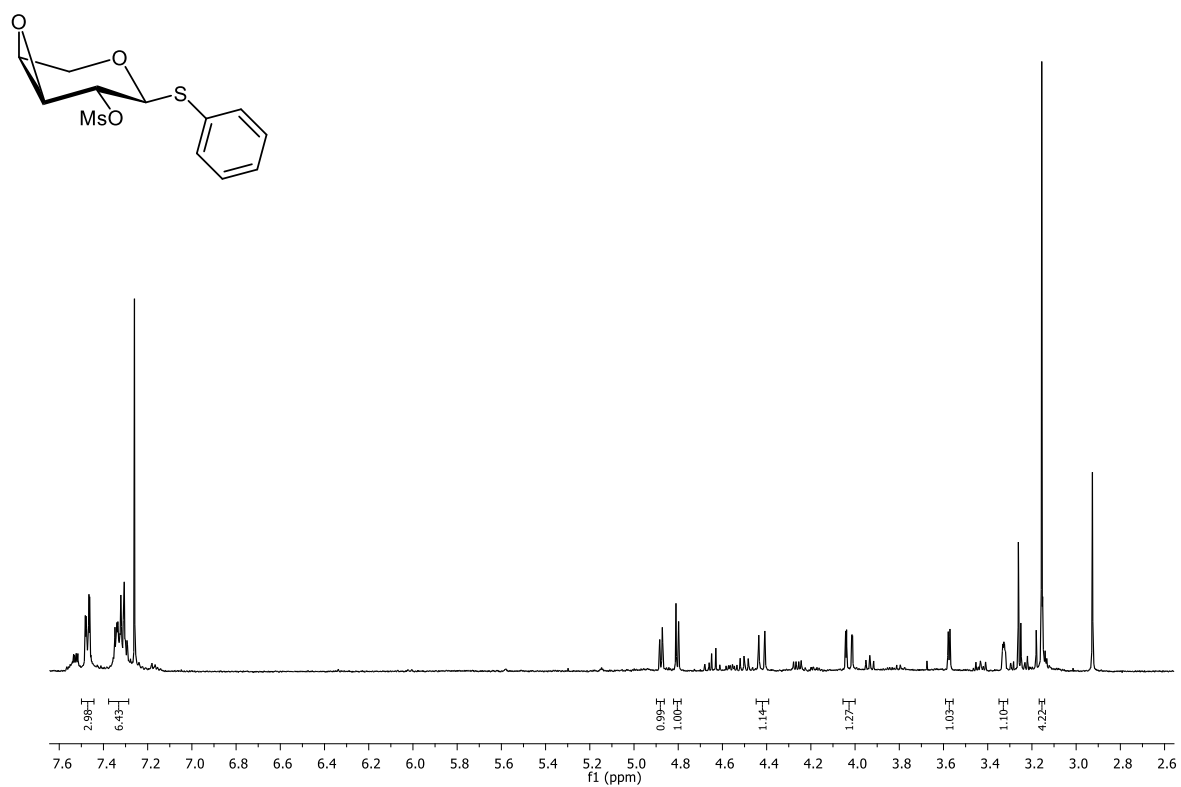
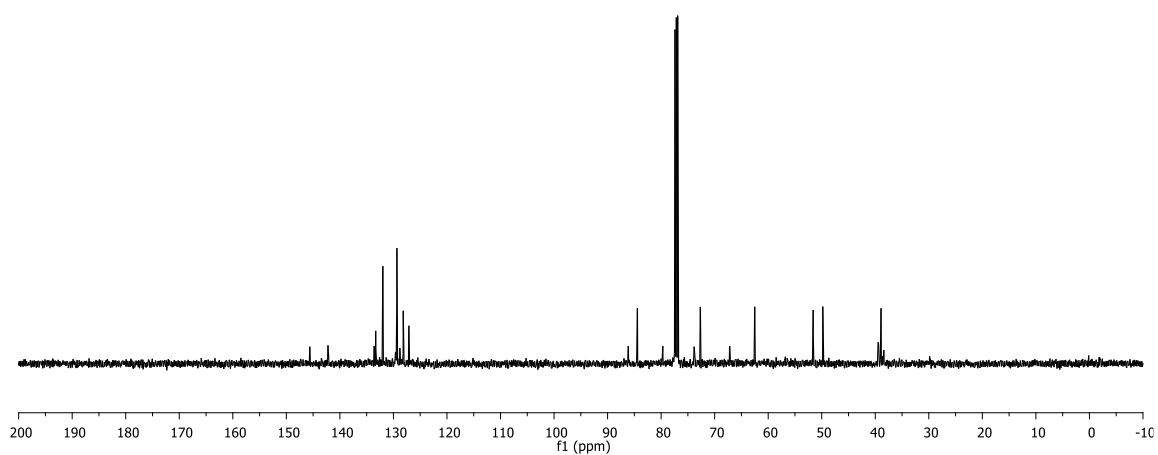


Figure 8.22.  $^{13}\text{C}$  NMR spectrum of **70** (125 MHz,  $\text{CDCl}_3$ , 298 K).



**Figure 8.23.** <sup>1</sup>H NMR spectrum of **71** (500 MHz, CDCl<sub>3</sub>, 298 K). Impurities due to instability in CDCl<sub>3</sub>.



**Figure 8.24.** <sup>13</sup>C NMR spectrum of **71** (125 MHz, CDCl<sub>3</sub>, 298 K).

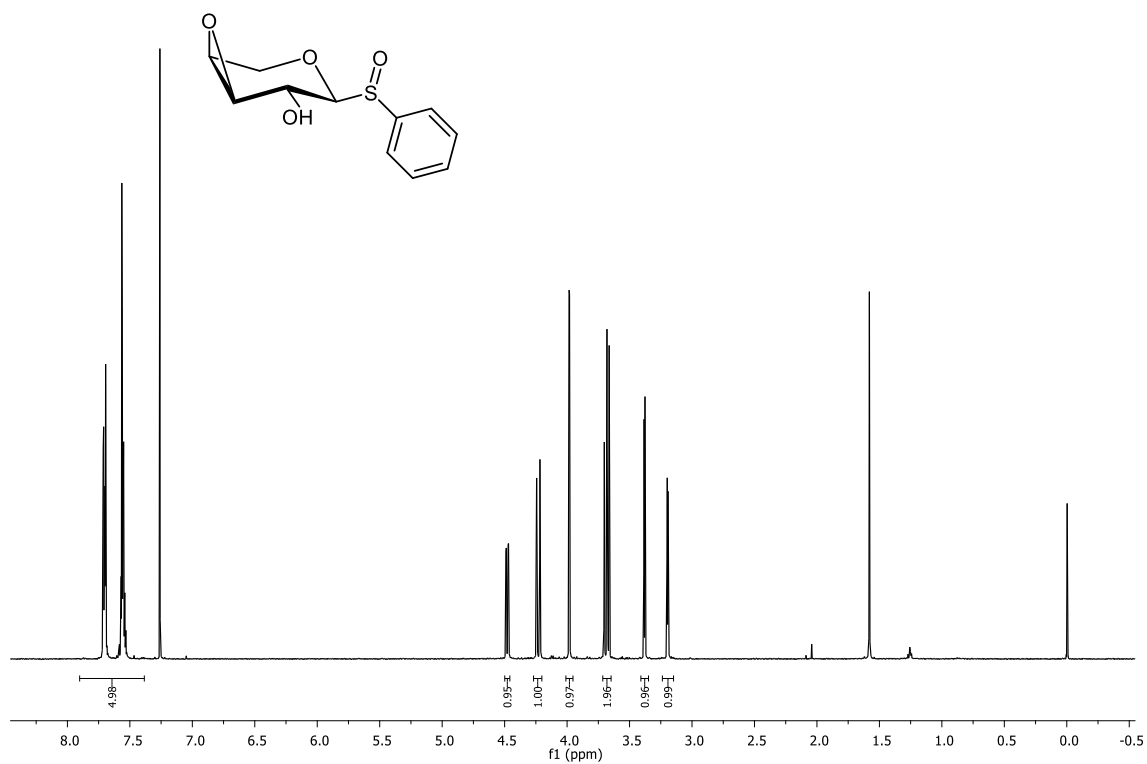


**Figure 8.25.** <sup>1</sup>H NMR spectrum of **81** (500 MHz, CDCl<sub>3</sub>, 298 K).

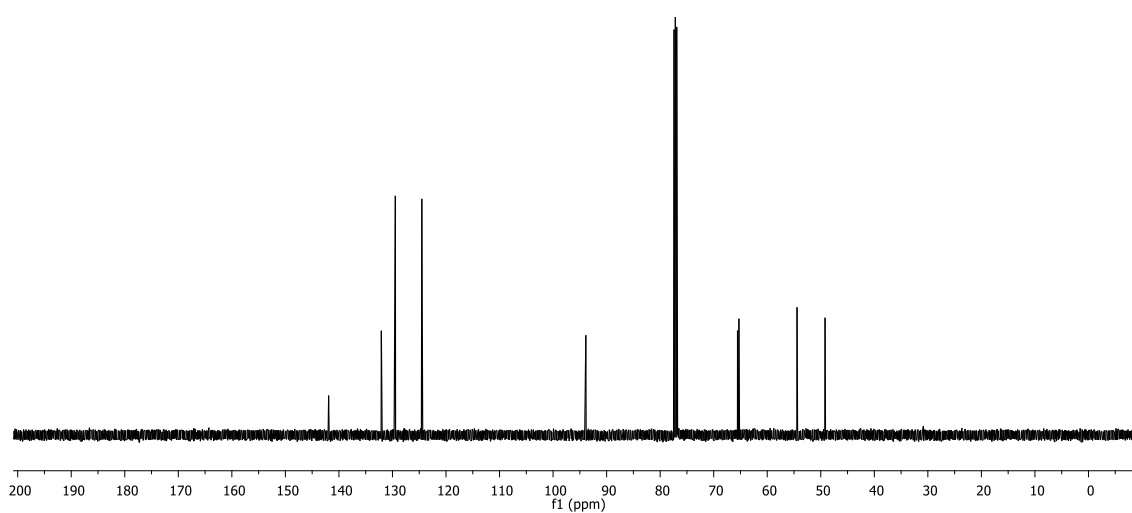


**Figure 8.26.** <sup>13</sup>C NMR spectrum of **81** (125 MHz, CDCl<sub>3</sub>, 298 K).

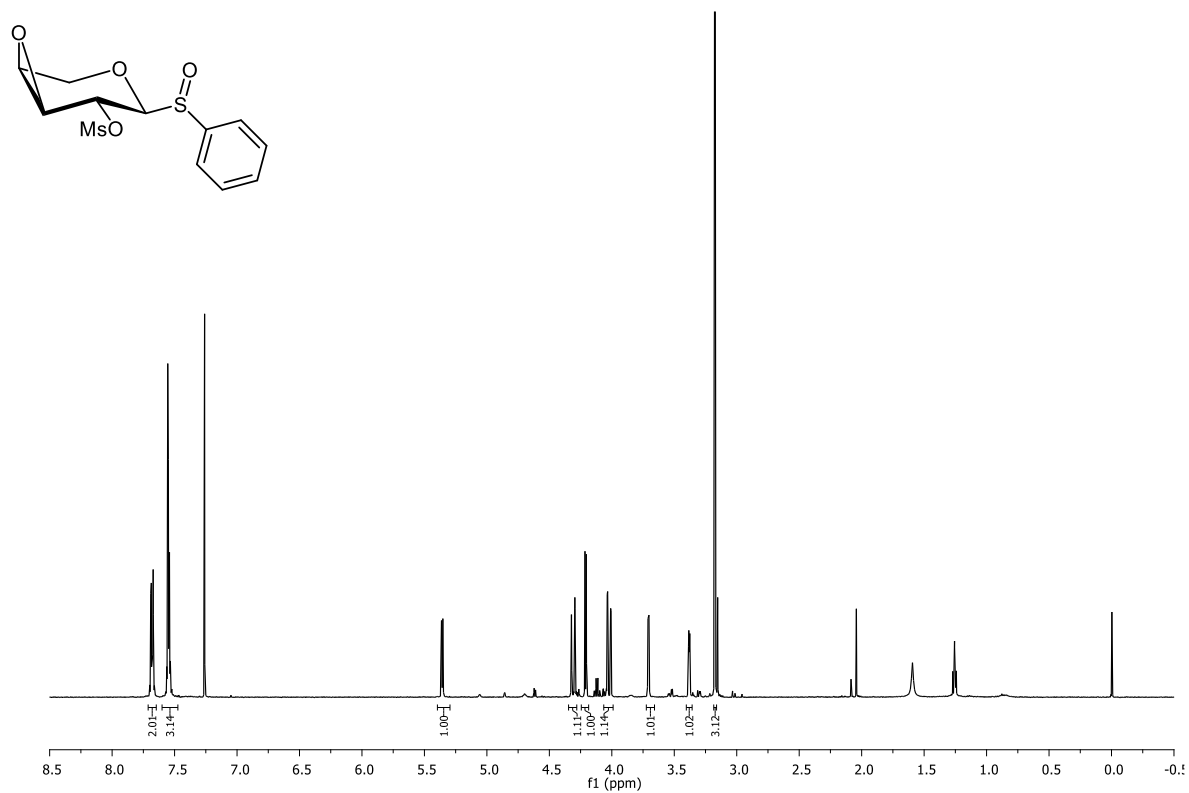


Figure 8.27. <sup>1</sup>H NMR spectrum of **82** (500 MHz, CDCl<sub>3</sub>, 298 K).

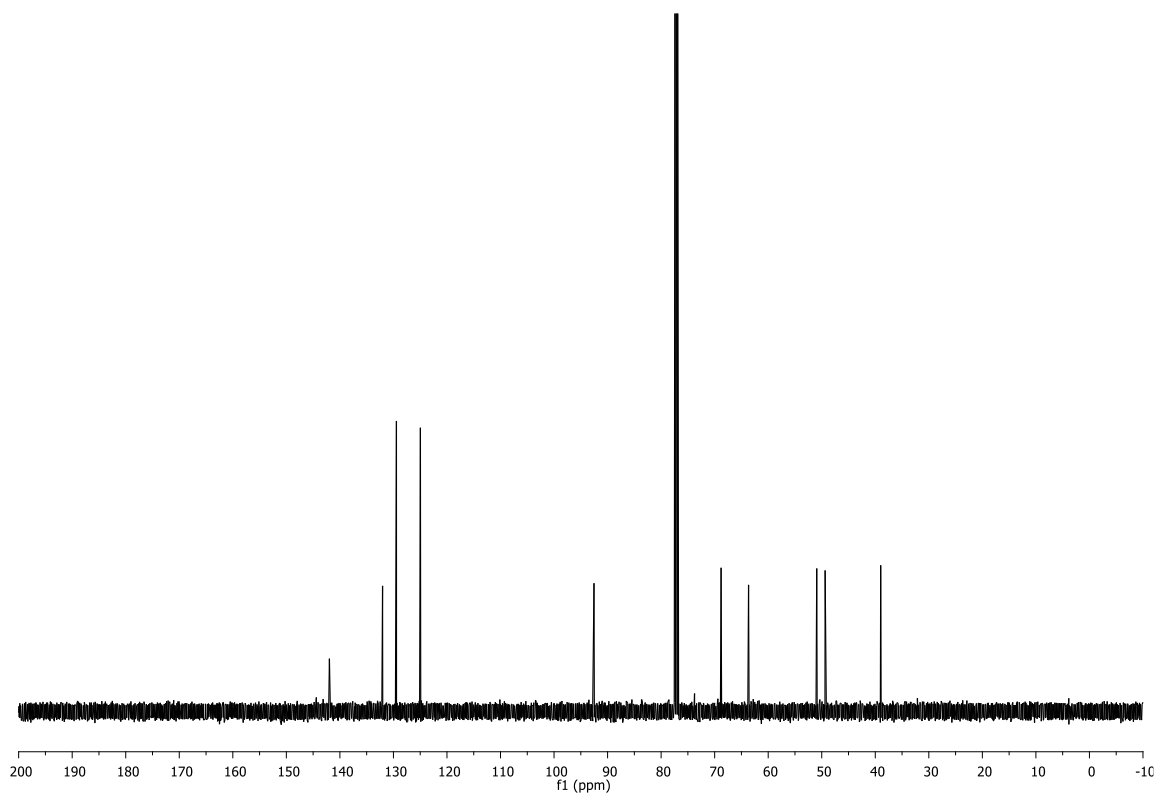


Figure 8.28. <sup>13</sup>C NMR spectrum of **82** (125 MHz, CDCl<sub>3</sub>, 298 K).

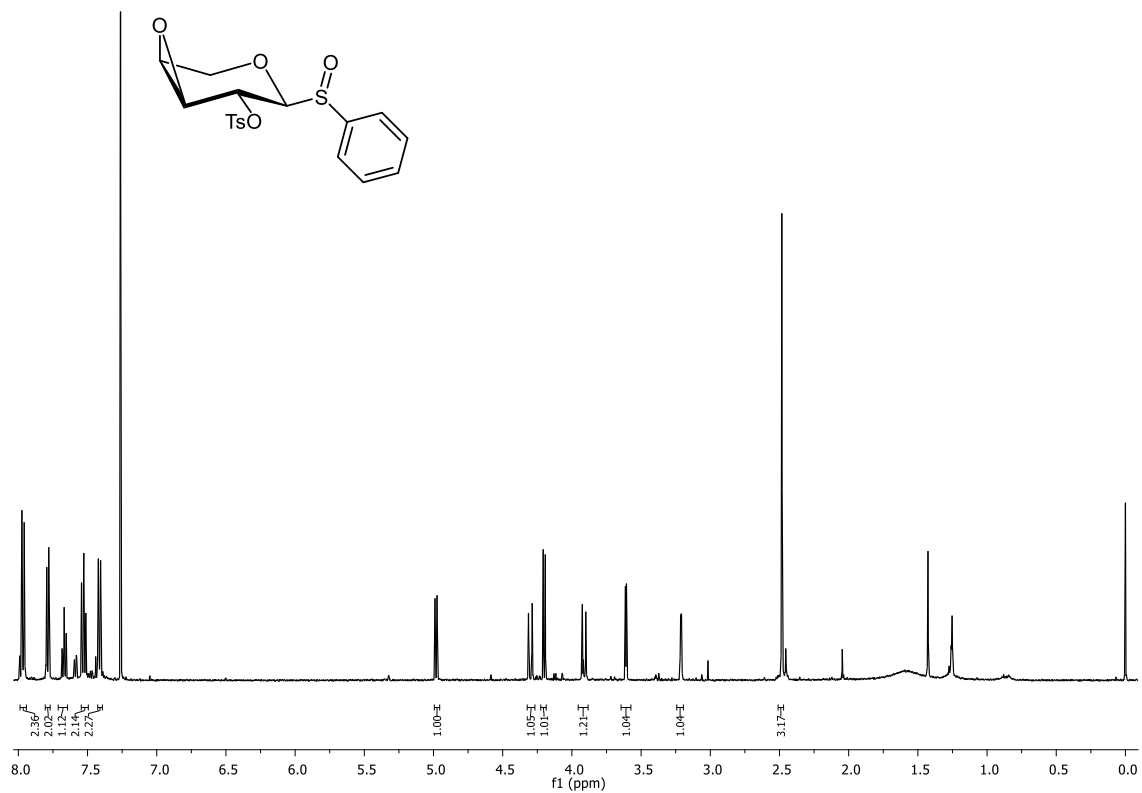


Figure 8.29.  $^1\text{H}$  NMR spectrum of **83** (500 MHz,  $\text{CDCl}_3$ , 298 K).

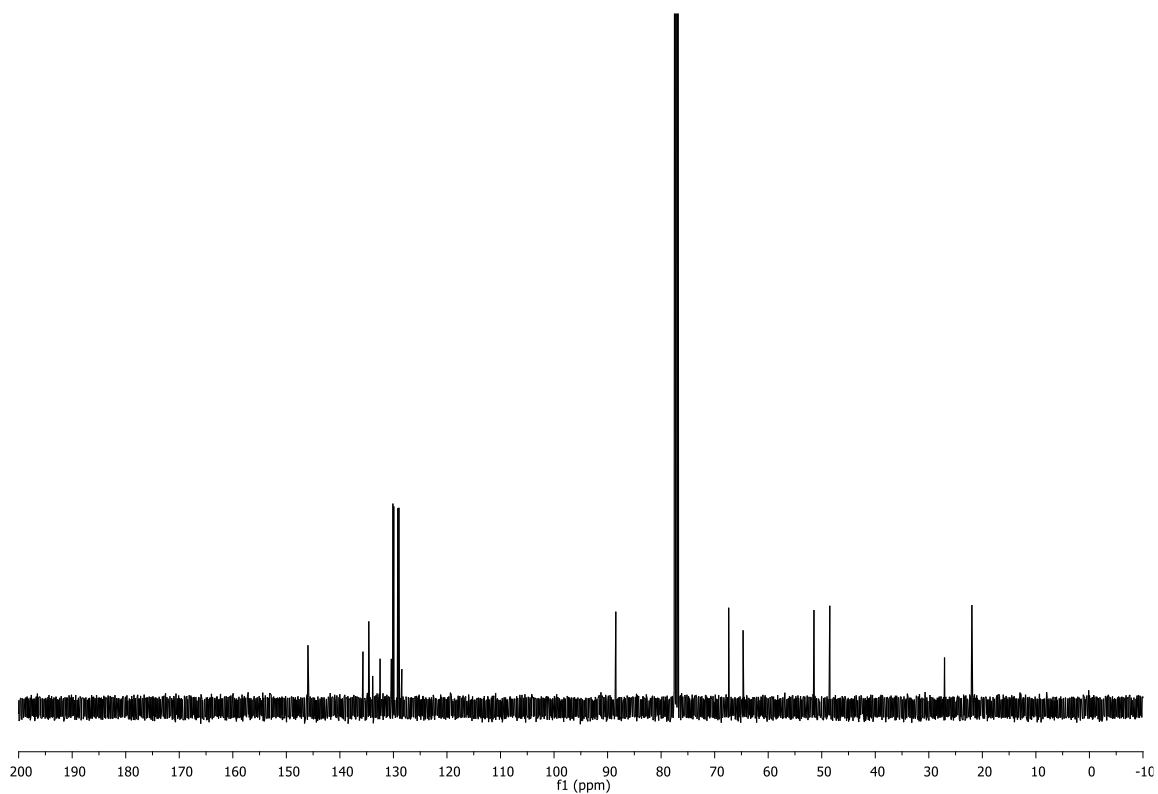


Figure 8.30.  $^{13}\text{C}$  NMR spectrum of **83** (125 MHz,  $\text{CDCl}_3$ , 298 K).

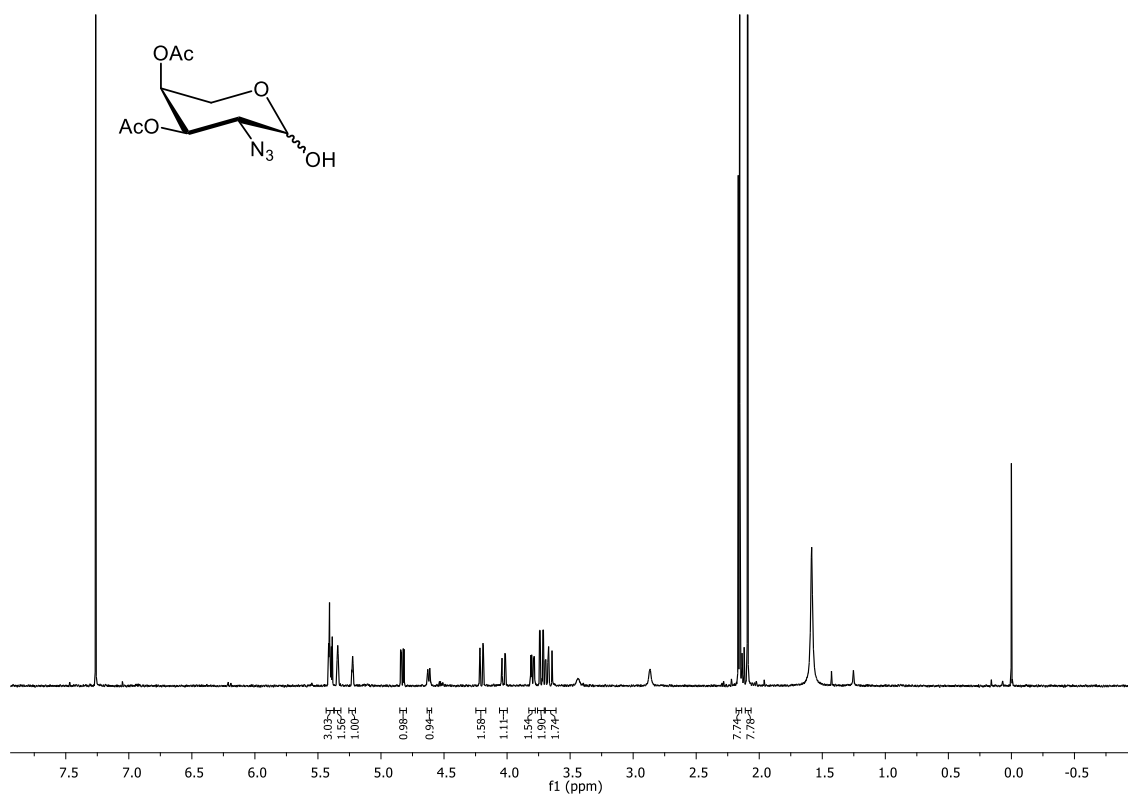


Figure 8.31. <sup>1</sup>H NMR spectrum of **96** (500 MHz, CDCl<sub>3</sub>, 298 K).

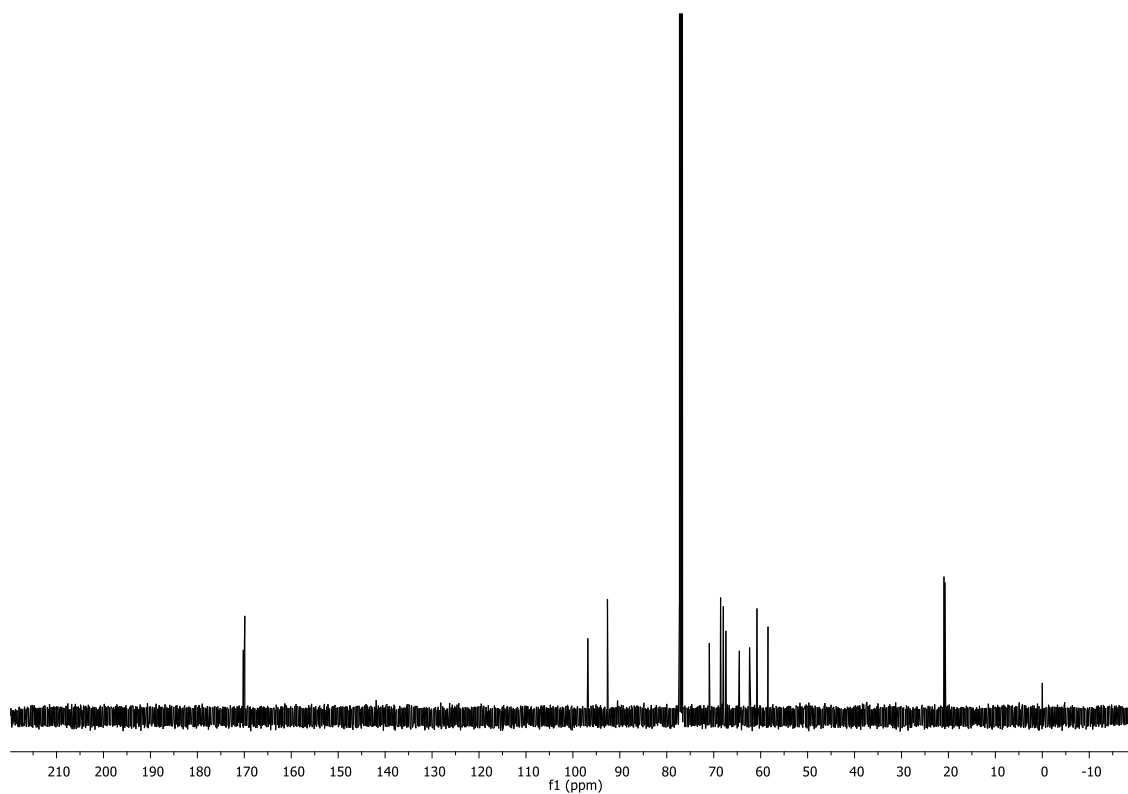
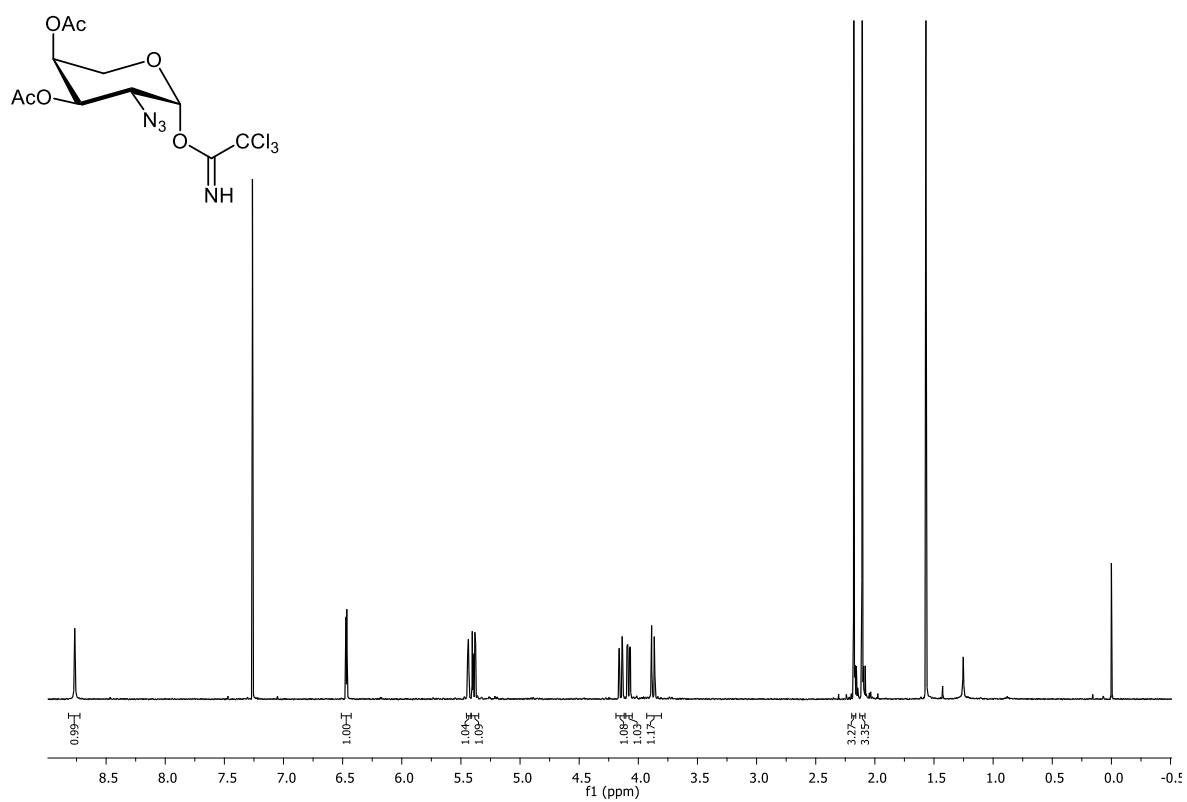
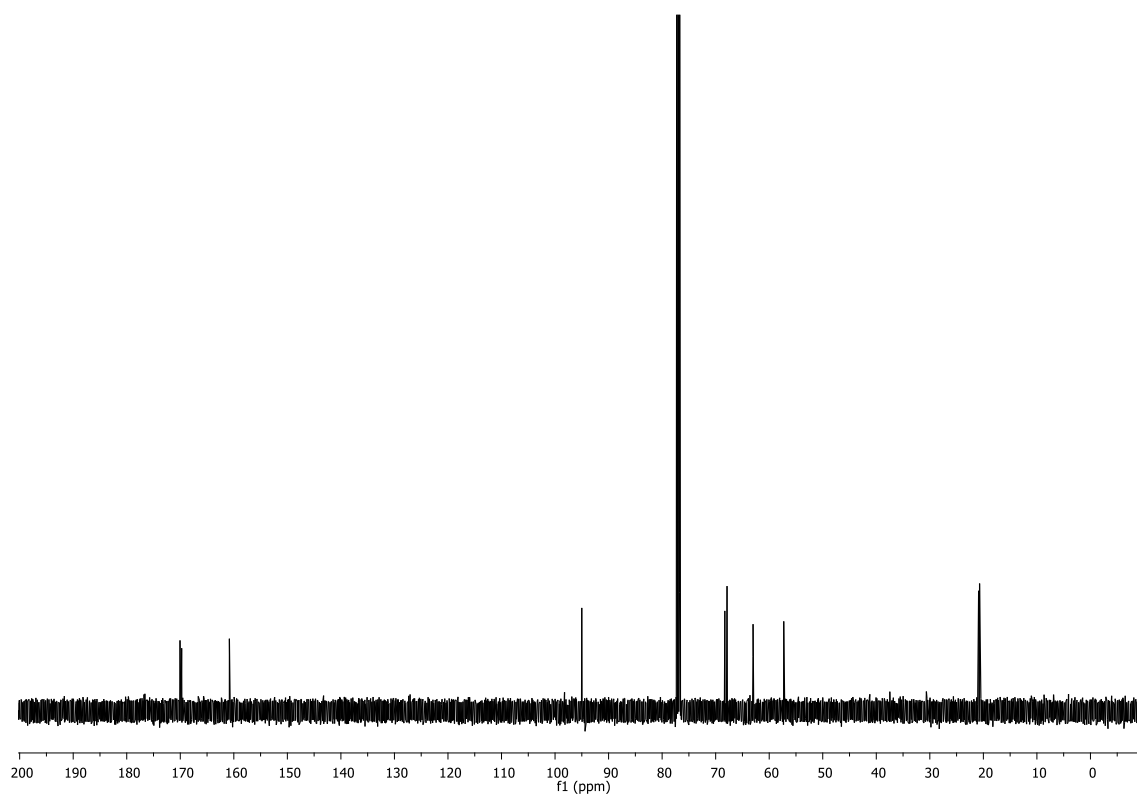


Figure 8.32. <sup>13</sup>C NMR spectrum of **96** (125 MHz, CDCl<sub>3</sub>, 298 K).



**Figure 8.33.**  $^1\text{H}$  NMR spectrum of **97** (500 MHz, CDCl<sub>3</sub>, 298 K).



**Figure 8.34.**  $^{13}\text{C}$  NMR spectrum of **97** (125 MHz, CDCl<sub>3</sub>, 298 K).

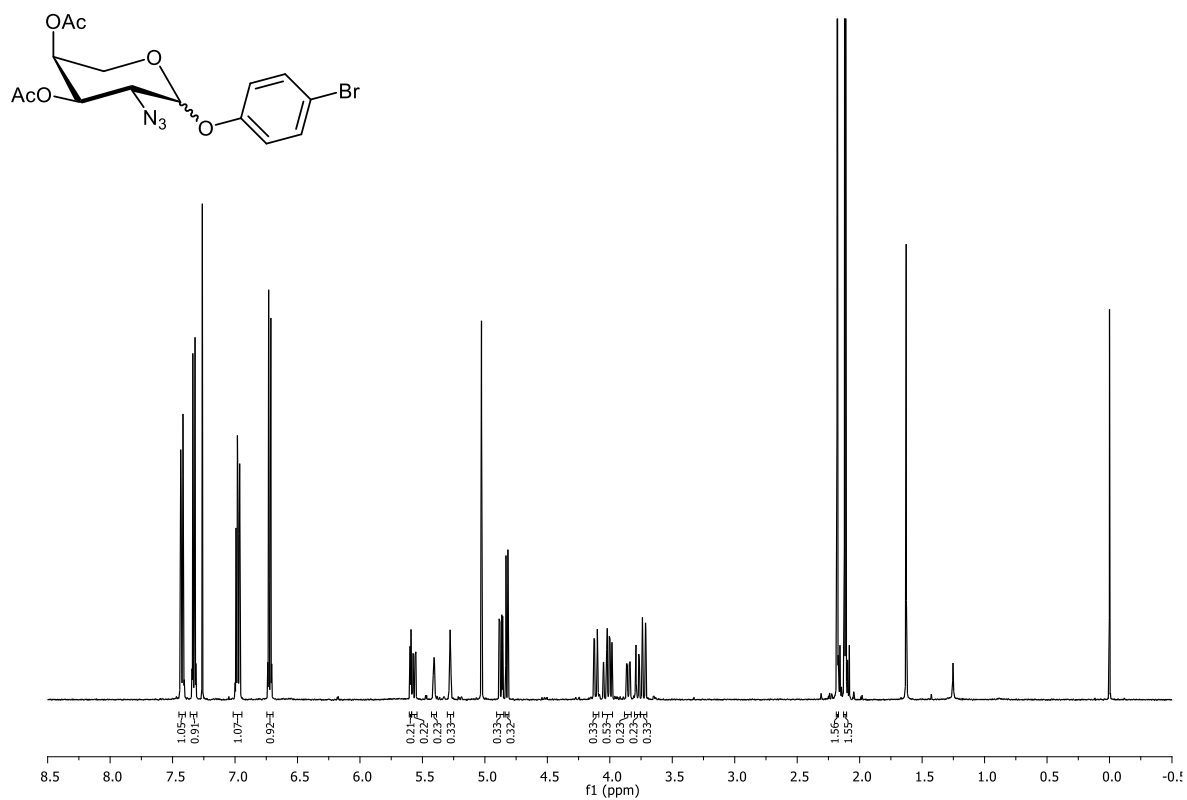


Figure 8.35. <sup>1</sup>H NMR spectrum of **99** (500 MHz, CDCl<sub>3</sub>, 298 K).

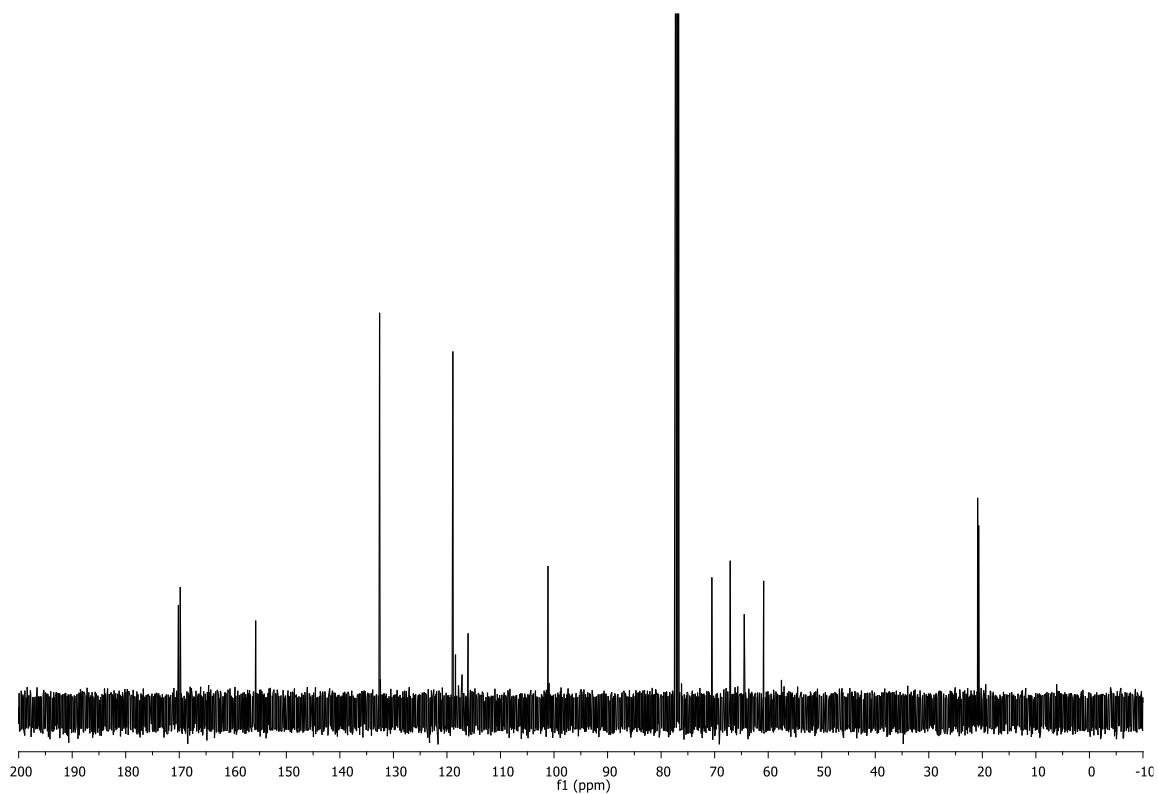
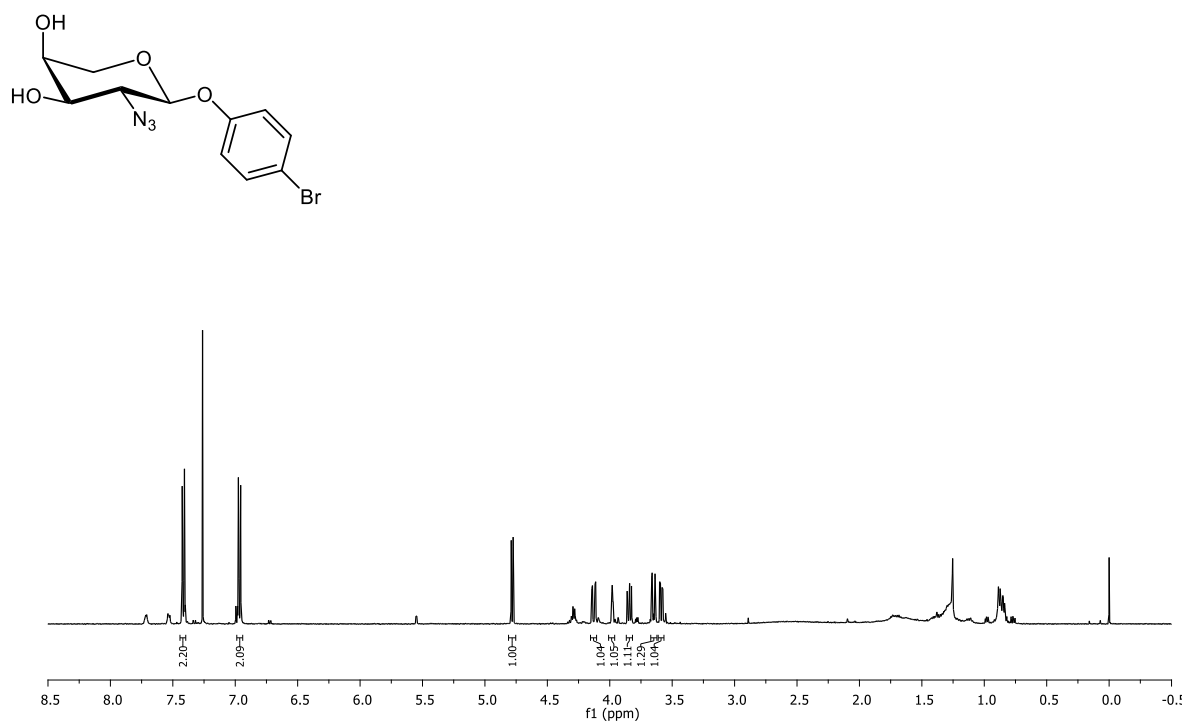
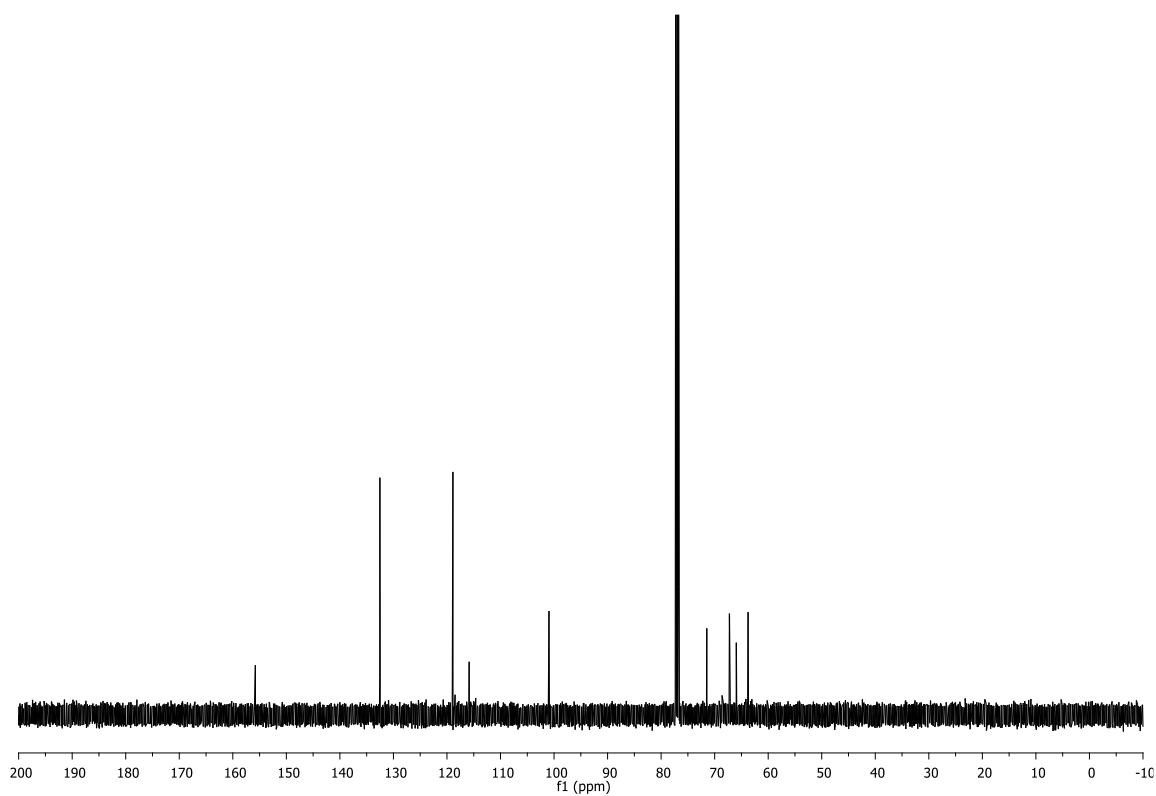


Figure 8.36. <sup>13</sup>C NMR spectrum of **99** (125 MHz, CDCl<sub>3</sub>, 298 K).



**Figure 8.37.** <sup>1</sup>H NMR spectrum of **100** (500 MHz, CDCl<sub>3</sub>, 298 K).



**Figure 8.38.** <sup>13</sup>C NMR spectrum of **100** (125 MHz, CDCl<sub>3</sub>, 298 K).

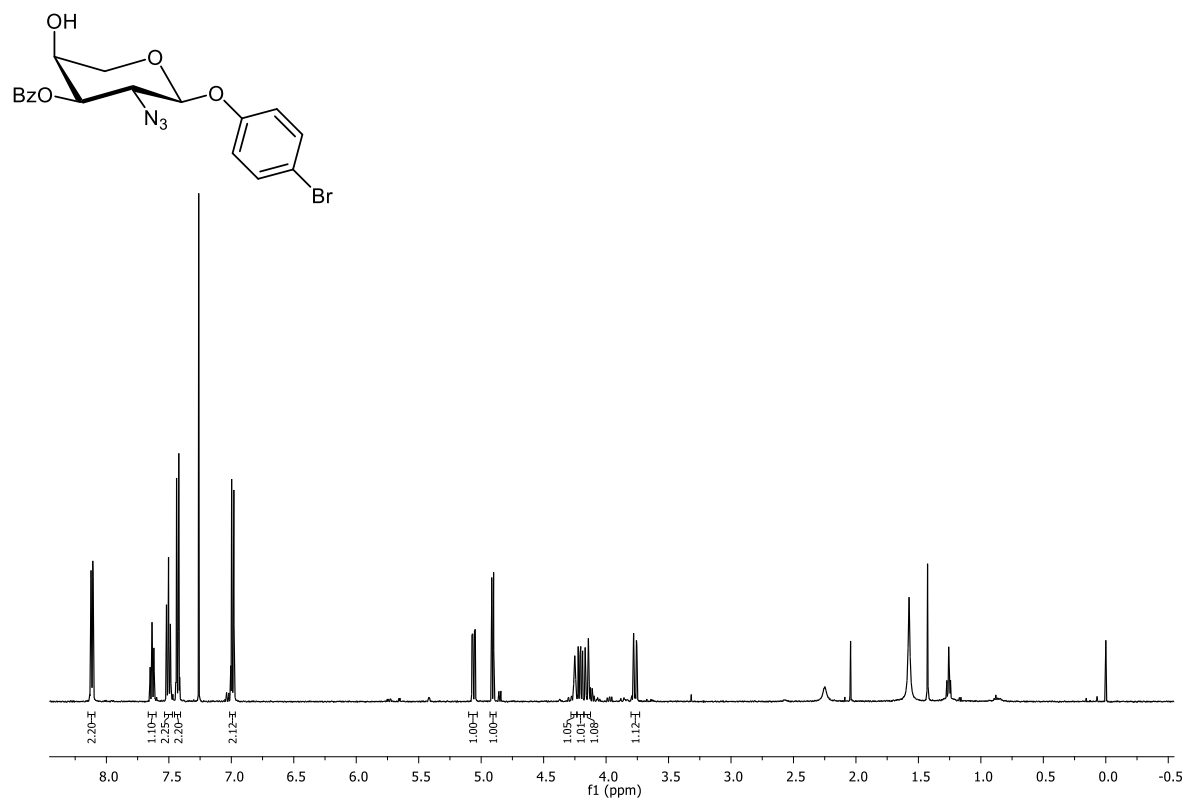


Figure 8.39. <sup>1</sup>H NMR spectrum of **101** (500 MHz, CDCl<sub>3</sub>, 298 K).

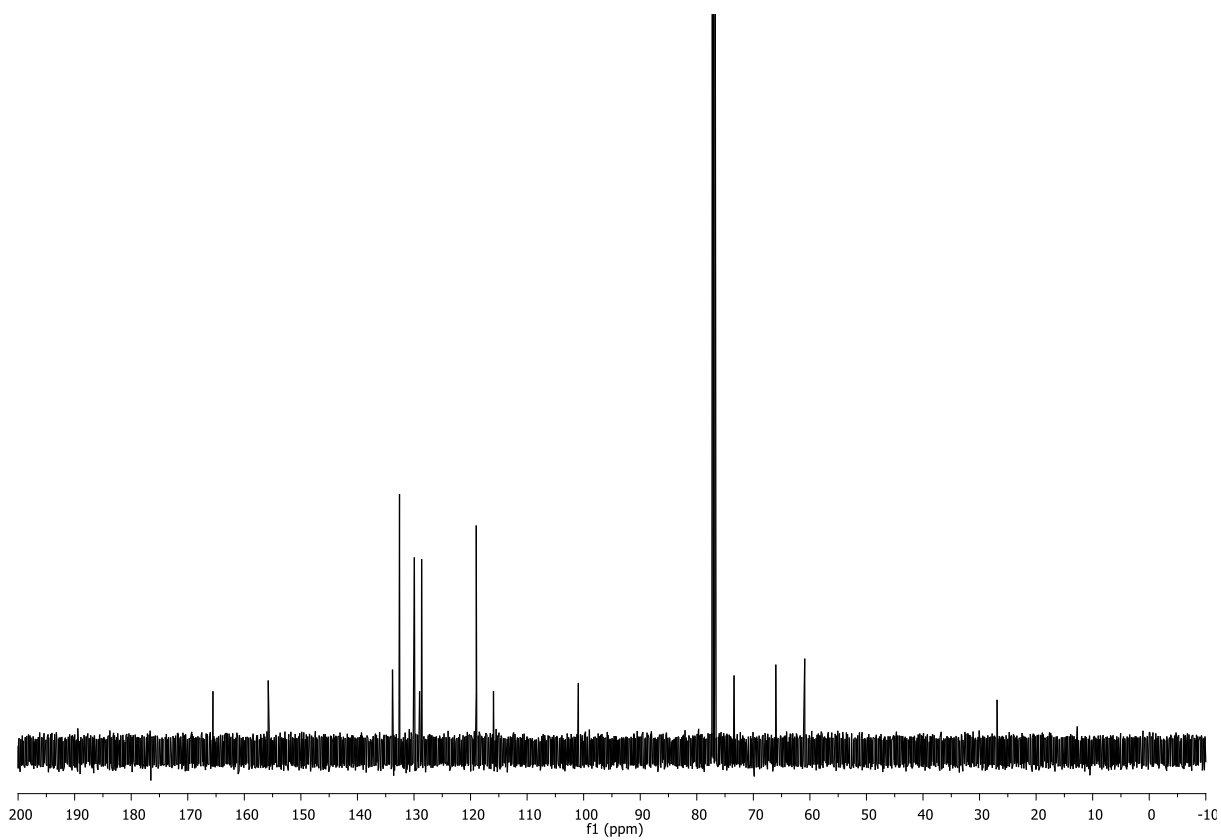
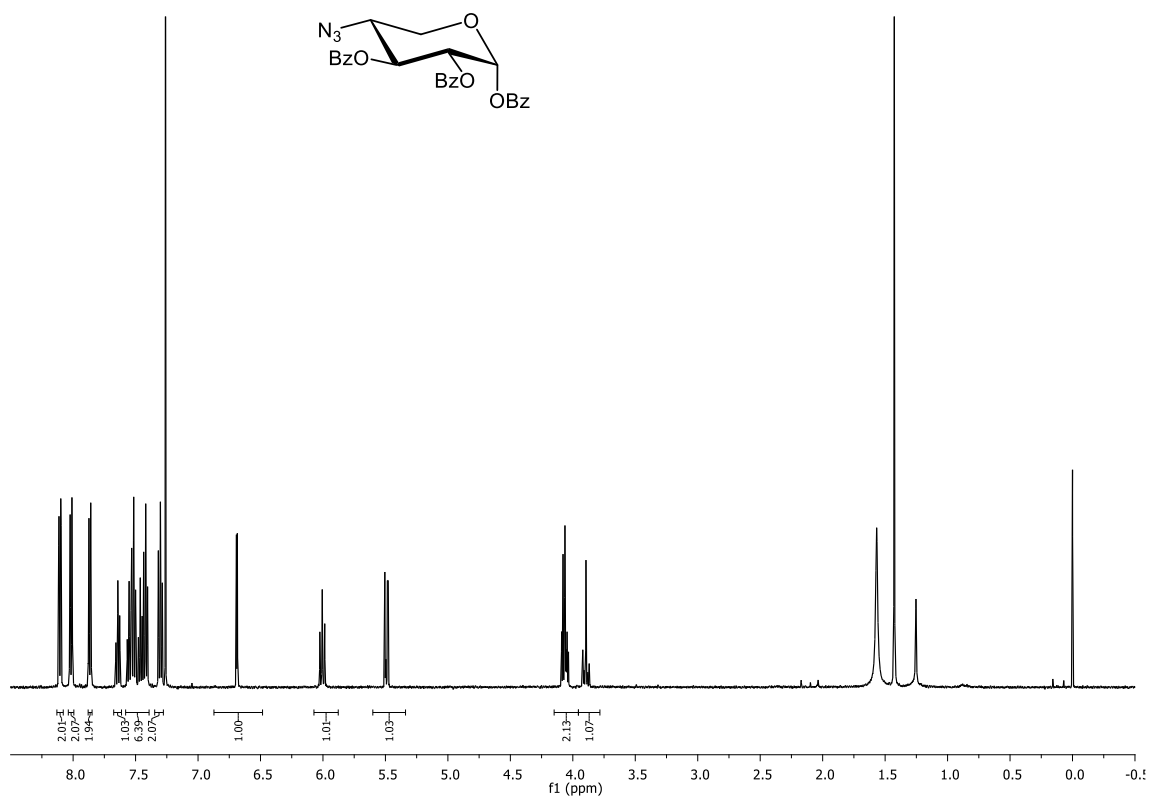
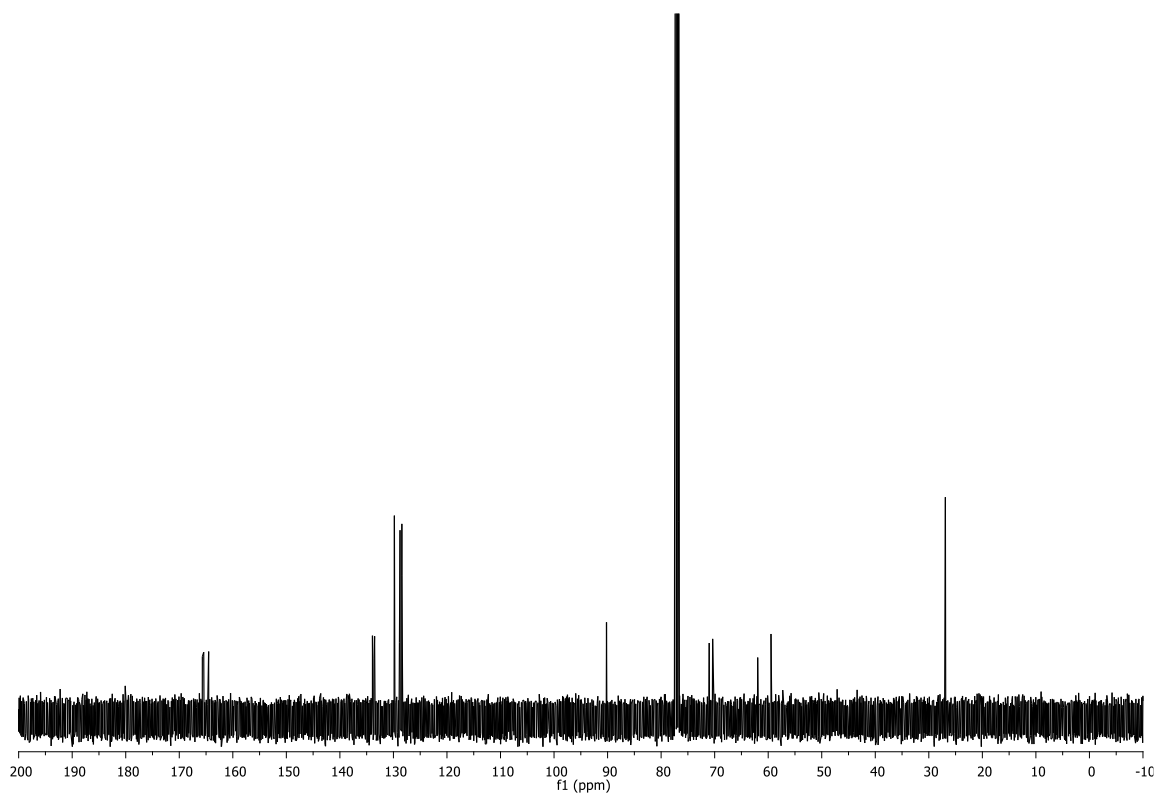


Figure 8.40. <sup>13</sup>C NMR spectrum of **101** (125 MHz, CDCl<sub>3</sub>, 298 K).



**Figure 8.41.** <sup>1</sup>H NMR spectrum of **105** (500 MHz, CDCl<sub>3</sub>, 298 K).



**Figure 8.42.** <sup>13</sup>C NMR spectrum of **105** (125 MHz, CDCl<sub>3</sub>, 298 K).

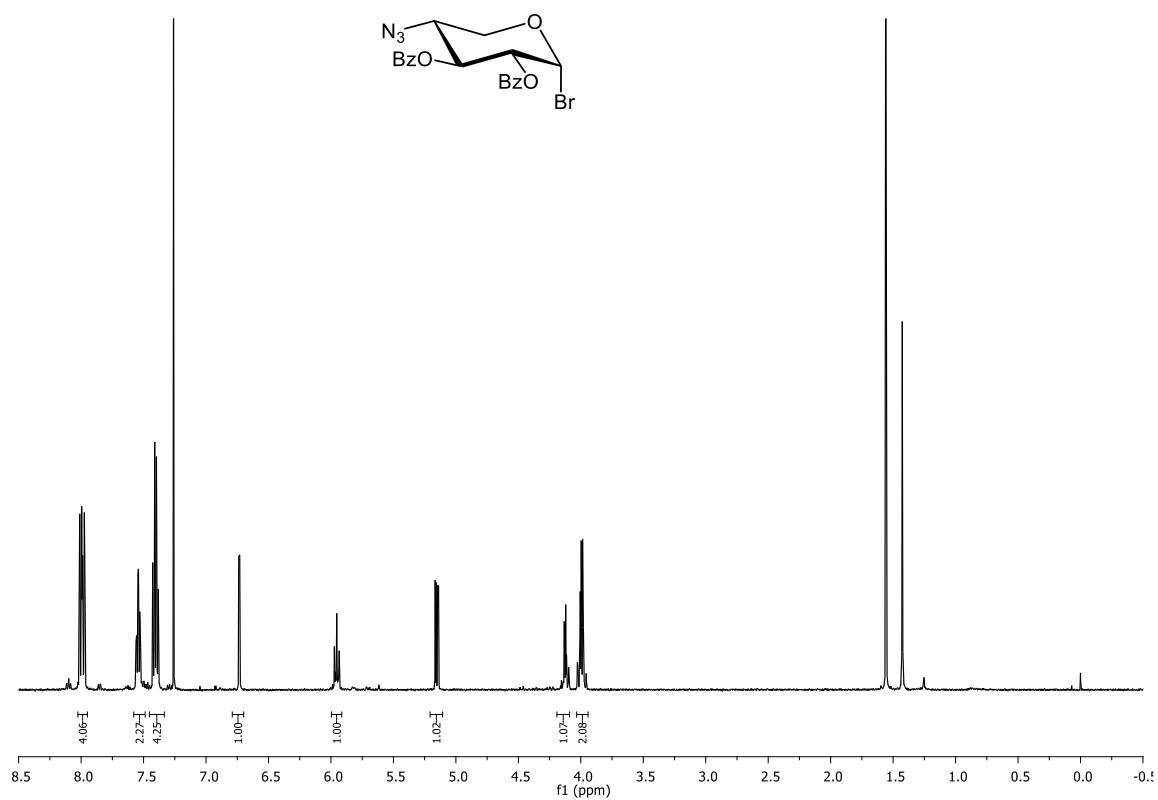


**Figure 8.43.** <sup>1</sup>H NMR spectrum of **106** (500 MHz, CDCl<sub>3</sub>, 298 K).

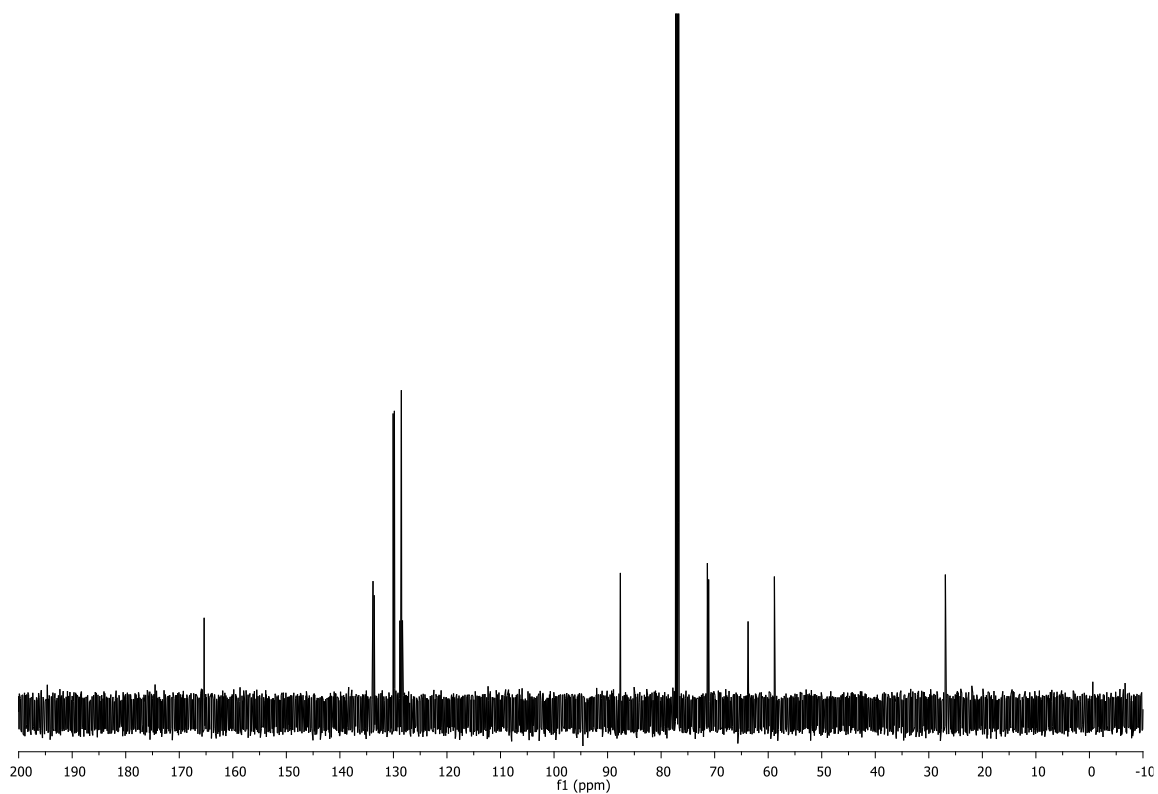


**Figure 8.44.** <sup>13</sup>C NMR spectrum of **106** (125 MHz, CDCl<sub>3</sub>, 298 K).

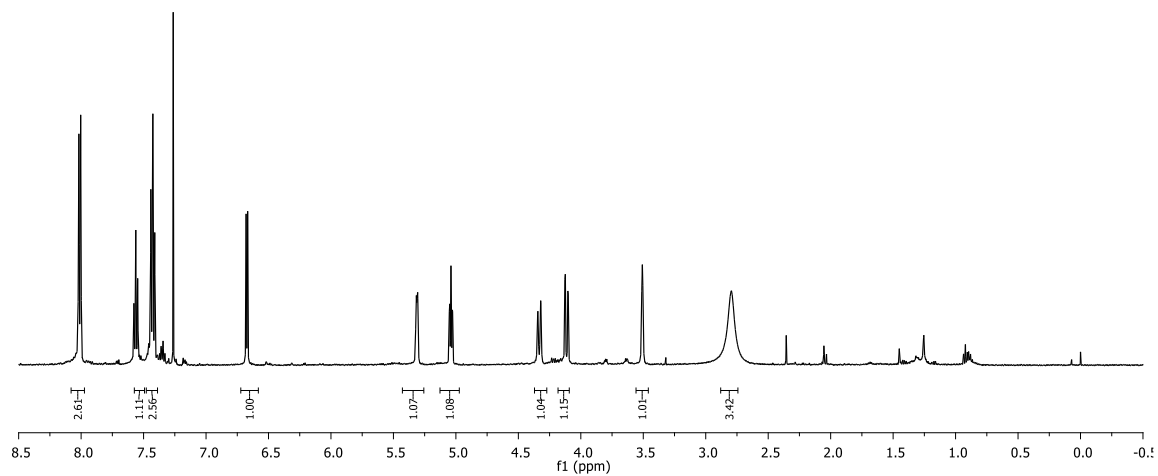


Figure 8.45.  $^1\text{H}$  NMR spectrum of **107** (500 MHz,  $\text{CDCl}_3$ , 298 K).

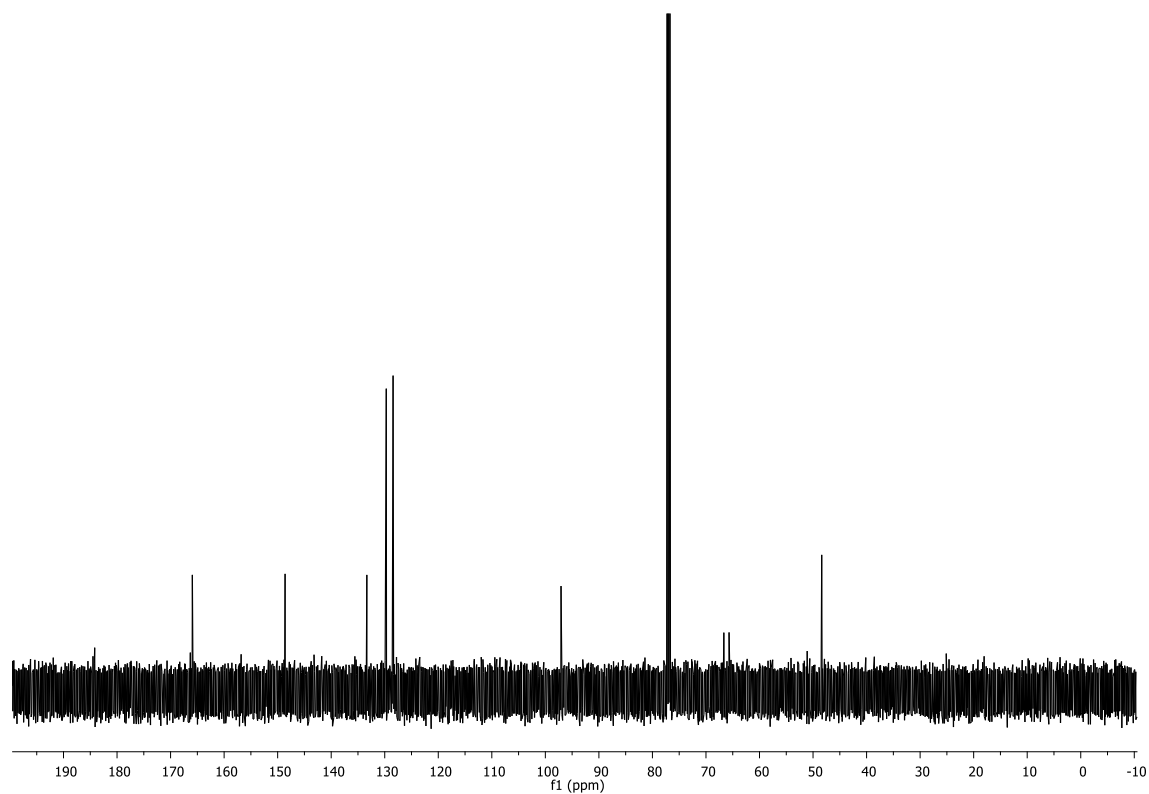


Figure 8.46.  $^{13}\text{C}$  NMR spectrum of **107** (125 MHz,  $\text{CDCl}_3$ , 298 K).

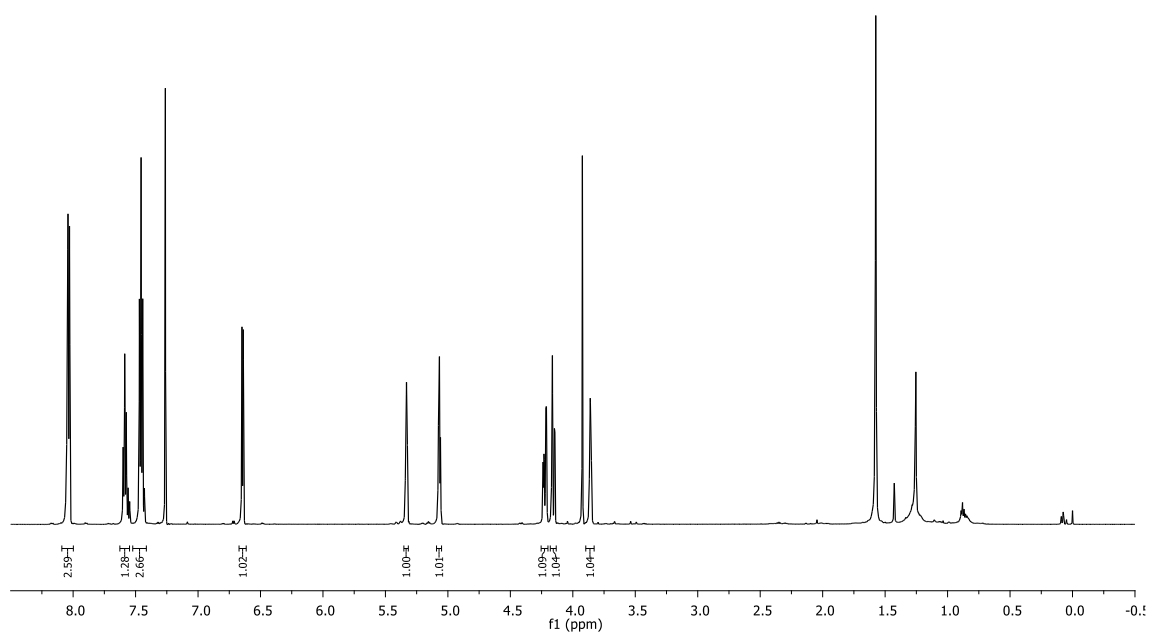


Figure 8.47. <sup>1</sup>H NMR spectrum of **109** (600 MHz, CDCl<sub>3</sub>, 298 K).

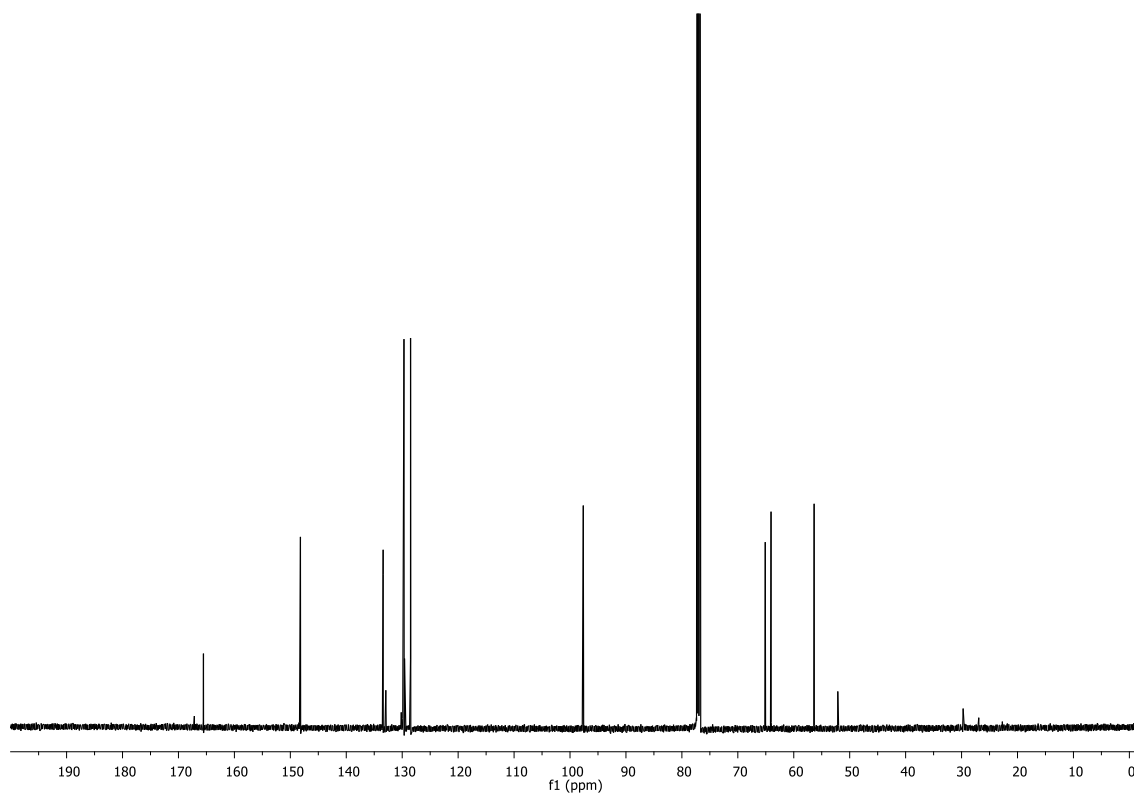


Figure 8.48. <sup>13</sup>C NMR spectrum of **109** (125 MHz, CDCl<sub>3</sub>, 298 K).

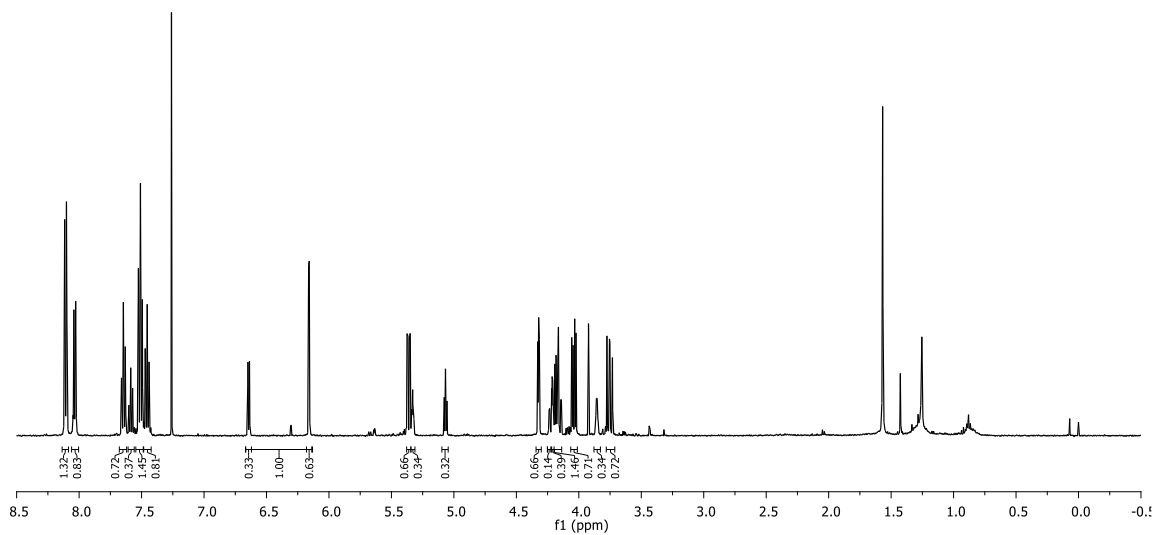
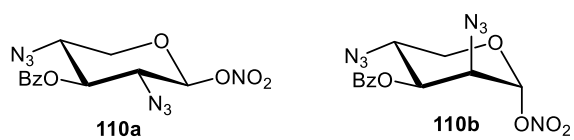


Figure 8.49. <sup>1</sup>H NMR spectrum of 110a/110b (500 MHz, CDCl<sub>3</sub>, 298 K).

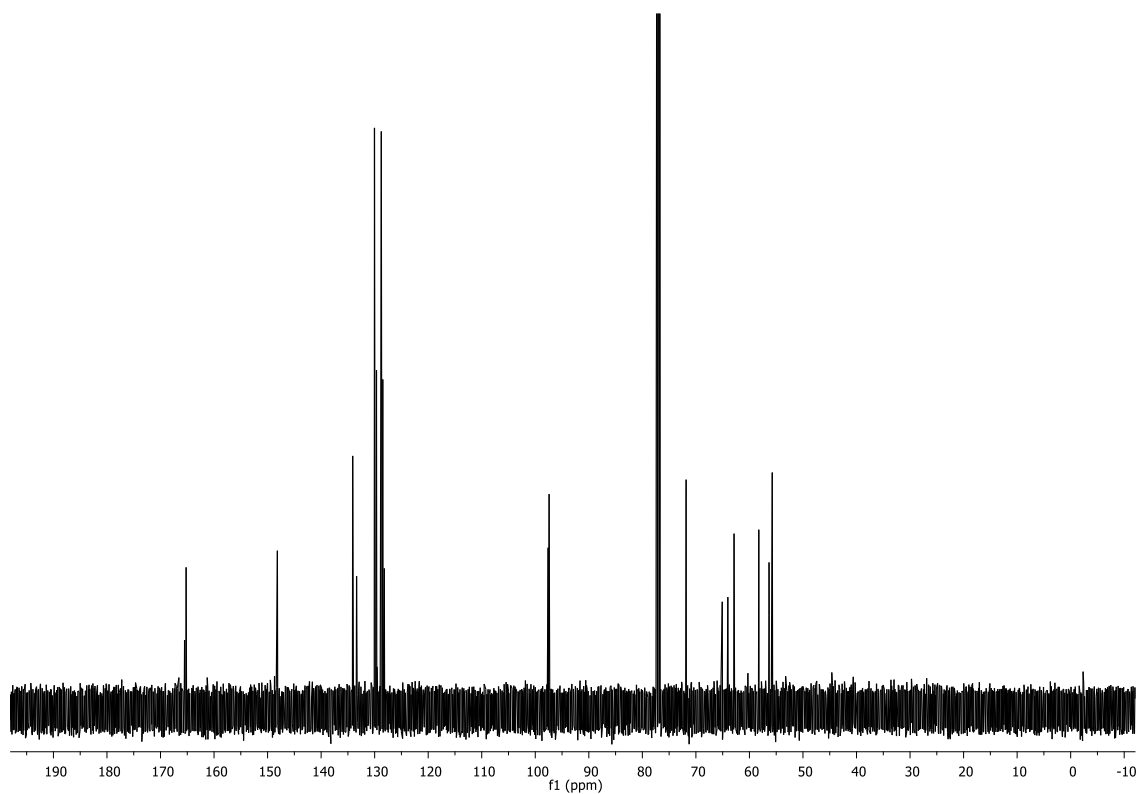


Figure 8.50. <sup>13</sup>C NMR spectrum of 110a/110b (125 MHz, CDCl<sub>3</sub>, 298 K).

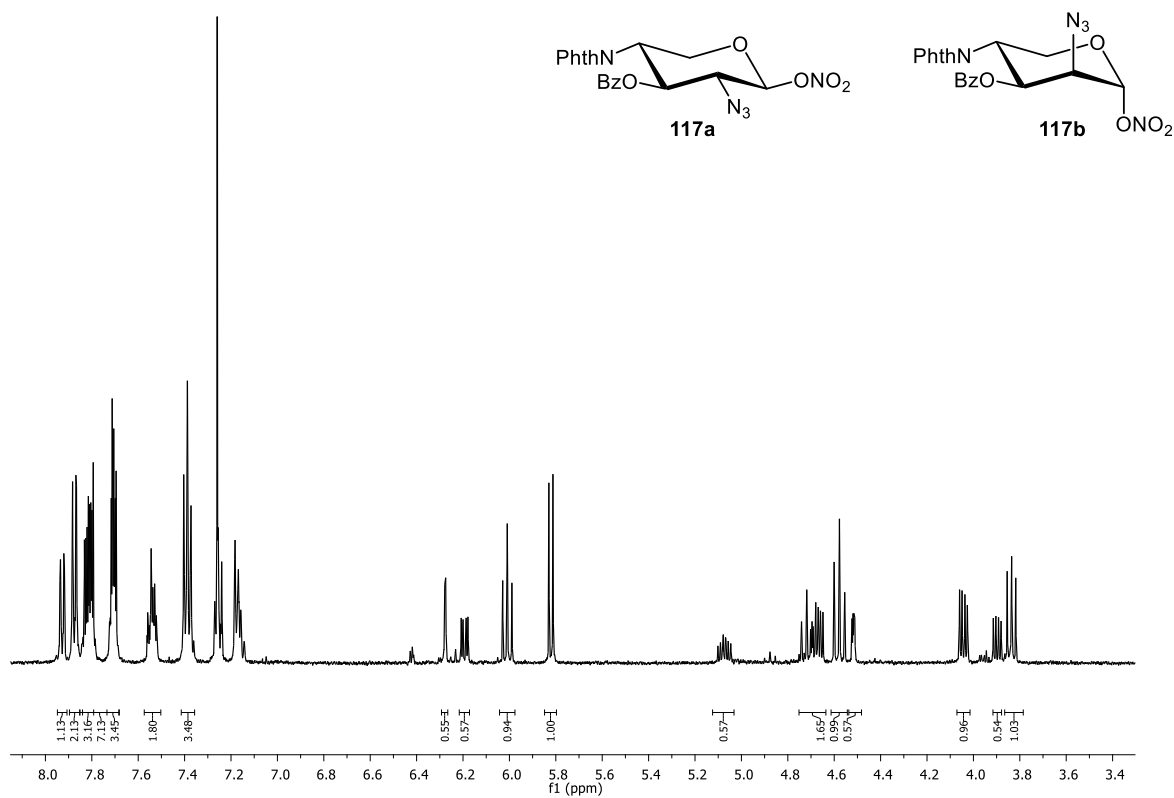


Figure 8.51. <sup>1</sup>H NMR spectrum of **117a/117b** (500 MHz, CDCl<sub>3</sub>, 298 K).

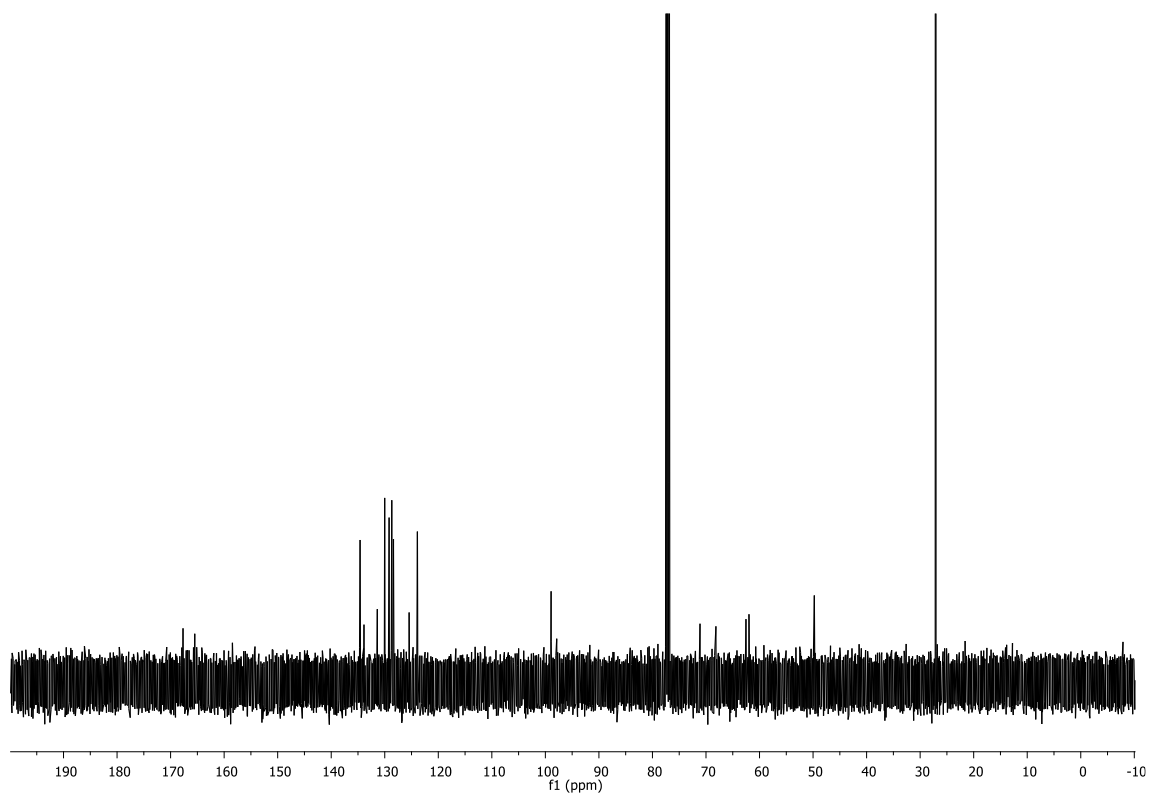
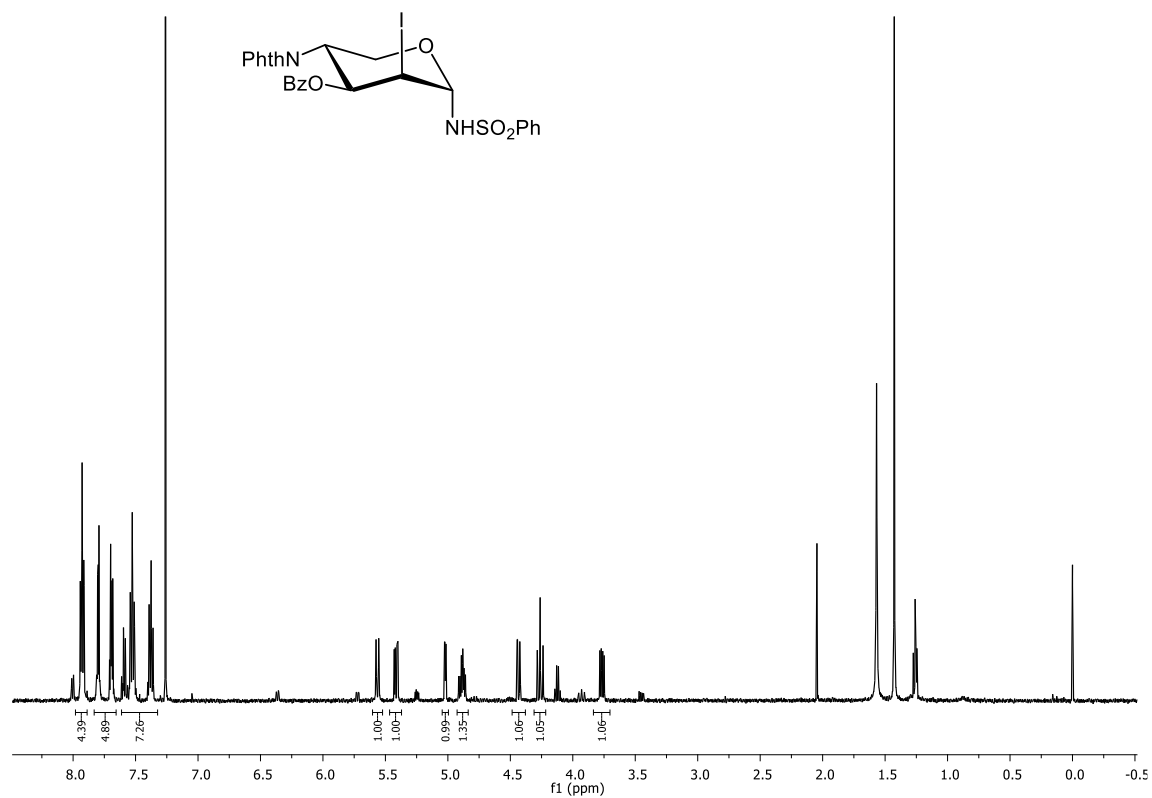
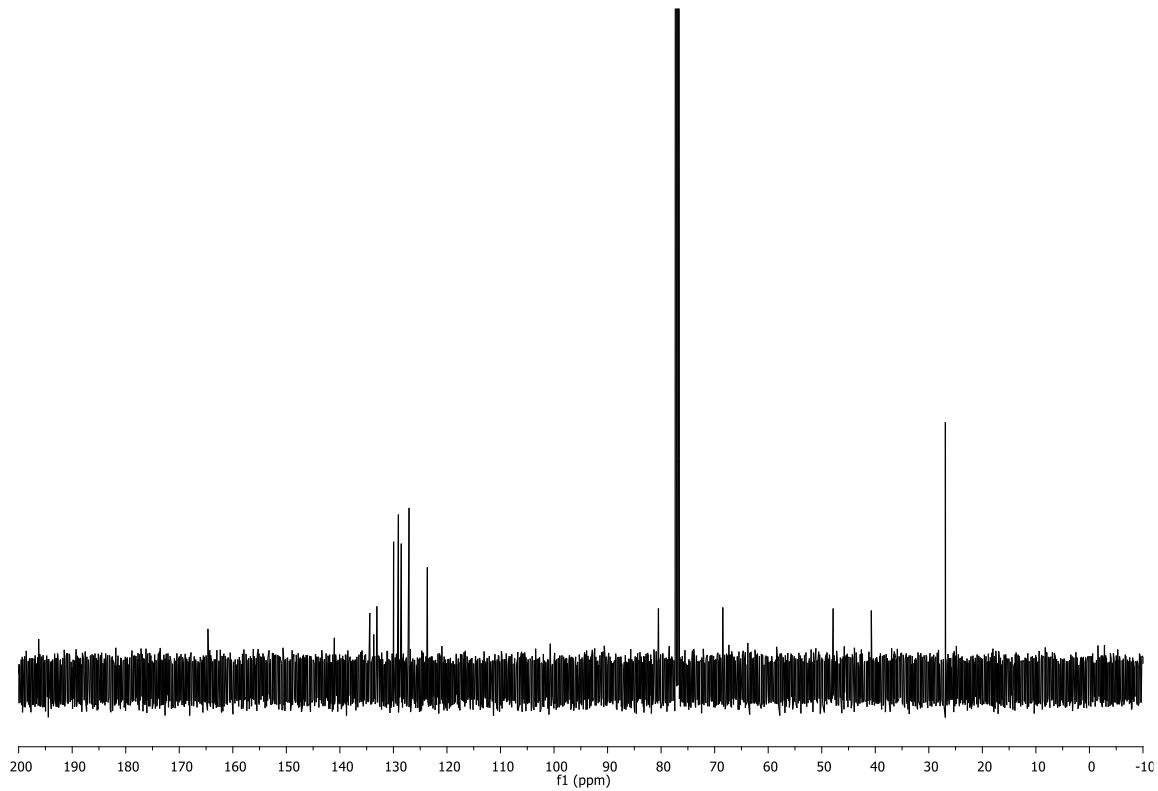


Figure 8.52. <sup>13</sup>C NMR spectrum of **117a/117b** (125 MHz, CDCl<sub>3</sub>, 298 K).



**Figure 8.53.** <sup>1</sup>H NMR spectrum of **126** (500 MHz, CDCl<sub>3</sub>, 298 K). Impurities due to isomerization in CDCl<sub>3</sub>.



**Figure 8.54.** <sup>13</sup>C NMR spectrum of **126** (125 MHz, CDCl<sub>3</sub>, 298 K).

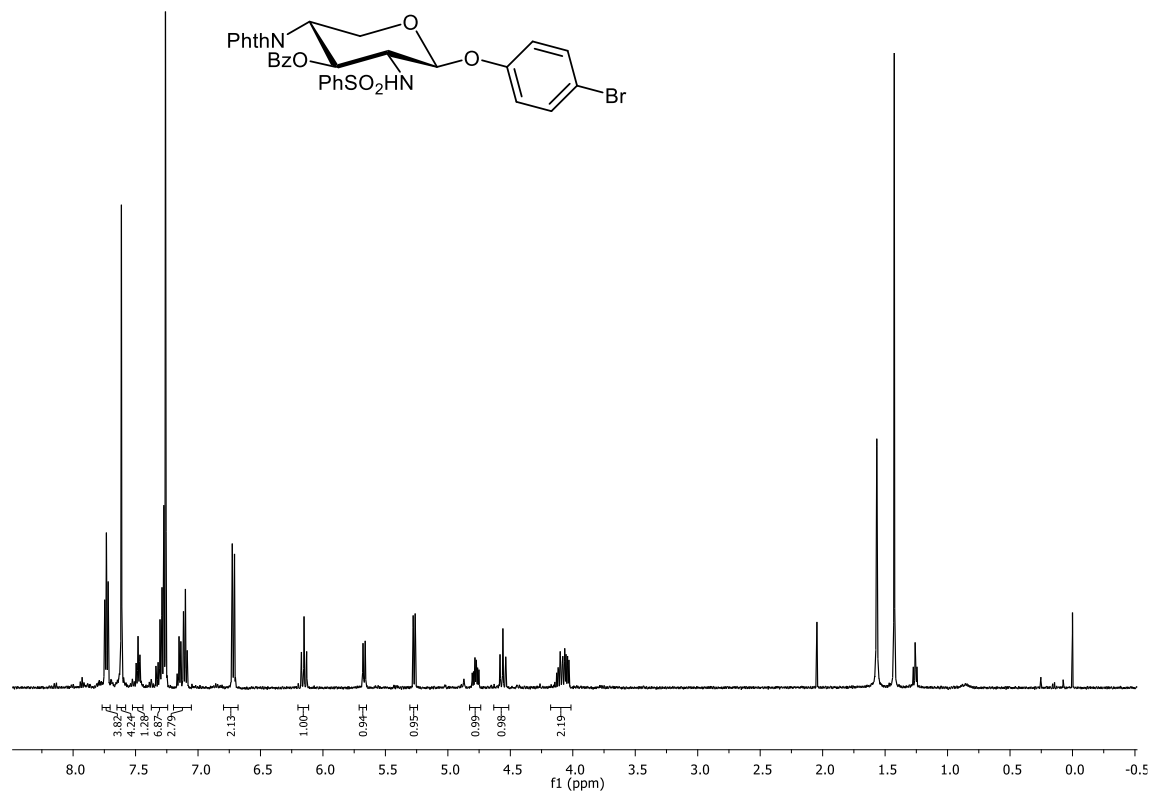


Figure 8.55. <sup>1</sup>H NMR spectrum of **127** (500 MHz, CDCl<sub>3</sub>, 298 K).

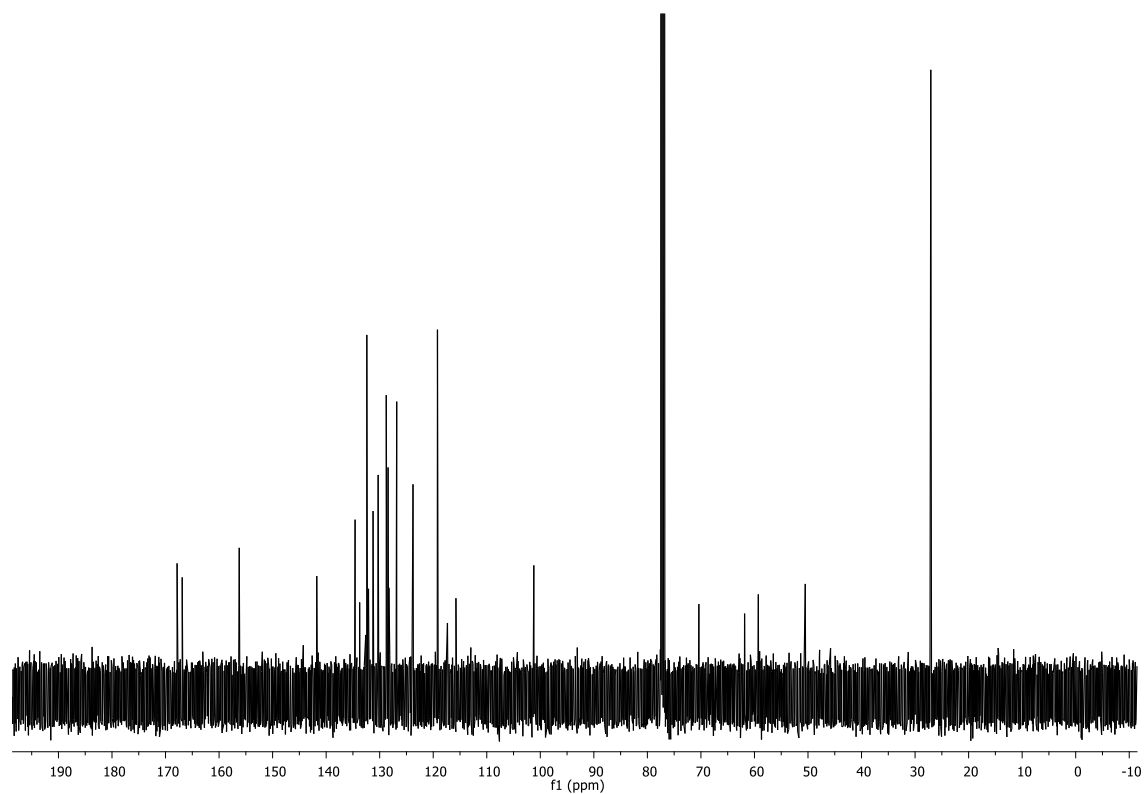


Figure 8.56. <sup>13</sup>C NMR spectrum of **127** (125 MHz, CDCl<sub>3</sub>, 298 K).

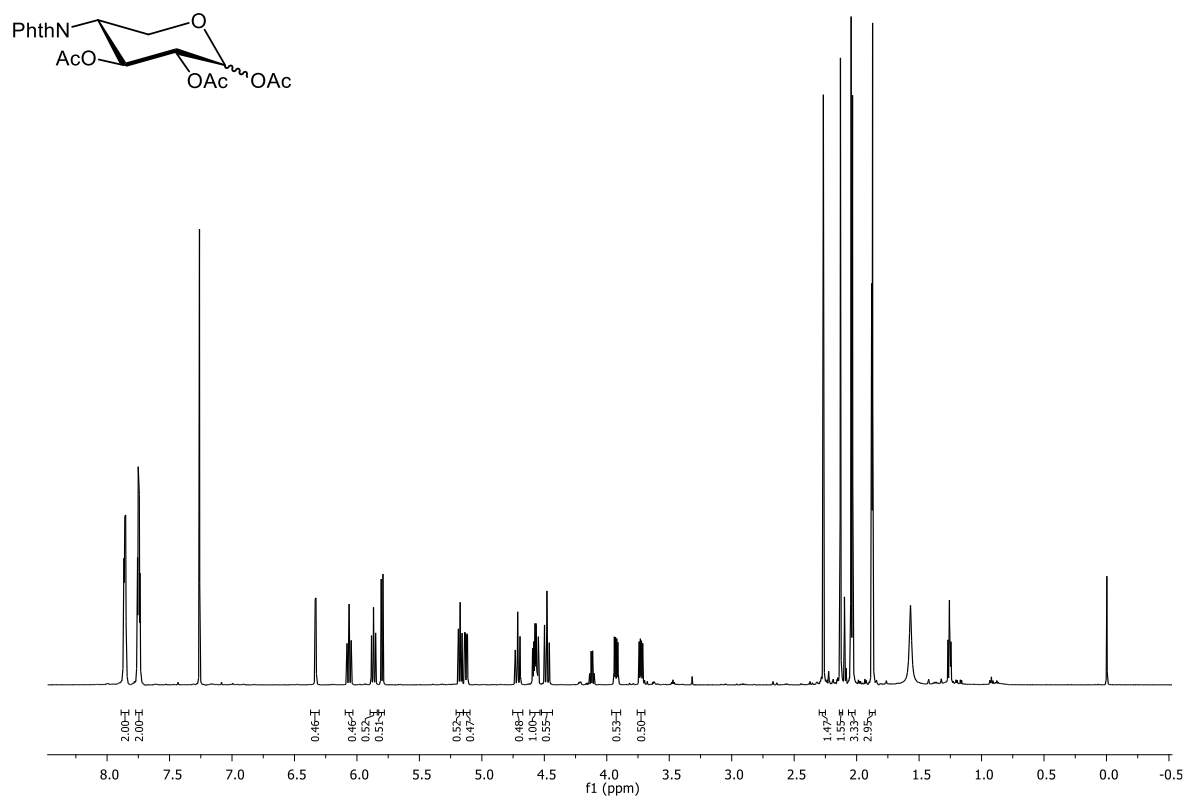


Figure 8.57. <sup>1</sup>H NMR spectrum of **131** (600 MHz, CDCl<sub>3</sub>, 298 K).

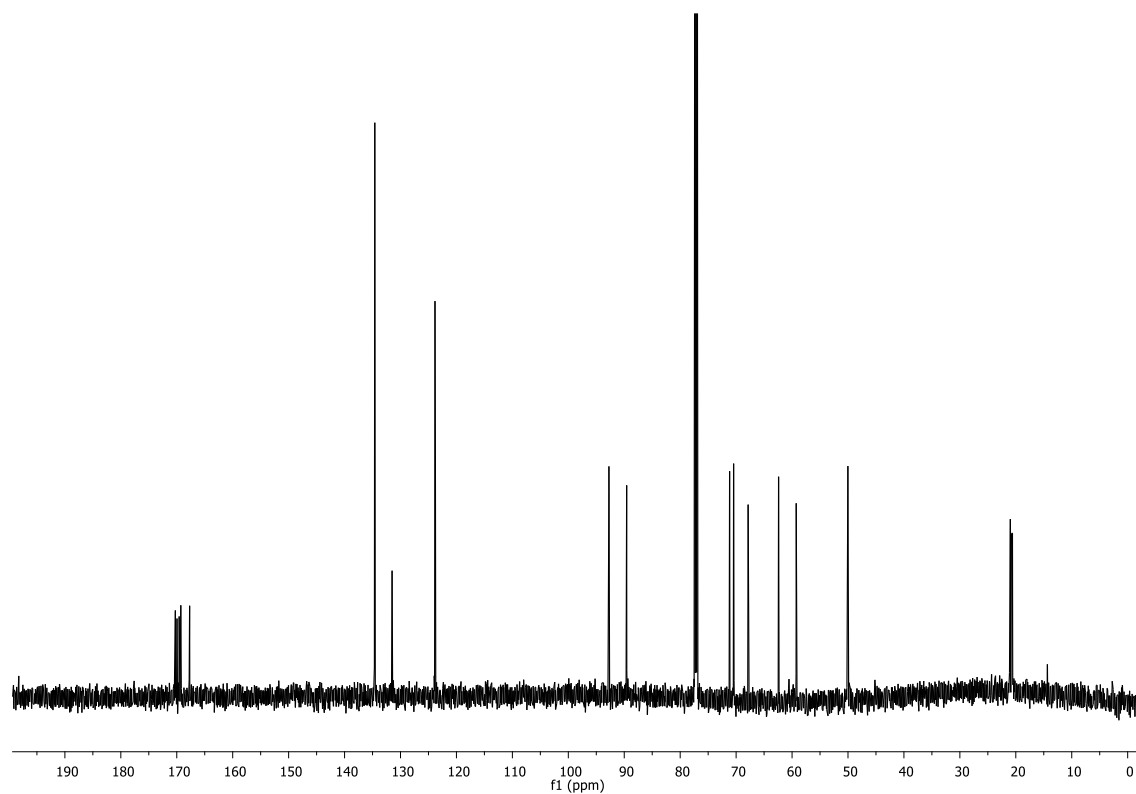
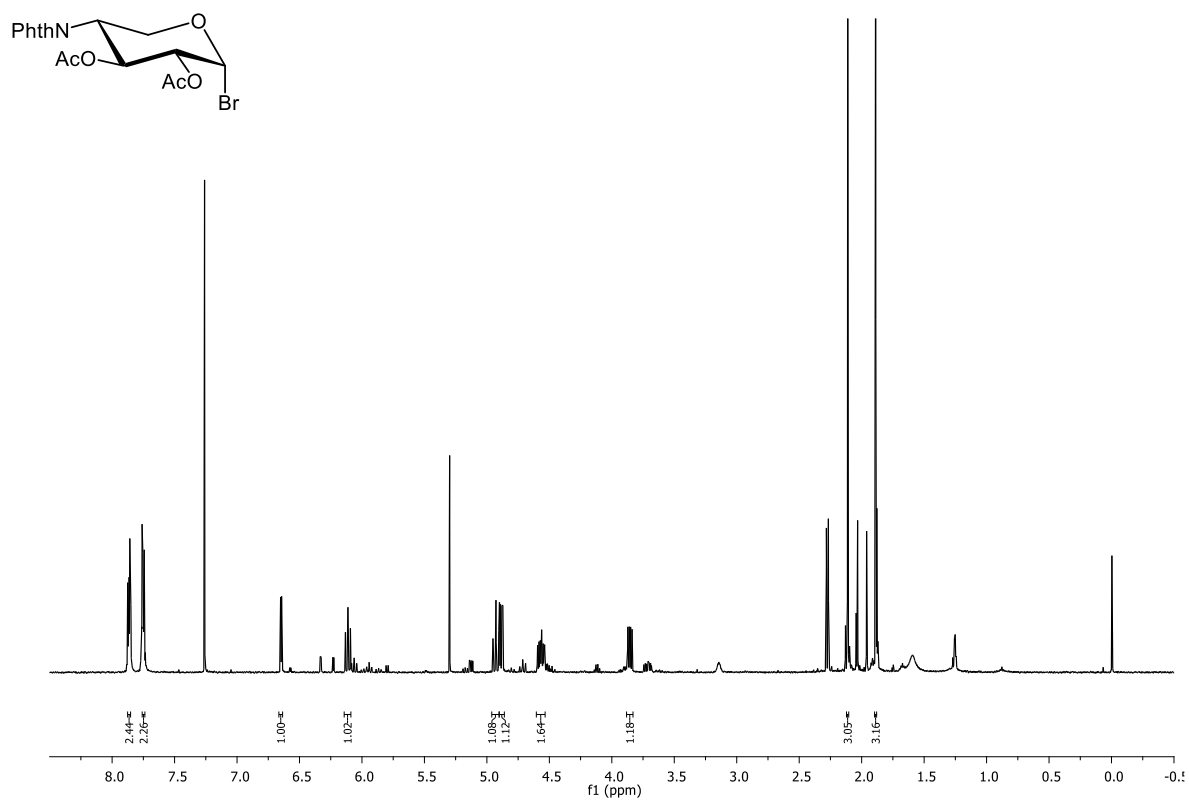
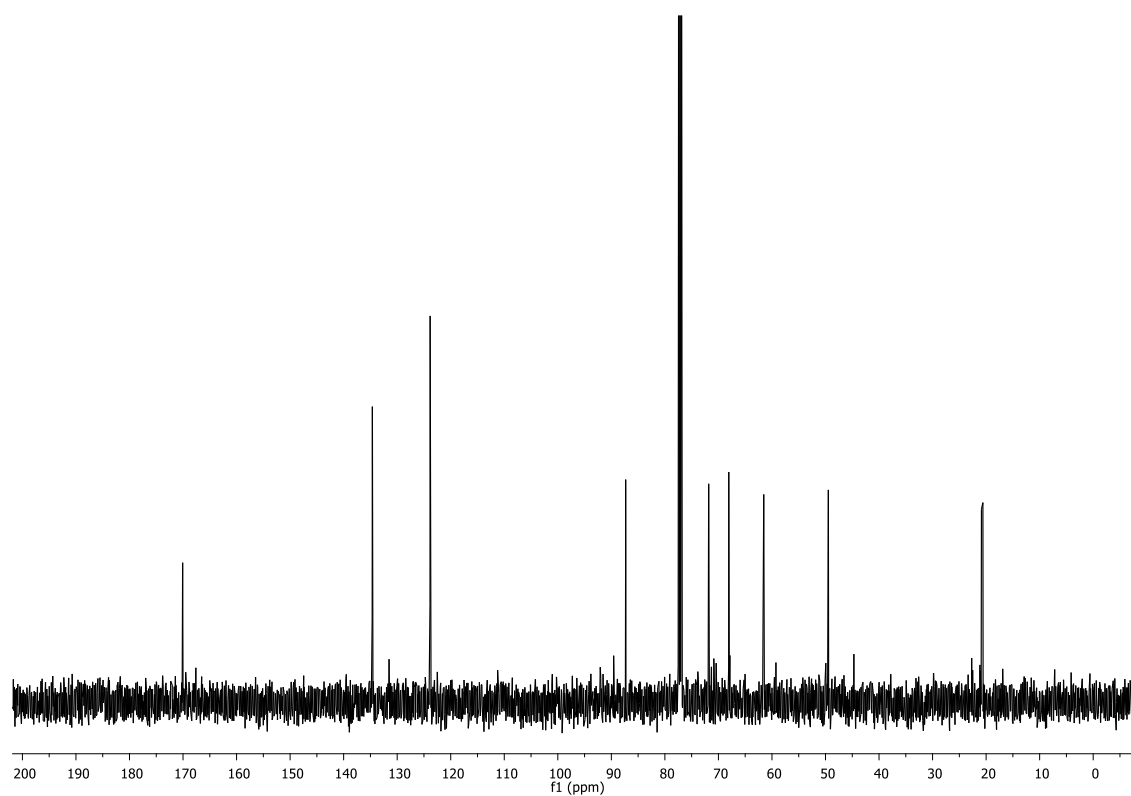


Figure 8.58. <sup>13</sup>C NMR spectrum of **131** (125 MHz, CDCl<sub>3</sub>, 298 K).

## Experimental section



**Figure 8.59.** <sup>1</sup>H NMR spectrum of **132** (500 MHz, CDCl<sub>3</sub>, 298 K). Impurities due to hydrolysis in CDCl<sub>3</sub>.



**Figure 8.60.** <sup>13</sup>C NMR spectrum of **132** (125 MHz, CDCl<sub>3</sub>, 298 K).

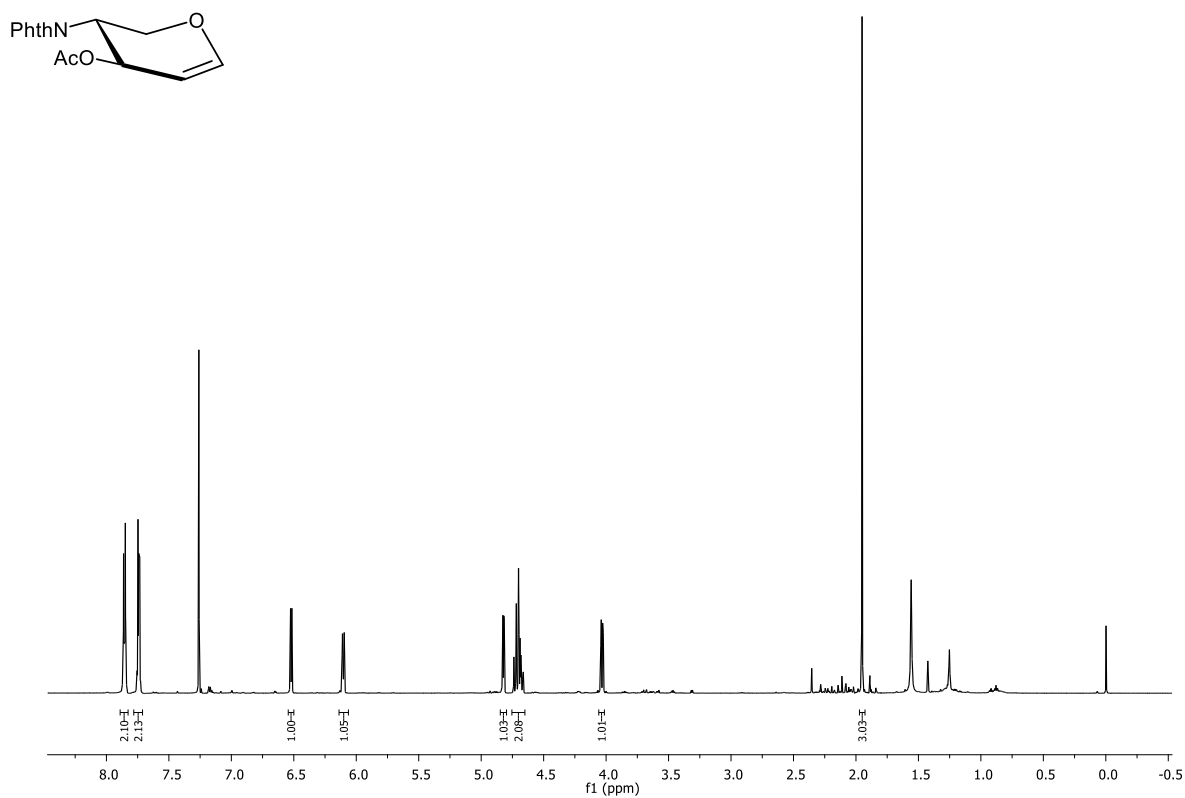


**Figure 8.61.** <sup>1</sup>H NMR spectrum of **133** (500 MHz, CDCl<sub>3</sub>, 298 K).

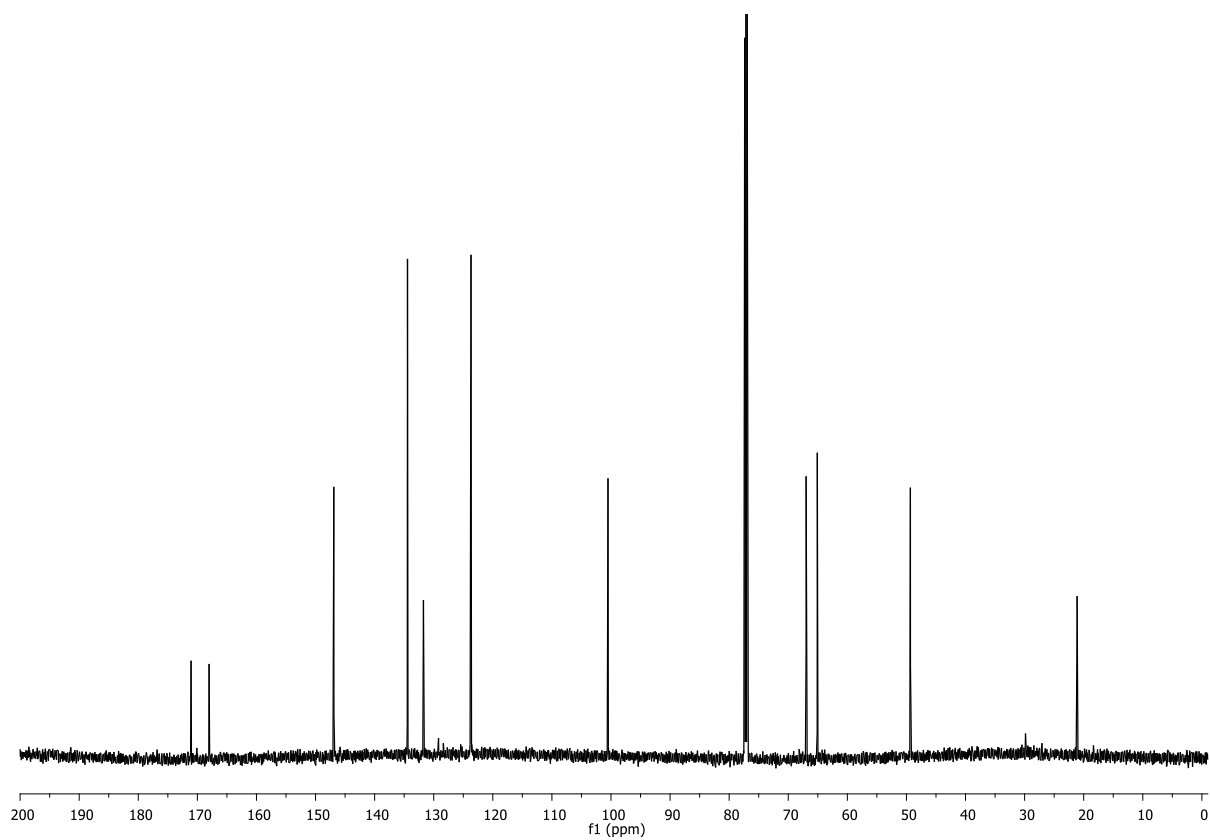


**Figure 8.62.** <sup>13</sup>C NMR spectrum of **133** (125 MHz, CDCl<sub>3</sub>, 298 K).

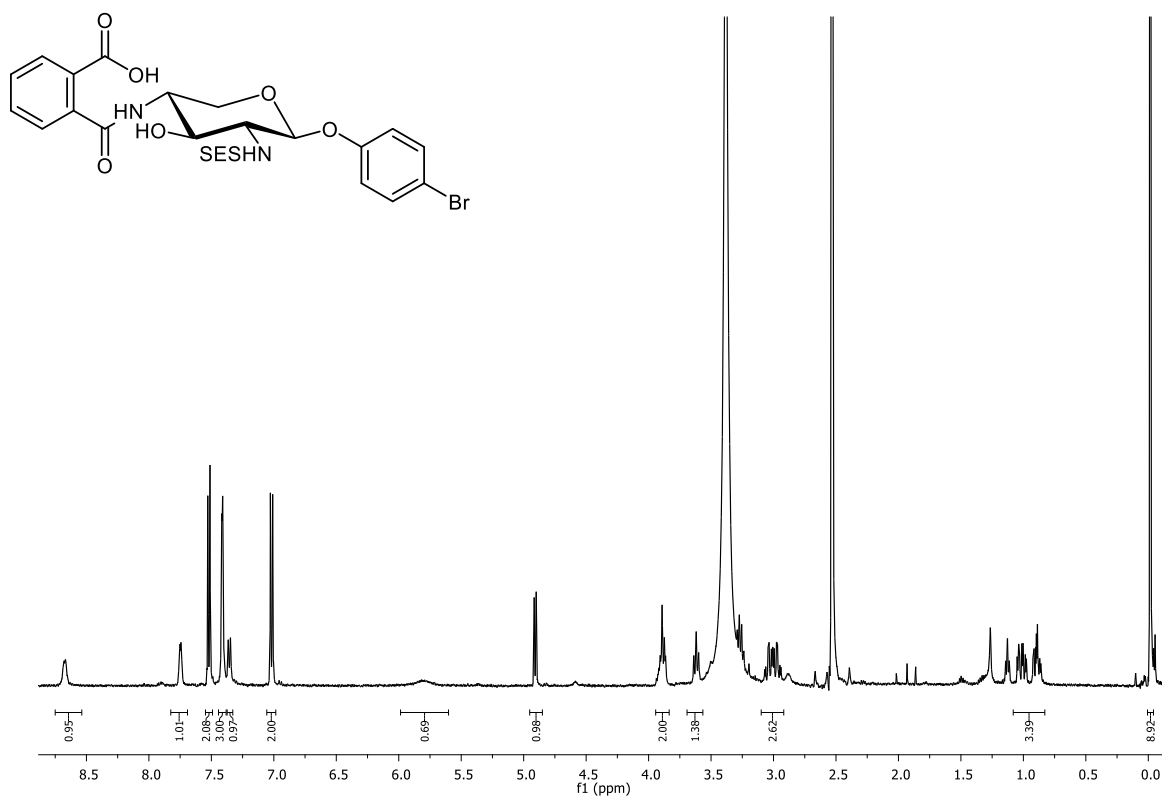


**Figure 8.63.**  $^1\text{H}$  NMR spectrum of **145** (500 MHz, DMSO- $d_6$ , 298 K).

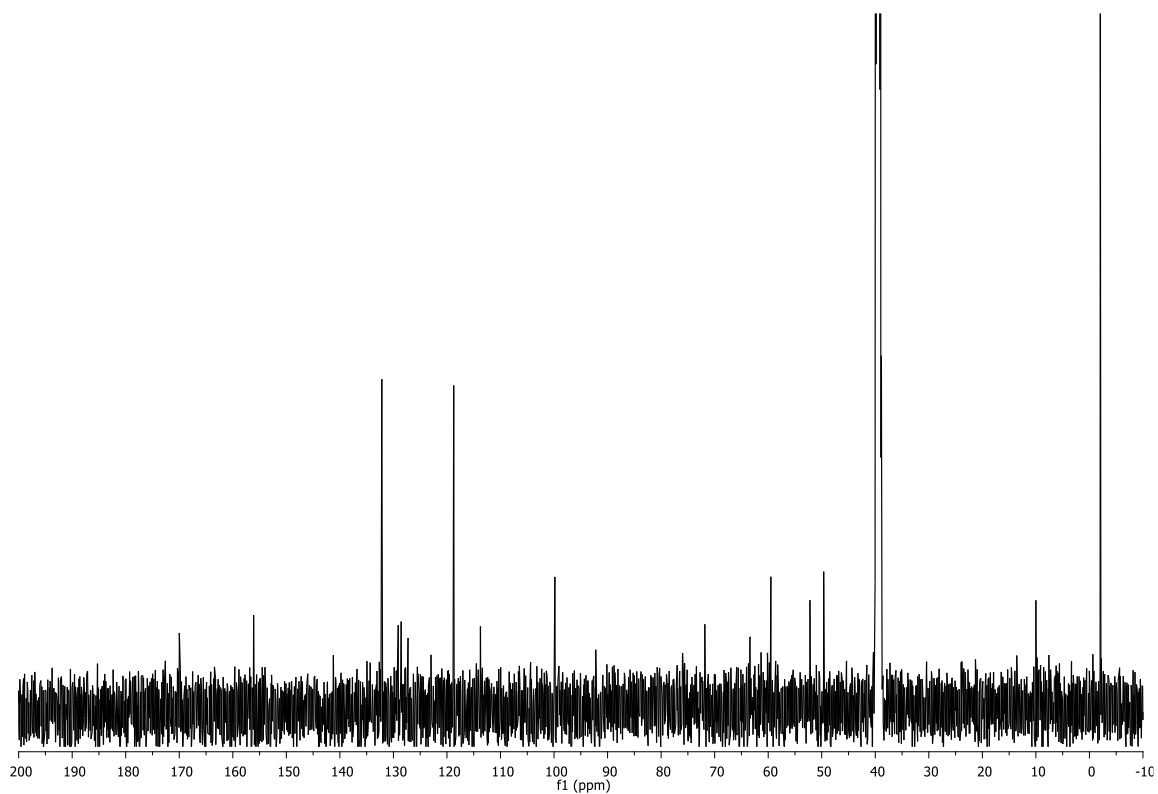


**Figure 8.64.**  $^{13}\text{C}$  NMR spectrum of **145** (125 MHz, DMSO- $d_6$ , 298 K).

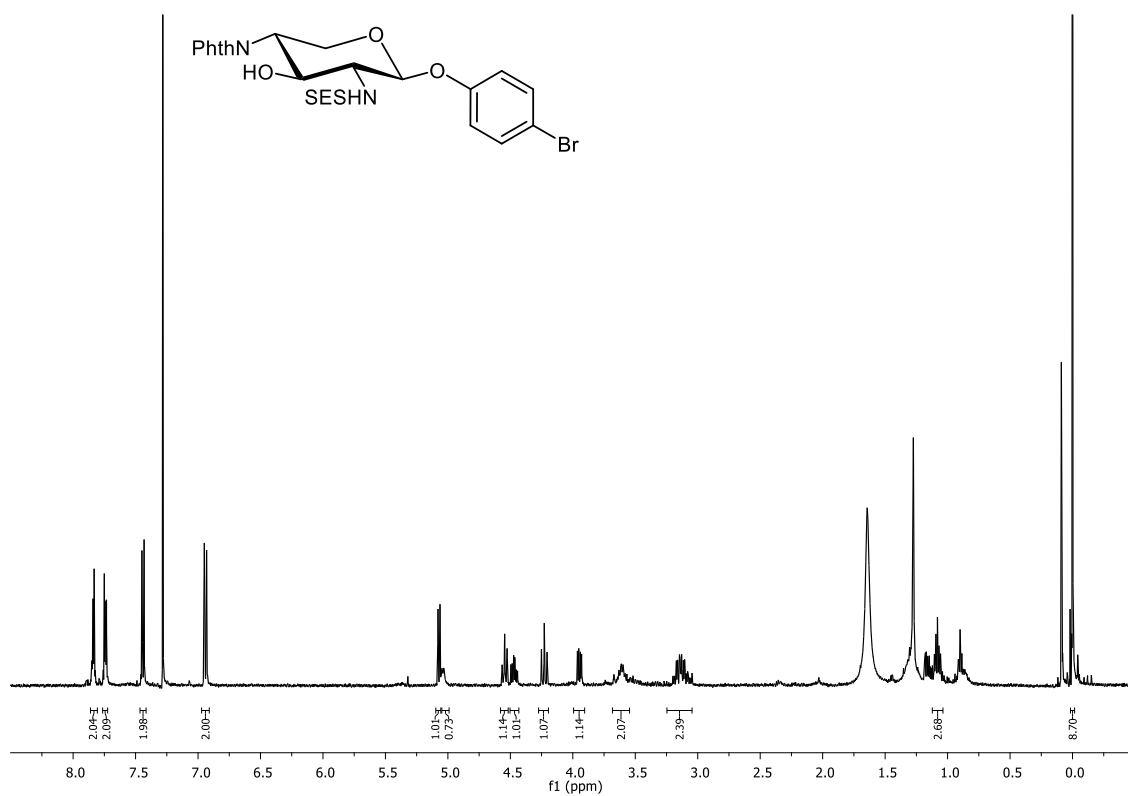


Figure 8.65.  $^1\text{H}$  NMR spectrum of **146** (500 MHz,  $\text{CDCl}_3$ , 298 K).

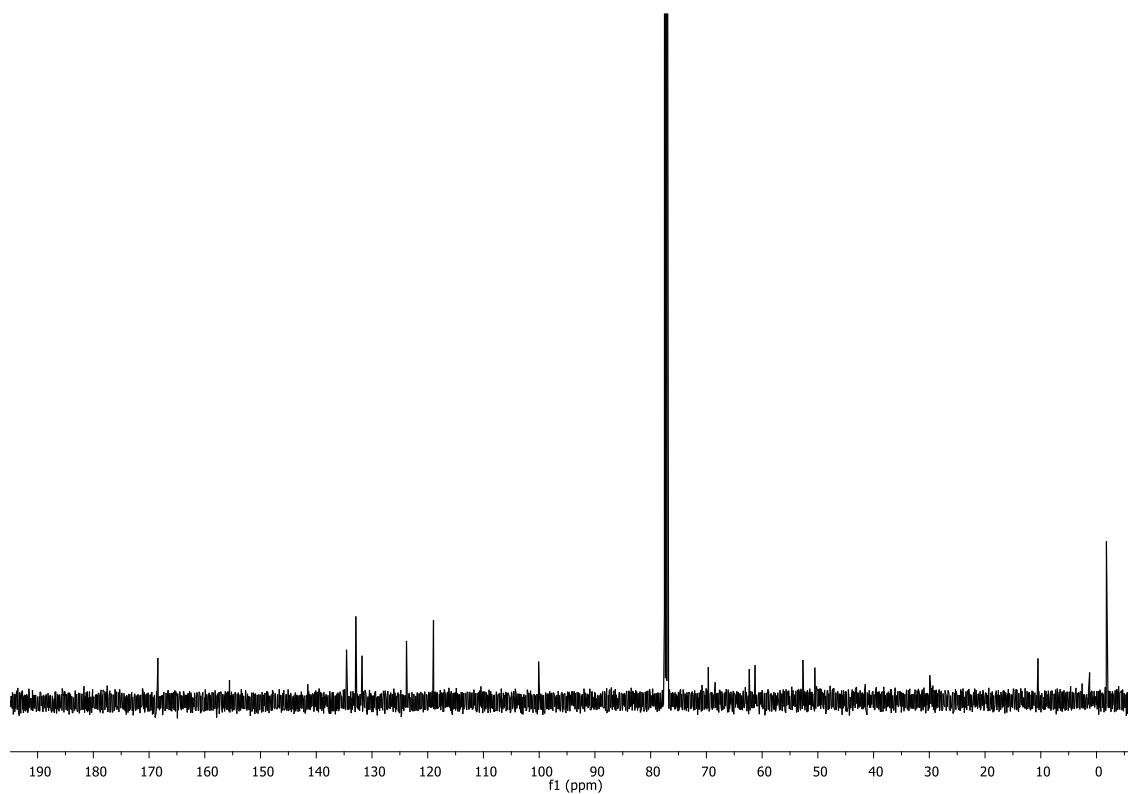


Figure 8.66.  $^{13}\text{C}$  NMR spectrum of **146** (125 MHz,  $\text{CDCl}_3$ , 298 K).

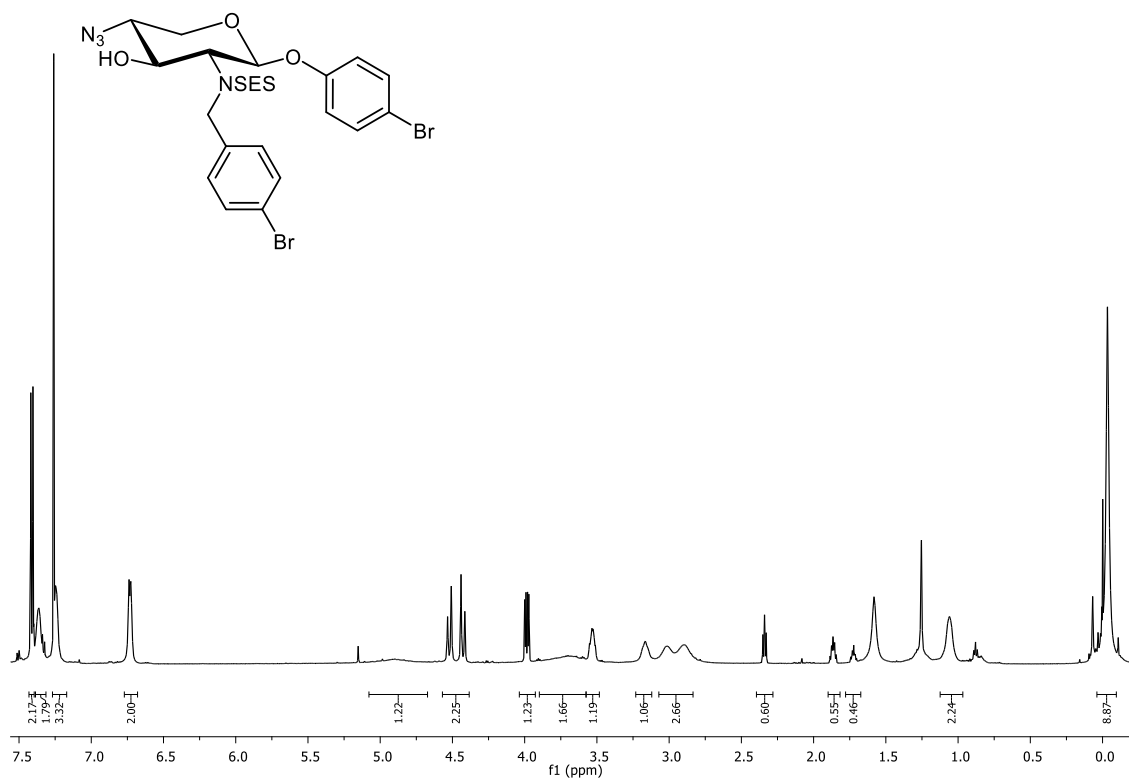


Figure 8.67.  $^1\text{H}$  NMR spectrum of **160** (600 MHz,  $\text{CDCl}_3$ , 298 K).

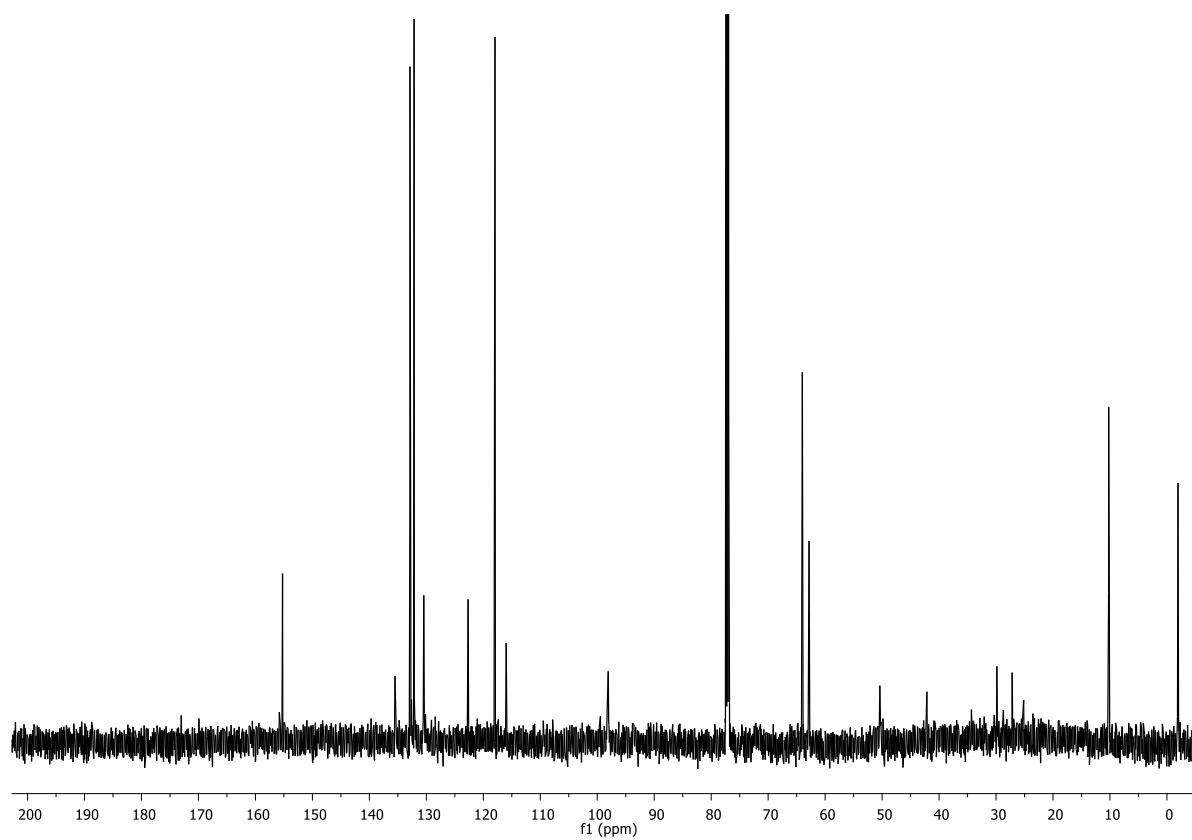
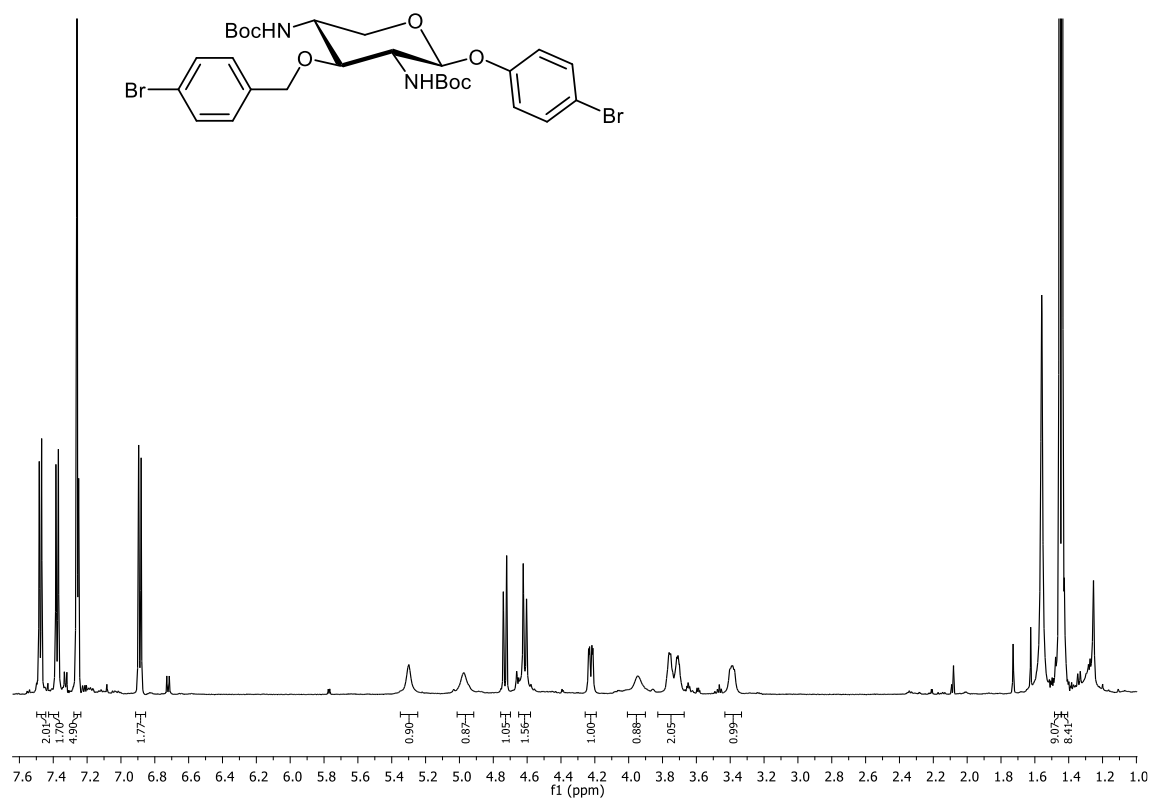
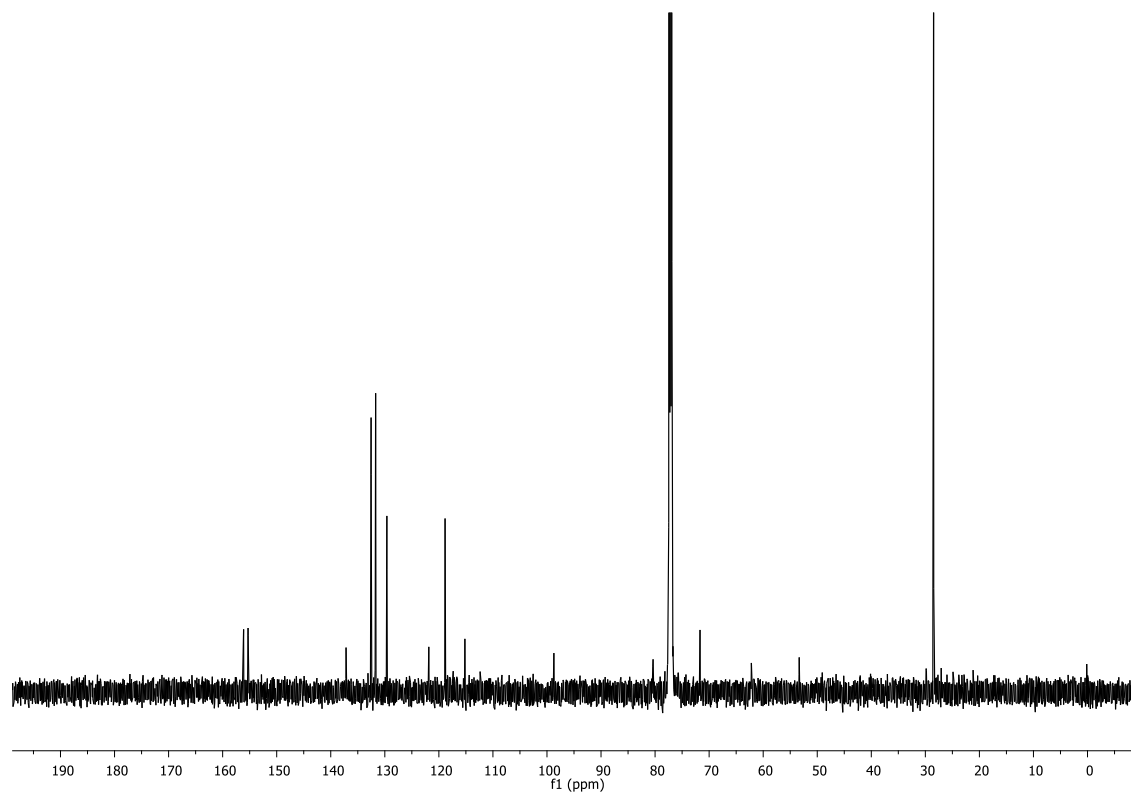


Figure 8.68.  $^{13}\text{C}$  NMR spectrum of **160** (125 MHz,  $\text{CDCl}_3$ , 298 K).



**Figure 8.69.** <sup>1</sup>H NMR spectrum of **165** (600 MHz, CDCl<sub>3</sub>, 298 K). Signal broadening is due to conformational equilibrium.



**Figure 8.70.** <sup>13</sup>C NMR spectrum of **165** (125 MHz, CDCl<sub>3</sub>, 298 K).

## Experimental section

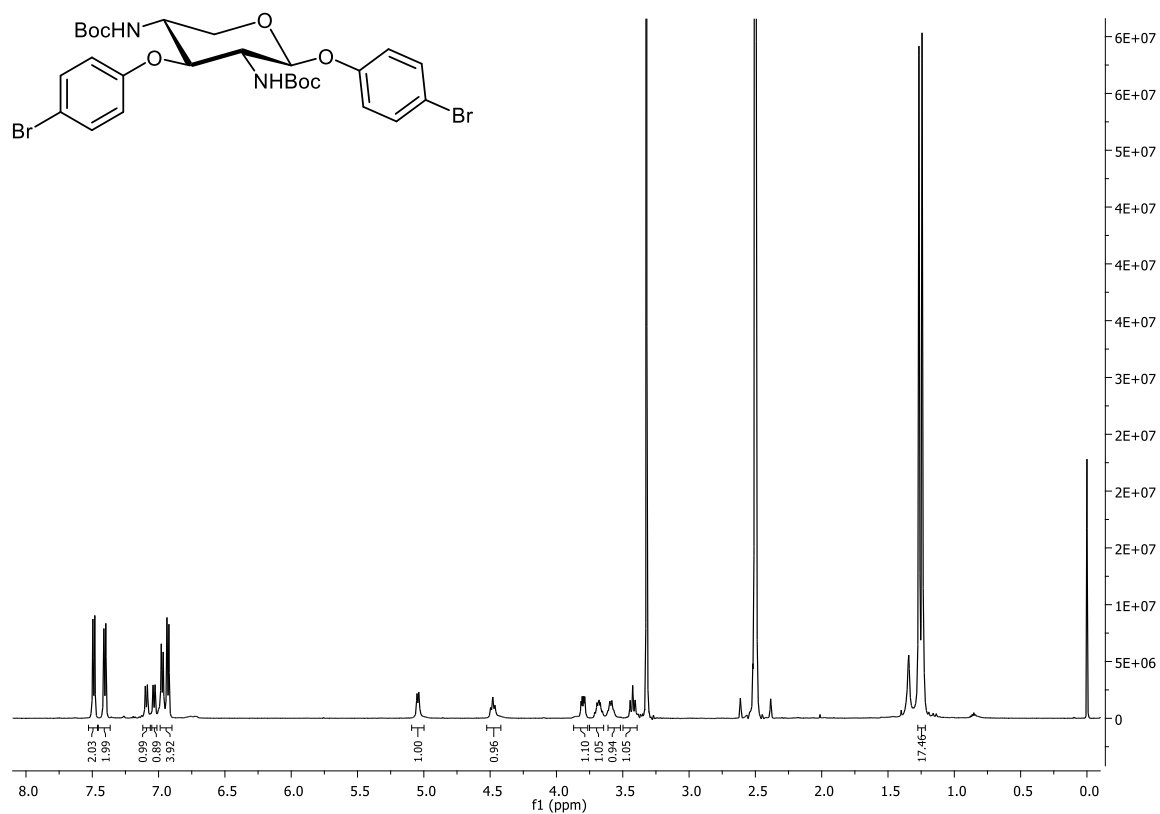


**Figure 8.71.** <sup>1</sup>H NMR spectrum of **166** (500 MHz, DMSO-d<sub>6</sub>, 298 K).

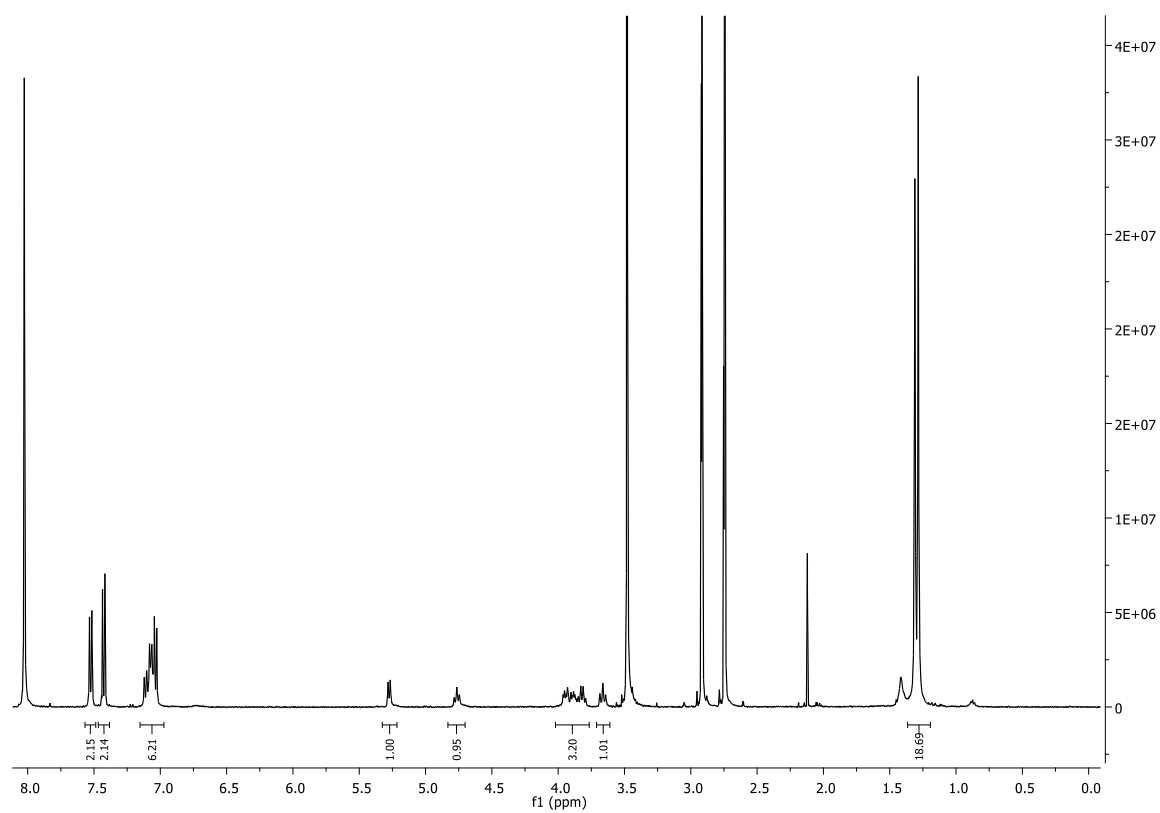


**Figure 8.72.** <sup>1</sup>H NMR spectrum of **166** (500 MHz, DMF-d<sub>7</sub>, 298 K).

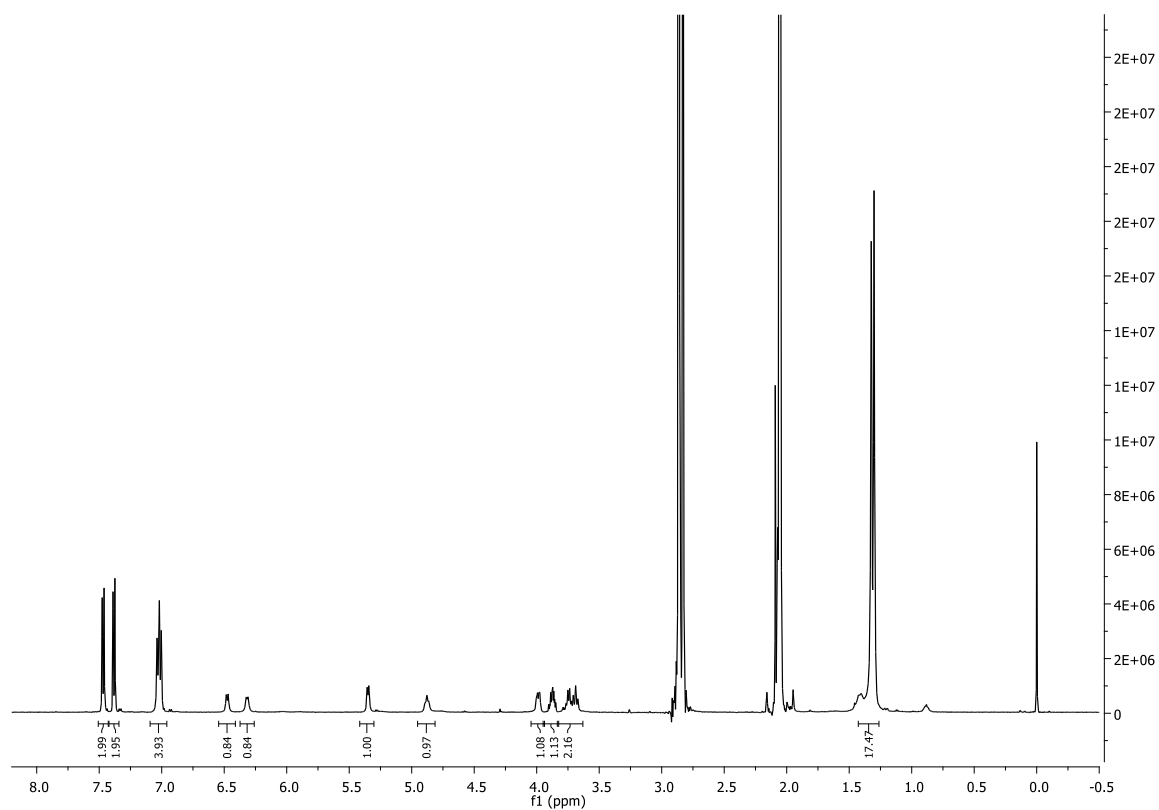


Figure 8.73.  $^1\text{H}$  NMR spectrum of **166** (500 MHz, acetone- $\text{d}_6$ , 298 K).

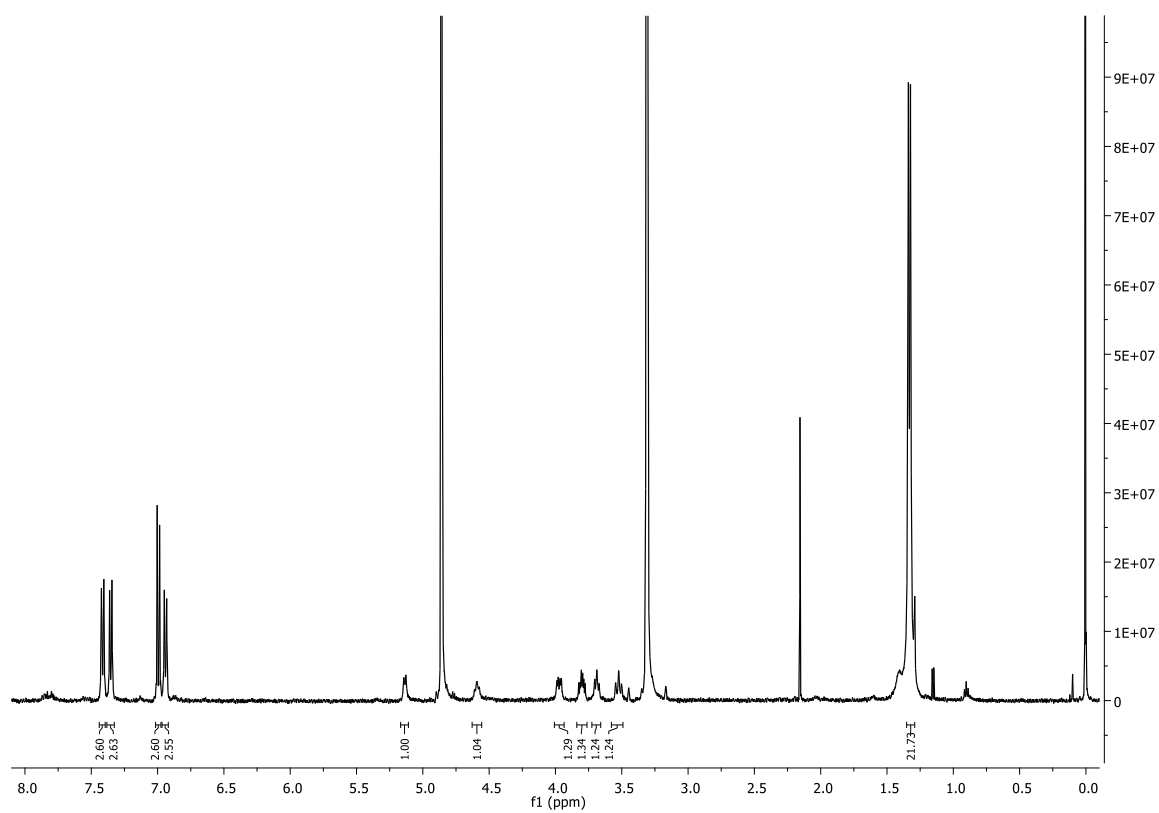


Figure 8.74.  $^1\text{H}$  NMR spectrum of **166** (500 MHz, MeOD- $\text{d}_4$ , 298 K).

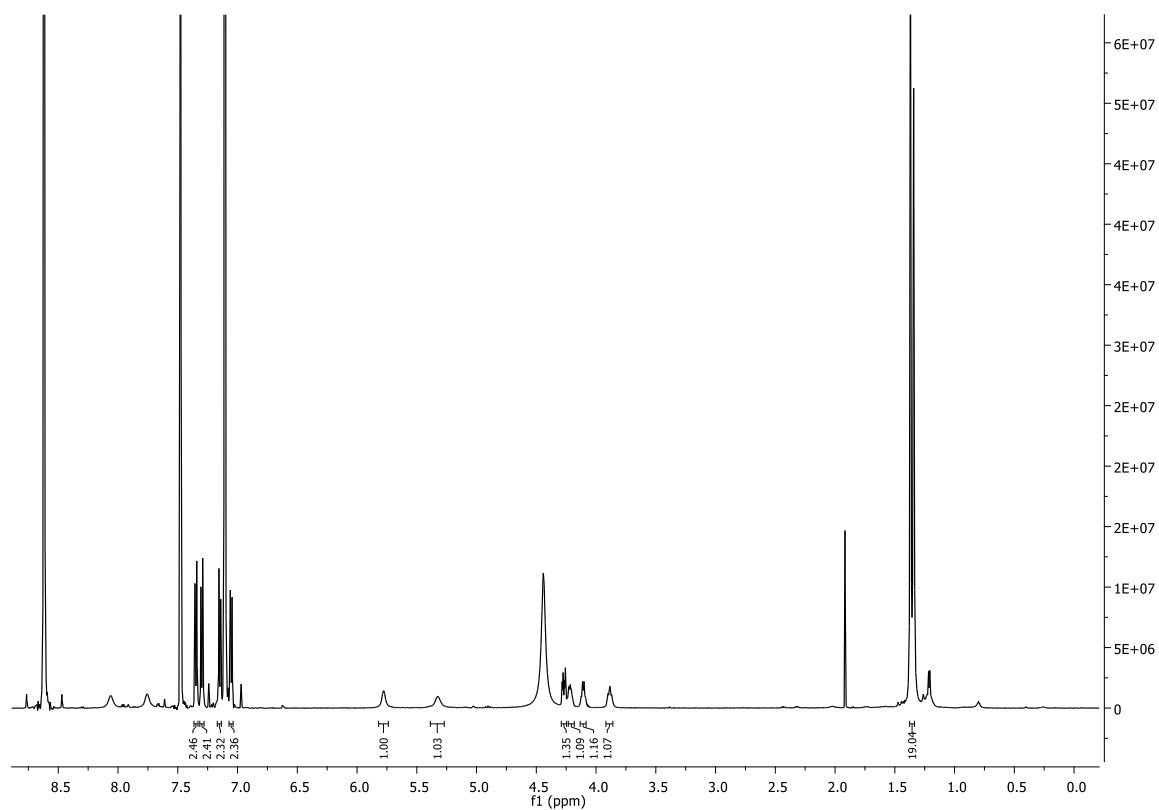


Figure 8.75.  $^1\text{H}$  NMR spectrum of **166** (500 MHz, pyridine- $d_5$ , 298 K).

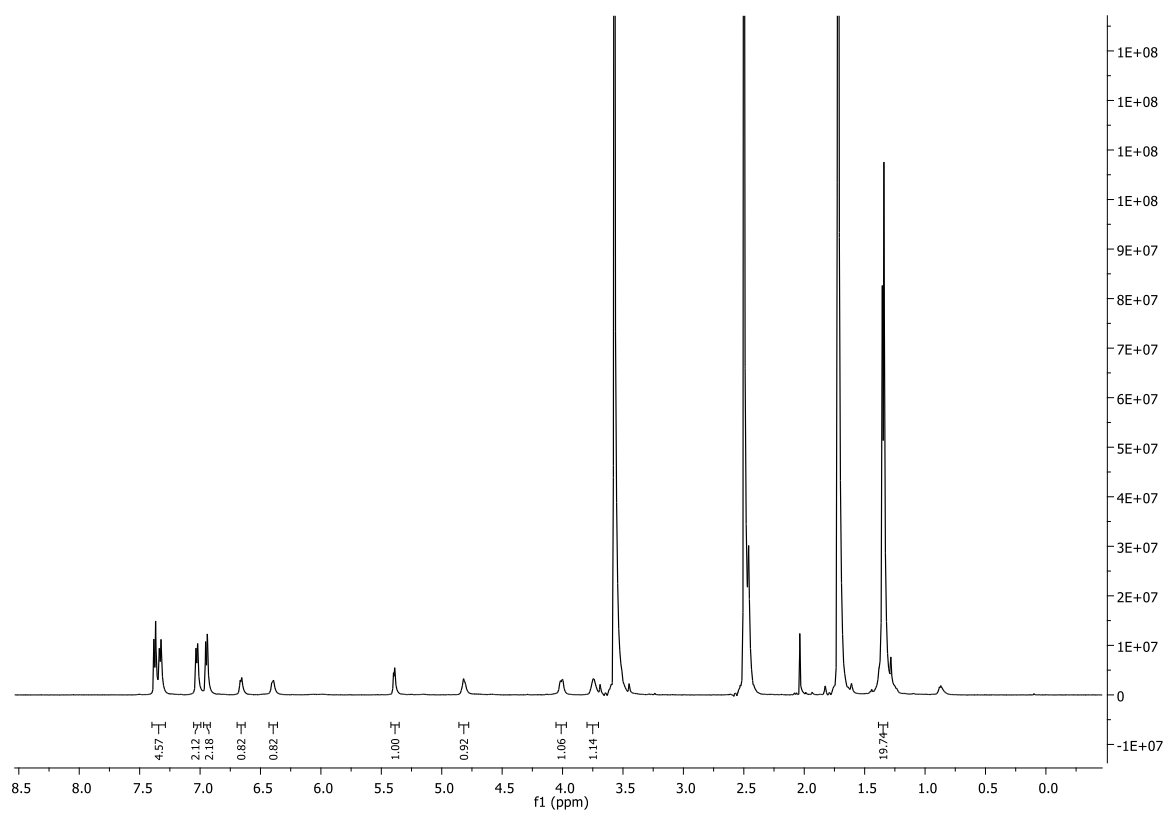


Figure 8.76.  $^1\text{H}$  NMR spectrum of **166** (500 MHz, THF- $d_8$ , 298 K).

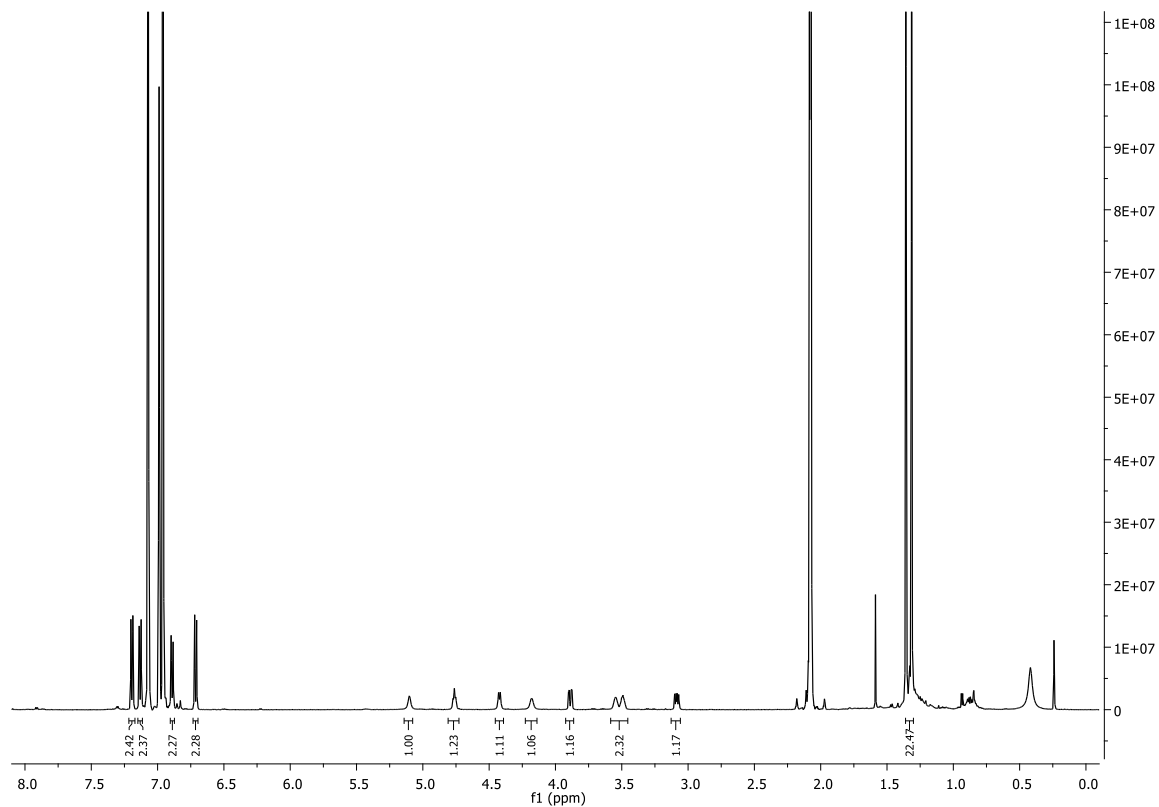


Figure 8.77.  $^1\text{H}$  NMR spectrum of 166 (500 MHz, toluene- $d_8$ , 328 K).

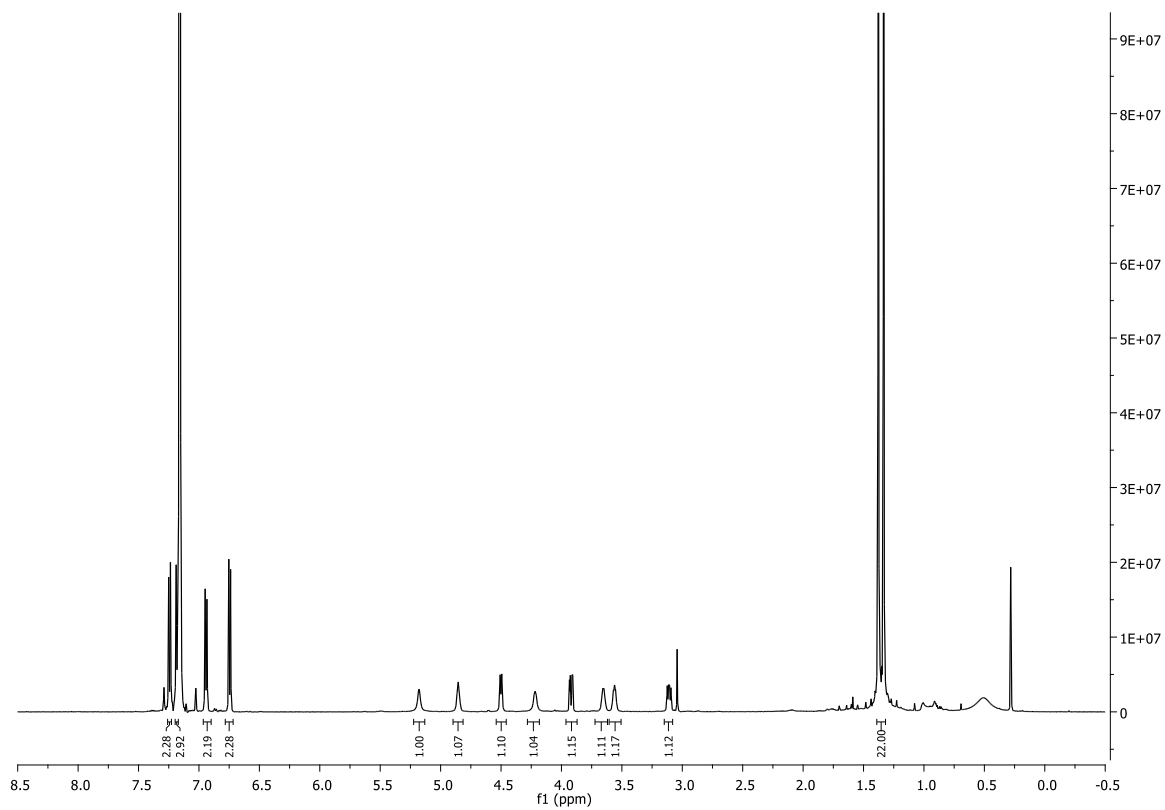


Figure 8.78.  $^1\text{H}$  NMR spectrum of 166 (500 MHz, benzene- $d_6$ , 328 K).

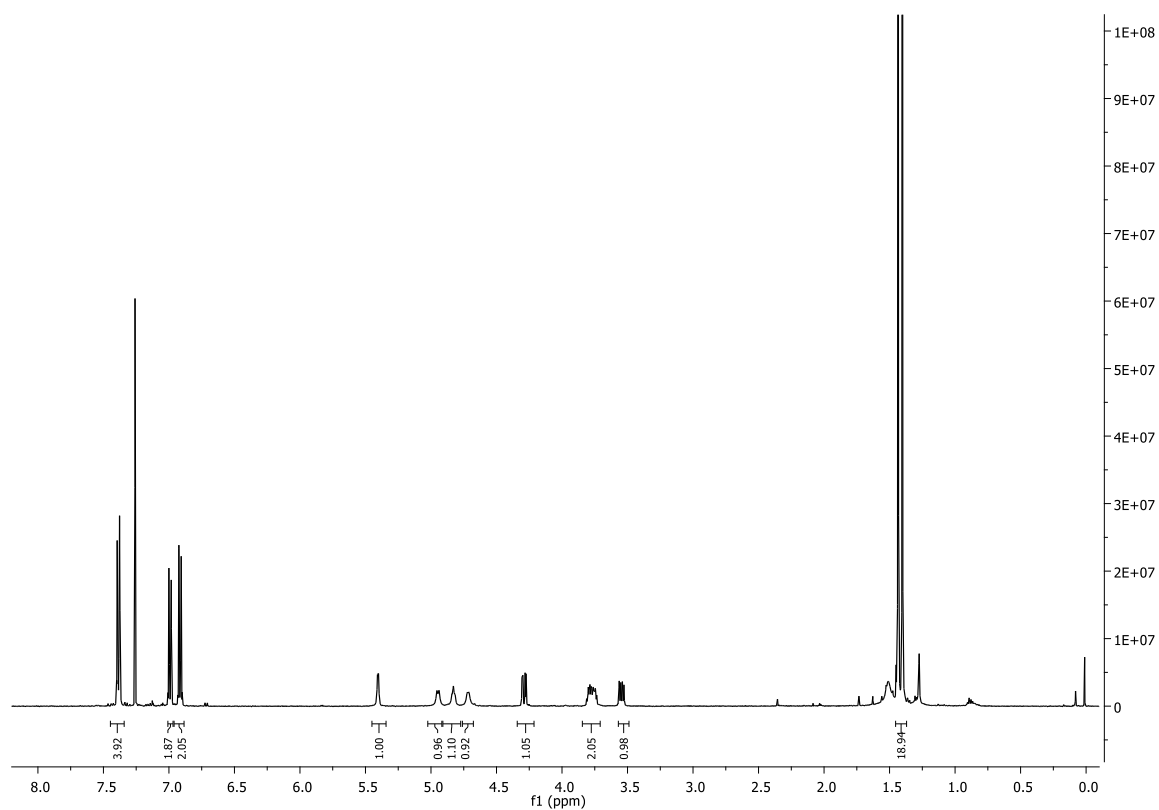


Figure 8.79.  $^1\text{H}$  NMR spectrum of **166** (500 MHz,  $\text{CDCl}_3$ , 328 K).

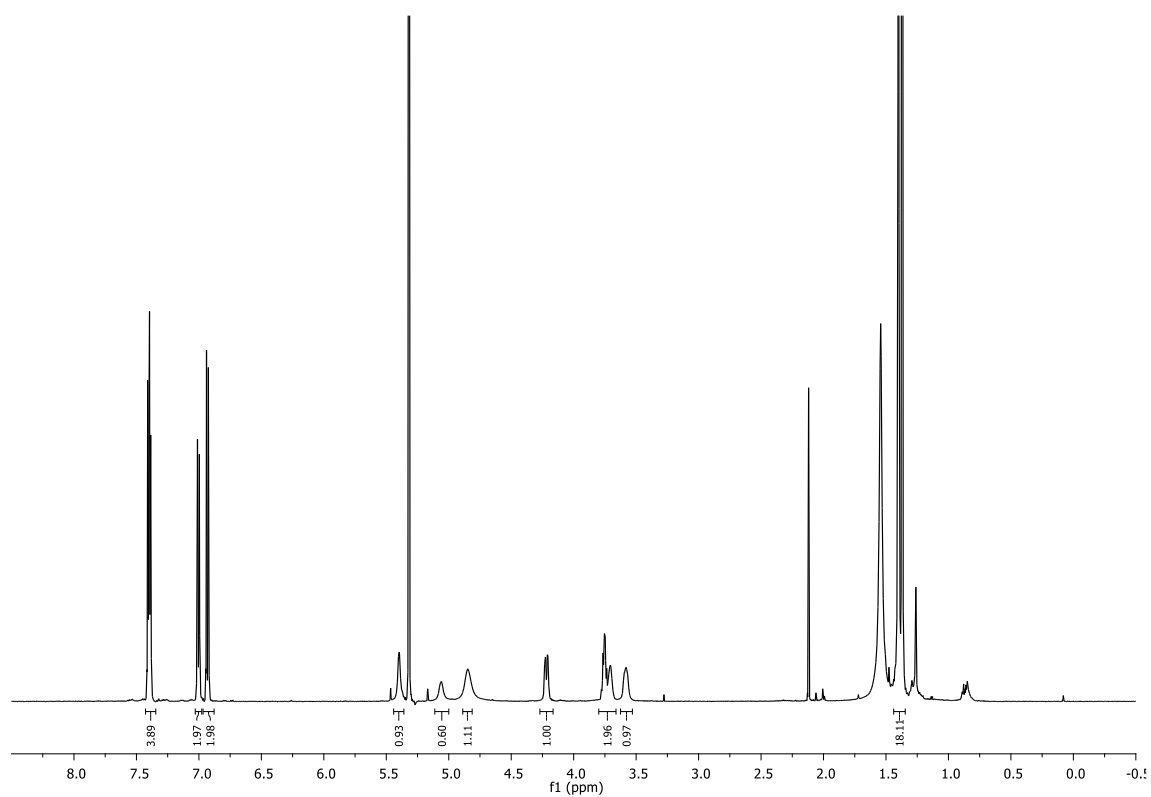


Figure 8.80.  $^1\text{H}$  NMR spectrum of **166** (500 MHz,  $\text{CD}_2\text{Cl}_2$ , 298 K).

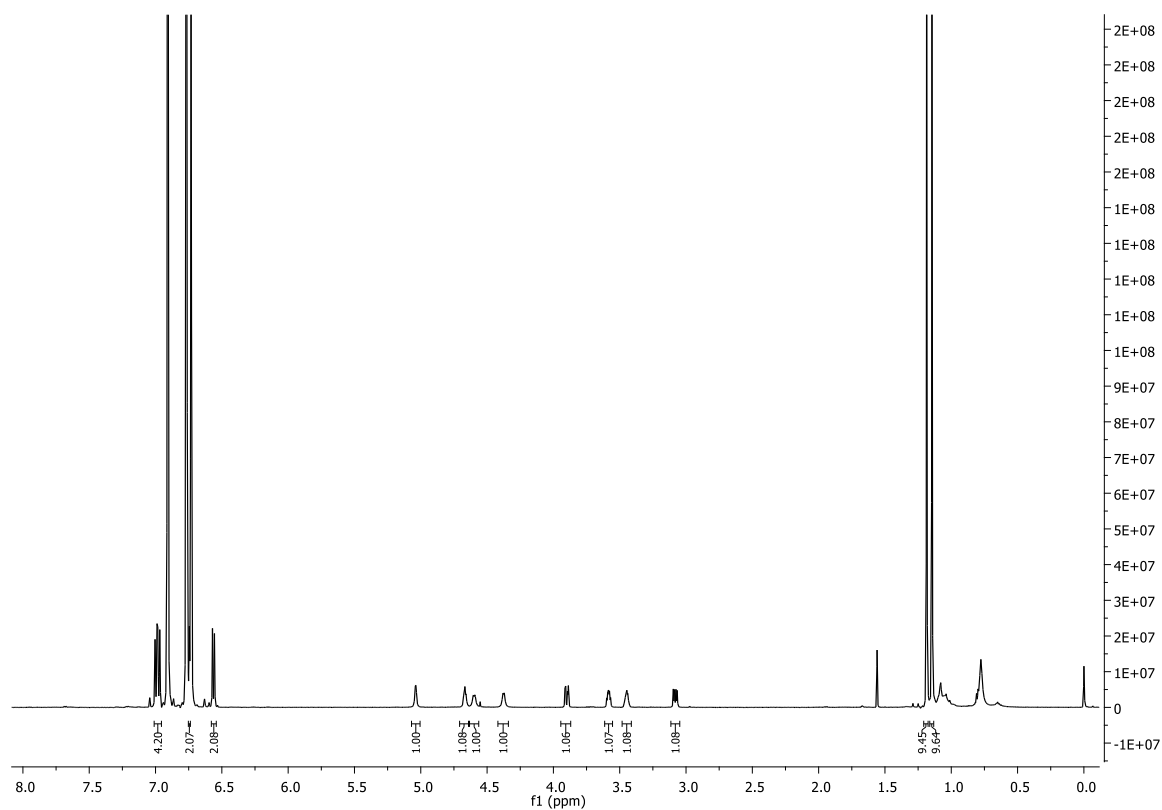


Figure 8.81.  $^1\text{H}$  NMR spectrum of **166** (500 MHz, chlorobenzene- $d_5$ , 328 K).

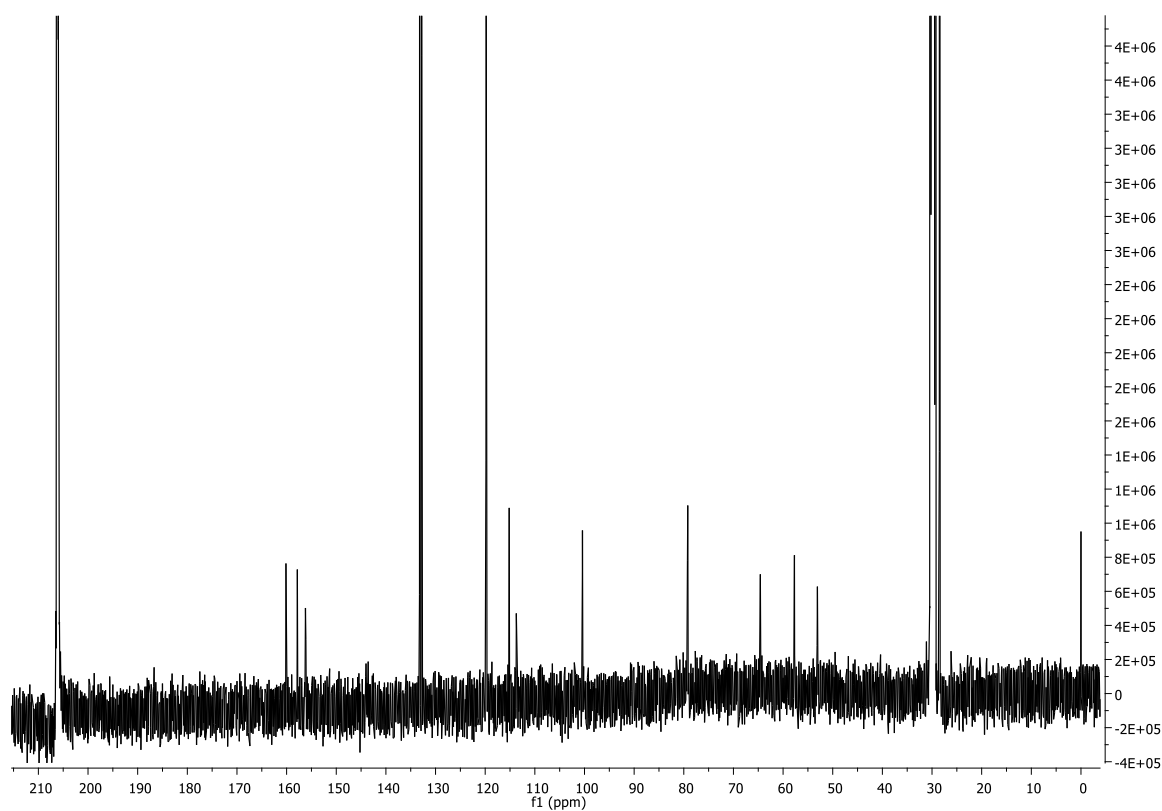


Figure 8.82.  $^{13}\text{C}$  NMR spectrum of **166** (125 MHz, acetone- $d_6$ , 298 K).

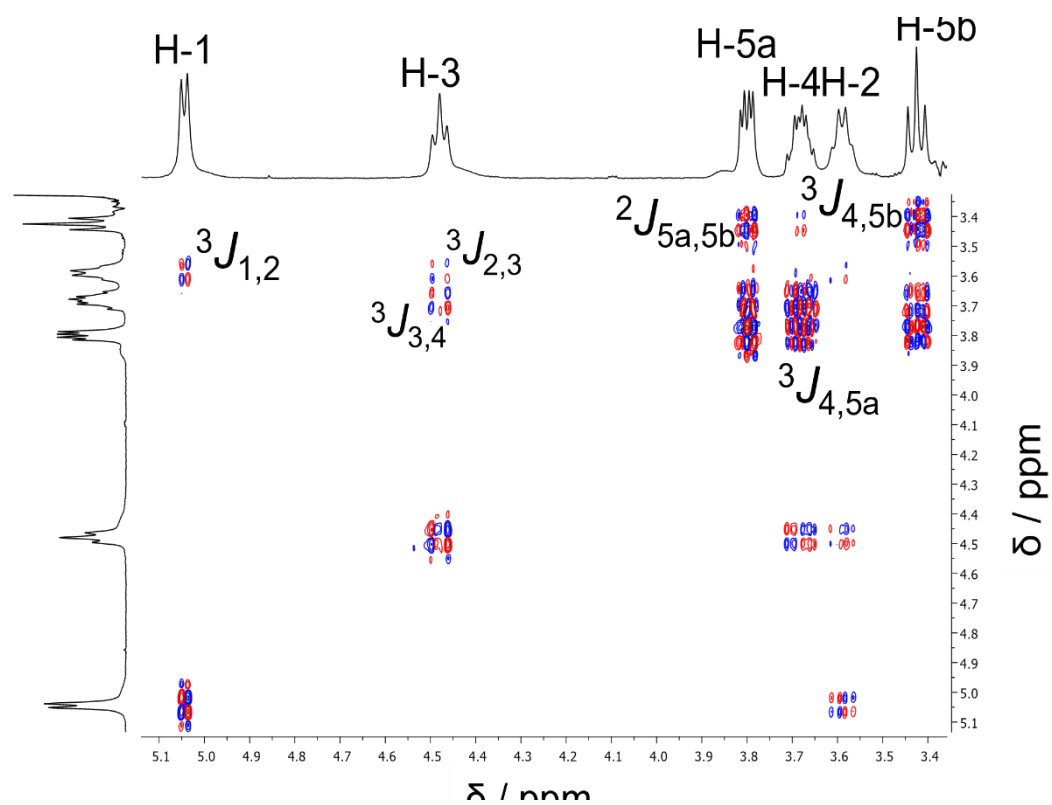


Figure 8.83. COSY-DQF NMR spectrum of **166** (500 MHz, DMSO- $d_6$ , 298 K).

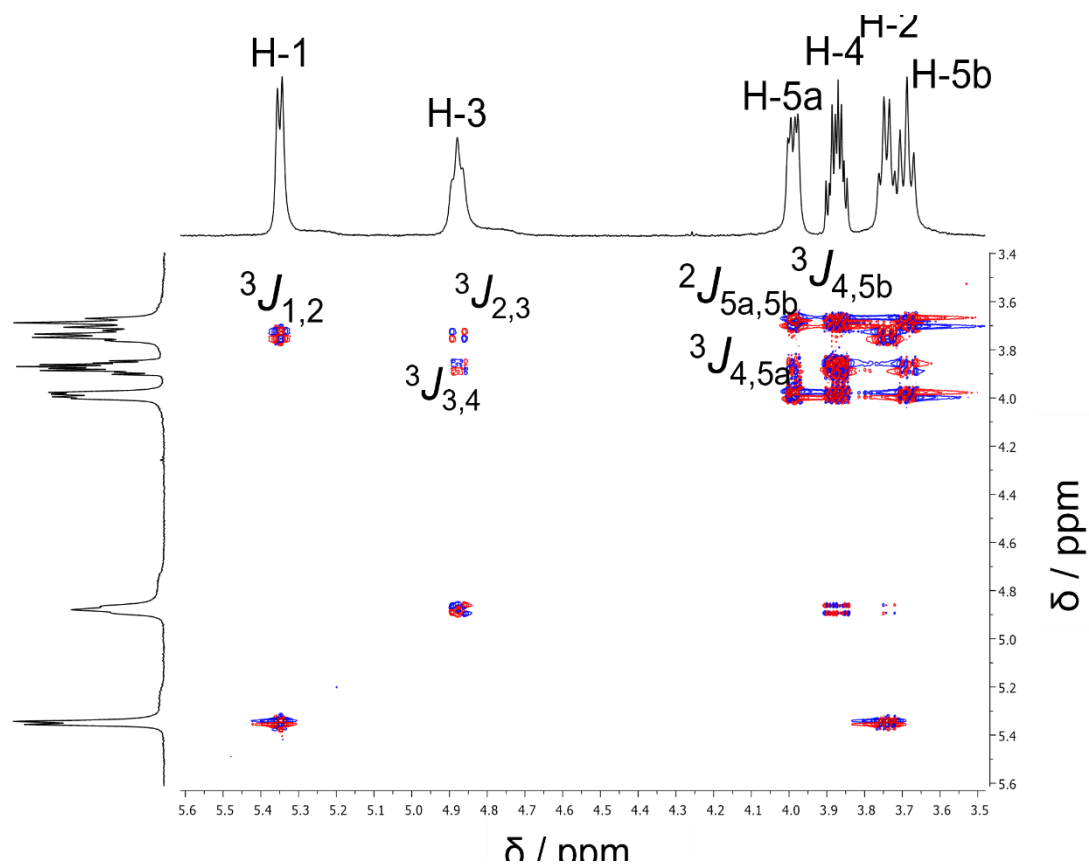


Figure 8.84. COSY-DQF NMR spectrum of **166** (500 MHz, acetone- $d_6$ , 298 K).

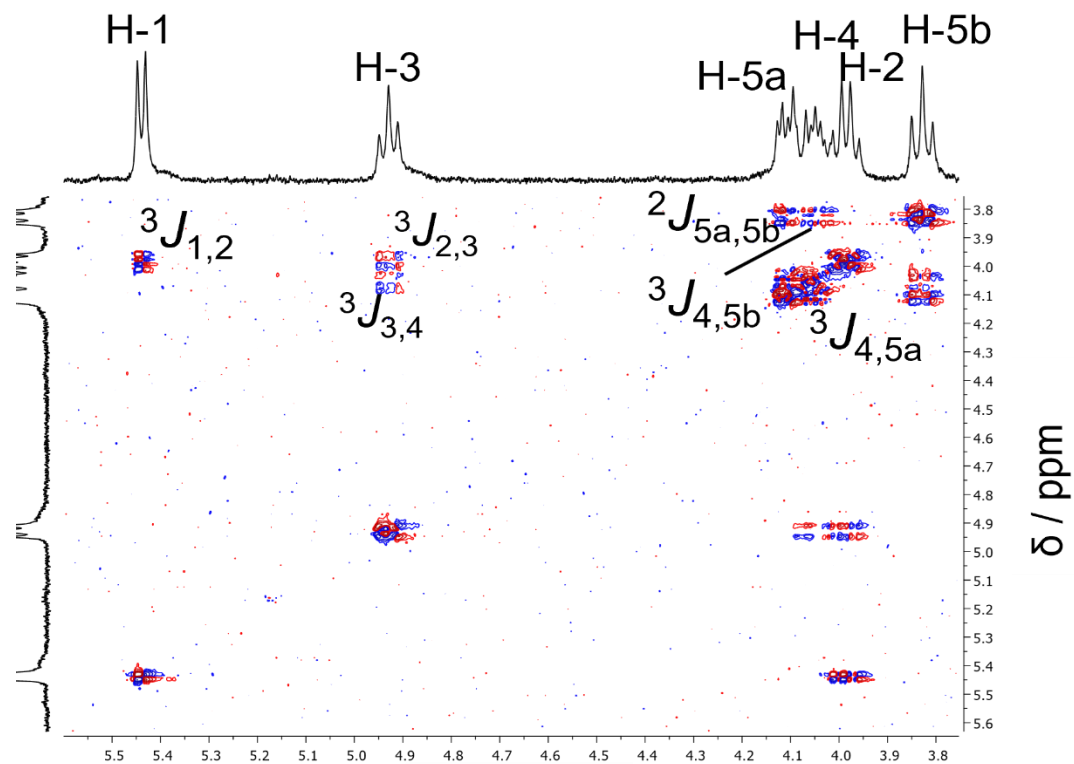


Figure 8.85. COSY-DQF NMR spectrum of **166** (500 MHz, DMF-d<sub>7</sub>, 298 K).

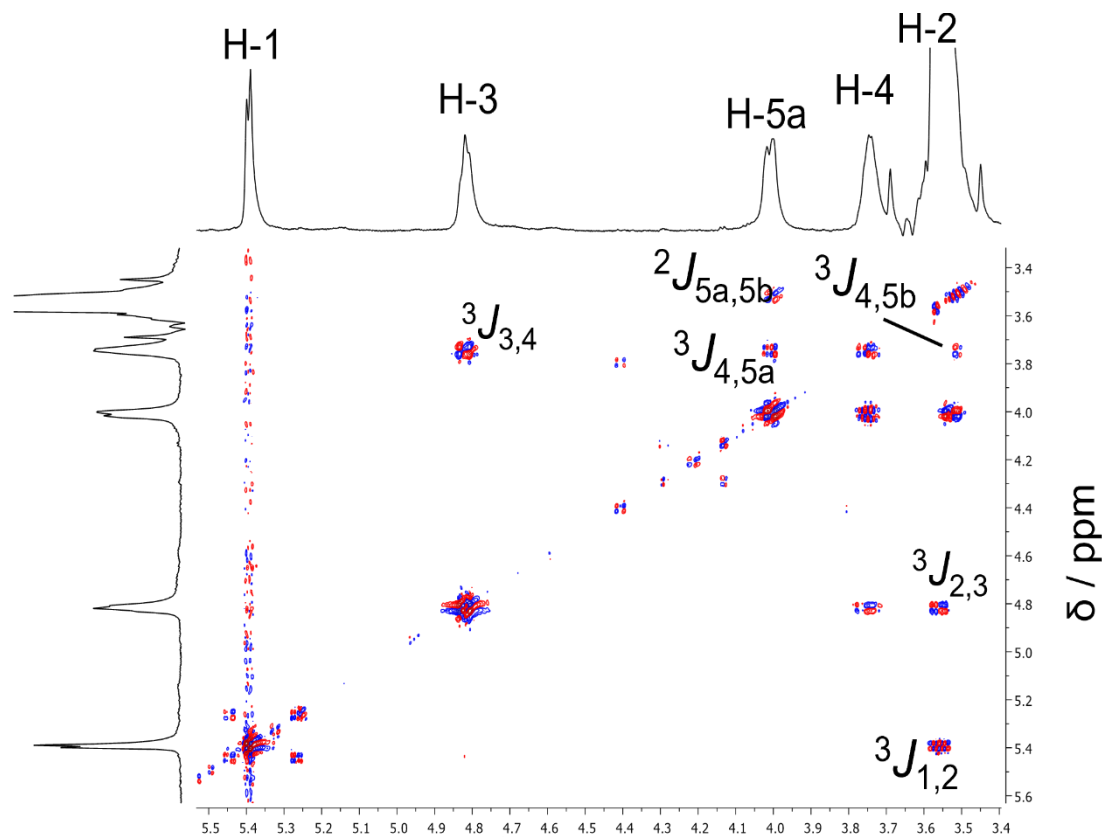


Figure 8.86. COSY-DQF NMR spectrum of **166** (500 MHz, THF-d<sub>8</sub>, 298 K).

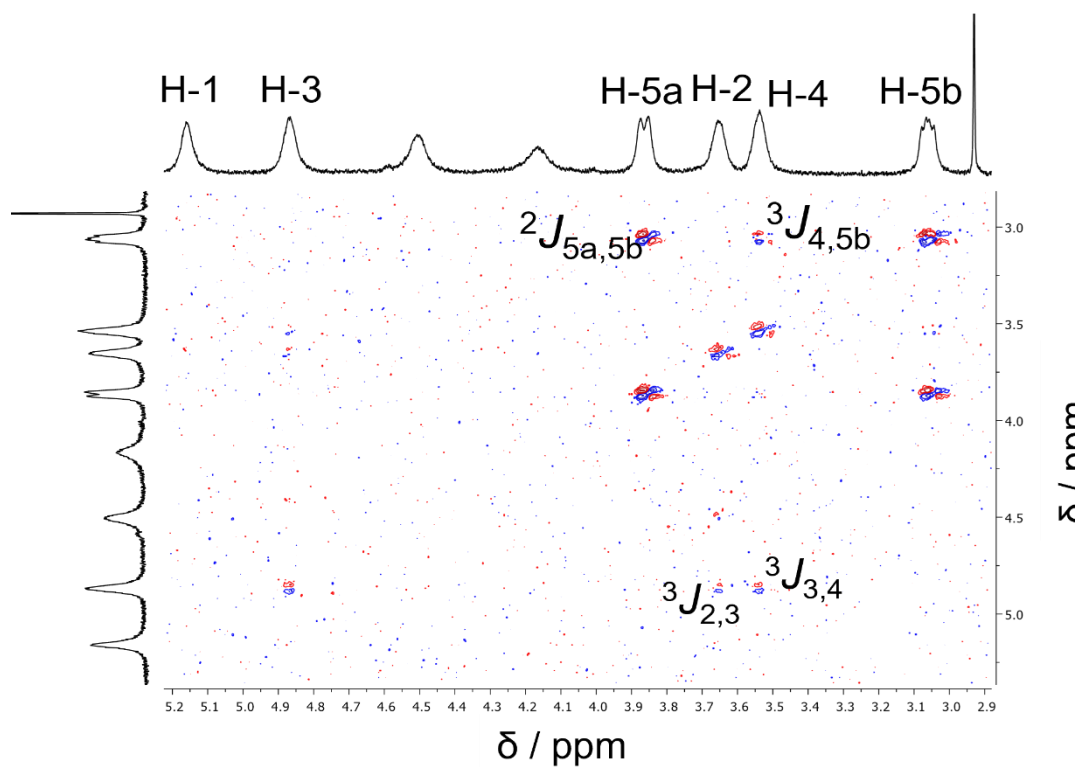


Figure 8.87. COSY-DQF NMR spectrum of **166** (500 MHz, benzene- $d_6$ , 298 K).

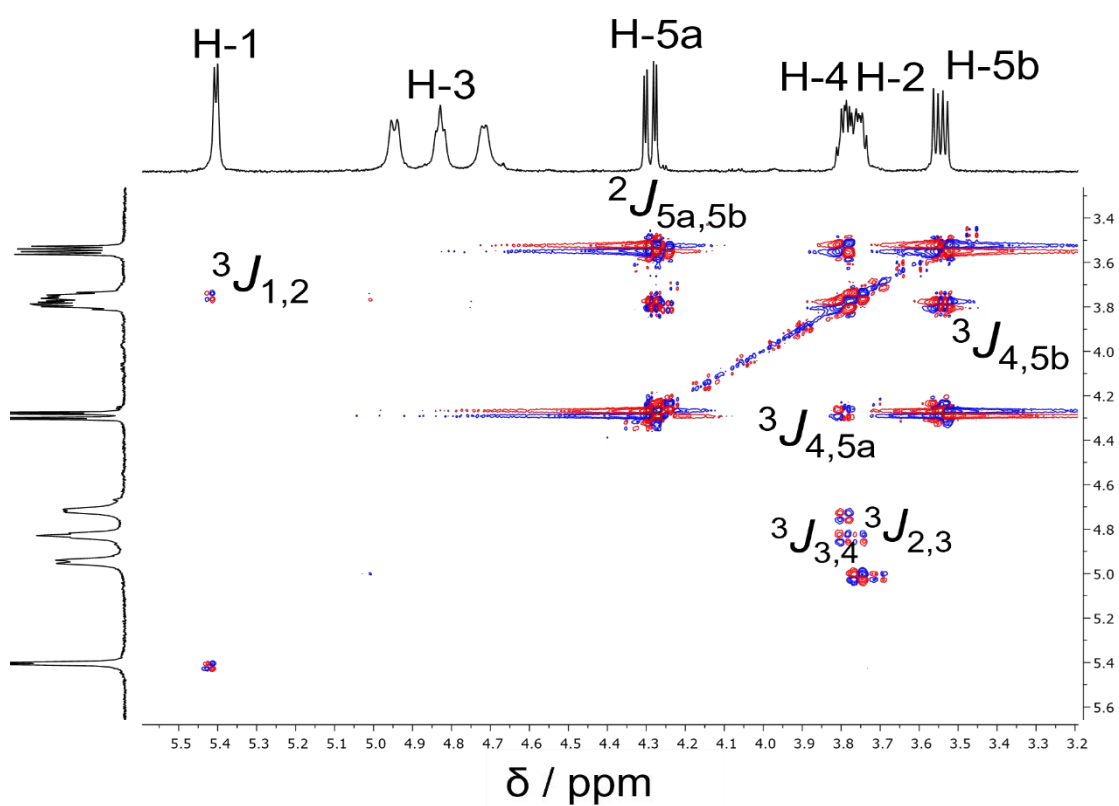


Figure 8.88. COSY-DQF NMR spectrum of **166** (500 MHz,  $CDCl_3$ , 298 K).

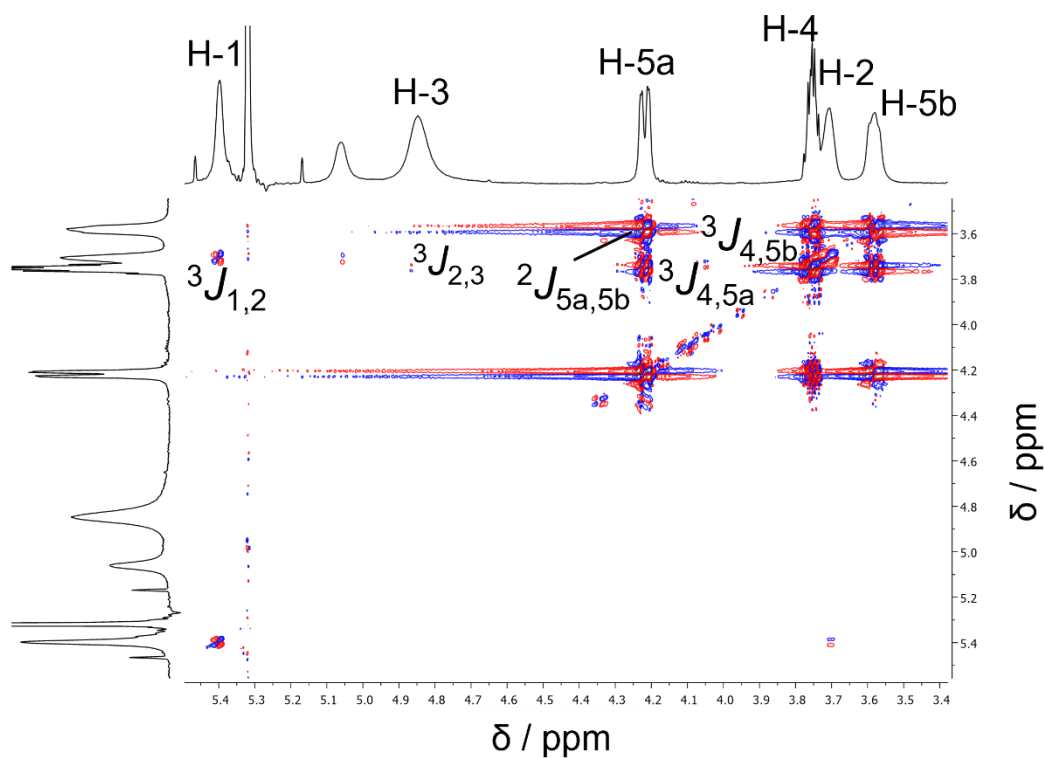


Figure 8.89. COSY-DQF NMR spectrum of **166** (500 MHz,  $\text{CD}_2\text{Cl}_2$ , 298 K).

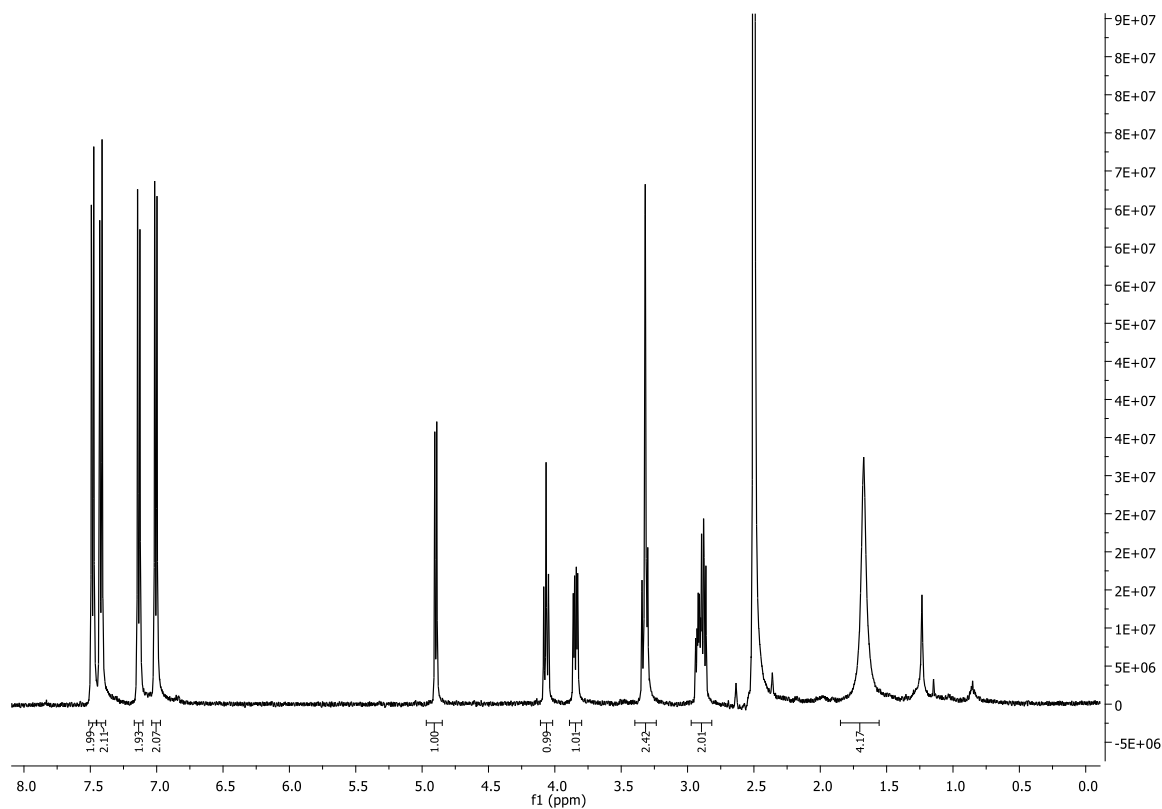


Figure 8.90.  $^1\text{H}$  NMR spectrum of **167** (500 MHz,  $\text{DMSO-d}_6$ , 298 K).

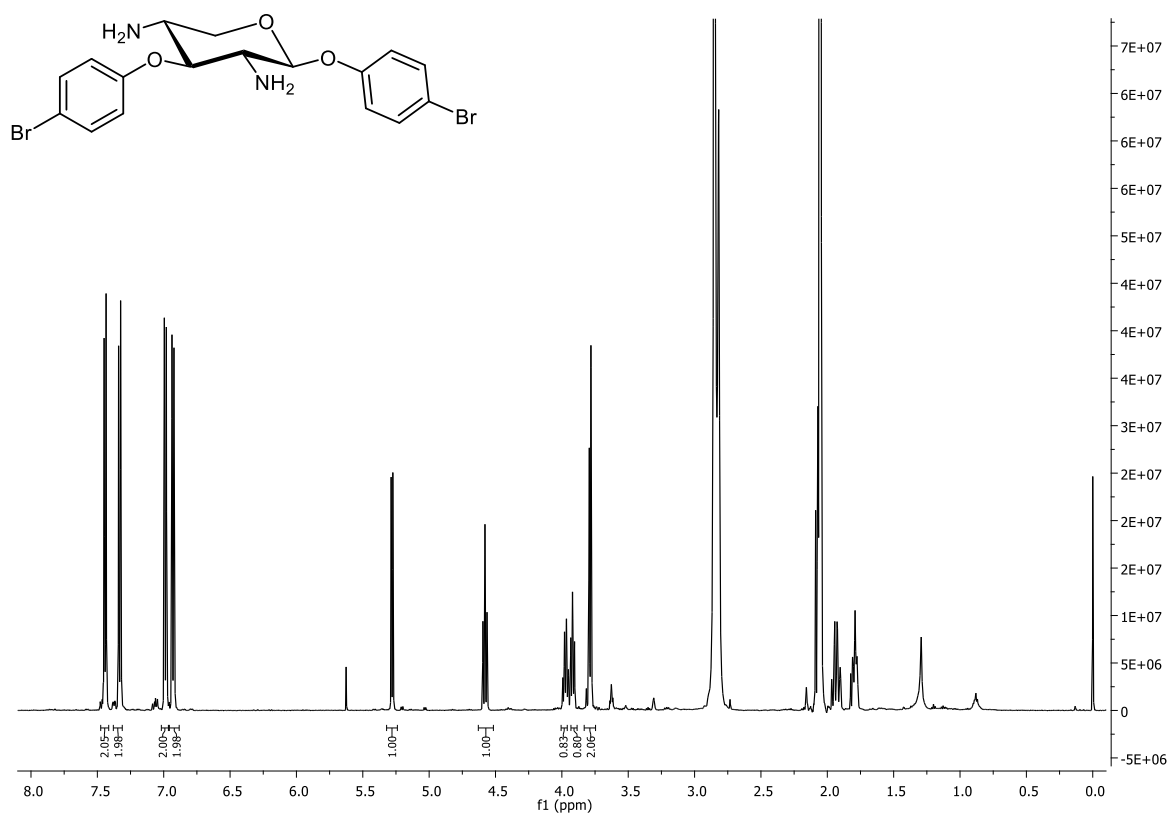


Figure 8.91. <sup>1</sup>H NMR spectrum of **167** (500 MHz, acetone-d<sub>6</sub>, 298 K).

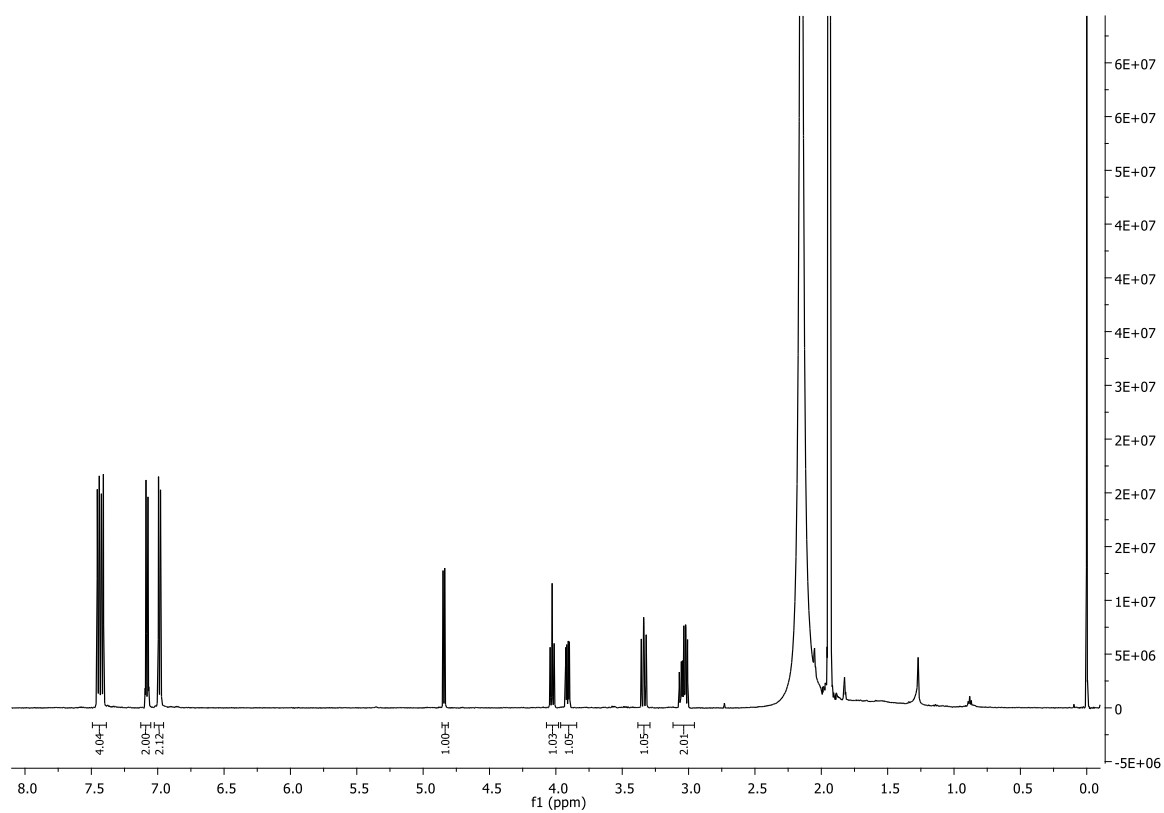


Figure 8.92. <sup>1</sup>H NMR spectrum of **167** (500 MHz, MeCN-d<sub>3</sub>, 298 K).

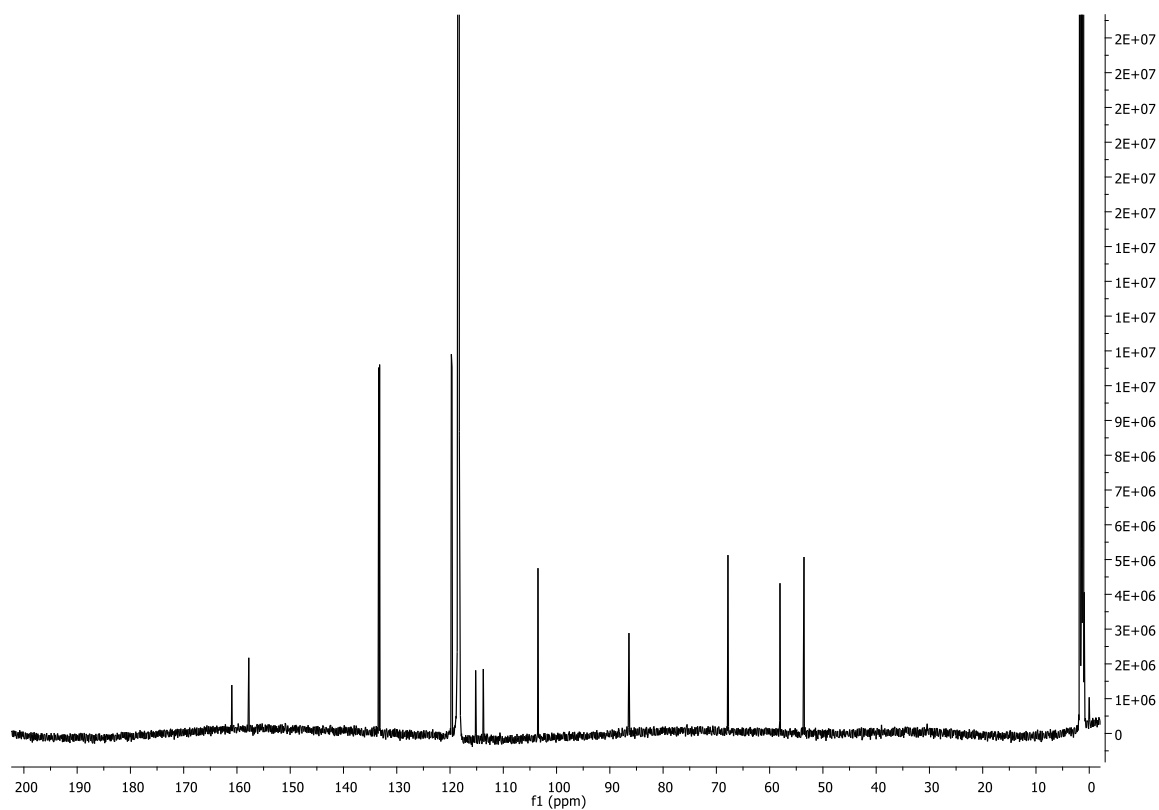


Figure 8.93.  $^{13}\text{C}$  NMR spectrum of **167** (125 MHz,  $\text{MeCN-d}_3$ , 298 K).

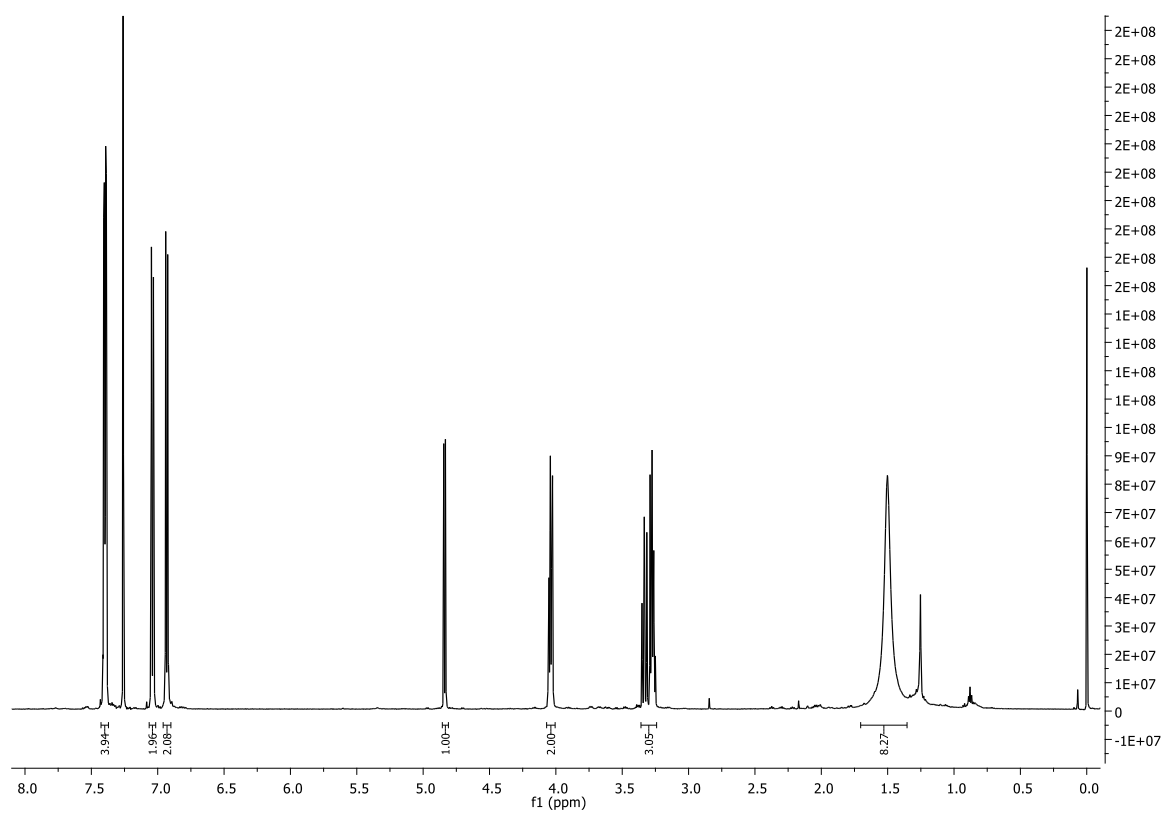


Figure 8.94.  $^1\text{H}$  NMR spectrum of **167** (500 MHz,  $\text{CDCl}_3$ , 298 K).

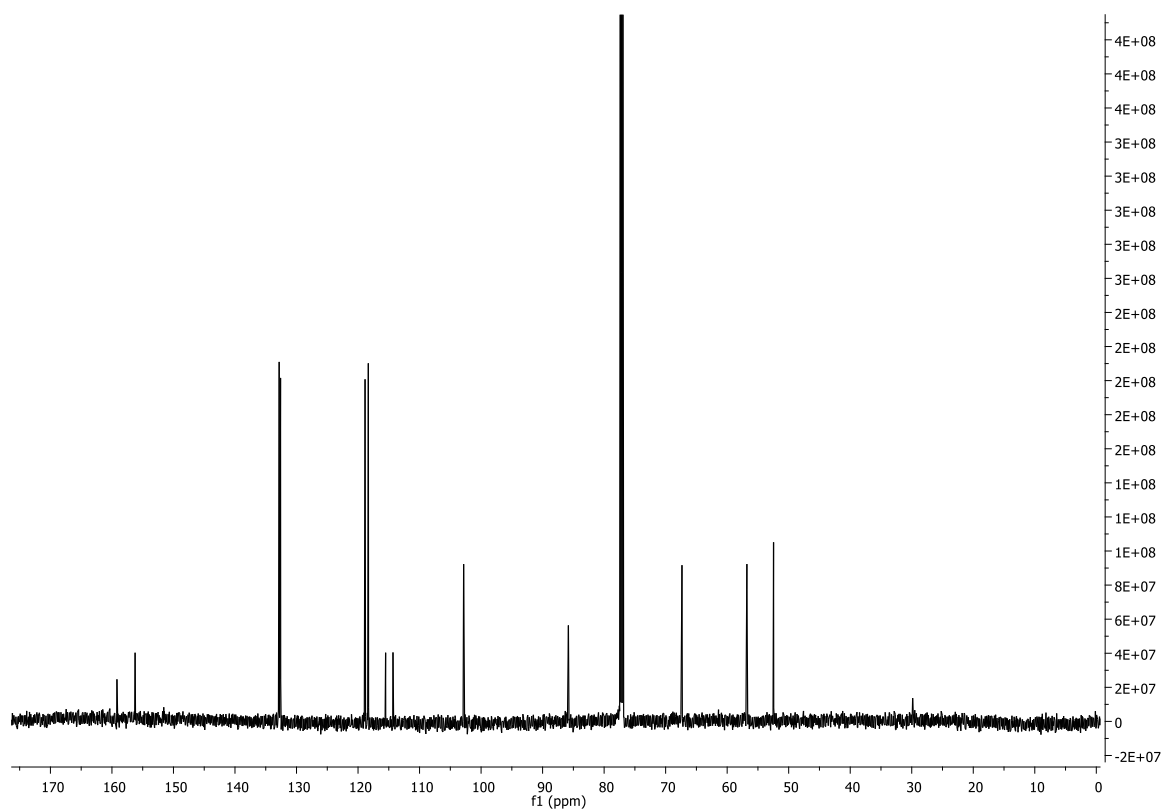


Figure 8.95.  $^{13}\text{C}$  NMR spectrum of **167** (125 MHz,  $\text{CDCl}_3$ , 298 K).

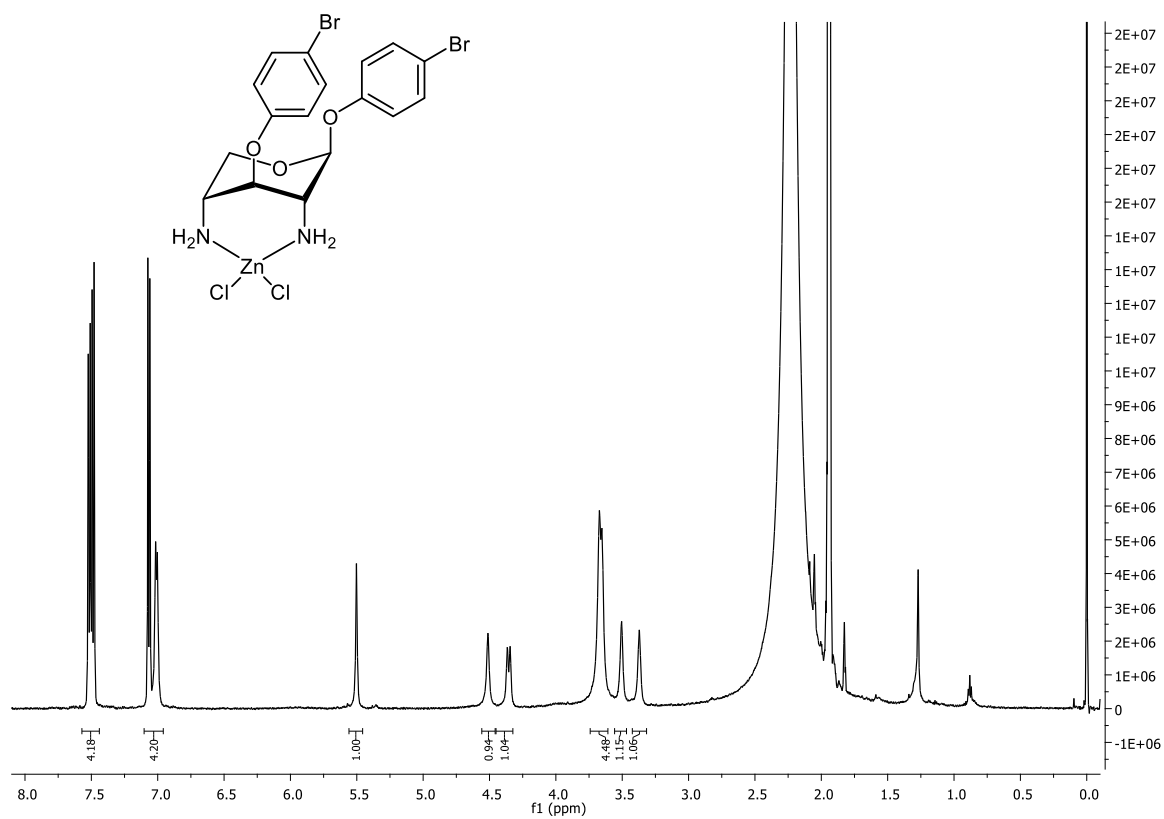


Figure 8.96.  $^1\text{H}$  NMR spectrum of **168** (500 MHz,  $\text{MeCN-d}_3$ , 298 K).

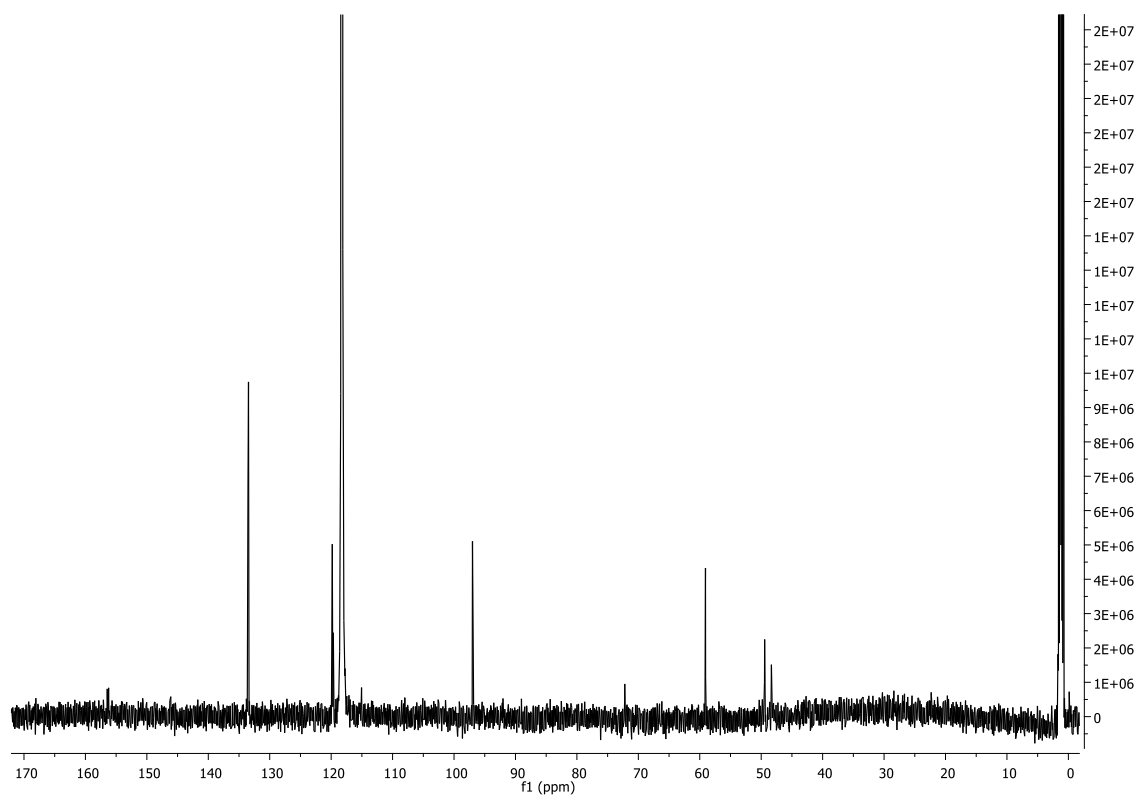


Figure 8.97.  $^{13}\text{C}$  NMR spectrum of **168** (125 MHz,  $\text{MeCN-d}_3$ , 298 K).

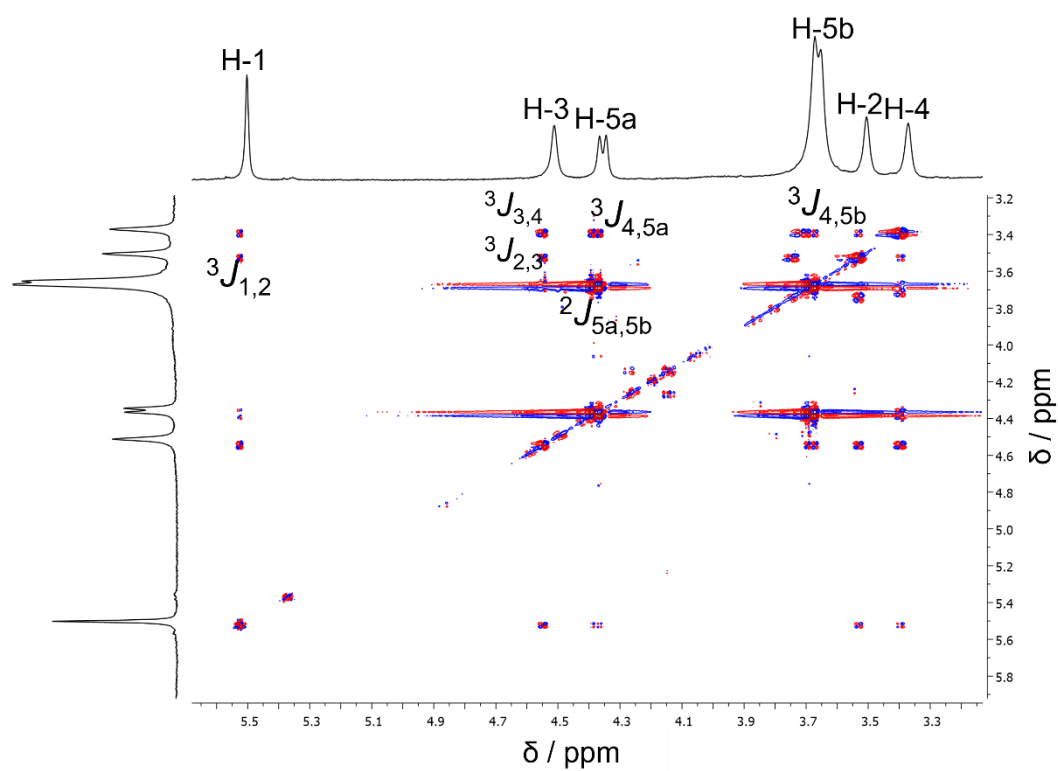


Figure 8.98. COSY-DQF NMR spectrum of **168** (500 MHz,  $\text{MeCN-d}_3$ , 298 K).

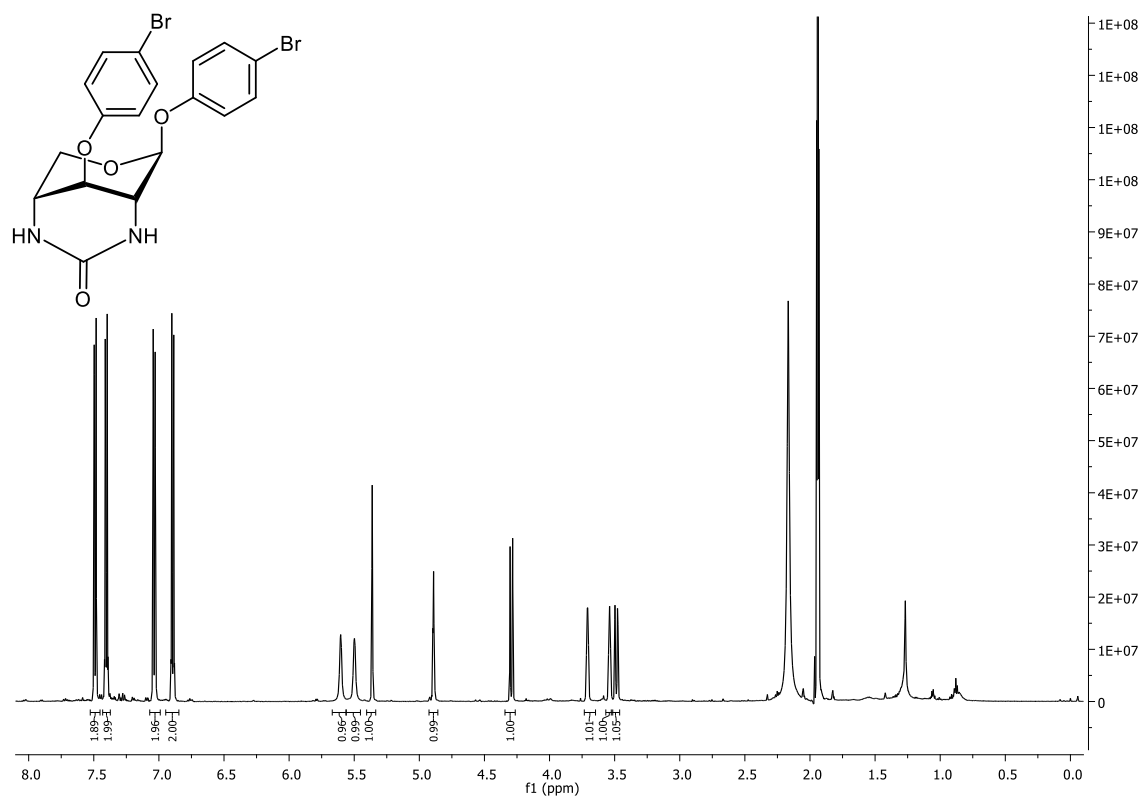


Figure 8.99.  $^1\text{H}$  NMR spectrum of **169** (600 MHz,  $\text{MeCN-d}_3$ , 298 K).

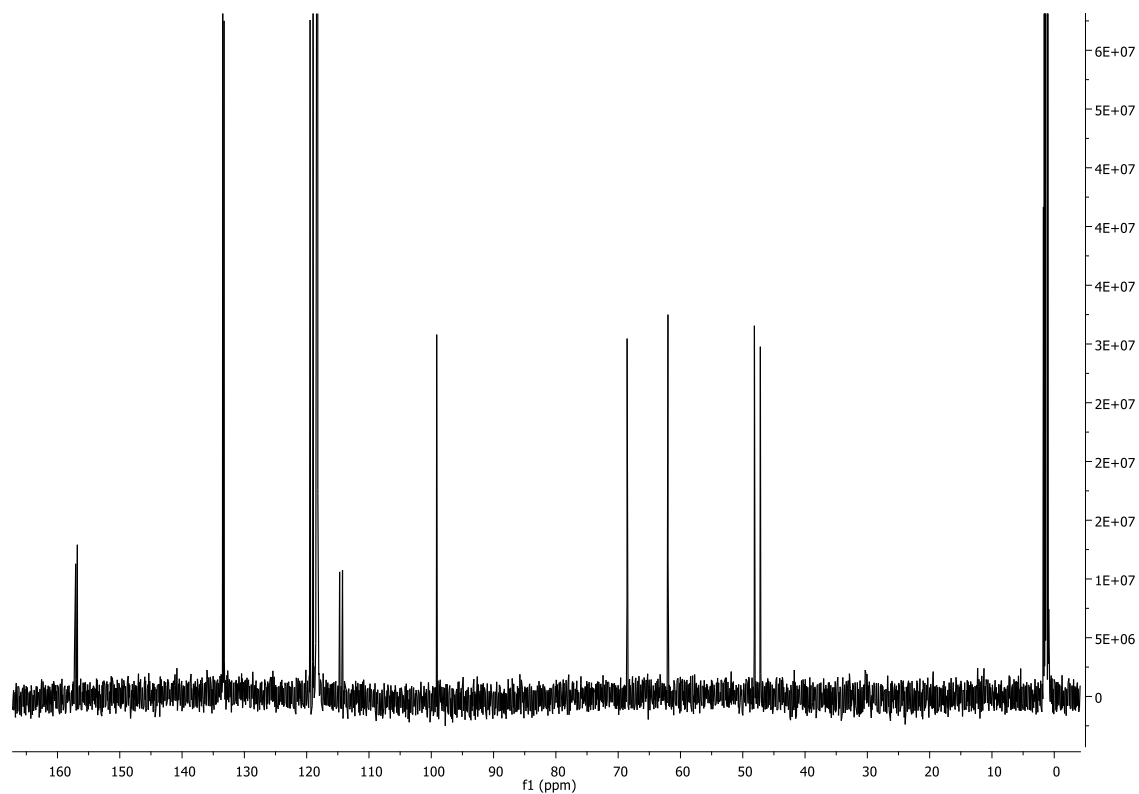


Figure 8.100.  $^{13}\text{C}$  NMR spectrum of **169** (125 MHz,  $\text{MeCN-d}_3$ , 298 K).

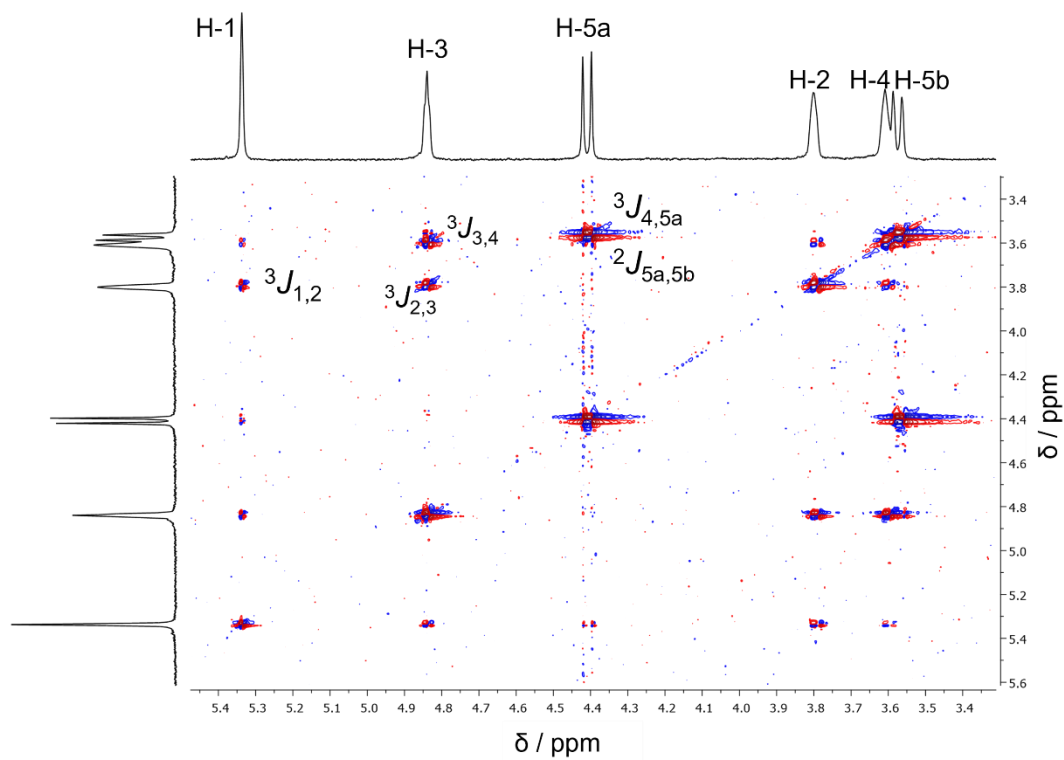


Figure 8.101. COSY-DQF NMR spectrum of **169** (500 MHz, MeCN- $d_3$ , 298 K).

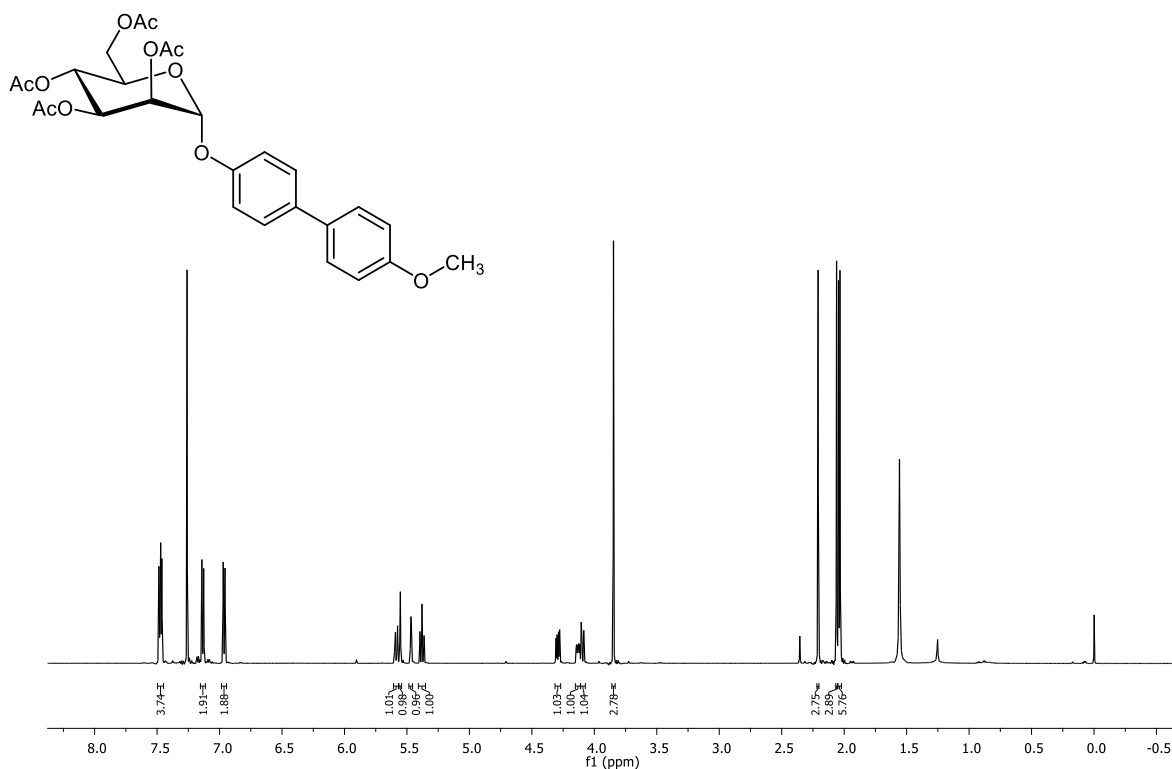


Figure 8.102.  $^1\text{H}$  NMR spectrum of **175** (600 MHz,  $\text{CDCl}_3$ , 298 K).

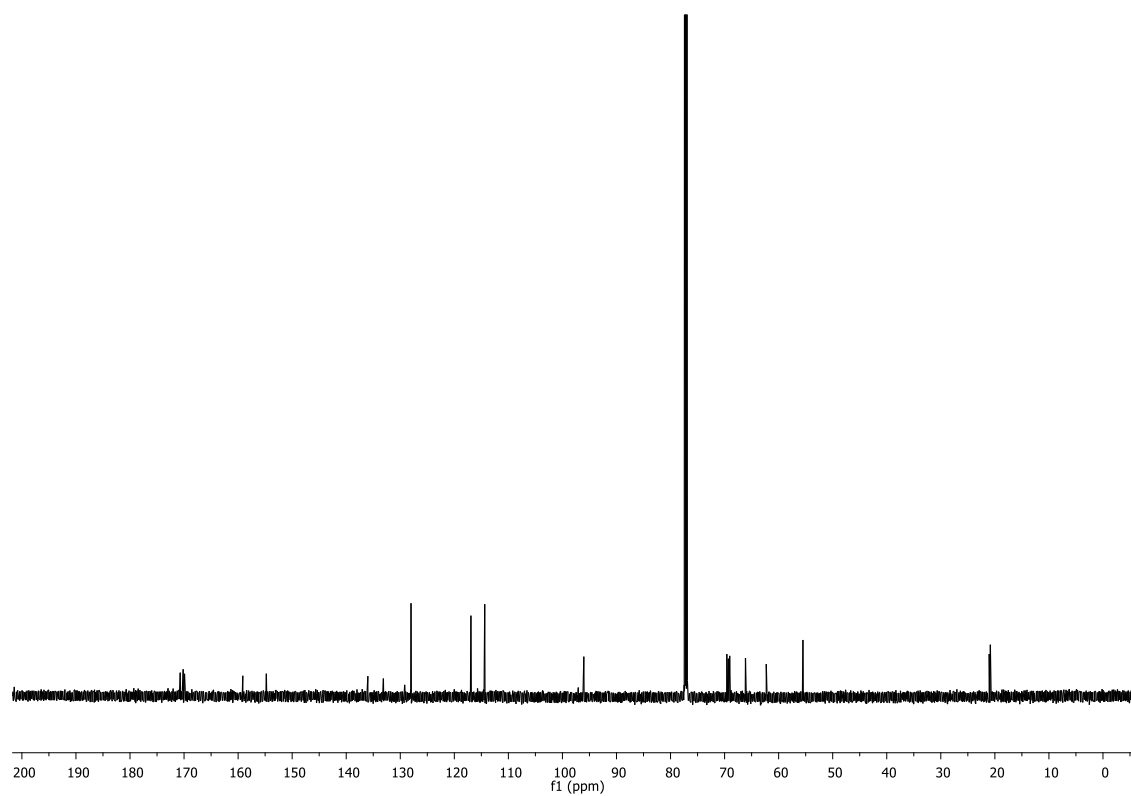


Figure 8.103.  $^{13}\text{C}$  NMR spectrum of **175** (125 MHz,  $\text{CDCl}_3$ , 298 K).

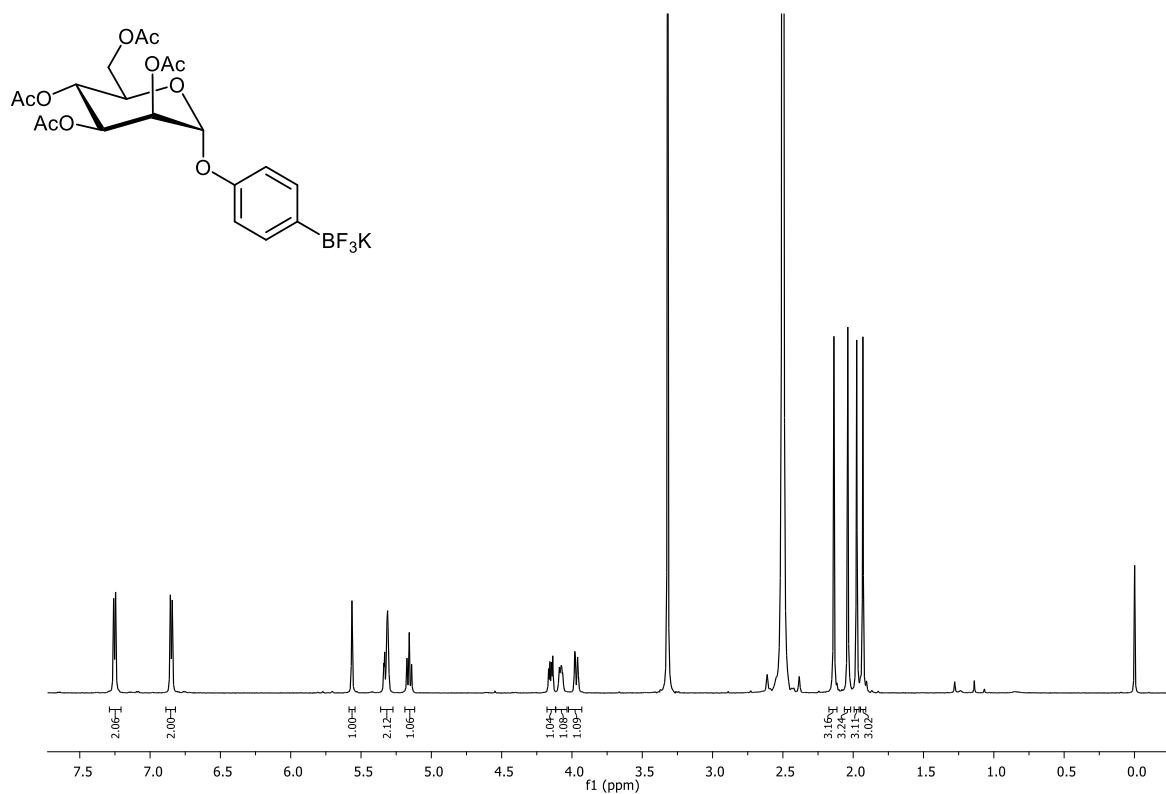


Figure 8.104.  $^1\text{H}$  NMR spectrum of **179** (600 MHz,  $\text{DMSO-d}_6$ , 298 K).

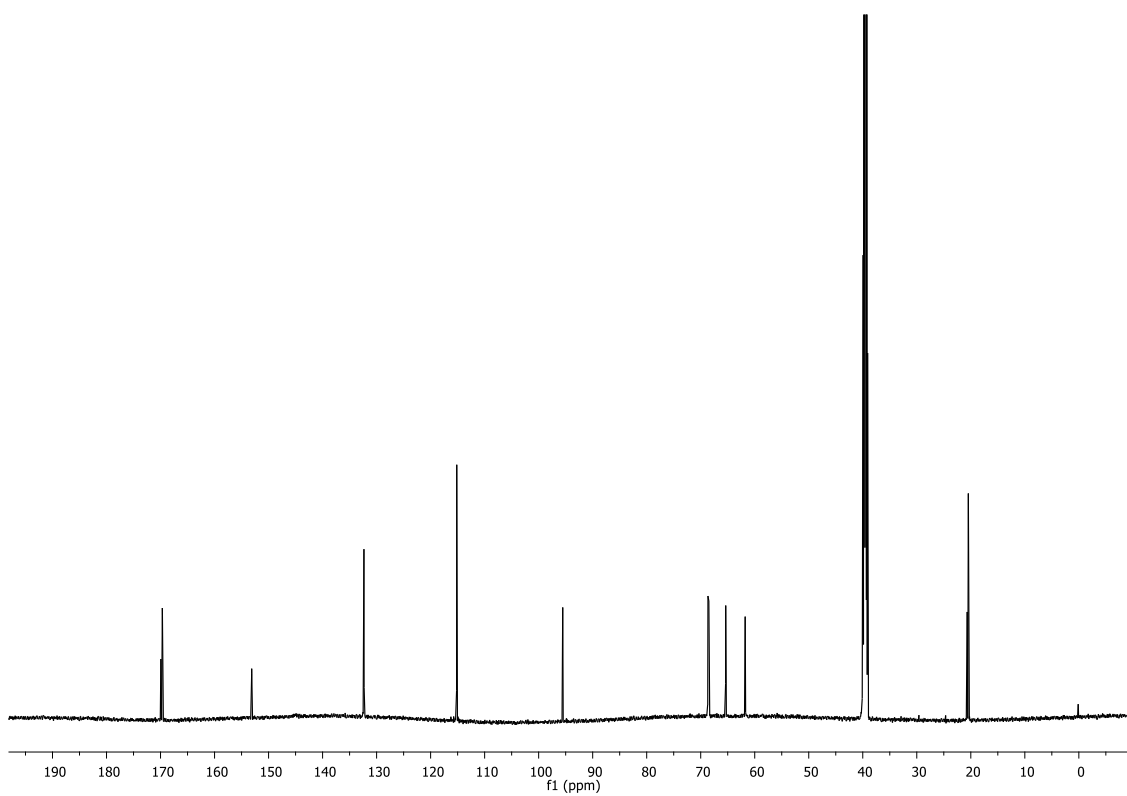


Figure 8.105.  $^{13}\text{C}$  NMR spectrum of **179** (125 MHz, DMSO- $d_6$ , 298 K).

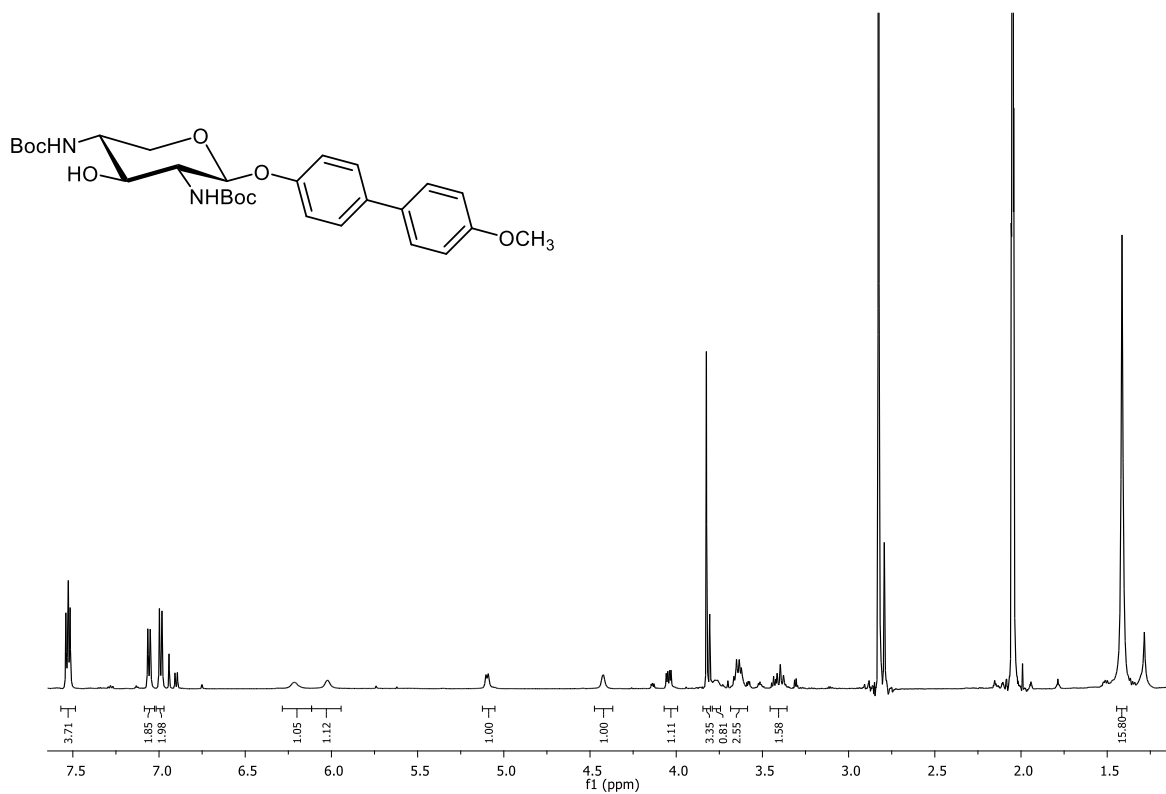


Figure 8.106.  $^1\text{H}$  NMR spectrum of **181** (500 MHz, acetone- $d_6$ , 298 K).

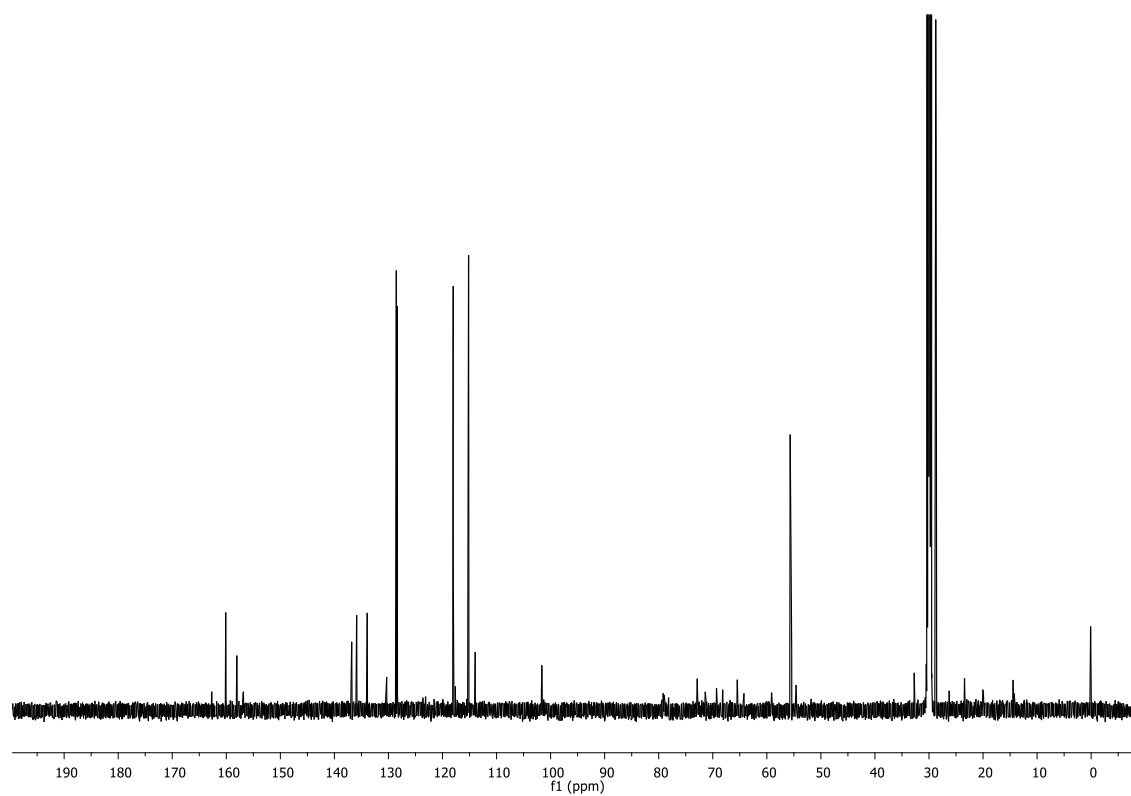


Figure 8.107.  $^{13}\text{C}$  NMR spectrum of **181** (125 MHz, acetone- $d_6$ , 298 K).

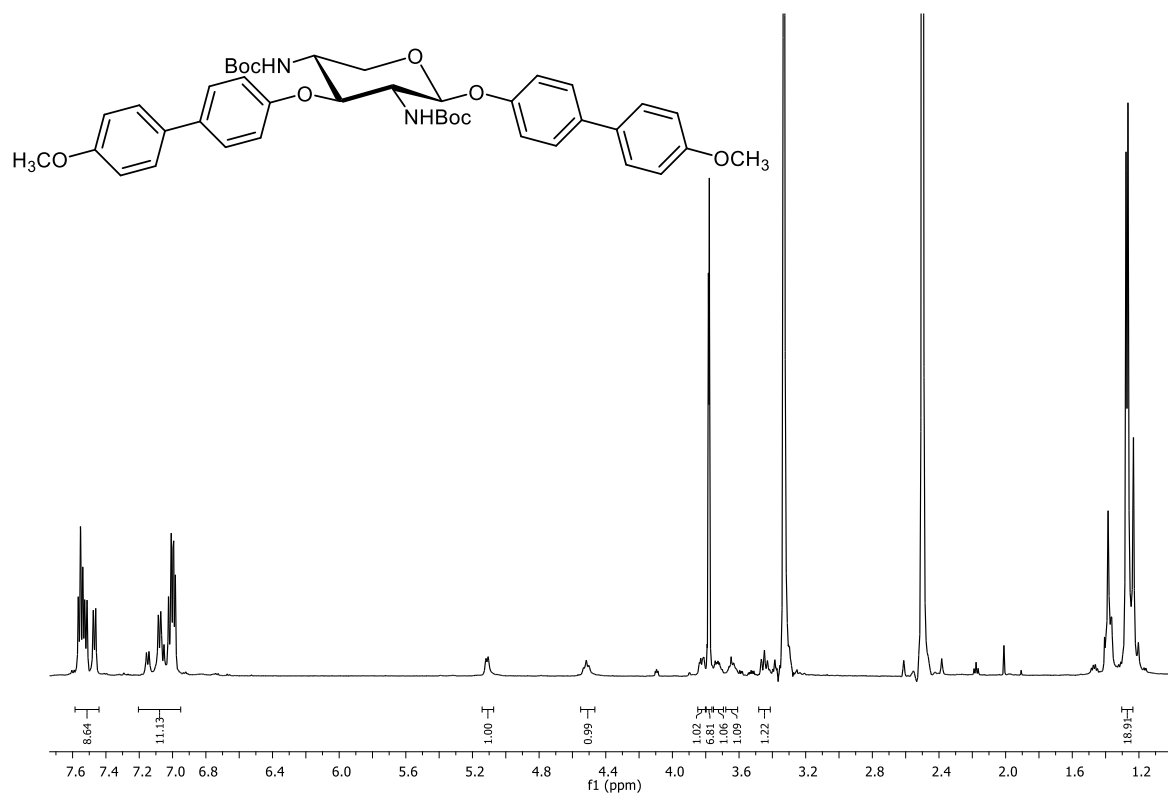


Figure 8.108.  $^1\text{H}$  NMR spectrum of **182** (600 MHz, DMSO- $d_6$ , 298 K).

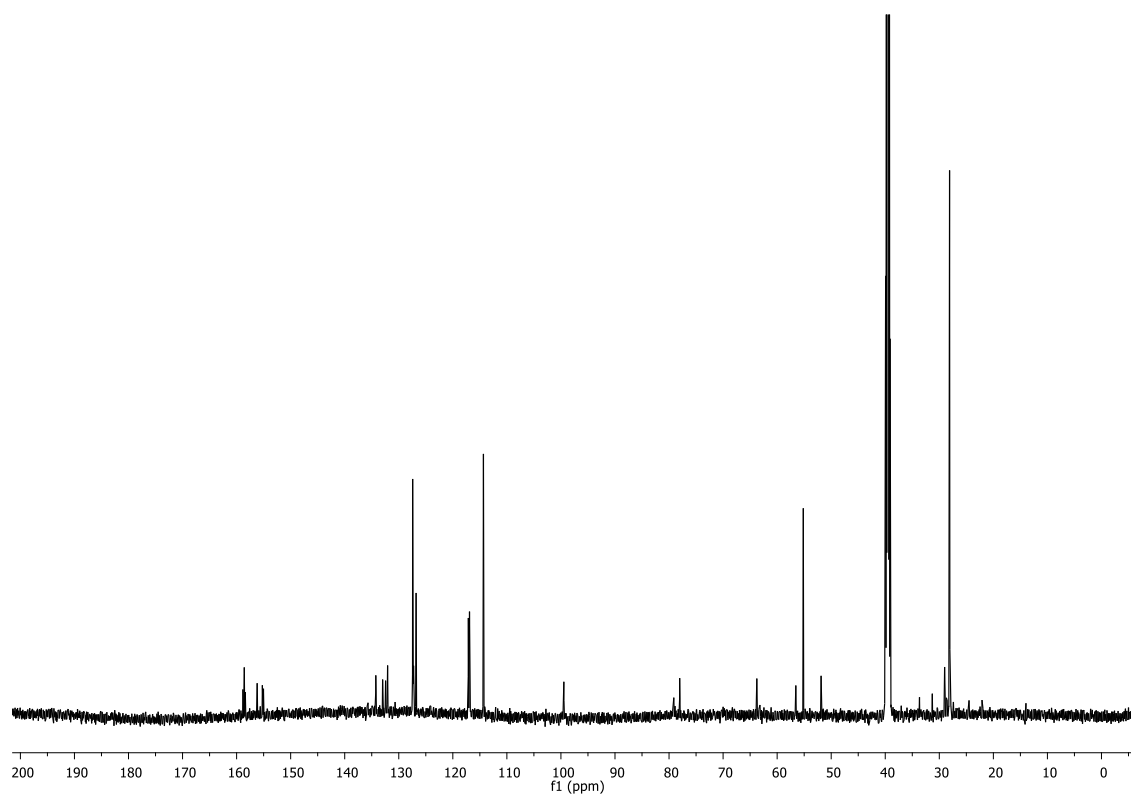


Figure 8.109.  $^{13}\text{C}$  NMR spectrum of **182** (125 MHz,  $\text{DMSO-d}_6$ , 298 K).

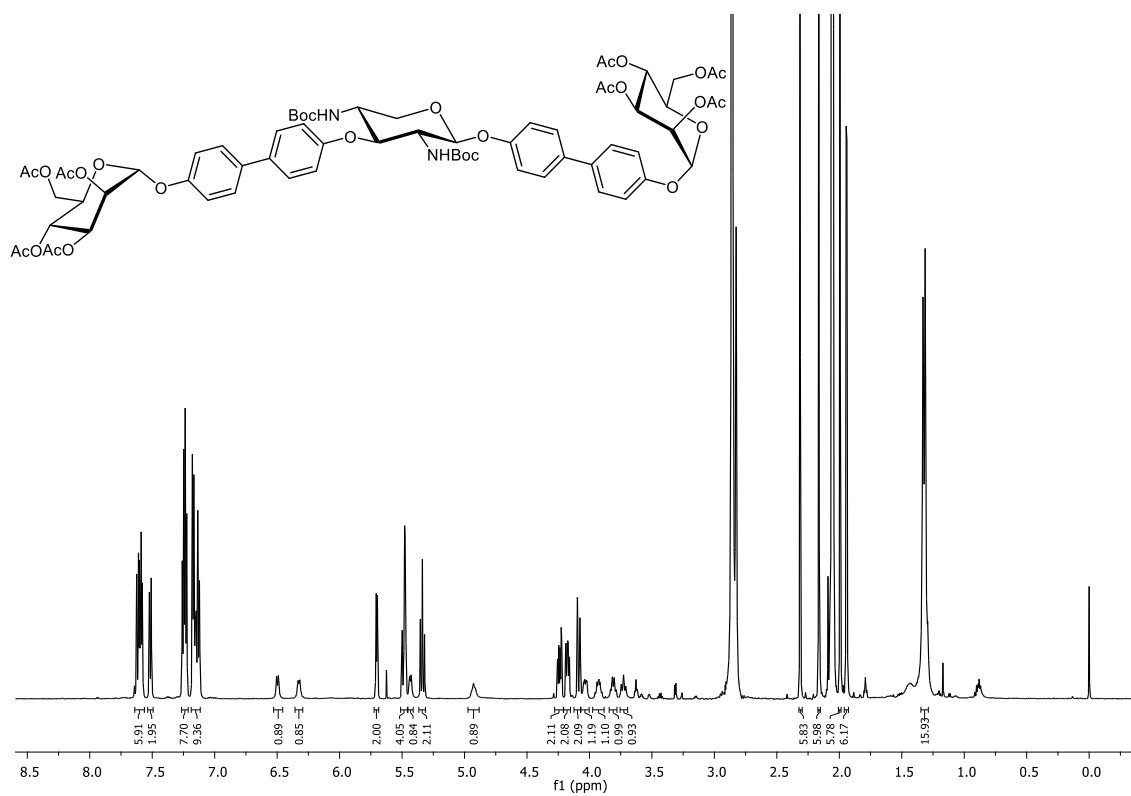


Figure 8.110.  $^1\text{H}$  NMR spectrum of **183** (600 MHz,  $\text{acetone-d}_6$ , 298 K).

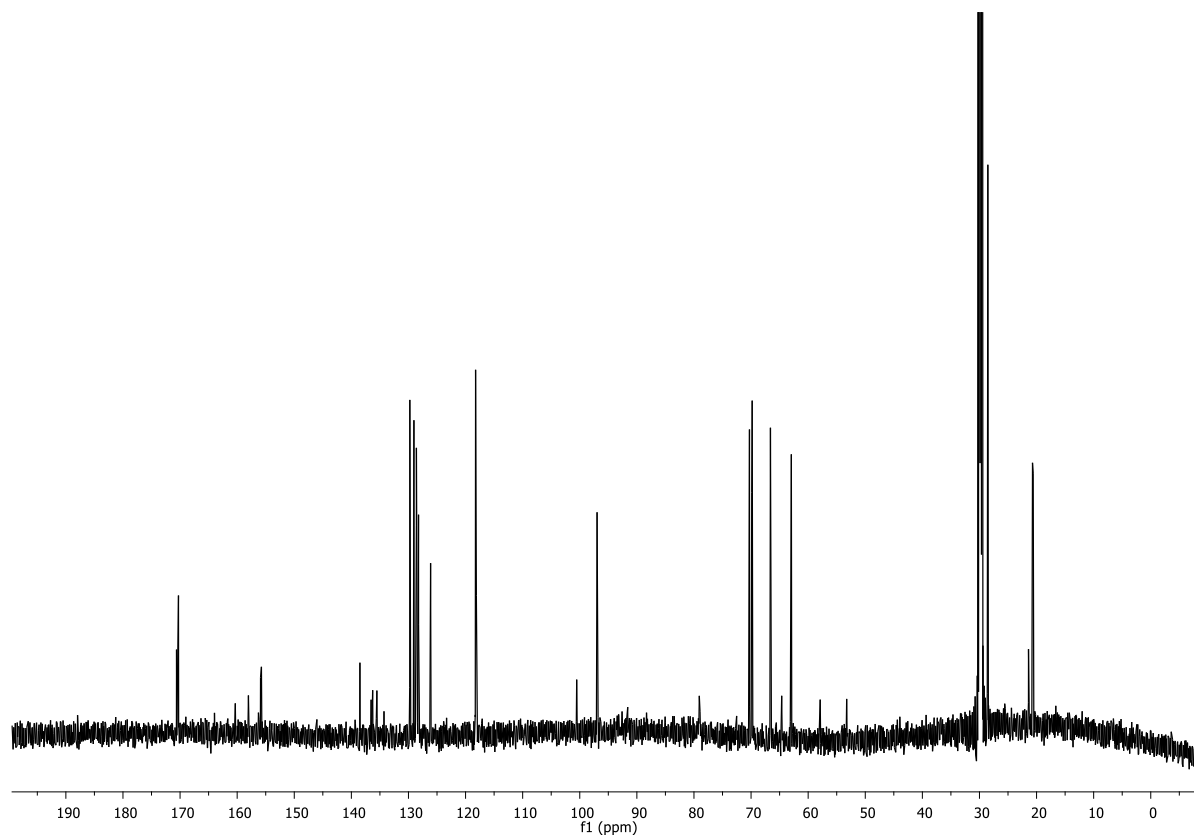


Figure 8.111.  $^{13}\text{C}$  NMR spectrum of **183** (125 MHz, acetone- $d_6$ , 298 K).

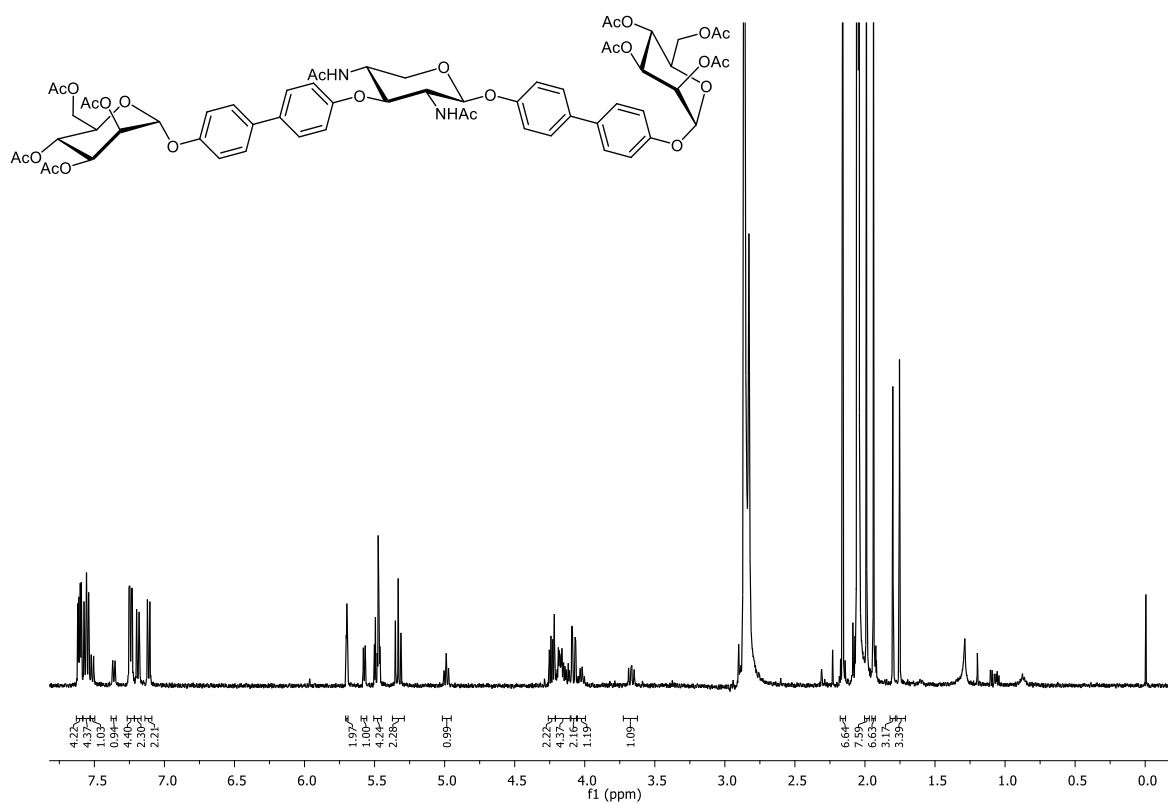


Figure 8.112.  $^1\text{H}$  NMR spectrum of **186** (500 MHz, acetone- $d_6$ , 298 K).

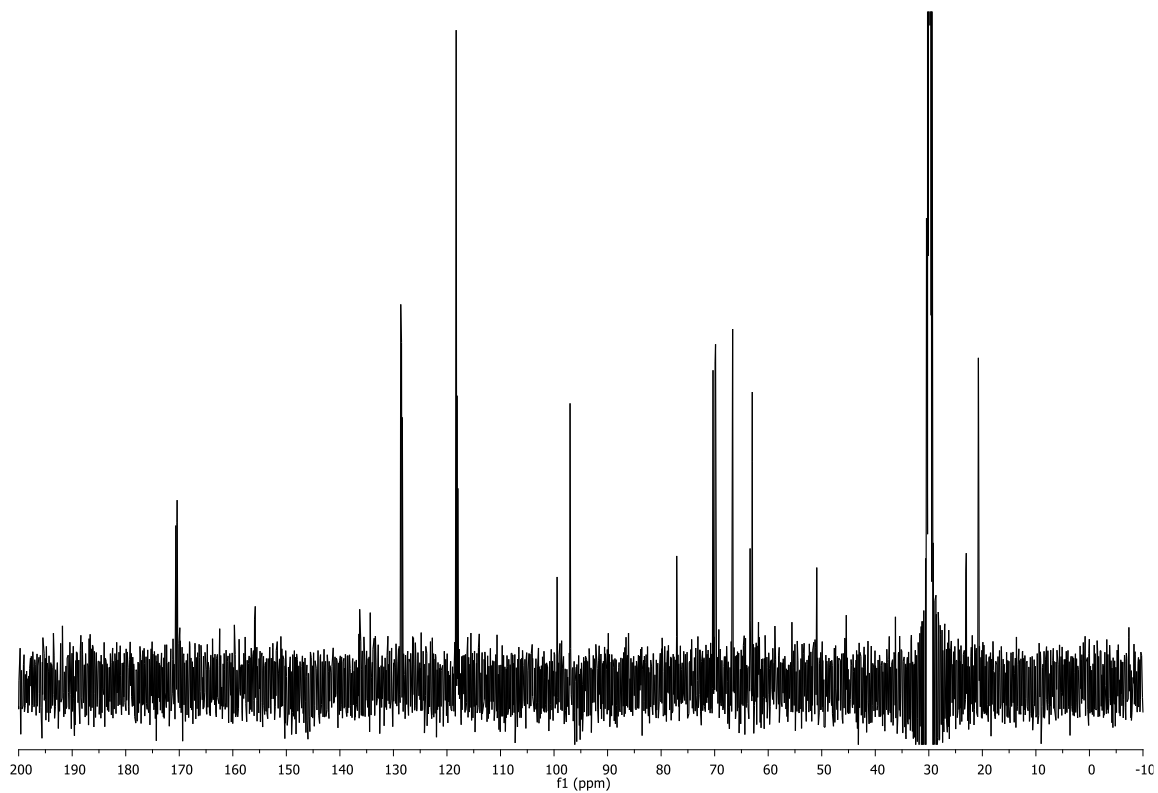


Figure 8.113.  $^{13}\text{C}$  NMR spectrum of **186** (125 MHz, acetone- $d_6$ , 298 K).

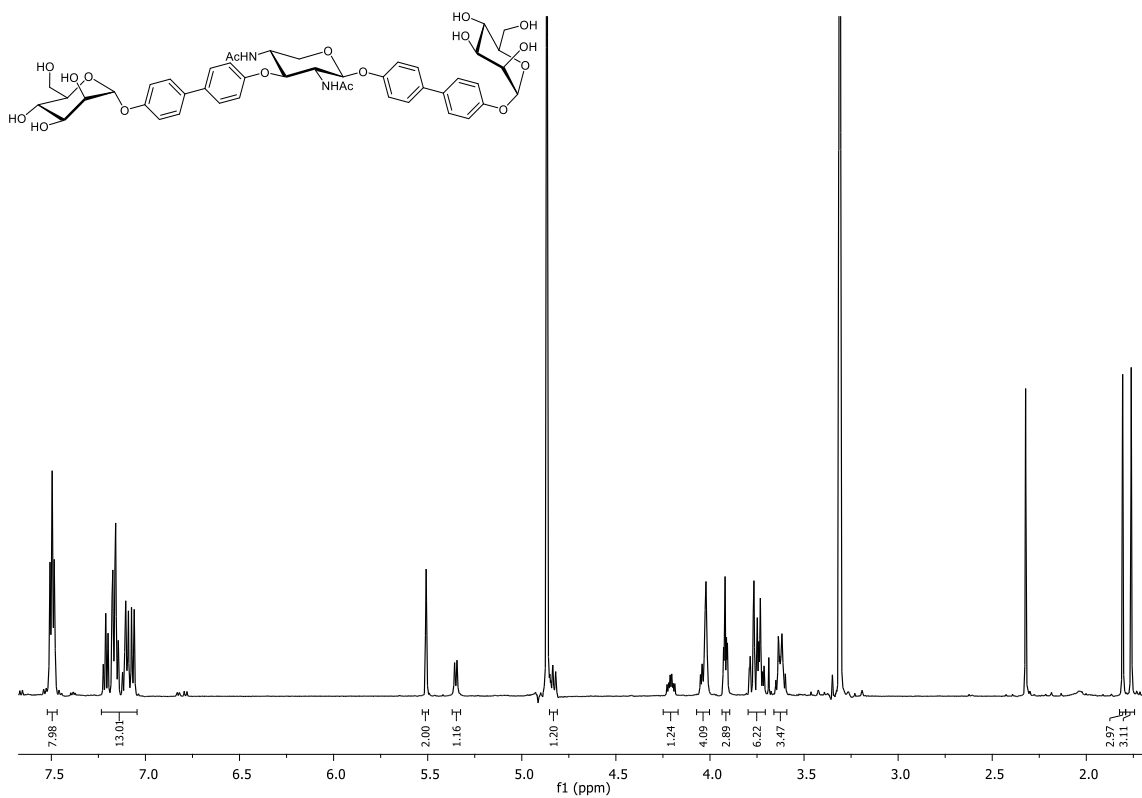


Figure 8.114.  $^1\text{H}$  NMR spectrum of **187** (600 MHz, MeOD, 298 K).

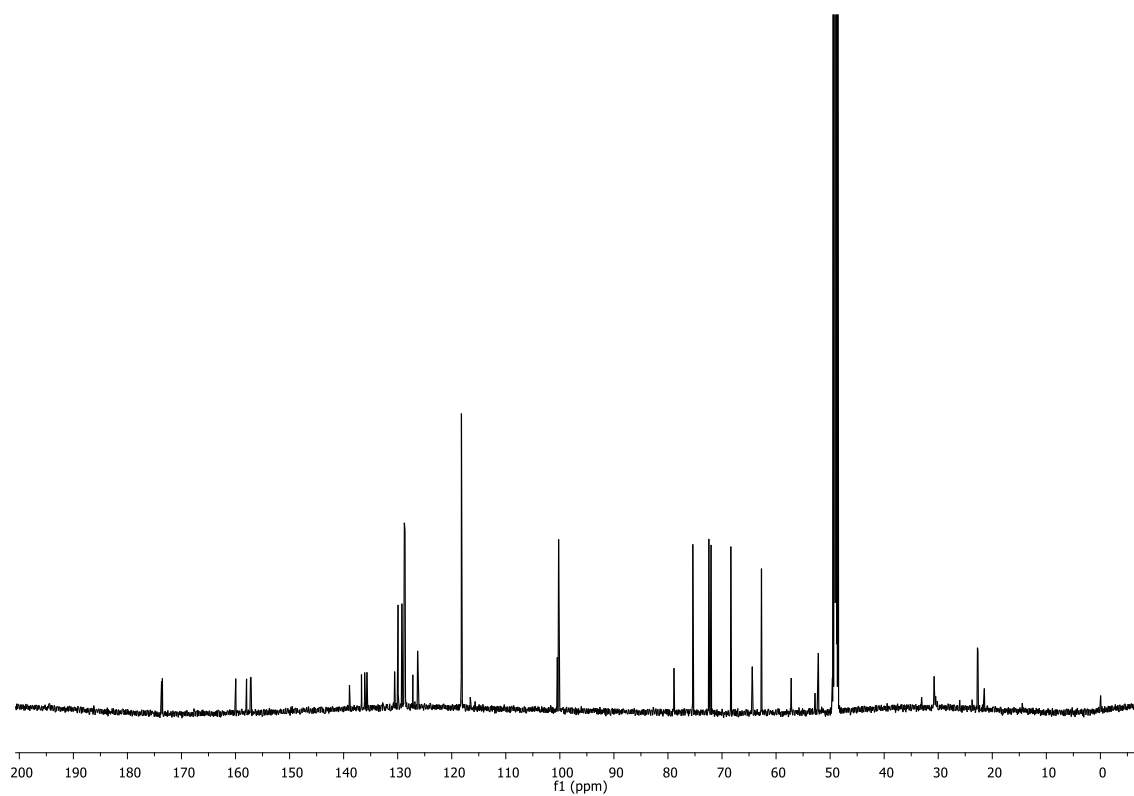


Figure 8.115. <sup>13</sup>C NMR spectrum of **187** (125 MHz, MeOD, 298 K).

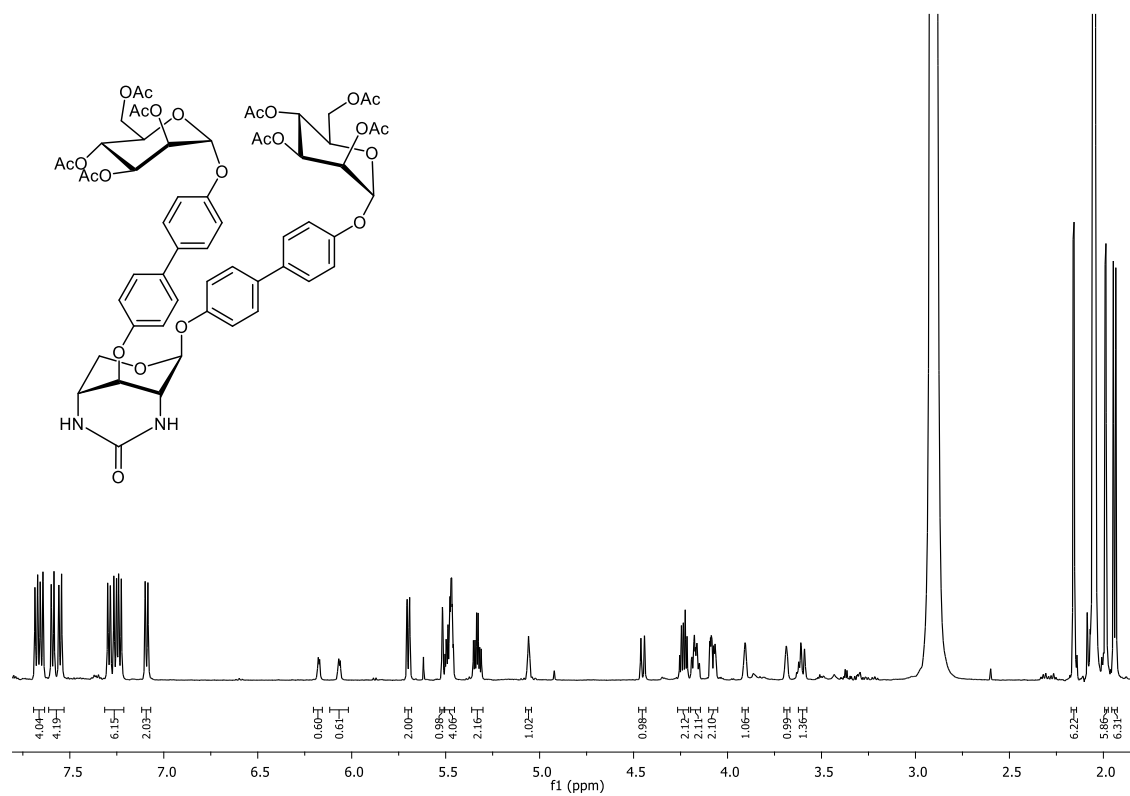


Figure 8.116. <sup>1</sup>H NMR spectrum of **184** (500 MHz, aceton-d<sub>6</sub>, 298 K).

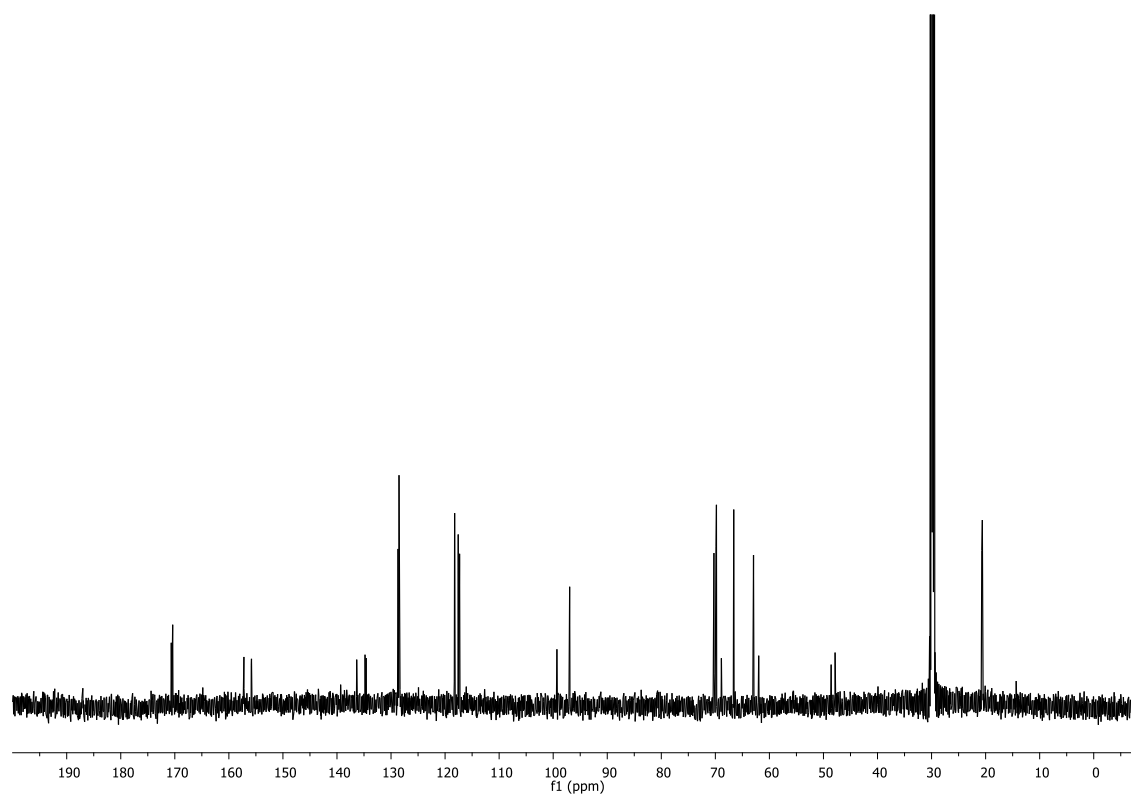


Figure 8.117.  $^{13}\text{C}$  NMR spectrum of **184** (125 MHz, aceton- $d_6$ , 298 K).

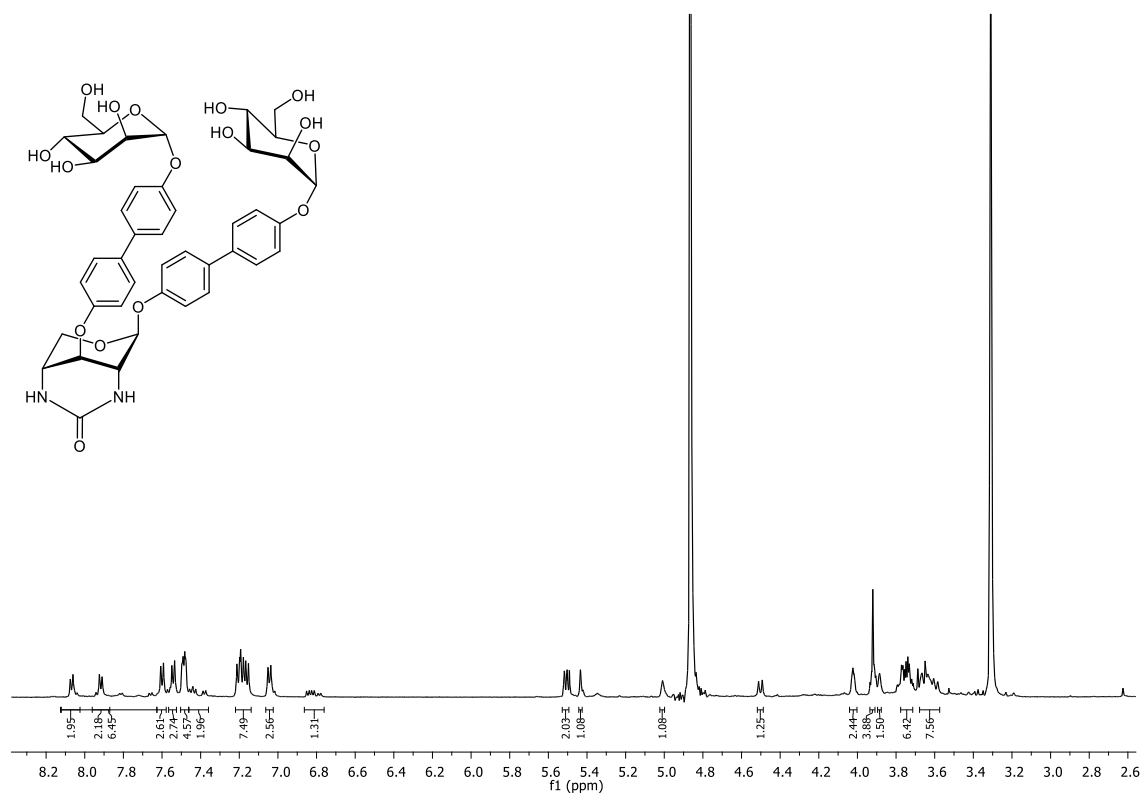
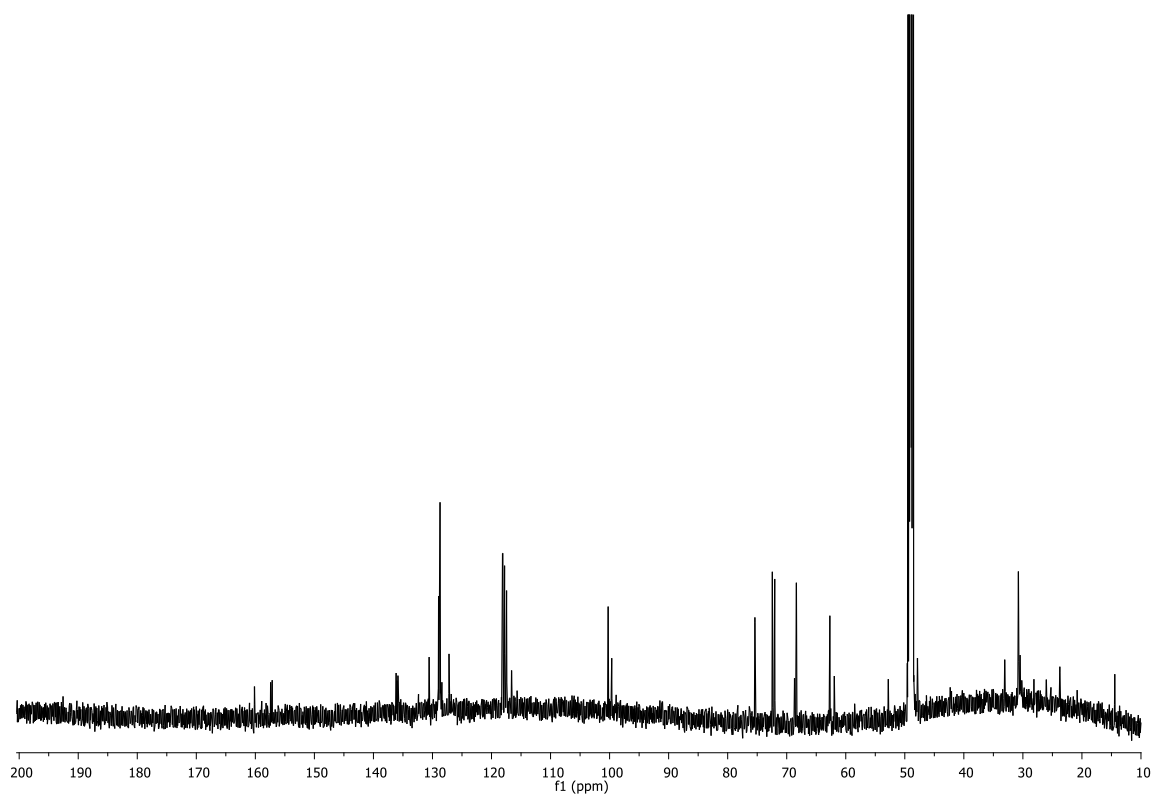
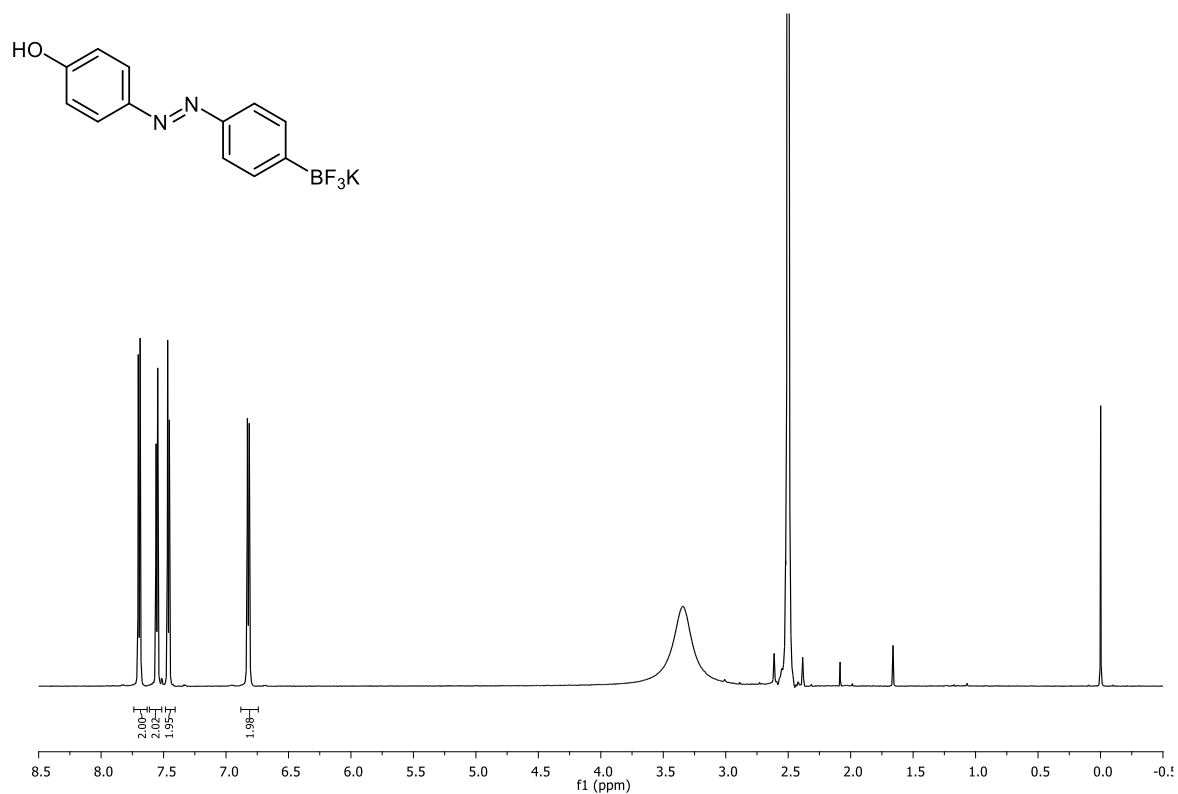


Figure 8.118.  $^1\text{H}$  NMR spectrum of **185** (600 MHz, MeOD, 298 K).



**Figure 8.119.**  $^{13}\text{C}$  NMR spectrum of **185** (125 MHz, MeOD, 298 K).



**Figure 8.120.**  $^1\text{H}$  NMR spectrum of **190** (600 MHz, DMSO- $d_6$ , 298 K).

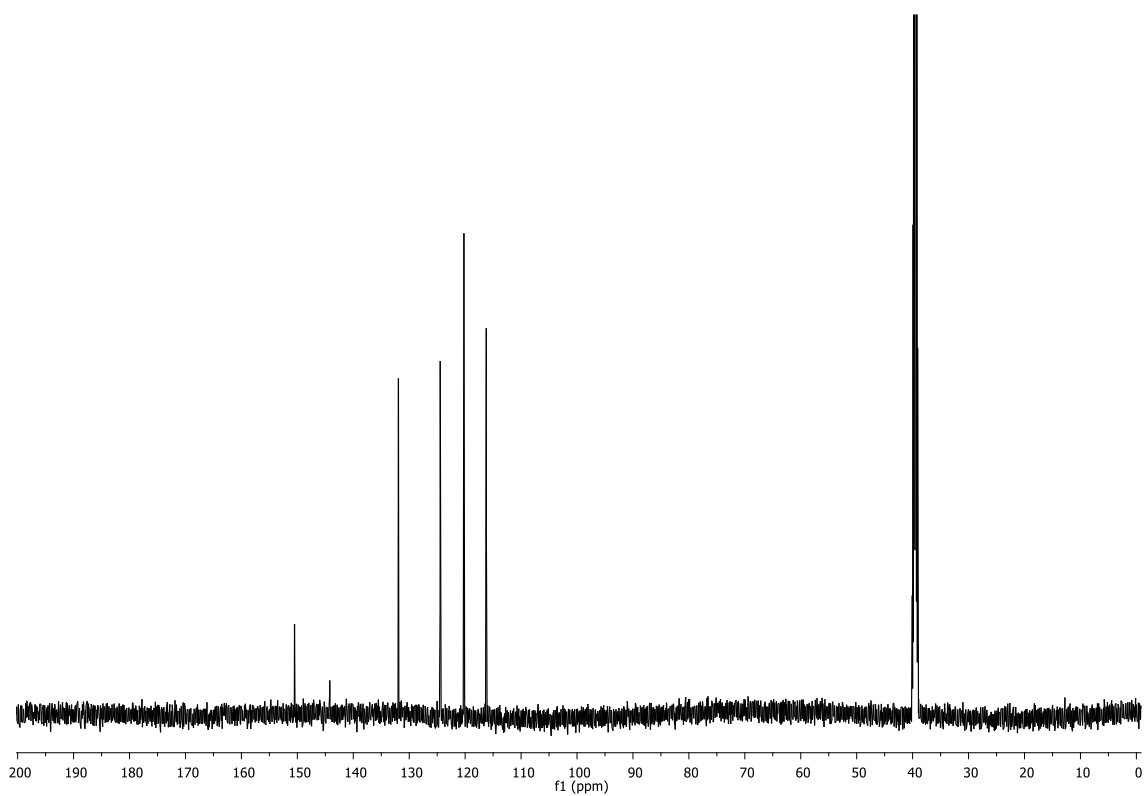


Figure 8.121.  $^{13}\text{C}$  NMR spectrum of **190** (125 MHz, DMSO- $d_6$ , 298 K).

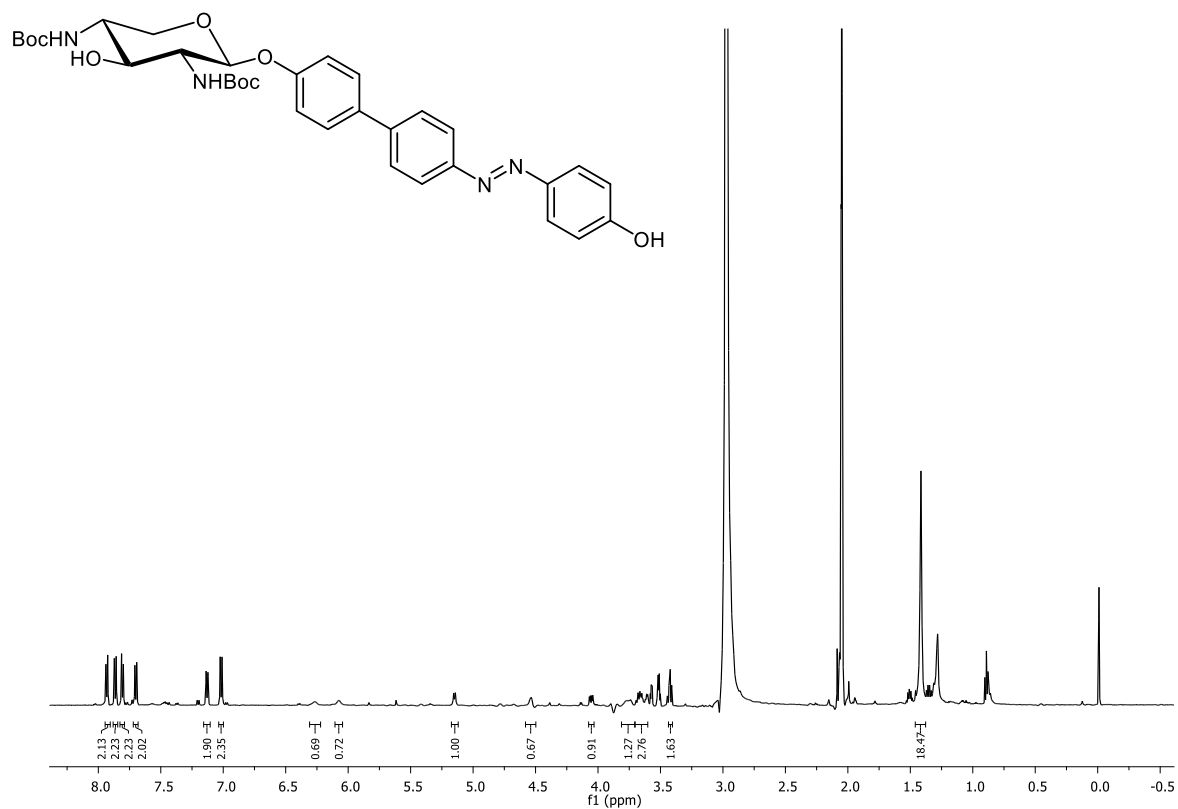
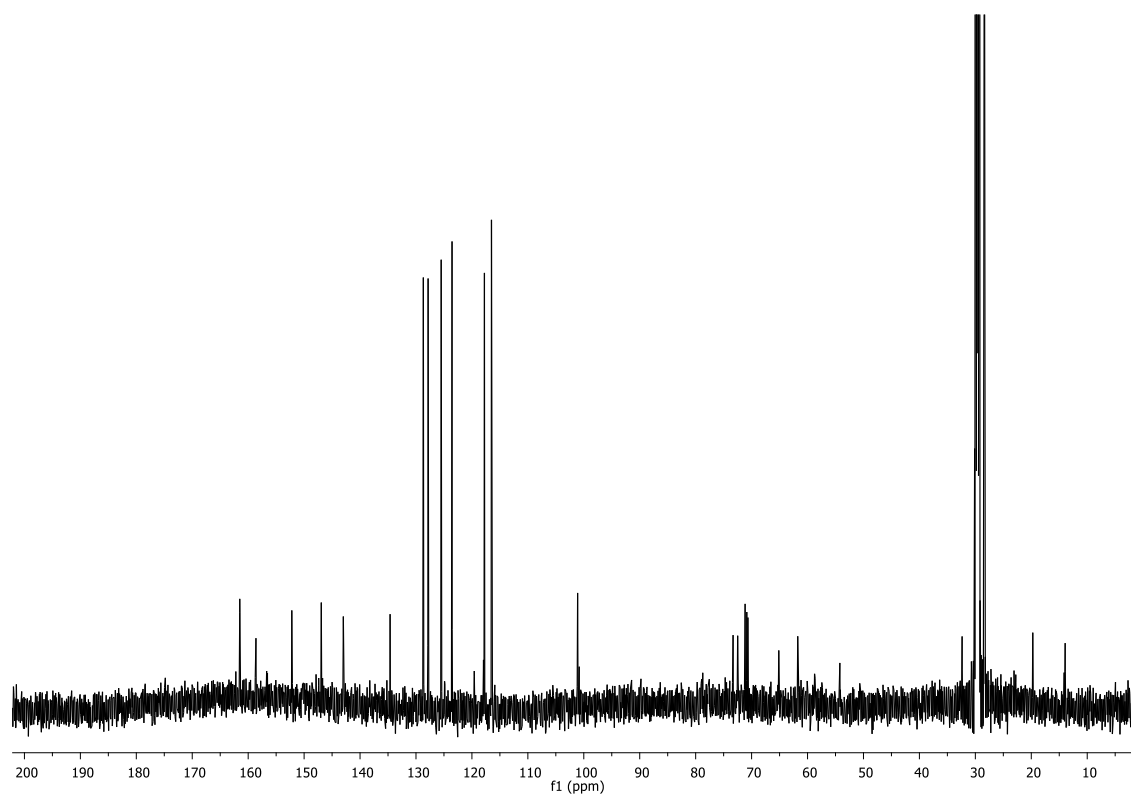


Figure 8.122.  $^1\text{H}$  NMR spectrum of **192** (600 MHz, aceton- $d_6$ , 298 K).



**Figure 8.123.**  $^{13}\text{C}$  NMR spectrum of 192 (125 MHz, acetone- $d_6$ , 298 K).

## 9 References

- [1] a) R. D. Cummings, J. M. Pierce, "The Challenge and Promise of Glycomics", *Chem. Biol.*, **2014**, 21, 1-15; b) A. Varki, "Biological roles of glycans", *Glycobiology*, **2017**, 27, 3-49.
- [2] D. B. Werz, R. Ranzinger, S. Herget, A. Adibekian, C.-W. von der Lieth, P. H. Seeberger, "Exploring the Structural Diversity of Mammalian Carbohydrates ("Glycospace") by Statistical Databank Analysis", *ACS Chem. Biol.*, **2007**, 2, 685-691.
- [3] a) N. Sharon, H. Lis, "Lectins as Cell Recognition Molecules", *Science*, **1989**, 246, 227-234; b) M. Ambrosi, N. R. Cameron, B. G. Davis, "Lectins: tools for the molecular understanding of the glycode", *Org. Biomol Chem.*, **2005**, 3, 1593-1608.
- [4] T. J. Wiles, R. R. Kulesus, M. A. Mulvey, "Origins and virulence mechanisms of uropathogenic *Escherichia coli*", *Exp. Mol. Pathol.*, **2008**, 85, 11-19.
- [5] a) C. J. Gray, L. G. Migas, P. E. Barran, K. Pagel, P. H. Seeberger, C. E. Eyers, G.-J. Boons, N. L. B. Pohl, I. Compagnon, G. Widmalm, S. L. Flitsch, "Advancing Solutions to the Carbohydrate Sequencing Challenge", *J. Am. Chem. Soc.*, **2019**, 141, 14463-14479; b) L. Möckl, "The Emerging Role of the Mammalian Glycocalyx in Functional Membrane Organization and Immune System Regulation", *Front. Cell Dev. Biol.*, **2020**, 8.
- [6] a) C. R. Bertozzi, L. L. Kiessling, "Chemical Glycobiology", *Science*, **2001**, 291, 2357-2364; b) H. J. Gabius, H. C. Siebert, S. André, J. Jiménez-Barbero, H. Rüdiger, "Chemical Biology of the Sugar Code", *ChemBioChem*, **2004**, 5, 740-764.
- [7] M. Kukkonen, T. Raunio, R. Virkola, K. Lähteenmäki, P. H. Mäkelä, P. Klemm, S. Clegg, T. K. Korhonen, "Basement membrane carbohydrate as a target for bacterial adhesion: binding of type I fimbriae of *Salmonella enterica* and *Escherichia coli* to laminin", *Mol. Microbiol.*, **1993**, 7, 229-237.
- [8] S. Weinbaum, J. M. Tarbell, E. R. Damiano, "The Structure and Function of the Endothelial Glycocalyx Layer", *Annu. Rev. Biomed. Eng.*, **2007**, 9, 121-167.
- [9] B. F. Becker, M. Jacob, S. Leipert, A. H. J. Salmon, D. Chappell, "Degradation of the endothelial glycocalyx in clinical settings: searching for the sheddases", *Br. J. Clin. Pharmacol.*, **2015**, 80, 389-402.
- [10] M. J. Paszek, C. C. DuFort, O. Rossier, R. Bainer, J. K. Mouw, K. Godula, J. E. Hudak, J. N. Lakins, A. C. Wijekoon, L. Cassereau, M. G. Rubashkin, M. J. Magbanua, K. S. Thorn, M. W. Davidson, H. S. Rugo, J. W. Park, D. A. Hammer, G. Giannone, C. R. Bertozzi, V. M. Weaver, "The cancer glycocalyx mechanically primes integrin-mediated growth and survival", *Nature*, **2014**, 511, 319-325.
- [11] N. Sharon, H. Lis, "Carbohydrates in cell recognition", *Sci. Am.*, **1993**, 268, 82-89.
- [12] I. Ofek, D. L. Hasy, N. Sharon, "Anti-adhesion therapy of bacterial diseases: prospects and problems", *FEMS Immunol. Med. Microbiol.*, **2003**, 38, 181-191.
- [13] D. Chappell, M. Jacob, K. Hofmann-Kiefer, M. Rehm, U. Welsch, P. Conzen, B. F. Becker, "Antithrombin reduces shedding of the endothelial glycocalyx following ischaemia/reperfusion", *Cardiovasc. Res.*, **2009**, 83, 388-396.

- [14] A. Varki, R. D. Cummings, M. Aebi, N. H. Packer, P. H. Seeberger, J. D. Esko, P. Stanley, G. Hart, A. Darvill, T. Kinoshita, J. J. Prestegard, R. L. Schnaar, H. H. Freeze, J. D. Marth, C. R. Bertozzi, M. E. Etzler, M. Frank, J. F. Vliegthart, T. Lütke, S. Perez, E. Bolton, P. Rudd, J. Paulson, M. Kanehisa, P. Toukach, K. F. Aoki-Kinoshita, A. Dell, H. Narimatsu, W. York, N. Taniguchi, S. Kornfeld, "Symbol Nomenclature for Graphical Representations of Glycans", *Glycobiology*, **2015**, 25, 1323-1324.
- [15] S. Neelamegham, K. Aoki-Kinoshita, E. Bolton, M. Frank, F. Lisacek, T. Lütke, N. O'Boyle, N. H. Packer, P. Stanley, P. Toukach, A. Varki, R. J. Woods, T. S. D. Group, "Updates to the Symbol Nomenclature for Glycans guidelines", *Glycobiology*, **2019**, 29, 620-624.
- [16] G. van Meer, D. R. Voelker, G. W. Feigenson, "Membrane lipids: where they are and how they behave", *Nature Rev. Mol. Cell Biology*, **2008**, 9, 112-124.
- [17] Y. D. Vankar, R. R. Schmidt, "Chemistry of glycosphingolipids—carbohydrate molecules of biological significance", *Chem. Soc. Rev.*, **2000**, 29, 201-216.
- [18] *Essentials of Glycobiology*, 3. ed. (Eds.: A. Varki, R. D. Cummings, J. D. Esko, P. Stanley, G. W. Hart, M. Aebi, A. G. Darvill, T. Kinoshita, N. H. Packer, J. H. Prestegard, R. L. Schnaar, P. H. Seeberger), Cold Spring Harbor Laboratory Press, Cold Spring Harbor (NY), **2015-2017**.
- [19] P. Stanley, N. Taniguchi, M. Aebi, N-Glycans, chapter 9, in *Essentials of Glycobiology*, 3. ed. (Ed.: R. C. A. Varki, J. Esko et al.), Cold Spring Harbor Laboratory Press, Cold Spring Harbor (NY), **2017**.
- [20] K. Brzezicka, U. Vogel, S. Serna, T. Johannssen, B. Lepenies, N.-C. Reichardt, "Influence of Core  $\beta$ -1,2-Xylosylation on Glycoprotein Recognition by Murine C-type Lectin Receptors and Its Impact on Dendritic Cell Targeting", *ACS Chem. Biol.*, **2016**, 11, 2347-2356.
- [21] a) M. Takahashi, Y. Kuroki, K. Ohtsubo, N. Taniguchi, "Core fucose and bisecting GlcNAc, the direct modifiers of the N-glycan core: their functions and target proteins", *Carbohydr. Res.*, **2009**, 344, 1387-1390; b) A. Cabanettes, L. Perkams, C. Spies, C. Unverzagt, A. Varrot, "Recognition of Complex Core-Fucosylated N-Glycans by a Mini Lectin", *Angew. Chem. Int. Ed.*, **2018**, 57, 10178-10181.
- [22] a) M. Bardor, C. Faveeuw, A.-C. Fichette, D. Gilbert, L. Galas, F. Trottein, L. Faye, P. Lerouge, "Immunoreactivity in mammals of two typical plant glyco-epitopes, core  $\alpha$ (1,3)-fucose and core xylose", *Glycobiology*, **2003**, 13, 427-434; b) A. K. Nyame, Z. S. Kwar, R. D. Cummings, "Antigenic glycans in parasitic infections: implications for vaccines and diagnostics", *Arch. Biochem. Biophys.*, **2004**, 426, 182-200.
- [23] L. Kjellén, U. Lindahl, "Proteoglycans: Structures and Interactions", *Annu. Rev. Biochem.*, **1991**, 60, 443-475.
- [24] P. Stanley, H. Schachter, N. Taniguchi, N-Glycans in *Essentials of Glycobiology*, 2nd ed. (Eds.: A. Varki, R. D. Cummings, J. D. Esko, H. H. Freeze, P. Stanley, C. R. Bertozzi, G. W. Hart, M. E. Etzler), Cold Spring Harbor (NY), **2009**.
- [25] a) Y. van Kooyk, G. A. Rabinovich, "Protein-glycan interactions in the control of innate and adaptive immune responses", *Nat. Immunol.*, **2008**, 9, 593-601; b) Y.-Y. Zhao, M. Takahashi, J.-G. Gu, E. Miyoshi, A. Matsumoto, S. Kitazume, N. Taniguchi, "Functional roles of N-glycans in cell signaling and cell adhesion in cancer", *Cancer Sci.*, **2008**, 99, 1304-1310.

- [26] N. Sharon, H. Lis, "History of lectins: from hemagglutinins to biological recognition molecules", *Glycobiology*, **2004**, *14*, 53R-62R.
- [27] J. B. Sumner, S. F. Howell, "Identification of Hemagglutinin of Jack Bean with Concanavalin A", *J. Bacteriol.*, **1936**, *32*, 227-237.
- [28] C. Szymanski, R. Schnaar, M. Aebi, Bacterial and Viral Infections, chapter 42 in *Essentials of Glycobiology*, 3. ed. (Eds.: A. Varki, R. Cummings, J. Esko, et al.), Cold Spring Harbor Laboratory Press, Cold Spring Harbor (NY), **2017**.
- [29] G. G. Anderson, K. W. Dodson, T. M. Hooton, S. J. Hultgren, "Intracellular bacterial communities of uropathogenic *Escherichia coli* in urinary tract pathogenesis", *Trends Microbiol.*, **2004**, *12*, 424-430.
- [30] P. T. Heath, N. K. Nik Yusoff, C. J. Baker, "Neonatal meningitis", *Arch. Dis. Child. Fetal Neonatal Ed.*, **2003**, *88*, F173.
- [31] V. Sperandio, Y. Nguyen, "Enterohemorrhagic *E. coli* (EHEC) pathogenesis", *Front. Cell. Infect. Microbiol.*, **2012**, *2*.
- [32] N. Firon, I. Ofek, N. Sharon, "Carbohydrate specificity of the surface lectins of *Escherichia coli*, *Klebsiella pneumoniae*, and *Salmonella typhimurium*", *Carbohydr. Res.*, **1983**, *120*, 235-249.
- [33] I. Ofek, D. Mirelman, N. Sharon, "Adherence of *Escherichia coli* to human mucosal cells mediated by mannose receptors", *Nature*, **1977**, *265*, 623-625.
- [34] D. Choudhury, A. Thompson, V. Stojanoff, S. Langermann, J. Pinkner, S. J. Hultgren, S. D. Knight, "X-ray Structure of the FimC-FimH Chaperone-Adhesin Complex from Uropathogenic *Escherichia coli*", *Science*, **1999**, *285*, 1061-1066.
- [35] W. J. Allen, G. Phan, G. Waksman, "Pilus biogenesis at the outer membrane of Gram-negative bacterial pathogens", *Curr. Opin. Struct. Biol.*, **2012**, *22*, 500-506.
- [36] N. Firon, S. Ashkenazi, D. Mirelman, I. Ofek, N. Sharon, "Aromatic alpha-glycosides of mannose are powerful inhibitors of the adherence of type 1 fimbriated *Escherichia coli* to yeast and intestinal epithelial cells", *Infect. Immun.*, **1987**, *55*, 472-476.
- [37] a) T. Tomašić, S. Rabbani, M. Gobec, I. M. Raščan, Č. Podlipnik, B. Ernst, M. Anderluh, "Branched  $\alpha$ -D-mannopyranosides: a new class of potent FimH antagonists", *MedChemComm*, **2014**, *5*, 1247-1253; b) L. K. Mydock-McGrane, T. J. Hannan, J. W. Janetka, "Rational design strategies for FimH antagonists: new drugs on the horizon for urinary tract infection and Crohn's disease", *Expert Opin. Drug Discov.*, **2017**, *12*, 711-731; c) M. Touaibia, E.-M. Krammer, T. C. Shiao, N. Yamakawa, Q. Wang, A. Glinschert, A. Papadopoulos, L. Mousavifar, E. Maes, S. Oscarson, G. Vergoten, M. F. Lensink, R. Roy, J. Bouckaert, "Sites for Dynamic Protein-Carbohydrate Interactions of O- and C-Linked Mannosides on the *E. coli* FimH Adhesin", *Molecules*, **2017**, *22*; d) T. Tomašić, S. Rabbani, R. P. Jakob, A. Reisner, Ž. Jakopin, T. Maier, B. Ernst, M. Anderluh, "Does targeting Arg98 of FimH lead to high affinity antagonists?", *Eur. J. Med. Chem.*, **2021**, *211*, 113093.
- [38] a) J. Bouckaert, J. Berglund, M. Schembri, E. De Genst, L. Cools, M. Wuhrer, C.-S. Hung, J. Pinkner, R. Slättegård, A. Zavialov, D. Choudhury, S. Langermann, S. J. Hultgren, L. Wyns, P. Klemm, S. Oscarson, S. D. Knight, H. De Greve, "Receptor binding studies disclose a novel class of high-affinity inhibitors of the *Escherichia coli* FimH adhesin", *Mol. Microbiol.*, **2005**, *55*, 441-

- 455; b) G. A. Rabinovich, M. A. Toscano, S. S. Jackson, G. R. Vasta, "Functions of cell surface galectin-glycoprotein lattices", *Curr. Opin. Struct. Biol.*, **2007**, 17, 513-520.
- [39] a) C. Fasting, C. A. Schalley, M. Weber, O. Seitz, S. Hecht, B. Koksche, J. Demedde, C. Graf, E.-W. Knapp, R. Haag, "Multivalency as a Chemical Organization and Action Principle", *Angew. Chem. Int. Ed.*, **2012**, 51, 10472-10498; b) M. Mammen, S.-K. Choi, G. M. Whitesides, "Polyvalent Interactions in Biological Systems: Implications for Design and Use of Multivalent Ligands and Inhibitors", *Angew. Chem. Int. Ed.*, **1998**, 37, 2754-2794.
- [40] Y. C. Lee, R. T. Lee, "Carbohydrate-Protein Interactions: Basis of Glycobiology", *Acc. Chem. Res.*, **1995**, 28, 321-327.
- [41] J. J. Lundquist, E. J. Toone, "The Cluster Glycoside Effect", *Chem. Rev.*, **2002**, 102, 555-578.
- [42] a) L. L. Kiessling, J. E. Gestwicki, L. E. Strong, "Synthetic Multivalent Ligands as Probes of Signal Transduction", *Angew. Chem. Int. Ed.*, **2006**, 45, 2348-2368; b) J. E. Gestwicki, C. W. Cairo, L. E. Strong, K. A. Oetjen, L. L. Kiessling, "Influencing Receptor-Ligand Binding Mechanisms with Multivalent Ligand Architecture", *J. Am. Chem. Soc.*, **2002**, 124, 14922-14933.
- [43] W. P. Jencks, "On the attribution and additivity of binding energies", *PNAS*, **1981**, 78, 4046.
- [44] S. Howorka, J. Nam, H. Bayley, D. Kahne, "Stochastic Detection of Monovalent and Bivalent Protein-Ligand Interactions", *Angew. Chem. Int. Ed.*, **2004**, 43, 842-846.
- [45] M. Hartmann, T. K. Lindhorst, "The Bacterial Lectin FimH, a Target for Drug Discovery – Carbohydrate Inhibitors of Type 1 Fimbriae-Mediated Bacterial Adhesion", *Eur. J. Org. Chem.*, **2011**, 2011, 3583-3609.
- [46] S. Cecioni, A. Imberty, S. Vidal, "Glycomimetics versus Multivalent Glycoconjugates for the Design of High Affinity Lectin Ligands", *Chem. Rev.*, **2015**, 115, 525-561.
- [47] C. Müller, G. Despras, T. K. Lindhorst, "Organizing multivalency in carbohydrate recognition", *Chem. Soc. Rev.*, **2016**, 45, 3275-3302.
- [48] J. L. Jiménez Blanco, C. Ortiz Mellet, J. M. García Fernández, "Multivalency in heterogeneous glycoenvironments: hetero-glycoclusters, -glycopolymers and -glycoassemblies", *Chem. Soc. Rev.*, **2013**, 42, 4518-4531.
- [49] S. Jiang, S. Niu, Z.-H. Zhao, Z.-J. Li, Q. Li, "Synthesis of a series of novel heteroglycoclusters and homoglycoclusters and the study of their anti-adhesion activities", *Carbohydr. Res.*, **2015**, 414, 39-45.
- [50] a) M. Gómez-García, J. M. Benito, D. Rodríguez-Lucena, J.-X. Yu, K. Chmurski, C. Ortiz Mellet, R. Gutiérrez Gallego, A. Maestre, J. Defaye, J. M. García Fernández, "Probing Secondary Carbohydrate-Protein Interactions with Highly Dense Cyclodextrin-Centered Heteroglycoclusters: The Heterocluster Effect", *J. Am. Chem. Soc.*, **2005**, 127, 7970-7971; b) M. Gómez-García, J. M. Benito, A. P. Butera, C. O. Mellet, J. M. G. Fernández, J. L. J. Blanco, "Probing Carbohydrate-Lectin Recognition in Heterogeneous Environments with Monodisperse Cyclodextrin-Based Glycoclusters", *J. Org. Chem.*, **2012**, 77, 1273-1288; c) M. I. García-Moreno, F. Ortega-Caballero, R. Rísquez-Cuadro, C. Ortiz Mellet, J. M. García Fernández, "The Impact of Heteromultivalency in Lectin Recognition and Glycosidase Inhibition: An Integrated Mechanistic Study", *Chem. Eur. J.*, **2017**, n/a-n/a.

- [51] G. Ragupathi, D. M. Coltart, L. J. Williams, F. Koide, E. Kagan, J. Allen, C. Harris, P. W. Glunz, P. O. Livingston, S. J. Danishefsky, "On the power of chemical synthesis: Immunological evaluation of models for multiantigenic carbohydrate-based cancer vaccines", *PNAS*, **2002**, *99*, 13699.
- [52] a) O. Renaudet, P. Dumy, "Chemoselectively Template-Assembled Glycoconjugates as Mimics for Multivalent Presentation of Carbohydrates", *Org. Lett.*, **2003**, *5*, 243-246; b) B. Thomas, M. Fiore, I. Bossu, P. Dumy, O. Renaudet, "Synthesis of heteroglycoclusters by using orthogonal chemoselective ligations", *Beilstein J. Org. Chem.*, **2012**, *8*, 421-427; c) B. Thomas, M. Fiore, G. C. Daskhan, N. Spinelli, O. Renaudet, "A multi-ligation strategy for the synthesis of heterofunctionalized glycosylated scaffolds", *Chem. Commun.*, **2015**, *51*, 5436-5439; d) D. Goyard, B. Thomas, E. Gillon, A. Imberty, O. Renaudet, "Heteroglycoclusters with dual nanomolar affinities for the lectins LecA and LecB from *Pseudomonas aeruginosa*", *Front. Chem.*, **2019**, *7*, 666.
- [53] "Conformational Nomenclature for Five and Six-Membered Ring Forms of Monosaccharides and Their Derivatives", *Eur. J. Biochem.*, **1980**, *111*, 295-298.
- [54] D. Cremer, J. A. Pople, "General definition of ring puckering coordinates", *J. Am. Chem. Soc.*, **1975**, *97*, 1354-1358.
- [55] A. Bérces, D. M. Whitfield, T. Nukada, "Quantitative description of six-membered ring conformations following the IUPAC conformational nomenclature", *Tetrahedron*, **2001**, *57*, 477-491.
- [56] J. F. Stoddart, *Stereochemistry of carbohydrates*, Vol. 1, Wiley, New York, **1971**.
- [57] C. M. Pedersen, L. U. Nordstrøm, M. Bols, "'Super Armed' Glycosyl Donors: Conformational Arming of Thioglycosides by Silylation", *J. Am. Chem. Soc.*, **2007**, *129*, 9222-9235.
- [58] A. F. Bochkov, Y. V. Voznyi, V. N. Chernetskii, V. M. Dashunin, A. V. Rodionov, "Orthoesters of Sugars .12. Use of Molecular-Sieves in Acid-Catalyzed Transesterification of Orthoesters of Sugars", *B Acad Sci Ussr Ch+*, **1975**, *24*, 348-351.
- [59] Y. Cao, Y. Kasai, M. Bando, M. Kawagoe, H. Yamada, "A 2,4-O-[(Z)-2-butenylene]-bridged glucopyranose: efficient construction of the bicyclic skeleton and its axial-rich twist-boat conformation", *Tetrahedron*, **2009**, *65*, 2574-2578.
- [60] F. W. Lichtenthaler, H. J. Lindner, "On the extent of chair distortion in "tetra-axial" derivatives of 2,3,4-tri-O-benzoyl- $\beta$ -D-xylopyranose", *Carbohydr. Res.*, **1990**, *200*, 91-99.
- [61] a) S. K. Das, J.-M. Mallet, J. Esnault, P.-A. Driguez, P. Duchaussoy, P. Sizun, J.-P. Héroult, J.-M. Herbert, M. Petitou, P. Sinaÿ, "Synthesis of Conformationally Locked Carbohydrates: A Skew-Boat Conformation of L-Iduronic Acid Governs the Antithrombotic Activity of Heparin", *Angew. Chem. Int. Ed.*, **2001**, *40*, 1670-1673; b) M. Remko, C.-W. von der Lieth, "Gas-Phase and Solution Conformations of the  $\alpha$ -L-Iduronic Acid Structural Unit of Heparin", *J. Chem. Inf. Model.*, **2006**, *46*, 1194-1200.
- [62] M. Rico, J. Santoro, "Complete analysis of the  $^1\text{H}$  NMR spectra of acetylated glycals—a conformational study", *Org. Magn. Reson.*, **1976**, *8*, 49-55.
- [63] S. J. Angyal, "The Composition and Conformation of Sugars in Solution", *Angew. Chem. Int. Ed.*, **1969**, *8*, 157-166.

- [64] a) T. Hansen, L. Lebedel, W. A. Remmerswaal, S. van der Vorm, D. P. A. Wander, M. Somers, H. S. Overkleeft, D. V. Filippov, J. Désiré, A. Mingot, Y. Bleriot, G. A. van der Marel, S. Thibaudeau, J. D. C. Codée, "Defining the SN1 Side of Glycosylation Reactions: Stereoselectivity of Glycopyranosyl Cations", *ACS Cent. Sci.*, **2019**, *5*, 781-788; b) H. Satoh, S. Manabe, "Design of chemical glycosyl donors: does changing ring conformation influence selectivity/reactivity?", *Chem. Soc. Rev.*, **2013**, *42*, 4297-4309.
- [65] a) D. J. Vocadlo, G. J. Davies, "Mechanistic insights into glycosidase chemistry", *Curr. Opin. Chem. Biol.*, **2008**, *12*, 539-555; b) G. J. Davies, A. Planas, C. Rovira, "Conformational Analyses of the Reaction Coordinate of Glycosidases", *Acc. Chem. Res.*, **2012**, *45*, 308-316.
- [66] B. Henrissat, G. Davies, "Structural and sequence-based classification of glycoside hydrolases", *Curr. Opin. Struct. Biol.*, **1997**, *7*, 637-644.
- [67] G. Sidhu, S. G. Withers, N. T. Nguyen, L. P. McIntosh, L. Ziser, G. D. Brayer, "Sugar Ring Distortion in the Glycosyl-Enzyme Intermediate of a Family G/11 Xylanase", *Biochemistry*, **1999**, *38*, 5346-5354.
- [68] E. Sabini, G. Sulzenbacher, M. Dauter, Z. Dauter, P. L. Jørgensen, M. Schülein, C. Dupont, G. J. Davies, K. S. Wilson, "Catalysis and specificity in enzymatic glycoside hydrolysis: a 2,5B conformation for the glycosyl-enzyme intermediate revealed by the structure of the *Bacillus agaradhaerens* family 11 xylanase", *Chem. Biol.*, **1999**, *6*, 483-492.
- [69] L. Amorim, F. Marcelo, C. Rousseau, L. Nieto, J. Jiménez-Barbero, J. Marrot, A. P. Rauter, M. Sollogoub, M. Bols, Y. Blériot, "Direct Experimental Evidence for the High Chemical Reactivity of  $\alpha$ - and  $\beta$ -Xylopyranosides Adopting a 2,5B Conformation in Glycosyl Transfer", *Chem. Eur. J.*, **2011**, *17*, 7345-7356.
- [70] Y. Yu, M. Delbianco, "Conformational Studies of Oligosaccharides", *Chem. Eur. J.*, **2020**, *26*, 9814-9825.
- [71] H. A. Taha, M. R. Richards, T. L. Lowary, "Conformational Analysis of Furanoside-Containing Mono- and Oligosaccharides", *Chem. Rev.*, **2013**, *113*, 1851-1876.
- [72] D. R. Ferro, A. Provasoli, M. Ragazzi, G. Torri, B. Casu, G. Gatti, J. C. Jacquinet, P. Sinay, M. Petitou, J. Choay, "Evidence for conformational equilibrium of the sulfated L-iduronate residue in heparin and in synthetic heparin mono- and oligo-saccharides: NMR and force-field studies", *J. Am. Chem. Soc.*, **1986**, *108*, 6773-6778.
- [73] a) S. J. Angyal, "Conformational analysis in carbohydrate chemistry. I. Conformational free energies. The conformations and  $\alpha$ : $\beta$  ratios of aldopyranoses in aqueous solution", *Aust. J. Chem.*, **1968**, *21*, 2737-2746; b) P. R. Sundararajan, V. S. R. Rao, "Theoretical studies on the conformation of aldopyranoses", *Tetrahedron*, **1968**, *24*, 289-295; c) K. Gaweda, W. Plazinski, "Pyranose ring conformations in mono- and oligosaccharides: a combined MD and DFT approach", *Physical Chemistry Chemical Physics*, **2017**, *19*, 20760-20772.
- [74] H. B. Mayes, L. J. Broadbelt, G. T. Beckham, "How Sugars Pucker: Electronic Structure Calculations Map the Kinetic Landscape of Five Biologically Paramount Monosaccharides and Their Implications for Enzymatic Catalysis", *J. Am. Chem. Soc.*, **2014**, *136*, 1008-1022.

- [75] I. Peña, S. Mata, A. Martín, C. Cabezas, A. M. Daly, J. L. Alonso, "Conformations of *d*-xylose: the pivotal role of the intramolecular hydrogen-bonding", *Physical Chemistry Chemical Physics*, **2013**, *15*, 18243-18248.
- [76] A. Siegbahn, U. Aili, A. Ochocinska, M. Olofsson, J. Rönnols, K. Mani, G. Widmalm, U. Ellervik, "Synthesis, conformation and biology of naphthoxylosides", *Biorg. Med. Chem.*, **2011**, *19*, 4114-4126.
- [77] P. Hobley, O. Howarth, R. N. Ibbett, "*1H* and *13C* NMR Shifts for Aldopyranose and Aldofuranose Monosaccharides: Conformational Analysis and Solvent Dependence", *Magn. Reson. Chem.*, **1996**, *34*, 755-760.
- [78] J. Rönnols, S. Manner, A. Siegbahn, U. Ellervik, G. Widmalm, "Exploration of conformational flexibility and hydrogen bonding of xylosides in different solvents, as a model system for enzyme active site interactions", *Org. Biomol. Chem.*, **2013**, *11*, 5465-5472.
- [79] A. D. Bain, "Chemical exchange in NMR", *Prog. Nucl. Magn. Reson. Spectrosc.*, **2003**, *43*, 63-103.
- [80] P. L. Durette, D. Horton, Conformational Analysis of Sugars and Their Derivatives in *Adv. Carbohydr. Chem. Biochem.*, Vol. 26 (Eds.: R. S. Tipson, D. Horton), Academic Press, **1971**, pp. 49-125.
- [81] C. A. G. Haasnoot, F. A. A. M. de Leeuw, C. Altona, "The relationship between proton-proton NMR coupling constants and substituent electronegativities—I: An empirical generalization of the Karplus equation", *Tetrahedron*, **1980**, *36*, 2783-2792.
- [82] V. V. Samoshin, "Conformational control of cyclohexane products by external stimuli", *Rev. J. Chem.*, **2011**, *1*, 250.
- [83] a) H. Yuasa, "Ring flip of carbohydrates: Functions and Applications", *Trends Glycosci. Glycobiol.*, **2006**, *18*, 353-370; b) T. Tyrikos-Ergas, G. Fittolani, P. H. Seeberger, M. Delbianco, "Structural Studies Using Unnatural Oligosaccharides: Toward Sugar Foldamers", *Biomacromolecules*, **2019**.
- [84] R. Sagar, S. Rudić, D. P. Gamblin, E. M. Scanlan, T. D. Vaden, B. Odell, T. D. W. Claridge, J. P. Simons, B. G. Davis, "Conformational effects in sugar ions: spectroscopic investigations in the gas phase and in solution", *Chem. Sci.*, **2012**, *3*, 2307-2313.
- [85] A. J. Ratcliffe, B. Fraser-Reid, "Generation of  $\alpha$ -D-glucopyranosylacetoneitrilium ions. Concerning the reverse anomeric effect", *J. Chem. Soc., Perkin Trans. 1*, **1990**, 747-750.
- [86] F. Coutrot, E. Busseron, "Controlling the Chair Conformation of a Mannopyranose in a Large-Amplitude [2]Rotaxane Molecular Machine", *Chem. Eur. J.*, **2009**, *15*, 5186-5190.
- [87] T. Holmstrøm, D. Raydan, C. M. Pedersen, "Easy access to a carbohydrate-based template for stimuli-responsive surfactants", *Beilstein J. Org. Chem.*, **2020**, *16*, 2788-2794.
- [88] T. Holmstrøm, M. Galsgaard Malle, S. Wu, K. J. Jensen, N. S. Hatzakis, C. M. Pedersen, "Carbohydrate-Derived Metal-Chelator-Triggered Lipids for Liposomal Drug Delivery", *Chem. Eur. J.*, **2021**, *27*, 6917-6922.
- [89] A. D. Bruyn, M. Anteunis, R. v. Rijsbergen, M. Claeysens, P. Kováč, "*1H* NMR Study of Methyl O-Acetyl- $\alpha$ - and - $\beta$ -D-Xylopyranosides Conformational Studies and Non Additivity of *1H*-Shift Increments", *J. Carbohydr. Chem.*, **1982**, *1*, 301-309.

- [90] H. Yuasa, H. Hashimoto, "Bending Trisaccharides by a Chelation-Induced Ring Flip of a Hinge-Like Monosaccharide Unit", *J. Am. Chem. Soc.*, **1999**, 121, 5089-5090.
- [91] a) T. Izumi, H. Hashimoto, H. Yuasa, "Switching extended 1,3-diequatorial and bent 1,3-diaxial states of a disubstituted hinge sugar by ligand exchange reactions on Pt(II)", *Chem. Commun.*, **2004**, 94-95; b) H. Yuasa, T. Izumi, N. Mitsuhashi, Y. Kajihara, H. Hashimoto, "An Improvement in the Bending Ability of a Hinged Trisaccharide with the Assistance of a Sugar—Sugar Interaction", *Chem. Eur. J.*, **2005**, 11, 6478-6490.
- [92] a) H. Yuasa, N. Miyagawa, T. Izumi, M. Nakatani, M. Izumi, H. Hashimoto, "Hinge Sugar as a Movable Component of an Excimer Fluorescence Sensor", *Org. Lett.*, **2004**, 6, 1489-1492; b) H. Yuasa, N. Miyagawa, M. Nakatani, M. Izumi, H. Hashimoto, "A tong-like fluorescence sensor for metal ions: perfect conformational switch of hinge sugar by pyrene stacking", *Org. Biomol. Chem.*, **2004**, 2, 3548-3556.
- [93] J. Takeuchi, A. Ohkubo, H. Yuasa, "A Ring-Flippable Sugar as a Stimuli-Responsive Component of Liposomes", *Chem. Asian J.*, **2015**, 10, 586-594.
- [94] K. Sakakibara, T. Fujisawa, J. P. Hill, K. Ariga, "Conformational interchange of a carbohydrate by mechanical compression at the air–water interface", *Physical Chemistry Chemical Physics*, **2014**, 16, 10286-10294.
- [95] a) S. Hakomori, "Carbohydrate-to-carbohydrate interaction in basic cell biology: a brief overview", *Arch. Biochem. Biophys.*, **2004**, 426, 173-181; b) N. Strömberg, P. G. Nyholm, I. Pascher, S. Normark, "Saccharide orientation at the cell surface affects glycolipid receptor function", *PNAS*, **1991**, 88, 9340-9344.
- [96] A. Regina Todeschini, S.-i. Hakomori, "Functional role of glycosphingolipids and gangliosides in control of cell adhesion, motility, and growth, through glycosynaptic microdomains", *Biochim. Biophys. Acta Gen. Subj.*, **2008**, 1780, 421-433.
- [97] Z. Wang, Z. S. Chinoy, S. G. Ambre, W. Peng, R. McBride, R. P. de Vries, J. Glushka, J. C. Paulson, G.-J. Boons, "A General Strategy for the Chemoenzymatic Synthesis of Asymmetrically Branched N-Glycans", *Science*, **2013**, 341, 379-383.
- [98] a) T. Weber, V. Chandrasekaran, I. Stamer, M. B. Thygesen, A. Terfort, T. K. Lindhorst, "Switching of Bacterial Adhesion to a Glycosylated Surface by Reversible Reorientation of the Carbohydrate Ligand", *Angew. Chem. Int. Ed.*, **2014**, 53, 14583-14586; b) L. Möckl, A. Müller, C. Bräuchle, T. K. Lindhorst, "Switching first contact: photocontrol of *E. coli* adhesion to human cells", *Chem. Commun.*, **2016**, 52, 1254-1257; c) G. Despras, L. Möckl, A. Heitmann, I. Stamer, C. Bräuchle, T. K. Lindhorst, "A Photoswitchable Trivalent Cluster Mannoside to Probe the Effects of Ligand Orientation in Bacterial Adhesion", *ChemBioChem*, **2019**, 20, 2373-2382; d) E. Fast, A. Schlimm, I. Lautenschläger, K. U. Clausen, T. Strunskus, C. Spormann, T. K. Lindhorst, F. Tucek, "Improving the Switching Capacity of Glyco-Self-Assembled Monolayers on Au(111)", *Chem. Eur. J.*, **2020**, 26, 485-501.
- [99] V. Chandrasekaran, H. Jacob, F. Petersen, K. Kathirvel, F. Tucek, T. K. Lindhorst, "Synthesis and surface-spectroscopic characterization of photoisomerizable glyco-SAMs on Au(111)", *Chemistry*, **2014**, 20, 8744-8752.

- [100] J. Brekalo, G. Despras, T. K. Lindhorst, "Pseudoenantiomeric glycoclusters: synthesis and testing of heterobivalency in carbohydrate–protein interactions", *Org. Biomol. Chem.*, **2019**, *17*, 5929-5942.
- [101] V. Ingrid, F. Barbara La, N. Francesco, "Carbohydrate-Based Molecular Scaffolding", *J. Carbohydr. Chem.*, **2006**, *25*, 97-138.
- [102] W. Meutermans, G. T. Le, B. Becker, "Carbohydrates as Scaffolds in Drug Discovery", *ChemMedChem*, **2006**, *1*, 1164-1194.
- [103] a) C. Kieburg, M. Dubber, T. K. Lindhorst, "A New Type of Carbohydrate Clustering: Synthesis of a Pentavalent Glycocluster Based on a Carbohydrate Core", *Synlett*, **1997**, *12*, 1447-1449; b) M. Dubber, T. K. Lindhorst, "Synthesis of octopus glycosides: core molecules for the construction of glycoclusters and carbohydrate-centered dendrimers", *Carbohydr. Res.*, **1998**, *310*, 35-41.
- [104] a) M. Dubber, T. K. Lindhorst, "Synthesis of carbohydrate-centered oligosaccharide mimetics equipped with a functionalized tether", *J. Org. Chem.*, **2000**, *65*, 6292; b) M. Dubber, T. K. Lindhorst, "Trehalose-Based Octopus Glycosides for the Synthesis of Carbohydrate-Centered PAMAM Dendrimers and Thiourea-Bridged Glycoclusters", *Org. Lett.*, **2001**, *3*, 4019-4022; c) T. K. Lindhorst, M. Dubber, "Octopus glycosides: multivalent molecular platforms for testing carbohydrate recognition and bacterial adhesion", *Carbohydr. Res.*, **2015**, *403*, 90-97.
- [105] R. P. McGeary, I. Jablonkai, I. Toth, "Carbohydrate-based templates for synthetic vaccines and drug delivery", *Tetrahedron*, **2001**, *57*, 8733-8742.
- [106] G. Thanh Le, G. Abbenante, B. Becker, M. Grathwohl, J. Halliday, G. Tometzki, J. Zuegg, W. Meutermans, "Molecular diversity through sugar scaffolds", *Drug Discov. Today*, **2003**, *8*, 701-709.
- [107] a) C. Kieburg, K. Sadalapure, T. K. Lindhorst, "Glucose-Based AB<sub>2</sub>-Building Blocks for the Construction of Branched Glycopeptidomimetics", *Eur. J. Org. Chem.*, **2000**, *2000*, 2035-2040; b) K. Sadalapure, T. K. Lindhorst, "A General Entry into Glycopeptide "Dendrons"", *Angew. Chem. Int. Ed.*, **2000**, *39*, 2010-2013; c) A. Patel, Thisbe K. Lindhorst, "Synthesis of "Mixed Type" Oligosaccharide Mimetics Based on a Carbohydrate Scaffold", *Eur. J. Org. Chem.*, **2002**, *2002*, 79-86; d) M. Dubber, O. Sperling, T. K. Lindhorst, "Oligomannoside mimetics by glycosylation of 'octopus glycosides' and their investigation as inhibitors of type 1 fimbriae-mediated adhesion of *Escherichia coli*", *Org. Biomol. Chem.*, **2006**, *4*, 3901-3912.
- [108] A. K. Ciuk, T.-E. Gloe, T. K. Lindhorst, "Carbohydrate-Scaffolded Thymine Multimers: Scope and Limitations of the Allylation–Hydroboration Sequence", *Eur. J. Org. Chem.*, **2018**, *2018*, 6971-6982.
- [109] T. Opatz, C. Kallus, T. Wunberg, W. Schmidt, S. Henke, H. Kunz, "D-Glucose as a pentavalent chiral scaffold", *Eur. J. Org. Chem.*, **2003**, 1527-1536.
- [110] N. Moitessier, C. Henry, N. Aubert, Y. Chapleur, "Orthogonally protected carbohydrate-based scaffolds", *Tetrahedron Lett.*, **2005**, *46*, 6191-6194.
- [111] S. O. Jaeschke, "Synthesis of multifunctional glycoconjugates, Master Thesis", CAU Kiel, **2016**.
- [112] S. O. Jaeschke, I. vom Sondern, T. K. Lindhorst, "Synthesis of regioisomeric maltose-based Man/Glc glycoclusters to control glycoligand presentation in 3D space", *Org. Biomol. Chem.*, **2021**, *19*, 7013-7023.

## References

---

- [113] T. Tanaka, W. C. Huang, M. Noguchi, A. Kobayashi, S.-i. Shoda, "Direct synthesis of 1,6-anhydro sugars from unprotected glycopyranoses by using 2-chloro-1,3-dimethylimidazolium chloride", *Tetrahedron Lett.*, **2009**, 50, 2154-2157.
- [114] G. Zemplén, E. Pascu, "Über die Verseifung acetylierter Zucker und verwandter Substanzen", *Ber. dtsch. Chem. Ges. A/B*, **1929**, 62, 1613-1614.
- [115] J. Gao, X. Li, G. Gu, S. Liu, M. Cui, H.-X. Lou, "Facile synthesis of triterpenoid saponins bearing  $\beta$ -Glu/Gal-(1 $\rightarrow$ 3)- $\beta$ -GluA methyl ester and their cytotoxic activities", *Bioorg. Med. Chem. Lett.*, **2012**, 22, 2396-2400.
- [116] B. Lal, B. N. Pramanik, M. S. Manhas, A. K. Bose, "Diphenylphosphoryl Azide - Novel Reagent for Stereospecific Synthesis of Azides from Alcohols", *Tetrahedron Lett.*, **1977**, 1976-1980.
- [117] A. S. Thompson, G. R. Humphrey, A. M. DeMarco, D. J. Mathre, E. J. J. Grabowski, "Direct conversion of activated alcohols to azides using diphenyl phosphorazidate. A practical alternative to Mitsunobu conditions", *J. Org. Chem.*, **1993**, 58, 5886-5888.
- [118] N. K. Richtmyer, The Altrose Group of Substances in *Adv. Carbohydr. Chem.*, Vol. Volume 1 (Eds.: W. W. Pigman, M. L. Wolfrom), Academic Press, **1945**, pp. 37-76.
- [119] R. R. Schmidt, "Neue Methoden zur Glycosid- und Oligosaccharidsynthese – gibt es Alternativen zur Koenigs-Knorr-Methode?", *Angew. Chem.*, **1986**, 98, 213-236.
- [120] G. Excoffier, D. Gagnaire, J.-P. Utile, "Coupure sélective par l'hydrazine des groupements acétyles anomères de résidus glycosyles acétylés", *Carbohydr. Res.*, **1975**, 39, 368-373.
- [121] R. R. Schmidt, J. Michel, "Facile Synthesis of  $\alpha$ - and  $\beta$ -O-Glycosyl Imidates; Preparation of Glycosides and Disaccharides", *Angew. Chem. Int. Ed.*, **1980**, 19, 731-732.
- [122] F. S. Ekholm, M. Poláková, A. J. Pawłowicz, R. Leino, "Synthesis of Divalent 2,2'-Linked Mannose Derivatives by Homodimerization", *Synthesis*, **2009**, 2009, 567-576.
- [123] N. E. Byramova, M. V. Ovchinnikov, L. V. Backinowsky, N. K. Kochetkov, "Selective Removal of O-Acetyl Groups in the Presence of O-Benzoyl Groups by Acid-Catalyzed Methanolysis", *Carbohydr Res*, **1983**, 124, C8-C11.
- [124] P. Pornsuriyasak, S. C. Ranade, A. Li, M. C. Parlato, C. R. Sims, O. V. Shulga, K. J. Stine, A. V. Demchenko, "STICS: surface-tethered iterative carbohydrate synthesis", *Chem. Commun.*, **2009**, 1834-1836.
- [125] D. L. Hughes, "Progress in the Mitsunobu Reaction. A Review", *Org. Prep. Proced. Int.*, **1996**, 28, 127-164.
- [126] M. A. Walker, "A High Yielding Synthesis of N-Alkyl Maleimides Using a Novel Modification of the Mitsunobu Reaction", *J. Org. Chem.*, **1995**, 60, 5352-5355.
- [127] J. S. Debenham, R. Madsen, C. Roberts, B. Fraser-Reid, "Two New Orthogonal Amine-Protecting Groups that can be Cleaved under Mild or Neutral Conditions", *J. Am. Chem. Soc.*, **1995**, 117, 3302-3303.
- [128] Z. J. Jia, S. Kelberlau, L. Olsson, G. Anilkumar, B. Fraser-Reid, "The Mitsunobu Reaction of Tetrachlorophthalimide", *Synlett*, **1999**, 1999, 565-566.
- [129] B. W. Greatrex, S. J. Brodie, R. H. Furneaux, S. M. Hook, W. T. McBurney, G. F. Painter, T. Rades, P. M. Rendle, "The synthesis and immune stimulating action of mannose-capped lysine-based dendrimers", *Tetrahedron*, **2009**, 65, 2939-2950.

- [130] Q. Wang, Z. Huang, J. Ma, X. Lu, L. Zhang, X. Wang, P. George Wang, "Design, synthesis and biological evaluation of a novel series of glycosylated platinum(IV) complexes as antitumor agents", *Dalton Trans.*, **2016**, 45, 10366-10374.
- [131] M. Zottola, B. V. Rao, B. Fraser-Reid, "A mild procedure for cleavage of 1,6-anhydro sugars", *J. Chem. Soc., Chem. Commun.*, **1991**, 969-970.
- [132] A. Y. Shaikh, S. Das, D. Pati, V. Dhaware, S. Sen Gupta, S. Hotha, "Cationic Charged Helical Glycopolyptide Using Ring Opening Polymerization of 6-Deoxy-6-azido-glyco-N-carboxyanhydride", *Biomacromolecules*, **2014**, 15, 3679-3686.
- [133] N. Röckendorf, T. K. Lindhorst, "Glucuronic Acid Derivatives as Branching Units for the Synthesis of Glycopeptide Mimetics", *J. Org. Chem.*, **2004**, 69, 4441-4445.
- [134] D. A. Fulton, A. R. Pease, J. F. Stoddart, "Cyclodextrin-based carbohydrate clusters by amide bond formation", *Isr. J. Chem.*, **2000**, 40, 325-333.
- [135] E. Saxon, C. R. Bertozzi, "Cell Surface Engineering by a Modified Staudinger Reaction", *Science*, **2000**, 287, 2007-2010.
- [136] H. Staudinger, J. Meyer, "Über neue organische Phosphorverbindungen III. Phosphinmethylenderivate und Phosphinimine", *Helv. Chim. Acta*, **1919**, 2, 635-646.
- [137] M. Mizuno, I. Muramoto, K. Kobayashi, H. Yaginuma, T. Inazu, "A Simple Method for the Synthesis of N $\beta$ -Glycosylated-Asparagine and -Glutamine Derivatives", *Synthesis*, **1999**, 1999, 162-165.
- [138] I. Aumüller, T. K. Lindhorst, "Chromophore-Supported Purification in Parallel Synthesis", *Eur. J. Org. Chem.*, **2006**, 2006, 1103-1108.
- [139] N. Rolland, G. Vass, J. Cleophax, A.-M. Sepulchre, S. D. Gero, A. Cier, "Synthèse totale d' $\alpha$ -disaccharidyles de tridésoxy-2,5,6-streptamine apparentés aux aminosides à partir du maltose et du lactose", *Helv. Chim. Acta*, **1982**, 65, 1627-1636.
- [140] S. G. Gouin, J. Kovensky, "Direct azidation of unprotected carbohydrates with PPh<sub>3</sub>/CBr<sub>4</sub>/NaN<sub>3</sub>. Modulation of the degree of substitution", *Tetrahedron Lett.*, **2007**, 48, 2875-2879.
- [141] D. H. Brauns, "Optical rotation and atomic dimension. VIII. Halogeno-hepta-acetyl derivatives of melibiose and maltose. The structures of bioses and cellulose", *J. Am. Chem. Soc.*, **1929**, 51, 1820-1831.
- [142] E. A. J. Post, S. P. Fletcher, "Controlling the Kinetics of Self-Reproducing Micelles by Catalyst Compartmentalization in a Biphasic System", *J. Org. Chem.*, **2019**, 84, 2741-2755.
- [143] J. Jiménez Blanco, J. García Fernández, A. Gadelle, J. Defaye, "A mild one-step selective conversion of primary hydroxyl groups into azides in mono- and oligo-saccharides", *Carbohydr. Res.*, **1997**, 303, 367-372.
- [144] S. Yan, N. Ding, W. Zhang, P. Wang, Y. Li, M. Li, "An efficient and recyclable catalyst for the cleavage of tert-butyl diphenylsilyl ethers", *Carbohydr. Res.*, **2012**, 354, 6-20.
- [145] M. Yamagami, H. Kamitakahara, A. Yoshinaga, T. Takano, "Thermo-reversible supramolecular hydrogels of trehalose-type diblock methylcellulose analogues", *Carbohydr. Polym.*, **2018**, 183, 110-122.
- [146] M. Hartmann, A. K. Horst, P. Klemm, T. K. Lindhorst, "A kit for the investigation of live *Escherichia coli* cell adhesion to glycosylated surfaces", *Chem Commun (Camb)*, **2010**, 46, 330-332.

- [147] A. Reisner, J. A. J. Haagenzen, M. A. Schembri, E. L. Zechner, S. Molin, "Development and maturation of *Escherichia coli* K-12 biofilms", *Mol. Microbiol.*, **2003**, *48*, 933-946.
- [148] M. González-Cuesta, C. Ortiz Mellet, J. M. García Fernández, "Carbohydrate supramolecular chemistry: beyond the multivalent effect", *Chem. Commun.*, **2020**, *56*, 5207-5222.
- [149] Schrödinger Release 2020-4: Glide, Schrödinger, New York, NY, **2020**.
- [150] Schrödinger Release 2020-4: Maestro, Schrödinger, LLC, New York, NY, **2020**.
- [151] Schrödinger Release 2020-4: LigPrep, Schrödinger, New York, NY, **2020**.
- [152] C.-S. Hung, J. Bouckaert, D. Hung, J. Pinkner, C. Widberg, A. DeFusco, C. G. Auguste, R. Strouse, S. Langermann, G. Waksman, S. J. Hultgren, "Structural basis of tropism of *Escherichia coli* to the bladder during urinary tract infection", *Mol. Microbiol.*, **2002**, *44*, 903-915.
- [153] Schrödinger Release 2020-4: Prime, Schrödinger, LLC, New York, NY, **2020**.
- [154] a) A. Wellens, M. Lahmann, M. Touaibia, J. Vaucher, S. Oscarson, R. Roy, H. Remaut, J. Bouckaert, "The Tyrosine Gate as a Potential Entropic Lever in the Receptor-Binding Site of the Bacterial Adhesin *FimH*", *Biochemistry*, **2012**, *51*, 4790-4799; b) S. Rabbani, E.-M. Krammer, G. Roos, A. Zalewski, R. Preston, S. Eid, P. Zihlmann, M. Prevost, M. F. Lensink, A. Thompson, B. Ernst, J. Bouckaert, "Mutation of Tyr137 of the universal *Escherichia coli* fimbrial adhesin *FimH* relaxes the tyrosine gate prior to mannose binding", *IUCrJ*, **2017**, *4*, 7-23.
- [155] a) Schrödinger Release 2020-4: Induced Fit Docking protocol; Glide, Schrödinger, LLC, New York, NY, **2020**; b) Schrödinger Release 2020-4: Induced Fit Docking protocol; Prime, Schrödinger, LLC, New York, NY, **2020**.
- [156] Schrödinger Release 2020-4: Desmond Molecular Dynamics System, D. E. S. Research, New York, **2020**.
- [157] A. J. Clark, P. Tiwary, K. Borrelli, S. Feng, E. B. Miller, R. Abel, R. A. Friesner, B. J. Berne, "Prediction of Protein-Ligand Binding Poses via a Combination of Induced Fit Docking and Metadynamics Simulations", *J. Chem. Theory Comput.*, **2016**, *12*, 2990-2998.
- [158] P. Tompa, "The principle of conformational signaling", *Chem. Soc. Rev.*, **2016**, *45*, 4252-4284.
- [159] a) S. A. Tatulian, "Structural Dynamics of Insulin Receptor and Transmembrane Signaling", *Biochemistry*, **2015**, *54*, 5523-5532; b) C. W. Ward, M. C. Lawrence, "Ligand-induced activation of the insulin receptor: a multi-step process involving structural changes in both the ligand and the receptor", *BioEssays*, **2009**, *31*, 422-434.
- [160] a) C. A. G. Haasnoot, R. de Gelder, H. Kooijman, E. R. Kellenbach, "The conformation of the idopyranose ring revisited: How subtle O-substituent induced changes can be deduced from vicinal <sup>1</sup>H-NMR coupling constants", *Carbohydr. Res.*, **2020**, *496*, 108052; b) P.-H. Hsieh, D. F. Thieker, M. Guerrini, R. J. Woods, J. Liu, "Uncovering the Relationship between Sulphation Patterns and Conformation of Iduronic Acid in Heparan Sulphate", *Sci. Rep.*, **2016**, *6*, 29602.
- [161] K. Skarbek, M. J. Milewska, "Biosynthetic and synthetic access to amino sugars", *Carbohydr. Res.*, **2016**, *434*, 44-71.
- [162] S. O. Jaeschke, T. K. Lindhorst, "Versatile Synthesis of Diaminoxylosides via Iodosulfonamidation of Xylal Derivatives", *Eur. J. Org. Chem.*, **2021**, *2021*, 6312-6318.
- [163] M. Jacobsson, J. Malmberg, U. Ellervik, "Aromatic O-glycosylation", *Carbohydr. Res.*, **2006**, *341*, 1266-1281.

- [164] A. Phanumartwiwath, T. W. Hornsby, J. Jamalis, C. D. Bailey, C. L. Willis, "Silyl Migrations in *d*-Xylose Derivatives: Total Synthesis of a Marine Quinoline Alkaloid", *Org. Lett.*, **2013**, 15, 5734-5737.
- [165] R. Lopez, A. Fernandez-Mayoralas, "Enzymic  $\beta$ -Galactosidation of Modified Monosaccharides: Study of the Enzyme Selectivity for the Acceptor and Its Application to the Synthesis of Disaccharides", *J. Org. Chem.*, **1994**, 59, 737-745.
- [166] E. N. Underlin, M. Böhm, R. Madsen, "Synthesis of Arabinoxylan Oligosaccharides by Preactivation-Based Iterative Glycosylations", *J. Org. Chem.*, **2019**, 84, 16036-16054.
- [167] M. Cerny, J. Stanek, J. Pacak, "Syntheses with Anhydro Sugars .6. Reactivity of *p*-Toluenesulfonyl Esters of 1,6-Anhydro- $\beta$ -D-Glucopyranose during Formation of Epoxy Derivatives in Alkaline Medium", *Collect. Czech. Chem. Commun.*, **1969**, 34, 849-8.
- [168] M. Cerny, "Chemistry of anhydro sugars", *Adv. Carbohydr. Chem. Biochem.*, **2003**, 58, 121-198.
- [169] Y. Nishida, J. Thiem, "Convenient synthetic approach towards C-3 modified methyl  $\beta$ -lactosides", *Carbohydr. Res.*, **1994**, 263, 295-301.
- [170] S. Arndt, L. C. Hsieh-Wilson, "Use of Cerny Epoxides for the Accelerated Synthesis of Glycosaminoglycans", *Org. Lett.*, **2003**, 5, 4179-4182.
- [171] P. K. Vasudeva, M. Nagarajan, "Ring opening reactions of benzyl 2,3-anhydro- $\alpha$ -D-ribofuranoside with nucleophiles", *Tetrahedron*, **1996**, 52, 5607-5616.
- [172] U. Zehavi, N. Sharon, "Synthesis of methyl 2,4-diacetamido-2,4,6-trideoxy hexopyranosides", *J. Org. Chem.*, **1972**, 37, 2141-2145.
- [173] G. Janairo, W. Kowolik, W. Voelter, "Reaction of Trimethylsilyl Azide with Anhydro Sugars, a Mild Method of Oxirane-Ring Opening", *Liebigs Ann. Chem.*, **1987**, 1987, 165-167.
- [174] A. Banaszek, V. Zaitsev, "2,4-Diazido-2,4,6-trideoxy-*l*-hexopyranoses as valuable building units in the synthesis of natural products", *Tetrahedron: Asymmetry*, **2004**, 15, 299-306.
- [175] V. Popsavin, G. Benedeković, M. Popsavin, B. Srećo, D. Djoković, "Regiochemistry of epoxide ring opening in methyl 2,3-anhydro-4-azido-4-deoxy- $\alpha$ - and  $\beta$ -*l*-lyxopyranosides", *Carbohydr. Res.*, **2005**, 340, 1866-1871.
- [176] H. M. Zuurmond, P. A. M. van der Klein, G. A. van der Marel, J. H. van Boom, "A stereospecific approach towards the synthesis of 2-deoxy  $\alpha$ - and  $\beta$ -glycosides based on a 1,2-ethyl (phenyl) thio group migration", *Tetrahedron*, **1993**, 49, 6501-6514.
- [177] C. Maioreanu, A. Kanai, J. M. Weibel, P. Pale, "Synthesis of 2-Deoxy-2-thiophenylglucosyl Azides through 1,2 Thio Migration of Thiophenyl Mannosides", *J. Carbohydr. Chem.*, **2005**, 24, 831-842.
- [178] F. Sajtos, L. Lázár, A. Borbás, I. Bajza, A. Lipták, "Glycosyl azides of sugar 2-sulfonic acids", *Tetrahedron Lett.*, **2005**, 46, 5191-5194.
- [179] D. Kahne, S. Walker, Y. Cheng, D. Van Engen, "Glycosylation of unreactive substrates", *J. Am. Chem. Soc.*, **1989**, 111, 6881-6882.
- [180] R. R. Gadikota, C. S. Callam, T. L. Lowary, "Stereocontrolled Synthesis of 2,3-Anhydro- $\beta$ -*d*-lyxofuranosyl Glycosides", *Org. Lett.*, **2001**, 3, 607-610.
- [181] M. Carpintero, I. Nieto, A. Fernández-Mayoralas, "Stereospecific Synthesis of  $\alpha$ - and  $\beta$ -C-Glycosides from Glycosyl Sulfoxides: Scope and Limitations", *J. Org. Chem.*, **2001**, 66, 1768-1774.

## References

---

- [182] A. Bouzide, N. LeBerre, G. Sauvé, "Silver(I) oxide-mediated facile and practical sulfonylation of alcohols", *Tetrahedron Lett.*, **2001**, 42, 8781-8783.
- [183] J. F. Moya-López, E. Elhalem, R. Recio, E. Álvarez, I. Fernández, N. Khiar, "Studies on the diastereoselective oxidation of 1-thio- $\beta$ -D-glucopyranosides: synthesis of the usually less favoured RS sulfoxide as a single diastereoisomer", *Org. Biomol. Chem.*, **2015**, 13, 1904-1914.
- [184] H. H. Kinfé, "Versatility of glycols in synthetic organic chemistry: coupling reactions, diversity oriented synthesis and natural product synthesis", *Org. Biomol. Chem.*, **2019**, 17, 4153-4182.
- [185] K. Parkan, R. Pohl, M. Kotora, "Cross-Coupling Reaction of Saccharide-Based Alkenyl Boronic Acids with Aryl Halides: The Synthesis of Bergenin", *Chem. Eur. J.*, **2014**, 20, 4414-4419.
- [186] R. L. Halcomb, S. J. Danishefsky, "On the direct epoxidation of glycols: application of a reiterative strategy for the synthesis of  $\beta$ -linked oligosaccharides", *J. Am. Chem. Soc.*, **1989**, 111, 6661-6666.
- [187] M. Gehrke, F. X. Aichner, "Über das Arabinal", *Ber. Dtsch. Chem. Ges.*, **1927**, 60, 918-922.
- [188] E. Fischer, K. Zach, "Reduction of acetobromoglucose", *Sitzber. Kgl. Preuss. Akad. Wiss.*, **1913**, 16, 311-317.
- [189] K. Bischofberger, R. H. Hall, "The preparation of stable furanoid glycols by the method of Fischer and Zach", *Carbohydr. Res.*, **1976**, 52, 223-227.
- [190] H. Chen, T. Xian, W. Zhang, W. Si, X. Luo, B. Zhang, M. Zhang, Z. Wang, J. Zhang, "An efficient method for the synthesis of pyranoid glycols", *Carbohydr. Res.*, **2016**, 431, 42-46.
- [191] R. U. Lemieux, R. M. Ratcliffe, "The azidonitration of tri-O-acetyl-D-galactal", *Can. J. Chem.*, **1979**, 57, 1244-1251.
- [192] T. Linker, D. Schanzenbach, E. Elamparuthi, T. Sommermann, W. Fudickar, V. Gyóllai, L. Somsák, W. Demuth, M. Schmittel, "Remarkable Oxidation Stability of Glycols: Excellent Substrates for Cerium(IV)-Mediated Radical Reactions", *J. Am. Chem. Soc.*, **2008**, 130, 16003-16010.
- [193] T. Linker, "Addition of Heteroatom Radicals to endo-Glycols †", *Chemistry*, **2020**, 2, 80-92.
- [194] H. Hashimoto, K. Araki, Y. Saito, M. Kawa, J. Yoshimura, "Preparation of 2-Azido-2-deoxypentose Derivatives", *Bull. Chem. Soc. Jpn.*, **1986**, 59, 3131-3136.
- [195] C. Plattner, M. Höfener, N. Sewald, "One-Pot Azidochlorination of Glycols", *Org. Lett.*, **2011**, 13, 545-547.
- [196] T. Toyokuni, S. Cai, B. Dean, "Use of Hydrazine Acetate as a Mild and Efficient Reagent for Anomeric Denitration of Carbohydrates", *Synthesis*, **1992**, 1992, 1236-1238.
- [197] F. Gauffeny, A. Marra, L. K. Shi Shun, P. Sinaÿ, C. Tabeur, "A novel and convenient method for the removal of a nitrate group at the anomeric position", *Carbohydr. Res.*, **1991**, 219, 237-240.
- [198] A. Chennaiah, Y. D. Vankar, "One-Step TEMPO-Catalyzed and Water-Mediated Stereoselective Conversion of Glycols into 2-Azido-2-deoxysugars with a PIFA-Trimethylsilyl Azide Reagent System", *Org. Lett.*, **2018**, 20, 2611-2614.
- [199] T. K. Page, T. Wirth, "Simple Direct Synthesis of [Bis(trifluoroacetoxy)iodo]arenes", *Synthesis*, **2006**, 2006, 3153-3155.

- [200] H. Gold, S. Munneke, J. Dinkelaar, H. S. Overkleef, J. M. F. G. Aerts, J. D. C. Codée, G. A. van der Marel, "A practical synthesis of capped 4-methylumbelliferyl hyaluronan disaccharides and tetrasaccharides as potential hyaluronidase substrates", *Carbohydr. Res.*, **2011**, *346*, 1467-1478.
- [201] J. F. Batey, C. Bullock, E. O'Brien, J. M. Williams, "The selective benzylation of monosaccharides", *Carbohydr. Res.*, **1975**, *43*, 43-50.
- [202] T. K. Lindhorst, J. Thiem, "Synthesis of 4-deoxy and 4-deoxy-4-halogeno derivatives of l-fucose as potential enzyme inhibitors", *Carbohydr. Res.*, **1991**, *209*, 119-129.
- [203] B. Elchert, J. Li, J. Wang, Y. Hui, R. Rai, R. Ptak, P. Ward, J. Y. Takemoto, M. Bensaci, C.-W. T. Chang, "Application of the Synthetic Aminosugars for Glycodiversification: Synthesis and Antimicrobial Studies of Pyranmycin", *J. Org. Chem.*, **2004**, *69*, 1513-1523.
- [204] T. Wang, A. V. Demchenko, "Synthesis of carbohydrate building blocks via regioselective uniform protection/deprotection strategies", *Org. Biomol. Chem.*, **2019**, *17*, 4934-4950.
- [205] B. J. Beahm, K. W. Dehnert, N. L. Derr, J. Kuhn, J. K. Eberhart, D. Spillmann, S. L. Amacher, C. R. Bertozzi, "A Visualizable Chain-Terminating Inhibitor of Glycosaminoglycan Biosynthesis in Developing Zebrafish", *Angew. Chem. Int. Ed.*, **2014**, *53*, 3347-3352.
- [206] N. Lunau, K. Seelhorst, S. Kahl, K. Tscherch, C. Stacke, S. Rohn, J. Thiem, U. Hahn, C. Meier, "Fluorescently Labeled Substrates for Monitoring  $\alpha$ 1,3-Fucosyltransferase IX Activity", *Chem. Eur. J.*, **2013**, *19*, 17379-17390.
- [207] J. Zhang, S. Singh, R. R. Hughes, M. Zhou, M. Sunkara, A. J. Morris, J. S. Thorson, "A Simple Strategy for Glycosyltransferase-Catalyzed Aminosugar Nucleotide Synthesis", *ChemBioChem*, **2014**, *15*, 647-651.
- [208] a) J. Zhao, S. Wei, X. Ma, H. Shao, "A simple and convenient method for the synthesis of pyranoid glycols", *Carbohydr. Res.*, **2010**, *345*, 168-171; b) J. Zhao, H. Shao, X. Wu, S. Shi, "A Rapid Synthesis of Pyranoid Glycols Promoted by  $\beta$ -Cyclodextrin and Ultrasound", *Chin. J. Chem.* **2011**, *29*, 1434-1440; c) H. Chen, T. Xian, W. Zhang, W. Si, X. Luo, B. Zhang, M. Zhang, Z. Wang, J. Zhang, "An efficient method for the synthesis of pyranoid glycols", *Carbohydr. Res.*, **2016**, *431*, 42-46.
- [209] a) R. P. Spencer, C. L. Cavallaro, J. Schwartz, "Rapid Preparation of Variously Protected Glycols Using Titanium(III)", *J. Org. Chem.*, **1999**, *64*, 3987-3995; b) R. P. Spencer, J. Schwartz, "Titanium(III) Reagents in Carbohydrate Chemistry: Glycal and C-Glycoside Synthesis", *Tetrahedron*, **2000**, *56*, 2103-2112.
- [210] L. Somsák, I. Németh, "A Simple Method for the Synthesis of Acylated Pyranoid Glycols Under Aprotic Conditions", *J. Carbohydr. Chem.*, **1993**, *12*, 679-684.
- [211] E. D. Goddard-Borger, R. V. Stick, "An Efficient, Inexpensive, and Shelf-Stable Diazotransfer Reagent: Imidazole-1-sulfonyl Azide Hydrochloride", *Org. Lett.*, **2007**, *9*, 3797-3800.
- [212] S. Kenso, O. Atsuhiko, K. Kyoko, "A Facile One-pot Synthesis of N-Substituted Phthalimides Using a Catalytic Amount of Crown Ether", *Bull. Chem. Soc. Jpn.*, **1982**, *55*, 1671-1672.
- [213] C. L. Forbes, R. W. Franck, "Improved Version of the Fischer-Zach Synthesis of Glycols: Vitamin B-12 Catalyzed Reductive Elimination of Glycosyl Bromides", *J. Org. Chem.*, **1999**, *64*, 1424-1425.

- [214] R. Scheffold, E. Amble, "Vitamin B12 and a Vitamin B12 Model Compound as Catalysts of Reductive Removal of  $\beta$ -Haloethyl Protecting Groups from Acids", *Angewandte Chemie International Edition in English*, **1980**, 19, 629-630.
- [215] H. Paulsen, J. P. Lorentzen, W. Kutschker, "Erprobte synthese von 2-azido-2-desoxy-d-mannose und 2-azido-2-desoxy-d-mannuronsäure als baustein zum aufbau von bakterien-polysaccharid-sequenzen", *Carbohydr. Res.*, **1985**, 136, 153-176.
- [216] I. Björk, U. Lindahl, "Mechanism of the anticoagulant action of heparin", *Mol. Cell. Biochem.*, **1982**, 48, 161-182.
- [217] D. A. Griffith, S. J. Danishefsky, "Sulfonamidoglycosylation of glycals. A route to oligosaccharides with 2-aminohexose subunits", *J. Am. Chem. Soc.*, **1990**, 112, 5811-5819.
- [218] a) D. A. Griffith, S. J. Danishefsky, "The Total Synthesis of Allosamidin. Expansions of the Methodology of Azaglycosylation Pursuant to the Total Synthesis of Allosamidin. A Surprising Enantiotopic Sense for a Lipase-Induced Deacetylation", *J. Am. Chem. Soc.*, **1996**, 118, 9526-9538; b) H. M. Kim, I. J. Kim, S. J. Danishefsky, "Total Syntheses of Tumor-Related Antigens N3: Probing the Feasibility Limits of the Glycal Assembly Method", *J. Am. Chem. Soc.*, **2001**, 123, 35-48; c) M. K. Spassova, W. G. Bornmann, G. Ragupathi, G. Sukenick, P. O. Livingston, S. J. Danishefsky, "Synthesis of Selected LeY and KH-1 Analogues: A Medicinal Chemistry Approach to Vaccine Optimization", *J. Org. Chem.*, **2005**, 70, 3383-3395; d) P. Nagorny, B. Fasching, X. Li, G. Chen, B. Aussedat, S. J. Danishefsky, "Toward Fully Synthetic Homogeneous  $\beta$ -Human Follicle-Stimulating Hormone ( $\beta$ -hFSH) with a Biantennary N-Linked Dodecasaccharide. Synthesis of  $\beta$ -hFSH with Chitobiose Units at the Natural Linkage Sites", *J. Am. Chem. Soc.*, **2009**, 131, 5792-5799.
- [219] R. U. Lemieux, B. Fraser-Reid, "The mechanisms of the halogenations and halogenmethoxylations of D-glucal triacetate, D-galactal triacetate, and 3,4-dihydropyran", *Can. J. Chem.*, **1965**, 43, 1460-1475.
- [220] D. Horton, W. Priebe, M. Sznajdman, "Iodoalkoxylation of 1,5-anhydro-2-deoxy-hex-1-enitols (glycals)", *Carbohydr. Res.*, **1990**, 205, 71-86.
- [221] F.-M. Gautier, F. Djedaïni-Pilard, C. Grandjean, "The iodosulfonamidation of peracetylated glycals revisited: access to 1,2-di-nitrogenated sugars", *Carbohydr. Res.*, **2011**, 346, 577-587.
- [222] G. D. Brayer, M. N. G. James, "A charge-transfer complex: bis(2,4,6-trimethyl-1-pyridyl)iodonium perchlorate", *Acta Crystallogr. B: Struct. Sci. Cryst.*, **1982**, 38, 654-657.
- [223] R. U. Lemieux, A. R. Morgan, "The synthesis of  $\beta$ -D-glucopyranosyl 2-deoxy- $\alpha$ -D-arabino-hexapyranoside", *Can. J. Chem.*, **1965**, 43, 2190-2197.
- [224] L. Laupichle, C. E. Sowa, J. Thiem, "Synthesis and structural studies of asparagine-modified 2-deoxy- $\alpha$ -N-glycopeptides associated with the renin-Angiotensin system", *Biorg. Med. Chem.*, **1994**, 2, 1281-1294.
- [225] R. Iwata, A. Doi, Y. Maeda, T. Wada, "Synthesis of oligodiaminomannoses and analysis of their RNA duplex binding properties and their potential application as siRNA-based drugs", *Org. Biomol. Chem.*, **2015**, 13, 9504-9515.
- [226] N. R. M. Reintjens, T. S. Koemans, N. Zilverschoon, R. Castelli, R. A. Cordfunke, J. W. Drijfhout, N. J. Meeuwenoord, H. S. Overkleeft, D. V. Filippov, G. A. van der Marel, J. D. C. Codée,

- "Synthesis of C-Glycosyl Amino Acid Building Blocks Suitable for the Solid-Phase Synthesis of Multivalent Glycopeptide Mimics", *Eur. J. Org. Chem.*, **2020**, 2020, 5126-5139.
- [227] S. J. Danishefsky, J. Gervay, J. M. Peterson, F. E. McDonald, K. Koseki, D. A. Griffith, T. Oriyama, S. P. Marsden, "Application of Glycals to the Synthesis of Oligosaccharides - Convergent Total Syntheses of the Lewis-X Trisaccharide Sialyl-Lewis-X Antigenic Determinant and Higher Congeners", *J. Am. Chem. Soc.*, **1995**, 117, 1940-1953.
- [228] J. M. Owens, B. K. S. Yeung, D. C. Hill, P. A. Petillo, "Facile C1 Epimerization of  $\alpha$ -1-Sulfonamidyl-2-deoxy-2-iodo-glycopyranosides", *J. Org. Chem.*, **2001**, 66, 1484-1486.
- [229] V. Kumar, N. G. Ramesh, "A glycal approach towards an efficient and stereodivergent synthesis of polyhydroxypyrrolidines", *Tetrahedron*, **2006**, 62, 1877-1885.
- [230] S. M. Weinreb, D. M. Demko, T. A. Lessen, J. P. Demers, " $\beta$ -Trimethylsilylethanesulfonyl chloride (SES-Cl): A new reagent for protection of amines", *Tetrahedron Lett.*, **1986**, 27, 2099-2102.
- [231] A. Nouvet, M. Binard, F. Lamaty, R. Lazaro, "Convenient introduction of 2-(trimethylsilyl)ethylsulfonyl (SES) amino protection on different amino acids and its use in peptidomimetic chemistry", *Lett. Pept. Sci.*, **1999**, 6, 239-242.
- [232] D. M. Dastrup, M. P. VanBrunt, S. M. Weinreb, "Preparation of Bis( $\beta$ -trimethylsilylethanesulfonyl)imide and Its Use in the Synthesis of Protected Amine Derivatives", *J. Org. Chem.*, **2003**, 68, 4112-4115.
- [233] S. J. Danishefsky, K. Koseki, D. A. Griffith, J. Gervay, J. M. Peterson, F. E. McDonald, T. Oriyama, "Azaglycosylation of complex stannyl alkoxides with glycal-derived iodo sulfonamides: a straightforward synthesis of sialyl-Lewis X antigen and other oligosaccharide domains", *J. Am. Chem. Soc.*, **1992**, 114, 8331-8333.
- [234] V. Declerck, P. Ribière, J. Martinez, F. Lamaty, "Sequential aza-Baylis-Hillman/Ring Closing Metathesis/Aromatization as a Novel Route for the Synthesis of Substituted Pyrroles", *J. Org. Chem.*, **2004**, 69, 8372-8381.
- [235] S. André, C. Grandjean, F.-M. Gautier, S. Bernardi, F. Sansone, H.-J. Gabius, R. Ungaro, "Combining carbohydrate substitutions at bioinspired positions with multivalent presentation towards optimising lectin inhibitors: case study with calixarenes", *Chem. Commun.*, **2011**, 47, 6126-6128.
- [236] V. Dimakos, M. S. Taylor, "Recent advances in the direct O-arylation of carbohydrates", *Org. Biomol. Chem.*, **2021**, 19, 514-524.
- [237] a) P. Beraud, A. Bourhim, S. Czernecki, P. Krausz, "Modification selective de mono- et de di-saccharides non proteges: Par l'intermédiaire de liaisons ester et ether", *Tetrahedron Lett.*, **1989**, 30, 325-326; b) H. Shi, B. Zhou, W. Li, Z. Shi, B. Yu, R. Wang, "Synthesis and anti-tumor activities of methyl 2-O-aryl-6-O-aryl'-d-glucopyranosides", *Bioorganic & Medicinal Chemistry Letters*, **2010**, 20, 2855-2858; c) C. O. R. Junior, S. B. R. Castro, A. A. Pereira, C. C. S. Alves, E. E. Oliveira, R. T. Rêgo, A. P. Ferreira, M. V. de Almeida, "Synthesis of genistein coupled with sugar derivatives and their inhibitory effect on nitric oxide production in macrophages", *Eur. J. Med. Chem.*, **2014**, 85, 615-620.
- [238] G. L. Tolnai, U. J. Nilsson, B. Olofsson, "Efficient O-Functionalization of Carbohydrates with Electrophilic Reagents", *Angew. Chem. Int. Ed.*, **2016**, 55, 11226-11230.

- [239] a) E. A. Merritt, B. Olofsson, "Diaryliodonium Salts: A Journey from Obscurity to Fame", *Angew. Chem. Int. Ed.*, **2009**, *48*, 9052-9070; b) E. Lindstedt, R. Ghosh, B. Olofsson, "Metal-Free Synthesis of Aryl Ethers in Water", *Org. Lett.*, **2013**, *15*, 6070-6073; c) E. Lindstedt, E. Stridfeldt, B. Olofsson, "Mild Synthesis of Sterically Congested Alkyl Aryl Ethers", *Org. Lett.*, **2016**, *18*, 4234-4237; d) E. Stridfeldt, E. Lindstedt, M. Reitti, J. Blid, P.-O. Norrby, B. Olofsson, "Competing Pathways in O-Arylations with Diaryliodonium Salts: Mechanistic Insights", *Chem. Eur. J.*, **2017**, *23*, 13249-13258.
- [240] W. Shang, Z.-D. Mou, H. Tang, X. Zhang, J. Liu, Z. Fu, D. Niu, "Site-Selective O-Arylation of Glycosides", *Angew. Chem.*, **2018**, *130*, 320-324.
- [241] D.-Y. Wang, Z.-K. Yang, C. Wang, A. Zhang, M. Uchiyama, "From Anilines to Aryl Ethers: A Facile, Efficient, and Versatile Synthetic Method Employing Mild Conditions", *Angew. Chem. Int. Ed.*, **2018**, *57*, 3641-3645.
- [242] M. Bielawski, M. Zhu, B. Olofsson, "Efficient and General One-Pot Synthesis of Diaryliodonium Triflates: Optimization, Scope and Limitations", *Adv. Synth. Catal.*, **2007**, *349*, 2610-2618.
- [243] A. Pees, C. Sewing, M. J. W. D. Vosjan, V. Tadino, J. D. M. Herscheid, A. D. Windhorst, D. J. Vugts, "Fast and reliable generation of [<sup>18</sup>F]triflyl fluoride, a gaseous [<sup>18</sup>F]fluoride source", *Chem. Commun.*, **2018**, *54*, 10179-10182.
- [244] J. Zhang, R. R. Schmidt, "O-Benzyl Trichloroacetimidates Having Electron-Withdrawing Substituents in Acid-Catalyzed Diarylmethane Synthesis", *Synlett*, **2006**, *2006*, 1729-1733.
- [245] D. E. Ward, Y. Gai, B. F. Kaller, "Synthetic Studies on Actinobolin and Bactobolin: Synthesis of N-Desalanyl-N-[2-(trimethylsilyl)ethanesulfonyl] Derivatives from a Common Intermediate and Attempted Removal of the SES Protecting Group", *J. Org. Chem.*, **1996**, *61*, 5498-5505.
- [246] D. L. Boger, J.-H. Chen, K. W. Saionz, "(–)-Sandramycin: Total Synthesis and Characterization of DNA Binding Properties", *J. Am. Chem. Soc.*, **1996**, *118*, 1629-1644.
- [247] S. K. Sundalam, A. Nilova, T. L. Seidl, D. R. Stuart, "A Selective C–H Deprotonation Strategy to Access Functionalized Arynes by Using Hypervalent Iodine", *Angew. Chem. Int. Ed.*, **2016**, *55*, 8431-8434.
- [248] A. Bhunia, S. R. Yetra, A. T. Biju, "Recent advances in transition-metal-free carbon–carbon and carbon–heteroatom bond-forming reactions using arynes", *Chem. Soc. Rev.*, **2012**, *41*, 3140-3152.
- [249] J. W. Wehner, M. Hartmann, T. K. Lindhorst, "Are multivalent cluster glycosides a means of controlling ligand density of glycoarrays?", *Carbohydr. Res.*, **2013**, *371*, 22-31.
- [250] a) C. Bannwarth, S. Ehlert, S. Grimme, "GFN2-xTB—An Accurate and Broadly Parametrized Self-Consistent Tight-Binding Quantum Chemical Method with Multipole Electrostatics and Density-Dependent Dispersion Contributions", *J. Chem. Theory Comput.*, **2019**, *15*, 1652-1671; b) S. Grimme, "Exploration of Chemical Compound, Conformer, and Reaction Space with Meta-Dynamics Simulations Based on Tight-Binding Quantum Chemical Calculations", *J. Chem. Theory Comput.*, **2019**, *15*, 2847-2862; c) P. Pracht, F. Bohle, S. Grimme, "Automated exploration of the low-energy chemical space with fast quantum chemical methods", *Phys. Chem. Chem. Phys.*, **2020**, *22*, 7169-7192.

- [251] Y.-L. Chen, J. Pyplo-Schnieders, H. Redlich, H. Luftmann, R. Fröhlich, "Preparation of 2-deoxystreptamine derivatives with all-axial substituents for desymmetrization", *Tetrahedron Lett.*, **2007**, *48*, 8145-8148.
- [252] a) U. Piantini, O. W. Sorensen, R. R. Ernst, "Multiple quantum filters for elucidating NMR coupling networks", *J. Am. Chem. Soc.*, **1982**, *104*, 6800-6801; b) M. Rance, O. W. Sørensen, G. Bodenhausen, G. Wagner, R. R. Ernst, K. Wüthrich, "Improved spectral resolution in COSY 1H NMR spectra of proteins via double quantum filtering", *Biochem. Biophys. Res. Commun.*, **1983**, *117*, 479-485.
- [253] a) Y. Kim, J. H. Prestegard, "Measurement of vicinal couplings from cross peaks in COSY spectra", *Journal of Magnetic Resonance (1969)*, **1989**, *84*, 9-13; b) S. Ravindranathan, X. Feng, T. Karlsson, G. Widmalm, M. H. Levitt, "Investigation of Carbohydrate Conformation in Solution and in Powders by Double-Quantum NMR", *J. Am. Chem. Soc.*, **2000**, *122*, 1102-1115.
- [254] J. P. Perdew, K. Burke, M. Ernzerhof, "Generalized Gradient Approximation Made Simple", *Phys. Rev. Lett.*, **1996**, *77*, 3865-3868.
- [255] J. P. Perdew, J. A. Chevary, S. H. Vosko, K. A. Jackson, M. R. Pederson, D. J. Singh, C. Fiolhais, "Atoms, molecules, solids, and surfaces: Applications of the generalized gradient approximation for exchange and correlation", *Phys. Rev. B*, **1992**, *46*, 6671-6687.
- [256] a) J. Tao, J. P. Perdew, V. N. Staroverov, G. E. Scuseria, "Climbing the Density Functional Ladder: Nonempirical Meta-Generalized Gradient Approximation Designed for Molecules and Solids", *Phys. Rev. Lett.*, **2003**, *91*, 146401; b) J. P. Perdew, J. Tao, V. N. Staroverov, G. E. Scuseria, "Meta-generalized gradient approximation: Explanation of a realistic nonempirical density functional", *J. Chem. Phys.*, **2004**, *120*, 6898-6911.
- [257] J. P. Perdew, M. Ernzerhof, K. Burke, "Rationale for mixing exact exchange with density functional approximations", *J. Chem. Phys.*, **1996**, *105*, 9982-9985.
- [258] a) A. D. Becke, "Density-functional exchange-energy approximation with correct asymptotic behavior", *Phys. Rev. A*, **1988**, *38*, 3098-3100; b) C. Lee, W. Yang, R. G. Parr, "Development of the Colle-Salvetti correlation-energy formula into a functional of the electron density", *Physical Review B*, **1988**, *37*, 785-789; c) A. D. Becke, "Density-functional thermochemistry. I. The effect of the exchange-only gradient correction", *J. Chem. Phys.*, **1992**, *96*, 2155-2160.
- [259] F. Jensen, "The optimum contraction of basis sets for calculating spin-spin coupling constants", *Theor. Chem. Acc.*, **2010**, *126*, 371-382.
- [260] a) F. London, "Théorie quantique des courants interatomiques dans les combinaisons aromatiques", *J. Phys. Radium*, **1937**, *8*, 397-409; b) H. F. Hamerka, "On the nuclear magnetic shielding in the hydrogen molecule", *Mol. Phys.*, **1958**, *1*, 203-215; c) R. Ditchfield, "Molecular Orbital Theory of Magnetic Shielding and Magnetic Susceptibility", *J. Chem. Phys.*, **1972**, *56*, 5688-5691; d) R. Ditchfield, "Self-consistent perturbation theory of diamagnetism", *Mol. Phys.*, **1974**, *27*, 789-807; e) G. L. Stoychev, A. A. Auer, R. Izsák, F. Neese, "Self-Consistent Field Calculation of Nuclear Magnetic Resonance Chemical Shielding Constants Using Gauge-Including Atomic Orbitals and Approximate Two-Electron Integrals", *J. Chem. Theory Comput.*, **2018**, *14*, 619-637; f) G. L. Stoychev, A. A. Auer, J. Gauss, F. Neese, "DLPNO-MP2 second

- derivatives for the computation of polarizabilities and NMR shieldings", *J. Chem. Phys.*, **2021**, *154*, 164110.
- [261] a) M. Kaupp, O. L. Malkina, V. G. Malkin, P. Pyykkö, "How Do Spin–Orbit-Induced Heavy-Atom Effects on NMR Chemical Shifts Function? Validation of a Simple Analogy to Spin–Spin Coupling by Density Functional Theory (DFT) Calculations on Some Iodo Compounds", *Chem. Eur. J.*, **1998**, *4*, 118-126; b) J. Vícha, J. Novotný, S. Komorovsky, M. Straka, M. Kaupp, R. Marek, "Relativistic Heavy-Neighbor-Atom Effects on NMR Shifts: Concepts and Trends Across the Periodic Table", *Chem. Rev.*, **2020**, *120*, 7065-7103.
- [262] a) F. Neese, A. Hansen, D. G. Liakos, "Efficient and accurate approximations to the local coupled cluster singles doubles method using a truncated pair natural orbital basis", *J. Chem. Phys.*, **2009**, *131*, 064103; b) F. Neese, A. Hansen, F. Wennmohs, S. Grimme, "Accurate Theoretical Chemistry with Coupled Pair Models", *Acc. Chem. Res.*, **2009**, *42*, 641-648; c) D. G. Liakos, A. Hansen, F. Neese, "Weak Molecular Interactions Studied with Parallel Implementations of the Local Pair Natural Orbital Coupled Pair and Coupled Cluster Methods", *J. Chem. Theory Comput.*, **2011**, *7*, 76-87; d) C. Riplinger, F. Neese, "An efficient and near linear scaling pair natural orbital based local coupled cluster method", *J. Chem. Phys.*, **2013**, *138*, 034106; e) C. Riplinger, B. Sandhoefer, A. Hansen, F. Neese, "Natural triple excitations in local coupled cluster calculations with pair natural orbitals", *J. Chem. Phys.*, **2013**, *139*, 134101; f) Y. Guo, C. Riplinger, U. Becker, D. G. Liakos, Y. Minenkov, L. Cavallo, F. Neese, "Communication: An improved linear scaling perturbative triples correction for the domain based local pair-natural orbital based singles and doubles coupled cluster method [DLPNO-CCSD(T)]", *J. Chem. Phys.*, **2018**, *148*, 011101.
- [263] a) M. Appell, G. Strati, J. L. Willett, F. A. Momany, "B3LYP/6-311++G\*\* study of  $\alpha$ - and  $\beta$ -d-glucopyranose and 1,5-anhydro-d-glucitol: 4C1 and 1C4 chairs, 3,OB and B3,O boats, and skew-boat conformations", *Carbohydr. Res.*, **2004**, *339*, 537-551; b) X. Biarnés, A. Ardèvol, A. Planas, C. Rovira, A. Laio, M. Parrinello, "The Conformational Free Energy Landscape of  $\beta$ -d-Glucopyranose. Implications for Substrate Preactivation in  $\beta$ -Glucoside Hydrolases", *J. Am. Chem. Soc.*, **2007**, *129*, 10686-10693; c) C. Calabrese, P. Écija, I. Compañón, M. Vallejo-López, Á. Cimas, M. Parra, F. J. Basterretxea, J. I. Santos, J. Jiménez-Barbero, A. Lesarri, F. Corzana, E. J. Cocinero, "Conformational Behavior of d-Lyxose in Gas and Solution Phases by Rotational and NMR Spectroscopies", *J. Phys. Chem. Lett.*, **2019**, *10*, 3339-3345.
- [264] N. Firon, I. Ofek, N. Sharon, "Interaction of mannose-containing oligosaccharides with the fimbrial lectin of *Escherichia coli*", *Biochem. Biophys. Res. Commun.*, **1982**, *105*, 1426-1432.
- [265] a) Z. Han, J. S. Pinkner, B. Ford, R. Obermann, W. Nolan, S. A. Wildman, D. Hobbs, T. Ellenberger, C. K. Cusumano, S. J. Hultgren, J. W. Janetka, "Structure-Based Drug Design and Optimization of Mannoside Bacterial FimH Antagonists", *J. Med. Chem.*, **2010**, *53*, 4779-4792; b) T. Klein, D. Abgottspon, M. Wittwer, S. Rabbani, J. Herold, X. Jiang, S. Kleeb, C. Lüthi, M. Scharenberg, J. Bezençon, E. Gubler, L. Pang, M. Smiesko, B. Cutting, O. Schwardt, B. Ernst, "FimH Antagonists for the Oral Treatment of Urinary Tract Infections: From Design and Synthesis to in Vitro and in Vivo Evaluation", *J. Med. Chem.*, **2010**, *53*, 8627-8641.
- [266] W. Schönemann, J. Cramer, T. Mühlethaler, B. Fiege, M. Silbermann, S. Rabbani, P. Dätwyler, P. Zihlmann, R. P. Jakob, C. P. Sager, M. Smieško, O. Schwardt, T. Maier, B. Ernst,

- "Improvement of Aglycone  $\pi$ -Stacking Yields Nanomolar to Sub-nanomolar FimH Antagonists", *ChemMedChem*, **2019**, *14*, 749-757.
- [267] Y. Bourne, B. Bolgiano, D.-I. Liao, G. Strecker, P. Cantau, O. Herzberg, T. Feizi, C. Cambillau, "Crosslinking of mammalian lectin (galectin-1) by complex biantennary saccharides", *Nature Structural Biology*, **1994**, *1*, 863-870.
- [268] S. K. Das, M. C. Trono, R. Roy, Transition Metal-Catalyzed Cross-Coupling Reactions toward the Synthesis of  $\alpha$ -d-Mannopyranoside Clusters in *Methods Enzymol.*, Vol. 362, Academic Press, **2003**, pp. 3-17.
- [269] R. Roy, M. C. Trono, D. Giguère, Effects of Linker Rigidity and Orientation of Mannoside Cluster for Multivalent Interactions with Proteins in *Glycomimetics: Modern Synthetic Methodologies*, Vol. 896, American Chemical Society, **2005**, pp. 137-150.
- [270] T. K. Dam, C. F. Brewer, "Thermodynamic Studies of Lectin–Carbohydrate Interactions by Isothermal Titration Calorimetry", *Chem. Rev.*, **2002**, *102*, 387-430.
- [271] A. J. J. Lennox, G. C. Lloyd-Jones, "Selection of boron reagents for Suzuki–Miyaura coupling", *Chem. Soc. Rev.*, **2014**, *43*, 412-443.
- [272] G. Berionni, B. Maji, P. Knochel, H. Mayr, "Nucleophilicity parameters for designing transition metal-free C–C bond forming reactions of organoboron compounds", *Chem. Sci.*, **2012**, *3*, 878-882.
- [273] G. A. Molander, B. Biolatto, "Palladium-Catalyzed Suzuki–Miyaura Cross-Coupling Reactions of Potassium Aryl- and Heteroaryltrifluoroborates", *J. Org. Chem.*, **2003**, *68*, 4302-4314.
- [274] a) G. A. Molander, I. Shin, "Pd-Catalyzed Suzuki–Miyaura Cross-Coupling Reactions between Sulfamates and Potassium Boc-Protected Aminomethyltrifluoroborates", *Org. Lett.*, **2013**, *15*, 2534-2537; b) A. K. L. Yuen, C. A. Hutton, "Deprotection of pinacolyl boronate esters via hydrolysis of intermediate potassium trifluoroborates", *Tetrahedron Lett.*, **2005**, *46*, 7899-7903.
- [275] G. Cutolo, F. Reise, M. Schuler, R. Nehmé, G. Despras, J. Brekalo, P. Morin, P. Y. Renard, T. K. Lindhorst, A. Tatibouët, "Bifunctional mannoside–glucosinolate glycoconjugates as enzymatically triggered isothiocyanates and FimH ligands", *Org. Biomol. Chem.*, **2018**, *16*, 4900-4913.
- [276] F. Sliman, D. Desmaële, "Synthesis of 5-Aryl- and 5-Heteroaryl-7-carboxyl-8-hydroxyquinaldines through Suzuki Cross-Coupling Reaction with Potassium Organotrifluoroborates", *Synthesis*, **2010**, *2010*, 619-630.
- [277] R. Roy, S. K. Das, F. Santoyo-González, F. Hernández-Mateo, T. K. Dam, C. F. Brewer, "Synthesis of "Sugar-Rods" with Phytohemagglutinin Cross-Linking Properties by Using the Palladium-Catalyzed Sonogashira Reaction", *Chem. Eur. J.*, **2000**, *6*, 1757-1762.
- [278] Z. Han, J. S. Pinkner, B. Ford, E. Chorell, J. M. Crowley, C. K. Cusumano, S. Campbell, J. P. Henderson, S. J. Hultgren, J. W. Janetka, "Lead Optimization Studies on FimH Antagonists: Discovery of Potent and Orally Bioavailable Ortho-Substituted Biphenyl Mannosides", *J. Med. Chem.*, **2012**, *55*, 3945-3959.
- [279] D. Schwizer, H. Gäthje, S. Kelm, M. Porro, O. Schwardt, B. Ernst, "Antagonists of the myelin-associated glycoprotein: A new class of tetrasaccharide mimics", *Biorg. Med. Chem.*, **2006**, *14*, 4944-4957.

## References

---

- [280] C. Amatore, A. Jutand, G. Le Duc, "The Triple Role of Fluoride Ions in Palladium-Catalyzed Suzuki–Miyaura Reactions: Unprecedented Transmetalation from [ArPdFL<sub>2</sub>] Complexes", *Angew. Chem. Int. Ed.*, **2012**, 51, 1379-1382.
- [281] T. Hirano, K. Hiromoto, H. Kagechika, "Development of a Library of 6-Arylcoumarins as Candidate Fluorescent Sensors", *Org. Lett.*, **2007**, 9, 1315-1318.
- [282] a) H. Nie, J. L. Self, A. S. Kuentler, R. C. Hayward, J. Read de Alaniz, "Multiaddressable Photochromic Architectures: From Molecules to Materials", *Adv. Opt. Mater.*, **2019**, 7, 1900224; b) M. Jeong, J. Park, S. Kwon, "Molecular Switches and Motors Powered by Orthogonal Stimuli", *Eur. J. Org. Chem.*, **2020**, 2020, 7254-7283.
- [283] a) G. S. Hartley, "The Cis-form of Azobenzene", *Nature*, **1937**, 140, 281-281; b) H. Rau, "Spectroscopic Properties of Organic Azo Compounds", *Angewandte Chemie International Edition in English*, **1973**, 12, 224-235.
- [284] A. Mostad, C. Romming, "Refinement of Crystal-Structure of Cis-Azobenzene", *Acta Chem. Scand.*, **1971**, 25, 3561-&.
- [285] J. H. Harvey, B. K. Butler, D. Trauner, "Functionalized azobenzenes through cross-coupling with organotrifluoroborates", *Tetrahedron Lett.*, **2007**, 48, 1661-1664.
- [286] T. Takeuchi, K. Akeda, S. Murakami, H. Shinmori, S. Inoue, W.-S. Lee, T. Hishiya, "Photoresponsive porphyrin-imprinted polymers prepared using a novel functional monomer having diaminopyridine and azobenzene moieties", *Org. Biomol. Chem.*, **2007**, 5, 2368-2374.
- [287] S. G. Gouin, E. Vanquelef, J. M. García Fernández, C. Ortiz Mellet, F.-Y. Dupradeau, J. Kovensky, "Multi-Mannosides Based on a Carbohydrate Scaffold: Synthesis, Force Field Development, Molecular Dynamics Studies, and Binding Affinities for Lectin Con A", *J. Org. Chem.*, **2007**, 72, 9032-9045.
- [288] B. K. Shull, Z. Wu, M. Koreeda, "A Convenient, Highly Efficient One-Pot Preparation of Peracetylated Glycals From Reducing Sugars", *J. Carbohydr. Chem.*, **1996**, 15, 955-964.
- [289] S. Darses, G. Michaud, J.-P. Genêt, "Potassium Organotrifluoroborates: New Partners in Palladium-Catalysed Cross-Coupling Reactions", *Eur. J. Org. Chem.*, **1999**, 1999, 1875-1883.
- [290] E. Harder, W. Damm, J. Maple, C. Wu, M. Reboul, J. Y. Xiang, L. Wang, D. Lupyan, M. K. Dahlgren, J. L. Knight, J. W. Kaus, D. S. Cerutti, G. Krilov, W. L. Jorgensen, R. Abel, R. A. Friesner, "OPLS3: A Force Field Providing Broad Coverage of Drug-like Small Molecules and Proteins", *J. Chem. Theory Comput.*, **2016**, 12, 281-296.
- [291] a) S. G. Gouin, G. Roos, J. Bouckaert, *Discovery and Application of FimH Antagonists in Carbohydrates as Drugs* (Eds.: P. H. Seeberger, C. Rademacher), Springer International Publishing, Cham, **2014**, pp. 123-168; b) G. Zhou, W.-J. Mo, P. Sebbel, G. Min, T. A. Neubert, R. Glockshuber, X.-R. Wu, T.-T. Sun, X.-P. Kong, "Uroplakin Ia is the urothelial receptor for uropathogenic *Escherichia coli*: evidence from *in vitro* FimH binding", *J. Cell Sci.*, **2001**, 114, 4095-4103.
- [292] a) Maestro-Desmond Interoperability Tools, Schrödinger, New York, NY, **2020**; b) Schrödinger Release 2020-4: Binding Pose Metadynamics protocol; Desmond Molecular Dynamics System, D. E. S. Research, New York, NY, **2020**.
- [293] Schrödinger Release 2020-4: MacroModel, Schrödinger, LLC, New York, **2020**.

- 
- [294] P. Mark, L. Nilsson, "Structure and Dynamics of the TIP3P, SPC, and SPC/E Water Models at 298 K", *J. Phys. Chem. A*, **2001**, *105*, 9954-9960.
- [295] a) F. Neese, "Software update: the ORCA program system, version 4.0", *WIREs Comput. Mol. Sci.*, **2018**, *8*, e1327; b) F. Neese, F. Wennmohs, U. Becker, C. Riplinger, "The ORCA quantum chemistry program package", *J. Chem. Phys.*, **2020**, *152*, 224108.
- [296] a) F. Weigend, M. Häser, H. Patzelt, R. Ahlrichs, "RI-MP2: optimized auxiliary basis sets and demonstration of efficiency", *Chem. Phys. Lett.*, **1998**, *294*, 143-152; b) S. Grimme, S. Ehrlich, L. Goerigk, "Effect of the damping function in dispersion corrected density functional theory", *J. Comput. Chem.*, **2011**, *32*, 1456-1465.
- [297] a) K. Wolinski, J. F. Hinton, P. Pulay, "Efficient implementation of the gauge-independent atomic orbital method for NMR chemical shift calculations", *J. Am. Chem. Soc.*, **1990**, *112*, 8251-8260; b) F. Jensen, "Segmented Contracted Basis Sets Optimized for Nuclear Magnetic Shielding", *J. Chem. Theory Comput.*, **2015**, *11*, 132-138.

**Abbreviations**

Ac	acetyl
aq.	aqueous
Boc	<i>tert</i> -butyloxycarbonyl
calc.	calculated
cf.	confer
CFG	Consortium for Functional Glycomics
CH <sub>2</sub> Cl <sub>2</sub>	dichloromethane
COSY	correlated spectroscopy
conc.	concentrated
CRD	carbohydrate recognition domain
CuAAC	copper(I)-catalyzed azide alkyne cycloaddition
d (NMR)	doublet
DBU	1,8-Diazabicyclo[5.4.0]undec-7-en
DEPT	distorsionless enhancement by polarization transfer
DFT	density functional theory
DIAD	diisopropyl azodicarboxylate
DMAP	<i>N,N</i> -dimethylaminopyridine
DMF	<i>N,N</i> -dimethylformamide
DMSO	dimethyl sulfoxide
<i>E. coli</i>	<i>Escherichia coli</i>
EDC	1-ethyl-3-(3-dimethylaminopropyl)carbodiimide
EtOAc	ethyl acetate
ESI	electrospray ionization
g	gram
GFP	green fluorescing protein
h	hour
HOBt	1-hydroxybenzotriazol
Hz	Hertz
IC <sub>50</sub>	half maximal inhibitory concentration
IFD	induced fit
IR	infrared spectroscopy
<i>J</i>	coupling constant
L	liter
lit.	literature
m (NMR)	multiplet

---

M	molarity
MALDI	matrix assisted laser desorption ionisation
MD	molecular dynamics
MeOH	methanol
min	minute
m.p.	melting point
MS	mass spectrometry
Ms	mesyl
m/z	mass-to-charge ratio
NHS	<i>N</i> -hydroxysuccinimide
NMR	nuclear magnetic resonance
OD	optical density
org.	organic
<i>p</i>	para
PBS	phosphate buffered saline
PBST	phosphate buffered saline with Tween <sup>®</sup>
pH	potentia Hydrogenii
pPKL	plasmid Per Klemm
ppm	parts per million
q (NMR)	quartet
quant.	quantitative
R	residue
R <sub>f</sub>	retardation factor
RIP	relative inhibitory potency
rpm	revolutions per minute
rt	room temperature
s (NMR)	singlet
SD	standard deviation
t (NMR)	triplet
TFA	trifluoroacetic acid
THF	tetrahydrofuran
TLC	thin layer chromatography
TMS	tetramethylsilan
ToF	time of flight
Ts	tosyl
Tyr	tyrosine
UV/Vis	ultraviolet/visible

## Danksagung

An dieser Stelle möchte ich mich bei einigen Personen bedanken, die mir besonders wichtig sind und mich während meiner Promotionszeit begleitet haben:

Mein besonderer Dank gilt Frau Prof. Dr. Thisbe K. Lindhorst, meiner Doktormutter, für die Betreuung dieser Arbeit und für die sehr gute Zusammenarbeit. Besonders möchte ich mich hier für die wissenschaftlichen Freiheiten, das große Vertrauen in meine Arbeit und meine Projekte, bereichernde Diskussionen und die großzügige Unterstützung über die gesamte Zeit meiner Promotion bedanken. Es hat mir großen Spaß gemacht, bei Ihnen meine Promotion durchzuführen.

Bei Herrn Prof. Dr. Frank D. Sönnichsen möchte ich mich für die Übernahme des Koreferats und für die vielen hilfreichen Ratschläge bei allen NMR-Fragen und Experimenten bedanken.

Zudem möchte ich mich an dieser Stelle bei meinem Kooperationspartner Herrn Prof. Dr. Alexander A. Auer vom MPI für Kohlenforschung in Mülheim bedanken. Diese gemeinsame Arbeit hat mir großen Spaß bereitet und besonders spannende Einblicke in das Feld der theoretischen Chemie gewährt.

Ich danke außerdem allen Mitarbeitern des Instituts für ihre Hilfsbereitschaft und die gute Zusammenarbeit. Besonders möchte ich mich hier bei den Mitarbeitern der spektroskopischen Abteilung Marion Höftmann, Gitta Kohlmeyer-Yilmaz, Holger Franzen, Rolf Schmied und Dirk Meyer für ihre Hilfe und die ein oder andere Last-Minute Messung bedanken. Auch bei Claus Bier möchte ich mich bedanken für viele Hilfestellungen und die interessanten Drehtage des Sicherheitsvideos.

Ein großer Dank gebührt zudem Christine Haug für die nette Zusammenarbeit und die großartige Unterstützung bei jeglichen organisatorischen Fragen. Außerdem möchte ich mich auch bei Elwira Klima-Bartczak bedanken, die als ehemalige gute Seele des AKs mit ihrer herzlichen Art immer für einen da war.

Natürlich möchte ich mich auch bei der gesamten Arbeitsgruppe Lindhorst in ihren unterschiedlichen Zusammensetzungen für die wunderbare Zeit, Feierabendbiere, Kaffeepausen, die fabelhafte Stimmung, angenehme Diskussionen und die gute Zusammenarbeit bedanken. Dabei gilt ein besonderer Dank der Truppe aus Labor 109 mit Jasna, Guillaume und Bohl für die produktive Arbeitsatmosphäre. Außerdem möchte ich mich noch bei Anne Heitmann bedanken, dass sie mich damals zur Kohlenhydratchemie überredet und in den Arbeitskreis geholt hat.

Außerdem möchte ich mich an dieser Stelle bei meinem Bachelorstudenten und (F3-) Praktikanten Sascha Koller, Frederik Wichter, Clemens Lütjohann und Ingo vom Sondern bedanken.

Ohne meine Freunde Justus, Bohl, Basti, Marc und meine Volleyballjungs von den #Mettenboys hätte mir meine Zeit während des Studiums und der Promotion wahrscheinlich nur halb so viel Spaß gemacht. Ich bin sehr froh, hier in Kiel so großartige Freunde kennengelernt zu haben!

Zum Schluss möchte ich mich besonders bei meinen Eltern und meiner Schwester bedanken, die mich immer unterstützt haben und denen ich sehr viel verdanke. Mein größter Dank gebührt schließlich Vanja, die immer für mich da ist, mich unterstützt, sich mit mir freut, mich aufbaut und einfach wundervoll ist.

Danke!